Alma Mater Studiorum – Università di Bologna

DOTTORATO DI RICERCA IN

Chimica

Ciclo XXVII

Settore Concorsuale di afferenza: 03/C1

Settore Scientifico disciplinare: CHIM/06

Synthesis of constrained peptidomimetics for therapeutic, diagnostic and theranostic applications

Presentata da: **Arianna Greco**

Coordinatore Dottorato

Aldo Roda

Relatore

Luca Gentilucci

Esame finale anno 2015

Index

Abbreviations and Acronyms

2D, 3D = two-, three-dimensional, respectively

Ala = alanine

AMBER = assisted model building with energy refinement

Amo = 5-aminomethyl-oxazolidine-2,4-dione

AMPUMP = 1-(4-(aminomethyl)phenyl)-3-(o-methylphenyl)urea

APTES = amnopropyltriethoxysilane

Asn = asparagine

Asp = aspartic acid

β^2-Pro = (*S*)-pyrrolidine-3-carboxylic acid

Boc = tert-butyloxycarbonyl

Boc_2O = Boc anhydride

Bn = benzyl

Bz = benzoyl

BSA = bovine serum albumin

Cbz or Z = carboxybenzyl

$CDCl_3$ = deuterated chloroform

CDI = 1,1′-carbonyldiimidazole

CMFDA = chloromethylfluorescein diacetate

c[RGDfK] = cyclo-(L)-Arg-(L)-Gly-(L)-Asp-(D)-Phe-(L)-Lys

ΔAbu = 2,3-dehydro-2-aminobutyric acid

ΔAla = dehydroalanine

ΔPhe = dehydroPhe

DBU = 1,5-diazabiciclo (5.4.0) undec-5-ene

DCM = dichlorometane

DGR = Asp-Gly-Arg

DIPEA = *N*,*N*-Diisopropylethylamine

DMA = dimethylamine

DMF = dimethylformamide

DMSO = dimethyl sulfoxide

DSC = disuccinimidyldicarbonate

DXP = *N,N'*-bis(2,6-dimethylphenyl)perylene-3,4,9,10-tetracarboxylic acid diimide

ECM = extracellular matrix

EDCI = 1-ethyl-3-(3-dimethylaminopropyl)carbodiimide

EDX = energy dispersive X-ray spectroscopy

EM-1 = endomorphin-1

ES-MS = electrospray ionization mass spectrometry

Et_2O = ether

EtOAc = ethyl acetate

Fmoc = 9H-fluoren-9-ylmethoxycarbonyl

FN = fibronectin

FT-IR = fourier transform infrared spectroscopy

gCOSY = gradient correlation spectroscopy

Gly = glycine

HATU = 1-[Bis(dimethylamino)methylene]-1H-1,2,3-triazolo[4,5-b]pyridinium 3-oxid hexafluorophosphate

HBTU = 2-(1H-Benzotriazole-1-yl)-1,1,3,3-tetramethyluronium hexafluorophosphate

HMBC = heteronuclear multiple bond correlation

HOBt = hydroxybenzotriazole

HSQC = heteronuclear single quantum coherence

IDS = Ile-Asp-Ser

Imd = 2-imidazolidinone

*i*Ser = isoserine

LDV = Leu-Asp-Val

MAOS = microwave-assisted organic synthesis

MD = molecular dynamics

MPUPA = o-methylphenylureaphenylacetyl

Mtr = 4-Methoxy-2,3,6-trimethylbenzenesulphonyl

MW = microwave

NCA = N-carboxyanhydride

NPs = nanoparticles

Oxd = 2-oxazolidinone

p-NBC = 4-Nitrobenzyl chloroformate

p-NPC = 4-Nitrophenyl chloroformate

PDMS = polydimethylsiloxane

PEG = polyethylene glycol

PFA = paraformaldehyde

PG = protecting group

Phe = phenyalanine

Phg = D-phenylGly

PhSer = Phenylserine

PPI = protein-protein interaction

Pro = proline

RGD = Arg-Gly-Asp

Rmsd = root-mean-square deviation

Roesy = rotating-frame nuclear overhauser effect correlation spectroscopy

RP = reversed phase;

rt = room temperature

SAM = self-assembled monolayer

Sar = sarcosine

SEM = scanning electron microscopy

Ser = serine

SP = solid phase

SPA = scintillation proximity-binding assay;

SPPS = solid phase peptide synthesis

TEA = triethilamine

TFA = trifluoroacetic acid

TGA = thermogravimetric analysis

THF = tetrahydrofuran

Thr = threonine

Trp = tryptophan

Ts = *N*-tosyl

Tyr = tyrosine

Val = valine

VCAM = vascular cell adhesion molecule

VCAM-1 = vascular cell adhesion molecule-1

VT = vitronectin or variable temperature

XPS = X-ray photoelectron spectroscopy

XRD = X-ray powder diffraction

Chapter 1

From peptides to drugs: peptidomimetics

The major striking features of the abundantly existing peptides and proteins are the enormous diversity in biological function, and the tremendous variations in structure. The biological functions range from hormones, toxins, and enzymes to antibodies, receptors, structural proteins, and beyond. Some of the most toxic compounds known are peptides,[1] and among the molecules capable of binding ligands noncovalently we also find proteins, such as avidin and antibodies. Similarly, their structural complexity varies from simple, small, randomly structured peptides, to turns and helices, and on to complicated assemblies of turns, helices, sheets, and structured assemblies of proteins. Responsible for this incredible diversity are "only" 20 different proteinogenic amino acids, which are linked by an identical, repeating, connecting amide linkage, often denoted as the "peptide bond". These 20 amino acids can lead to 8000 different tripeptides and as many as 64 million possible hexapeptides and one can easily imagine the structural diversity as larger peptides assume more defined structures. It is therefore self-evident that, together with the large diversity of amino acid residues, which contain a wide range of side chain functional groups, this structural diversity will lead to a gigantic plurality in biological function. Furthermore, nature increases the diversity of both structure and function of peptides and proteins even further by post-translational modifications; this allows, for example, the introduction of an on–off switch for the activity of a protein by phosphorylation.

In addition, the set of the 20 amino acids that are present in proteins is greatly expanded and also includes the damino acids found in many small natural products and peptides, which are synthesized by non-ribosomal biosynthetic pathways. The situation is even more complicated, since different peptides can affect the same physiological function.[2]

Finally, nowadays, with the exciting methods of expanding the genetic code, the set of 20 proteinogenic amino acid residues has been increased to well over 20.[3]

Nevertheless there is the need to expand this impressive diversity of peptides and proteins even more by entering the realm of peptidomimetics and protein mimics. The reason can be found in their biological properties and structures, which are reminiscent of the structural features of peptides, proteins and their constituent amino acid residues. In many cases the structural and biological properties have to be improved or altered. In fact, despite of their clinical potential, seldom native peptides may be used directly as drugs, especially for oral administration. This is due to some very important limitations, such as: limitate stability toward proteolysis by peptidase; poor absorbition from intestine to the blood and across the blood-brain barrier, due for example to the high molecular weight; rapid excretion through the liver and/or kidneys; rapid photolytic degradation; high conformational flexibility, which often allows interactions with multiple receptors, resulting in several undesired side-effects.[4]

Therefore, solubility, stability, bioavailability, and affinity of peptides and proteins were and still are important properties that limit, to a considerable extent, the development of peptides and proteins as drugs, and in many pharmaceutical companies this was considered to be a "no-go" area and the Lipinski "Rule of Five" was used to underpin it. Much effort has been expended to find ways to replace portions of biologically active peptides with non-peptide structures, with the aim of obtaining orally bioavailable entities. Such compounds, containing non-peptidic structural elements, that are capable of mimicking or antagonizing the biological action of a natural parent peptide are defined as peptidomimetics.[4a] Peptidomimetics might be able to remedy, at least partly, the objections pointed out by the Rule of Five.

The Rule of Five states that poor absorption or permeation is more likely when more than five H-bond donors (sum of OHs and NHs) and more than ten H-bond acceptors (sum of Os and Ns) are present, in addition to a molecular weight greater than 500, and a log P greater than 5.

Thus, there is still a lot to gain when peptidomimetics of a particular bioactive peptide can be developed, because peptides usually contain plenty of hydrogen bond donors and acceptors, have a molecular weight greater than 500 (even with only four residues), and can be very hydrophilic or hydrophobic. Nevertheless, the last two decades have also shown tremendous developments with respect to "biologics" such as hormones, monoclonal antibodies, nanobodies (variable domains of camelid heavychain-only antibodies), etc. None of them obeys the Rule of Five, and there is usually more than a problem with respect to solubility, stability, bioavailability and affinity; however, all are often used in extremely valuable treatments of severe diseases.

Anyway the rational design of mimetics would be great if one could "transform" any conceivable amino acid sequence (a peptide chain) into a corresponding peptidomimetic chain, while retaining the required peptide properties, such as the presence of the amino acid side chains, its repetitive nature, the possibility for interaction with and by the backbone, as well

as eradicating or diminishing at least some unfavorable characteristics such as biodegradability. In this optic, modified peptides have been commonly obtained by different modifications of amino acids and peptide structures.

The first approaches were based on simple modifications of N- or C- terminus, N- and Cα- methylation, or single amino acid replacement with its D-amino acid equivalent.[5] The introduction of these variants in an aminoacidic sequence provides an increased stability to peptides, since enzymes have difficult to hydrolyze unnatural amino acids. Moreover, the above mentioned modifications, such as the insertion of D-residues, often enforce a different conformation of the peptide,[6] and strongly influence receptor affinity and selectivity.[7]

The introduction of isosteric groups represents another peptide bond modifications approach.[21,8] The replacement of a labile peptide bond with an isoster was of great help for designing therapeutic agents targeting proteases; very often, the isoster imitates the transition state of peptide bond cleavage, including the hydroxyl group resulting from enzyme nucleophilic addition.This strategy resulted in the development of a variety of peptidomimetic classes, the most common and studied are peptoids,[9] introduced by Zuckermann, in which the side chain of an amino acid is "shifted" to the α-amino group. This leads to alkylated peptide amide bonds, thereby explaining the resistance towards degradation by proteases. In fact, alkylation, in particular methylation, of amino acids in biologically active peptides is a useful principle to reduce biodegradation and increase bioavailability, for example in cyclosporine and somatostatin analogues.[10]

Also peptide-bond reversal represents an important structural alteration for peptides,[11] and proved to be useful to reduce the degradation rate of the peptides by peptidases. Retro-inverso peptides have found applications as immunogens, immunomodulators, immunostimulators, antimicrobial, and diagnostic reagents, as well as modified isomers of membrane-penetrating peptides as delivery systems.[12]

Finally azapeptides,[13] urea-peptidomimetics,[14] and sulphonamide peptides/peptoids,[15] are part of this class of mimetics (Figure 1).

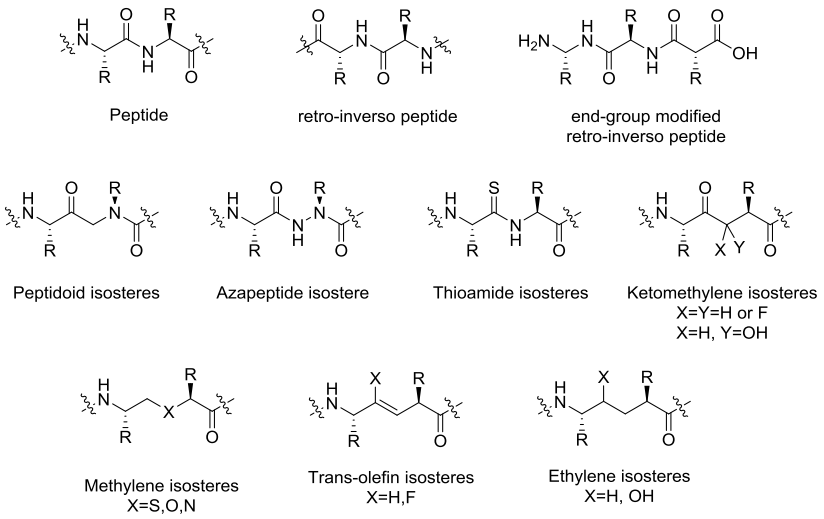

Figure 1. Some common peptide bond isoster.

Peptide analogs have also been obtained by introducing unusual residues, which can be achieved by a number of ways,[16] such as β-,[17] γ- and δ-amino acids,[18] or α- or β-substituted amino acids.[19] These particular amino acids have been utilized to construct the mimetics of naturally occurring peptide hormones, MHC-binding beta-peptides, opioid peptides, somatostatin, or amphipathic β-peptide inhibitors of membrane-bound proteins.[20]

Unfortunately, the major problem and collateral effect of the great part of peptidomimetic strategies illustrated until now is that, in principle, a mimetic, just like its corresponding peptide, is very flexible. In particular, the high flexibility of peptides is due to the multiple conformations that are energetically possible for each residue of the incorporated amino acids. To get an idea of how important the issue of conformational freedom, just think that inasmuch as every amino acid has two degrees of conformational freedom, N–Cα (Φ) and Cα–CO (Ψ), are possible approximately 9 (3^2) stable local conformations. For a polypeptide with only 40 amino acids in length the number of possible conformations which need to be considered escalates to nearly 10^{40}.[5a]

Pioneering work by Ramachandran et al. resulted in the so-called Ramachandran plots which restrict the allowed values for the torsion angles Φ and Ψ and with that the conformational space accessible to the amino acids to about one third of the

total structural space. Nevertheless the remaining degrees of freedom still make a prediction of the structure extremely difficult.

This extraordinary high flexibility leads to the fact that short polypeptides rarely form any stable 3D structures in solution.[5b] There are only few examples reported in the literature where short to medium-sized peptides (<30-50 amino acids) were able to form stable structures. In most cases they exist in aqueous solution in numerous dynamically interconverting conformations. Additionally, the number of stable short peptide structures, which are accessible, is very limited because of the need to use amino acids having a strong structure inducing effect, like for example helix-inducing amino acids as leucine, glutamic acid or lysine. Finally, it is questionable whether the solid state conformations determined by X-ray analysis are identical to those occurring in solution or during the interactions of proteins with each other.[21]

This tricky trouble is extended also to the great part of peptidomimetics illustrated until now, for example in peptoids the side chain on the α-carbon atom is missing, thereby leading to a large range of allowable ϕ and ψ angles, despite the presence of the side chain on the amide-nitrogen atom that affects the range of allowable ϕ angles.[22] Understandably, increased conformational flexibility will lead to decreased binding affinity, as described above.

The problem was resolved with two interesting approaches, which purpose was reduce flexibility: by cyclization to afford cyclic peptoids or by noncovalent intramolecular interactions.

Rigid molecules are considered promising also for the evidence that a lot of biological processes are controlled by interactions between proteins (protein-protein interaction PPI), that, in most cases, are due to the contribution of just few amino acid residues, often arranged in a well defined folding structure (turn).

According to the most common definition, a turn is a structural motif where the Cα atoms of two residues separated by few, usually 1 to 5, peptide bonds are in close approach, less than 7 Å, while the corresponding residues do not form a regular secondary structure element such as in an α-helix or β-sheet (Figure 2).

The most renowned PPI processes are, for instance, the formation of hormone-receptor, protease-inhibitor, or antibody-antigen complexes.[23] Others, less specific, occur when proteins aggregate, like in amyloid fibrils which form in the tissues in several diseases such as Alzheimer's, familial amyloidotic polyneuropathy, the spongiform encephalopathies, familial Mediterranean fever, and some forms of rheumatoid arthritis.[24]

It's therefore self-evident how important it could be to interact and interfere with this kind of mechanisms in order to play a key role in their control and modulation.

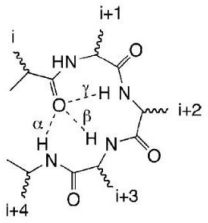

Figure 2. A fast way to distinguish between α-, β-, and γ-turns.

The first class of rigid mimics consists in the peptide cyclic analogues that are much more stable respect to the native peptides, conformationally more defined, and more selective towards the specific target. In addition, these covalent constraints also play a decisive role in controlling the three-dimensional structure of a molecule, for example by forming cavity or shell-like structures that are capable of binding other (small) molecules.

Peptide cyclization has been performed by simple condensation of the N- and C- terminus or by connecting functionalized side chains.[25] Another efficient method for preparing both small and macrocyclic rings, is the ring-closing metathesis approach,[26] though in certain cases the occurrence of inappropriate secondary structural elements precluding peptide cyclization required introducing a reversible backbone protection.[27]

Examples of cyclopeptidomimetics prepared by simple condensation are the RGD integrin inhibitors developed by Kessler for treatment of human tumor metastasis and tumor induced angiogenesis, bone remodelling and osteoporosis.[28] N-methylation scan on some cyclic peptides provided c[Arg-Gly-Asp-D-Phe-NMeVal], Cilengitide, with enhanced biological activity and affinity. The conformationally defined RGD mimetics have been utilized also for investigating the relationship between the 3D display of the pharmacophores and the different selectivity towards different kinds of RGD-binding integrins.[29]

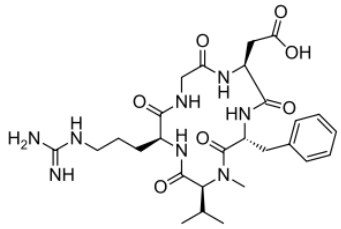

Figure 3. Chemical structure of Cilengitide, developed by Kessler.

Noteworthy advancements have been recently reported also in the development of non-cyclic conformationally defined peptidomimetics, designed to interfere with cell adhesion mechanisms, therefore constituting interesting tools in the synthesis of imaging biomarkers and assessment of therapy response as well as in the engineering of cell-targeted agents.[30] To induce the peptide folding were proposed constraining elements like dehydro amino acids, cyclic amino acids,[31] and other mimics of specific residues, which have been used to design acyclic peptides because of their turn-inducing or helix-forming propensity (Figure 4).[32]

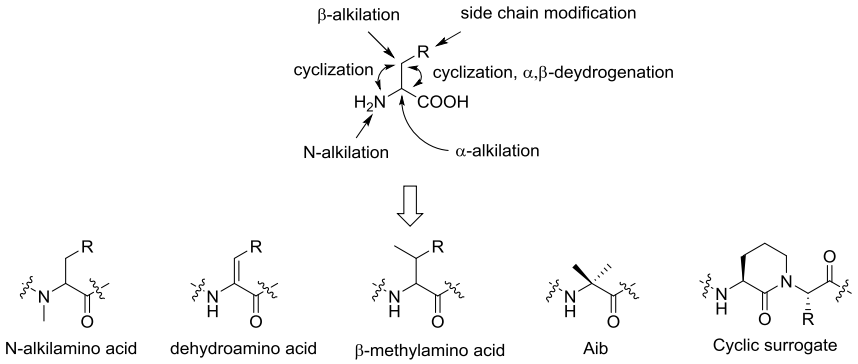

Figure 4. Some of the conformationally constrained residues aforementioned.

An important role among the backbone elements, which induce constrained conformations, is played by Pro and its derivatives. The peculiar features of this cyclic amino acid (among others the ability to induce cis peptide bond conformation)[33] makes it a priceless ally while looking for rigidity. A number of pseudo-Pro building blocks have also been assessed in several occasions and with various results, giving libraries of compounds with different properties, and with the capability to induce either the trans or the cis conformation[34] depending on the type of heterocycle used.
Another powerful element, widely used to constrain angles in peptidomimetics, is the so called Freidinger lactam. This lactam's peculiarity is the fact of being a bridge between the α carbon and the following amide nitrogen, resulting in five- six- or seven-membered heterocycles. Contrary to the pseudo-Pro, Freidinger lactam directly constrains the Ψ and the ω angles.[35] Since its introduction in the early 80's it has been widely used to constrain peptide conformations, stabilizing β- and γ-turn structures and acting as a β-strand mimetic in linear peptides,[36] with lots of applications in the medicinal chemistry field, especially in the interaction with G-protein coupled receptors, as reported in a study aiming to reproduce the active conformation of the Growth hormone-releasing peptides (GHRPs) by incorporating a Freidinger lactam in it.[37] Some more recent work also focused on the development of new analogues of the Freidinger lactam, by introducing several kinds of modifications on its initial structure, such as heteroatoms substituting the simple sp^3 carbons, in order to give rigidity to the ring, or the use of fused bicyclic or spirocyclic extensions.[4a]

As seen, in recent years, research in the field of peptidomimetics is expanding always more and accordingly also its chemistry is growing. This led to the development of different synthetic methods for obtaining oligomeric peptidomimetics, such as the solid-phase peptide synthesis (SPPS), developed by B. Merrifield between 1950 and 1960, that made possible to synthesize polypeptides, with fifty or more amino acids in length, in large quantities making them available for pharmacological and clinical testing.[4b]
In addition, in the early 1990's, the Kent group reported a chemoselective ligation of unprotected peptides.[38] They later developed the ''native chemical ligation'' method for the conjugation of unprotected polypeptide/peptoid molecules. This new strategy initiated an era of chemical protein synthesis,[39] during which a variety of proteins and mimics have been prepared.[40]

Moreover, the ever-increasing demand of techniques to obtain a large number of compounds in relatively short time, allowed microwaves to gain importance among the synthetic technologies. In fact, MAOS (Microwave-Assisted Organic Synthesis) is been successfully coupled with the SPPS or with in solution peptide synthesis, enabling to reduce significantly the reaction time, because this kind of technique, raising the temperature very quickly, allows to fasten the reaction and may give access to different reaction routes, leading to unexpected yields, conversions and selectivities.
Analyzing these aspects, it is evident that the development of synthetic procedures for the synthesis of unnatural amino acids and peptides/mimetics, for istance with a milder environmental impact, is a field of actual interest.

The context shown and analized, highlights the developments on this area that might now also have a strong impetus on the growth and significance of modified peptides, peptidomimetics, and protein mimics as drugs. Moreover, this will also be favorably influenced by the recent enormous developments in drug delivery methods for these compounds, that guarantees the preservation of their biological activity during an acceptable shelf-life and ideally the effective and safe transport and delivery to its site of action.
However, during the last three decades, there has been an exponential growth in an average number of peptide therapeutics entering clinical studies. Peptide and mimics drugs are being investigated in a wide variety of therapeutic areas, with the highest number of them entering clinical trials for metabolic disorders and cancer treatments (Figure 4).[41]

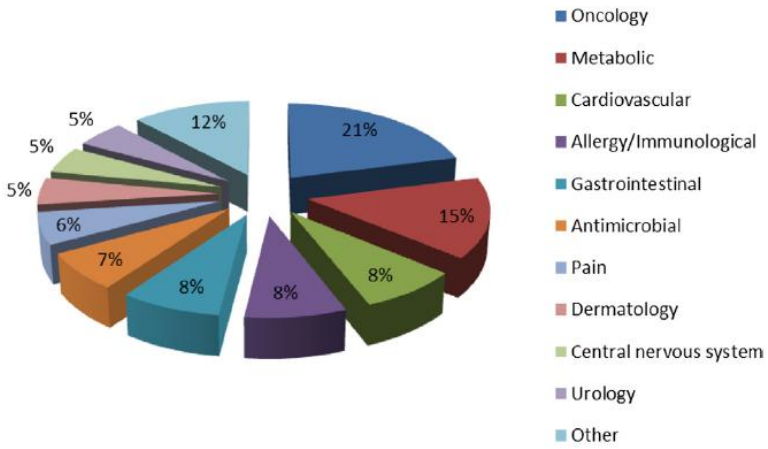

Figure 4. The distribution of peptide pipeline drugs by therapeutic areas. Other indications that are not specified on the chart include: Endocrinology, Respiratory, Bones, Hematology, Ophthalmology, OB-GYN (obstetrics and gynecology). The highest number of peptides has entered clinical study for cancer treatments and metabolic disorders. Data was taken from a 2012 report provided by the Peptide Therapeutic Foundation.[42]

These results prove that peptidomimetic approach represents a well-established strategy for developing novel, effective non-toxic therapeutic agents.
Apart from their uses as drugs, it is important to mention that peptidomimetic derivatives may have other applications such as in the study of binding mode, in the diagnostic and in the foldamers field. For example, determining the receptor-bound structure of biologically active peptides is fundamental in drug design. In fact, recent evidences have stated that the peptidomimetic strategy is the front runner in biotechnology and nanotechnology, for creating new biomaterials and biodevices, biosensors, bioelectronics, to perform specific operations within a physiological environment.
The field is so vast that it would be reductive to even try to make an overall view of it in this introductive chapter, but there is good literature that covers it all (see references herein).

References

[1] N. Sewald, H.-D. Jakubke, Peptides: Chemistry and Biology, Wiley-VCH, Weinheim, **2002**, Chapter 3.

[2] Liskamp R. M. J., *ChemBioChem*, **2011**, *12*, 1626.

[3] L. Wang, P. G. Schultz, *Angew. Chem.* **2004**, *117*, 34 ; *Angew. Chem. Int. Ed.* **2004**, *44*, 34.

[4] a) Danijel Kikely, *Curr. Med. Chem.*, **2006**, *13*, 1525; b) Gentilucci L., Tolomelli A., *Curr. Med. Chem*, **2006**, *13*, 2449.

[5] a) Sasubilli R., Gutheil W.G., *J. Comb. Chem*., **2004**, *6*, 911; b) Sagan S., *Curr. Med. Chem.*, **2004**, *11*, 2799; c) Luthman K., Hacksell U., *Textbook of Drug Design and Discover*, **2002**, 459.

[6] Durani, S. *Acc Chem Res*, **2008**, *41*,1301.

[7] Gentilucci, L.; Cardillo, G.; Squassabia, F.; et al. *Bioorg Med Chem Lett,* **2007**, *17*, 2329.

[8] a) Ahn J.M., Boyle N. A., *Mini Rev. Med. Chem.*, **2002**, *2*, 463; b) [8] Guichard G., *Solid-Phase Synthesis*, **2000**, 649.

[9] Horwell, D. C., Howson W., *Drug Des. Discov.*, **1994**, *2*, 63.

[10] a) A. Ruegger, M. Kuhn, H. Lichti, H.-R. Loosli, R. Huguenin, C. Quiquerez, A. von Wartburg, *Helv. Chim. Acta* **1976**, *59*, 1075 ; b) E. Biron, J. Chatterjee, O. Ovadia, D. Langenegger, J. Brueggen, D. Hoyer, H. A. Schmid, R. Jelinek, C. Gilon, A. Hoffman, H. Kessler, *Angew. Chem.* **2008**, *120*, 2633 ; *Angew. Chem. Int. Ed.* **2008**, *47*, 2595.

[11] Fletcher M. D., Campbell M., *Chem. Rev*., **1998**, *98*, 763.

[12] Chorev, M. *Biopolymers*, **2005**, *80*, 67.

[13] a) Gante J., Krug M. Lauterbach G., *J. Pept. Sci.*, **1995**, *1*, 201; b) Zega A., *Curr. Med. Chem.*, **2005**, *12*, 589.

[14] a) Bakshi P., Wolfe M. S., *J. Med. Chem.*, **2004**, *47*, 6485; b) Boeijen A, Liskamp R. M. J., Eur. *J. Org. Chem.*, **1999**, *9*, 2127.

[15] a) Brouwer, A. J., Liskamp R. M. J., *J. Org. Chem***, 2004**, *69*, 3662; b) Van Ameijde J., Liskamp R. M. J., *Tetrahedron Lett*., **2000**, *41*, 1103.

[16] a) Cardillo G., Gentilucci L., Tolomelli A., *Aldrich. Acta*, **2003**, *36*, 39; b) Cardillo G., Gentilucci L., Tolomelli A., *Tetrahedron A.*, **2004**, *15*, 593.

[17] Lelais G., Seebach D., *Biopolymers*, **2004**, *76*, 206.

[18] Trabocchi A., Guarna F., Guarna A., *Curr. Org. Chem.*, **2005**, *9*, 1127.

[19] a) Cardillo G., Gentilucci L., *Eur. J. Org. Chem.*, **2001**, *18*, 3545;b) Cardillo G., Gentilucci L., *J. Org. Chem.*, **2002**, *67*, 5957; c) Cardillo G., Gentilucci L., Tolomelli A., *Synletters*, **1999**, *11*, 1727; d) Cardillo, G.; Gentilucci L., Tolomelli A., *Tetrahedron*, **1999**, *55*, 15151.

[20] Seebach, D.; Beck, A.K.; Bierbaum, D.J. *Chem Biodivers*, **2004**, *1*, 1111.

[21] Felix A., Moroder L., Toniolo C., *Methods in Organic chemistry*, ***2003***, *Vol. E 22c-d*.

[22] a) R. J. Simon, R. S. Kania, R. N. Zuckermann, V. D. Huebner, D. A. Jewell, S. Banville, S. Ng, L. Wang, S. Rosenberg, C. K. Marlowe, D. C. Spellmeyer, R. Tan, A. D. Frankel, D. V. Santi, F. E. Cohen, P. A. Bartlett, *Proc. Natl. Acad. Sci. USA* **1992**, *89*, 9367; b) R. N. Zuckermann, J. M. Kerr, S. B. H. Kent, W. H. Moos, *J. Am. Chem. Soc*. **1992**, *114*, 10646.

[23] W.E.Stites, *Chem. Rev*. **1997**, 1233.

[24] A.S.Cohen, *Curr. Opin. Rheumatol*. **1994**, 68.

[25] Tavassoli A., Naumann T. A., *In Nucleic Acid sand Molecular Biology,*, **2005**, *16*, 293.

[26] a) Phillips A. J., Abell A. D., *Aldric. Acta*, **1999**, *32*, 75; b) Liskamp R. M. J., *Bioorganic & Medicinal Chem*istry, **2005**, *13*, 4221; c) Stymiest J. L., Mitchell B. F., *J. Org. Chem.*, **2005**, *70*, 7799.

[27] Schmiedeberg N., Kessler H., *Organic Let*ters, **2002**, *4*, 59.

[28] a) Schaffner, P.; Dard, M.M. *Cell Mol Life Sci*, **2003**, *6*, 119; b) Aummailley, M.; Gurrath, M.; Müller, G.; Calvete, J.; Timpl, R.; Kessler, H. *FEBS Lett*, **1991**, *291*, 50.

[29] Dechantsreiter, M.A.; Planker, E.; Mathä, B.; et al. *J Med Chem*, **1999**, *42*, 3033.

[30] A.Tolomelli, L.Gentilucci, E.Mosconi, et al., *ChemMedChem* **2011**, 2264.

[31] a) Maechling S., Norman S. E., *Tetrahedron Lett*., **2006**, *47*, 189; b) Labudda-Dawidowska O., *J. Med. Chem.*, **2005**, *48*, 8055.

[32] Aube J., *Organic Letters*, **2005**, *7*, 1059.

[33] D. K. Chalmers, G. R. Marshall, *J. Am. Chem. Soc*. **1995**, 5927.

[34] R.De Marco, A.Tolomelli, L.Gentilucci, et al., *Org. Biomol. Chem.* **2012**, 2307.

[35] R.M.Freidinger, D.F.Veber, D.S.Perlow, et al., *Science* **1980**, 656.

[36] R.M.Freidinger, *J. Med. Chem.* **2003**, 5553.

[37] F.Galaud, A.Demers, H.Ong, et al., *Proceedings of the 19th American Peptide Symposium* **2006**, 188.

[38] Schnolzer, M.; Kent, S. B. *Science* **1992**, *256*, 221.

[39] Dawson, P. E.; Muir, T. W.; Clark-Lewis, I.; Kent, S. B. *Science* **1994**, *266*, 776.

[40] Kent, S. B. *Chem Soc Rev* **2009**, *38*, 338.

[41] N. Tsomaia, Eur. *J. Med. Chem*., **2015**, 1.

[42] J.M. Reichert, The Peptide Therapeutics Foundation: Mapping the Future of Peptide Therapeutics, Peptide Therapeutic Foundation, 2012. http:// peptidereview.com/PDF/PTF_IPR12_23_7.pdf.

Chapter 2

Solid phase peptide synthesis using *N*-carboxyanhydrides and PEG resins in water

The increasing need for large quantities of biologically active peptides for the market strongly raised the problem of the environmental sustainability of their synthesis. In this respect, in this chapter is described a solid phase procedure in water, using PEG peptide amide resins and NCAs under controlled conditions. This procedure afforded with reasonable yield and purity a short peptide amide, without the need of coupling reagents nor protecting groups.

2.1. Introduction

The market for biologically active peptides is expected to grow rapidly in the next years. Besides to the current interest in peptide as drugs and active pharmaceutical ingredients, and as cosmeceuticals, recent findings suggest a wide range of novel applications in medicine, biotechnology, and surgery.[1] Peptides do not persist in the environment, giving innocuous degradation products; their components are the amino acids, which are renewable feedstocks available from biomasses[2] or agricultural byproduct streams.[3]

However, peptides are typical examples of products that impose an environmental burden during their manufacture. Both the solution and the solid phase (SP) syntheses[4] require large amounts of organic solvent, the use of reagents to activate the coupling between the residues, and the massive use of protecting groups (PGs), resulting in very poor atom economy and the release of harmful organic wastes.[5] As a consequence, the development of environmentally benign conditions has emerged as an important issue in green chemistry.[6]

One of the major problems concerns the huge amount of solvents needed, particularly for synthesis on solid supports. A convenient approach would be to carry out solvent-free reactions; this can be done with techniques such as mixing, grinding, or ball-milling.[7] So far, most of the efforts focused on the development of synthetic procedures in water. Since the common carbamate PGs are hydrophobic, reactivity can be improved suspending in water nanoparticle reactants generated by using a planetary ball mill,[8] or by MW activation.[9] Alternatively, new hydrophilic PGs have been proposed to improve water solubility.[10]

Also the reagents for coupling and protection/deprotection steps should be reduced wherever possible. Significant reductions of organic wastes have been obtained using enzymatic catalysis for coupling reactions,[11] or for PG removal.[12]

The use of PGs was partially reduced on performing peptide coupling in aqueous solution utilizing the *N*-acylbenzotriazole derivatives and unprotected amino acids,[13] or by using the native chemical ligation reaction of unprotected peptides in solution[14] on a water-compatible solid support.[15]

In this chapter is reported the SP preparation of peptides-amides in water on a PEG resin, by using *N*-carboxyanhydride (NCA) derivatives, conveniently prepared in turn under solvent-free conditions and MW irradiation. NCA, or Leuch's anhydrides, constitute a special class of α-amino acid mixed anhydrides in which the amino group is protected and the carboxylate is activated at the same time.[16] The attractiveness of peptide synthesis by NCA lies in its simplicity and atom economy; the molecular bulk of the reactants remains with the newly formed peptide, the only byproduct being carbon dioxide, and the condensation sequence may be rapidly repeated to build polypeptides requiring only control to avoid NCA polymerization.

To test the efficacy of different kinds of PEG-based resins for peptide amides, we synthesized the endogenous opioid peptide endomorphin-1 (EM1), H-Tyr-Pro-Trp-Phe-NH_2. This tetrapeptide was isolated from mammalian brain and it was found to activate μ-opioid receptors with high affinity and selectivity.[17]

2.2. Results and discussion

In the last years, our research group have been involved in the synthesis and investigation of EM-1 and mimetics as potential remedies for pain relief devoid of unwanted side-effects.[18] Since we became aware of the environmental impact of the classical syntheses, we faced the opportunity to develop a more sustainable procedure. We designed a very simple SP methodology in water, using PEG resins for the preparation of peptide amides, and the NCAs of the amino acids Tyr, Pro, Trp, and Phe.

These NCAs were prepared in almost quantitative yields from the unprotected amino acids and one third of triphosgene (Scheme 1). Though still hazardous (GHS05, GHS06), triphosgene can be used as a safe-to-handle phosgene substitute, and in recent years emerged as an important green chemical.[19] The classic procedure reported in the literature[20] was modified in that the condensation was performed under solvent-free conditions and MW irradiation. In the case of Pro, the *N*-carbamoyl

intermediate did not cyclize spontaneously, and the use of a non nucleophilic base was required; eventually, the use of polymer-supported bases has been also proposed.[21] The resulting NCAs were checked by ^{1}H-NMR, and ESI-MS, and the spectra are reported in Experimental section; purities (70-85%) were determined by RP-HPLC. The analyses of the byproducts were compatible with the presence of amino acid salts, isocyanatoacyl chlorides, *N*-chloroformyl amino acids,[22] and for Pro triethylammonium chloride. Polymerization at this stage was excluded on the basis of the HPLC-ESI analyses. Interestingly, the crude NCAs were utilized without purification, a significant advantage consented by the SP approach.

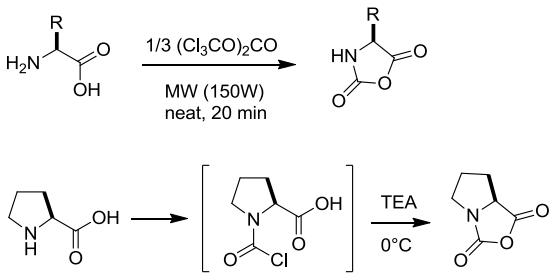

Scheme 1. MW-assisted synthesis of NCAs.

The NCAs are prone to polymerization; indeed, poly-amino acids can be conveniently synthesized from NCAs.[23] As a consequence, we operated under carefully controlled conditions; the key factor is the relative stability of the intermediate carbamic acid in an aqueous environment at a basic pH, that prevents the formation of the free aminopeptide while the NCA is still present in the reaction mixture (Scheme 2).

The PEG-based resins are highly chemically stable and allow the use of almost any kind of solvent, including water.[9,24] PEG has a very low toxicity and is used in a variety of biocompatible products.[25] Three different peptide ChemMatrix® amide resins were tested, H-Rink Amide, H-PAL, and H-Ramage (Table 1). A suspension of the amino-free resin in borate buffer pH = 10.2 was treated with a 3 equiv. of PheNCA, and the suspension was mechanically shaken at 5°C. After 3 h the resin was filtered and washed three times with citrate buffer pH = 3.0, rapidly to avoid peptide cleavage.

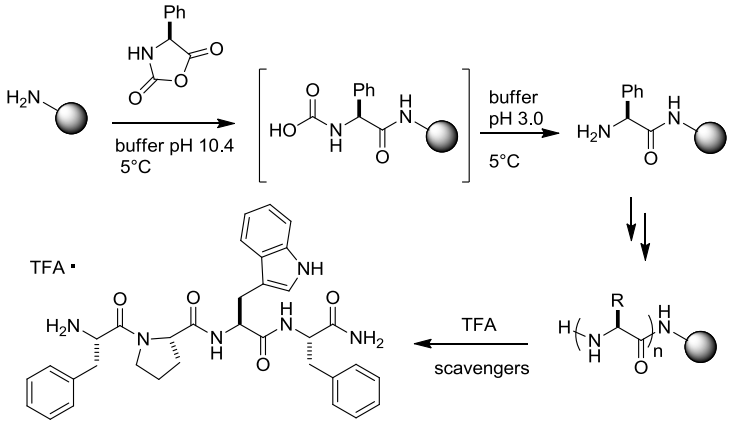

Scheme 2. SPPS of EM-1 in aqueous medium by coupling NCAs on a PEG peptide-amide resin.

Table 1. SPPS of EM-1 on different PEG based ChemMatrix® peptide-amide resins.

entry	resin	loading (mmol/g)	bead size (mesh)[a]	cleavage mixture TFA/H_2O/Et_3SiH (%)	purity, crude (%)[b]	yield, isolated (%)[c,d]	purity, isolated (%)[d]
1	H-Rink Amide	0.4-0.60	100-200	95.0/2.5/2.5	70	68	95
2	H-PAL	0.4-0.5	100-200	95.0/2.5/2.5	65	66	95
3	H-Ramage	0.25-0.50	100-200	5.0/2.5/2.5[e]	73	52	97

[a] Dry. [b] After crystallization, determined by analytical RP-HPLC. [c] Based on the average loading. [d] After semi-preparative RP-HPLC. [e] The rest being DCM.

The remaining NCAs were added in turn under the same conditions. The cleavage of the peptide amide from the resin was performed with TFA in the presence of scavengers. The crude peptides were analyzed by reversed phase HPLC and ESI. The analyses were compatible with the presence of traces of peptide byproducts, in particular failure sequences, and sequences with duplicate amino acids, possibly arising from NCA polymerization during the coupling step, and excluded racemization.

Final purification was performed by semi-preparative reversed phase HPLC, which afforded EM-1, ≥ 95% pure; EM-1 was identified by ESI-MS, ^{1}H-NMR, and gCOSY spectroscopy (Experimental section). The ^{1}H-NMR spectra of the isolated peptides excluded the presence of epimers.

Figure 1 shows the chromatogram of the preparation performed with the H-Ramage resin (Entry 3). This afforded the highest purity but a slightly reduced yield, possibly due to the comparatively lower stability in the decarboxylation step (Scheme 2).

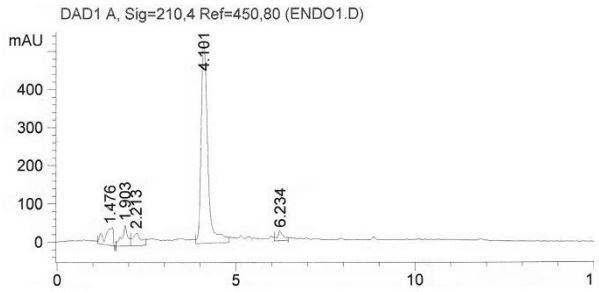

Figure 1. RP-HPLC analysis of crude EM-1 as obtained from entry 3 of Table 1.

From the general point of view of sustainability, the proposed synthetic protocol gives some advantages respect to the standard SP approach. The entire protocol was conducted in the almost complete absence of organic solvents. The solvent-free preparation of the NCAs required only the amino acids and one third of triphosgene, apart for Pro which required 1 equiv. of TEA. Swelling and coupling were conducted in borate buffer, and the washes were performed with citrate buffer. The high reactivity of the NCAs allowed using a reasonable excess of 3 equiv. for the couplings, comparable or inferior to classic SP synthesis.[2b,9,24] The cleavage step was done as usual with TFA and scavengers; EtOH, Et_2O, and CH_3CN were utilized in the conclusive stages to recover and isolate the peptides.

2.3. Conclusions

A short peptide-amide was synthesized in SP and in aqueous conditions, by employing a PEG resin and NCAs as activated/protected derivatives of the amino acids. These NCAs have been prepared with triphosgene under MW irradiation, a very convenient method also for its efficient energy use. EM-1 was obtained with moderate yield and purity, so that for the moment the method seems less competitive than the classic procedures for longer sequences. Nevertheless, the entire protocol is attractive for its environmental sustainability; apart from the amino acids and some reagents used occasionally, the only bulk chemical was triphosgene, a relatively safe reagent which danger and toxicity is justified by excellent atom economy and the absence of wastes of the overall protocol, including organic solvents.

2.4. Experimental section

2.4.1. General Methods

Unless stated otherwise, chemicals were obtained from commercial sources and used without further purification. The solid phase syntheses were conducted on ChemMatrix®, 100% PEG based resin from PCAS BioMatrix. The MW-assisted synthesis was performed using a Milestone Mycrosynth multimode labstation. Purities were determined by analytical RP-HPLC performed on a C18 column, 4.6 μm particle size, 100 Å pore diameter, 250 μm, DAD 210 nm, from a 9:1 H_2O/CH_3CN to a 2:8 H_2O/CH_3CN in 20 min, (for the analysis of EM-1: from a 9:1 H_2O/CH_3CN/0.1% TFA to 2:8 H_2O/CH_3CN/0.1% TFA) at a flow rate of 1.0 mL/min, followed by 10 min at the same composition. Semipreparative RP-HPLC was performed on a C18 column (7 μm particle size, 21.2 mm × 150 mm, from 8:2 H_2O/CH_3CN/0.1% TFA to 100% CH_3CN/0.1% TFA in 10 min) at a flow rate of 12 mL/min. Mass analysis was done by ESI. ^{1}H NMR were recorded at 400 MHz, in 5 mm tubes, at rt. Chemical shifts are reported as δ values relative to the solvent peak.

2.4.2. Synthetic procedures

Synthesis of the NCAs. A limp mixture of triphosgene (0.35 mmol) and the amino acid (1.0 mmol) was mixed under MW irradiation in an open vessel equipped with a refrigerator under a fume hood, while gently blowing with nitrogen. The microwave-assisted reaction was performed keeping irradiation power fixed at 150W and monitoring internal reaction temperature 80°C with a built-in ATC-FO advanced fiber optic automatic temperature control. After 20 min. the mixture was cooled at rt and the resulting NCA (90-95 %, 80-85 % pure by analytical RP-HPLC) was used as a waxy solid without further purification.

Procedure for the synthesis of ProNCA. Proline (1.0 mmol) was treated with triphosgene as described above. After 20 min the mixture was cooled at 0°C, TEA (1.0 mmol) was added and the limp mixture was mixed for additional 30 minutes. Crude ProNCA (90 %, 70 % pure by analytical RP-HPLC) was used without further purification.

SP synthesis of EM-1. NCA coupling: The PEG resin or PEG resin-peptide (0.3 mmol in free amino group) was swollen with borate buffer pH=10.2 (4.0 ml). The NCA (0.9 mmol) was added at 5°C and the suspension was mechanically shaken for 3 hours. Then the mixture was filtered, and the resin was washed three times with citrate buffer pH=3.0, and finally with borate buffer pH=10.2.

Cleavage procedure. The resin-peptide was suspended in mixture of TFA and scavengers (5 mL, Table 1), and mechanically shaken at rt. After 2 h, the mixture was filtered, the resin was washed twice with 10% TFA in Et_2O (5 mL), and the collected filtrates were poured into 50 mL of ice-cold Et_2O. The precipitate was filtered, and the crude peptide TFA salt was re-crystallized from EtOH/Et_2O and collected by centrifugation (65-73 % pure by analytical RP-HPLC, Table 1). The peptide was isolated after semi-preparative RP-HPLC (52-68 % yield, 95-97% pure by analytical RP-HPLC, Table 1).

TyrNCA.[26] ^{1}H-NMR (400 MHz, $CDCl_3$) δ: 2.99 (dd, 1H, J = 6.9, 13.9 Hz, TyrHβ), 3.20 (d, 1H, J = 4.6, 13.9 Hz, TyrHβ), 4.54 (m, 1H, TyrHα), 6.02 (br s, 1H, TyrNH), 6.91 (d, 2H, J = 8.2 Hz, $TyrArH_{3,5}$), 7.14 (d, 2H, J = 8.2 Hz, $TyrArH_{2,6}$).
ES-MS *m*/*z* [M+1]; 208.1; calcd. for $C_{10}H_{10}NO_4$: 208.1.

ProNCA.[27,28] ^{1}H-NMR (400 MHz, $CDCl_3$) δ: 2.04 (m, 1H, ProHγ), 2.11-2.32 (m, 2H, ProHβ + ProHγ), 2.44 (m, 1H, ProHβ), 3.31 (m, 1H, ProHδ), 3.69 (dd, J = 7.5, 10.4 Hz, 1H, ProHδ), 4.35 (dd, J = 7.2, 9.2 Hz, 1H, ProHα).
ES-MS *m*/*z* [M+1]: 142.1; calcd. $C_6H_8NO_3$: 142.0.

TrpNCA.[28] ^{1}H-NMR (400 MHz, $CDCl_3$) δ: 3.13 (dd, 1H, J = 9.1, 14.9 Hz, TrpHβ), 3.49 (dd, 1H, J = 3.6, 14.9 Hz, TrpHβ), 4.55 (dd, J = 3.6, 9.1 Hz, 1H, TrpHα), 5.99 (br.s, 1H, TrpNH), 7.11 (s, 1H, TrpH2), 7.15-7.31 (m, 2H, TrpH5+TrpH6), 7.41 (d, J = 8.0 Hz, 1H, TrpH7), 7.57 (d, J = 7.6 Hz, 1H, TrpH4), 8.27 (br. s, 1H, TrpH1).
ES-MS *m*/*z* [M+1]; 232.2; calcd. for $C_{12}H_{11}N_2O_3$: 232.1.

PheNCA.[29,30] ^{1}H-NMR (400 MHz, $CDCl_3$) δ: 3.00 (dd, 1H, J = 8.4, 13.8 Hz, PheHβ), 3.32 (dd, 1H, J = 4.1 13.8 Hz, PheHβ), 4.54 (dd, J = 4.1, 8.4 Hz, 1H, PheHα), 5.95 (br s, 1H, PheNH), 7.18-7.26 (m, 2H, ArH), 7.27-7.41 (m, 3H, ArH).
ES-MS *m*/*z* [M+1]: 192.1; calcd. for $C_{11}H_9NO_3$: 192.1.

EM-1, H-Tyr-Pro-Trp-PheNH_2.[31] ^{1}H-NMR (400MHz, DMSO-d6); 3:1 trans:cis δ:[a] 1.38-1.56 (m, $4H_<$, Proγ$_<$ + Proβ$_<$), 1.57-1.78 (m, $3H_>$, Proβ$_>$ + Proγ$_>$), 1.92 (m, $1H_>$, Proβ$_>$), 2.66-2.79 (m, $2H_<$, TyrHβ$_<$ + $1H_>$, TyrHβ$_>$ + $1H_{><}$, PheHβ$_{><}$), 2.80-2.90 (m, $1H_<$, TrpHβ$_<$, + $2H_>$, TyrHβ$_>$ + TrpHβ$_>$), 2.90-2.95 (m, $1H_{><}$, PheHβ$_{><}$), 3.01 (m, $1H_>$, ProHδ$_>$ + $1H_{><}$, TrpHβ$_{><}$), 3.20-3.32 (m, $2H_<$, ProHδ$_<$), 3.45-3-62 (m, $1H_>$, ProHδ$_>$ + $2H_<$, ProHα$_<$ + TyrHα$_<$), 4.18 (br.t, $1H_>$, TyrHα$_>$), 4.32-4.53 (m, $2H_{><}$, TrpHα$_{><}$ + PheHα$_{><}$ + $1H_>$, ProHα$_>$), 6.61 (d, J = 8.4 Hz, $2H_{><}$, $TyrArH_{3,5><}$), 6.84 (d, J = 8.4 Hz, $2H_<$, $TyrArH_{2,6<}$), 6.92-7.00 (m, $2H_{><}$, TrpH6$_{><}$ + TrpH5$_{><}$, + $2H_>$, $TyrArH_{2,6>}$), 7.15-7.00 (m, $7H_{><}$, PheArH$_{><}$ + $CONH_{2><}$ + TrpH2$_{><}$),7.20-7.30 (m, $2H_{><}$, TrpH7$_{><}$ + $CONH_{2><}$), 7.51 (d, J = 7.6 Hz, $1H_{><}$, TrpH4$_{><}$), 7.85 (d, J = 7.1 Hz, $1H_>$, $PheNH_>$), 8.05-7.94 (m, $1H_>$, TrpNH$_>$ + $1H_<$, PheNH$_<$ + $2H_{><}$, TyrNH$_{><}$), 8.20 (d, J = 6.9 Hz, $1H_<$, TrpNH$_<$), 9.36 (s, $1H_>$, TyrOH$_>$), 9.43 (s, $1H_<$, TyrOH$_<$), 10.72 (s, $1H_<$, TrpH1$_<$), 10.80 (s, $1H_>$, TrpH1$_>$).
[a] $_>$ = major isomer, $_<$ = minor isomer, $_{><}$ = the resonances of major and minor conformers for the same proton appear under the same peak. ES-MS *m*/*z* [M+1]: 611.1; calcd. for $C_{34}H_{39}N_6O_5$: 611.3.

References

[1] a) Hruby, V. J. *Nat. Rev. Drug Discov*., **2002**, *1*, 847; b) Gentilucci, L.; Tolomelli, A.; Squassabia, F. *Curr. Med. Chem.*, **2006**, *13*, 2449; c) Zhang, L.; Falla, T. J. *Clin. Dermatol*., **2009**, *27*, 485; d) Stevenson, C. L. *Curr. Pharm. Biotechnol*., **2009**, *10*, 122.

[2] a) Scott, E.; Peter, F.; Sanders, J. *Appl. Microbiol. Biotechnol*., **2007**, *75*, 751; b) Williams, P. J. le B.; Laurens, L. M. L. *Energy Environ. Sci*., **2010**, *3*, 554.

[3] Lammens, T.M.; Franssen, M.C.R.; Scott, E.L.; Sanders, J.P.M. *Biomass Bioenergy*, **2012**, *44*, 168.

[4] Synthesis of peptides and peptidomimetics, Vol. E22 (Eds.: M. Goodman, A. Felix, L. Moroder, C. Toniolo), Thieme, Stuttgart, 2002.

[5] Green chemistry: Frontiers in benign chemical syntheses and processes (Eds.: P. T. Anastas, T. C. Williamson), Oxford University Press, New York, 1999.

[6] a) Dunn, P. J.; Wells, A. S.; Williams, M. T.; Eds. Green chemistry in the pharmaceutical industry; WILEY-VCH Verlag GmbH & Co.: Weinheim, 2010; b) Silpi, D.; Abha, S.; Torok, M. *Curr. Org. Synth.*, **2011**, *8*, 262.

[7] a) Declerck, V.; Nun, P.; Martinez, J.; Lamaty, L. *Angew. Chem. Int. Ed.*, **2009**, *48*, 9318; b) Štrukil, V.; Bartolec, B.; Portada, T.; Đilović, I.; Halaszc, I.; Margetić, D. *Chem. Commun.* **2012**, *48*, 12100; c) Bonnamour, J.; Métro, T.-X.; Martinez, J.; Lamaty, F. *Green Chem.*, **2013**, *15*, 1116.

[8] Hojo, K.; Ichikawa, H.; Onishi, M.; Fukumori, Y.; Kawasaki, K. *J. Pept. Sci.*, **2011**, *17*, 487, and references herein.

[9] Athanassios, S.; Albericio, F.; Grøtli, M. Solid*Org. Lett.*, **2009**, *11*, 4488.

[10] Hojo, K.; Maeda, M.; Tanakamaru, N.; Mochida, K.; Kawasaki, K. *Prot. Pept. Lett.*, **2006**, *13*, 189, and references herein.

[11] a) Schellenberger, V.; Jakubke, H. D. *Angew. Chem. Int. Ed. Engl.*, **1991**, *30*, 1437; b) Wong, C. H. *Science*, **1989**, *244*, 1145.

[12] Góngora-Benítez, M.; Basso, A.; Bruckdorfer, T.; Royo, M.; Tulla-Puche, J.; Albericio, F. *Chem. Eur. J.*, **2012**, *18*, 16166.

[13] Katritzky, A. R.; Zhang, Y.; Singh, S. K. *Synthesis*, **2003**, *48*, 2795.

[14] Dawson, P. E.; Muir, T. W.; Clark-Lewis, I.; Kent, S. B. *Science*, **1994**, *266*, 776.

[15] Johnson, E. C. B.; Durek, T.; Kent, S. B. H. *Angew. Chem. Int. Ed*., **2006**, *45*, 3283.

[16] a) Denkewalter, R. G.; Schwam, H.; Strachan, R. G., Beesley, T. E.; veber, D. F.; Schoenwaldt, E. F.; Barkemeyer, H.; Paleveda, Jr. W. J.; Jacob, T. A.; Hirschmann, R. *J. Am. Chem. Soc*., **1966**, *83*, 3163; b) Montalbetti, C. A. G. N.; Falque, V. *Tetrahedron*, **2005**, *61*, 10827; c) Spina, R.; Colacino, E.; Gabriele, B.; Salerno, G.; Martinez, J.; Lamaty, F. *J. Org. Chem.*, **2013**, *78*, 2698.

[17] a) Zadina, J. E.; Hackler, L.; Lin-Jun, G.; Kastin, A. J. *Nature*, **1997**, *386*, 499; b) Keresztes, A.; Borics, A.; Tóth, G. *Chem. Med. Chem*., **2010**, *5*, 1176.

[18] a) Gentilucci, L. In *Neuropeptides in neuroprotection and neuroregeneration.* Nyberg, F. Ed.; CRC Press, Boca Raton USA, pp 229-252; b) De Marco, R.; Tolomelli, A.; Spampinato, S.; Bedini, A.; Gentilucci, L. *J. Med. Chem.*, **2012**, *55*, 10292.

[19] a) Trotzki, R.; Nüchter, M.; Ondruschka, B. *Green Chem.*, **2003**, *5*, 285; b) Fuse, S.; Tanabe, N.; Takahashi, T. *Chem. Commun*., **2011**, *47*, 12661.

[20] Wilder, R.; Mobashery, S. *J. Org. Chem.*, **1992**, *57*, 2755.

[21] Gulin, P. O.; Rabanal, F.; Giralt, E. *Org. Lett*., **2006**, *8*, 5385.

[22] Kramer, J. R.; Deming, T. J. *Biomacromolecules***, 2010**, *11*, 3668.

[23] Palacios, P.; Bussat, P.; Bichon, D. Synthesis *Angew. Chem. Int. Ed*., **1991**, *193*, 77.

[24] García-Ramos, Y.; Paradís-Bas, M.; Tulla-Puche. J.; Albericio, F. *J. Pept. Sci*., **2010**, *16*, 675.

[25] Webster, R.; Elliott, V.; Park, B. K.; Walker, D.; Hankin, M.; Taupin, *Milestones in Drug Therapy*, Veronese, F. M., Ed.; Birkhäuser: Basel, Swiss, **2009**.

[26] Lu, Y.-S.; Lin, Y.-C.; Kuo, S.-W. *Macromolecules*, **2012**, *45*, 6547.

[27] Gulin, P. O.; Rabanal, F.; Giralt, E. *Org. Lett*., **2006**, *8*, 5385.

[28] Our spectra for ProNCA and TrpNCA appear different from that reported in the following paper: Akssira, M.; Boumzebra, M.; Kasmi, H.; Dahdouh, A. *Tetrahedron*, **1994**, *50*, 9051.We argue that the spectral data reported in this Ref. 3 are rather rough. On the other hand, our data for ProNCA nicely agree with Ref. 2; for instance (δ in $CDCl_3$), the two ProHδ are described as 3.50 (m, 2H) in Ref. 3, while they are at 3.33 (1H), and 3.79 (1H) in Ref. 2; ProHα is at 4.15 in Ref. 3, while it is at 4.36 in Ref. 2.

[29] Wilder, R.; Mobashery, S. *J. Org. Chem.*, **1992**, *57*, 2755.

[30] Daly, W. H.; Poché, D. *Tetrahedron Lett*., **1998**, *29*, 5859.

[31] Podlogar, B. L.; Paterlini, M. G.; Ferguson; D. M.; Leo, G. C.; Demeter, D. A.; Brown, F. K.; Reitz, A. B. *FEBS Lett*., **1998**, *439*, 13.

Chapter 3

Preparation of ΔAla equipped with Oxd chiral auxiliaries for the stereoselective synthesis of substituted tryptophans

Chiral dehydroamino acid building blocks are versatile starting materials for the preparation of optically active unusual amino acids and other compounds of pharmacological interest. In this chapter is disclosed the expedient preparation of dehydroalanines (ΔAla) equipped with oxazolidin-2-one (Oxd) chiral auxilixaries, Ts-Oxd-ΔAla-OMe. These compounds have been obtained in high yields from dipeptides Ts-Ser/Thr/phenylSer-Ser-OMe by the one-pot cyclization-elimination reaction with *N,N*-disuccinimidyl carbonate and catalytic DIPEA. To test the efficacy of the chiral auxiliaries in controlling asymmetric transformations, the Friedel-Crafts alkylations of indoles carrying diverse substituents were performed in the presence of Lewis and Brønsted acids. The reactions proceeded with good to excellent diastereomeric ratios giving (*S*)- or (*R*)-tryptophan derivatives, isolated very conveniently by simple flash chromatography. To verify the utility of this approach, optically pure (*S*)-2-methyltryptophan and (*S*)-5-fluorotryptophan were obtained and utilized to prepare analogues of endogenous opioid peptide endomorphin-1, H-Tyr-Pro-Trp-PheNH_2.

3.1. Introduction

Among the unusual amino acids, the α,β-dehydroamino acids (or Δaas) represent a noteworthy class for their presence in naturally occurring toxins and antibiotics, and for their important role in the biosynthesis of other non-proteinogenic amino acids.[1]

Δaas display unusual conformational features; when inserted into peptides, they induce conformational constrains which lead to changes in the secondary structure. The double bond rigidifies the conformation of the side chain; χ is fixed to 0° (*Z*) or 180° (*E*), and favors the formation of β- or γ-turns when the Δaas are placed at the *i+2* position of the putative turn sequence (Figure 1a). Besides, the presence of these unnatural and constrained residues confer resistance to enzymatic degradation. The folding properties of Δaas have been utilized for the design of foldamers, oligomers which have a tendency to form well-defined secondary structures stabilized by non-covalent, nonadjacent interactions. For instance, it was reported that the sequential introduction in oligomers of ΔPhe gave repeated β-turns, forming a 3_{10} helix.[2]

Besides, Δaas have demonstrated their utility in organic synthesis as versatile intermediates, giving access to a variety of derivatives.[1] The double bond permits to perform several reactions (Figure 1b), which can be utilized for the preparation of interesting biologically active compounds, such as the oligosaccharide-peptide ligation by the addition of complex oligosaccharide thiolates to dehydroalanine (ΔAla)-containing peptides,[3] or the synthesis of a lanthionine-bridged enkephalin mimetics.[4]

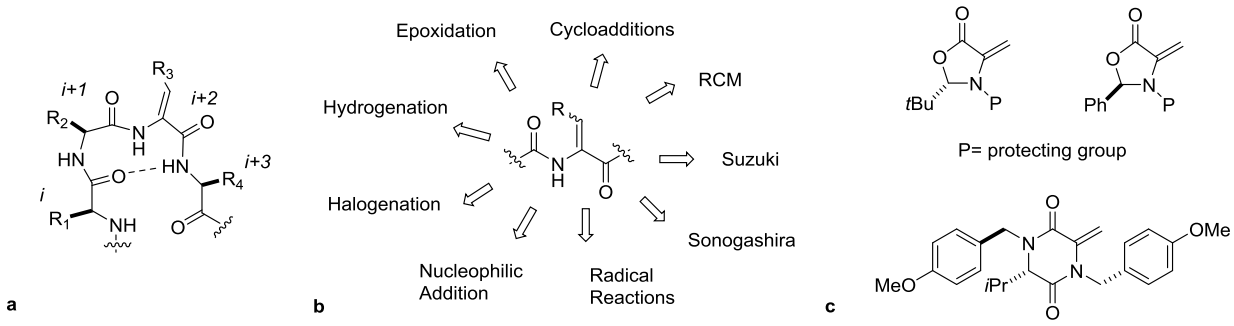

Figure 1 a) Δaas are β-turn inducers when placed at the position *i+2* of the putative turn; b) Δaas as substrates for different synthetic reactions; c) selected examples of chiral cyclic Δaas recently utilized for C-C bond formation (Michael-additions).

Non-functionalized Δaas are enamines prone to hydrolysis; on the other hand, *N*-acyl derivatives or Δaas already incorporated into peptide sequences, are more stable, therefore several protocols for their preparations have been reported, including elimination reactions, Horner-Wadsworth-Emmons and Wittig reactions, Erlenmeyer synthesis and ring-opening

of oxazolones, Schöllkopf formylamino-methylenation, etc.[1] One of the most direct methods is the dehydration of β-hydroxy-α-amino acids (e.g. Ser or Thr). For instance, Ferreira et al. reported the *anti* selective elimination with Boc_2O/DMAP, that afforded only one of the two possible *E*/*Z* isomers,[5] the *Z* isomer being practically more accessible from *threo* reagents than the *E*.

Chiral ΔAla derivatives constitute suitable starting materials for many asymmetric transformations.[1] Selected examples from the literature of compounds containing ΔAla recently utilized for diastereoselective Michael additions are shown in Figure 1c. The addition of the benzophenone glycine-*tert*-butylester imine to 2-phenyloxazolidin-5-one gave the Michael adduct with control of the two new stereocenters and a diastereoselectivity of 97:3;[6] the 2-tert-butyloxazolidin-5-one underwent addition of enamine in a preferentially *cis* manner with a ratio of 83:17;[7] the organocuprate addition to dehydrodiketopiperazine gave the *cis* product in high yields and >95% diastereomeric excess.[8]

In this chapter is reported the expedient preparation of ΔAla equipped with Oxd chiral auxilixaries (**3**), by one-pot cyclization-elimination of dipeptides of sequence Ts-Ser (or Thr, phenylSer)-Ser-OMe (**1**). To test the efficacy of these chiral building blocks for the preparation of non-racemic and non-natural amino acids, it is been performed the tandem Friedel-Crafts (F.-C.) alkylation/asymmetric protonation of substituted indoles,[9] to afford tryptophans functionalized at the indole with alkyl, aryl groups, halogens, or their combinations. Modified tryptophans are present in peptides of microbial or marine origins (e.g. halotryptophans),[10] and unnatural Trp analogs have been utilized as important building blocks for the total synthesis of biologically active products,[11] as biological probes,[12] and finally as chiral small molecule catalysts.[13] Several authors developed asymmetric syntheses of optically pure indole-substituted tryptophans.[14] Halotryptophans can be obtained by palladium-mediated heteroannulation of a chiral auxiliary,[15] by electrochemical oxidation of proline followed by Fischer indole synthesis,[16] from serine and commercially available microorganism containing tryptophan synthase,[17] by enzymatic resolutions.[18] The F.-C. alkylation of substituted indoles with methyl acetamidoacrylate[19] gave Trp derivatives in non-stereoselective fashion. On the other hand, non-racemic tryptophan derivatives were prepared with moderate stereoselectivities by F.-C. alkylation when ΔAla was incorporated into peptides.[20] Some asymmetric catalytic syntheses have been reported to afford with high levels of enantioselectivity (*S*)- or (*R*)-tryptophans carrying a limited number of distinct modifications.[21] Heck reaction between *N*-Ts-indoles and methyl 2-acetamidoacrylate furnished the dehydrotryptophans, whose asymmetric catalytic hydrogenation with [(COD)Rh(*R*,*R*)-Et-DuPHOS]$^+$TfO$^-$ as catalyst furnished enantiomerically pure (*R*)-5-and 6-substituted tryptophans.[22] More recently, the F.-C. alkylation of methyl acetamidoacrylate catalyzed by 3,3-dibromo-BINOL·$SnCl_4$ complex furnished 2-substituted tryptophans in good yields and high enantioselectivity.[23]

Finally, herein is described the synthesis of two analogues of the endogenous agonist of the μ-opioid receptor endomorphin-1 (EM1), H-Tyr-Pro-Trp-PheNH_2.[24] Among the opioid peptides, EM1 shows a unique sequence and extraordinary receptor affinity and selectivity. In fact, as mentioned above, our research group have been interested in the preparation, conformational analysis and pharmacological characterization of EM1 analogues[25] as potential drugs for pain management.[26] Since none of the other endogenous opioid peptides contain a Trp in the sequence, SAR studies on EM1 analogues containing modified Trp could shed light into the role of this pharmacophore in ligand-receptor recognition.[27] Besides, the introduction of substituents at the indole of Trp could improve metabolic stability, bioavailability, and CNS exposure.[25d,28]

3.2. Results and discussion

Recently, in our research group, was observed that the reaction of the *N*-tosyl (Ts) dipeptide ester Ts-Ser-Ser-OMe (**1a**) with *N*,*N*-disuccinimidyl carbonate (DSC) and a catalytic amount of DIPEA in DCM/DMF, gave a 1:1 mixture of the compound containing two oxazolidin-2-one-4-carboxylate rings (Oxd), Ts-Oxd-Oxd-OMe (**2a**), and of the compound containing one Oxd and a ΔAla, Ts-Oxd-ΔAla-OMe (**3a**) (Figure 2, and Table 1, entry 1). This compound **3a** can be regarded as a ΔAla equipped with a oxazolidin-2-one chiral auxiliary, [29,30] potentially useful for the asymmetric synthesis of optically active unusual α-amino acids.[1,20] This opportunity prompted us to preparare dipeptides Ts-Oxd-ΔAla-OMe carrying different substituents at the position 5 of the Oxd (Figure 2).

The dipeptides **1a-c**, precursors of **3a-c** (Figure 2), were easily prepared by coupling in solution Ts-Ser (R = H), Ts-Thr (R = Me), and (*S*/*R*)-Ts-phenylSer (R = Ph), respectively, with H-Ser-OMe. Amino acid tosylation was performed according to the literature.[31] The two β-hydroxy-α-amino acid building blocks were incorporated without a protection for the OH function, according to a protocol largerly emploied by us (chapter 4, 5 and 6),[32] using HOBt, HBTU, and DIPEA, as activating agents, at 80°C under MW irradiation.[33] Under these expedient conditions, acylation of the OH-function and thus the formation of a depsipeptide side product was not observed, as confirmed by the ^{1}H NMR and RP-HPLC MS analyses of the crude reaction mixture.

The reaction of **1a** with DSC/DIPEA was performed in different solvents (Figure 2), giving different outcomes: in pure DCM the reaction gave a 92:8 mixture of **2a** and **3a** (Table 1, entry 2), while in DMF the situation was completely reversed, giving a 5:95 ratio in favor of **3a** (entry 3). Finally, the slow addition of DSC to a solution of **1a-c** and catalytic DIPEA in DMF at 0°C further reduced the amount of **2** (traces), as determined by HPLC-MS analysis of the reaction mixture, while the corresponding Ts-Oxd-ΔAla esters **3a** were obtained in almost quantitative yields after isolation by flash chromatography (entry 4). In a similar way, the reaction of **1b** and **1c** performed under the same conditions gave the corresponding **3b** (entry 5) and **3c** (entry 6) in very good yields.

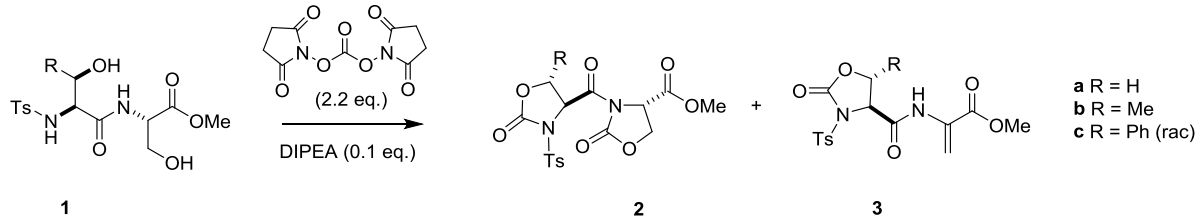

Figure 2. One-pot synthesis of ΔAla equipped with Oxd chiral auxiliaries **3a-c**.

Table 1. Reactions of **1a-c** with DSC/DIPEA under different conditions.

entry	**1**	solvent	Temp (°C)	**2**+**3** (%)[a]	**2**:**3** (%)[b]
1	**a**	DCM/DMF	20	93	51.49
2	**a**	DCM	20	88	92:8
3	**a**	DMF	20	86	5:95
4[c]	**a**	DMF	0	94	2:98
5[c]	**b**	DMF	0	92	3:97
6[c]	**c**	DMF	0	90	2:98

[a] determined after isolation by flash chromatography over silica gel. [b] Determined by RP- HPLC of the reaction mixtures. [c] Slow addition of DSC to **1**.

The analysis of the reaction mixtures at successive reaction times indicated that the reaction proceeds via the cyclization of Ts-Ser mojety promoted by DIPEA, followed by the dehydration of Ser-OMe to ΔAla (Figure 3). It was proposed that the cyclization of the Ts-Ser moiety can be promoted by the presence of the arylsulfonyl group,[25b,31] while the comparatively higher acidity of the Hα of Ser-ester respect to that of the Hα of Ser-amide accounts for the elimination of the intermediate Ser-*O*-succinimidyl carbonate to ΔAla.[5]

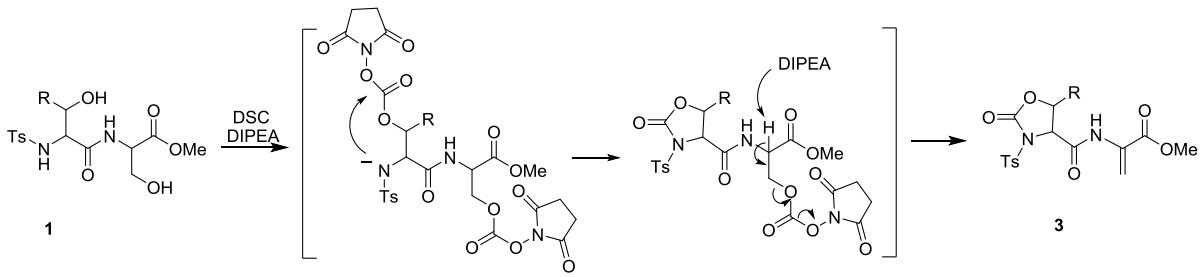

Figure 3. Synthesis of peptides Ts-Oxd-ΔAlaOMe (**3**) from dipeptides Ts-Ser/Thr/PhSer-SerOMe (**1**): proposed two-step mechanism.

As anticipated in the introduction, we decided to assess the utility of the Oxd-equipped ΔAla as chiral building blocks for the preparation of non-racemic non-natural amino acids. In particular, we tested the efficacy of **3a** (R = H), **3b** (R = Me), or **3c** (R = Ph), to furnish optically active tryptophan derivatives by the Lewis acids-promoted F.-C. alkylation of substituted indoles[9,19,20] in the presence of a Lewis acids-assisted Brønsted acid.[23] In essence, the process consists in a tandem Michael addition-enolate protonation, a process which is very difficult to control under the point of view of the stereochemistry.[11a,23,34] Initially, we screened different conditions for the reaction of **3a** with un-substituted indole. The reactions were carried out in DCM, in the presence of different Lewis acids,[19,20,23] of molecular sieves,[34] of phenol as

protonating agent (Lewis acid-assisted Brønsted acid[23]), and afforded the dipeptide Ts-Oxd-Trp-OMe as a mixture of diastereoisomers (*S*,*S*)-**4a** and (*S*,*R*)-**5a** (Figure 4).

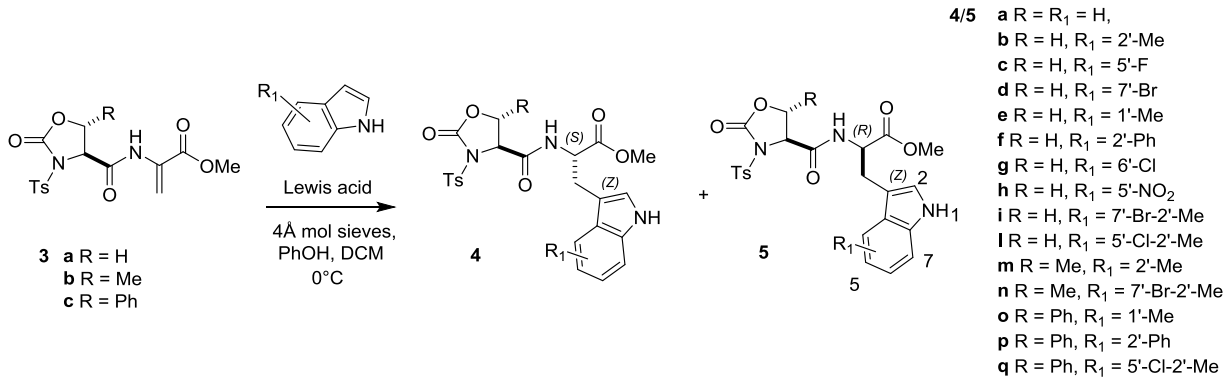

Figure 4. Lewis-Brønsted acid-promoted asymmetric F.-C. alkylation of substituted indoles with dipeptides **3a-c**.

Yields and d.r. strongly varied depending on the Lewis acid selected. $Yb(OTf)_3$, $Sc(OTf)_3$, $ZnCl_4$, $MgBr_2$, $SnBu_2Cl_2$, $ZnOTf_2$, $FeCl_3$, $InCl_3$, $CeCl_3$, $RuCl_3$ gave no products; other Lewis acids, $MgBr_2$, BBu_2OTf, $TiCl_4$, $Cu(OTf)_2$, gave **4a** and **5a** in traces. Finally, the reaction gave reasonable-to-good yields with $AlEtCl_2$, $AlEt_2Cl$,[19,20] or $SnCl_4$,[23] as reported in Table 2. The reaction with 1.5 equiv. of $AlEt_2Cl$ gave a 18:82 mixture of the diastreoisomers in favor of (*S*,*R*)-**5a** (entry 1), as determined by the HPLC analyses of the reaction mixtures; **4a** and **5a** were isolated by flash chromatography over silica gel in 10% and 45% yield, respectively. The use of $AlEtCl_2$ gave a higher yield (**4a** 17%, **5a** 52%) but a reduced selectivity of 25:75 (entry 2). On the other hand, $SnCl_4$ (1.05 equiv.) gave **4a** and **5a** in good yield (7% and 67%) after flash chromatography, with a d.r. of 90:10 in favor of (*S*,*R*)-**5a** (entry 3).

The configuration of the newly created stereocentre on Trp was determined by comparison with authentic samples of Ts-(*S*)-Oxd-(*S*)-Trp-OMe and Ts-(*S*)-Oxd-(*R*)-Trp-OMe, prepared by standard peptide synthesis in solution from the commercially available amino acids. The analyses of the crude reaction mixtures revealed no evidence of concurrent α-amidoalkylation reaction.[19,35] Increasing time and temperature did not lead to significantly higher yields; on the other hand, lower temperatures gave negligible improvements in terms of streoselectivity. The reduction of the amounts of Lewis acids to less than 1.0 equiv. gave reduced yields, consistent with the observation that stoichiometric Lewis-Brønsted acid was required due to its binding to the product, resulting in product inhibition.[23] As for aluminum Lewis acids, a moderate excess was recommended for good reactivity and high selectivity in the conjugate addition reactions.[36] In the absence of molecular sieves, the reactions gave scarce d.r., and variable quantities of by-products arising from peptide bond and/or ester hydrolysis, as revealed by reversed phase (RP)-HPLC and electro-spray (ESI)-MS analyses. Finally, the absence of the proton donor phenol gave similar yields but accompanied by a significant drop of stereoselectivity, while the substitution of phenol with 2-naphthol or 2,2′-biphenol did not alter the reaction outcome.

Consequently, the reactions of **3a** with substituted indoles (Table 2, entries 4-25 were performed with $AlEt_2Cl$, or $AlEtCl_2$, or with $SnCl_4$ in the presence of phenol and activated molecular sieves in DCM. In all cases (including **4a**, **5a**), the analyses of the diastereoisomers **4** and **5** by reversed-phase HPLC under different conditions was unfeasible. However, the separation was possible by normal phase-HPLC using an analytical Kromasil Diol column, so allowing the determination of d.r. (Table 2). Gratifying, in most cases the diastereoisomers were easily isolated in preparative scale by low-pressure flash chromatography over silica-gel using standard solvents.

The reaction of **3a** with 2-methylindole (entries 4-6) gave the dipeptides Ts-Oxd-(*S*)-2-Me-Trp-OMe (**4b**) and Ts-Oxd-(*R*)-2-Me-Trp-OMe (**5b**) in good to excellent yields and d.r. up to 8:92 with $SnCl_4$ in favor of the (*S*,*R*)-stereoisomer **5b** (entry 6), while $AlEt_2Cl$ and $AlEtCl_2$ gave inferior results (entries 4 and 5). A similar trend was observed for the reaction of **3a**, 5-fluoroindole, and the same Lewis acids, which gave **4c** and **5c** (entries 7-9). The reactions of **3a** with 7-bromoindole (entries 10-12) and 1-methylindole (entries 13-15) gave good yields and outstanding d.r. In particular, in the presence of $SnCl_4$ 7-bromoindole gave **4d**/**5d** in 6:94 ratio (entry 12). In a similar way, the reaction of 1-methylindole and **3a** with $SnCl_4$ (entry 15) afforded **5e** as the largely predominant product, being the diastereoisomer **4e** present only in traces.

On the contrary, 2-phenylindole or 6-chloroindole reacted with **3a** in the presence of $AlEtCl_2$ and $SnCl_4$, but not $AlEt_2Cl$, giving the corresponding products **4f**/**5f**,[23] or **4g**/**5g** in modest yields, albeit the diastereoselectivities were comparable to that of the previous experiments (not shown). As for 5-nitroindole, the reaction with **3a** gave only traces of **4h**/**5h** with all of the Lewis acids utilized. For these low-yielding reactions the analyses of the reaction mixtures by HPLC, ESI-MS, and ^{1}H NMR, excluded the formation of large quantities of by-products and confirmed the presence of un-reacted **3a**.

Finally, we tested the F.-C. alkylation of indoles carrying two substituents, 7-bromo-2-methylindole (entries 16-18) and 5-chloro-2-methylindole (entries 19-21). Interestingly, the reaction of 7-bromo-2-methylindole with **3a** afforded the best yield and d.r. with $AlEtCl_2$ (**4i** 9% and **5i** 75%, **4i**/**5i** 11:89, entry 17), while the reaction of 5-chloro-2-methylindole gave the best d.r. with $AlEt_2Cl$ (**4l**/**5l** 9:91, entry 19), but the best yield with $AlEtCl_2$ (**4l** 13% and **5l** 68%, entry 20).

Table 2 Yields and d.r. for the F.-C. reaction of R-indoles with **3a-c** with different Lewis Acids.

Entry	**3**	L.A. (eq.)	R_1-Indole (eq.)	**4**/**5** (%)[a]	**4**, **5**	**4** (%)[b]	**5** (%)[b]	**4**+**5** (%)[b]
1	**a**	$AlEt_2Cl$ (1.5)	H	18:82	**a**	10	45	54
2	**a**	$AlEtCl_2$ (1.5)	H	25:75	**a**	17	52	69
3	**a**	$SnCl_4$ (1.05)	H	10:90	**a**	7	67	74
4	**a**	$AlEt_2Cl$ (1.5)	2-Me	15:85	**b**	10	59	69
5	**a**	$AlEtCl_2$ (1.5)	2-Me	23:77	**b**	20	68	88
6	**a**	$SnCl_4$ (1.05)	2-Me	8:92	**b**	7	82	89
7	**a**	$AlEt_2Cl$ (1.5)	5-F	16:85	**c**	8	47	55
8	**a**	$AlEtCl_2$ (1.5)	5-F	22:78	**c**	17	62	79
9	**a**	$SnCl_4$ (1.05)	5-F	10:90	**c**	8	74	82
10	**a**	$AlEt_2Cl$ (1.5)	7-Br	11:89	**d**	6	51	60
11	**a**	$AlEtCl_2$ (1.5)	7-Br	8:92	**d**	6	69	75
12	**a**	$SnCl_4$ (1.05)	7-Br	6:94	**d**	4.5	71	75
13	**a**	$AlEt_2Cl$ (1.5)	1-Me	5[c]:95	**e**	-[c]	76	80
14	**a**	$AlEtCl_2$ (1.5)	1-Me	9[c]:91	**e**	-[c]	85	93
15	**a**	$SnCl_4$ (1.05)	1-Me	3[c]:97	**e**	-[c]	92	95
16	**a**	$AlEt_2Cl$ (1.5)	7-Br-2-Me	17:83	**i**	12	61	73
17	**a**	$AlEtCl_2$ (1.5)	7-Br-2-Me	11:89	**i**	9	75	84
18	**a**	$SnCl_4$ (1.05)	7-Br-2-Me	14:86	**i**	12	71	82
19	**a**	$AlEt_2Cl$ (1.5)	5-Cl-2-Me	9:91	**l**	6	63	69
20	**a**	$AlEtCl_2$ (1.5)	5-Cl-2-Me	16:84	**l**	13	68	81
21	**a**	$SnCl_4$ (1.05)	5-Cl-2-Me	12:88	**l**	9	68	78
22	**b**	$AlEt_2Cl$ (1.5)	2-Me	19:81	**m**	11	46	57
23	**b**	$AlEtCl_2$ (1.5)	2-Me	27:73	**m**	16	43	59
24	**b**	$SnCl_4$ (1.05)	2-Me	15:85	**m**	9	51	60
25	**b**	$AlEt_2Cl$ (1.5)	7-Br-2-Me	18:82[d]	**n**		49[d]	49
26	**b**	$AlEtCl_2$ (1.5)	7-Br-2-Me	18:82[d]	**n**		54[d]	54
27	**b**	$SnCl_4$ (1.05)	7-Br-2-Me	22:78[d]	**n**		60[d]	60
28	**c**	$AlEt_2Cl$ (1.5)	1-Me	23:77[d]	**o**		55[d]	55
29	**c**	$AlEtCl_2$ (1.5)	1-Me	30:70[d]	**o**		62[d]	62
30	**c**	$SnCl_4$ (1.05)	1-Me	20:80[d]	**o**		64[d]	64
31	**c**	$AlEt_2Cl$ (1.5)	2-Ph	20:80[d]	**p**		50[d]	50

32	**c**	$AlEtCl_2$ (1.5)	2-Ph	25:75[d]	**p**	64[d]	64
33	**c**	$SnCl_4$ (1.05)	2-Ph	20:80[d]	**p**	65[d]	65
34	**c**	$AlEt_2Cl$ (1.5)	5-Cl-2-Me	16:84[d]	**q**	54[d]	54
35	**c**	$AlEtCl_2$ (1.5)	5-Cl-2-Me	28:72[d]	**q**	60[d]	60
36	**c**	$SnCl_4$ (1.05)	5-Cl-2-Me	21:79[d]	**q**	66[d]	66

[a] Diastereomeric ratios determined by normal phase HPLC of the reaction mixtures, using a Kromasil Diol column. [b] Yields calculated after isolation by flash chromatography over silica gel. [c] Not isolated. [d] The diastereoisomers were not separated. n.d.: not determined.

Subsequently, to check any effects of diverse groups at the position 5 of the Oxd chiral auxiliary, we repeated the F.-C. alkylation of some selected substituted indoles with the dipeptides Ts-5-Me-Oxd-ΔAla-OMe (**3b**) and (*S*/*R*)-Ts-5-Ph-Oxd-ΔAla-OMe (**3c**) with $AlEt_2Cl$, $AlEtCl_2$, and $SnCl_4$, under the same conditions utilized for **3a**. The reaction of **3b** with 2-methylindole gave in all cases lower yields and reduced diastereoselectivities (entries 22-24) compared to the corresponding results observed for **3a** (entries 4-6). The isolation of the diastereomeric dipeptides **4m** and **5m** by flash chromatography over silica-gel was still feasible. Similarly, moderate yields and d.r. were obtained also for the reaction of **3b** with 7-Br-2-Me indole (entries 25-27). Nevertheless, the separation of the diastereoisomers by flash chromatography was not possible, and **4n**, **5n** were obtained as a mixture. Finally, the F.-C. reactions of **3c** and 1-methylindole (entries 28-30), 2-phenylindole (entries 31-33), and 5-Cl-2-Me-indole (entries 34-36) afforded the products **4o**/**5o**, **4p**/**5p**, and **4q**/**5q**, respectively. In all cases, the isolation of the diastereoisomers (*S*,*S*)-**4** and (*S*,*R*)-**5** by flash chromatography over silica-gel was not possible. As observed for **3b**, yields and d.r. for the reactions of **3c** with 1-methylindole and 5-Cl-2-Me-indole were modest compared to the corresponding results for **3a**. In contrast, the moderate reactivity of 2-phenylindole with **3c** to give **4p**/**5p** (entries 31-33) can be regarded as a improvement compared to the reaction with **3a**, since the latter gave inferior yields. Possibly, the moderate yields and d.r. of the reactions of **3b** and **3c** and all the indoles can be correlated to a significant instability of the respective 5-Me-Oxd and 5-Ph-Oxd auxiliaries; indeed, the analyses of the crude reaction mixtures (entries 26-40) by NMR and HPLC-ESI-MS revealed the presence of variable amounts of dipeptides containing Thr or phenylserine, possibly resulting from the degradation of the 5-substituted Oxd rings.

In summary, from the comparison of the results of the tandem F.-C. alkylation/asymmetric enolate protonation reported in Table 2, it appears that in most cases the substrate **3a** is the most performing both in terms of yields and d.r. Besides, the un-substituted Ts-Oxd chiral auxilixary of **3a** allowed a very easy separation of the stereoisomers. Reaction yields strongly varied depending on the nature of the substituents at the indole ring. As expected, activating groups such as 1-methyl or 2-methyl gave very good yields, while weakly deactivating group such as 5-fluoro or 7-bromo still gave reasonable to good yields, in some cases superior to indole, albeit 6-chloroindole reacted poorly under the same conditions. Not surprisingly, the strongly deactivating 5-nitro group prevented the reaction. On the other hand, the modest reactivity of 2-phenylindole and **3a** with all of the Lewis acids tested was unexpected.[23] Also unexpected was the comparatively higher reactivity of 2-phenylindole and **3c**. Possibly, these reactions can be improved by increasing the amounts of Lewis acid and/or indoles;[19] for the moment, the reactions have been not optimized further. As for the disubstituted indoles (5-Cl-2-Me-indole and 7-Br-2-Me-indole), the F.-C. reactions with **3a** proceeded with good yields possibly for the activating effect of the 2-methyl group.

In general, the stereochemical trend was very similar for all of the tested indoles, giving predominantly the (*S*,*R*)-**5** stereoisomers. For the monosubstituted indoles, the best d.r. were obtained with $SnCl_4$, including 7-bromoindole and 1-methylindole which reacted with **3a** very nicely giving a outstanding d.r., so that the minor (*S*,*S*)-stereoisomer could not be recovered after purification of the reaction mixture by flash chromatography. The disubstituted indoles behaved differently; for 7-bromo-2-methylindole and 5-chloro-2-methylindole the best d.r. were obtained with $AlEtCl_2$, and $AlEt_2Cl$, respectively.

The absolute configurations of all diastereoisomers **4** and **5** were determined by comparison of the HPLC analyses on Kromasil Diol column, and of the chiral HPLC analyses on CHIRALPAK IC column, with that of compounds **4a** and **5a**; the latter analysis also excluded racemization. Some representative examples of chiral HPLC analyses are reported in Figure 5: the analyses of 2'-methyl substituted **4b** and **5b**, of 5'-chloro-2'-methyl-**4l** and -**5l**, and of compounds **4m** and **5m** equipped with 5-methyl oxazolidin-2-one, clearly match the analyses of **4a** and **5a**. The latter were confirmed in turn by comparison with authentic samples of Ts-(*S*)-Oxd-(*S*)-Trp-OMe (**4a**) and Ts-(*S*)-Oxd-(*R*)-Trp-OMe (**5a**), prepared from the commercially available (*S*)- or (*R*)-tryptophan. The absolute stereochemistry of **4b** and **5b**, and of **4c** and **5c**, was also

confirmed after removal of the chiral auxiliary, by comparing the specific optical rotations of enantiopure (*S*)-2-methyltryptophan and (*S*)-5-fluorotryptophan with the values reported in the literature.[15,17a,b,18a,37]

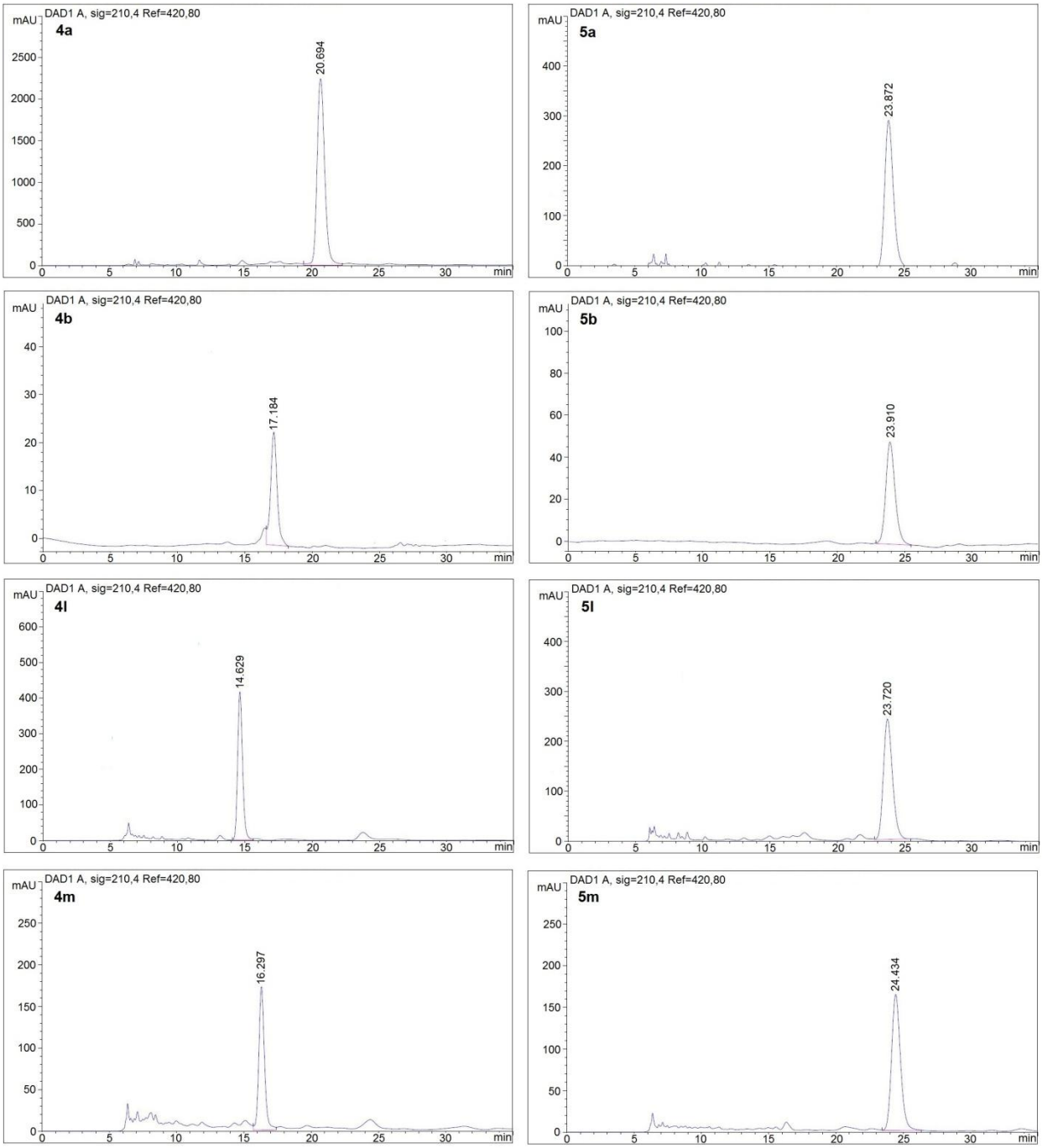

Figure 5 HPLC analyses of the representative compounds **4a**, **5a 4b**, **5b**, **4l**, **5l, 4m**, **5m**, performed on a chiral stationary phase, using CHIRALPAK IC column (cellulose *tris* 3,5-dichlorophenylcarbamate, particle size 5 µm, lenght 250 mm, internal diameter 4.6 mm, DAD 210); mobile phase: 1:1 n-hexane/2-propanol, at 0.8 mL min^{-1}.

To rationalize the stereochemical outcome of the reactions, we analyzed the in solution conformation of Ts-Oxd-ΔAla-OMe (**3a**). Previous analyses including Electronic Circular Dichroism, 2D NMR, and molecular dynamics computations[30] showed Ts group of **3a** facing the double bond of ΔAla at a distance of about 3.7 Å (Figure 6), perfectly compatible with the values reported in the literature for π-stacking interactions.[38]

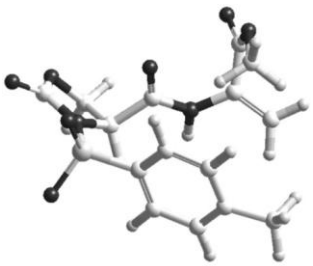

Figure 6. Representative low-energy structure of **3a** consistent with ROESY analysis (see also Figure 7), calculated by restrained molecular dynamics. The calculated geometry of the ΔAla residue matches the structures reported in the literature.[39]

Reasonably, the Lewis acid effectively promotes the conjugate addition of the indoles by forming a complex with the carbonyl oxygen of ΔAla.[19,34b,40] The Michael addition gives rise to a intermediate enolate (Figure 7). The ability of arylsulfonamido groups to form sandwich structures with enolates by π-stacking interactions is well known.[41] Electron-poor aromatic rings have been reported to promote the reactivity of delocalized anions such as enolates by means of a donor-acceptor π-stacking stabilization of the transition states.[42] As proposed in Figure 7, the Ts group could shield the *Si* face of the enolate, leaving the *Re* face more accessible to the PhOH-Lewis acid complex that serves as a Brønsted acid to protonate the intermediate enolate.[11a,13,23]

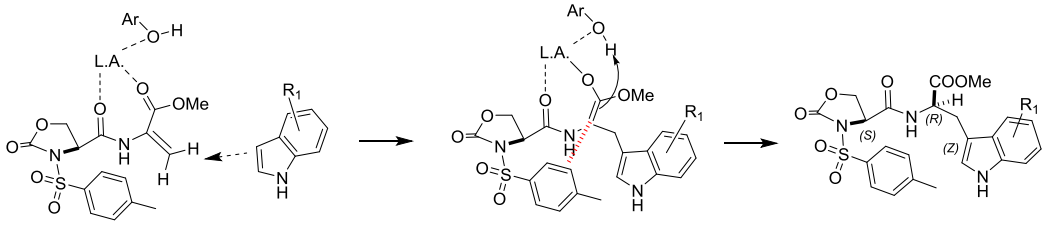

Figure 7. Proposed model for the tandem Michael addition-enolate protonation of indoles and ΔAla, and role of the oxazolidin-2-one chiral auxilixary.

The F.-C. reaction between the indoles and Ts-Oxd-ΔAla-OMe appears as a practical method to give access to peptides containing modified Trp. To exploit this opportunity, we synthesized in a few steps the analogues of the opioid peptide H-Tyr-Pro-Trp-PheNH_2 (EM1) containing 2-methyltryptophan or 5-fluorotryptophan[15,17a,b,18a,c,37a,b] [2-Me-Trp^3]-EM1 (**8**), and [5-F-Trp^3]-EM1 (**9**), respectively (Figure 8 and 9). Since we were interested in (*S*)-configures amino acids, we performed the F.-C. reactions of the indoles with the (*R*)-enantiomer of **3a**, in the presence of $SnCl_4$ and PhOH. (*R*)-**3a** was obtained in turn by treatment of (*R*,*R*)-**1a** with DSC and DIPEA as described for **3a**. The reactions of 2-methylindole and 5-fluoroindole afforded (*R*,*S*)-**5b** or (*R*,*S*)-**5c**, respectively, as the major products, with the same yields and d.r. as reported in Table 2, entries 6 and 9. After isolation by flash chromatography, (*R*,*S*)-**5b** or (*R*,*S*)-**5c** were treated with 10% HBr at reflux under conventional heating, giving 2-methyltryptophan (**6b**) or 5-fluorotryptophan (**6c**) in moderate yields. Gratifyingly, heating at 95°C under MW irradiation afforded **6b** or **6c** in more satisfactory yields (Figure 8). The reaction mixture was adjusted to pH 3, and crude Ts-Ser-OH was easily separated from **6b** or **6c** and recovered in almost quantitative yield by extraction with EtOAc (Figure 8). The tryptophans **6b** or **6c** were isolated using a Dowex H^+ form resin.[18c] Spectroscopic characterization and specific optical rotation were found to match with the literature above reported, confirming the absolute stereochemistry attributed in the previous paragraph.

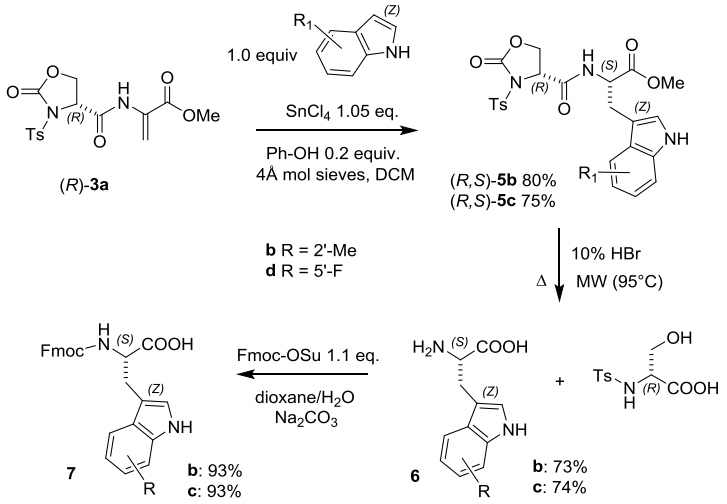

Figure 8. Synthesis of Fmoc-2-Me-Trp-OH, and Fmoc-5-F-Trp-OH, by F.-C. reaction of the indoles with (*R*)-**3a**.

Finally, **6b** or **6c** were protected at the *N*-terminus with the Fmoc group under standard conditions,[18c] and the resulting **7b** or **7c** were utilized for the solid-phase peptide synthesis (SPPS) of modified EM1.
The tetrapeptide-amides [2-Me-Trp[3]]-EM1 (**8b**), and [5-F-Trp[3]]-EM1 (**8c**) were rapidly obtained by standard SPPS on a Rink amide resin in DCM/DMF, using Fmoc-protected amino acids, and HBTU/HOBt/DIPEA as coupling agents (Figure 9). The reaction was performed under MW-assisted conditions, keeping temperature at 45°C while mechanically shaking, which allowed to complete the reactions in 10 min. Coupling efficiency was monitored by the Kaiser or Chloranyl tests. After each coupling, Fmoc was removed very rapidly (1 min) with DMF/piperidine at 45°C under MW irradiation. Peptide cleavage was performed by treatment with trifluoroacetic acid (TFA) in the presence of scavengers. After filtration, the crude peptides were precipitated from ice-cold Et_2O, and collected by centrifuge. The peptide **8b** or **8c** were isolated >95% pure by semi-preparative RP-HPLC on a C18 column.

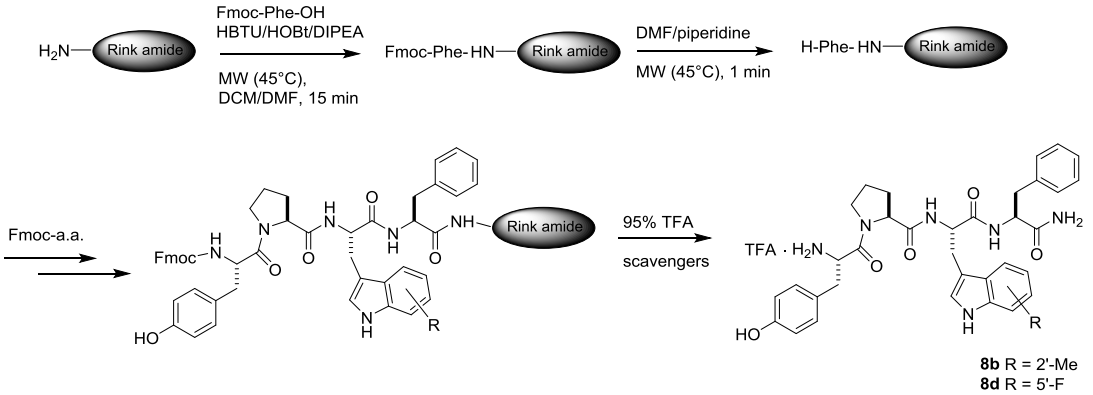

Figure 9. Solid phase synthesis of the EM1 analogues **8b** and **8c** containing substituted Trp[3].

3.3. Conclusions

In summary, we proposed a practical route for the preparation of dehydroalanine equipped with a oxazolidinone chiral auxiliary, by one-pot cyclization-elimination of the dipeptide Ts-Ser-Ser-OMe, and we demonstrated the efficacy of the resulting Ts-Oxd-ΔAla-OMe chiral building block for the preparation of non-racemic non-natural amino acids. The F.-C. alkylation of substituted indoles with ΔAla carrying (*S*)-configured chiral auxiliary in the presence of Lewis/Brønsted acids allowed obtaining (*R*)-tryptophans with diverse substituents at different positions of the indole, in good to excellent d.r over the (*S*)-isomers. The tryptophans were easily isolated in optical pure form after simple flash chromatography and cleavage of the chiral auxiliary. As a preliminary demonstration of the utility of this protocol, we introduced 2-methyl or 5-fluoro tryptophan into a peptide sequence of pharmacological interest, the opioid peptide EM1. The procedure can be utilized to synthesize a library of EM1 analogues, aiming at obtaining new opioid peptides with improved in vivo performances, as well as to deduce information about the role of Trp in peptide-receptor recognition and activation by SAR studies.

3.4. Experimental section

3.4.1. General methods

Standard chemicals were purchased from commercial sources and used without further purification. The reactions were monitored by thin layer chromatography. Flash chromatography was performed on silica gel (230-400 mesh), using mixtures of distilled solvents. Analytical RP-HPLC was performed on an Agilent 1100 series apparatus, using a RP column Phenomenex mod. Gemini 3µ C18 110A 100x3.0 mm (P/No 00D-4439-Y0); column description: stationary phase octadecyl carbon chain-bonded silica (C18) with TMS endcapping, fully porous organo-silica solid support, particle size 3 µm, pore size 110 Å, length 100 mm, internal diameter 3 mm; DAD 210 nm; mobile phase: from a 9:1 H_2O-MECN to a 2:8 H_2O-MECN in 20 min at a flow rate of 1.0 mL min^{-1}, followed by 10 min at the same composition. Semi-preparative RP-HPLC was performed on an Agilent 1100 series apparatus, using a RP column ZORBAX mod. Eclipse XDB-C18 PrepHT cartridge 21.2x150 mm 7µ (P/No 977150-102); column description: stationary phase octadecyl carbon chain-bonded silica (C18), double endcapped, particle size 7 µm, pore size 80 Å, lenght 150 mm, internal diameter 21.2 mm; DAD 210 nm; mobile phase from 8:2 H_2O-MeCN with 0.1% TFA to 100% MECN/0.1% TFA in 10 min at a flow rate of 12 mL min^{-1}. Chiral HPLC analysis was performed on an Agilent 1200 series apparatus, using a CHIRALPAK IC column (P/No 83325); column description: chiral stationary phase cellulose *tris* (3,5-dichlorophenylcarbamate) immobilized on silica, particle size 5 µm, lenght 250 mm, internal diameter 4.6 mm, DAD 210/254 nm; mobile phase: 1:1 n-hexane/2-propanol, at 0.8 mL min^{-1}. Direct phase-HPLC analyses were performed on an Agilent 1100 series apparatus, using a Kromasil 60-5Diol column (P/No E42500); column description: stationary phase silica, particle size 5 µm, pore size 60 Å, lenght 250 mm, internal diameter 4.6 mm, DAD 210 nm; mobile phase hexane/2-propanol 60:40, at a flow rate of 0.6 mL min^{-1}. ESI analysis was performed using a MS single quadrupole HP 1100MSD detector, with a drying gas flow of 12.5 l/min, nebulizer pressure 30 psgi, drying gas temp. 350°C, capillary voltage 4500 (+) and 4000 (-), scan 50-2600 amu. Elemental analyses were performer using a Thermo Flash 2000 CHNS/O analyzer. The synthetic procedures by MW irradiation were performed using a microwave oven (MicroSYNTH Microwave Labstation for Synthesis) equipped with a built-in ATC-FO advanced fiber optic automatic temperature control. ^{1}H NMR spectra were recorded using a Varian Gemini apparatus at 400 MHz in 5 mm tubes, using 0.01 M peptide at room temperature. Solvent suppression was performed by the solvent presaturation procedure implemented in Varian (PRESAT). ^{13}C NMR spectra were recorded at 100 MHz. Chemical shifts are reported as δ values relative to residual $CHCl_3$ δH (7.26 p.p.m.), DMSO δH (2.50 p.p.m.) and $CDCl_3$ δC (77.16 p.p.m.) as internal standards. The unambiguous assignment of ^{1}H NMR resonances was performed by 2D gCOSY.

3.4.2. Synthetic procedures

General procedure for the synthesis of Ts-Ser/Thr/phenylSer-Ser-OMe (**1**). A stirred solution of the *N*-tosylamino acid (1.0 mmol) in 4:1 DCM/DMF (5 mL) was treated with HOBt (1.2 mmol) and HBTU (1.2 mmol), at r.t. and under inert atmosphere. After 5 min, the amino acid esters (1.1 mmol), and DIPEA (2.4 mmol) were added and the reaction was stirred under MW irradiation.[33] The microwave-assisted reaction was performed by setting maximum irradiation power at 150W and monitoring the internal reaction temperature at 80°C. After 10 min, the mixture was concentrated at reduced pressure, and the residue was diluted with EtOAc (25 mL). The solution was washed with 0.1 M HCl (5 mL), and a saturated solution of $NaHCO_3$ (5 mL). The organic layer was dried over Na_2SO_4 and the solvent was evaporated at reduced pressure. The crude peptides (80-90 % yield, 70-80 % pure by analytical RP-HPLC) were identified by ESI-MS and ^{1}H NMR analysis, and were used without further purifications.

Ts-L-Ser-L-Ser-OMe (**1a**). ^{1}H NMR ($CDCl_3$) δ: 2.31 (s, 3H, TsMe), 3.49 (m, 1H, SerHα), 3.62 (s, 3H, OMe), 3.70-3.90 (m, 4H, SerHβ), 4.41 (m, 1H, SerHα), 6.66 (d, J=7.2 Hz, 1H, SerNH), 7.18-7.22 (m, 2H, TsArH), 7.63-7.69 (m, 3H, TsArH+SerNH); ES-MS *m/z:* 361.1 $[M+H]^+$, calcd 361.0.

Ts-L-Thr-L-Ser-OMe (**1b**). ^{1}H NMR ($CDCl_3$) δ: 1.00 (d, J=6.4 Hz, 3H, ThrMe), 2.38 (s, 3H, TsMe), 3.72 (s, 3H, OMe), 3.74 (t, J=3.0 Hz, 1H, ThrHα), 3.85-3.89 (m, 2H, SerHβ), 4.18-4.24 (m, 2H, ThrHβ), 4.46 (q, J=3.8 Hz, 1H, SerHα), 6.31 (d, J= 8.0 Hz, 1H, ThrNH), 7.21-7.25 (m, 2H, TsArH), 7.60 (d, J=7.6 Hz, SerNH), 7.69-7.63 (m, 2H, TsArH); ES-MS *m/z:* 375.2 $[M+H]^+$, calcd 375.1.

Ts-L/D-phenylSer-L-Ser-OMe (**1c**). ^{1}H NMR ($CDCl_3$) δ (*two diastereoisomers*): 2.39+2.40 (s, 3H, TsMe), 3.80 (s, 3H, OMe), 3.90-4.06 (m, 3H, PhSerHβ+SerHβ), 4.63-4.65 (m, 1H, SerHα), 5.27+5.31 (m, 1H, PhSerHα), 7.02-7.40 (m, 10H, TsArH+PhSerArH+PhSerNH), 7.90+7.93 (d, J=7.6 Hz, 1H, SerNH); ES-MS *m/z:* 437.3 $[M+H]^+$, calcd 437.1.

General procedure for the synthesis of Ts-Oxd-ΔAla-OMe (**3**). *N,N*-disuccinimidyl carbonate (0.73 mmol) was added in 60 min by using a temporized syringe to a stirred solution of **1** (0.33 mmol) in DMF (4 mL) and a catalytic amount of DIPEA (0.07 mmol) at 0°C and under inert atmosphere. After 60 min, the solvent was removed under reduced pressure. The residue was diluted with 0.1 M HCl (5 mL), and the mixture was extracted three times with DCM (5 mL). The combined organic layers were dried over Na_2SO_4, filtered, and concentrated at reduced pressure. The residue was purified by flash chromatography over silica-gel (eluant cyclohexane/EtOAc 70:30), giving **3** (yields: see Table 1; 94-96 % pure by analytical RP-HPLC) as waxy solids.

Ts-L-Oxd-ΔAla-OMe (**3a**). $[\alpha]_D^{20}$ -26.8 (*c* 1.0, MeOH); ^{1}H NMR ($CDCl_3$) δ: 2.42 (s, 3H, Me), 3.88 (s, 3H, COOMe), 4.45 (dd, J=4.6, 9.0 Hz, 1H, $OxdH_5$), 4.52 (t, J=9.1 Hz, 1H, $OxdH_5$), 4.99 (dd, J=4.4, 9.2 Hz, 1H, $OxdH_4$), 6.05 (s, 1H, =CH), 6.65 (s, 1H, =CH), 7.33-7.37 (m, 2H, TsArH), 7.92-7.96 (m, 2H, TsArH), 8.54 (s, 1H, ΔAlaNH); ^{13}C NMR ($CDCl_3$) δ: 21.4, 52.6, 57.9, 66.0, 111.0, 128.7, 128.9, 129.1, 129.1, 131.0, 133.8, 145.4, 151.5, 163.6, 166.8; ES-MS *m/z:* 369.1 $[M+H]^+$, calcd 369.1. Elem. Anal. for $C_{15}H_{16}N_2O_7S$, calcd: C 48.91, H 4.38, N 7.60, S 8.70; found: C 49.15, H 4.51, N 7.51, S 8.57.

Ts-L-5-Me-Oxd-ΔAla-OMe (**3b**). $[\alpha]_D^{20}$ -18.3 (*c* 0.5, MeOH); ^{1}H NMR ($CDCl_3$) δ: 1.44 (d, J=12.4 Hz, 3H, 5-Me), 2.44 (s, 3H, TsMe), 3.86 (s, 3H, COOMe), 4.54 (d, J=10.0 Hz, 1H, $OxdH_4$), 4.71 (m, 1H, $OxdH_5$), 6.03 (s, 1H, =CH), 6.65 (s, 1H, =CH), 7.33-7.37 (m, 2H, TsArH), 7.92-7.96 (m, 2H, TsArH), 8.55 (s, 1H, ΔAlaNH); ^{13}C NMR ($CDCl_3$) δ: 20.7, 20.8, 53.5, 65.4, 75.1, 111.4, 129.2, 130.0, 130.1, 130.9, 133.8, 146.5, 151.4, 164.2, 166.2; ES-MS *m/z:* 400.2 [M+18], calcd 400.4. Elem. Anal. for $C_{16}H_{24}N_2O_7S$, calcd: C, 50.26; H, 4.74; N, 7.33; S, 8.39. found: C, 49.97; H, 4.89; N, 7.45; S, 8.22.

Ts-L/D-5-Ph-Oxd-ΔAla-OMe (**3c**). ^{1}H NMR ($CDCl_3$) δ: 2.47 (s, 3H, TsMe), 3.88 (s, 3H, OMe), 4.71 (d, J=4.6 Hz, 1H, $OxdH_4$), 5.64 (d, J=4.6 Hz, 1H, $OxdH_5$), 6.08 (s, 1H, =CH), 6.72 (s, 1H, =CH), 7.14-7.21 (m, 2H, TsArH), 7.32-7.39 (m, 5H, 5-Ph), 7.86-7.90 (m, 2H, TsArH), 8.55 (s, 1H, ΔAlaNH); ^{13}C NMR ($CDCl_3$) δ: 21.8, 53.2, 66.3, 78.1, 111.1, 125.0, 128.8, 129.3, 129.6, 129.8, 130.6, 133.4, 136.5, 151.2, 163.7, 165.6; ES-MS *m/z* 445.2 $[M+H]^+$, calcd 445.1. Elem. Anal. for $C_{21}H_{20}N_2O_7S$, calcd: C, 56.75; H, 4.54; N, 6.30; S, 7.21; found: C, 56.45; H, 4.58; N, 6.33; S, 7.12.

General procedure for the Michael addition with substituted indoles. A flame-dried flask containing freshly activated powdered 4 Å molecular sieves (200 wt %) under inert atmosphere was charged with anhydrous DCM (5 mL), then the indole (Table 2, 1.0 mmol), **3** (1.0 mmol) and, PhOH (0.20 mmol) were added under inert atmosphere at r.t. The Lewis acid (1 M in DCM, 1.0 mmol) was slowly added under inert atmosphere at 0°C. The reaction was stirred at 0°C for 24 h, then it was quenched with 0.5 M HCl (5 mL). The mixture was filtered over celite®, and concentrated at reduced pressure to a final volume of 5 mL. The residual aqueous layer was extracted with EtOAc (3×15 mL), the combined organic layers were washed with saturated $NaHCO_3$ (5 mL), and dried over Na_2SO_4. The solvent was evaporated at reduced pressure, and the crude residue was purified by flash chromatography over silica-gel (eluant cyclohexane/EtOAc 70:20) giving **4** and **5** (Table 2, 94-97% pure by analytical HPLC) as waxy solids.

Ts-L-Oxd-L-Trp-OMe (**4a**). $[\alpha]_D^{20}$ +44.0 (*c* 1.0, $CHCl_3$); ^{1}H NMR ($CDCl_3$) δ: 2.40 (s, 3H, TsMe), 3.38 (d, J=5.0 Hz, 2H, TrpHβ), 3.67 (s, 3H, OMe), 4.10-4.15 (m, 2H, $OxdH_5$), 4.73 (dd, J=6.4, 7.6 Hz, 1H, $OxdH_4$), 4.94 (dt, J=5.0, 7.6 Hz, 1H, TrpHα), 6.94 (d, J=7.6 Hz, 1H, TrpNH), 7.12 (t, J=7.6 Hz, 1H, $TrpH_5$), 7.16 (m, 2H, $TrpH_{2,6}$), 7.21-7.23 (m, 2H, TsArH), 7.36 (d, J=8.0 Hz, 1H, $TrpH_7$), 7.54 (d, J=8.0 Hz, 1H, $TrpH_4$), 7.83-7.85 (m, 2H, TsArH), 8.47 (s, 1H, $TrpH_1$); ^{13}C NMR ($CDCl_3$) δ: 21.7, 27.5, 52.6, 53.0, 57.8, 65.9, 108.8, 111.5, 118.2, 119.6, 122.2, 124.0, 127.2, 128.9, 129.6, 136.1, 151.8, 167.4, 171.9; ESI-MS *m/z* 486.2 $[M+H]^+$, calcd 486.1. Elem. Anal. for $C_{23}H_{23}N_3O_7S$, calcd: C, 56.90; H, 4.77; N, 8.65; S, 6.60; found: C, 57.47; H, 4.80; N, 8.59; S, 6.55.

Ts-L-Oxd-D-Trp-OMe (**5a**). $[\alpha]_D^{20}$ -22.0 (*c* 0.5, $CHCl_3$); ^{1}H NMR ($CDCl_3$) δ: 2.41 (s, 3H, TsMe), 3.37 (dd, J=6.4, 15.5 Hz, 1H, TrpHβ), 3.39 (dd, J=6.2, 15.5 Hz, 1H, TrpHβ), 3.73 (s, 3H, OMe), 4.05 (dd, J=5.0, 9.0 Hz, 1H, $OxdH_5$), 4.20 (m, 1H, $OxdH_5$), 4.77 (dd, J=5.0, 9.0 Hz, 1H, $OxdH_4$), 4.93 (ddd, J=6.2, 6.4, 7.6 Hz, 1H, TrpHα), 7.03 (d, J= 7.6 Hz, 1H, TrpNH), 7.10 (t, J=7.2 Hz, 1H, $TrpH_6$), 7.12 (br.s, 1H, $TrpH_2$), 7.18 (t, J=7.4 Hz, 1H, $TrpH_5$), 7.24-7.26 (m, 2H, TsArH), 7.35 (d, J=8.0 Hz, 1H, $TrpH_7$), 7.49 (d, J=8.0 Hz, 1H, $TrpH_4$), 7.84-7.86 (m, 2H, TsArH), 8.54 (br.s, 1H, $TrpH_1$); ^{13}C NMR ($CDCl_3$) δ: 22.1, 27.6, 38.1, 53.5, 58.3, 66.1, 109.6, 111.9, 118.7, 120.0, 122.7, 123.9, 128.0, 129.3, 130.1, 133.9, 136.6, 146.5, 167.7, 170.2, 171.3; ESI-MS *m/z* 486.2 $[M+H]^+$, calcd 486.1. Elem. Anal. for $C_{23}H_{23}N_3O_7S$, calcd: C, 56.90; H, 4.77; N, 8.65; S, 6.60; found: C, 56.34; H, 4.84; N, 8.73; S, 6.45.

Ts-L-Oxd-L-2-Me-Trp-OMe (**4b**): $[\alpha]_D^{20}$ -65.0 (*c* 0.7, $CHCl_3$); ^{1}H NMR ($CDCl_3$) δ: 2.39 (s, 3H, TrpMe), 2.40 (s, 3H, TsMe), 3.26 (dd, J=6.2, 14.8 Hz, 1H, TrpHβ), 3.35 (dd, J=6.0, 14.8 Hz, 1H, TrpHβ), 3.73 (s, 3H, OMe), 4.12 (m, 1H,

$OxdH_5$), 4.29 (t, J=9.0 Hz, 1H, $OxdH_5$), 4.75 (dd, J=4.4, 9.0 Hz, 1H, $OxdH_4$), 4.91 (ddd, J=6.0, 6.2, 8.0 Hz, 1H, TrpHα), 6.69 (d, J=8.0 Hz, 1H, TrpNH), 7.10-7.17 (m, 6H, $TrpH_{4-7}$+TsArH), 7.76-7.78 (m, 2H, TsArH), 8.00 (s, 1H, $TrpH_1$); ^{13}C NMR ($CDCl_3$) δ: 11.6, 21.7, 29.7, 52.6, 57.7, 65.8, 105.2, 110.5, 117.6, 119.8, 121.5, 128.5, 128.9, 129.6, 133.2, 133.6, 135.3, 145.9, 151.6, 167.2, 171.9; ESI-MS *m/z* 500.2 $[M+H]^+$, calcd 500.1. Elem. Anal. for $C_{24}H_{25}N_3O_7S$, calcd: C, 57.70; H, 5.04; N, 8.41; S, 6.42. found : C, 58.68; H, 4.98; N, 8.52; S, 6.39.

Ts-L-Oxd-D-2-Me-Trp-OMe (**5b**): $[\alpha]_D^{20}$ +13.8 (*c* 0.13, $CHCl_3$); ^1H NMR ($CDCl_3$) δ: 2.40 (s, 3H, TrpMe), 2.41 (s, 3H, TsMe), 3.24 (dd, J=6.6, 14.6 Hz, 1H, TrpHβ), 3.36 (dd, J=5.8, 14.6 Hz, 1H, TrpHβ), 3.73 (s, 3H, OMe), 3.94 (dd, J=4.8 8.8 Hz, 1H, $OxdH_5$), 4.11 (dd, J=8.8, 9.4 Hz, 1H, $OxdH_5$), 4.64 (dd, J=4.8, 9.4 Hz, 1H, $OxdH_4$), 4.88 (ddd, J=5.8, 6.6, 7.2 Hz, 1H, TrpHα), 6.73 (d, J=7.2 Hz, 1H, TrpNH), 7.08-7.18 (m, 4H, $TrpH_{4-7}$), 7.20-7.22 (m, 2H, TsArH), 7.80-7.82 (m, 2H, TsArH), 7.98 (s, 1H, $TrpH_1$); ^{13}C NMR ($CDCl_3$) δ: 12.0, 22.1, 27.3, 53.0, 53.7, 58.1, 65.7, 105.7, 111.0, 118.0, 120.0, 121.8, 128.8, 129.2, 129.3, 130.0, 133.7, 135.7, 146.3, 152.0, 172.1, 172.3; ESI-MS *m/z* 500.2 $[M+H]^+$, calcd: 500.1. Elem. Anal. for $C_{24}H_{25}N_3O_7S$, calcd: C, 57.70; H, 5.04; N, 8.41; S, 6.42. found: C, 57.61; H, 5.10; N, 8.46; S, 6.30.

Ts-L-Oxd-L-5-F-Trp-OMe (**4c**). $[\alpha]_D^{20}$ +16.2 (*c* 0.5, $CHCl_3$); ^1H NMR ($CDCl_3$) δ: 2.44 (s, 3H, TsMe), 3.37 (d, J=4.8 Hz, 2H, TrpHβ), 3.76 (s, 3H, OMe), 4.28 (dd, J=4.4, 9.8 Hz, 1H, $OxdH_5$), 4.39 (t, J=9.6 Hz, 1H, $OxdH_5$), 4.76 (dd, J=4.4, 9.0 Hz, 1H, $OxdH_4$), 4.92 (m, 1H, TrpHα), 6.88 (br.d, 1H, TrpNH), 6.93 (d, J=6.8 Hz, 1H, $TrpH_6$), 7.05 (s, 1H, $TrpH_2$), 7.12 (s, 1H, $TrpH_4$), 7.28-7.29 (m, 2H, TsArH), 7.53 (d, J=6.8 Hz, 1H, $TrpH_7$), 7.84-7.86 (m, 2H, TsArH), 8.16 (s, 1H, $TrpH_1$); ^{13}C NMR ($CDCl_3$) δ: 22.1, 30.1, 53.3, 53.8, 58.3, 66.1, 103.3, 110.4, 113.2, 115.0, 123.0, 127.6, 128.1, 129.3, 130.2, 133.7, 137.6, 151.9, 157.6, 170.2, 171.7; ES-MS *m/z* 504.0 $[M+H]^+$, calcd 504.1. Elem. Anal. for $C_{23}H_{22}FN_3O_7S$, calcd: C, 54.87; H, 4.40; N, 8.35; S, 6.37; found: C, 54.58; H, 4.68; N, 8.38; S, 6.33.

Ts-L-Oxd-D-5-F-Trp-OMe (**5c**) $[\alpha]_D^{20}$ +38.5 (*c* 0.2, $CHCl_3$); ^1H NMR ($CDCl_3$) δ: 2.44 (s, 3H, TsMe), 3.36 (d, J=5.2 Hz, 2H, TrpHβ), 3.76 (s, 3H, OMe), 4.27 (dd, J=5.6, 8.2 Hz, 1H, $OxdH_5$), 4.37 (dd, J=8.2, 9.4 Hz, 1H, $OxdH_5$), 4.75 (dd, J=5.6, 9.4 Hz, 1H, $OxdH_4$), 4.91 (m, 1H, TrpHα), 7.04 (br.d, 1H, TrpNH), 6.96-7.10 (m, 2H, $TrpH_{2,6}$), 7.12 (s, 1H, $TrpH_4$), 7.28-7.30 (m, 2H, TsArH), 7.54 (d, J=8.0 Hz, 1H, $TrpH_7$), 7.84-7.87 (m, 2H, TsArH), 8.48 (s, 1H, $TrpH_1$); ^{13}C NMR ($CDCl_3$) δ: 21.0, 28.0, 51.1, 52.9, 56.9, 60.8, 101.6, 107.9, 110.6, 113.2, 121.0, 125.5, 126.1, 127.1, 130.0, 131.5, 135.3, 149.3, 155.0, 168.6, 168.8; ES-MS *m/z* 504.0 $[M+H]^+$, calcd 504.1. Elem. Anal. for $C_{23}H_{22}FN_3O_7S$, calcd: C, 54.87; H, 4.40; N, 8.35; S, 6.37; found: C, 55.16; H, 4.43; N, 8.29; S, 6.30.

Ts-L-Oxd-L-7-Br-Trp-OMe (**4d**). $[\alpha]_D^{20}$ +51.0 (*c* 0.1, $CHCl_3$); ^1H NMR ($CDCl_3$, 400 MHz) δ: 2.40 (s, 3H, TsMe), 3.38 (d, J=4.8 Hz, 2H, TrpHβ), 3.73 (s, 3H, OMe), 4.34 (dd, J=4.4, 7.8 Hz, 1H, $OxdH_5$), 4.44 (dd, J=7.8, 10.0 Hz, 1H, $OxdH_5$), 4.83 (dd, J=4.4, 10.0 Hz, 1H, $OxdH_4$), 4.98 (m, 1H, TrpHα), 6.71 (br.d, 1H, TrpNH), 6.90 (t, J=8.0 Hz, 1H, $TrpH_5$), 7.16 (br.s, 1H, $TrpH_2$), 7.22-7.31 (m, 3H, TsArH+$TrpH_6$), 7.51 (d, J=8.0 Hz, 1H, $TrpH_4$), 7.81 (d, J=8.0 Hz, 2H, TsAr), 8.30 (s, 1H, $TrpH_1$); ^{13}C NMR ($CDCl_3$, 400 MHz) δ: 20.8, 28.0, 50.9, 51.3, 56.6, 60.7, 98.1, 107.5, 115.4, 118.7, 120.5, 122.0, 125.7, 126.7, 127.0, 131.0, 132.8, 134.8, 149.0, 168.1, 168.3; ES-MS *m/z* 563.8/565.8 $[M+H]^+$, calcd 564.0/566.0. Elem. Anal. for $C_{23}H_{22}BrN_3O_7S$, calcd: C, 48.94; H, 3.93; N, 7.45; S, 5.68; found: C, 49.34; H, 3.96; N, 7.37; S, 5.61.

Ts-L-Oxd-D-7-Br-Trp-OMe (**5d**). $[\alpha]_D^{20}$ -11.0 (*c* 0.5, $CHCl_3$ ^1H NMR ($CDCl_3$) δ: 2.45 (s, 3H, TsMe), 3.40 (d, J=4.8 Hz, 2H, TrpHβ), 3.73 (s, 3H, OMe), 4.30 (dd, J=5.0, 8.4 Hz, 1H, $OxdH_5$), 4.38 (dd, J=8.4, 9.0 Hz, 1H, $OxdH_5$), 4.75 (dd, J=5.0, 9.0 Hz, 1H, $OxdH_4$), 4.93 (dt, J=4.8, 7.6 Hz, 1H, TrpHα), 6.83 (d, J=7.6 Hz, 1H, TrpNH), 6.91 (t, J=7.8 Hz, 1H, $TrpH_5$), 7.16 (br.s, 1H, $TrpH_2$), 7.22-7.31 (m, 3H, TsArH+$TrpH_6$), 7.47 (d, J=8.0 Hz, 1H, $TrpH_4$), 7.85-7.88 (m, 2H, TsArH), 8.30 (br.s, 1H, $TrpH_1$); ^{13}C NMR ($CDCl_3$) δ: 21.0, 28.1, 51.1, 51.6, 57.0, 61.0, 98.5, 108.1, 116.1, 119.3, 121.2, 122.6, 126.4, 127.4, 127.7, 131.7, 133.5, 135.5, 149.6, 169.0, 169.2; ES-MS *m/z* 563.9/565.9 $[M+H]^+$, calcd 564.0/566.0. Elem. Anal. for $C_{23}H_{22}BrN_3O_7S$, calcd: C, 48.94; H, 3.93; N, 7.45; S, 5.68; found: C, 49.55; H, 3.90; N, 7.49; S, 5.63.

Ts-L-Oxd-D-1-Me-Trp-OMe (**5e**). $[\alpha]_D^{20}$ +20.7 (*c* 0.3, $CHCl_3$); ^1H NMR ($CDCl_3$) δ: 2.43 (s, 6H, TrpMe+ TsMe), 3.41 (d, J= 4.4 Hz, 2H, TrpHβ), 3.73 (s, 3H, OMe), 4.24 (dd, J=4.4, 9.6 Hz, 1H, $OxdH_5$), 4.35 (t, J=9.2 Hz, 1H, $OxdH_5$), 4.74 (dd, J=4.8, 9.0 1H, $OxdH_4$), 4.90 (dt, J=4.4, 8.0 Hz, 1H, TrpHα), 6.51 (br.s, 1H, $TrpH_2$), 6.78 (d, J=8.0 Hz, 1H, TrpNH), 7.02-7.12 (m, 2H, $TrpH_{5,7}$), 7.32-7.36 (m, 2H, TsArH), 7.48 (d, J=8.0 Hz, 1H, $TrpH_6$), 7.59 (d, J=7.6 Hz, 1H, $TrpH_4$), 7.61-7.66 (m, 2H, TsArH); ^{13}C NMR ($CDCl_3$) δ: 20.9, 28.2, 33.3, 50.9, 52.7, 56.6, 60.7, 107.4, 107.5, 116.4, 117.4, 119.3, 122.7, 125.1, 125.7, 126.7, 131.0, 134.8, 135.0, 149.0, 168.1, 168.3; ESI-MS *m/z* 500.1 $[M+H]^+$, calcd: 500.1, Elem. Anal. for $C_{24}H_{25}N_3O_7S$, calcd: C, 57.70; H, 5.04; N, 8.41; S, 6.42. found: C, 58.54; H, 5.08; N, 8.35; S, 6.39.

Ts-L-Oxd-L-7-Br-2-Me-Trp-OMe (**4i**). $[\alpha]_D^{20}$ +7.0 (*c* 0.4, $CHCl_3$); ^1H NMR ($CDCl_3$) δ: 2.42 (s, 3H, TrpMe), 2.44 (s, 3H, TsMe), 3.25 (dd, J=4.8, 13.2 Hz, 1H, TrpHβ), 3.31 (dd, J=3.6, 13.2 Hz, 1H, TrpHβ), 3.74 (s, 3H, OMe), 4.20 (dd, J=4.5,

8.8 Hz, 1H, $OxdH_5$), 4.40 (dd, J=8.8, 9.1 Hz, $OxdH_5$), 4.75 (dd, J=4.5, 9.1 Hz, 1H, $OxdH_4$), 4.94 (ddd, J=3.6, 4.8, 7.6, 1H, TrpHα), 6.63 (d, J=7.6 Hz, 1H, TrpNH), 6.98-7.15 (m, 2H, $TrpH_{4,5}$), 7.22-7.24 (m, 2H, TsArH), 7.46 (d, J=7.6 Hz, 1H, $TrpH_6$), 7.78-7.82 (m, 2H, TsArH), 8.03 (br.s, 1H, $TrpH_1$); ^{13}C NMR ($CDCl_3$) δ: 12.2, 22.4, 28.0, 51.7, 53.8, 59.2, 62.5, 100.9, 108.0, 118.6, 121.8, 123.1, 128.0, 130.0, 131.5, 136.9, 138.7, 153.2, 170.7. ES-MS *m/z* 591.1 [M+Na] calcd 591.0, Elem. Anal. for $C_{24}H_{24}BrN_3O_7S$, calcd: C, 49.83; H, 4.18; N, 7.26; S, 5.54. found: C, 49.51; H, 4.21; N, 7.35; S, 5.49.

Ts-L-Oxd-D-7-Br-2-Me-Trp-OMe (**5i**). $[\alpha]_D^{20}$ -38.0 (*c* 0.5, $CHCl_3$); ^{1}H NMR ($CDCl_3$) δ: 2.47 (s, 3H, TrpMe), 2.49 (s, 3H, TsMe), 3.24 (dd, J=5.8, 14.9 Hz, 1H, TrpHβ), 3.34 (dd, J=6.4, 14.9 Hz, 1H, TrpHβ), 3.73 (s, 3H, OMe), 4.19 (dd, J=4.8, 8.8 Hz, 1H, $OxdH_5$), 4.26 (t, J=8.9 Hz, $OxdH_5$), 4.68 (dd, J=4.8, 8.9 Hz, 1H, $OxdH_4$), 4.93 (ddd, J=5.8, 6.4, 7.2 Hz, 1H, TrpHα), 6.73 (d, J=7.2 Hz, 1H, TrpNH), 7.00-7.20 (m, 2H, $TrpH_{4,5}$), 7.44 (m, 2H, TsArH), 7.46 (d, J=7.6 Hz, 1H, $TrpH_6$), 7.84 (d, J=8.0 Hz, 2H, TsArH), 8.47 (s, 1H, $TrpH_1$); ^{13}C NMR ($CDCl_3$) δ: 12.2, 22.4, 28.0, 51.7, 53.8, 59.2, 62.5, 100.9, 108.0, 118.6, 121.8, 123.1, 127.9, 128.2, 130.0, 131.5, 136.9, 138.7, 153.2, 167.7, 170.7. ES-MS *m/z* 591.1 [M+Na] calcd 591.0, Elem. Anal. for $C_{24}H_{24}BrN_3O_7S$, calcd: C, 49.83; H, 4.18; N, 7.26; S, 5.54 found: C, 49.42; H, 4.22; N, 7.19; S, 5.54.

Ts-L-Oxd-L-5-Cl-2-Me-Trp-OMe (**4l**). $[\alpha]_D^{20}$ -13.6 (c 0.6, $CHCl_3$); ^{1}H NMR ($CDCl_3$) δ: 2.39 (s, 3H, TrpMe), 2.43 (s, 3H, TsMe), 3.23 (dd, J=7.0, 14.6 Hz, 1H, TrpHβ), 3.28 (dd, J=6.0, 14.6 Hz, 1H, TrpHβ), 3.76 (s, 3H, OMe), 4.26 (dd, J=4.5, 9.2 Hz, 1H, $OxdH_5$), 4.37 (t, J=9.1 Hz, $OxdH_5$), 4.75 (dd, J=4.5, 9.0 Hz, 1H, $OxdH_4$), 4.89 (ddd, J=6.0, 7.0, 7.6 Hz, 1H, TrpHα), 6.64 (d, J=7.6 Hz, 1H, TrpNH), 7.10 (d, J=8.4 Hz, $TrpH_6$), 7.18 (d, J=8.4 Hz, 1H, $TrpH_7$), 7.19-7.23 (m, 2H, TsArH), 7.46 (s, 1H, $TrpH_4$), 7.75-7.79 (m, 2H, TsArH), 7.97 (s, 1H, $TrpH_1$); ^{13}C NMR ($CDCl_3$) δ: 11.7, 21.7, 26.9, 52.7, 53.2, 57.8, 65.7, 105.2, 111.5, 117.2, 121.7, 125.5, 128.8, 129.6, 129.7, 133.6, 134.9, 151.5, 167.2, 171.7; ESI-MS *m/z* 534.0 $[M+H]^+$, calcd 534.1. Elem. Anal. for $C_{24}H_{24}ClN_3O_7S$, calcd: C, 53.98; H, 4.53; N, 7.87; S, 6.00. found: C, 54.58; H, 4.50; N, 7.79; S, 6.06.

Ts-L-Oxd-D-5-Cl-2-Me-Trp-OMe (**5l**). $[\alpha]_D^{20}$ -12.0 (c 0.2, $CHCl_3$); ^{1}H NMR ($CDCl_3$) δ: 2.39 (s, 3H, TrpMe), 2.42 (s, 3H, TsMe), 3.22 (dd, J= 5.8, 14.6 Hz, 1H, TrpHβ), 3.33 (dd, J=6.2, 14.6 Hz, 1H, TrpHβ), 3.78 (s, 3H, OMe), 4.15 (dd, J=4.6, 8.8 Hz, 1H, $OxdH_5$), 4.29 (t, J=9.0 Hz, 1H, $OxdH_5$), 4.70 (dd, J=4.6, 9.0 Hz, 1H, $OxdH_4$), 4.87 (ddd, J=5.8, 6.2, 7.6 Hz, 1H, TrpHα), 6.76 (d, J=7.6 Hz, 1H, TrpNH), 7.08 (d, J=8.4 Hz, 1H, $TrpH_6$), 7.19 (d, J=8.4 Hz, 1H, $TrpH_7$), 7.20-7.24 (m, 2H, TsArH), 7.32 (s, 1H, $TrpH_4$), 7.80-7.83 (m, 2H, TsArH), 8.00 (s, 1H, $TrpH_1$); ^{13}C NMR ($CDCl_3$) δ: 11.5, 21.5, 29.5, 52.2, 53.0, 57.3, 65.5, 105.2, 111.4, 117.0, 120.5, 124.3, 128.8, 129.2, 129.9, 133.4, 133.9, 135.0, 145.3, 151.6, 167.3, 171.7; ESI-MS *m/z* 534.0 $[M+H]^+$, calcd 534.1. Elem. Anal. for $C_{24}H_{24}ClN_3O_7S$, calcd: C, 53.98; H, 4.53; N, 7.87; S, 6.00; found: C, 53.67; H, 4.50; N, 7.91; S, 6.05.

Ts-L-5-Me-Oxd-L-2-Me-Trp-OMe (**4m**). $[\alpha]_D^{20}$ +37.9 (c 0.2, $CHCl_3$); ^{1}H NMR ($CDCl_3$) δ: 1.11 (d, J=6.4 Hz, 3H, OxdMe), 2.36 (s, 3H, TrpMe), 2.41 (s, 3H, TsMe), 3.29 (dd, J=6.4, 14.8 Hz, 1H, TrpHβ), 3.32 (dd, J=6.0, 14.8 Hz, 1H, TrpHβ), 3.70 (s, 3H, OMe), 4.26 (d, J=4.8 Hz, 1H, $OxdH_4$), 4.36 (m, 1H, $OxdH_5$), 4.92 (ddd, J=6.0, 6.4, 7.6 Hz, 1H, TrpHα), 6.71 (d, J=7.6 Hz, 1H, TrpNH), 7.10-7.16 (m, 4H, $TrpH_{4-7}$), 7.18-7.22 (m, 2H, TsArH), 7.79-7.83 (m, 2H, TsArH), 7.95 (s, 1H, $TrpH_1$); ^{13}C NMR ($CDCl_3$) δ: 11.6, 14.1, 21.6, 27.3, 52.3, 58.8, 64.0, 75.0, 105.2, 110.7, 118.5, 119.0, 120.7, 127.1, 128.5, 128.9, 129.4, 129.6, 133.9, 135.6, 137.5, 151.4, 167.3, 172.3; ESI-MS *m/z* 534.1 $[M+H]^+$, calcd 534.1. Elem. Anal. for $C_{25}H_{27}N_3O_7S$, calcd: C, 58.47; H, 5.30; N, 8.18; S, 6.24; found: C, 58.05; H, 5.33; N, 8.25; S, 6.18.

Ts-L-5-Me-Oxd-D-2-Me-Trp-OMe (**5m**). $[\alpha]_D^{20}$ -6.5 (c 0.1, $CHCl_3$); ^{1}H NMR ($CDCl_3$) δ: 1.18 (d, J=6.4 Hz, 3H, OxdMe), 2.41 (s, 3H, TrpMe), 2.41 (s, 3H, TsMe), 3.27 (dd, J=6.0, 14.8 Hz, 1H, TrpHβ), 3.37 (dd, J=6.4, 14.8 Hz, 1H, TrpHβ), 3.74 (s, 3H, OMe), 4.18 (d, J=4.4 Hz, 1H, $OxdH_4$), 4.34 (m, 1H, $OxdH_5$), 4.87 (ddd, J=6.0, 6.4, 7.2 Hz, 1H, TrpHα), 6.67 (d, J=7.2 Hz, 1H, TrpNH), 7.10-7.15 (m, 4H, $TrpH_{4-7}$), 7.19-7.22 (m, 2H, TsArH), 7.80 (m, 2H, TsArH), 7.96 (s, 1H, $TrpH_1$); ^{13}C NMR ($CDCl_3$) δ: 11.7, 14.2, 21.7, 28.8, 53.3, 60.4, 64.4, 110.6, 117.5, 119.7, 121.4, 128.8, 129.7, 135.2, 164.5, 167.1, 171.8; ES-MS *m/z* 514.4 $[M+H]^+$, calcd 514.2. Elem. Anal. for $C_{25}H_{27}N_3O_7S$, calcd: C, 58.47; H, 5.30; N, 8.18; S, 6.24; found: C, 59.00; H, 5.26; N, 8.22; S, 6.19.

Ts-L-5-Me-Oxd-L/D-7-Br-2-Me-Trp-OMe (**4n**, **5n**). ^{1}H NMR ($CDCl_3$) δ (*two diastereoisomers*): 1.11 (d, J=6.4 Hz, 3H, OxdMe), 2.40 (s, 3H, TsMe), 2.47 (s, 3H, TrpMe), 3.13+3.23 (d, J=6.0 Hz, 2H, TrpHβ), 3.67 (s, 3H, OMe), 4.27+4.33 (d, J=4.6 Hz, 1H, $OxdH_4$), 4.34 (m, 1H, $OxdH_5$), 4.71+4.79 (m, 1H, TrpHα), 6.94+7.00 (t, J=7.8 Hz, 1H, $TrpH_5$), 7.08 (d, J=8.0 Hz, 1H, $TrpH_4$), 7.06-7.09 (m, 1H, TrpNH), 7.22-7.31 (m, 3H, TsArH+$TrpH_6$), 7.65-7.69 (m, 2H, TsArH), 8.11+8.20 (s, 1H, $TrpH_1$). ES-MS *m/z* 609.2 [M+18], calcd 609.1.

Ts-L/D-5-Ph-Oxd-L/D-1-Me-Trp-OMe (**4o**, **5o**). ^{1}H NMR ($CDCl_3$) δ (*racemic*, *two diastereoisomers*): 2.42 (s, 6H, TsMe+TrpMe), 3.35-3.46 (m, 2H, TrpHβ), 3.69+3.71 (s, 3H, OMe), 4.53+4.54 (d, J=4.0 Hz, 1H, $OxdH_4$), 4.91-4.98 (m, 1H, TrpHα), 5.42+5.44 (d, J=4.0 Hz, 2H, $OxdH_5$), 6.63+6.79 (d, J=7.0 Hz, 1H, TrpNH), 6.81+6.82 (br.s, 1H, $TrpH_2$), 6.97 (t, J=7.2 Hz, 1H, $TrpH_5$), 7.00-7.05 (m, 2H, TsArH), 7.30-7.61 (m, 8H, Ph+$TrpH_{4,6,7}$), 7.68-7.72 (m, 2H, TsArH); ES-MS *m*/*z* 576.3 $[M+H]^+$, calcd 576.2, found 576.3.

Ts-L/D-5-Ph-Oxd-L/D-2-Ph-Trp-OMe (**4p**, **5p**). ^{1}H NMR ($CDCl_3$) δ (*racemic*, *two diastereoisomers*): 2.43+2.47 (s, 3H, TsMe), 3.88 (s, 3H, OMe), 3.42-3.61 (m, 2H, TrpHβ), 4.83+4.87 (m, 1H, TrpHα), 4.90 (br.d, 1H, $OxdH_4$), 5.34+5.43 (br.d, 1H, $OxdH_5$), 6.91 (d, J=7.6 Hz, 1H, TrpNH), 7.10 (t, J = 7.2 Hz, 1H, $TrpH_6$), 7.13-7.20 (m, 3H, $TrpH_5$+TsArH), 7.22-7.40 (m, 10H, Ph), 7.52+7.54 (br.d, 1H, $TrpH_7$), 7.75+7.80 (d, J=7.8 Hz, 1H, $TrpH_4$), 7.86-7.88 (m, 2H, TsArH), 8.57 (s, 1H, $TrpH_1$); ES-MS *m*/*z* 638.3 $[M+H]^+$, calcd 638.2.

Ts-L/D-5-Ph-Oxd-L/D-5-Cl-2-Me-Trp-OMe (**4q**, **5q**). ^{1}H NMR ($CDCl_3$) δ (*racemic*, *two diastereoisomers*): 2.37+2.39 (s, 3H, TsMe), 2.43 (s, 3H, TrpMe), 3.22-3.37 (m, 2H, TrpHβ), 3.77+3.78 (s, 3H, OMe), 4.51+4.52 (d, J=4.0 Hz, 1H, $OxdH_4$), 4.88+4.95 (m, 1H, TrpHα), 5.44+5.50 (d, J=4.0 Hz, 1H, $OxdH_5$), 6.62+6.86 (d, J=7.4 Hz, 1H, TrpNH), 6.97 (d, J=7.2 Hz, 2H, $TrpH_6$), 7.07-7.50 (m, 8H, Ph+TsArH+$TrpH_7$), 7.69-7.72 (m, 2H, TsArH), 7.95+7.99 (s, 1H, $TrpH_1$); ES-MS *m*/*z* 627.1 [M+Na], found 627.3.

Synthesis of modified EM1. *(S)-2-methyltryptophan (**6b**), (S)-5-fluorotryptophan (**6c**).* 10% HBr (4.0 ml) was added to (*R*,*S*)-**5b** or (*R*,*S*)-**5c** (1.0 mmol), and the mixture was heated while stirring for 45 min by MW irradiation at 150 W, while monitoring the internal reaction temperature at 95°C. The pH of the mixture was adjusted to about 3 with 1 M NaOH, and the aqueous mixture was washed three times with EtOAc (5 mL) to recover (*R*)-Ts-Ser-OH (not isolated). The aqueous layer was concentrated at reduced pressure and passed through Dowex 50X2-200 resin H^+ form. The resin washed with water (100 ml). The amino acids were eluted using 10% ammonia in methanol (200 ml), and the solvent removed in vacuo to afford **6b** (0.73 mmol, 73%) or **6c** (0.74 mmol, 74%).
6b (commercially available). Optical rotation $[\alpha]^D_{20}$ = -9.8 (*c* 0.26 in H_2O) was found to match with the literature;[37a] NMR characterization was found to match with the literature;[37b] ES-MS *m*/*z* 219.2 $[M+H]^+$, calcd 219.1.
6c. Optical rotation $[\alpha]^D_{20}$ = +5.6 (*c* 1.0 in 0.1 M HCl) was found to match with the literature;[15] NMR characterization was found to match with the literature;[15,18c] ES-MS *m*/*z* 223.2 $[M+H]^+$, found 223.2.

*N-Fmoc-(S)-2-methyltryptophan (**7b**), N-Fmoc-(S)-5-fluorotryptophan (**7c**).* $NaHCO_3$ (118 mg, 1.4 mmol) and 9-fluorenylmethyloxycarbonyl succinimide (270 mg, 0.8 mmol) were added to the a suspension of amino acid **6b** or **6c** (0.7 mmol) in 1:1 water/dioxane (6 mL) at 0°C, and the mixture was stirred overnight at r.t. Dioxane was removed at reduced pressure, and the pH of the aqueous mixture was adjusted to 3 with 1 M HCl. The mixture was extracted three times with EtOAc (10 mL), and the collected organic layers were dried over Mg_2SO_4. The solvent was evaporated at reduced pressure, affording the crude Fmoc-protected amino acid. The residues were purified by flash-chromatography over silica-gel (eluant: EtOAc/MeOH 97:3), giving **7b** or **7c** (for both 95% yield, 92% pure by RP-HPLC).

N-Fmoc-(*S*)-2-methytryptophan (**7b**). ^{1}H NMR (DMSO-d_6) δ: 1.90 (s, 3H, TrpMe), 2.73 (dd, J=7.0, 14.5 Hz, 1H, TrpHβ), 2.99 (dd, J=2.5, 14.5 Hz, 1H, TrpHβ), 4.12-4.33 (m, 3H, FmocH), 4.65 (m, 1H, TrpHα), 6.05 (br.d, 1H, TrpNH), 7.00 (br.t, 1H, $TrpH_6$), 7.19-7.30 (m, 4H, FmocArH+$TrpH_{4,5}$), 7.36 (t, J=7.5 Hz, 2H, FmocArH), 7.56 (d, J=7.5 Hz, 2H, FmocArH), 7.76 (d, J=7.5 Hz, 2H, FmocArH), 8.01 (d, J=7.0 Hz, 1H, $TrpH_7$), 8.55 (s, 1H, $TrpH_1$); ES-MS m/z 441.3 $[M+H]^+$, calcd 441.2.

N-Fmoc-(*S*)-5-fluorotryptophan (**7c**). ^{1}H NMR characterization was found to match with the literature;[18c] ES-MS *m*/*z* 444.2 $[M + H]^+$, calcd 444.2.

*[2-Me-Trp^3]-EM1 (**8**), [5-F-Trp^3]-EM1 (**9**).* A measure of Fmoc-Rink amide resin (0.3 g, 1.1 mmol/g, resin particle size: 100-200 mesh) was introduced into a reactor for SPPS. Fmoc was removed with 4:1 DMF/piperidine (4 mL) under MW irradiation (40W) for 1 min under mechanical shaking, monitoring the internal temperature at 45°C. The suspension was filtered, the resin was washed with DCM (5 mL) and treated with a second portion of DMF/piperidine as above described. Then the suspension was filtered, and the resin was washed three times in sequence with DCM (5 mL) and MeOH (5 mL).

All coupling steps were performed according to the following general procedure. The resin was swollen in DCM (5 mL), and a solution of **7b** or **7c** (0.6 mmol) and HOBt (0.1 g, 0.7 mmol) in DMF (4 mL) was added at r.t. and under nitrogen atmosphere, followed by HBTU (0.26 g, 0.7 mmol) and DIPEA (0.2 mL, 1.2 mmol). The mixture was mechanically

shaken under MW irradiation with a initial irradiation power of 40W and monitoring the internal reaction temperature at 45°C, and after 10 min the resin was filtered and washed three times with the sequence DCM (5 mL) and MeOH (5 mL). Coupling efficacy was determined by Kaiser or Chloranyl test. All subsequent Fmoc deprotection steps were performed as above reported. The resin-bound peptide was suspended in a solution of TFA (9.0 mL), TIPS (0.40 mL), H_2O (0.40 mL), and PhOH (0.20 g), and mechanically shaken at r.t. After 2 h, the mixture was filtered, the resin was washed twice with 10% TFA in Et_2O (10 mL) and twice Et_2O (10 mL). Filtrate and washes were collected, and solvent and volatiles were removed under N_2 flow at r.t. The resulting residue was suspended in ice-cold Et_2O, and the crude solid which precipitated was triturated and collected by centrifuge. The peptide **8** or **9** was isolated by semi-preparative RP-HPLC (80% yield based on the average resin loading; >95% pure by analytical RP-HPLC, see General Methods).

[2-Me-Trp^3]-EM1 (**8**). ^{1}H NMR (DMSO-d6) δ (about *3:1 mixture of two conformers, t = major-trans isomer, c = minor-cis isomer*): 1.38-1.62 (m, $4H_c$+$1H_t$), 1.72-1.84 (m, $2H_t$), 1.95 (m, $1H_t$), 2.09 (s, $3H_c$), 2.10 (s, $3H_t$), 2.62 (dd, J=6.5, 14.5 Hz, $1H_t$), 2.65-2.76 (m, $3H_c$), 2.78 (dd, J=7.5, 15.0 Hz, $1H_t$), 2.82 (dd, J=8.0, 14.0 Hz, $1H_t$), 2.86 (m, $1H_c$), 2.90 (m, $1H_t$), 2.93 (m, $1H_c$), 2.95-3.09 (m, $2H_t$+$1H_c$), 3.09 (dd, J=7.0, 15.5 Hz, $1H_t$), 3.21-3.32 (m, $2H_c$), 3.45-3.61 (m, $1H_t$+$2H_c$), 4.35-4.47 (m, $3H_t$+$2H_c$), 4.55 (m, $1H_t$), 6.68 (m, $2H_t$+$2H_c$), 6.90 (dd, J= 4.8, 7.2 Hz, $1H_t$), 6.98-7.05 (m, $2H_t$+$1H_c$), 7.10 (m, $2H_t$+$2H_c$), 7.10-7.25 (m, $7H_t$+$7H_c$), 7.50 (d, J=7.2 Hz, $1H_t$+$1H_c$), 7.81 (d, J=7.8 Hz, $1H_t$), 7.87 (br.d, $2H_t$), 7.94-8.05 (m, $3H_c$), 8.20 (br.d, $1H_c$), 8.21 (d, J=9.0 Hz, $1H_t$), 9.31 (s, $1H_c$), 9.33 (s, $1H_t$), 10.60 (s, $1H_c$). 10.66 (s, $1H_t$); ES-MS m/z: 625.3 $[M+H]^+$; calcd: 625.3.

[5-F-Trp^3]-EM1 (**9**). ^{1}H NMR (DMSO-d6) δ (about *3:1 mixture of two conformers, t = major-trans isomer, c = minor-cis isomer*): 1.42-1.55 (m, $4H_c$), 1.62-1.73 (m, $3H_t$), 1.91 (m, $1H_t$), 2.68-2.83 (m, $3H_t$+$2H_c$), 2.83-2.95 (m, $2H_t$+$2H_c$), 2.95-3.05 (m, $2H_t$+$2H_c$), 3.20 (m, $1H_c$), 3.30 (m, $1H_c$), 3.40-3.67 (m, $1H_t$+$2H_c$), 4.15 (m, $1H_t$), 4.35 (dd, J=4.6, 8.2 Hz, $1H_t$), 4.37-4.40 (m, $1H_t$ + $1H_c$), 4.40-4.48 (m, $1H_t$ + $1H_c$), 6.60 (m, $2H_t$+$2H_c$), 6.87 (m, $2H_c$), 7.07 (m, $2H_t$), 7.10-7.35 (m, $9H_t$+$9H_c$), 7.90 (d, J=8.4 Hz, $1H_t$), 7.95 (d, J=8.0 Hz, $1H_t$), 8.01 (br.s, $2H_t$), 8.11 (d, J=8.4 Hz, $1H_c$), 8.25- 8.32 (m, $3H_c$), 9.30 (br.s, $1H_t$ + $1H_c$), 10.80 (s, $1H_c$), 10.88 (s, $1H_t$); ES-MS m/z: 629.2 $[M+H]^+$; calcd: 629.7.

References

1 a) Stammer C. H. In *Chemistry and Biochemistry of Amino Acids, Peptides, and Proteins*; Weinstein B., Ed.; Dekker: New York, **1982**, 33; b) Schmidt U., Lieberknecht A., Wild J. *Synthesis* **1988**, *3*, 159; c) Humphrey J. M., Chamberlin A. R., *Chem. Rev.*, **1997**, *97*, 2243; d) Bonauer C., Walenzyk T., König B. *Synthesis*, **2006**, *1*, 1.

2 Rajashankar K. R., Ramakumar S., Chauhan V. S. *J. Am. Chem. Soc.*, **1992**, *114*, 9225.

3 Galonić D. P., van der Donk W. A., Gin D .Y. *Chem. Eur. J.*, **2003**, *9*, 5997.

4 Polinsky A., Cooney M. G., Toy-Palmer A., Osapay G., Goodman M., *J. Med. Chem.*, **1992**, *35*, 4185-4194.

5 Ferreira P. M.T., Maia H. L. S., Monteiro L. S., Sacramento J., *High J Chem Soc, Perkin Trans 1*, **1999**, *24*, 3697.

6 Javidan A., Schafer K., Pyne S. G., *Synlett*, **1997**, *1*, 100.

7 Pyne S. G., Javidan A., Skeleton B. W., White A. H., *Tetrahedron*, **1995**, *51*, 5157.

8 Bull S. D., Davies S. G., Garner A. C., O'Shea M. D., *J. Chem. Soc., Perkin Trans.*, **2001**, *1*, 3281-3287.

9 Bandini M., Melloni A., Tommasi S., Umani-Ronchi A., *Synlett.*, **2005**, *8*, 1199.

10 a) Yeh E., Garneau S., Walsh C. T., *Proc. Natl. Acad. Sci. U.S.A.*, **2005**, *102*, 3960; b) Bittner S., Scherzer R., Harlev E., *Amino Acids*, **2007**, *33*, 19.

11 a) Xu Z., Zhang F., Zhang L., Jia Y., *Org. Biomol. Chem*,. **2011**, *9*, 2512; b) Artman G. D., Grubbs A. W., Williams R. M., *J. Am. Chem. Soc.*, **2007**, *129*, 6336; c) He B., Hao S., Yu D., Yong Q. *J. Org. Chem.*, **2009**, *74*, 298-304; d) De Marco R., Bedini A., Spampinato S., Gentilucci L., *J. Med. Chem.*, **2014**, *57*, 6861.

12 Royer C. A., *Chem. Rev.*, **2006**, *106*, 1769.

13 Ishihara K., Fushimi N., Akakura M., *Acc. Chem. Res.*, **2007**, *40*, 1049.

14 a) Perry C. W., Brossi A., Deitcher K. H., Tautz W., Teitel S., *Synthesis*, **1977**, *7*, 492; b) Li X., Yin W., Srirama Sarma P. V. V., Zhou H., Ma J., Cook J. M., *Tetrahedron Lett*., **2004**, *45*, 8569.

15 Ma C., Liu X., Li X., Flippen-Anderson J., Yu S., Cook J., *J. Org. Chem.*, **2001**, *66*, 4525.

16 Irie K., Ishida A., Nakamura T., Oh-Ishi T., *Chem. Pharm. Bull.*, **1984**, *32*, 2126.

17 a) Goss R. J. M., Newil P. L. A., *Chem. Commun.*, **2006**, *47*, 4924; b) Smith D. R., Willemse T., Gkotsi D. S., Schepens W., Maes B. U., Ballet S., Goss R. J., *Org. Lett.*, **2014**, *16*, 2622.

18 a) Porter J., Dykert J., Rivier J., *J. Pept. Prot. Res.*, **1987**, *30*, 13; b) Konda-Yamada Y., Okada C., Yoshida K., Umeda Y., Arima S., Sato N., Kai T., Takayanagi H., Harigaya Y., *Tetrahedron*, **2002**, *58*, 7851; c) Blaser G., Sanderson J. M., Batsanov A. S., Howard J. A. K., *Tetrahedron Lett.*, **2008**, *49*, 2795.

19 Angelini E., Balsamini C., Bartoccini F., Lucarini S., Piersanti G., *J. Org. Chem.*, **2008**, *73*, 5654.

20 Gentilucci L., Cerisoli L., De Marco R., Tolomelli A., *Tetrahedron Lett.*, **2010**, *51*, 2576.

21 a) Drury W. J., Ferraris D., Cox C., Young B., Lectka T., *J. Am. Chem. Soc.*, **1998**, *120*, 11006; b) Castle S. L., Srikanth G. S. C., *Org. Lett.*, **2003**, *5*, 3611; c) Zheng B. H., Ding C. H., Hou, X. L., Dai L. X., Org. Lett., 2010, 12, 1688.

22 Prieto M., Mayor S., Lloyd-Williams P., Giralt E., *J. Org. Chem.*, **2009**, *74*, 9202.

23 Kieffer ME, Repka LM, Reisman SE (2012) J Am Chem Soc 134:5131-5137.

24 a) Zadina J. E., Hackler L., Ge L. J., Kastin A. J., *Nature*, **1997**, *383*, 499; b) Fichna J., Janecka A., Costentin J., Do Rego J. C., *Pharmacol. Rev.*, **2007**, *59*, 88.

25 a) Gentilucci L., Squassabia F., Demarco R., Artali R., Cardillo G., Tolomelli A., Spampinato S., Bedini A., *FEBS Journal*, **2008**, *275*, 2315; b) Gentilucci L., Tolomelli A., De Marco R., Spampinato S., Bedini A., Artali R., *Chem.Med.Chem.*, **2011**, *6*, 1640; c) De Marco R., Tolomelli A.,

Spampinato S., Bedini A., Gentilucci L., *J. Med. Chem.*, **2012**, *55*, 10292; d) De Marco R., Bedini A., Spampinato S., Gentilucci L., *J. Med. Chem.*, **2014**, *57*, 6861.

[26] a) Gentilucci L., *Curr. Topics Med. Chem.*, **2004**, *4*, 19; b) Lipkowski A. W., Misicka A., Carr D. B., Ronsisvalle G., Kosson D., Bonney M. I., *Pure Appl. Chem*., **2004**, *76*, 941.

[27] Keresztes A., Borics A., Tóth G., *Chem.Med.Chem.*, **2010**, *5*, 1176.

[28] Witt K. A., Gillespie T. J., Huber J. D., Egleton R. D., Davis T. P., *Peptides*, **2001**, *22*, 2329.

[29] Zappia G., Cancelliere G., Gacs-Baitz E., Delle Monache G., Misiti D., Nevola L., Botta B., *Curr. Org. Synthesis*, **2007**, *4*, 238.

[30] De Marco R., Tolomelli A., Campitiello M., Rubini P., Gentilucci L., *Org. Biomol. Chem.*, **2012**, *10*, 2307.

[31] a) Ousmer M., Braun N. A., Bavoux C., Perrin M., Ciufolini M. A., *J. Am. Chem. Soc.*, **2001**, *123*, 7534; b) Deng X., Mani N. S., *Green Chem.*, **2006**, *8*, 835.

[32] a) Greco A., Tani S., De Marco R., Gentilucci L., *Chem. Eur. J.*, **2014**, *20*, 13390; b) Greco A., De Marco R., Tani S., Giacomini D., Galletti P., Tolomelli A., Juaristi E., Gentilucci L., *Eur. J. Org. Chem.*, **2014**, *34*, 7614.

[33] Bacsa B., Horváti K., Bõsze S., Andreae F., Kappe C. O., *J. Org. Chem.*, **2008**, *73*, 7532.

[34] a) Duhamel L., Duhamel P., Plaquevent J. C., *Tetrahedron: Asymmetry*, **2004**, *15*, 3653; b) Sibi M. P., Coulomb J., Stanley L. M., *Angew. Chem. Int. Ed.*, **2008**, *47*, 9913.

[35] Jia Y. X., Zhong J., Zhu S. F., Zhang C. M., Zhou Q. L., *Angew. Chem. Int. Ed.*, **2007**, *46*, 5565.

[36] Castellino S., Dwight W. J., *J. Am. Chem. Soc.*, **1993**, *115*, 2986.

[37] a) Yabe Y., Miura C., Horikoshi H., Miyagawa H., Baba Y., *Chem. Pharm. Bull.*, **1979**, *27*, 1907; b) Mocek U., Zeng Z., O'Hagan D., Zhou P., Fan L. D. G., Beale J. M., Floss H. G., *J. Am. Chem. Soc.*, **1993**, *115*, 7992.

[38] Jones G. B., Chapman B. J., *Synthesis*, **1995**, *5*, 475.

[39] a) Alemán C., Casanovas J. C. A., *Biopolymers*, **1995**, *36*, 71; b) Rzeszotarska B., Siodlak D., Broda M. A., Dybala I., Koziol A. E., *J. Pept. Res.*, **2002**, *59*, 79; c) Padmanabhan B., Dey S., Khandelwal B., Rao G. S., Singh T. P., *Biopolymers*, **1992**, *32*, 1271.

[40] a) Tabatabaeian K., Mamaghani M., Mahmoodi N. O., Khorshidi A., *J. Mol. Cat. A*, **2007**, *270*, 112; b) Blay G., Cano J., Cardona L., Fernández I., Muñoz M. C., Pedro J. R., Vila C., *J. Org. Chem.*, **2012**, *77*, 10545.

[41] Mahrwald R., (2004) Modern aldol reactions Vol. 1: enolates, organocatalysis, biocatalysis and natural product synthesis. Wiley, Weinheim, pp 1-328.

[42] a) Ojima I., Kwon H. B., *J. Am. Chem. Soc.*, **1988**, *110*, 5617; b) Krenske E. H., Houk K. N., *Acc. Chem. Res.*, **2013**, *46*, 979.

Chapter 4

In-peptide synthesis of constraining motives containing di-Oxd and ΔAbu-Oxd as β-turn inducers

Small and easy-to-do mimetics of the β-turns are of great interest to interfere with protein-protein recognition events mediated by β-turn recognition motifs. Herein is proposed a straightforward procedure for constraining the conformation of tetrapeptides lacking a pre-formed scaffold. According to the stereochemistry array, *N*-Ts tetrapeptides including Thr or PhSer (phenylserine) at the positions 2 or 3 gave rise in a single step to the sequences Oxd^2-Oxd^3 or ΔAbu^2-Oxd^3 (Oxd, oxazolidin-2-one; ΔAbu, 2,3-dehydro-2-aminobutyric). These pseudo-Pro residues displayed highly constrained ϕ, ψ, and χ dihedral angles, and induced clear β-turns or inverse turns of type I or II, as determined by extensive spectroscopic and computational analyses.

4.1. Introduction

Interactions between proteins (PPI) are important for the majority of biological functions and cellular signaling.[1] Systematic studies have revealed that there is typically a small cluster of residues at the interface of the proteins that contributes the majority of the recognition or binding affinity. Very often, these key regions adopt well defined turn structures.[2] As a consequence, small molecules mimicking the 3D features of the turn regions can find applications as therapeutic agents.

The β-turn occurs where the polypeptide backbone reverses direction, and consists of four amino acid residues *i* to *i+3* in which the distance between Cαi and C$\alpha i+3$ is about 7Å; according to the dihedral angles ϕ and ψ of the residues *i+1* and *i+2*, the turns are classified in different types. Small mimetics of β-turns, such as the privileged structures benzodiazepines, Freidinger lactams, internal or external bicyclic dipeptide mimetics, spirocyclic dipeptides, etc., have been extensively investigated and utilized to discover compounds that can mimic or disrupt β-turn-mediated recognition events.[3]

However, the preparation of the scaffolds and their incorporation in the sequence may require multi-step procedures, resulting in low overall yields. Besides, most synthetic methods lack flexibility and are therefore not suited to introduce diversity.[3] As a consequence, the development of a high yielding, single step procedure for the introduction of a conformational constraint that forces the peptide to adopt a β-turn is currently of considerable interest.

In this thesis chapter is reported a straightforward procedure for constraining the conformation of tetrapeptides lacking a pre-formed scaffold. The resulting β-turn mimetics include 2-oxo-1,3-oxazolidine-4-carboxylate rings (or oxazolidin-2-one, in short: Oxd), that can be proposed as constrained pseudo-Pro residues.[4] Pro strongly impacts the structural and conformational properties of peptide and protein backbones and their molecular recognition.[5] It does not have a hydrogen on the amide group and therefore cannot act as a H-bond donor. The cyclic structure forces the ϕ angle to about -65°, therefore Pro is known as a classical breaker of both the α-helical and β-sheet structures in proteins and peptides, while it promotes the formation of β-turns.[2,6] Besides, due to the small free enthalpy difference between the cis and trans Xaa-Pro bond isomers of 2.0 $kJ \cdot mol^{-1}$ (compared to 10.0 $kJ \cdot mol^{-1}$ for other peptide bonds), there is a relatively high intrinsic probability of 30% cis conformation at r.t.[7] Interestingly, the cis-trans interconversion of X-Pro is one of the rate-determining steps in protein folding.[8]

In order to understand the relationship between peptide bond geometry and bioactivity, many synthetic Pro analogues have been developed that provide restrictions of the Xaa-Pro conformation. In general, the modifications consist in ring substitutions with alkyl and aromatic groups, incorporation of heteroatoms, or the expansion or contraction of the five-membered ring.[9]

To take advantage of the conformational bias exerted by the Oxd pseudo-Pro, we planned to synthesize diastereomeric *N*-sulfonyl tetrapeptides containing two consecutive Oxd rings, as β-turn inducers. According to the stereochemistry array of the amino acids, the reaction of two β-hydroxy α-amino acids (Thr or *threo*-phenylserine, PhSer) already present within the sequences at the positions 2 and 3, with bis(succinimidyl)carbonate (DSC), afforded two consecutive Oxd or a 2,3-dehydro-2-aminobutyric acid (ΔAbu) in 2 and a Oxd in 3. These combinations resulted in highly constrained extended or folded structures, in particular turns or inverse turns of type I and II, and are especially interesting because they can control not only the ϕ and ψ dihedral angles of the backbone but also the χ angles of the side chains.

Peptides containing Oxd rings constitute a infrequent but remarkable class of peptidomimetics. They have found some applications in medicinal chemistry,[10] in the construction of foldamers[11] or as self-assembling scaffolds forming nanostructures.[12] Also the compounds with the ΔAbu-Oxd sequence are of some interest, since they contain two distinct secondary structure-forming elements. The dehydroamino acids are well known β-turn inducers; for instance, sequential placement of dehydroPhe (ΔPhe) in oligomers gave repeated β-turns forming 3_{10} helices.[13]

4.2. Results and Discussion

4.2.1. Synthesis of tetrapeptides containing di-Oxd and ΔAbu-Oxd.

Few years ago our research group has published the synthesis of Oxd rings directly within peptide sequences, by treatment of *N*-arylsulfonyl peptides containing L- or D-configured Ser with DSC and a catalytic amount of a base, in solution or in the solid phase (Scheme 1, path a).[4]

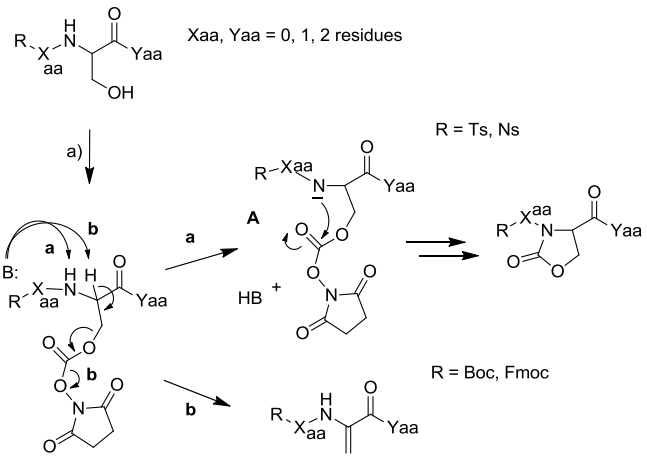

Scheme 1. Different reactivity of the N-carbamate and N-sulfonyl oligopeptides. a) DSC, cat. base (B:).

Apparently, the reaction was due to the presence of the *N*-sulfonyl group; indeed, the reaction of the corresponding Fmoc- or Boc-peptides under the same conditions with carbonates or dicarbonates gave elimination to dehydroalanine (ΔAla), as reported in the literature (Scheme 1, path b).[13] Interestingly, peptides having the sulfonyl group directly connected to the Ser or separated by one or two amino acids, gave similar results (Scheme 1, Xaa = 0, 1, or 2 residues).[4] This observation prompted us to perform in a single step the contemporary cyclization of sulfonyl-oligopeptides containing two consecutive ring-forming residues, to afford highly rigid structures.

Accordingly, we prepared a series of distereomeric tetrapeptides containing two Thr residues, or Thr and *threo*-PhSer, at the positions 2 and 3, and we reacted the tetrapeptides (Scheme 2) with a moderate excess of DSC and a catalytic amount of diisopropylethylamine (DIPEA). The preparation of the *N*-tosyl tetrapeptides **1a-g** was conducted by coupling the amino acids under MW irradiation, using a microwave oven specifically designed for organic synthesis,[14] with HBTU/HOBt as activating agents (Experimental Section, Table 4). *N*-tosyl (Ts)-Ala was prepared as described in the literature;[15] L- or D-*threo*-PhSer were obtained via optical resolution of the racemate,[16] since the resolution by enzymatic hydrolysis[17] gave poor results.

The reaction of Ts-Ala-Thr-Thr-PheOMe (**1a**) with 2.2 equiv. of DSC in 3:1 DCM/DMF and in the presence of 0.1 equiv of DIPEA (Scheme 2, entry 1) provided the corresponding di-Oxd-containing Ts-Ala-Oxd-Oxd-PheOMe (**2a**) in excellent yield after isolation by flash chromatography (Table 1).

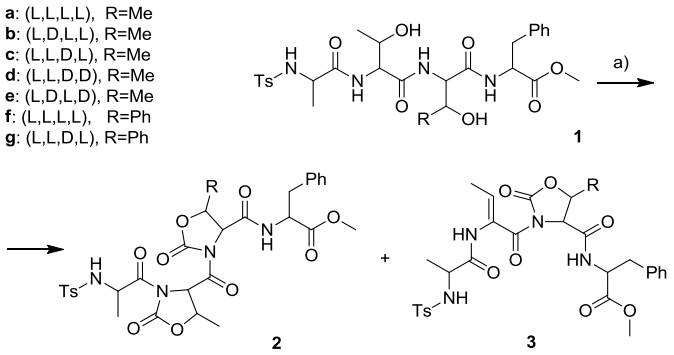

Scheme 2. Reactions of the sulfonyl-peptides **1a-e**, containing L- or D-Thr at the positions 2 and 3, and of **1f**,**g** containing L-Thr in 2 and *threo* L- or D-PhSer in 3, respectively. a) DSC, cat. DIPEA.

On the other hand, the reaction of Ts-Ala-D-Thr-Thr-PheOMe (**1b**), under the same reaction conditions, gave exclusively a tetrapeptide containing ΔAbu at position 2, Ts-Ala-ΔAbu-Oxd-PheOMe (**3b**), while the tetrapeptide containing two Oxd (**2b**) was observed only in traces. (Scheme 2, and Table 1, entry 2).
The reaction of Ts-Ala-Thr-D-Thr-PheOMe (**1c**) under the same conditions gave a 74:26 mixture of Ts-Ala-Oxd-D-Oxd-PheOMe (**2c**) and Ts-Ala-ΔAbu-D-Oxd-PheOMe (**3c**) (entry 3). The reaction outcome changed upon varying the solvent utilized; in pure DCM the yield of **2c** increased up to 85% (entry 4), while in DMF the reaction afforded mainly **3c**, with a 78% yield (entry 5).
The tetrapeptide Ts-Ala-Thr-D-Thr-D-PheOMe (**1d**) exclusively gave Ts-Ala-Oxd-D-Oxd-D-PheOMe (**2d**) (entry 6), while Ts-Ala-D-Thr-Thr-D-PheOMe (**1e**) failed in giving either **2** or **3** in significant amounts (entry 7) under diverse reaction conditions (not shown).

Table 1. Synthesis of the constrained peptidomimetics **2** or **3** from the stereoisomers **1**.

entry	**1**	Ala[1]	Thr[2]	Xaa[3],	R	Phe[4]	Solvent[a]	**2** (%)[b]	**3** (%)[b]
1	**a**	L	L	L	Me	L	DCM/DMF	87	tr.
2	**b**	L	D	L	Me	L	DCM/DMF	-	90
3	**c**	L	L	D	Me	L	DCM/DMF	67	23
4	**c**	"	"	"	Me	"	DCM	85	9
5	**c**	"	"	"	Me	"	DMF	5	78
6	**d**	L	L	D	Me	D	DCM/DMF	90	-
7	**e**	L	D	L	Me	D	DCM and/or DMF	tr.[c]	tr.[c]
8	**f**	L	L	L	Ph	L	DCM/DMF	92	-
9	**g**	L	L	D	Ph	L	DCM/DMF	93	tr.

[a] All compounds **1a-g** were tested in different solvent mixtures (3:1 DCM/DMF, DCM, DMF); with the exception of entries 3-5, the reaction outcomes were practically unaffected, therefore these results are not shown. [b] Determined after purification by flash chromatography over silica-gel; tr. = traces. [c] The rest being the reagent.

Finally, the reaction was repeated with the sequences Ts-Ala-Thr-PhSer-PheOMe (**1f**) or Ts-Ala-Thr-D-PhSer-PheOMe (**1g**), which gave the di-Oxd compounds **2f** and **2g** in very satisfactory yields (entries 8 and 9). These peptides include a 2-oxo-5-phenyloxazolidine-4-carboxylate residue at position 3, which might effectively represent a constrained Phe mimetic, with fixed ϕ, ψ and χ dihedral angles (Table 2).

Table 2. Angles ϕ and ψ of the residues *i+1*, *i+2* observed for the compounds analyzed and ideal values.

compd	ϕ_{i+1}	ψ_{i+1}	χ_{i+1}	ϕ_{i+2}	ψ_{i+2}	χ_{i+2}
2a (A)	-73	158	-114	-81	76	-115
2a (B)	-104	-179	-90	-40	-50	-140
2c (C)	-45	129	-122	69	-86	118
2c (D)	-51	144	-117	77	-27	110
2d	-55	139	-117	77	-29	113
3b	-38	-59	-2	-96	29	-114
3c (E)	61	55	2	93	-2	117
3c (F)	37	63	0	81	-36	113
I	-60	-30	-	-90	0	-
II	-60	120	-	80	0	-

This result suggests the opportunity to develop analogues of proteinogenic or unusual amino acids, carrying the side chain at the position 5 of the Oxd ring. Indeed, the literature reports many procedures for the stereocontrolled preparation of a variety of β-hydroxy α-amino acids.[18] Nevertheless, the synthesis of Oxds functionalized with different side chains is beyond the scope of this work, which is primarily addressed to the synthesis of model tetrapeptides and investigation of the secondary structures.

Epimerization during the reactions was excluded on the basis of the comparison of the NMR and HPLC analyses of the compounds, including the HPLC analysis on a chiral stationary phase (see General methods).

From the comparison of the results (entries 1-9) it appeared that the stereochemistry array exerted a major bias in determining the cyclization versus the elimination in 2. Homochiral sequences at the positions 1 and 2 tended to give exclusively or predominantly the di-Oxd compounds, as observed for **1a**, **1c**, and **1d**. On the contrary, the peptide **1e** containing the sequence L-Ala-D-Thr failed in giving **2** or **3** in significant amounts, and **1b** solely afforded the ΔAbu-Oxd sequence. The diastereomeric peptides **1f**, **1g** containing PhSer behaved in a similar way as the corresponding peptides **1a** and **1c** (the formation of **3g** was observed only in traces in different solvents).

The proposed reaction mechanism of Scheme 1 path **a**, postulates that for n = 1 or 2, as occurring for the compounds **1a-g**, the electron-poor aromatic ring of the arylsulfonylamido group might effectively stabilize the anionic intermediate **A** by π-stacking interaction, thus driving to the Oxd ring. Possibly, the diastereoisomer **1b** adopted in solution a conformation which allowed promoting the cyclization at position 3, but not in 2, therefore giving elimination, as expected on the basis of the literature. For **1c**, the different results observed for the entries 3 to 5 could be attributed to a preference for different conformations in the different solvents. As for **1e**, showing alternated absolute stereochemistry, it appeared that the compound was unable to attain the cyclization either in 2 or 3; the compound did not eliminate in a significant extent as well, as observed by treatment with different bases in different solvents at r.t. or under heating.

The tosyl group was removed in good yield with iodotrimethylsilane,[19] while the treatment with SmI_2-pyrrolidine-water[20] was less efficient.

4.2.2. Conformational analyses of the di-Oxd and ΔAbu-Oxd peptides.

To investigate the conformational bias exerted by the two consecutive L- or D-configured Oxd, or ΔAbu and L- or D-Oxd residues at positions 2 and 3, on the overall structure of the peptides, we analyzed the model compounds **2a**, **2c**, **2d**, and **3b**, **3c**, by FT-IR and NMR spectroscopy.

FT-IR spectroscopy was utilized to analyze the amide N-H stretching regions; generally, non H-bonded amide protons show a peak above 3400 cm^{-1}, while H-bonded amide NH bonds exhibit a peak below 3400 cm^{-1}.[21]

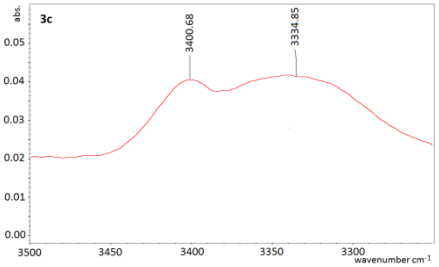

Figure 1. Amide NH stretching regions of the IR absorption spectra for samples of tetrapeptide **3c** (3 mM in DCM, r.t.).

The FT-IR absorption spectra of **2d** only showed a strong band above 3400 cm^{-1} (Experimental section Figure 6). The spectra of **2a**, **2c**, **3b**, and **3c** (Experimental section Figure 6) showed a mayor peak at about 3400 cm^{-1}, and a second peak at about 3340 cm^{-1}. The latter became predominant in **3c**, suggestive of a significant population of H-bonded conformations in equilibrium with non bonded structures. The spectra of **3c** dissolved in DCM is reported in Figure 1.

The ^{1}H-NMR experiments were done at 400 MHz in $CDCl_3$ or in 8:2 DMSO-d_6/H_2O. 2D gCOSY experiments were utilized for the unambiguous assignment of the resonances. In each solvent, all spectra showed a single set of sharp resonances, consistent with conformational homogeneity or a fast equilibrium between slightly different conformers. For most compounds, the ^{1}H-NMR resonances showed modest variations of the chemical shifts in the two solvents (Table 5) suggesting that the peptidomimetic sequences were conformationally stable; exceptions are highlighted in Table 5.

It has been shown that the Oxd confers the preceding amide bond a exclusive trans conformation.[11] The ^{1}H-NMR analyses of all of the compounds showed a significantly downfield position of the Hα proton of the residues preceding the Oxd rings (Experimental section Table 5). For instance, the resonances of AlaHα in Ts-Ala-Thr-Thr-PheOMe (**1a**) and Ts-Ala-ΔAbu-L-(5'-Me-Oxd)-PheOMe (**3b**) appeared at about 3.9 and 3.8 p.p.m. ($CDCl_3$), respectively, while in Ts-

Ala-(5'-Me-Oxd[2])-(5'-Me-Oxd[3])-PheOMe (**2a**) AlaHα was at about 5.2 p.p.m. On the other hand, in the same compound **2a**, Oxd[3]H4 was at 4.2 p.p.m, while Oxd[2]H4 was at about 5.3 p.p.m., for the deshielding effect of Oxd[3]C=O. These observations were compatible with a non-conventional, CH···O=C intramolecular H-bond,[22] confirming the trans conformation of the amide bond between the Oxd and the preceding, deshielded residue.

The occurrence of intramolecular H-bonds in **2a**, **2c**, **2d**, **3b**, and **3c**, was evaluated by analyzing the variation of the NH proton chemical shifts upon addition of increasing percentages of DMSO-d_6 to 2 mM solutions of the compounds in $CDCl_3$. As representative example, the titration curves of **3c** are shown in Figure 2. The titration of **2a** gave no evidence of H-bonds involving PheNH nor AlaNH, since these signals exhibited a considerable downfield shift;[23] **2c**, **2d** gave similar results (Figure 8). On the contrary, the titration of **3c** (Figure 2) and **3b** (Figure 8) revealed that PheNH, but not AlaNH nor ΔAbuNH, was much less sensitive, therefore less accessible, accounting for a H-bonded structure.

Variable temperature (VT)-^{1}H-NMR experiments in $CDCl_3$ and 8:2 DMSO-d_6/H_2O were also utilized to deduce the presence of intramolecular H-bonds (Table 3). For almost all compounds, the comparatively lower VT-^{1}H-NMR Δδ/Δt parameters of PheNH with respect to AlaNH (and ΔAbuNH) were suggestive of a moderate preference for conformations having PheNH involved in a H-bond (|Δδ/Δt| < or close to 2.5 p.p.b./K).[21,24] The only exception was observed for **2d** in $CDCl_3$, since the Δδ/Δt (p.p.b./K) of AlaNH was lower than that of PheNH (-1.7 and -2.7, respectively).

From the comparison of the results above discussed for the Oxd-Oxd compounds (**2**), it appeared that the possible existence or not of H-bonds was differently supported by the methods employed. Reasonably, the inconsistencies reflected the existence of equilibria between H-bonded and non H-bonded structures. As for the ΔAbu-Oxd compounds (**3**), all of the evidences were highly coherent in support of a H-bonded PheNH.

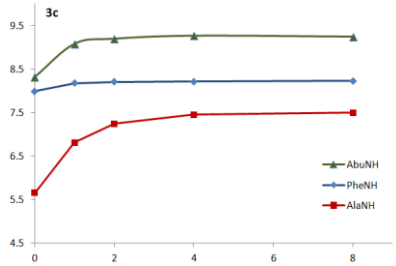

Figure 2. Variation of NH proton chemical shift (p.p.m.) of **3c** as a function of increasing percentages of DMSO-d_6 to the CDCl3 solution (v/v).

Table 3. Δδ/Δt values (p.p.b./K) for the amide protons of **2a**, **2c**, **2d**, and **3b**, **3c**, in $CDCl_3$ and 8:2 DMSO-d_6/H_2O; solvents: S1 = $CDCl_3$; S2 = 8:2 DMSO-d_6/H_2O; amino acid stereochemistry has been omitted.

compd	solvent	Ala[1]NH	ΔAbu[2]NH	Phe[4]NH
2a	S1	-2.7	-	-2.4
	S2	-6.1	-	-3.9
3b	S1	-13.5	-8.0	-3.8
	S2	-5.0	-7.2	-4.1
2c	S1	-2.3	-	-1.2
	S2	-6.3	-	-3.8
3c	S1	-9.0	-4.4	-4.0
	S2	-6.5	-7.0	-4.1
2d	S1	-1.7	-	-2.7
	S2	-6.0	-	-4.2

To determine the preferred conformations in solution and their dynamic behaviours, the compounds were analyzed by 2D-ROESY in 8:2 DMSO-d_6/H_2O and molecular dynamics (MD) simulations. DMSO-d_6 or DMSO-d_6/H_2O mixtures have been recommended by several authors as biomimetic media.[25] Structures consistent with the spectroscopic analyses were obtained by MD using the distances derived from ROESY as constraints. The intensities of the ROESY cross-peaks were ranked to infer the distances (Tables 6-10). The ω bonds were set at 180°, since the absence of Hαi-H$\alpha(i+1)$ cross-peaks excluded cis peptide bonds. Simulations were conducted in a box of explicit water molecules. Random structures were generated by unrestrained high-temperature MD; the structures were subjected to high-temperature restrained MD with a scaled force field, followed by a simulation with full restraints. Finally, the system was gradually cooled, and the structures were minimized with the AMBER force field.[26] The results were clustered by the RMSD analysis of the backbone atoms.

For Ts-Ala-(5'-Me-Oxd)-(5'-Me-Oxd)-PheOMe (**2a**), the analysis gave two clusters comprising all-together more than 90% of the structures. For each cluster, the representative geometries A and B with the lowest internal energy were selected and analyzed (Figure 3). The occurrence of these two different structures, which differ almost exclusively by the opposite orientation of the Phe residue, reflected the observation of contradictory cross-peaks: the cross-peaks PheNH-Oxd^3H_4 and PheNH-Oxd^3H_5 accounted for the conformation A, while the cross peak PheNH-Oxd^2H_5 was coherent with B. Possibly, the two structures represented conformers in fast equilibrium.

To investigate the dynamic behaviour of **2a** (A) and (B), unrestrained MD were performed for 10 ns in a box of standard TIP3P water molecules. The simulations showed the conversion of one conformation into the other. The analyses of the trajectories of the conformer (A) revealed very few structures compatible with a γ-turn centered on Oxd^3 with a explicit H-bond between PheNH and Oxd^2C=O, while (B) gave no evidence of secondary structures.

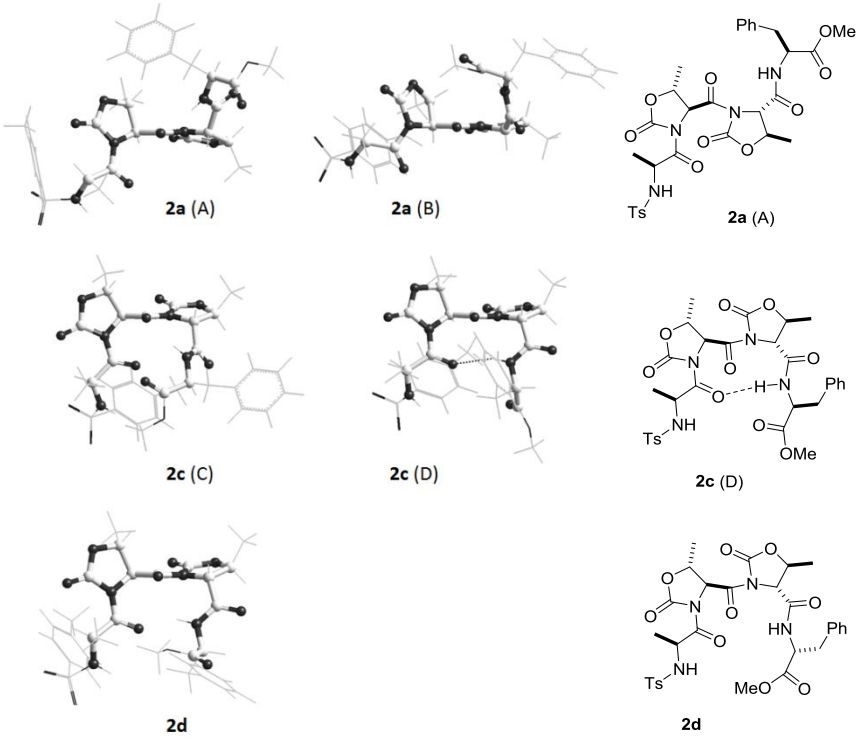

Figure 3. Left. Representative low-energy structures of **2a** (A and B), **2c** (C), and **2d** consistent with ROESY analysis, calculated by restrained MD; low energy structure of **2c** (D) calculated by unrestrained MD. All structures determined in a 30×30×30 box of standard TIP3P water molecules. Backbones and Oxd are rendered in balls-and cylinders, the rest in sticks. The peptide bond connecting Oxd^2-Oxd^3 are shown horizontally and perpendicularly with respect to the viewer. Right. Schetches of the extended structure of **2a** (A), and of the folded **2c** (D) and **2d**.

For Ts-Ala-(5'-Me-Oxd)-D-(5'-Me-Oxd)-PheOMe (**2c**) and Ts-Ala-(5'-Me-Oxd)-(5'-Me-Oxd)-D-PheOMe (**2d**), the analyses gave one mayor clusters each comprising about 80% of the structures. For each compound's cluster, the representative geometries with the lowest internal energy are shown in Figure 3. These structures **2c** (C) and **2d** are compatible with a well-defined type II β-turn secondary structure (Table 10). The structures **2c** (C) and **2d** were analyzed by unrestrained MD; besides to the different random conformations, the analysis of the trajectories of **2c** (C), but not of **2d**, revealed a explicit H-bond between PheNH and the AlaC=O, as shown in **2c** (D), Figure 3.

The conformational analyses of the peptides **3b**, **3c** containing in their sequences ΔAbu^2 and L- or D-Oxd^3, respectively, gave one cluster each, comprising the large majority of the structures; the representative geometries are shown in Figure 4. The calculated geometry of ΔAbu closely matched that of dehydroamino acids reported in the literature.[13,27]

The structure **3b**, stabilized by a explicit H-bond between AlaC=O and PheNH, was compatible with a type I β-turn. The structure of **3c** (E) nicely reproduced a inverse type I β-turn (Table 10), and showed a H-bond between AlaC=O and PheNH. The unrestrained MD simulations revealed also a tendency for structures characterized by a H-bond between PheC=O and AlaNH, such as the representative **3c** (F), Figure 4.

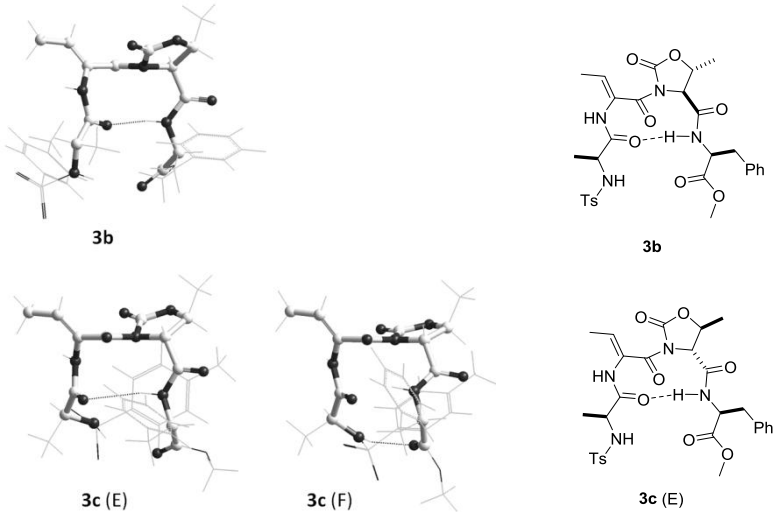

Figure 4. Left. Representative low-energy structures of **3b** and **3c** (E) consistent with ROESY analysis, calculated by restrained MD; low energy structure of **3c** (F) calculated by unrestrained MD. All structures determined in a 30×30×30 box of standard TIP3P water molecules. Backbones and Oxd are rendered in balls-and cylinders, the rest in sticks. The peptide bond connecting ΔAbu[2]-Oxd[3] are shown horizontally and perpendicularly with respect to the viewer. Right. Schetches of the folded structures **3b** and **3c** (E).

To further confirm the presence of folded structures, we used Electronic Circular Dichroism (ECD) spectroscopy. Spectra of model peptides **2a**, **2d**, and **3b**, were recorded both in dichloromethane and in methanol.
The spectra in dichloromethane (Figure 5) showed a negative band centered at about 230 nm, less intense for **2a**. These spectral features could be indicative of a significant population of bent conformers, in particular in the case of **2d** and **3b**. In fact, a negative nπ* ECD band near 225 nm is generally observed in the presence of β-turn structures (I or II type).[21,28]
The observed different intensities of ECD signals were in agreement with ROESY and MD data which evidenced homogeneous conformations for **2d** and **3b**.
By moving from dichloromethane to methanol, intensities of the negative ECD bands slightly reduced for all compounds (Experimental section, Figure 7). This spectral behavior could be ascribed to a dependence of the conformer population on the polarity and/or the competitive nature of the solvent.

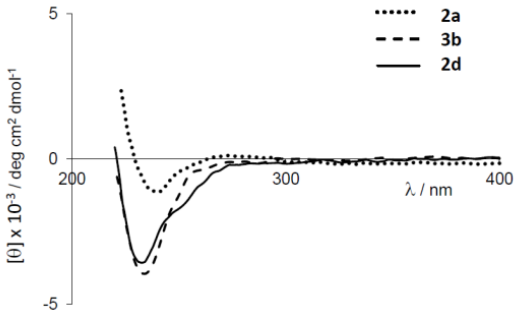

Figure 5. ECD spectra recorded in dichloromethane at room temperature (**2a** dotted line, **3b** dashed line, **2d** full line).

Taken together, all of the experimental evidences support that the peptides **3** containing the ΔAbu at the position 2 formed highly stable type I β-turns reinforced by H-bonds, normal or inverse depending on the stereochemistry of the Oxd[3]. This result is particularly gratifying, since the formation of the ΔAbu-Oxd motif was somewhat unpredictable.
On the other hand, the data of the peptides **2** collected by ROESY/MD analyses confirmed a certain flexibility of the Phe[4] residue. This observation could explain the discrepancies in the determination of H-bonds by IR, VT-NMR, and NMR titration experiments. Nevertheless, the results highlighted the rigidity of the Ala-Oxd-Oxd portions; the rotation of the Ala and the two Oxd rings one respect to the other was not observed during the unrestrained MD simulations. The conformational homogeneity was correlated to the strong preference for all-trans conformations stabilized by the weak interactions between the Oxd carbonyls and the Hα protons of the preceding residues.
In particular, the heterochiral Oxd[2]-D-Oxd[3] scaffold induced a stable and well defined type II β-turn, albeit the H-bond between the residues *i-i+3* was relatively loose. This ability to promote folded structures makes sense, and is consistent

with the observations on previously described Oxd-peptides.[11,12] The Oxd ring can be regarded to as a pseudo-Pro; it is well known that heterochiral linear oligopeptides including a Pro show higher propensity to fold compared to the homochiral sequences.[21,24]

4.3. Conclusions

In this chapter is reported a straightforward, one-step procedure for constraining a peptide backbone without the need for a pre-formed scaffold. The cyclization of two consecutive β-hydroxy amino acid residues (L/D-Thr or *threo*-L/D-PhSer) embedded in *N*-arylsulfonyl tetrapeptide sequences, afforded in excellent yields the peptides containing Oxd^2-L/D-Oxd^3 (**2**) or ΔAbu^2-L/D-Oxd^3 (**3**), according to the stereochemistry array of the precursors.

Conformational analyses of the model peptides revealed that the homochiral Oxd^2-Oxd^3 dipeptidomimetic induced a extended disposition of the backbone. The heterochiral sequences exerted a strong conformational control, giving rise to type II β-turns. The unrestrained MD simulations confirmed the rigidity of the conformations, since the rotation of the two Oxd rings one with respect to the other was not observed during the simulations. On the other hand, the sequence ΔAbu^2-Oxd^3 induced highly stable β-turns of type I, stabilized by clear H-bonds.

For their ability to control the ϕ and ψ dihedral angles of the backbone as well as the χ dihedral angles of side chains, peptide mimetics based on the structures of the model peptides **2** and **3** might find applications in medicinal chemistry as 3D rigid scaffolds, in the field of the foldamers, or as self-assembling scaffolds to form nanostructures.

4.4. Experimental section

4.4.1. General Methods

Unless stated otherwise, standard chemicals were obtained from commercial sources and used without further purification. Flash chromatography was performed on silica gel (230-400 mesh), using mixtures of distilled solvents. Analytical RP-HPLC was performed on an ODS column (4.6 μm particle size, 100 Å pore diameter, 250 μm, DAD 210 nm, from a 9:1 H_2O-CH_3CN to a 2:8 H_2O-CH_3CN in 20 min) at a flow rate of 1.0 mL min-1, followed by 10 min at the same composition. Semi-preparative RP-HPLC was performed on a C18 column (7 μm particle size, 21.2 mm × 150 mm, from 8:2 H_2O-CH_3CN to 100% CH_3CN in 10 min) at a flow rate of 12 mL min^{-1}. Purities were assessed by analytical RP-HPLC under the above reported conditions and elemental analysis. Chiral HPLC analysis was performed on a CHIRALPAK IC column (0.46 cm × 25 cm), 1:1 n-hexane/2-propanol, at 0.8 mL min-1. Semi-preparative and analytical RP-HPLC of the peptide 14 was performed as reported above, with the addition of 0.1% TFA in the mobile phase. Elemental analyses were performer using a Thermo Flash 2000 CHNS/O analyzer. High-quality IR were obtained at 2 cm^{-1} resolution using a FT-IR spectrometer and 1 mm NaCl solution cell. ^{1}H-NMR spectra were recorded on a Varian instrument at 400MHz, ^{13}C-NMR spectra at 100 MHz. Circular Dichroism (CD) spectra were recorded on a Jasco J-710 spectropolarimeter. The synthetic procedure by MW irradiation was performed using a microwave oven (MicroSYNTH Microwave Labstation for Synthesis).

4.4.2. Synthetic procedures

*Synthesis of the peptides **1a-g***.A stirred solution of the N-protected amino acid in 4:1 DCM-DMF (5 mL) was treated with HOBt (1.2 equiv.) and HBTU (1.2 equiv.), at r.t. and under inert atmosphere. After 5 min, the C-protected amino acid (1.1 equiv.) and DIPEA (2.4 equiv.) were added, and the mixture was stirred under inert atmosphere and under MW irradiation (150W). After 10 min, the mixture was concentrated at reduced pressure, and the residue was diluted with EtOAc (25 mL). The solution was washed with 0.1 M HCl (5 mL), and a saturated solution of $NaHCO_3$ (5 mL). The organic layer was dried over Na_2SO_4 and the solvent was evaporated at reduced pressure. The crude peptides were analyzed by HPLC-MS analysis, and were used without further purifications.

Table 4. RP-HPLC and ES-MS analyses of the linear peptides **1a-f.**

1	ES-MS m/z [M+1] vs calcd	Purity[a] (%)	**1**	ES-MS [M+1] vs calcd	Purity[a] (%)
a	607.3/607.2	85	**e**	607.2/607.2	84
b	607.2/607.2	83	**f**	669.3/669.3	84
c	607.3/607.2	81	**g**	669.4/669.3	83
d	607.1/607.2	80			

[a] Determined by analytical RP-HPLC, see General methods.

The intermediate N-Boc peptides were deprotected by treatment with 1:2 TFA-DCM (5 mL), while stirring at r.t. After 15 min, the solution was evaporated under reduced pressure, and the treatment was repeated. The residue was suspended in Et_2O (20 mL). The peptide-TFA salts were collected by centrifuge, and used for the next couplings without further purifications (80-85% pure, Table 4).

*Synthesis of Ts-Ala-Oxd-(5'-R-Oxd)-PheOMe (**2a,c,d,f,g**), Ts-Ala-ΔAbu-(5'-Me-Oxd)-PheOMe (**3b,c**).* DSC (0.73 mmol) was added to a stirred solution of **1** (0.33 mmol) in the solvent mixture of Table 1 (4 mL) followed by DIPEA (0.07 mmol) at r.t. and under inert atmosphere. After 3 h, the solvent was removed under reduced pressure, the residue was diluted with 0.1 M HCl (5 mL), and the mixture was extracted three times with DCM (5 mL). The combined organic layers were dried over sodium sulfate, filtered, and concentrated at reduced pressure. The residue was purified by semi-preparative RP-HPLC (see General methods), giving **2** (85-93%, see Table 1, 94-97% pure by analytical RP-HPLC) or **3** (78-90%, see Table 1, 95-98% pure by analytical RP-HPLC), as waxy solids.

Ts-Ala-(5'-Me-Oxd^2)-(5'-Me-Oxd^3)-PheOMe (**2a**). IR (CH_2Cl_2) ν: 3406, 3335, 1789, 1736, 1703, 1670 cm^{-1}; ^{1}H-NMR ($CDCl_3$) δ: 1.43 (d, J=6.8 Hz, 3H, AlaMe), 1.52 (d, J=6.3 Hz, 6H, Oxd^2Me+Oxd^3Me), 2.43 (s, 3H, TsMe), 3.11 (dd, J=5.5, 14.1 Hz, 1H, PheHβ), 3.15 (dd, J=5.4, 14.1 Hz, 1H, PheHβ), 3.77 (s, 3H, OMe), 4.26 (d, J=3.7 Hz, 1H, Oxd^3H_4), 4.58 (dq, J=2.1, 6.3 Hz, 1H, Oxd^2H_5), 4.75 (dq, J=3.7, 6.3 Hz, 1H, Oxd^3H_5), 4.85 (q, J=7.6 Hz, 1H, PheHα), 5.22 (dq, J=6.8, 10.4 Hz, 1H, AlaHα), 5.26 (d, J=2.1 Hz, 1H, Oxd^2H_4), 5.39 (d, J=10.4 Hz, 1H, AlaNH), 6.28 (d, J=7.6 Hz, 1H, PheNH), 7.04-7.11 (m, 2H, PheArH), 7.21-7.26 (m, 3H, PheArH), 7.31 (d, J=8.0 Hz, 2H, TsArH), 7.75 (d, J=8.0 Hz, 2H, TsArH); ^{1}H-NMR (8:2 DMSO-d_6/H_2O) δ: 1.18 (d, J=6.7 Hz, 3H, AlaMe), 1.44-1-47 (m, 6H, Oxd^3Me+Oxd^2Me), 2.37 (s, 3H, TsMe), 2.94 (dd, J=8.4, 13.9 Hz, 1H, PheHβ), 3.01 (dd, J=5.7, 13.9 Hz, 1H, PheHβ), 3.56 (s, 3H, OMe), 4.48-4.52 (m, 2H, PheHα+Oxd^3H_5), 4.57 (d, J=1.9 Hz, 1H, Oxd^3H_4), 4.66 (dq, J=2.0, 7.0 Hz, 1H, Oxd^2H_5), 5.02 (dq, J=6.7, 8.5 Hz, 1H, AlaHα), 5.17 (d, J=2.0 Hz, 1H, Oxd^2H_4), 7.11 (d, J=7.6 Hz, 2H, PheArH), 7.14-7.26 (m, 3H, PheArH) 7.37 (d, J=8.0 Hz, 2H, TsArH), 7.63 (d, J=8.0 Hz, 2H, TsArH), 8.36 (d, J=8.5 Hz, 1H, AlaNH), 8.98 (d, J=7.0 Hz, 1H, PheNH). ^{13}C-NMR (DMSO-d_6) δ: 18.5, 20.5, 21.3, 21.4, 36.9, 50.1, 52.5, 54.3, 61.0, 61.6, 74.7, 76.6, 126.0, 127.2, 128.6, 128.8, 129.6, 130.1, 137.0, 138.2, 143.5, 152.0, 153.2, 167.4, 167.7, 171.7, 172.4; ES-MS (m/z) 659.3 [M+1], calcd 659.2; Elem. Anal. for $C_{30}H_{34}N_4O_{11}S$, calcd: C 54.70, H 5.20, N 8.51, S 4.87; found: C 54.67, H 5.17, N 8.45, S 4.81.

Ts-Ala-ΔAbu-(5'-Me-Oxd)-PheOMe (**3b**). IR (CH_2Cl_2) ν: 3407, 3318, 1789, 1748, 1708 cm^{-1}; ^{1}H-NMR ($CDCl_3$) δ: 1.23 (d, J=6.8 Hz, 3H, AlaMe), 1.43 (d, J=6.0 Hz, 3H, OxdMe), 1.79 (d, J=7.2 Hz, 3H, ΔAbuMe), 2.43 (s, 3H, TsMe), 3.03 (dd, J=8.2, 13.8 Hz, 1H, PheHβ), 3.23 (dd, J=5.4, 13.8 Hz, 1H, PheHβ), 3.71 (s, 3H, OMe), 3.85 (quint, J=7.2 Hz, 1H, AlaHα), 4.36-4.41 (m, 2H, $OxdH_{4,5}$), 4.84 (q, J=8.2 Hz, 1H, PheHα), 5.92 (d, J=6.8 Hz, 1H, AlaNH), 6.04 (q, J=7.2 Hz, 1H, ΔAbuHβ), 7.14-7.22 (m, 2H, PheArH), 7.24-7.34 (m, 5H, PheArH+TsArH), 7.64 (d, J=8.0 Hz, 1H, PheNH), 7.77 (d, J=7.6 Hz, 2H, TsArH), 8.66 (s, 1H, ΔAbuNH); ^{1}H-NMR (8:2 DMSO-d_6/H_2O) δ: 1.03 (d, J=7.2 Hz, 3H, AlaMe), 1.36 (d, J=6.2 Hz, 3H, OxdMe), 1.66 (d, J=7.2 Hz, 3H, ΔAbuMe), 2.40 (s, 3H, TsMe), 2.98 (dd, J=7.2, 14.0 Hz, 1H, PheHβ), 3.04 (dd, J=6.0, 14.0 Hz, 1H, PheHβ), 3.59 (s, 3H, OMe), 3.90 (quint, J=6.4 Hz, 1H, AlaHα), 4.33 (dq, J=2.8, 6.2 Hz, 1H, $OxdH_5$), 4.42 (d, J=2.8 Hz, 1H, $OxdH_4$), 4.54 (q, J=7.4 Hz, 1H, PheHα), 5.71 (q, J=7.2 Hz, 1H, ΔAbuHβ), 7.18-7.25 (m, 3H, PheArH), 7.31 (t, J=7.4 Hz, 2H, PheArH), 7.38 (d, J=8.1 Hz, 2H, TsArH), 7.68 (d, J=8.1 Hz, 2H, TsArH), 7.94 (d, J=7.6 Hz, 1H, AlaNH), 8.78 (d, J=7.2 Hz, 1H, PheNH), 9.53 (s, 1H, ΔAbuNH). ^{13}C-NMR (DMSO-d_6) δ: 12.8, 19.4, 20.3, 37.0, 51.9, 52.4, 54.1, 62.1, 75.0, 120.5, 126.9, 127.2, 128.8, 129.6, 130.1, 130.5, 134.1, 137.1, 138.7, 143.2, 151.8, 168.6, 170.8, 170.9, 171.9; ES-MS (m/z) 615.4 [M+1], calcd 615.2; Elem. Anal. for $C_{29}H_{34}N_4O_9S$, calcd: C 56.67, H 5.58, N 9.11, S 5.22; found: C 56.78, H 5.56, N 9.08, S 5.18.

Ts-Ala-(5'-Me-Oxd^2)-D-(5'-Me-Oxd^3)-PheOMe (**2c**) IR (CH_2Cl_2) ν 3406, 3347, 1793, 1736, 1707 cm^{-1}; ^{1}H-NMR ($CDCl_3$) δ: 1.33 (d, J=6.6 Hz, 3H, AlaMe), 1.47 (d, J=6.2 Hz, 3H, Oxd^2Me), 1.53 (d, J=6.4 Hz, 3H, Oxd^3Me), 2.42 (s, 3H, TsMe), 3.01 (dd, J=6.4, 14.1 Hz, 1H, PheHβ), 3.20 (dd, J=6.4, 14.1 Hz, 1H, PheHβ), 3.77 (s, 3H, OMe), 4.29 (d, J=4.8 Hz, 1H, Oxd^3H_4), 4.53 (dq, J=2.4, 6.4 Hz, 1H, Oxd^2H_5), 4.64 (quint, 1H, J=6.2 Hz, Oxd^3H_5), 4.82 (q, J=6.4 Hz, 1H, PheHα), 5.11 (dq, J=6.8, 13.6 Hz, 1H, AlaHα), 5.24 (d, J=2.4 Hz, 1H, Oxd^2H_4), 5.44 (d, J=10.0 Hz, 1H, AlaNH), 6.55 (d, J=7.6 Hz, 1H, PheNH), 7.09 (d, J=7.2 Hz, 2H, PheArH), 7.24-7.31 (m, 5H, PheArH+TsArH), 7.73 (d, J=7.6 Hz, 2H, TsArH); ^{1}H-NMR(8:2 DMSO-d_6/H_2O) δ: 1.17 (d, J=6.8 Hz, 3H, AlaMe), 1.35 (d, J=6.2 Hz, 3H, Oxd^2Me), 1.39 (d, J=6.4 Hz, 3H, Oxd^3Me), 2.36 (s, 3H, TsMe), 2.83 (dd, J=8.1, 13.8 Hz, 1H, PheHβ), 3.11 (dd, J=8.1, 13.8 Hz, 1H, PheHβ), 3.63 (s, 3H, OMe), 3.84 (quint, J=5.6 Hz, 1H, Oxd^3H_5), 4.36 (d, J=4.8 Hz, 1H, Oxd^3H_4), 4.51 (dq, J=8.1, 9.6 Hz, 1H, PheHα), 4.95-5.03 (m, 2H, Oxd^2H_4+AlaHα), 5.06 (q, 1H, J=6.2 Hz, Oxd^2H_5), 7.17 (d, J=6.8 Hz, 2H, PheArH), 7.19-7.30 (m, 3H, PheArH), 7.37 (d, J=8.2 Hz, 2H, TsArH), 7.62 (d, J=8.2 Hz, 2H, TsArH), 8.42 (d, J=9.2 Hz, 1H, AlaNH), 8.94 (d, J=8.1 Hz, 1H, PheNH).^{13}C-NMR (DMSO-d_6) δ: 18.5, 20.4, 20.5, 21.4, 37.4, 50.3, 52.6, 53.8, 61.3, 62.0, 69.4, 70.1, 127.2, 128.4, 128.7, 129.8, 130.1, 137.4, 138.3, 143.5, 152.3, 153.3, 166.5, 167.1, 171.7, 172.0; ES-MS (m/z) 659.4 [M+1],

calcd 659.2; Elem. Anal. for $C_{30}H_{34}N_4O_{11}S$, calcd: C 54.70, H 5.20, N 8.51, S 4.87; found: C 54.60, H 5.14, N 8.44, S 4.81.

Ts-Ala-ΔAbu-D-(5'-Me-Oxd)-PheOMe (**3c**). IR (CH_2Cl_2) ν: 3400, 3334, 1781, 1744, 1707 cm^{-1}; ^{1}H-NMR ($CDCl_3$) δ: 1.28 (d, J=7.2 Hz, 3H, AlaMe), 1.54 (d, J=6.0 Hz, 3H, OxdMe), 1.89 (d, J=7.2 Hz, 3H, ΔAbuMe), 2.46 (s, 3H, TsMe), 3.09 (dd, J=9.0, 13.8 Hz, 1H, PheHβ), 3.18 (dd, J=6.2, 13.8 Hz, 1H, PheHβ), 3.72 (s, 3H, OMe), 3.87 (m, 1H, AlaHα), 4.45 (d, J=7.2 Hz, 1H, $OxdH_4$), 4.59 (quint, J=6.5 Hz, 1H, $OxdH_5$), 4.79 (q, J=8.4 Hz, 1H, PheHα), 5.66 (br.d, 1H, AlaNH), 6.27 (q, J=6.6 Hz, 1H, ΔAbuHβ), 7.21 (d, J=8.4, 2H, PheArH), 7.23-7.33 (m, 3H, PheArH), 7.35 (d, J=7.8 Hz, 2H, TsArH), 7.80 (d, J=7.8 Hz, 2H, TsArH), 7.98 (d, J=8.0 Hz, 1H, PheNH), 8.28 (s, 1H, ΔAbuNH); ^{1}H-NMR(8:2 DMSO-d_6/H_2O) δ: 1.03 (d, J=7.2 Hz, 3H, AlaMe), 1.20 (d, J=6.0 Hz, 3H, OxdMe), 1.67 (d, J=7.2 Hz, 3H, ΔAbuMe), 2.36 (s, 3H, TsMe), 2.85 (dd, J=10.4, 13.5 Hz, 1H, PheHβ), 3.12 (dd, J=4.8, 13.5 Hz, 1H, PheHβ), 3.58-3.69 (m, 4H, $OxdH_5$+OMe), 3.99 (quint, J=7.1 Hz, 1H, AlaHα), 4.25 (d, J=2.0 Hz, 1H, $OxdH_4$), 4.58 (m, 1H, PheHα), 5.65 (q, J=6.8 Hz, 1H, ΔAbuHβ), 7.13-7.24 (m, 2H, PheArH), 7.28 (t, J=7.0 Hz, 2H, PheArH), 7.35 (d, J=6.6 Hz, 2H, TsArH), 7.65 (d, J=6.6 Hz, 2H, TsArH), 7.93 (d, J=8.4 Hz, 1H, AlaNH), 8.85 (d, J=8.4 Hz, 1H, PheNH), 9.73 (s, 1H, ΔAbuNH). ^{13}C-NMR (DMSO-d_6) δ: 12.8, 16.9, 21.5, 25.7, 37.8, 52.8, 54.7 56.9, 62.0, 75.2, 121.9, 126.0, 127.0, 128.7, 129.9, 132.0, 134.4, 136.3, 143.0, 154.8, 168.4, 170.8, 171.6; ES-MS (m/z) 615.4 [M+1], calcd 615.2; Elem. Anal. for $C_{29}H_{34}N_4O_9S$, calcd: C 56.67, H 5.58, N 9.11, S 5.22; found: C 56.60, H 5.52, N 9.02, S 5.15.

Ts-Ala-(5'-Me-Oxd^2)-D-(5'-Me-Oxd^3)-D-PheOMe (**2d**). IR (CH_2Cl_2) ν: 3409, 1776, 1747, 1707, 1608, 1420 cm^{-1}; ^{1}H-NMR ($CDCl_3$) δ: 1.40 (d, J=7.0 Hz, 3H, AlaMe), 1.46 (d, J=6.0 Hz, 3H, Oxd^3Me), 1.58 (d, J=6.3 Hz, 3H, Oxd^2Me), 2.44 (s, 3H, TsMe), 3.05 (dd, J=8.3, 13.9 Hz, 1H, PheHβ), 3.17 (dd, J=5.3, 13.9 Hz, 1H, PheHβ), 3.74 (s, 3H, OMe), 4.29-4.37 (m, 2H, $Oxd^3H_{4,5}$), 4.58 (dq, J=3.5, 6.3 Hz, 1H, Oxd^2H_5), 4.88 (ddd, J=5.3, 8.3, 8.5 Hz, 1H, PheHα), 5.16 (dq, J=7.0, 10.8 Hz, 1H, AlaHα), 5.42 (d, J=3.5 Hz, 1H, Oxd^2H_4), 5.61 (d, J=10.8 Hz, 1H, AlaNH), 6.63 (d, J=8.5 Hz, 1H, PheNH), 7.14 (d, J=6.6 Hz, 2H, PheArH), 7.22-7.37 (m, 5H, PheArH+TsArH), 7.76 (d, J=8.0 Hz, 2H, TsArH); ^{1}H-NMR (8:2 DMSO-d_6/H_2O) δ: 1.15 (d, J=6.6 Hz, 3H, AlaMe), 1.40 (d, J=6.2 Hz, 3H, Oxd^2Me), 1.46 (d, J=6.0 Hz, 3H, Oxd^3Me), 2.37 (s, 3H, TsMe), 2.97 (d, J=6.8 Hz, 2H, PheHβ), 3.58 (s, 3H, OMe), 4.46-4.52 (m, 3H, PheHα+$Oxd^3H_{4,5}$), 5.02 (m, 1H, AlaHα), 5.03 (d, J=1.6 Hz, 1H, Oxd^2H_4), 5.10 (dq, J=1.6, 6.2 Hz, 1H, Oxd^2H_5), 7.18 (d, J=6.7 Hz, 2H, PheArH), 7.19-7.23 (m, 3H, PheArH), 7.37 (d, J=8.2 Hz, 2H, TsArH), 7.62 (d, J=8.2 Hz, 2H, TsArH), 8.41 (d, J=9.6 Hz, 1H, AlaNH), 8.89 (d, J=7.6 Hz, 1H, PheNH). ^{13}C-NMR ($CDCl_3$) δ: 18.9, 20.6, 20.9, 21.5, 37.9, 51.1, 52.6, 53.4, 61.1, 62.4, 74.2, 76.0, 127.2, 127.4, 128.6, 129.3, 129.7, 135.6, 136.9, 143.8, 151.1, 152.0, 165.7, 168.1, 171.4, 173.8; ES-MS (m/z) 659.3 [M+1], calcd 659.2; Elem. Anal. for $C_{30}H_{34}N_4O_{11}S$, calcd: C 54.70, H 5.20, N 8.51, S 4.87; found: C 54.65, H 5.26, N 8.50, S 4.82.

Ts-Ala-(5'-Me-Oxd^2)-(5'-Ph-Oxd^3)-PheOMe (**2f**). IR (CH_2Cl_2) ν: 3407, 3350, 1790, 1740, 1699, 1660 cm^{-1}; ^{1}H-NMR ($CDCl_3$) δ: 1.41 (d, J=7.2 Hz, 3H, AlaMe), 1.55 (d, J=6.2 Hz, 6H, Oxd^2Me), 2.43 (s, 3H, TsMe), 3.12 (d, J=5.6 Hz, 2H, PheHβ), 3.78 (s, 3H, OMe), 4.53 (d, J=4.4 Hz, 1H, Oxd^3H_4), 4.66 (dq, J=2.0, 6.2 Hz, 1H, Oxd^2H_5), 4.90 (q, J=7.6 Hz, 1H, PheHα), 5.24 (dq, J=7.6, 10.8 Hz, 1H, AlaHα), 5.35 (d, J=2.0 Hz, 1H, Oxd^2H_4), 5.41 (d, J=10.8 Hz, 1H, AlaNH), 5.57 (d, J=4.4 Hz, 1H, Oxd^3H_5), 6.31 (d, J=7.7 Hz, 1H, PheNH), 7.04-7.12 (m, 2H, PheArH), 7.20-7.30 (m, 5H, PheArH+5'-PhArH), 7.31 (d, J=8.0 Hz, 2H, TsArH), 7.39-7.44 (m, 3H, 5'-PhArH), 7.77 (d, J=8.0 Hz, 2H, TsArH); ^{13}C-NMR ($CDCl_3$) δ: 19.5, 21.1, 21.5, 37.2, 50.6, 52.7, 53.7, 61.2, 65.8, 73.8, 79.0, 125.2, 127.3, 127.6, 129.1, 129.4, 129.5, 129.9, 130.1, 135.9, 136.6, 143.8, 151.1, 152.3, 166.1, 167.4, 173.1, 173.4; ES-MS (m/z) 721.2 [M+1], calcd 721.2; Elem. Anal. for $C_{35}H_{36}N_4O_{11}S$, calcd: C 58.32, H 5.03, N 7.77, S, 4.45; found: C 58.29, H 5.09, N 7.80, S, 4.40.

Ts-Ala-(5'-Me-Oxd^2)-D-(5'-Ph-Oxd^3)-PheOMe (**2g**). IR (CH_2Cl_2) ν: 3409, 3345, 1779, 1730, 1700, 1656 cm^{-1}; ^{1}H-NMR ($CDCl_3$) δ: 1.30 (d, J=7.3 Hz, 3H, AlaMe), 1.52 (d, J=6.4 Hz, 3H, Oxd^2Me), 2.43 (s, 3H, TsMe), 3.03 (dd, J=7.2, 14.4 Hz, 2H, PheHβ), 3.23 (dd, J=6.0, 14.4 Hz, 2H, PheHβ), 3.76 (s, 3H, OMe), 4.53-4.61 (m, 2H, Oxd^2H_5+Oxd^3H_4), 4.88 (q, J=7.6 Hz, 1H, PheHα), 5.13 (dq, J=7.6, 10.8 Hz, 1H, AlaHα), 5.29 (d, J=2.4 Hz, 1H, Oxd^2H_4), 5.50-5.58 (m, 2H, AlaNH+Oxd^3H_5), 6.63 (d, J=7.7 Hz, 1H, PheNH), 7.04-7.11 (m, 2H, PheArH), 7.15-7.20 (m, 2H, 5'-PhArH), 7.20-7.25 (m, 3H, PheArH), 7.31 (d, J=8.0 Hz, 2H, TsArH), 7.39-7.43 (m, 3H, 5'-PhArH), 7.76 (d, J=8.0 Hz, 2H, TsArH); ^{13}C-NMR ($CDCl_3$) δ: 19.3, 20.6, 21.5, 37.6, 50.7, 53.3, 53.5, 60.8, 63.4, 71.8, 79.0, 125.3, 127.4, 128.7, 129.2, 129.5, 129.7, 130.1, 134.7, 135.7, 136.7, 143.6, 151.3, 152.3, 165.4, 167.0, 171.2, 173.1; ES-MS (m/z) 721.3 [M+1], calcd 721.2; Elem. Anal. for $C_{35}H_{36}N_4O_{11}S$, calcd: C 58.32, H 5.03, N 7.77, S, 4.45; found: C 58.22, H 5.07, N 7.71, S, 4.49.

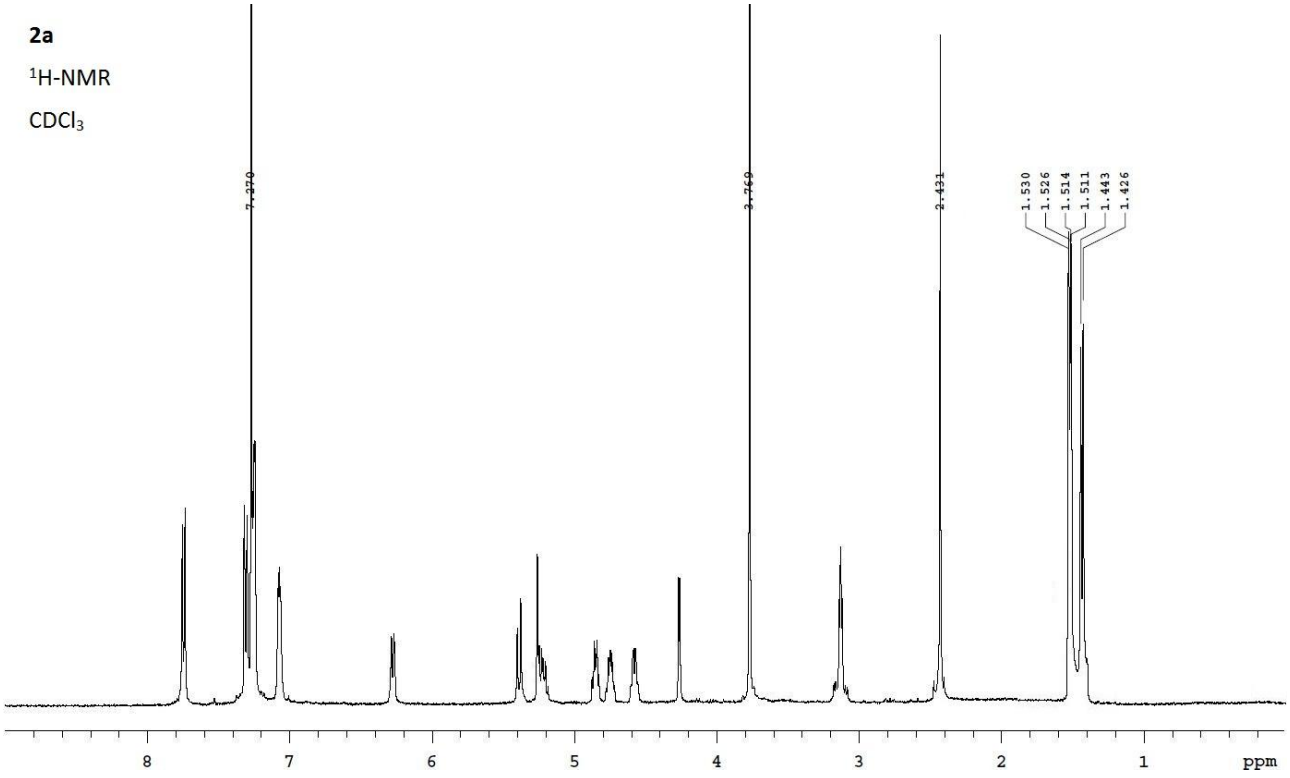
2a
^{1}H-NMR
$CDCl_3$
7.270
3.769
2.431
1.530
1.526
1.514
1.511
1.443
1.426
8
7
6
5
4
3
2
1
ppm

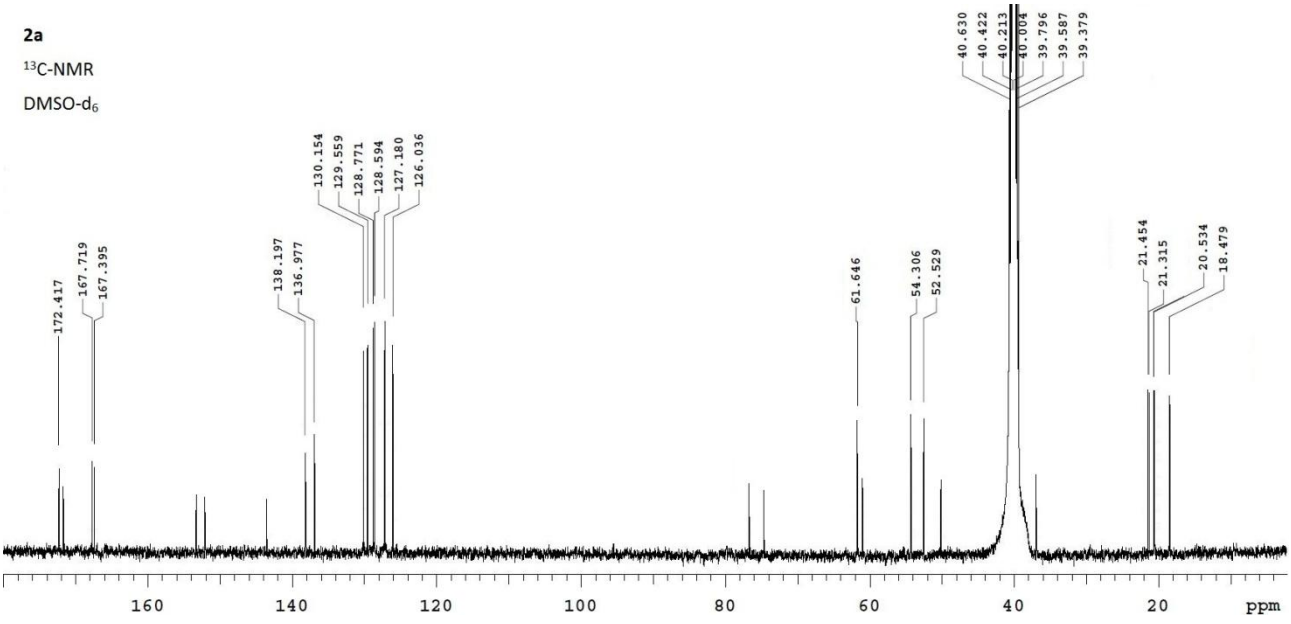
2a
^{13}C-NMR
DMSO-d_6
172.417
167.719
167.395
138.197
136.977
130.154
129.559
128.771
128.594
127.180
126.036
61.646
54.306
52.529
40.630
40.422
40.213
40.004
39.796
39.587
39.379
21.454
21.315
20.534
18.479
160
140
120
100
80
60
40
20
ppm

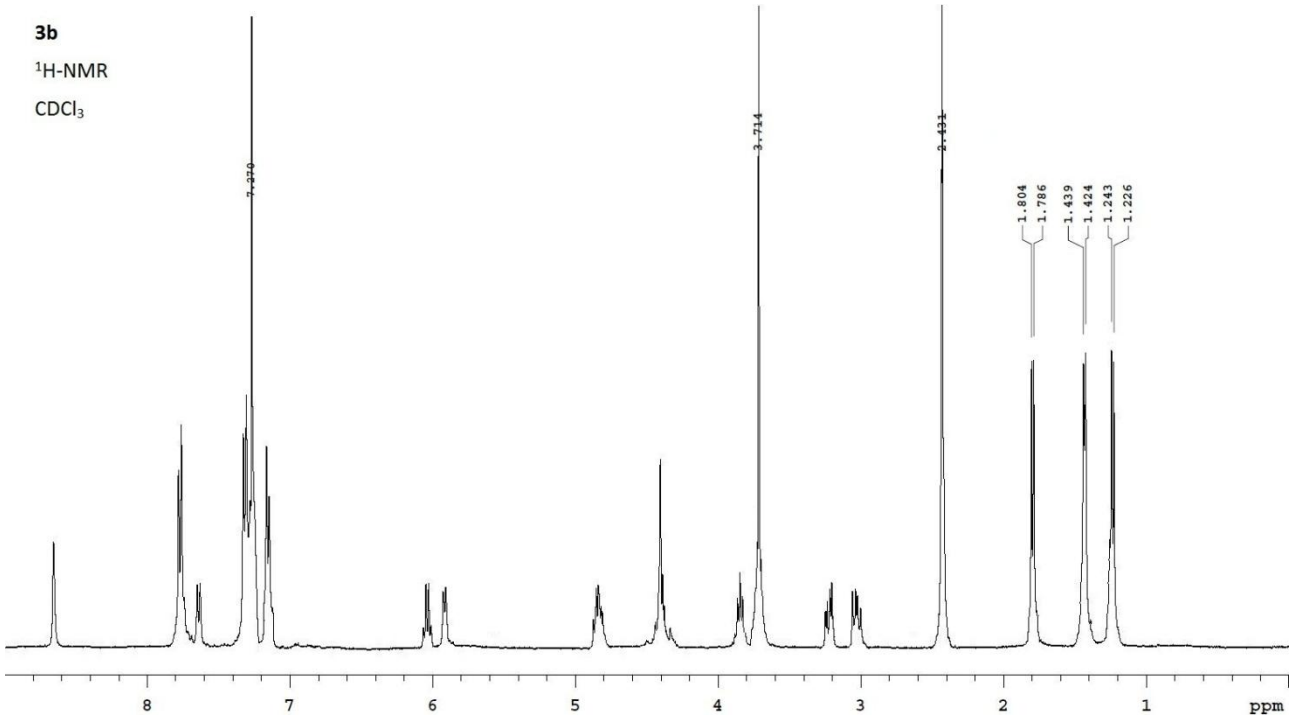
3b
1H-NMR
CDCl3
7.270
3.714
2.431
1.804
1.786
1.439
1.424
1.243
1.226
8
7
6
5
4
3
2
1
ppm

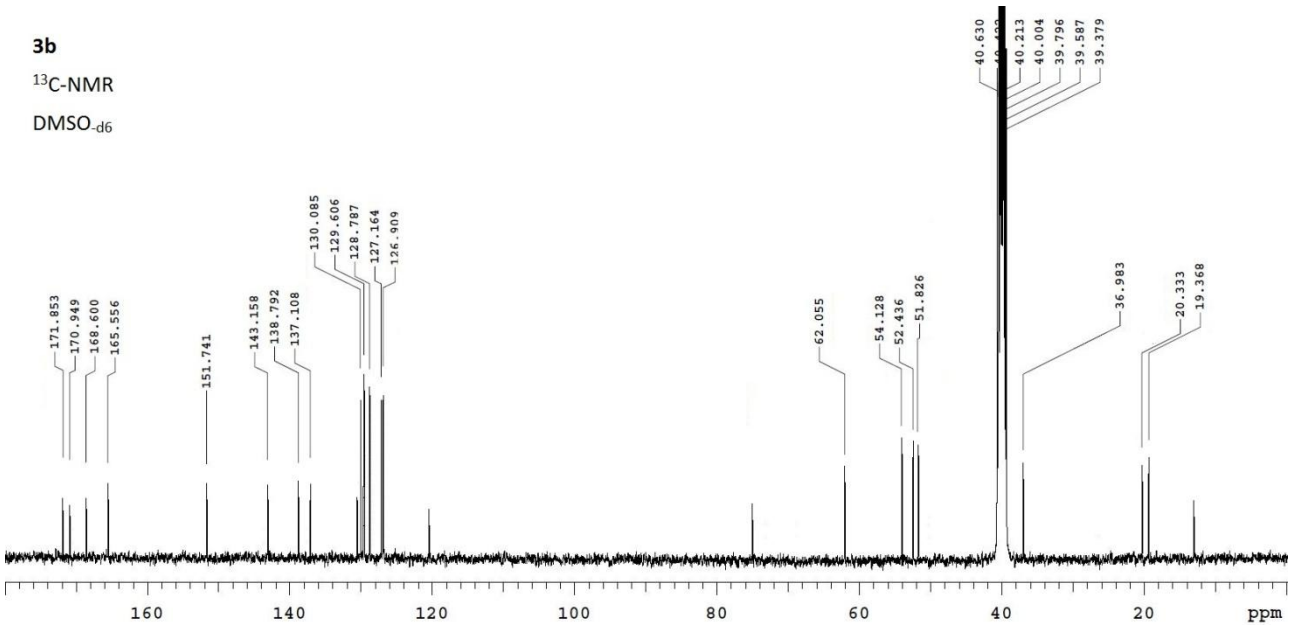
3b
13C-NMR
DMSO-d6
171.853
170.949
168.600
165.556
151.741
143.158
138.792
137.108
130.085
129.606
128.787
127.164
126.909
62.055
54.128
52.436
51.826
40.630
40.213
40.004
39.796
39.587
39.379
36.983
20.333
19.368
160
140
120
100
80
60
40
20
ppm

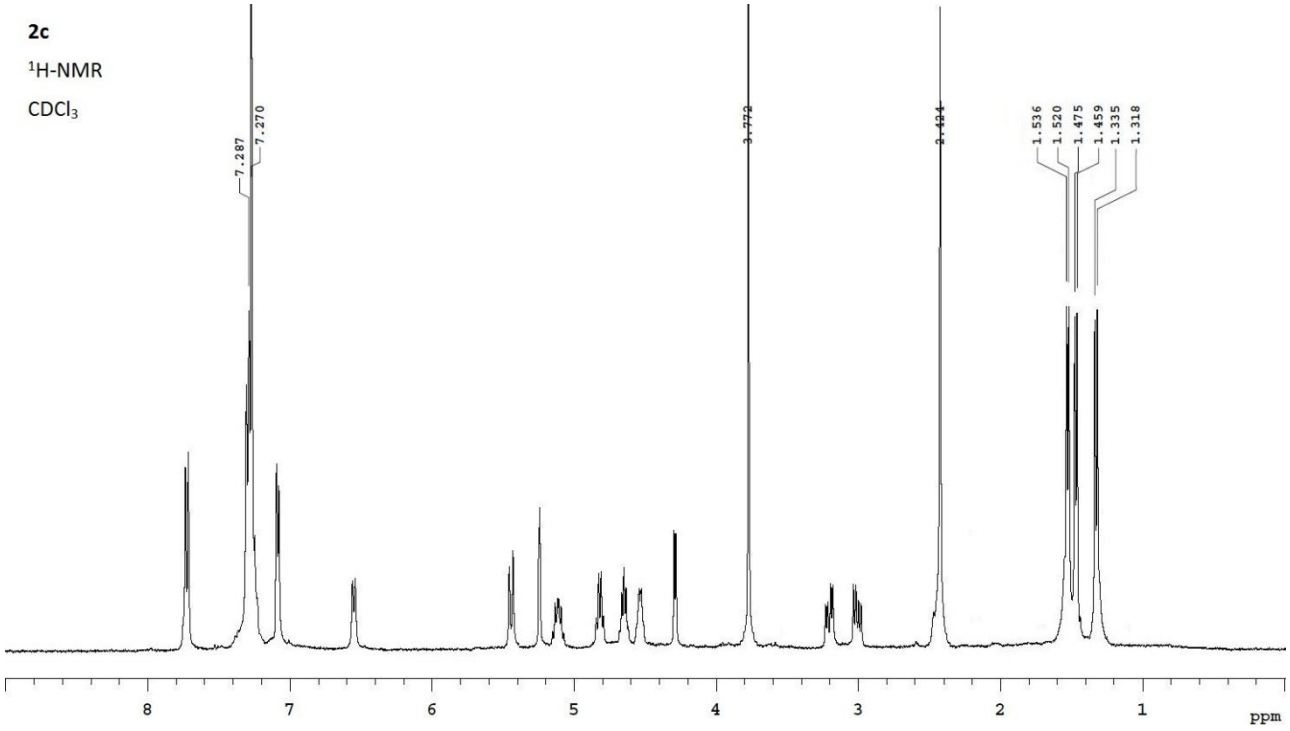
2c
^{1}H-NMR
$CDCl_3$
7.287
7.270
3.772
2.434
1.536
1.520
1.475
1.459
1.335
1.318
8
7
6
5
4
3
2
1
ppm

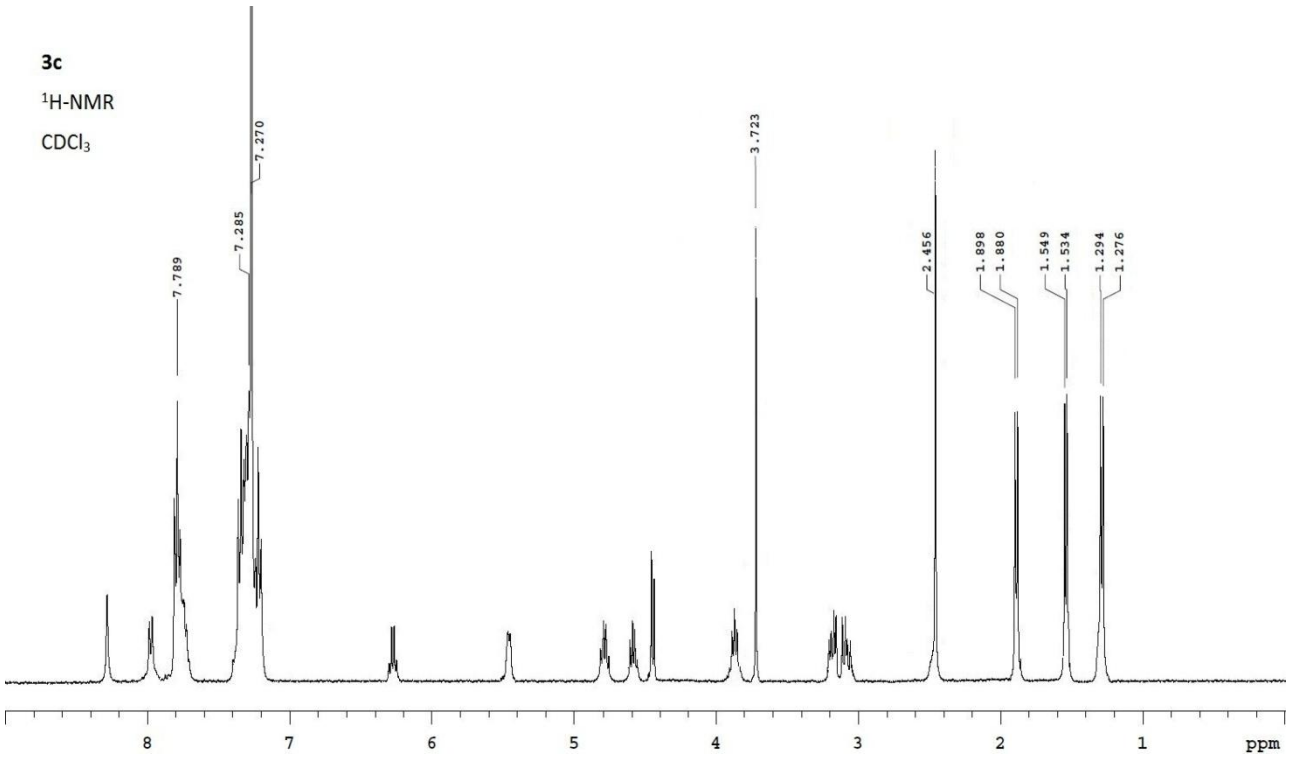
3c
^{1}H-NMR
$CDCl_3$
7.789
7.285
7.270
3.723
2.456
1.898
1.880
1.549
1.534
1.294
1.276
8
7
6
5
4
3
2
1
ppm

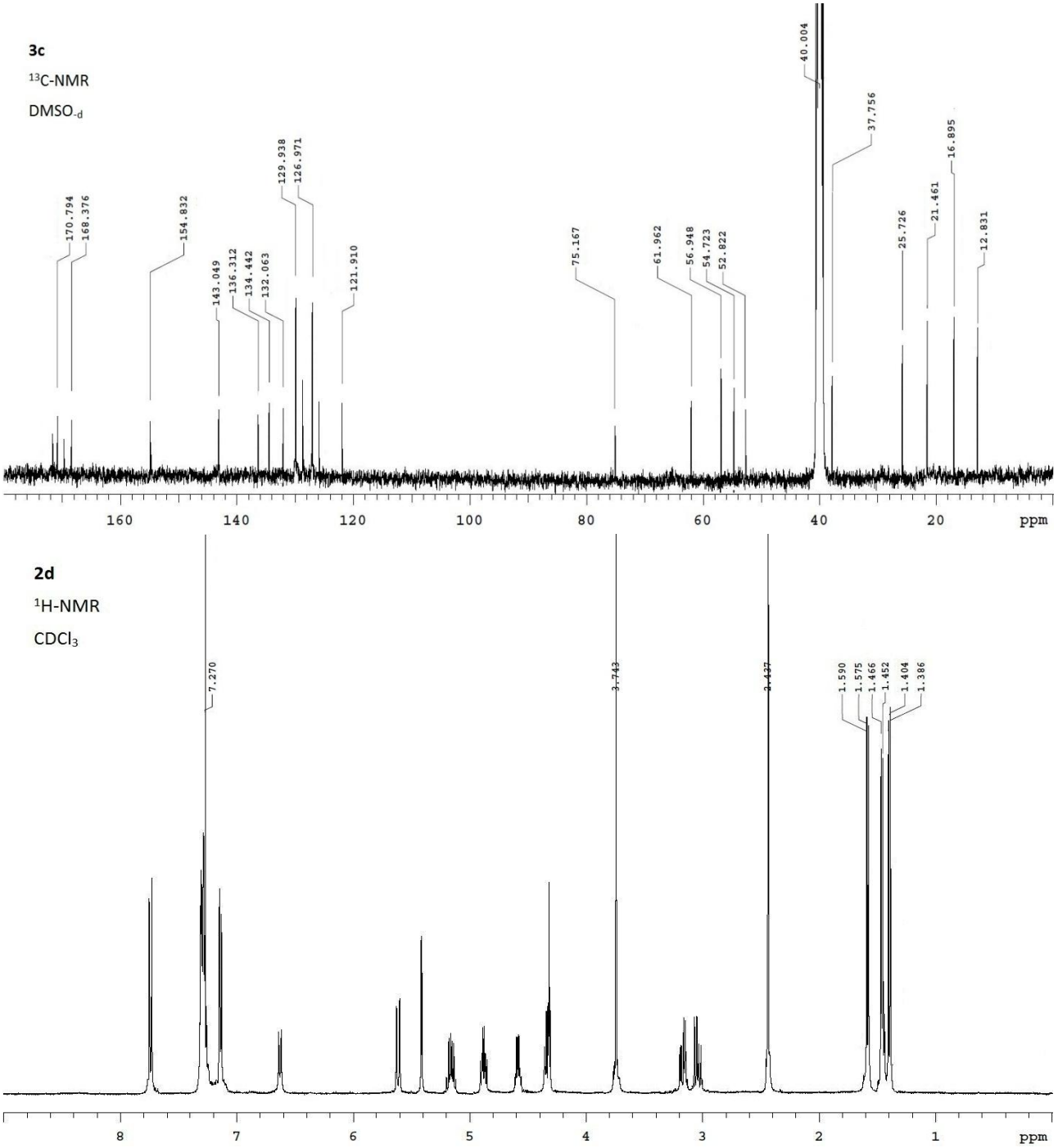
3c
13C-NMR
DMSO-d
170.794
168.376
154.832
143.049
136.312
134.442
132.063
129.938
126.971
121.910
75.167
61.962
56.948
54.723
52.822
40.004
37.756
25.726
21.461
16.895
12.831
160
140
120
100
80
60
40
20
ppm
2d
1H-NMR
CDCl3
7.270
3.743
3.437
1.590
1.575
1.466
1.452
1.404
1.386
8
7
6
5
4
3
2
1
ppm

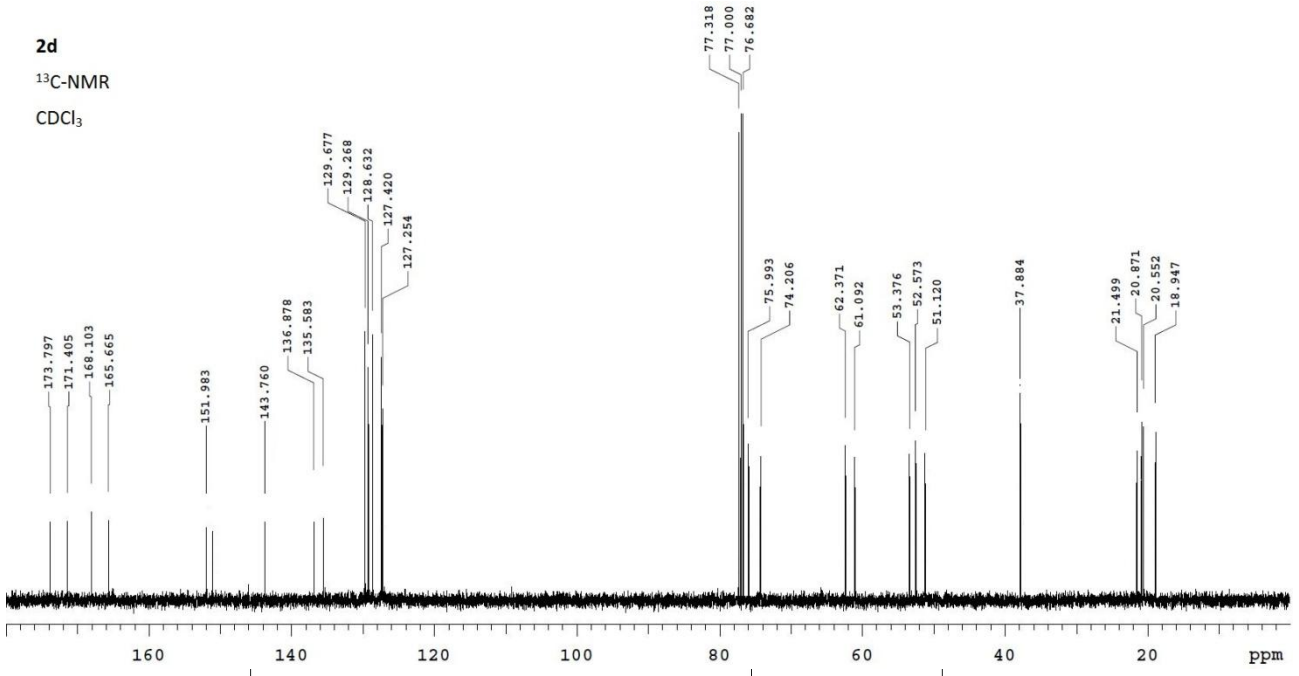
2d
^{13}C-NMR
$CDCl_3$
77.318
77.000
76.682
129.677
129.268
128.632
127.420
127.254
75.993
74.206
62.371
61.092
53.376
52.573
51.120
37.884
21.499
20.871
20.552
18.947
173.797
171.405
168.103
165.665
151.983
143.760
136.878
135.583
160
140
120
100
80
60
40
20
ppm

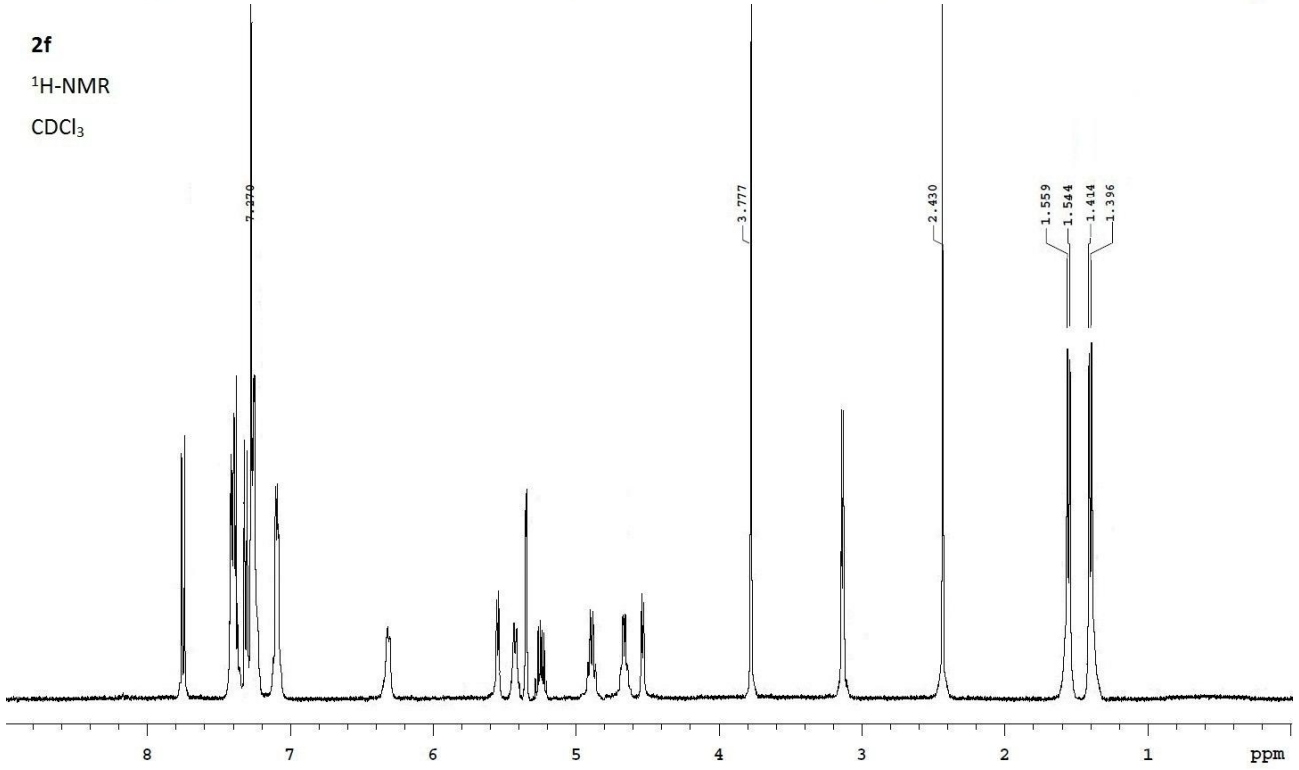
2f
^{1}H-NMR
$CDCl_3$
7.239
3.777
2.430
1.559
1.544
1.414
1.396
8
7
6
5
4
3
2
1
ppm

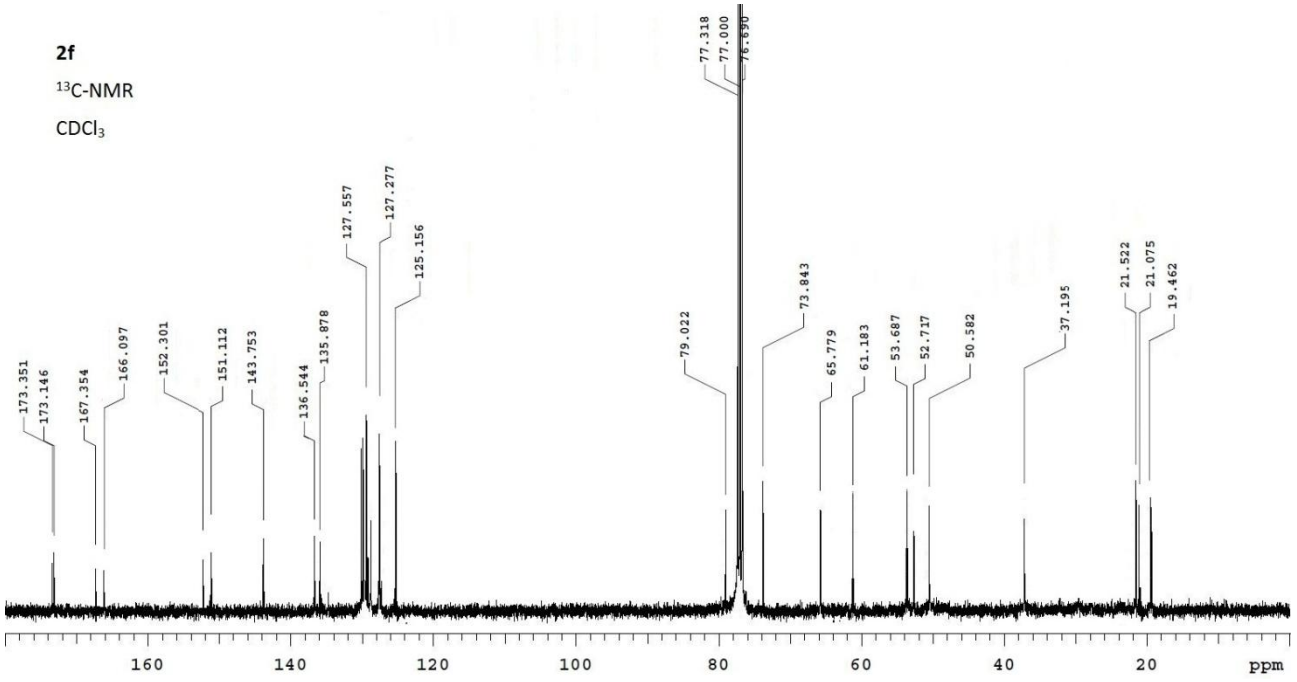
2f
13C-NMR
CDCl3
77.318
77.000
76.690
173.351
173.146
167.354
166.097
152.301
151.112
143.753
136.544
135.878
127.557
127.277
125.156
79.022
73.843
65.779
61.183
53.687
52.717
50.582
37.195
21.522
21.075
19.462
160
140
120
100
80
60
40
20
ppm

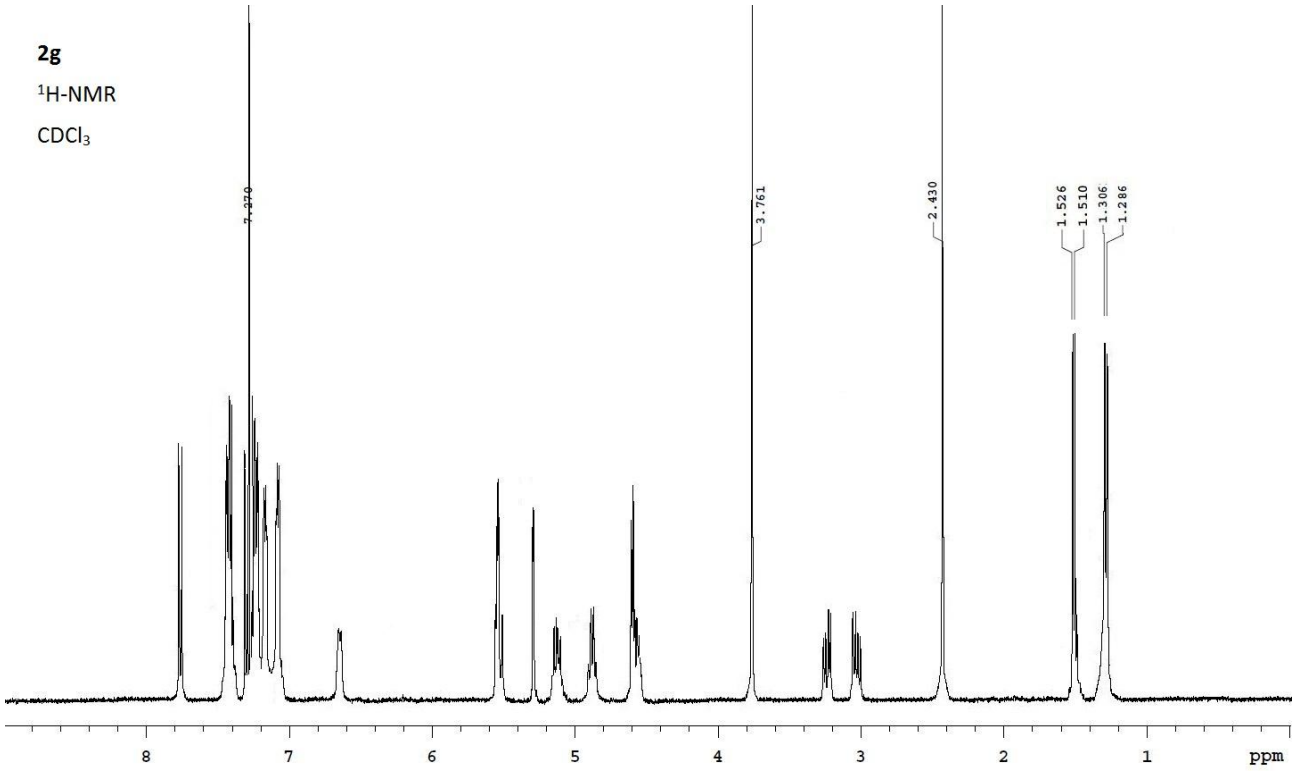
2g
1H-NMR
CDCl3
7.370
3.761
2.430
1.526
1.510
1.306
1.286
8
7
6
5
4
3
2
1
ppm

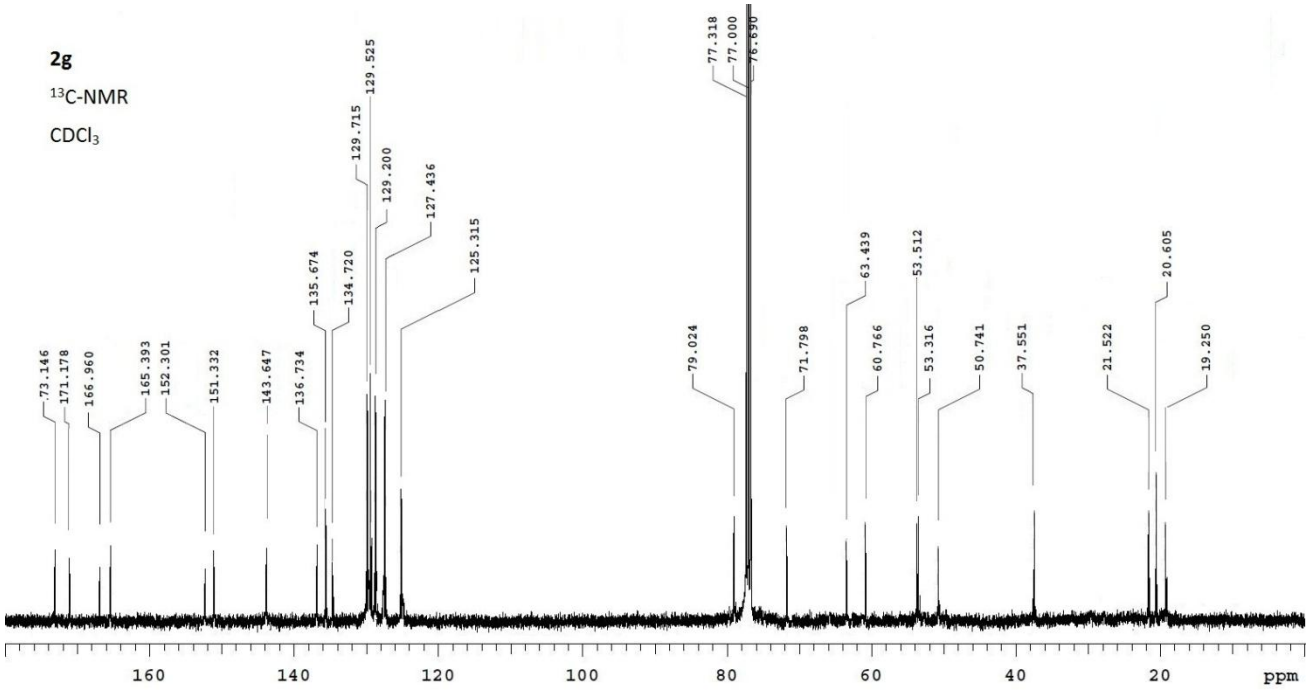

4.4.3. Conformational analysis

IR analyses. Infrared spectra were obtained at 2 cm^{-1} resolution using a 1 mm NaCl solution cell and a FT-IR spectrometer (64 scans). All spectra were obtained in 3 mM solutions in dry CH_2Cl_2 at 297 K. The compounds were dried in vacuo, and all the sample preparations were performed in a inert atmosphere.

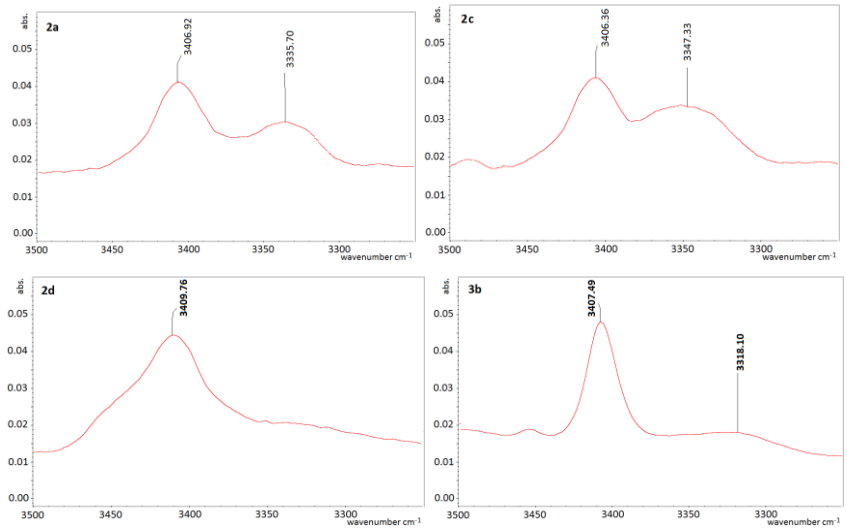

Figure 6. Amide NH stretching regions of the IR absorption spectra for samples of tetrapeptides **2a**, **2d** and **3b** (3 mM in DCM) at room temperature.

Circular Dichroism. ECD spectra were recorded from 200 to 400 nm at 25 °C. 1 mM solutions were made up in spectral grade solvents and run in a 0.1 cm quartz cell. Data are reported in molar ellipticity [θ] (deg·cm^2·$dmol^{-1}$).

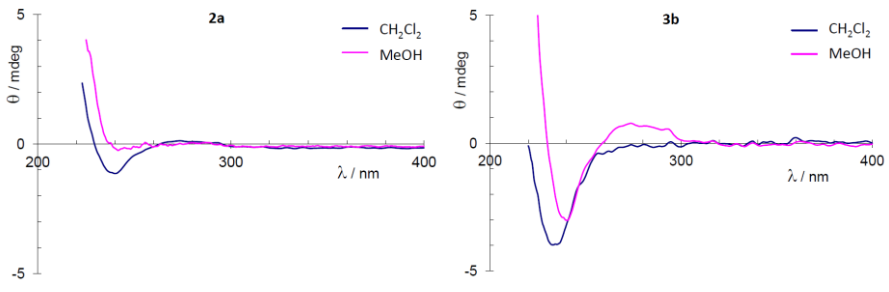

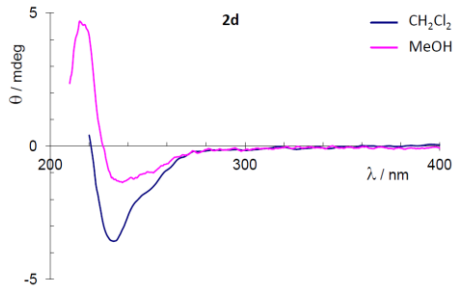

Figure 7. ECD spectra of **2a**, **3b**, and **2d**; 1 mM in DCM or MeOH, path length 0.1 cm.

NMR analyses. ^{1}H-NMR spectra were recorded at 400 MHz in 5 mm tubes, using 0.01 M peptide at room temperature. Solvent suppression was performed by the solvent presaturation procedure implemented in Varian (PRESAT). ^{13}C-NMR spectra were recorded at 100 MHz. Chemical shifts are reported as δ values. The unambiguous assignment of ^{1}H-NMR resonances was performed by 2D gCOSY, HMBC, and HSQC. gCOSY experiments were conducted with a proton spectral width of 3103 Hz. VT-^{1}H-NMR experiments were performed over the range of 298-348 °K. 2D spectra were recorded in the phase sensitive mode and processed using a 90°-shifted, squared sine-bell apodization. 2D ROESY experiments were recorded in 8:2 DMSO-d_6/H_2O, with a 250 ms mixing time with a proton spectral width of 3088 Hz. Peaks were calibrated on DMSO.

Table 5. Selected ^{1}H-NMR chemical shifts (δ) of the model compds **2a**, **2c**, **2d**, and **3b**, **3c**; solvents: S1 = $CDCl_3$; S2 = 8:2 DMSO-d_6/H_2O; amino acid stereochemistry has been omitted.

	2a		**2c**		**2d**		**3b**		**3c**	
	S1	S2	S1	S2	S1	S2	S1	S2	S1	S2
Ala^{1}NH	5.39	8.36	5.44	8.42	5.61	8.41	5.92	7.94	5.66	7.93
Ala^{1}Hα	5.22	5.02	5.11	5.0	5.16	5.02	3.85	3.90	3.87	3.99
Oxd^{2}H4	5.26	5.17	5.24	5.0	5.42	5.03	-	-	-	-
Oxd^{2}H5	4.58	4.66	4.53	5.06	4.58	5.10	-	-	-	-
ΔAbuNH	-	-	-	-	-	-	8.66	9.53	8.28	9.73
ΔAbuHβ	-	-	-	-	-	-	6.04	5.71	6.27	5.65
Oxd^{3}H4	4.26	4.57	4.29	4.36	4.3	4.5	4.38	4.42	4.4	4.25
Oxd^{3}H5	4.75	4.5	4.64	3.84	4.3	4.5	4.4	4.33	4.6	3.6
Phe^{4}NH	6.28	8.98	6.55	8.94	6.63	8.89	7.64	8.78	7.98	8.85
Phe^{4}Hα	4.85	4.5	4.82	4.51	4.88	4.5	4.84	4.54	4.79	4.58

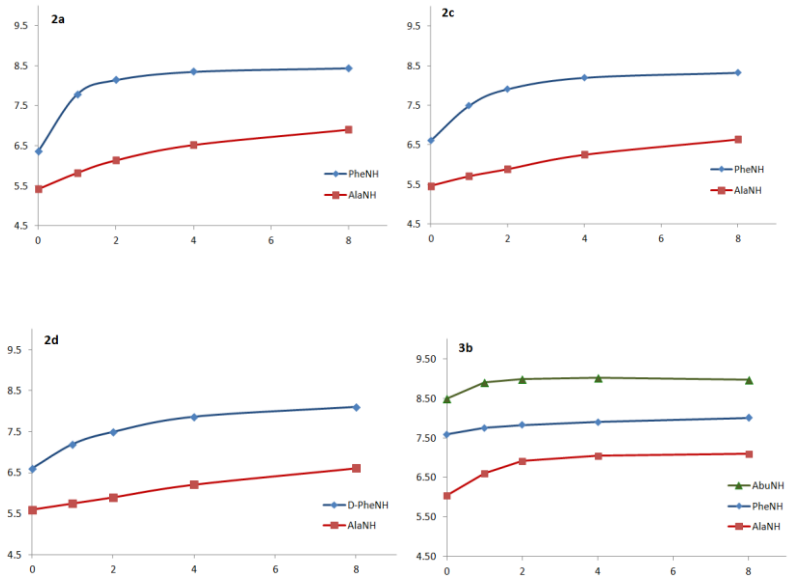

Figure 8. Variation of NH proton chemical shift (p.p.m.) of **2a**, **2c**, **2d** and **3b** as a function of increasing percentages of DMSO-d_6 to the $CDCl_3$ solution (v/v).

ROESY and molecular dynamics. Only ROESY-derived constraints were included in the restrained molecular dynamics. Cross-peak intensities were classified very strong, strong, medium, and weak, and were associated with distances of 2.2, 2.6, 3.0, and 4.5 Å, respectively. Geminal couplings and other obvious correlations were discarded. For the absence of Hα(i, i+1) ROESY cross peaks, all of the ω bonds were set at 180° (force constant: 16 kcal $mol^{-1}Å^{-2}$). The restrained MD simulations were conducted using the AMBER force field in a 30×30×30 Å box of standard TIP3P models of equilibrated water.[29] All water molecules with atoms that come closer than 2.3 Å to a solute atom were eliminated. A 100 ps simulation at 1200 °K was used for generating 50 random structures that were subsequently subjected to a 50 ps restrained MD with a 50 % scaled force field at the same temperature, followed by 50 ps with full restraints (distance force constant of 7 kcal mol^{-1} $Å^{-2}$), after which the system was cooled in 20 ps to 50 °K. H-bond interactions were not included, nor were torsion angle restraints. The resulting structures were minimized with 3000 cycles of steepest descent and 3000 cycles of conjugated gradient (convergence of 0.01 kcal $Å^{-1}$ mol^{-1}). The backbones of the structures were clustered by the RMSD analysis module of HyperChem.[30] Unrestrained MD simulation was performed in a 30×30×30 Å box of standard TIP3P water for 10 ns at 298 °K, at constant temperature and pressure (Berendsen scheme,[31] bath relaxation constant of 0.2). For 1-4 scale factors, van der Waals and electrostatic interactions are scaled in AMBER to half their nominal value. The integration time step was set to 0.1 fs.

Table 6. Non-obvious ROESY cross-peaks observed for **2a**.[a]

Cross-peak	intensity	Cross-peak	intensity
PheNH-Oxd^{3}Me	w	PheNH-PheHβ(up)	s
PheNH-PheHβ(dw)	m	PheNH-PheHα	m
PheNH-Oxd^{3}H4	s	PheNH-Oxd^{3}H5	m
PheNH-Oxd^{2}H5	w	PheNH-PheArH	m
AlaNH-AlaMe	vs	AlaNH-AlaHα	s
AlaNH-TsArH2,6	s	TsArH2,6-AlaMe	w
TsArH2,6-Oxd^{2}Me	w	TsArH2,6-AlaHα	m
TsArH3,5-Oxd^{2}Me	s	TsArH3,5- Oxd^{2}H4	w
PheArH-PheHα	s	Oxd^{2}H4-Oxd^{3}H4	w
Oxd^{2}H4-AlaHα	w	AlaHα-Oxd^{2}H5	w
Oxd^{2}H5-Oxd^{3}H5	w	COOMe-PheHα	w

[a] Stereochemistry has been omitted; [b] up = upfield, dw = downfield; [c] vs = very strong, s = strong, m = medium, w = weak.

Table 7. Non-obvious ROESY cross-peaks observed for **2c**.[a]

Cross-peak	intensity	Cross-peak	intensity
PheNH-PheArH	w	PheNH-PheHα	m
PheNH-Oxd^{3}H4	vs	PheNH-Oxd^{3}H5	w
PheNH-PheHβ(dw)	w	PheNH-PheHβ(up)	s
PheNH-Oxd^{3}Me	w	PheNH-COOMe	w
AlaNH-TsArH2,6	m	AlaNH-AlaHα	m
AlaNH-AlaMe	s	TsArH2,6-AlaMe	w
TsArH2,6-Oxd^{2}Me	w	TsArH2,6-AlaHα	m
TsArH3,5-Oxd^{2}Me	w	TsArH3,5-AlaHα	w
PheArH2,4,6- Oxd^{3}Me	w	PheArH2,4,6- PheHβ(up)	s
PheArH2,4,6- PheHβ(dw)	s	PheArH2,4,6- AlaMe	w
PheArH2,4,6- PheHα	m	PheArH2,4,6-COOMe	w
PheArH2,4,6-Oxd^{3}H5	w	Oxd^{2}H4-Oxd^{3}H5	w
Oxd^{2}H4-Oxd^{3}H4	w	Oxd^{2}H5-Oxd^{3}H4	w
Oxd^{2}H5-PheHα	w	AlaHα-PheHα	w
PheHα-PheHβ(dw)	s	PheHα-PheHβ(up)	m
PheHα-COOMe	w	PheHα- Oxd^{3}H5	w
PheHα-Oxd^{3}H4	w	Oxd^{3}H5-PheHβ(dw)	w
COOMe-AlaMe	m	COOMe-TsMe	w
COOMe-PheHβ(dw)	m	COOMe-PheHβ(up)	m
TsMe- Oxd^{2}Me	w		

[a] Stereochemistry has been omitted; [b] up = upfield, dw = downfield; [c] vs = very strong, s = strong, m = medium, w = weak.

Table 8. Non-obvious ROESY cross-peaks observed for **2d**.[a]

Cross-peak	intensity	Cross-peak	intensity
PheNH-AlaMe	w	PheNH-Oxd^{3}Me	w
PheNH-PheHβ	vs	PheNH-COOMe	w
PheNH-PheHα	m	PheNH-Oxd^{3}H4	m
PheNH-Oxd^{3}H5	w	PheNH-PheArH	s
AlaNH-AlaMe	s	AlaNH-COOMe	w
AlaNH-AlaHα	s	AlaNH-TsArH2,6	s
AlaNH-TsArH3,5	w	TsArH2,6-AlaMe	m
TsArH2,6-Oxd^{2}Me	w	TsArH2,6-AlaHα	s
TsArH2,6-OxdH4	w	TsArH3,5-Oxd^{2}Me	s
TsArH3,5-AlaHα	m	PheArH3,5-AlaMe	m
PheArH3,5-COOMe	w	PheArH3,5-PheHα	m
PheArH-Oxd^{3}Me	w	PheArH-COOMe	s
Oxd^{2}H4-TsMe	m	PheHα-AlaMe	w
COOMe-AlaMe	w	COOMe-PheHβ	s
PheHβ-AlaMe	m	TsMe-AlaMe	w
Oxd^{2}Me-AlaMe	w		

[a] Stereochemistry has been omitted; [b] up = upfield, dw = downfield; [c] vs = very strong, s = strong, m = medium, w = weak.

Table 9. Non-obvious ROESY cross-peaks observed for **3b.**[a]

Cross-peak	intensity	Cross-peak	intensity
ΔAbuNH-AlaMe	m	ΔAbuNH-ΔAbuMe	s
ΔAbuNH-AlaHα	vs	ΔAbuNH-AlaNH	s
ΔAbuNH-PheNH	w	ΔAbuNH-TsArH2,6	w
PheNH-Oxd^{3}H5	w	PheNH-PheHβ	vs
PheNH-Oxd^{3}H4	vs	PheNH-PheHα	s
PheNH-PheArH	m	PheNH-AlaNH	w
AlaNH-AlaMe	vs	AlaNH-AlaHα	s
AlaNH-TsArH2,6	w	TsArH2,6-AlaMe	w
TsArH2,6-AlaHα	m	PheArH-COOMe	w
PheArH-PheHβ	vs	PheArH-PheHα	s
PheArH-Oxd^{3}H5	w	ΔAbuHb-Oxd^{3}H4	w
COOMe-PheHβ	m	COOMe-PheHα	w
PheHβ-Oxd^{3}H4	w	COOMe-Oxd^{3}Me	w
ΔAbuMe-TsMe	w	ΔAbuMe-AlaMe	s
ΔAbuMe-Oxd^{3}Me	w		

[a] Stereochemistry has been omitted; [b] up = upfield, dw = downfield; [c] vs = very strong, s = strong, m = medium, w = weak.

Table 10. Non-obvious ROESY cross-peaks observed for **3c**.[a]

Cross-peak	intensity	Cross-peak	intensity
ΔAbuNH-AlaMe	m	ΔAbuNH-ΔAbuMe	s
ΔAbuNH-Oxd^{3}Me	w	ΔAbuNH-AlaNH	vs
ΔAbuNH-ΔAbuHβ	w	ΔAbuNH-TsArH2,6	w
ΔAbuNH-PheNH	w	PheNH-PheArH	m
PheNH-PheHβ(up)	s	PheNH-PheHβ(dw)	w
PheNH-Oxd^{3}H5	m	PheNH-Oxd^{3}H4	s
PheNH-PheHα	s	PheNH-PheArH	m
AlaNH-AlaMe	m	AlaNH-AlaHα	m
TsArH2,6-AlaMe	m	TsArH2,6-AlaHα	s
TsArH2,6-AlaNH	m	TsArH3,5-AlaNH	w
PheArH3,5-Oxd^{3}Me	w	PheArH3,5-PheHβ(up)	w
PheArH3,5-PheHα	w	PheArH2,6-Oxd^{3}Me	w
PheArH2,6-PheHβ(up)	vs	PheArH2,6-PheHβ(dw)	vs
PheArH2,6-Oxd^{3}H5	w	PheArH2,6-PheHα	s
PheHα-PheHβ(dw)	vs	PheHα-PheHβ(up)	s
Oxd3H5-PheHβ(up)	w	COOMe-PheNH	w
COOMe-PheHα	m	COOMe-PheHβ(dw)	w
COOMe-PheHβ(up)	w		

[a] Stereochemistry has been omitted; [b] up = upfield, dw = downfield; [c] vs = very strong, s = strong, m = medium, w = weak.

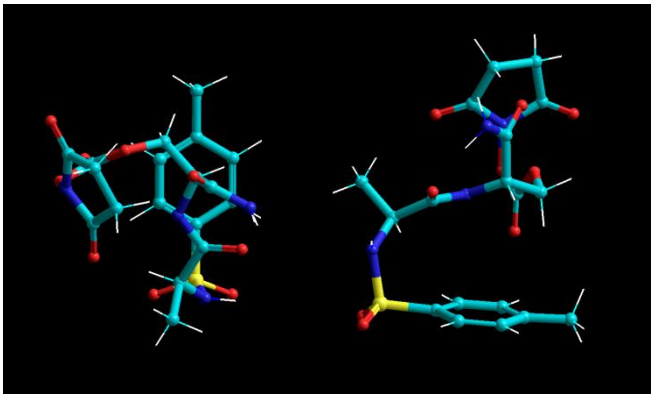

Figure 9. Top (left) and side (right) view of the intermediate anion **A** of Scheme 1, calculated for the cyclization of the model peptide Ts-Ala-Ser-NH_2 with DSC and DIPEA, employing ab initio molecular orbital (MO) theory. A systematic conformational analysis for the structures was done at the HF/6-31G* level. The conformers were re-optimized at the HF/6-31G** level. Backbones are rendered in balls-and-cylinders, hydrogen atoms in sticks. Optimization was performed by conjugate gradient algorithm, convergence at 0.001; energies are expressed in Kcal mol^{-1}. $DIPEAH^+$ was included in the computations, but is not visualized for clarity.

References

[1] W. E. Stites, *Chem. Rev*., **1997**, *97*, 1233.

[2] K. Suat, and S. D. S. Jois, *Curr. Pharm. Des*., **2003**, *9*, 1209; J. D. A. Tyndall, B. Pfeiffer, G. Abbenante, and D. P. Fairlie, *Chem. Rev*., **2005**, *105*, 793 and update(s); J. A. Robinson, *Acc. Chem. Res*., **2008**, *41*, 1278; Y. Che, and G. R. Marshall, *Expert Opin. Ther. Targets*, **2008**, *12*, 101.

[3] For some reviews: A. J. Souers, and J. A. Ellman, *Tetrahedron*, **2001**, *57*, 7431; M. MacDonald, and J. Aubé, *Curr. Org. Chem*. **2001**, *5*, 417; W. A. Loughlin, J. D. A. Tyndall, M. P. Glenn, and D. P. Fairlie, *Chem. Rev*. **2004**, *104*, 6085; A. Perdih, and D. Kikelj, *Curr. Med. Chem*., **2006**, *13*, 1525; R. F. Hirschmann, K. C. Nicolaou, A. R. Angeles, J. S. Chen, and A. B. Smith III, *Acc. Chem. Res*., **2009**, *42*, 1511; R. M. J. Liskamp, D. T. S. Rijkers, J. A. W. Kruijtzer, and J. Kemmink, *Chem. Bio. Chem*., **2011**, *12*, 1626.
For some selected, recent examples: D. Blomberg, M. Hedenstro, P. Kreye, I. Sethson, K. Brickmann, and J. Kihlberg, *J. Org. Chem*., **2004**, *69*, 3500; G. Xuyuan, J. Ying, R. S. Agnes, E. Navratilova, P. Davis, G. Stahl, F. Porreca, H. I. Yamamura, and V. J. Hruby, *Org. Lett*., **2004**, *19*, 3285; U. Rosenström, C. Sköld, G. Lindeberg, M. Botros, F. Nyberg, A. Karlén, and A. Hallberg, *J. Med. Chem*., **2006**, *49*, 6133; A. S. M. Ressurreição, A. Bordessa, M. Civera, L. Belvisi, C. Gennari, and U. Piarulli, *J. Org. Chem*., **2008**, *73*, 652; L. Lomlim, J. Einsiedel, F. W. Heinemann, K. Meyer, and P. Gmeiner, *J. Org. Chem*., **2008**, *73*, 3608; Y. Angell, D. Chen, F. Brahimi, H. U. Saragovi, and K. Burgess, *J. Am. Chem. Soc*., **2008**, *30*, 556; R. Scheffelaar, R. A. K. Nijenhuis, M. Paravidino, M. Lutz, A. L. Spek, A. W. Ehlers, F. J. J. de Kanter, M. B. Groen, R. V. A. Orru, and E. Ruijter, *J. Org. Chem.*, **2009**, *74*, 660; M. Sañudo, M. G. Valverde, S. Marcaccini, J. J. Delgado, J. Rojo, and T. Torroba, *J. Org. Chem.*, **2009**, *74*, 2189; G. Lesma, N. Landoni, T. Pilati, A. Sacchetti, and A. Silvani, *J. Org. Chem*., **2009**, *74*, 8098; J. Y. Lee, I. Im, T. R. Webb, D. McGrath, M. Song, and Y. Kim, *Bioorg. Chem*., **2009**, *37*, 90; A. Mieczkowski, W. Koźmiński, and J. Jurczak, *Synthesis* **2010**, *2*, 221; A. Pinsker, J. Einsiedel, S. Harterich, R. Waibel, and P. Gmeiner, *Org. Lett*., **2011**, *13*, 3502; L. R. Whitby, Y. Ando, V. Setola, P. K. Vogt, Roth, and B. L. Boger D. L. *J. Am. Chem. Soc.*, **2011**, *133*, 10184.

[4] R. De Marco, A. Tolomelli, M. Campitiello, P. Rubini, and L. Gentilucci, *Org. Biomol. Chem.*, **2012**, *10*, 2307.

[5] B. K. Kay, M. P. Williamson, and M. Sudol, *FASEB J.*, **2000**, *14*, 231; A. Zarrinpar, R. P. Bhattacharyya, and W. A. Lim, *Sci. STKE*, **2003**, re8.

[6] J. S. Richardson, and D. C. Richardson, Prediction of Protein structure and the Principle of Protein Conformation, G. D. Fasman. Ed, Plenum Press, New York, **1989**.

[7] D. E. Stewart, A. Sarkar and J. E. Wampler, *J. Mol. Biol.*, **1990**, *214*, 253; M. W. MacArthur and J. M. Thornton, *J. Mol. Biol*., **1991**, *218*, 397; D. K. Chalmers, and G. R. Marshall, *J. Am. Chem. Soc.*, **1995**, *117*, 5927; T. Hoffmann, H. Lanig, R. Waibel, and P. Gmeiner, *Angew. Chem. Int. Ed.*, **2001**, *40*, 3361; K. Wookhyun, R. A. McMillan, J. P. Snyder, and V. P. Conticello, *J. Am. Chem. Soc.*, **2005**, *127*, 18121; H. Bittermann, and P. Gmeiner, *J. Org. Chem.*, **2006**, *71*, 97; A. P. Vartak, and L. L. Johnson, *Org. Lett.*, **2006**, *8*, 983.

[8] W. J. Wedemeyer, E. Welker, and H. A. Scheraga, *Biochemistry*, **2002,** *41*, 14637.

[9] P. Karoyan, S. Sagan, O. Lequin, J. Quancard, S. Lavielle, and G. Chassaing, Substituted Prolines: Syntheses and Applications in Structure-Activity Relationship Studies of Biologically Active Peptides. In: O. A. Attanasi, D. Spinelli Eds, Targets in Heterocyclic Systems-Chemistry and Properties, Royal Society of Chemistry, Cambridge, **2005**; 8: pp 216-273; P. Thamm, H. J. Musiol and L. Moroder, Synthesis of Peptides Containing Proline Analogues. In: Goodman, M. Ed, Methods of Organic Chemistry: Synthesis of Peptides and Peptidomimetics. Georg Thieme Verlag Stuttgart New York **2003**; 22: pp 52-86; for selected examples: J. Samanen, T. Cash, D. Narindray, E. Brandeis, Jr. W. Adams, H. Weideman, T. Yellin, D. Regoli, *J. Med. Chem*., **1991**, *34*, 3036; D. Seebach, T. L. Sommerfeld, Q. Jiang and L. M. Venanzi, *Helv. Chim. Acta*, **1994**, *77*, 1313; E. Beausoleil and W. Lubell, *J. Am. Soc.*, **1996**, *118*, 12902; P. Dumy, M. Keller, D. E. Ryan, B. Rohwedder, T. Wöhr and M. Mutter, *J. Am. Chem. Soc*., **1997**, *119*, 918; M. Keller, C. Sager, P. Dumy, M. Schutkowski, G.S. Fischer and M. Mutter, *J. Am. Soc.*, **1998**, ***120***, 2714; Y. J. Chung, B. R. Huck, L. A. Christianson, H. E. Stanger, S. Krautha1user, D. R. Powell, and S. H. Gellman, *J. Am. Chem. Soc.*, **2000**, *122*, 3995; M. Keller, C. Boissard, L. Patiny, N. N. Chung, C. Lemieux, M. Mutter, P. W. Schiller, *J. Med. Chem*., **2001**, *44*, 3896; M. Doi, A. Asano, E. Komura, Y. Ueda, *Biochem. Biophys, Res. Commun.*, **2002**, ***297***, 138; L. Halab, and D. W. Lubell, *J. Am. Chem. Soc*., **2002**, *124*, 2474; F. Cavelier, B. Vivet, J. Martinez, A. Aubry, C. Didierjean, A. Vicherat, M. Marraud, *J. Am. Chem. Soc*., **2002**, *124*, 2917; J. Quancard, A. Labonne, Y. Jacquot, G. Chassaing, S. Lavielle, P. Karoyan, *J. Org. Chem.*, **2004**, *69*, 7940; P. Grieco, L. Giusti, A. Carotenuto, P. Campiglia, V. Calderone, T. Lama, I. Gomez-Monterrey, G. Tartaro, M. R. Mazzoni and E. Novellino, *J. Med. Chem*., **2005**, *48*, 3153; J. L. Baeza, G. Gerona-Navarro, M. J. Pérez de Vega, M. T. García-López,

R. González-Muñiz, and M. Martín-Martínez, *J. Org. Chem.*, **2008**, *73*, 1704; D. Torino, A. Mollica, F. Pinnen, G. Lucente, F. Feliciani, P. Davis, J. Lai, S.-W. Mad, F. Porreca and V. J. Hruby, *Bioorg. Med. Chem. Lett.*, **2009**, *19*, 4115.

[10] Selected examples: J. Gante, H. Juraszyk, P. Raddatz, H. Wurziger, S. Bernotat-Danielowski, G. Melzer, and F. Rippmann, *Bioorg. Med. Chem. Lett*., **1996**, *6*, 2425; W. Kamm, P. Raddatz, J. Gante, and T. Kissel, *Pharm. Res*., **1999**, *16*, 1527; T. Mittag, K. L. Christensen, K. B. Lindsay, N. C. Nielsen, and T. Skrydstrup, *J. Org. Chem*., **2008**, *73*, 1088; A. Ali, G. S. Reddy, M. N. Nalam, S. G. Anjum, H. Cao, C. A. Schiffer, and T. M. Rana, *J. Med. Chem*., **2010**, *53*, 7699.

[11] G. Luppi, D. Lanci, V. Trigari, M. Garavelli, A. Garelli, and C. Tomasini, *J. Org. Chem*., **2003**, *68*, 1982; G. Luppi, M. Villa, and C. Tomasini, *Org. Biomol. Chem.*, **2003**, *1*, 247; C. Tomasini, G. Luppi, and M. Monari, *J. Am. Chem. Soc.*, **2006**, *128*, 2410; G. Angelici, G. Luppi, B. Kaptein, Q. B. Broxterman, H. J. Hofmann, and C. Tomasini, *Eur. J. Org. Chem*., **2007**, *16*, 2713.

[12] G. Angelici, G. Falini, H. J. Hofmann, D. Huster, M. Monari, and C. Tomasini, *Angew. Chem. Int. Ed*., **2008**, *22*, 8075; G. Angelici, G. Falini, H. J. Hofmann, D. Huster, M. Monari, and C. Tomasini, *Chem. Eur. J.*, **2009**, *15*, 8037.

[13] K. R. Rajashankar, S. Ramakumar, and V. S. Chauhan, *J. Am. Chem. Soc*., **1992**, *114*, 9225; U. Schmidt, A Lieberknecht, and J. Wild, *Synthesis*, **1988**, *3*, 159; A. Polinsky, M. G. Cooney, A. Toy-Palmer, G. Osapay, and M. Goodman, *J. Med. Chem.*, **1992**, *35*, 4185; J. M. Humphrey, and A. R. Chamberlin, *Chem. Rev*., **1997**, *97*, 2243; C. Bonauer, T. Walenzyk, and B. König, *Synthesis*, **2006**, *1*,1; R. Ramapanicker, R. Mishra, and S. Chandrasekaran, *J. Pept. Sci*., **2010**, *16*, 123.

[14] V. Santagada, F. Fiorino, E. Perissutti, B. Severino, V. De Filippis, B. Vivenzio, and G. Caliendo, *Tetrahedron Lett*., **2001**, *42*, 5171; B. Bacsa, K. Horváti, S. Bõsze, F. Andreae, and C. O. Kappe, *J. Org. Chem*., **2008**, *73*, 7532.

[15] T. Połoński, *Tetrahedron*, **1985**, *41*, 603; M. Ousmer, N. A. Braun, C. Bavoux, M. Perrin, and M. A. Ciufolini, *J. Am. Chem. Soc*., **2001**, *123*, 7534; X. Deng, and N. S. Mani, *Green Chem*., **2006**, *8*, 835.

[16] T. Shiraiwa, R. Saijoh, M. Suzuki, K. Yoshida, S. Nishimura, and H. Nagasawa, *Chem. Pharm. Bull*., **2003**, *51*, 1363.

[17] R. Chênevert, M. Létourneau, and S. Thiboutot, *Can. J. Chem*., **1990**, *68*, 960.

[18] P. F. Hughes, S. H. Smith, and J. T. Olson *J. Org. Chem.*, **1994**, *59*, 5799; G. Cardillo, L. Gentilucci, A. Tolomelli, and C. Tomasini *Synlett.*, **1999**, *11*, 1727; S. Armaroli, G. Cardillo, L. Gentilucci, M. Gianotti, and A. Tolomelli, *Org. Lett*., **2000**, *8*, 1105; G. Cardillo, L. Gentilucci, M. Gianotti and A. Tolomelli, *Tetrahedron: Asymmetry*, **2001**, *12*, 563; N. Yoshikawa, and M. Shibasaki, *Tetrahedron*, **2002**, *58*, 8289; K. Koketsu, H. Oguri, K. Watanabe, and Hi. Oikawa, *Org. Lett.*, **2006**, *8*, 4719; D. Crich and A. Banerjee, *J. Org. Chem.*, **2006**, *71*, 7106; S.-H. Baik, and H. Yoshioka, *Biotechnol, Lett*., **2009**, *31*, 443; A. Lemke, M. Büschleb, and C. Ducho *Tetrahedron*, **2010**, *66*, 208; B. Seashore-Ludlow, P. Villo, and P. Somfai, *Chem. Eur. J.*, **2012**, *18*, 7219; R. Rahmani, M. Matsumoto, Y. Yamashita, and S. Kobayashi, *Chem. Asian J*., **2012**, *7*, 1191.

[19] G. Sabitha, B. V. S. Reddy, S. Abraham, and J. S. Yadav, *Tetrahedron Lett*., **1999**, *40*, 1569.

[20] T. Ankner, and G. Hilmersson, *Org. Lett.*, **2009**, *11*, 503.

[21] C. Toniolo, and E. Benedetti, *Crit. Rev. Biochem*., **1980**, *9*, 1; B. Imperiali, R. A. Moats, S. L. Fisher, and T. J. Prins, *J. Am. Chem. Soc.*, **1992**, *114*, 3182; J. Yang, and S. H. Gellman, *J. Am. Chem. Soc*., **1998**, *120*, 9090; I. G. Jones, W. Jones, and M. North, *J. Org. Chem*., **1998**, *63*, 1505; L. Belvisi, C. Gennari, A. Mielgo, D. Potenza, and C. Scolastico, *Eur. J. Org. Chem.*, **1999**, 389.

[22] F. Bernardi, M. Garavelli, M. Scatizzi, C. Tomasini, V. Trigari, M. Crisma, F. Formaggio, C. Peggion, and C. Toniolo, *Chem. Eur. J.*, **2002**, *8*, 2516.

[23] K. D. Kopple, M. Ohnishi, and A. Go, *Biochemistry*, **1969**, *8*, 4087; D. Martin, and H. G. Hauthal, In *Dimethyl Sulphoxide*; Van Nostrand-Reinhold: Wokingham, U.K., **1975**.

[24] J. A. Smith, and L. G. Pease, *J. Mol. Biol*., **1980**, *203*, 221; D. K. Chalmerst, and G. R. Marshall, *J. Am. Chem. Soc*., **1995**, *117*, 5927; J. Venkatraman, S. C. Shankaramma, and P. Balaram, *Chem. Rev*., **2001**, *101*, 3131; R. Rai, S. Raghothama, and P. Balaram, *J. Am. Chem. Soc.*, **2006**, *128*, 2675.

[25] P. A. Temussi, D. Picone, G. Saviano, P. Amodeo, A. Motta, T. Tancredi, S. Salvadori, and R. Tomatis, *Biopolymers*, **1992**, *32*, 367, and references herein; A. Borics, and G. Töth, *J. Mol. Graph. Modell*., **2010**, *28*, 495.

[26] W. D. Cornell, P. Cieplak, C. I. Bayly, I. R. Gould, K. M. Merz, D. M. Ferguson, D. C. Spellmeyer, T. Fox, J. W. Caldwell, and P. A. Kollman. *J. Am. Chem. Soc.*, **1995**, *117*, 5179.

[27] B. Padmanabhan, S. Dey, B. Khandelwal, G. S. Rao, and T. P. Singh, *Biopolymers*, **1992**, *32*, 1271; C. Alemán, and J. Casanovas, *Biopolymers*, **1995**, *36*, 71; R. Jain, and V. S. Chauhan, *Biopolymers*, **1996**, *40*, 105; B. Rzeszotarska, D. Siodlak, M. A. Broda, I. Dybala, and A. E. Koziol, *J. Pept. Res.*, **2002**, *59*, 79.

[28] R. Kuroda, and Y. Saito, Circular Dichroism of Peptides and Proteins. In *Circular Dichroism Principles and Applications*, 2nd ed.; (Eds: N. Berova, K. Nakanishi, R. Woody); Wiley-VCH: New York, **2000**; pp 601-615; O. Pieroni, A. Fissi, R. M. Jain, and V. S. Chauhan, *Biopolymers*, **1996**, *38*, 97; A. Perczel, M. Hollosi, B. M. Foxman, and G. D. Fasman, *J. Am. Chem. Soc*., **1991**, *113*, 9772.

[29] W. L. Jorgensen, J. Chandrasekhar, J. Madura, R. W. Impey, and M. L. J. Klein, *Chem. Phys*., **1983**, *79*, 926.

[30] HyperChem Release 8.0.3, **2007**, Hypercube Inc. 1115 NW 4th St. Gainesville, FL 32608 (USA).

[31] H. J. C. Berendsen, J. P. M. Postma, W. F. van Gunsteren, A. Di Nola, and J. R. J. Haak, *Chem. Phys*., **1984**, *81*, 3684.

Chapter 5

First example of β^2-Freidinger lactam analogs: synthesis and conformational analysis of Amo ring

Constrained peptidomimetic scaffolds are of considerable interest for the design of therapeutically useful analogues of bioactive peptides. In this chapter is presented the single step cyclization of (*S*)- or (*R*)-α-hydroxy-β^2- or α-substituted-α-hydroxy-$\beta^{2,2}$-amino acids already incorporated within oligopeptides to 5-aminomethyl-oxazolidine-2,4-dione (Amo) rings. These scaffolds can be regarded as unprecedented β^2- or $\beta^{2,2}$-*homo* Freidinger lactam analogs, and can be equipped with a proteinogenic side chain at each residue. In a biomimetic environment Amo rings act as inducers of extended, semi-bent or folded geometries, depending on the relative stereochemistry and the presence of α-substituents.

5.1. Introduction

Although native biologically active peptides have a great potential for medical and biotechnological applications,[1] their utility is reduced by severe inherent limitations, in particular poor stability against proteolytic breakdown and scarce biodistribution and bioavailability properties.[2] Besides, peptides tend to be quite flexible, and conformations are highly dependent on environment, leading to modest receptor selectivity. These issues have been addressed by the design of highly stable and conformationally constrained peptidomimetics,[1,2] i.e. compounds whose pharmacophoric and stereostructural elements mimic the bioactive structure of the parent peptides.[3]

One approach to obtaining more rigid peptidomimetics[1-3] is to incorporate local constraints using conformationally restricted amino acid units or modified peptide backbones. Global constraints are introduced for instance *via* cyclization or by replacing portions of the peptides with non-peptide structures. In this context, large effort has been dedicated to design scaffolds mimicking turn structures. β-Turns are common motifs in peptide structures (Figure 1), and very often are critical to peptide conformational stability and many interactions correlated to a variety of biological processes.[3,4] Native β-turns involve four residues with Cα(*i*) to Cα(*i+3*) distances of less than 7.0 Å, and form a hydrogen-bond C=**O**(*i*)· · ·**H**-N(*i+4*) (1->4-type).[5] As a consequence, small scaffolds which reproduce these features have been extensively investigated to discover compounds that can mimic or disrupt turn-mediated recognition events.[6] For instance, the prototypic Freidinger lactam dipeptides[2,4,7] have been widely used to constrain peptide conformations, stabilizing turn structures and acting as strand inducers (Figure 1).[8]

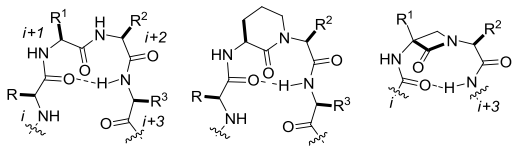

Figure 1. Sketch of a β-turn, a classic Freidinger lactam, and the α-amino-β-lactam approach.

However, the scaffold-strategy resulted in limited success with bioactive peptide ligands where the non-peptide or pseudopeptide scaffold itself contains most of the pharmacophore elements.[3,6] Frequently, the side chains at some fundamental positions are not maintained, or one of the amino acids is omitted on the basis of the hypothesis that some residues play a structural rather than a recognition role, e.g. Pro or Gly at position *i+1* of a β-turn.[6,9] Therefore, the structures of the turn mimetics may lack some relevant pharmacophores for specific targets. An example is represented by the early Freidinger lactams, (Figure 1) obtained by sacrificing the *i+1* side chain with the formation of 5- to 8-membered rings. To overcome this limit, many efforts have been dedicated to the preparation of α-substituted lactams;[10] for instance, Palomo et al. proposed the separation of constraint and recognition elements, and introduced a α-alkyl-α-amino-β-lactam rings placed at the position *i+1* residue as potent nucleators of β-turns (Figure 1).[11]

Besides, the preparation of the constrained mimetics may require multi-step procedures, resulting in low overall yields, and many synthetic methods lack flexibility and are therefore not suited to introduce diversity.[6] As a consequence, the development of a expedient procedure to constrain a peptide while maintaining all of the pharmacophores is of considerable interest.

During my thesis work, we have been interested in the rapid and simple ring closure of β-hydroxy-α-amino acids into turn-inducer scaffolds. In the previous chapter is illustrated that the reaction of *N*-arylsulfonyl-peptides containing L- or D-configured Ser and/or other β-hydroxy-α-amino acids (Thr, PhSer), with *N,N′*-disuccinimidyl carbonate (DSC) and a catalytic amount of DIPEA, gave rise in a single step to the formation of oxazolidinone (Oxd) ring(s) (Scheme 1).[12] Under the same

conditions, the corresponding Fmoc- or Boc-peptides gave elimination to dehydroalanine, in agreement to the literature,[13] suggesting that the *N*-sulfonyl group effectively promoted the cyclization.

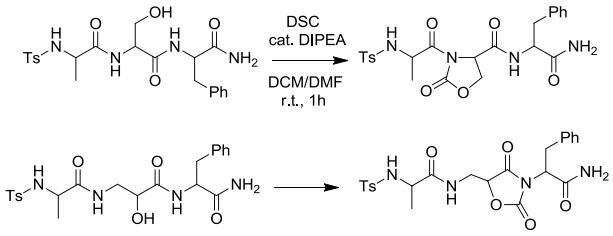

Scheme 1. Reaction of peptides containing Ser (top) or *iso*Ser (bottom) with DSC.

Another part of this project is been the development of a single step procedure to lock the geometry of a oligopeptide by cyclization of α-hydroxy-β^2-amino acids or α-substituted-α-hydroxy-$\beta^{2,2}$-amino acids, already present in the sequence, to 5-aminomethyloxazolidine-2,4-dione rings (Amo). These unusual heterocyclic scaffolds (Scheme 1 and Figure 2) can be regarded as β^2- or $\beta^{2,2}$-*homo* variants of a classic Freidinger lactam and can be equipped with a side chains at each α-position.

5.2. Results and Discussion

5.2.1. Synthesis

On repeating the same protocol of Scheme 1 on a peptide containing the α-hydroxy-β^2-amino acid *iso*Ser, we observed, not totally unexpected, a different outcome: the reaction gave exclusively the cyclization to 5-aminomethyloxazolidine-2,4-dione (Amo) comprising *iso*Ser and the following amino acid (Scheme 1). To our knowledge, this peptide represents the first example of conformationally constrained peptide containing a oxazolidine-2,4-dione scaffold; in general, this heterocycle has been described and utilized very few times in organic or medicinal chemistry.[14]

Under the structural point of view Amo can be regarded as a novel constrained β^2-amino acid. Among the β-amino acids, the β^2-amino acids are less synthetically feasible respect to their β^3-counterparts (Figure 2).[15] Besides, the cyclic structure of Amo, achieved *via* acylation of the backbone nitrogen atom, embraces two consecutive amino acids, therefore introducing a global constraint of C(*i*)-N(*i+1*)-type[3a] in the sequence. This kind of short range cyclizations[16] can significantly reduce the conformational space accessible to the peptide segment in which they are incorporated. In this perspective, the Amo ring can be regarded as a novel β^2-*homo*-analogue of a Freidinger lactam (Figure 2).[17] Structures combining the conformational properties of the Freidinger lactams with the stability of the β-amino acids have been the subject of much interest by Gmeiner and co. and some other groups;[18] however, in all cases the reported structures were β^3-*homo* variants of Freidinger lactams (Figure 2).

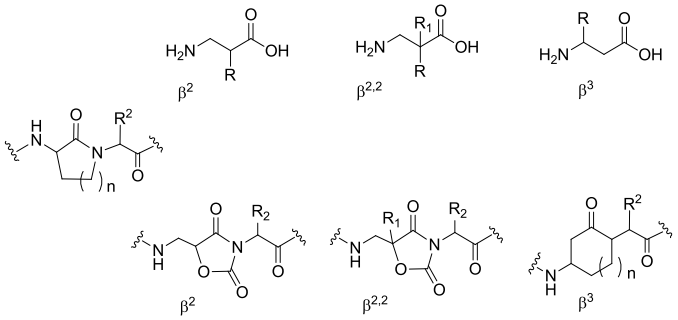

Figure 2. Structures of β^2-, $\beta^{2,2}$-, and β^3-amino acids (top), and comparison of a classic Freidinger lactam composed of all α-amino acids (middle), with the β^2- and $\beta^{2,2}$-*homo* Amo variants, and with a Gmeiner's β^3-*homo* lactams[18] (bottom).

Finally, the Amo-Phe sequence of Scheme 1 might also represent a constrained dipeptide unit composed of β^2 and α residues, of potential interest for the design of α/β-hybrid foldamers[19] showing unprecedented secondary structures (see also the section "Conformational properties"). Indeed, unexpected conformational effects have been often observed when β^2-amino acids were present in the backbone instead of the more common β^3 residues.[15a]

This potential interest prompted us to exploit the cyclization to prepare oligopeptide sequences containing the unusual scaffold under different reaction conditions. Accordingly, we prepared a mini-library of di-, tri- or tetrapeptides containing (*S*)- or (*R*)-configured *iso*Ser, equipped with different groups at the *N*-terminus, amide or ester at the *C*-terminus (Scheme 2), and we reacted these peptides with different carbonates or dicarbonates, in solution (Scheme 3, Table 1) or in the solid phase (Scheme 4, Table 1).

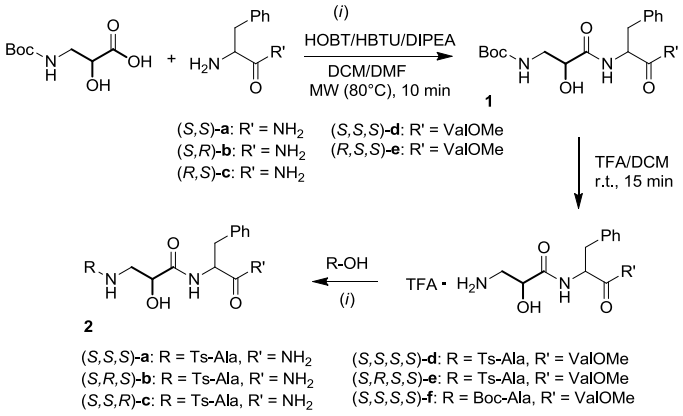

Scheme 2. Synthesis of *iso*Ser-containing peptides **1** and **2.**

The dipeptide Boc-*iso*Ser-PheNH$_2$ (**1a**) was prepared in solution by coupling Boc-*iso*SerOH and H-PheNH$_2$ under MW irradiation,[20] using HBTU/HOBt/DIPEA as activating agents (Scheme 2, *i*). Boc-*iso*SerOH[21] was prepared according to the literature. The *iso*Ser building block was incorporated without a protection for the OH function. Under these reaction conditions,[12] the acylation of the OH-function and thus the formation of a depsipeptide side product was not observed, as confirmed by the ^{1}H NMR and RP-HPLC MS analyses of the crude reaction mixture. After purification by flash chromatography over silica gel, **1a** was utilized for the following cyclization step (Scheme 3, Table 1).

By using the same protocol, Boc-*iso*SerOH and (*R*)-H-PheNH$_2$ gave **1b**, while (*R*)-Boc-*iso*SerOH[21] and H-PheNH$_2$ gave **1c**. The tripeptides **1d** and **1e** were prepared from Boc-*iso*SerOH and H-Phe-ValOMe (**1d**), or (*R*)-Boc-*iso*SerOH and H-Phe-ValOMe (**1e**). The crude **1b-e** were analysed by RP-HPLC MS and utilized as intermediates for the preparation of longer sequences without further purifications. The dipeptide H-Phe-ValOMe was prepared in turn from Boc-Phe-ValOMe,[22] by treatment with 25% TFA in DCM. The same conditions were utilized for Boc deprotection of the di- or tripeptides **1a-e** (Scheme 2).

The peptide-TFA salts from **1a-e** were subjected to coupling with Tosyl (Ts)-AlaOH under the above described conditions, giving the corresponding tri- or tetrapeptides **2a-e** (Scheme 2). Ts-AlaOH was prepared as described in the literature.[23] Finally, the tetrapeptide **2d** was obtained from **1d** and Boc-AlaOH. The tri- or tetrapeptides **2a-f** were isolated by flash chromatography over silica gel, and their structures were assigned by ^{1}H NMR and HPLC-MS.

The reaction of the Ts-tripeptides **2a**, **b** containing (*S*)- or (*R*)-*iso*Ser, and of the diastereoisomeric **2c**, with DSC and DIPEA for 1 h in DCM/DMF gave the corresponding Amo-peptides **3a-c** with excellent yields (Scheme 3, Table 1, entries 1-3). Other carbonates or dicarbonates gave inferior results (Table 1: entry 4, triphosgene 55%; entry 5, Boc$_2$O traces; entry 6, CDI 70%). Good yields were obtained with DSC for the synthesis of tetrapeptides **3d-f** having Val methyl ester at the *C*-terminus (entries 7 to 9), and for the minimalist dipeptide Boc-Amo-PheNH$_2$ **3g** (entry 10).

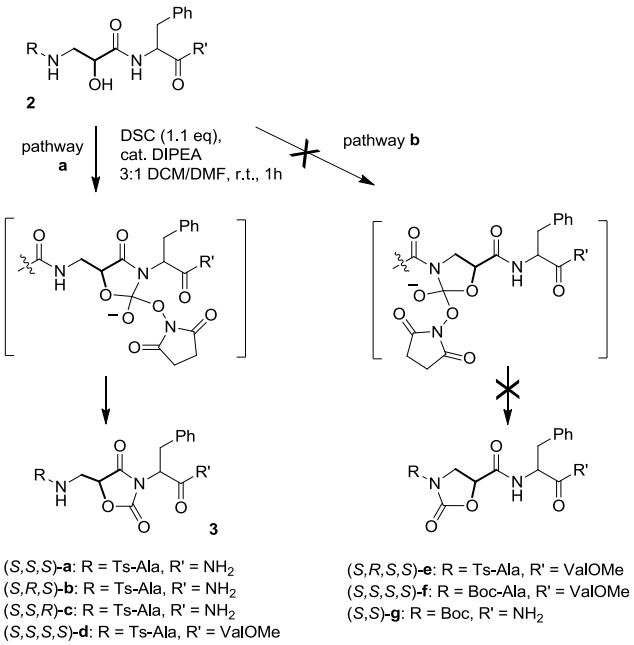

Scheme 3. Regioselective cyclization of *iso*Ser-containing peptides **2** to Amo-peptides **3**.

Different protecting groups at the *N*-terminus such as Boc (entries 9 and 10) and Ac (entry 11), gave results very close to Ts. Clearly, for the comparatively simpler cleavage, carbamate protecting groups represent the most obvious choice.[24] Nevertheless, the literature reports several methods for the mild cleavage of arylsulfonyl groups.[24,25] Recently, we successfully removed the Ts group from peptides containing the Oxd ring with iodotrimethylsilane,[12,26] while the treatment with SmI_2-pyrrolidine-water[27] was less efficient.

Table 1. Cyclization of peptides **1a** and **2** containing *iso*Ser to Amo-peptides **3.**

Entry	**1/2**	R	*isoSer*	*Phe*	R'	carbonate	**3**	(%)[a]
1	**2a**	Ts-Ala	*S*	*S*	NH_2	DSC	**a**	93
2	**2b**	Ts-Ala	*R*	*S*	NH_2	DSC	**b**	90
3	**2c**	Ts-Ala	*S*	*R*	NH_2	DSC	**c**	93
4	**2a**	Ts-Ala	*S*	*S*	NH_2	triphosgene	**a**	55
5	**2a**	Ts-Ala	*S*	*S*	NH_2	Boc_2O	**a**	traces
6	**2a**	Ts-Ala	*S*	*S*	NH_2	CDI	**a**	70
7	**2d**	Ts-Ala	*S*	*S*	ValOMe	DSC	**d**	90
8	**2e**	Ts-Ala	*R*	*S*	ValOMe	DSC	**e**	93
9	**2f**	Boc-Ala	*S*	*S*	ValOMe	DSC	**f**	91
10	**1a**	Boc	*S*	*S*	NH_2	DSC	**g**	91
11	**2h**[b]	Ac-Ala	*S*/*R*	*S*	Phe-Wang	DSC	**h**[c]	80[d]

The Ac-peptide **2h** was prepared as a mixture of diastereoisomers from racemic *iso*Ser (not protected at the OH function) by solid-phase synthesis (Scheme 4). *N*-Fmoc-protected amino acids were coupled on a standard Wang resin with HBTU/HOBt/DIPEA under MW irradiation (45°C).[12] Fmoc deprotection was performed with 20% piperidine in DMF under MW irradiation. The resulting resin-bound peptide Ac-Ala-(*S*/*R*)-*iso*Ser-Phe-Wang was then utilized for the following cyclization prior to cleavage by treatment with a moderate excess of DSC (3 equiv.) and DIPEA (1 equiv.) in 4:1 DCM/DMF for 2 h. The cleavage from resin was performed with TFA in DCM in the presence of scavengers.
Analysis of the crude reaction mixture by RP-HPLC and ESI-MS revealed the presence of the two diastereomeric Amo-peptide acids Ac-Ala-(*S*/*R*)-Amo-PheOH (**3h**) in 1:1 ratio, recovered in very satisfactory yield (80%, based on an average resin loading of 0.6 mmol/g) after semipreparative RP-HPLC (General Methods).

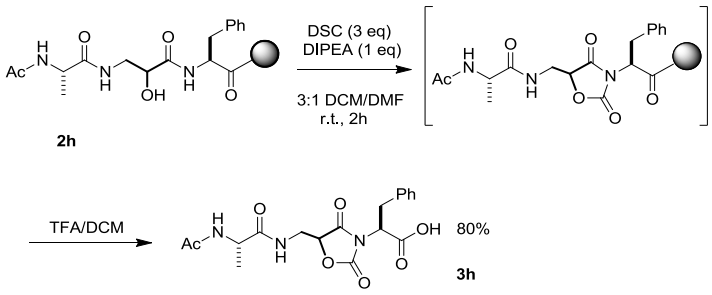

Scheme 4. Solid-phase synthesis of Ac-tripeptides **3h**.

In all cases, epimerization during the cyclization of **2a**-**h** was excluded on the basis of the NMR and HPLC analyses, including the HPLC on a chiral stationary phase (see General Methods).
The structure of the ring closing products **3** was readily determined by ^{1}H NMR and gCOSY. The disappearance of the PheNH resonance in the ^{1}H NMR-spectrum, a significant downfield shift of PheHα, and the loss of the PheHα-PheNH coupling constant, accounted for the acylation of the adjacent Phe nitrogen. On the contrary, the proton pattern of the *iso*Ser residue was maintained (apart from OH group), while the resonances of the Ala residue were practically unaffected.
In principle, the cyclization of the *iso*Ser residue with DSC could give rise also to the formation of a oxazolidin-2-one (Oxd) ring (Scheme 3, path **b**); this was obtained as the only product in peptides containing Ser (Scheme 1) or other β-hydroxy-α-amino acids. The concomitant formation of traces of oxazolidinones by alternative cyclization was excluded on the basis of the HPLC, MS, and ^{1}H NMR analyses of the crude reaction mixtures. Apparently, all reactions of **2a**-**h** proceeded with complete regioselectivity giving exclusively the Amo ring. This observation prompted us to verify whether the ring closure to Oxd would occur when the former would be prevented by choosing sarcosine (Sar, *N*-methylglycine), as the *C*-terminal amino acid. Consequently, we synthesized the tripeptide Ts-Ala-*iso*Ser-SarNH_2 (**2i**), and we attempted the cyclization reaction under the same conditions as before (Scheme 5). In effect, after 1h the cyclization to the corresponding peptide Ts-Ala-Oxd-SarNH_2 (**4**) was observed, albeit in low yield (25%) compared to the Amo-peptides **3**, the rest being the intermediate *iso*Ser-*O*-carbonate. The yield was improved to 55% by using 1 equiv. of DBU (1,8-diazabicyclo[5.4.0]undec-7-ene) instead of catalytic DIPEA, an excess of DSC (3 equiv.), higher temperatures (40ºC), and prolonged reaction times (6h). Apparently, the cyclization to Amo **3** seems to be favored respect to the alternative cyclization to Oxd **4**.

Scheme 5. Reaction of sarcosine-containing **2i** to Oxd-peptide **4.**

Presumably, the cyclization to Amo proceeds *via* the five-membered anionic intermediate with endocyclic C=O (Scheme 3, path **a**, and Scheme 8). The loss of 2,5-dioxopyrrolidin-1-olate leaving group, rapidly protonated by $DIPEAH^+$, leads to the Amo-peptide **3** and DIPEA, which can be utilized in catalytic amount. The detailed study of the reaction mechanism is beyond the scope of this work. Preliminary computations (Scheme 8) suggested that the intermediate with endocyclic C=O is significantly more stable than the alternative intermediate with hexocyclic C=O (Scheme 3, path **b**), precursor of the Oxd.
The Amo ring proved to be remarkably stable when dissolved in common organic solvents and in water. On the other hand, it was reported in the literature that the carbamate increased the reactivity of the inner peptide bond towards reduction by $NaBH_4$.[14] Accordingly, **3b** was regioselectively reduced at the position 4 of the 5-membered ring in very satisfactory yield,

giving exclusively the 4-hydroxy-5-aminomethyl oxazolidin-2-one **5** in *trans* relative stereochemistry (Scheme 6). The *trans*-relationships between the two substituents was substantiated by the very small coupling constant $J_{H4\text{-}H5}$ in the ^{1}H NMR spectra. 4,5-Disubstituted *trans*-oxazolidin-2-ones are characterized by coupling constants much lower than that of the *cis*-stereoisomers[28] (equilibrium between anomers was not observed).

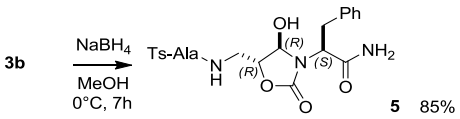

Scheme 6. Regio and stereoselective reduction of the Amo ring.

The ring closure to Amo ring was made possible by the sacrifice of the OH group of the α-hydroxy-β^2-amino acid *iso*Ser. Therefore, Amo represents a constrained β^2-amino acid deprived of a side chain.[15] For this reason, we exploited the opportunity to utilize α-substituted-α-hydroxy-β^{2,2}-amino acids for preparing Amo-derivatives carrying a explicit proteinogenic side chain. The *iso*Ser derivatives are interesting members of the β^2-amino acid family present in many bioactive compounds, e.g. Taxol, bestatin, protease inhibitors, etc., therefore several synthetic protocols have been developed for their synthesis in optically active form, including asymmetric catalysis, enzymatic resolution, and the use of chiral auxiliaries and building blocks.[15,29]

As a prototype for a side chain substituted amino acid surrogate, we prepared the model non-racemic (*S*)- or (*R*)-α-methyl-*iso*Ser from a keto ester and nitromethane, using an adaptation of the catalytic enantioselective Henry reaction reported by Jørgensen, Scheme 5.[30] Methyl pyruvate was reacted with nitromethane in the presence of Cu(II), TEA, and (*R*)- or (*S*)-*t*-Bu-bisoxazoline (Box), giving in high yields (*S*)- or (*R*)-configured β-nitro-α-hydroxy ester **6a** or **6b**, respectively.[31] The reduction of the nitro group gave the (*S*)- or (*R*)-β^{2,2}-amino ester **7a**[32] or **7b**, and the coupling with the other residues under MW irradiation and standard coupling agents gave the linear homochiral tetrapeptide **9a** or the heterochiral **9b**, respectively. The treatment with DSC and the base afforded the β^{2,2}-*homo* Freidinger lactam analogues **10a** and **10b** bearing a substituent at each α-position, Scheme 7.

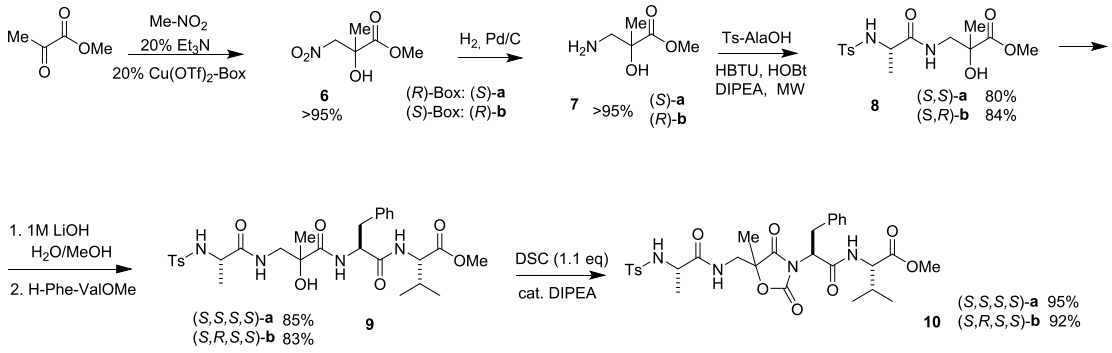

Scheme 7. Synthesis of peptides **10** containing the (*S*)- or (*R*)-configured 5-methylAmo scaffold.

5.2.2. Conformational properties

For the novelty represented by the Amo scaffolds which incorporate (*S*)- or (*R*)-β^2- or a β^{2,2}-amino acid, we decided to investigate the conformations of the Amo-containing tetrapeptides. Indeed, it is well known that the introduction of a β^2-residue in a peptide sequence can lead to secondary structures quite different from that of sequences composed of all α-residues.[15,19,33]

Hofmann et al. have investigated by systematic theoretical analyses the intrinsic conformational preferences of Ac-β-amino amide monomers carrying single or multiple substitutions at the Cα and Cβ backbone atoms. The most stable conformations were found to be different types of six- and eight-membered ring hydrogen bonded structures (C6, C8) corresponding to gauche rotamers around the Cα-Cβ bond, a feature which is expected to promote local folding when incorporated into peptides.[33d,i]

In a similar way, initially we performed theoretical studies to analyze the conformational preferences of representative models of unsubstituted and α-substituted Amo monomers, that we identified in the structures Ac-3-methylAmo (**11a**) and Ac-3,5-dimethylAmo (**11b**). According to the convention of Banerjee and Balaram,[33a] the soft torsional degrees of freedom in

a β-amino acid are defined as ϕ (N-Cβ), θ (Cβ-Cα), and ψ (Cα-C=O), respectively (Figure 3). It is apparent that the central torsion angle θ represents the most relevant geometric variable of Amo monomers.

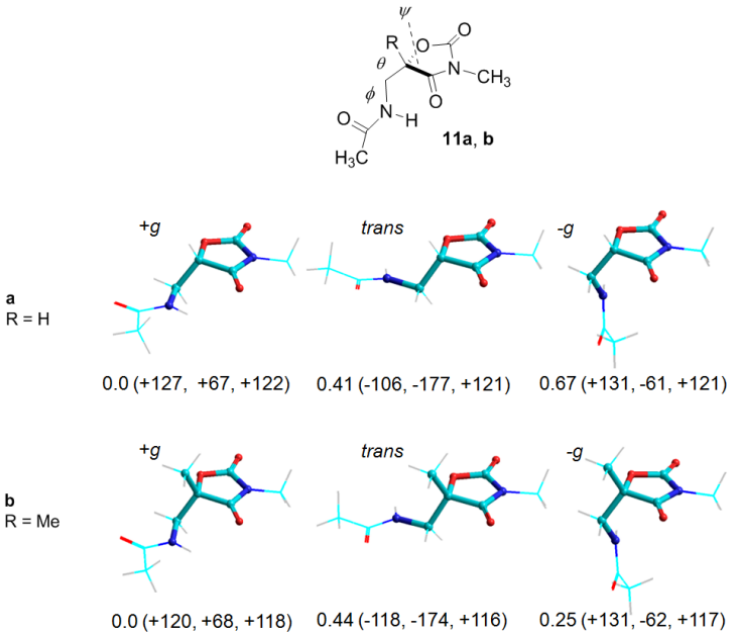

Figure 3. Minimum-energy conformations and relative energies of the *+g*, *trans*, and *-g* rotamers around the central backbone dihedral angle θ of model compounds **11a** and **11b**. A systematic conformational analysis around ϕ and θ was performed in gas-phase employing DFT; ΔE are given in kcal/mol; ϕ, θ, and ψ, are given into brackets in degrees; Amo is rendered in balls and cylinders, the rest in sticks.

The relative energies of the minimum-energy conformations of the *+g*, *trans*, and *-g* rotamers around angle θ of **11a** and **11b** have been estimated in the gas-phase with the aid of theoretical studies,[34] employing the density functional theory. The calculated relative energies in increasing order were: for **11a**, *+g* < *trans* < *-g*; for **11b**, *+g* < *-g* < *trans* (Figure 3). For both structures the global minimum was a *+g* conformer of θ, which is consistent with the calculated geometries reported in the literature for β[2]- and disubstituted β[2,2]-amino acids, albeit the rigid angle ψ prevents the formation of the commonly observed 6-membered hydrogen bonded pseudocycles (C6).[33] For **11a**, the *-g* conformer was by far the less stable. On the other hand, the presence of the methyl substituent at the position 5 of the Amo ring in **11b** strongly reduced the ΔE between the *+g* global minimum and the *-g* rotamer, while the ΔE of the *trans* geometry was slightly higher (Figure 3).

It is plausible that the geometric preferences of the Amo monomers could impact the conformations of Amo-containing oligopeptides. The computations indicated that the introduction of a bulk at the position α of the scaffold should increase the population of folded structures compared to unsubstituted Amo (Figure 3), since in the former the more extended *trans* rotamer was the least stable. Likely, when a α-substituted Amo scaffold as **11b** is inserted into a peptide, the preponderance of *+g* and *-g* rotamers should consent to further stabilize folded geometries by intra-molecular hydrogen-bonding. In oligomers, the occurrence of inter-residue hydrogen bonds or other interactions between monomers may significantly influence the stability relationships between competing alternatives, albeit they are not the main driving force for the formation of the corresponding conformers themselves.[19,33] Besides, polar solvents are expected to have a influence on the stability and conformation of molecules, and generally tend to reduce the ΔE between conformers.[33]

In order to experimentally determine the conformations of oligomers containing the Amo scaffolds, we performed a conformational analysis by NMR spectroscopy of the model tetrapeptides **3d** and **3e**, which include the unsubstituted (*S*)- or (*R*)-configured Amo scaffold, respectively, and **10a** and **10b** containing (*S*)- or (*R*)-5-methylAmo. To gain more information, analyses were occasionally performed on other Amo-peptides. The ^{1}H NMR of the model compounds were recorded either in $CDCl_3$ or in 8:2 [D_6]DMSO/H_2O; [D_6]DMSO or mixtures of [D_6]DMSO and H_2O have been recommended by several authors as excellent representatives of biological fluids.[35] The spectra showed a single set of resonances, suggestive of conformational homogeneity or a rapid equilibrium between conformers.

In 100% $CDCl_3$ amide protons that are hydrogen bonded are found downfield respect to non bonded protons. For all Amo-oligopeptides, the chemical shifts of the amide protons appeared in the order AmoNH > ValNH > AlaNH. In particular, the

all-(*S*)- sequences **3d** and **10a** showed AmoNH resonances > 7.0 p.p.m., suggesting that these amide proton were bonded to a significant extent.

The occurrence of intramolecular hydrogen bonding was deduced by analyzing the variations of the NH chemical shifts upon addition of increasing percentages of $[D_6]$DMSO to solutions of the compounds in $CDCl_3$ (Figure 4).

During the titration of **3e** and **10b** AlaNH and AmoNH exhibited a moderate downfield shift, while ValNH was much more sensitive. For **3d**, AmoNH was significantly less sensitive than AlaNH and ValNH. On the other hand, for **10a** the chemical shifts of AlaNH and ValNH showed a marked variation, while that of AmoNH remained practically constant and is therefore less accessible. This suggested that in **10a** AmoNH could be involved in a H-bond.[36]

To gain more information, also the tripeptide **3a** and **3c** were analyzed by titration experiments (Figure 5). They both behaved as the tetrapeptides **3d** and **10a**, namely showing AmoNH possibly involved in a hydrogen bond, this observation reasonably excluding ValOMe as H-bond acceptor in the tetrapeptides. The reversal of configuration of the residue 3, from (*S*) in **3a** to (*R*) in **3c**, seemed to be well tolerated.

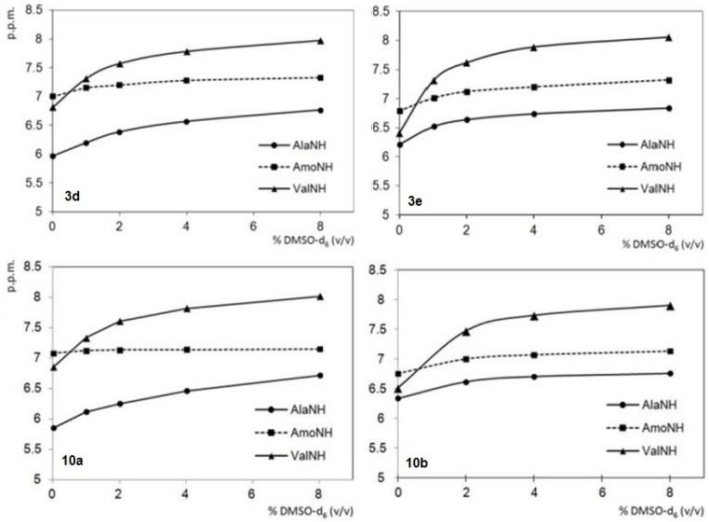

Figure 4. Titration experiments: variation of NH proton chemical shift (p.p.m.) of 2 mM **3d**, **3e**, **10a**, and **10b** in $CDCl_3$ as a function of increasing $[D_6]$DMSO (% v/v).

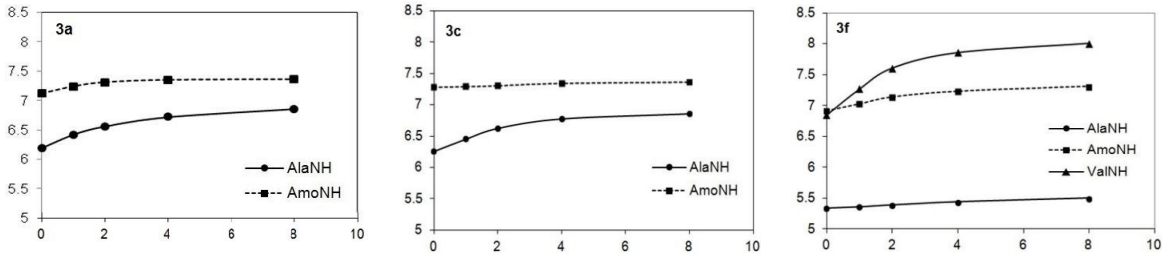

Figure 5. Titration experiments: variation of NH proton chemical shift (p.p.m.) of 2 mM **3a**, **3c**, **3f**, in $CDCl_3$ as a function of increasing $[D_6]$DMSO (from 0 to 8 % v/v).

Variable temperature (VT) NMR experiments were used to detect if amide protons were involved in intramolecular hydrogen bonding or are solvent exposed. The analyses were performed in $CDCl_3$ and 8:2 $[D_6]$DMSO/H_2O (Table 1). In $CDCl_3$, **3e** and **10b** showed comparatively lower $\Delta\delta/\Delta t$ values for ValNH respect to AlaNH and AmoNH (for **3e**, $\Delta\delta/\Delta t$ = -0.5 p.p.b./K; for **10b**, $\Delta\delta/\Delta t$ = -1.0 p.p.b./K),[37] suggestive of a preference for conformations having hydrogen bonded ValNH ($|\Delta\delta/\Delta t|$ < or close to 2.0 p.p.b./K). For **3d** and **10a**, the $\Delta\delta/\Delta t$ parameters in $CDCl_3$ did not allow clear deductions. In $[D_6]$DMSO/H_2O, the $\Delta\delta/\Delta t$ parameters of **3d**, **3e**, and **10b** did not reveal any H-bonded amide proton. On the contrary, for **10a** the chemical shift of AmoNH was significantly less sensitive to increasing temperature ($\Delta\delta/\Delta t$ in $[D_6]$DMSO/H_2O = -2.1 p.p.b./K), indicating a plausible conformation having this amide proton involved in a hydrogen bond.

Table 2. Δδ/Δt values (p.p.b./K) for the amide protons of **3d**, **3e**, **10a**, **10b**, in $CDCl_3$ or 8:2 $[D_6]DMSO/H_2O$.

compd	solvent	AlaNH	AmoNH	ValNH
3d	$CDCl_3$	-5.1	-4.9	-2.9
	8:2 $[D_6]DMSO/H_2O$	-7.0	-6.3	-4.5
3e	$CDCl_3$	-7.0	-4.0	-0.5
	8:2 $[D_6]DMSO/H_2O$	-7.0	-6.6	-5.0
10a	$CDCl_3$	-4.2	-4.1	-2.4
	8:2 $[D_6]DMSO/H_2O$	-6.8	-2.1	-4.7
10b	$CDCl_3$	-6.7	-3.9	-1.0
	8:2 $[D_6]DMSO/H_2O$	-7.1	-5.8	-4.5

Table 3. Δδ/Δt values (p.p.b./°K) for the amide protons of peptides **3a**, **3b**, **3c**, **3f**, **5**, in $CDCl_3$.

Compd	sequence	AlaNH	AmoNH	ValNH	$CONH_2$
3a	Ts-Ala-(S)-Amo-$PheNH_2$	-15.1	-8.1	-	-14.3/-9.7
3b	Ts-Ala-(*R*)-Amo-$PheNH_2$	-8.6	-6.2	-	-8.6/-8.0
3c	Ts-Ala-(S)-Amo-(*R*)-$PheNH_2$	-8.4	-6.0	-	-7.7/-9.5
3f	Boc-Ala-(*S*)-Amo-Phe-ValOMe	-4.5	-5.0	-4.5	-
5	Ts-Ala-(*R*)-5-hydroxyAmo-$PheNH_2$	-14.7	-10.0	-	-13.7/-11.0

The model compounds were analyzed by 2D-ROESY. In $CDCl_3$ the spectra displayed a modest number of non-obvious inter-residue cross-peaks (not shown), which was indicative of conformational freedom. On the contrary, in the biomimetic 8:2 $[D_6]DMSO/H_2O$ the spectra were much more satisfactory, and revealed meaningful inter-residue cross-peaks.

Very often, changes in solvent composition cause meaningful changes in the shape of the peptides. Generally, apolar solvents such as chloroform are expected to increase hydrogen bonding, due to the absence of competitive solvation of donors and acceptors by individual solvent molecules.[19,36-38] Apparently, for the Amo-tetrapeptides, VT NMR and titration experiments in chloroform differently supported the possible existence or not of hydrogen bonds, accounting for a scarce conformational definition, as suggested also by ROESY analyses. This behavior was investigated and confirmed by means of FT-IR spectroscopy and Electronic Circular Dichroism (ECD) in a non competitive solvent (DCM).

FT-IR spectroscopy in DCM was utilized to analyze the amide stretching regions. Normally, non bonded amide protons show a peak above 3400 cm^{-1}, while bonded amide NH exhibit a peak below 3400 cm^{-1}.[39] The spectra of each tetrapeptide showed a peak > 3400 cm^{-1} and one or more peaks < 3400 cm^{-1} (Figure 6), indicative of equilibria between non bonded and multiple bonded structures.

The compounds were dried in vacuo, and all the sample preparations were performed under nitrogen atmosphere. All infrared spectra were obtained for 1 mM solutions in dry DCM at 297 °K at 2 cm^{-1} resolution, using a 1 mm NaCl solution cell and a FT-IR spectrometer (64 scans). (Figure 6).

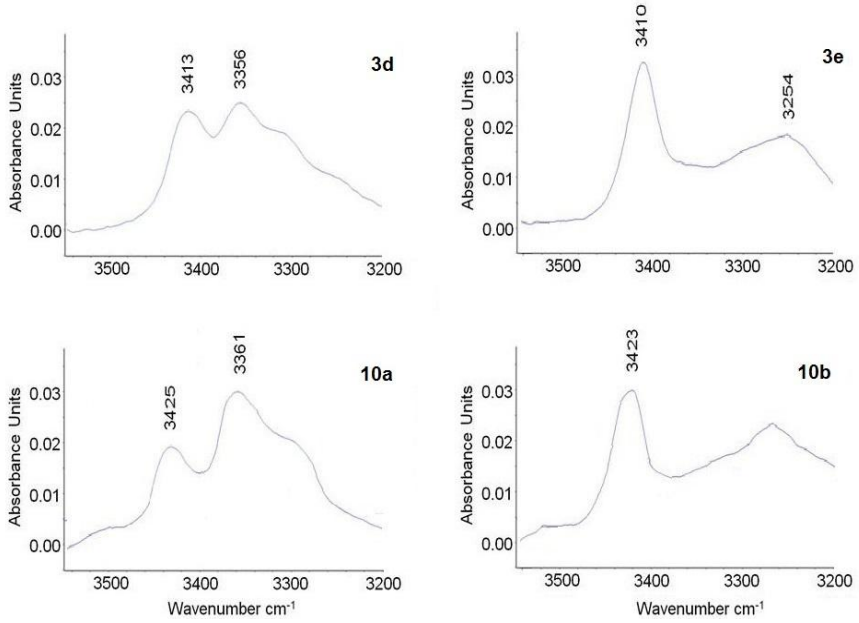

Figure 6. Amide NH stretching regions of the IR absorption spectra for samples of 2 mM **3d**, **3e**, **10a**, and **10b** in DCM at r.t.

Electronic Circular Dichroism (ECD) is a widely used technique for studying protein and peptide conformations. This technique is intrinsically a low-resolution method; however, it can furnish qualitative information on the presence of ordered secondary structures, although not too many examples on short peptides are reported.[40] ECD spectra of the model tetrapeptides in DCM (Figure 7) showed a smooth negative band centered at about 240 nm. This observation could be compatible with the occurrence of non-classic β-turns, since the n-π* band of the latter generally appear near 225 nm.[40]
ECD spectra were recorded from 200 to 400 nm at 25 °C. 1 mM solutions were made up in spectral grade solvents and run in a 0.1 cm quartz cell (Figure 7). Data are reported in molar ellipticity [θ] (deg cm^2 $dmol^{-1}$).

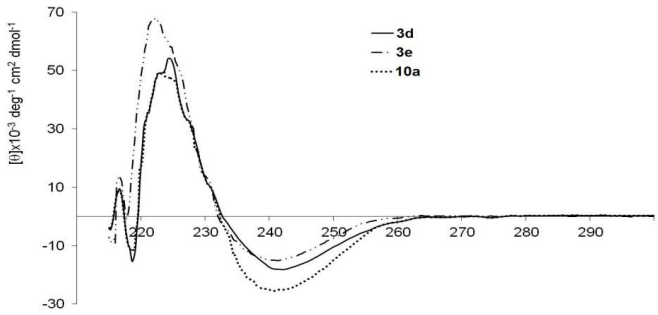

Figure 7. ECD spectra of **3d**, **3e, 10a,** and **10b** recorded in DCM at r.t.; **3d** and **10b** are practically superimposed.

Plausibly, the results of the various experiments in non competitive environments reflected the existence of equilibria between diverse hydrogen bonded and non-bonded structures, as well as distorted or weak intra-residue hydrogen bonds, which can be observed in peptides composed of α- and β-residues.[19,33,41] On the other hand, in DMSO/water the analyses gave clues of higher conformational homogeneity. It has been demonstrated that cryoprotective mixtures of high viscosities, such as DMSO/water, showed a remarkable ability to favor compact structures representative of the bioactive conformers over disordered ones.[35,42]

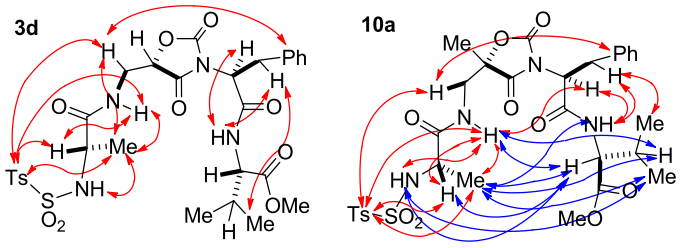

Figure 8. Sketches of the structures of **3d** and **10a**, and short-range (distances ≤ 3 Å) proton-proton ROESY correlations, indicated by arrows. Intra-residue and long-range (> 3 Å) correlations are not shown. Grey dashed arrows connect protons belonging to consecutive residues (*i*-*i*+*1*), while black solid arrows connect protons of non-consecutive residues (*i*-*i*+*2* or *i*-*i*+*3*).

As anticipated, the 2D-ROESY of the model compounds in 8:2 [D_6]DMSO/H_2O gave analyzable cross-peaks. Compared to the tetrapeptides **3e** and **10b** (not shown), the homochiral **3d** and **10a** showed a comparatively larger number of short-range inter-residue proton-proton correlations (Figure 8). In particular, **10a** displayed also several short-range cross-peaks between remote residues (for the complete list of cross-peaks, see Tables 4-7), suggestive of a folded structure.

Cross-peak intensities were ranked to infer plausible inter-proton distances as restraints (Tables 4-7). Structures (50) consistent with ROESY were obtained by simulated annealing with restrained molecular dymamics (MD) in a box of explicit TIP3P equilibrated water molecules. With the exception of Amo-Phe, the ω bonds were set at 180°; indeed, it is well established that peptides comprising only secondary amide bonds adopt all-trans conformations.[43] In any case, the absence of Hα(*i*)-Hα(*i+1*) cross-peaks reasonably excluded the occurrence of *cis* peptide bonds.[44] The structures were minimized with the AMBER force field[45] and clustered by the rmsd analysis of backbone atoms. For each peptide, this procedure essentially gave one major cluster comprising the large majority of the structures. The representative structures of **3d**, **3e**, **10a**, and **10b**, with the lowest energy, were selected and analyzed (Figure 9).

In the ROESY-derived structures of the homochiral tetrapeptides **3d** and **10a**, the Ts-Ala and Val-OMe moieties occupied the same side underneath the heterocycle. The Amo residue of **3d** displayed a +*g* conformation about the central dihedral angle (θ = +42°), and a partially bent disposition of the backbone (Figure 9). On the other hand, in **10a** the central dihedral angle of Amo presented a -*g* conformation (θ = -53°), and the peptide adopted a folded geometry compatible with an atypical turn centered on the dipeptide mimetic Amo-Phe. This secondary structure was stabilized by a clear 2->1-type H-bond between AmoNH and PheC=O, in agreement to the VT NMR temperature coefficient (Table 2). The representative structure of **10a** shown in Figure 9 is characterized by the following dihedral angles (in degrees): Amo (ϕ, θ, ψ): -106, -53, -119; Phe (ϕ, ψ): +83, +143 (see also Figure 10). The distance between the amide nitrogen of Amo and the carbonyl oxygen of Phe is 3.0 Å, while that between AlaCα and PheCα is about 4.3 Å.

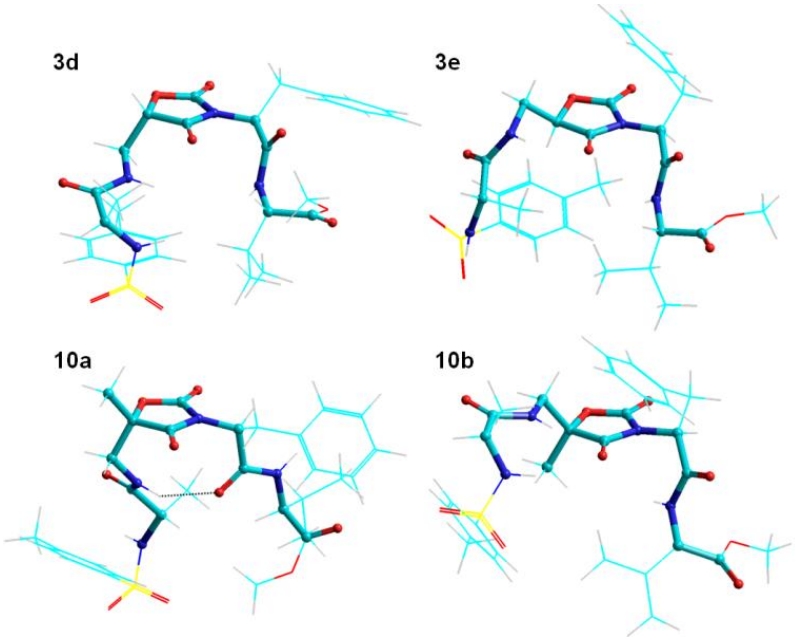

Figure 9. Top, representative lowest energy structures **3d**, **3e**, **10a**, and **10b**, calculated by restrained MD in a 30x30x30 Å box of standard TIP3P water molecules. Backbones and Amo rings are rendered in balls and cylinders, the rest in sticks.

As for the tetrapeptides **3e** and **10b**, which include (*R*)-Amo scaffolds, the ROESY derived structures revealed more extended backbone conformations, with Ts-Ala and Val-OMe positioned at the opposite sides of Amo ring. For both compounds, the central dihedral angle of Amo adopted a *-g* conformation (**3e**: θ = -64°; **10b**: θ = -55°). The marked differences between *homo* and *hetero*-chiral peptides are not unexpected, since it is well-known that short sequences may experience dramatic changes of backbone conformation by reversal of the configuration of even a single residue.[2,6,11]

To analyze the dynamic behavior of the peptides, starting from the structures of Figure 9 we performed unrestrained MD simulations for 10 ns at 300 K in a box of explicit TIP3P water molecules. For all compounds, during the simulations the complete rotation of the Phe-Val moiety around the Amo-Phe bond was not observed; possibly, the two carbonyls at positions 2 and 4 of the Amo ring prevented this movement. The analyses of the trajectories of **10a** showed that the folded geometry of the backbone was maintained during the simulation, albeit AmoNH and PheC=O were prone to rotate about the dihedral angles Amoϕ and Pheψ, respectively, leading to a occasional fluctuation of the distance PheC=***O***-Amo***N*** (Figure 8). The analyses of the trajectories of **3d**, **3e**, and **10b**, did not reveal the occurrence of clear secondary structures (not shown), and confirmed the higher backbone mobility of heterochiral **3e** and **10b**.

The role exerted by the residue *i+3* on peptide conformation was not investigated. It can be expected that substitution of Phe[3] with other amino acids could modify the stability and geometry of the folded conformation.[8a,11c] It was shown that peptides incorporating a central -lactam-Gly- pair can exhibit high conformational heterogeneity around the lactam-Gly bond, depending on the presence and relative disposition of the substituents of the lactam scaffold.[8a,11b]

On resuming the evidences of experimental results and theoretical computations, it can be perceived that the conformational features of **3d**, **3e**, and **10b**, seem to be governed mainly by the stereochemistry and geometric preferences of the Amo scaffold, which preferentially adopt a *+g* orientation of the central torsion angle θ (the *-g* conformation of (*R*)-Amo is equivalent to the *+g* of the (*S*)-enantiomer). For **10a**, a significant population of bent conformers was expected on the basis of the higher stability of the *-g* conformer (Figure 3), correlated in turn to the presence of the α-substituent onto the Amo scaffold. This effect and the stabilization exerted by the 9-membered hydrogen bond appear as the major contributors to the folding of peptide **10a**.

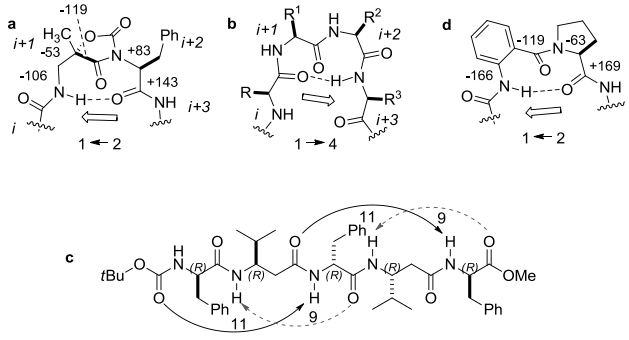

Figure 10. Sketch of the *pseudo* β-turn of **10a** stabilized by a 9-membered 2->1 H-bond induced by the (*S*)-Amo scaffold, and relevant dihedral angles (deg) (**a**); a ideal β-turn showing the 10-membered 1->4 H-bond (**b**); the peptide in ref.[46] is characterized by 9-membered 2->1 H-bonds (grey dashed arrows) as observed for **10a**, and distinct 11-membered i->i+3 hydrogen bonds with opposite orientation (**c**); anthranilic acid-Pro[47] scaffold showing the 9-membered 2->1 H-bond, and relevant dihedral angles (deg) (**d**).

The conformation adopted by the model peptide **10a** in a solvent mimetic of biological fluids can be regarded as a *pseudo* β-turn, being characterized by a Cα(*i*) to Cα(*i+3*) distance < 7.0 Å.[47] This structure requires only the mixed β/α-dipeptide to display the closed hydrogen-bonded network (Figure 10**a**). The dipeptide Amo-Phe contains a 9-membered hydrogen bonded ring between AmoNH and PheC=O of type 2->1. This structure is in contrast to native β-turns (Figure 10**b**), which involve four residues to form the hydrogen-bonded structure in the opposite direction (residues 1->4). To our knowledge, **10a** represents a very rare example of short sequence showing this kind of *pseudo* β-turn,[48] while it was observed in linear oligomers composed of repetitive α/β-units (e.g. Figure 10**c**, **d**).

The secondary structure formed by a given type of hybrid α/β-oligomer depends on the number and substitution of the α- or β-residues within the units, on their stereochemistry pattern, and conformational restraints such as the incorporation of cyclic structures within the amino acid. A variety of secondary structures have been reported in the literature, stabilized by 10- to 15-membered hydrogen bonded rings in both orientations of the backbone direction, while 9-membered H-bonded rings of type 2->1 have been described more seldom.[19,33]

Hofmann et al. have carried out a detailed theoretical study of α/β-peptides, demonstrating the stability of a mixed helix with a 9-membered hydrogen bond in the forward direction and an 11-membered hydrogen bond in the backward direction of the peptide chain in apolar solvents.[33f] On the other hand, the peptide Boc-[(*R*)-Phe-(*R*)-β^3-*homo*-Val]$_2$-(*R*)-PheOMe (Figure 10**c**),[46] 'heterochiral' because the β^3-residues derived from L-α-residues, was shown to adopt a mixed structure characterized by one classic 11-membered i->i+3 hydrogen bond, and a distinct 9-membered 2->1 H-bond with opposite orientation.[49]
More recently, the 2->1 9-membered hydrogen bond was described by Sanjayan and Rajamohanan[49] in oligopeptide foldamers consisting of the repeating building blocks L-Pro and anthranilic acid, the latter as a rigid β-amino acid (Figure 10**d**). The structure was explained as the result of the combined intrinsic conformational preferences of two local constraints and the repetitive α/β-hybrid structure.[19] Replacing Pro with other residues had an adverse effect on the stabilization of this architecture. Later studies confirmed the stability of the turn motifs featuring the 9-membered hydrogen-bond also in tripeptides containing a distinct Ant-Pro scaffold.[48]
Remarkably, the characteristic Freidinger-lactam-like structure of the mixed β^2/α-dipeptide mimetic Amo-Phe consented **10a** to adopt in a very competitive and biomimetic environment a significant population of folded geometries, without the concomitant assistance of further constraint-inducers, and without the cooperative effect of repetitive units.

5.3. Conclusions

The cyclization of *iso*Ser incorporated into short peptides with DSC and DIPEA was performed either in solution or in solid phase with very good yields, and allowed preparing in a single step peptidomimetics containing the unusual aminomethyloxazolidin-2,4-dione (Amo) scaffold comprising *iso*Ser and the following residue. This unusual scaffold represents a unprecedented β^2-*homo* variant of the classic Freidinger lactam. Besides, the availability of optically pure α-substituted α-hydroxy-$\beta^{2,2}$-amino acids allowed preparing peptidomimetics carrying a single proteinogenic side chain at each residue. Conformational analyses indicated that the constrained α-substituted Amo tends to favour in homochiral oligomers a rare *pseudo* β-turn stabilized by a 9-membered hydrogen bond of type 2->1 in the opposite direction of the sequence.
For the simple synthetic protocol and the atypical geometric features, the Amo ring deserves to be exploited for the design of new conformationally biased peptidomimetics or foldamers. The scope of the Amo scaffold could be extended by introducing a substituent with defined stereochemistry in the β-position of the Amo motif, thus providing a constrained $\beta^{2,3}$-amino acids building block. Further studies could include the preparation and analysis of the conformational preference of oligopeptides composed of repetitive Amo units, alone or in combination with other residues.

5.4. Experimental Section

5.4.1. General Methods

Standard chemicals (including Boc- or Fmoc-protected α-amino acids, (S)- and (R)-H-isoSerOH, Fmoc-rac-H-isoSerOH, (S)- and (R)-H-PheNH_2, H-ValOMe, H-SarNH_2), were purchased from commercial sources and used without further purification. Flash chromatography was performed on silica gel (230-400 mesh), using mixtures of distilled solvents. Compounds purities were assessed by analytical RP-HPLC and elemental analysis. Analytical RP-HPLC was performed on an Agilent 1100 series apparatus, using a RP column Phenomenex mod. Gemini 3μ C18 110A 100x3.0 mm (P/No 00D-4439-Y0); column description: stationary phase octadecyl carbon chain-bonded silica (C18) with TMS endcapping, fully porous organo-silica solid support, particle size 3 μm, pore size 110 Å, length 100 mm, internal diameter 3 mm; DAD 210 nm; mobile phase: from a 9:1 H_2O-CH_3CN to a 2:8 H_2O-CH_3CN in 20 min at a flow rate of 1.0 mL min^{-1}, followed by 10 min at the same composition. Semi-preparative RP-HPLC was performed on an Agilent 1100 series apparatus, using a RP column ZORBAX mod. Eclipse XDB-C18 PrepHT cartridge 21.2x150 mm 7μ (P/No 977150-102); column description: stationary phase octadecyl carbon chain-bonded silica (C18), double endcapped, particle size 7 μm, pore size 80 Å, lenght 150 mm, internal diameter 21.2 mm; DAD 210 nm; mobile phase from 8:2 H_2O-CH_3CN to 100% CH_3CN in 10 min at a flow rate of 12 mL min^{-1}. Chiral HPLC analysis was performed on an Agilent 1200 series apparatus, using a CHIRALPAK IC column (P/No 83325); column description: chiral stationary phase cellulose tris (3,5-dichlorophenylcarbamate) immobilized on silica, particle size 5 μm, lenght 250 mm, internal diameter 4.6 mm, DAD 210/254 nm; mobile phase: 3:1 n-hexane/2-propanol, at 0.8 mL min^{-1}.The RP-HPLC of compounds 3h, H-Phe-ValOMe, 7, Ts-Ala-α-Me-isoSerOH, was performed as reported above, with the addition of 0.1% TFA in the mobile phase, and setting DAD at 254 nm. ESI analysis was performed using a MS single quadrupole HP 1100MSD detector, with a drying gas flow of 12.5 l/min, nebulizer pressure 30 psgi, drying gas temp. 350°C, capillary voltage 4500 (+) and 4000 (-), scan 50-2600 amu. Elemental analyses were performer using a Thermo Flash 2000 CHNS/O analyzer. High quality IR were obtained at 2 cm^{-1} resolution using a FT-IR

spectrometer and 1 mm NaCl solution cell. Electronic circular dichroism (ECD) spectra were recorded on a Jasco J-710 spectropolarimeter. The synthetic procedures by MW irradiation were performed using a microwave oven (MicroSYNTH Microwave Labstation for Synthesis) equipped with a built-in ATC-FO advanced fiber optic automatic temperature control. ^{1}H NMR spectra were recorded using a Varian Gemini apparatus at 400 MHz in 5 mm tubes, using 0.01 M peptide at room temperature. Solvent suppression was performed by the solvent presaturation procedure implemented in Varian (PRESAT). ^{13}C NMR spectra were recorded at 100 MHz. Chemical shifts are reported as δ values relative to residual $CHCl_3$ δH (7.26 p.p.m.), DMSO δH (2.50 p.p.m.) and $CDCl_3$ δC (77.16 p.p.m.) as internal standards. The unambiguous assignment of ^{1}H NMR resonances was performed by 2D gCOSY. VT-^{1}H NMR experiments were performed over the range of 298-348 K; temperature calibration was done with the ethylene glycol OH-CHn chemical-shift separation method. 4.6 μm particle.

5.4.2. Synthetic procedures

Boc-(S)-isoSer-(S)-$PheNH_2$ (**1a**). A stirred solution of Boc-isoSer-OH (0.20 g, 1.0 mmol) in 4:1 DCM/DMF (5 mL) was treated with HOBt (0.16 g, 1.2 mmol.) and HBTU (0.46 g, 1.2 mmol.), at r.t. and under nitrogen atmosphere. After 5 min, H-$PheNH_2$ (0.18 g, 1.1 mmol.) and DIPEA (0.42 mL, 2.4 mmol) were added, and the mixture was stirred under nitrogen atmosphere and under MW irradiation. The microwave-assisted reaction was performed with a initial irradiation power of 150W, and monitoring the internal reaction temperature at 80°C with a built-in ATC-FO advanced fiber optic automatic temperature control. After 10 min, the mixture was concentrated at reduced pressure, and the residue was diluted with EtOAc (25 mL). The solution was washed with 0.1 M HCl (5 mL), and a saturated solution of $NaHCO_3$ (5 mL). The organic layer was dried over Na_2SO_4 and the solvent was evaporated at reduced pressure. Peptide **1a** was isolated (0.29 g, 80%, 91% pure by analytical RP-HPLC, see General Methods, Rt = 4.33 min) by flash chromatography over silica gel (eluant EtOAc/MeOH 95:5). ^{1}H NMR ($CDCl_3$) δ = 1.34 (s, 9H, t-Bu), 3.00-3.17 (m, 2H, PheHβ), 3.20-3.36 (m, 2H, isoSerHβ), 4.10 (m, 1H, isoSerHα), 4.59 (q, J = 6.8 Hz, 1H, PheHα), 5.38 (br.t, 1H, isoSerNH), 6.29 (s, 1H, $CONH_2$), 6.79 (s, 1H, $CONH_2$), 7.08-7.12 (m, 3H, PheArH), 7.12-7.20 (m, 2H, PheArH), 7.61 (br.d, 1H, PheNH). ESI-MS m/z 374.4 $(M+ Na)^+$, calcd 374.4

Boc-(S)-isoSer-(R)-$PheNH_2$ (**1b**); Boc-(R)-isoSer-(S)-$PheNH_2$ (**1c**). The reaction of Boc-isoSerOH and (R)-H-$PheNH_2$, or (R)-Boc-isoSerOH and H-$PheNH_2$, using the same reagent quantities and under same MW-assisted conditions described for the preparation of **1a**, afforded dipeptides **1b** or **1c**, respectively. After the same work up, the crude **1b,c** were precipitated from MeOH/Et_2O and collected by filtration. The crude peptides were identified by ESI-MS, and purity was assessed by analytical RP-HPLC (General Methods). **1b** (86%, 76% pure, Rt = 4.01 min) ESI-MS m/z 352.2 $(M+1)^+$, calcd 352.4. **1c** (85%, 78% pure, Rt = 3.49 min) ESI-MS m/z 352.3 $(M+1)^+$, calcd 352.4.

Boc-(S)-isoSer-(S)-Phe-ValOMe (**1d**); Boc-(R)-isoSer-(S)-Phe-ValOMe (**1e**). Boc- Phe-ValOMe[22] (1.13 g, 3.0 mmol) was N-deprotected according to the General Procedure for Boc Deprotection, giving H-Phe-ValOMe-TFA salt in quantitative yield (90% pure by analytical RP-HPLC, see General methods, Rt = 1.82 min), identified by ESI analysis. ESI-MS m/z 279.2 $(M+1)^+$, calcd 279.2. The crude dipeptide was coupled with Boc-isoSerOH or Boc-(R)-isoSerOH using the same quantities and under same conditions described for the preparation of **1a**, affording dipeptides **1d** or **1e**, respectively. After the same work up, the crude **1d,e** were analyzed by RP-HPLC ESI-MS (General Methods). **1d** (82%, 75% pure, Rt = 4.30 min) ESI-MS m/z 466.1 $(M+1)^+$, calcd 466.2. **1e** (80%, 73% pure, Rt = 4.62 min) ESI-MS m/z 466.2 $(M+1)^+$, calcd 466.2.

General Procedure for Boc Deprotection. The intermediate N-Boc peptides 1 (1.0 mmol) were deprotected by treatment with 25% TFA in DCM (5 mL) while stirring at r.t. After 15 min, the solution was evaporated under reduced pressure, and the treatment was repeated. The residue was suspended in ice-cold Et_2O (20 mL). The intermediate peptide-TFA salts which precipitated in almost quantitative yields were collected by centrifuge, and used for the next couplings without further purifications (80-85% pure by analytical RP-HPLC, General Methods).

General Procedure for the Synthesis of Peptides **2e-f**. The N-deprotected peptides-TFA salts prepared from peptides **1** as described above were subjected to coupling with Tosyl (Ts)-AlaOH or Boc-AlaOH in the same number of mmol and using the same procedure utilized for **1a**, giving the corresponding tri- or terapeptides **2a-e** or **2f**, respectively. After the usual work-up, the peptides were isolated (80-85%) by flash chromatography over silica gel (eluant EtOAc/MeOH 95:5).

Ts-(S)-Ala-(S)-isoSer-(S)-$PheNH_2$ (**2a**). 90% pure by RP-HPLC (General Methods), Rt = 4.86 min. ^{1}H NMR ($CDCl_3$) δ = 1.00 (d, J=6.8 Hz, 3H, AlaMe), 2.37 (s, 3H, TsMe), 2.71 (ddd, J=5.0, 8.2, 13.8 Hz, 1H, isoSerHβ), 2.88 (dd, J=7.8, 13.8 Hz, 1H PheHβ), 3.02 (dd, J=5.0, 13.8 Hz, 1H, PheHβ), 3.20 (ddd, J=4.4, 6.2, 13.8 Hz, 1H, isoSerHβ), 3.73 (dq, J=5.2, 6.8 Hz, 1H, AlaHα), 3.79 (dd, J=4.4, 8.2 Hz, 1H, isoSerHα), 4.49 (ddd, J=5.0, 5.6, 7.8, 1H, PheHα), 5.86 (d, J=5.2 Hz, 1H, AlaNH), 7.16-7.27 (m, 5H, PheArH), 7.35 (m, 2H, $TsArH_{3,5}$), 7.51 (s, 1H, $CONH_2$), 7.63-7.69 (m, 3H, $TsArH_{2,6}$+PheNH), 7.77 (dd, J=5.0, 6.2 Hz, 1H, isoSerNH), 7.86 (s, 1H, $CONH_2$). ESI-MS m/z 477.4 $(M+H)^+$, calcd 477.2.

Ts-(S)-Ala-(R)-isoSer-(S)-PheNH$_2$ (**2b**). 88% pure by RP-HPLC (General Methods), Rt = 4.16 min. ^{1}H NMR ($CDCl_3$) δ = 0.99 (d, J=6.8 Hz, 3H, AlaMe), 2.36 (s, 3H, TsMe), 2.86-2.98 (m, 2H, isoSerHβ+PheHβ), 3.01 (dd, J=4.8, 13.9 Hz, 1H, PheHβ), 3.22 (ddd, J=4.6, 6.2, 13.8 Hz, 1H, isoSerHβ), 3.74 (dq, J=5.0, 6.8 Hz, 1H, AlaHα), 3.78 (dd, J=4.6, 8.0 Hz, 1H, isoSerHα), 4.46 (ddd, J=4.8, 5.7, 7.6 Hz, 1H, PheHα), 5.79 (d, J=5.0 Hz, 1H, AlaNH), 7.16-7.27 (m, 5H, PheArH), 7.35 (m, 2H, TsArH$_{3,5}$), 7.51 (s, 1H, CONH$_2$), 7.64-7.67 (m, 3H, TsArH$_{2,6}$+PheNH), 7.75 (dd, J=4.8, 6.2 Hz, 1H, isoSerNH), 7.85 (s,1H, CONH$_2$). ESI-MS m/z 477.4 $(M+H)^+$, calcd 477.2.

Ts-(S)-Ala-(S)-isoSer-(R)-PheNH$_2$ (**2c**). 91% pure by RP-HPLC (General Methods), Rt = 4.45 min. ^{1}H NMR ($CDCl_3$) δ = 1.18 (d, J=7.0 Hz, 3H, AlaMe), 2.42 (s, 3H, TsMe), 3.04 (dd, J=8.2, 14.0 Hz, 1H, PheHβ), 3.23 (dd, J=6.0, 14.0 Hz, 1H, PheHβ), 3.63 (ddd, J=4.8, 8.2, 13.8 Hz, 1H, isoSerHβ), 3.68-3.78 (m, 2H, AlaHα+isoSerHβ), 4.16 (m, 1H, isoSerHα), 4.49 (dd, J=6.0, 6.4, 8.2 Hz, 1H, PheHα), 5.32 (d, J=2.4 Hz, 1H, isoSerOH), 5.93 (d, J=7.6 Hz, 1H, AlaNH), 6.34 (s, 1H, CONH$_2$), 6.79 (s, 1H, CONH$_2$), 7.18-7.31 (m, 7H, TsArH$_{3,5}$+PheArH), 7.61 (d, J=6.4 Hz, 1H, PheNH), 7.68 (dd, J=4.8, 6.0 Hz, 1H, isoSerNH), 7.75 (m, 2H, TsArH$_{2,6}$). ESI-MS m/z 477.4 $(M+H)^+$, calcd 477.2.

Ts-(S)-Ala-(S)-isoSer-(S)-Phe-(S)-ValOMe (**2d**). 89% pure by RP-HPLC (General Methods), Rt = 4.90 min. ^{1}H NMR ($CDCl_3$) δ = 0.84 (d, J=6.6 Hz, 3H, ValMe), 0.87 (d, J=6.8 Hz, 3H, ValMe), 1.17 (d, J=6.8 Hz, 3H, AlaMe), 2.10 (m, 1H, ValHβ), 2.41 (s, 3H, TsMe), 3.13 (d, J=7.6 Hz, 2H, PheHβ), 3.41 (ddd, J=5.6, 6.4, 14.0 Hz, 1H, isoSerHβ), 3.49 (ddd, J=6.0, 8.0, 14.0 Hz, 1H, isoSerHβ), 3.69 (s, 3H, OMe), 3.79 (dq, J=6.8, 7.6 Hz, 1H, AlaHα), 4.13 (ddd, J=4.6, 6.0, 6.4 Hz, 1H, isoSerHα), 4.44 (dd, J=5.2, 8.4 Hz, 1H, ValHα), 4.70 (dt, J=7.6, 8.0 Hz, 1H, PheHα), 5.04 (d, J=4.6 Hz, 1H, isoSerOH), 6.14 (d, J=7.6 Hz, 1H, AlaNH), 6.92 (d, J=8.4 Hz, 1H, ValNH), 7.18-7.30 (m, 7H, PheArH+TsArH$_{3,5}$), 7.51 (dd, J=5.6, 8.0 Hz, 1H, isoSerNH), 7.52 (d, J=8.0 Hz, 1H, PheNH), 7.73 (m, 2H, TsArH$_{2,6}$). ESI-MS m/z 591.3 $(M+H)^+$, calcd 591.4.

Ts-(S)-Ala-(R)-isoSer-(S)-Phe-(S)-ValOMe (**2e**). 92% pure by RP-HPLC (General Methods), Rt = 4.78 min. ^{1}H NMR ($CDCl_3$) δ = 0.93 (d, J=6.8 Hz, 3H, ValMe), 0.95 (d, J=7.2 Hz, 3H, ValMe), 1.15 (d, J=7.2 Hz, 3H, AlaMe), 2.15 (m, 1H, ValHβ), 2.45 (s, 3H, TsMe), 3.00 (dd, J=7.4, 13.9 Hz, 1H, PheHβ), 3.08 (dd, J=6.9, 13.9 Hz, 1H, PheHβ), 3.43 (ddd, J=3.0, 5.2, 14.2 Hz, 1H, isoSerHβ), 3.74 (s, 3H, OMe), 3.87-3.95 (m, 2H, AlaHα+isoSerHβ), 4.20 (dd, J=3.0, 6.2 Hz, 1H, isoSerHα), 4.51 (dd, J=5.8, 8.1 Hz, 1H, ValHα), 4.55 (ddd, J=6.9, 7.4, 8.0 Hz, 1H, PheHα), 6.39 (d, J=8.1 Hz, 1H, ValNH), 7.19-7.34 (m, 10H, PheArH+TsArH$_{3,5}$+AlaNH+PheNH+isoSerNH), 7.77 (m, 2H, TsArH$_{2,6}$). ESI-MS m/z 590.3 $(M+H)^+$, calcd 591.4

Boc-(S)-Ala-(S)-isoSer-(S)-Phe-(S)-ValOMe (**2f**). 87% pure by RP-HPLC (General Methods), Rt = 4.86 min. ^{1}H NMR ($CDCl_3$) two conformers in 6:4 ratio δ = 0.80 (d, J=7.2 Hz, 3H, ValMe), 0.83 (d, J=6.8 Hz, 3H, ValMe), 1.21$_{\text{major conf}}$+1.26$_{\text{minor conf}}$ (d, J =6.8 Hz, 3H, AlaMe), 1.37 (s, 9H, t-Bu), 2.05 (m, 1H, ValHβ), 3.01-3.11 (m, 2H, PheHβ), 3.35 (m, 1H, isoSerHβ), 3.48 (m, 1H, isoSerHβ), 3.65 (s, 3H, OMe), 4.03-4.08 (m, 2H, AlaHα+isoSerHα), 4.38 (m, 1H, ValHα), 4.63 (br.q, 1H, PheHα), 5.05$_{\text{minor conf}}$+5.31$_{\text{major conf}}$ (br.d, 1H, AlaNH), 6.84 (br.d, 1H, ValNH), 7.19-7.23 (m, 6H, PhArH+isoSerNH), 7.55 (br.d, J=8.4 Hz, 1H, PheNH). ESI-MS m/z 536.6 $(M+H)^+$, calcd 536.7

Solid-phase synthesis of Ac-(S)-Ala-(S/R)-Amo-(S)-Phe-Wang (**2h**). Wang resin pre-loaded with Fmoc-PheOH (0.5 g, 0.4-0.8 mmol/g, resin particle size: 100-200 mesh) was introduced into a reactor for SPPS. Fmoc was removed with 4:1 DMF/piperidine (5 mL) under MW irradiation for 1 min under mechanical shaking (40W, monitoring the internal temperature at 45°C with a built-in ATC-FO advanced fiber optic automatic temperature control). The suspension was filtered, the resin was washed with DCM (5 mL) and treated with a second portion of DMF/piperidine as above described. Then the suspension was filtered, and the resin was washed three times in sequence with DCM (5 mL) and MeOH (5 mL).

All coupling steps were performed according to the following General Procedure. The resin was swollen in DCM (5 mL), and a solution of the Fmoc-N-protected amino acid (0.6 mmol) and HOBt (0.6 mmol) in DMF (4 mL) was added at r.t. and under nitrogen atmosphere, followed by HBTU (0.6 mmol.) and DIPEA (1.2 mmol). The mixture was mechanically shaken under MW irradiation as above described, and after 10 min the resin was filtered and washed three times with the sequence DCM (5 mL) and MeOH (5 mL). Coupling efficacy was determined by means of the Kaiser test. All subsequent deprotection steps were performed as above reported.

Ts-Ala-isoSer-SarNH$_2$ (**2i**). Boc-isoSerOH and H-SarNH$_2$ were coupled in the same quantities and by the same procedure utilized for the preparation of 1a (MW assisted peptide synthesis). The crude Boc-isoSer-SarNH$_2$ was recovered as descrived for **1b,c** (85%, 78% pure by analytical RP-HPLC, General methods, Rt =3.17 min). The dipeptide was N-deprotected according to the General Procedure for Boc Deprotection, and the corresponding peptide-TFA salt was coupled with Ts-AlaOH under above described conditions. **2i** was isolated (70%, 92% pure by analytical RP-HPLC, see General Methods, Rt = 3.54 min) by flash chromatography over silica gel (eluant EtOAc/MeOH 95:5). ^{1}H NMR ($CDCl_3$) major conformer δ =

1.11 (d, J=7.2 Hz, 3H, AlaMe), 2.37 (s, 3H, TsMe), 3.45 (s, 3H, SarMe), 3.64-3.76 (m, 2H, isoSerHβ+AlaHα), 3.82 (J=4.4, 6.2, 13.8 Hz, 1H, isoSerHβ), 4.14 (d, J=18.2 Hz, 1H, SarHα), 4.20 (d, J=18.2 Hz, 1H, SarHα), 4.90 (br.t, 1H, isoSerHα), 6.31 (d, J=6.8 Hz, 1H, AlaNH), 6.90 (s, 1H, $CONH_2$), 7.20 (s, 1H, $CONH_2$), 7.35 (m, 2H, $TsArH_{3,5}$), 7.53 (dd, J=5.0, 6.2 Hz, 1H, isoSerNH), 7.66 (m, 2H, $TsArH_{2,6}$). ESI-MS m/z 401.2 $(M+H)^+$, calcd 401.1.

In-solution synthesis of Amo-peptides **3a-g**, **10a** and **10b**. DSC (0.36 mmol) was added to a stirred solution of **1** (0.33 mmol) in 3:1 DCM/DMF (4 mL) followed by DIPEA (0.07 mmol) at r.t. and under nitrogen atmosphere. After 1 h, the solvent was removed under reduced pressure, the residue was diluted with 0.1 M HCl (5 mL), and the mixture was extracted three times with DCM (5 mL). The combined organic layers were dried over Na_2SO_4, solvent was evaporated at reduced pressure. The residue was purified by semi-preparative RP-HPLC (General Methods).

Ts-(S)-Ala-(S)-Amo-(S)-$PheNH_2$ (**3a**). 95% pure by RP-HPLC (General Methods), Rt = 6.41 min. ^{1}H NMR ($CDCl_3$) δ = 1.17 (d, J=6.8 Hz, 3H, AlaMe), 2.42 (s, 3H, TsMe), 3.48-3.58 (m, 3H, PheHβ+AmoHβ), 3.69 (ddd, J=4.0, 6.4, 13.8 Hz, 1H, AmoHβ), 3.78 (dq, J=6.4, 6.8 Hz, 1H, AlaHα), 4.73 (dd, J=4.0, 7.6 Hz, 1H, AmoHα), 4.93 (t, J=8.4 Hz, 1H, PheHα), 6.10 (br.d, J=6.4 Hz, 1H, AlaNH), 6.24 (s, 1H, $CONH_2$), 6.52 (s, 1H, $CONH_2$), 7.09 (br.t, 1H, AmoNH), 7.19 (m, 2H, $TsArH_{3,5}$), 7.20-7.34 (m, 5H, PhArH), 7.72 (m, 2H, $TsArH_{2,6}$); ^{13}C NMR ($CDCl_3$) δ = 18.4, 21.5, 33.8, 38.9, 52.7, 56.8, 76.7, 127.2, 127.5, 128.9, 129.5, 129.9, 135.8, 136.3, 144.0, 154.7, 170.1, 171.6, 172.9. Elem. Anal. for $C_{23}H_{26}N_4O_7S$; calcd: C 54.97, H 5.21, N 11.15, S 6.38; found: C 54.14, H 5.28, N 11.28, S 6.51. ESI-MS m/z 503.3 $(M+H)^+$, calcd 503.2.

Ts-(S)-Ala-(R)-Amo-(S)-$PheNH_2$ (**3b**). 96% pure by RP-HPLC (General Methods), Rt = 6.32 min. ^{1}H NMR ($CDCl_3$) δ = 1.15 (d, J=7.1 Hz, 3H, AlaMe), 2.43 (s, 3H, TsMe), 3.37 (ddd, J=4.4, 4.8, 14.6 Hz, 1H, AmoHβ), 3.52 (d, J=8.7 Hz, 2H, PheHβ), 3.80 (dq, J=7.1, 8.2 Hz, 1H, AlaHα), 4.12 (ddd, J=4.2, 7.6, 14.6 Hz, 1H, AmoHβ), 4.70 (dd, J=4.2, 4.4 Hz, 1H, AmoHα), 4.97 (t, J=8.7 Hz, 1H, PheHα), 6.28 (m, 2H, $CONH_2$+AlaNH), 6.41 (s, 1H, $CONH_2$), 6.99 (dd, J=4.8, 7.6 Hz, 1H, AmoNH), 7.23-7.31 (m, 5H, PheArH), 7.33 (m, 2H, $TsArH_{3,5}$), 7.73 (m, 2H, $TsArH_{2,6}$); ^{13}C NMR ($CDCl_3$) δ = 18.7, 21.3, 33.2, 38.5, 52.5, 55.8, 76.7, 126.8, 127.0, 128.5, 128.6, 129.5, 136.1, 137.0, 143.3, 153.9, 169.3, 170.8, 172.6. Elem. Anal. for $C_{23}H_{26}N_4O_7S$; calcd: C 54.97, H 5.21, N 11.15, S 6.38, found: C 56.07, H 5.11, N 10.93, S 6.27. ESI-MS m/z 503.3 $(M+H)^+$, calcd 503.2.

Ts-(S)-Ala-(S)-Amo-(R)-$PheNH_2$ (**3c**). 95% pure by RP-HPLC (General Methods), Rt = 6.88 min. ^{1}H NMR ($CDCl_3$) δ = 1.11 (d, J=7.2 Hz, 3H, AlaMe), 2.42 (s, 3H, TsMe), 3.45-3.52 (m, 3H, AmoHβ+PheHβ), 3.75-3.84 (m, 2H, AlaHα+AmoHβ), 4.69 (dd, J=4.0, 4.4 Hz, 1H, AmoHα), 4.91 (dd, J=6.4, 9.9 Hz, 1H, PheHα), 6.25 (d, J=7.2 Hz, 1H, AlaNH), 6.47 (s, 1H, $CONH_2$), 6.79 (s, 1H, $CONH_2$), 7.18-7.31 (m, 8H, $TsArH_{3,5}$+PheArH+AmoNH), 7.73 (m, 2H, $TsArH_{2,6}$); ^{13}C NMR ($CDCl_3$) δ = 18.3, 21.0, 33.0, 38.5, 52.2, 55.6, 76.6, 126.6, 126.7, 128.3, 128.4, 129.3, 136.0, 136.8, 143.0, 153.8, 169.1, 170.3, 172.4. Elem. Anal. for $C_{23}H_{26}N_4O_7S$; calcd: C 54.97, H 5.21, N 11.15, S 6.38; found: C 55.62, H 5.16, N 11.24, S 6.20. ESI-MS m/z 503.3 $(M+H)^+$, calcd 503.2.

Ts-(S)-Ala-(S)-Amo-(S)-Phe-(S)-ValOMe (**3d**). 96% pure by RP-HPLC (General Methods), Rt = 6.55 min. ^{1}H NMR ($CDCl_3$) δ = 0.81 (d, J=6.4 Hz, 3H, ValMe), 0.88 (d, J=6.8 Hz, 3H, ValMe), 1.13 (d, J=7.2 Hz, 3H, AlaMe), 2.14 (m, 1H, ValHβ), 2.39 (s, 3H, TsMe), 3.44 (ddd, J=3.5, 5.2, 14.4 Hz, 1H, AmoHβ), 3.53 (d, J=8.6 Hz, 2H, PheHβ), 3.63 (ddd, J=4.0, 6.0, 14.4 Hz 1H, AmoHβ), 3.73 (s, 3H, OMe), 3.82 (dq, J=7.2, 8.6 Hz, 1H, AlaHα), 4.51 (dd, J=4.8, 8.6 Hz, 1H, ValHα), 4.67 (dd, J=3.5, 4.0 Hz, 1H, AmoHα), 4.95 (t, J=8.6 Hz, 1H, PheHα), 5.79 (d, J=8.6 Hz, 1H, AlaNH), 6.81 (d, J=8.6 Hz, 1H, ValNH), 7.00 (dd, J=5.2, 6.0 Hz, 1H, AmoNH), 7.23-7.33 (m, 7H, $PheArH_2$+$TsArH_{3,5}$), 7.68 (m, 2H, $TsArH_{2,6}$); ^{13}C NMR ($CDCl_3$) δ = 17.8, 18.8, 18.9, 21.4, 30.9, 34.1, 38.9, 52.3, 52.4, 57.4, 57.9, 77.3, 127.0, 127.4, 128.8, 128.9, 129.6, 135.7, 136.9, 143.5, 154.4, 167.5, 171.1, 172.2, 172.5. Elem. Anal. for $C_{29}H_{36}N_4O_9S$; calcd: C 56.48, H 5.88, N 9.09, S 5.20; found: C 55.35, H 5.76, N 9.27, S 5.32. ESI-MS m/z 617.5 $(M+H)^+$, calcd 617.2.

Ts-(S)-Ala-(R)-Amo-(S)-Phe-(S)-ValOMe (**3e**). 94% pure by RP-HPLC (General Methods), Rt = 6.98 min. ^{1}H NMR ($CDCl_3$) δ = 0.81 (d, J=6.8 Hz, 3H, ValMe), 0.89 (d, J=6.4 Hz, 3H, ValMe), 1.14 (d, J=7.0 Hz, 3H, AlaMe), 2.14 (m, 1H, ValHβ), 2.44 (s, 3H, TsMe), 3.28 (ddd, J=3.0 3.4, 14.4 Hz, 1H, AmoHβ), 3.54 (dd, J=8.0, 14.6 Hz, 1H, PheHβ), 3.58 (dd, J=8.4, 14.6 Hz, 1H, PheHβ), 3.77 (s, 3H, OMe), 3.87 (dq, J=7.0, 8.8 Hz, 1H, AlaHα), 4.28 (ddd, J=4.1, 9.0, 14.4 Hz, 1H, AmoHβ), 4.49 (dd, J=5.0, 8.2 Hz, 1H, ValHα), 4.76 (dd, J=3.0, 4.1 Hz, 1H, AmoHα), 5.03 (dd, J=8.0, 8.4 Hz, 1H, PheHα), 6.21 (d, J=8.8 Hz, 1H, AlaNH), 6.41 (d, J=8.2 Hz, 1H, ValNH), 6.78 (dd, J=3.4, 9.0 Hz, 1H, AmoNH), 7.30-7.34 (m, 5H, PheArH), 7.38 (m, 2H, $TsArH_{3,5}$), 7.72 (m, 2H, $TsArH_{2,6}$); ^{13}C NMR ($CDCl_3$) δ = 17.8, 18.7, 18.9, 21.5, 30.9, 34.0, 38.3, 52.4, 52.9, 55.5, 58.3, 77.8, 127.0, 127.1, 127.9, 128.8, 128.9, 129.2, 129.4, 129.8, 129.9, 135.3, 137.1, 143.7, 153.9, 167.4, 171.2, 171.5, 172.5. Elem. Anal. for $C_{29}H_{36}N_4O_9S$; calcd: C 56.48, H 5.88, N 9.09, S 5.20; found: C 55.57, H 5.97, N 8.90, S 5.04. ESI-MS m/z 617.5 $(M+H)^+$, calcd 617.2.

Boc-(S)-Ala-(S)-Amo-(S)-Phe-(S)-ValOMe (**3f**). 95% pure by RP-HPLC (General Methods), Rt = 7.02 min. ^{1}H NMR ($CDCl_3$) δ = 0.84 (d, J=6.4 Hz, 3H, ValMe), 0.92 (d, J=6.8 Hz, 3H, ValMe), 1.25 (d, J=6.0 Hz, 3H, AlaMe), 1.42 (s, 9H, t-Bu), 2.18 (m, 1H, ValHβ), 3.42 (ddd, J=4.4, 5.6, 14.4 Hz, 1H, AmoHβ), 3.53 (d, J=8.5 Hz, 2H, PheHβ), 3.76 (s, 3H, OMe), 3.84 (ddd, J=4.8, 7.2, 14.4 1H, AmoHβ), 4.16 (m, 1H, AlaHα), 4.56 (dd, J=4.8, 8.2 Hz, 1H, ValHα), 4.74 (dd, J=4.4, 4.8 Hz, 1H, AmoHα), 4.95 (t, J=8.5 Hz, 1H, PheHα), 5.30 (br.d, 1H, AlaNH), 6.81 (d, J=8.2 Hz, 1H, ValNH), 6.87 (dd, J=5.6, 7.2 Hz, 1.H, AmoNH), 7.23-7.34 (m, 5H, PheArH); ^{13}C NMR ($CDCl_3$) δ = 17.6, 18.5, 18.9, 25.4, 25.5, 28.2, 30.9, 34.2, 38.8, 50.0, 52.4, 57.3, 57.7, 76.6, 127.5, 128.6, 128.8, 129.0, 135.5, 152.1, 154.4, 168.7, 171.4, 172.3, 173.9. Elem. Anal. for $C_{27}H_{38}N_4O_9$; calcd: C 57.64, H 6.81, N 9.96; found: C 56.66, H 6.95, N 10.11. ESI-MS m/z 585.3 $(M+Na)^+$, calcd 585.3.

Boc-(S)-Amo-(S)-PheNH$_2$ (**3g**). 96% pure by RP-HPLC (General Methods), Rt = 6.88 min. ^{1}H NMR ($CDCl_3$) δ = 1.42 (s, 9H, t-Bu), 3.23 (ddd J=4.4, 5.4, 14.6 Hz, 1H, AmoHβ), 3.43 (ddd, J=4.0, 7.8, 14.6 Hz, 1H, AmoHβ), 3.46-3.53 (m, 2H, PheHβ), 4.70 (dd, J=4.0, 4.8 Hz, 1H, AmoHα), 4.85-4.94 (m, 2H, AmoNH+PheHα), 5.84 (br.s, 1H, $CONH_2$), 6.43 (br.s, 1H, $CONH_2$), 7.20 (d, J=6.8 Hz, 2H, PheArH), 7.26-7.35 (m, 3H, PheArH); ^{13}C NMR ($CDCl_3$) δ = 28.2, 33.5, 38.5, 56.0, 79.8, 80.9, 127.1, 128.7, 128.4, 136.5, 154.3, 155.7, 169.4, 171.1. Elem. Anal. for $C_{18}H_{23}N_3O_6$; calcd: C 57.29, H 6.14, N 11.13; found: C 58.43, H 6.26, N 10.91. ESI-MS m/z 400.4 $(M+Na)^+$, calcd 400.2.

Solid-phase synthesis of Ac-(S)-Ala-(S/R)-Amo-(S)-PheOH (**3h**). The resin-bound peptide **2h** was suspended in 3:1 DCM/DMF (4 mL), and DSC (0.9 mmol) and DIPEA (0.3 mmol) were added at r.t. and under nitrogen atmosphere. The reaction was conducted under mechanical shaking for 2 h, then the suspension was filtered, and the resin was washed three times in sequence with DCM (5 mL) and MeOH (5 mL).

The resin-bound peptide was suspended in a solution of TFA (4.8 mL), H_2O (0.20 mL), and PhOH (0.050 g), in DCM (5 mL), and mechanically shaken at r.t. After 2 h, the mixture was filtered, the resin was washed twice with 10% TFA in Et_2O (5 mL) and twice Et_2O (5 mL). Filtrate and washes were collected, and solvent and volatiles were removed under N_2 flow at r.t. The resulting residue was suspended in ice-cold Et_2O, and the crude solid which precipitated was triturated and collected by centrifuge. The Amo-peptide acid **3h** was isolated as a 1:1 mixture of diastereoisomers by semipreparative RP-HPLC (see General Methods) (80% based on the average resin loading of 0.6 mmol/g; >95% pure by analytical RP-HPLC). ^{1}H NMR ([D_6]DMSO) δ = 1.14+1.16 (d, J=8.0 Hz, 6H, AlaMe), 1.81 (s, 6H, Ac), 2.83 (ddd, J=3.2, 4.0, 14.2 Hz, 1H, AmoHβ), 3.17-3.29 (m, 3H, AmoHβ+PheHβ), 3.38-3.48 (m, 3H, AmoHβ+PheHβ), 3.49 (ddd, J=3.6, 8.6, 14.4 Hz 1H, AmoHβ), 4.17-4.26 (m, 2H, AlaHα), 4.82-4.94 (m, 2H, PheHα), 4.97 (dd, J=3.6, 7.2 Hz, 1H, AmoHα), 5.10 (dd, 3.2, 7.6, 1H, AmoHα), 7.18-7.30 (m, 10H, PhArH), 7.90 (br.d, 1H, AlaNH), 7.92-8.04 (m, 2H, AlaNH+AmoNH), 8.19 (br.t, 1H, AmoNH); ^{13}C NMR ([D_6]DMSO) δ = 18.1, 18.2, 33.0, 33.1, 48.0, 48.1, 54.2, 54.5, 77.8, 78.1, 126.9, 128.1, 128.5, 128.8, 128.9, 129.1, 136.6, 136.7, 154.0, 168.9, 169.0, 170.3, 170.4, 172.1, 172.7. 173.0, 173.1. Elem. Anal. for $C_{18}H_{21}N_3O_7$; C 55.24, H 5.41, N 10.74; found: C 54.14, H 5.52, N 10.55. ESI-MS m/z 392.2 $(M+H)^+$, calcd 392.2.

Ts-Ala-Oxd-SarNH$_2$ (**4**). A solution of peptide **2i** (0.1 g, 0.25 mmol) in 3:1 DCM/DMF (4 mL) was treated with DSC (0.20 g, 0.75 mmol) and DBU (38 μL, 0.25 mmol) at 40°C and under nitrogen atmosphere. After 6 h the reaction was stopped and work-up was done as described for the synthesis of **3a-g**. The Oxd-peptide **4** was isolated by semi-preparative RP-HPLC (58 mg, 55 %, 94% pure by RP-HPLC, general Methods, Rf = 4.60 min). ^{1}H NMR ($CDCl_3$) major conformer δ = 1.32 (d, J=7.3 Hz, 3H, AlaMe), 2.40 (s, 3H, TsMe), 3.47 (s, 3H, SarMe), 3.90 (dd, J=4.2, 8.6 Hz, 1H, $OxdH_4$), 4.09 (d, J=18.0 Hz, 1H, SarHα), 4.12 (dd, J=8.6, 9.3 Hz, 1H, $OxdH_4$), 4.24 (d, J=18.0 Hz, 1H, SarHα), 5.11 (dq, J=7.3, 8.8 Hz, 1H, AlaHα), 5.45 (dd, J=4.2, 9.3 Hz, 1H, $OxdH_5$), 6.07 (br.s, 1H, $CONH_2$), 6.38 (br.s, 1H, $CONH_2$), 6.44 (m, 2H, $CONH_2$+AlaNH), 7.18 (m, 2H, $TsArH_{3,5}$), 7.75 (m, 2H, $TsArH_{2,6}$); ^{13}C NMR ([D_6]DMSO) δ = 18.5, 20.8, 39.1, 38.6, 50.7, 60.5, 85.4, 128.3, 129.3, 137.6, 141.5, 153.1, 168.4, 169.1, 175.0. Elem. Anal. for $C_{17}H_{22}N_4O_7S$; C 47.88, H 5.20, N 13.14; found: C 47.11, H 5.12, N 13.29. ESI-MS m/z 427.1 $(M+H)^+$, calcd 427.1.

Ts-(S)-Ala-(4R,5R)-4-hydroxy-5-aminomethylOxd-(S)-PheNH$_2$ (**5**). $NaBH_4$ (4 mmol) was added to a solution of the **3b** (0.4 mmol) in MeOH (4 mL) at 0°C under nitrogen atmosphere. The mixture was stirred for 7 h, then the reaction was stopped with acetone (4 mL). The reaction mixture was concentrated at reduced pressure, and the residue was diluted with water (5mL), and extracted three times with DCM (5mL). The collected organic layers were dried with Na_2SO_4, filtered, and concentrated at reduced pressure. The residue was purified by semi-preparative RP-HPLC (see General Methods) giving **5** (85%, 95% pure by RP-HPLC, general Methods, Rf = 5.12 min). ^{1}H NMR ($CDCl_3$) δ = 1.17 (d, J=6.8 Hz, 3H, AlaMe), 2.44 (s, 3H, TsMe), 3.04 (ddd, J=3.4, 5.0, 14.6 Hz, CH_2N), 3.14-3.25 (m, 2H, CH_2N+PheHβ) 3.34 (dd, J= 7.6, 14.0 Hz, 1H, PheHβ), 3.73 (dq, J=6.8, 7.2 Hz, 1H, AlaHα), 4.35 (br.t, 1H, OxdH5), 4.84 (dd, J=7.6, 8.6 Hz, 1H, PheHα), 5.21 (br.s, 1H, OxdH4), 5.95 (br.s, 1H, $CONH_2$), 6.03 (d, J=7.2 Hz, 1H, AlaNH), 6.63 (br.s, 1H, $CONH_2$), 7.08 (dd, J=5.0, 6.8 Hz, 1H, CH_2NH), 7.27-7.35 (m, 7H, PhArH+$TsArH_{3,5}$), 7.73 (m, 2H, $TsArH_{2,6}$); ^{13}C NMR ($CDCl_3$) δ = 19.2, 20.8, 34.8, 40.1, 52.7,

60.2, 79.7, 81.6, 125.7, 127.0, 127.6, 128.8, 129.0, 129.3, 130.1, 135.5, 138.1, 144.2, 157.3, 171.2, 172.9. Elem. Anal. for $C_{23}H_{28}N_4O_7S$; calcd: C 54.75, H 5.59, N 11.10, S 6.36; found: C 53.98, H 5.64, N 11.32, S 6.55. ESI-MS m/z 527.0 $(M+Na)^+$, calcd 527.2.

Ts-(S)-Ala-(S)-α-Me-isoSerOMe (**8a**). Nitromethane (1.5 mL), methyl pyruvate (50 μL, 0.5 mmol, and TEA (14 μL, 0.1 mmol) were mixed in the presence of $Cu(OTf)_2$ (36 mg, 0.10 mmol) and 2,2'-isopropylidenebis[(4R)-4-tert-butyl-2-oxazoline] (31 mg, 0.10 mmol), as described in the literature (Ref.[30] main text). The reaction mixture was filtered through a plug of silica, and solvent was removed at reduced pressure. The resulting crude α-nitro-(S)-hydroxy ester **6a** obtained in quantitative yield was identified by RP-HPLC-ESI analysis, and was utilized without further purifications (81 mg, 99%, 85% pure by RP-HPLC analysis, Rt = 2.04 min, 87% e.e. as determined by chiral HPLC analysis of the crude mixture, see General Methods). ESI-MS m/z 186.2 $(M+Na)^+$, calcd 186.1. Compound **6a** was dissolved in EtOH (6 mL) and treated with 10% Pd/C (100 mg) and H_2 at atmospheric pressure for 6 h at r.t. giving after filtration over celite and evaporation of solvent at reduced pressure the 3-amino-2-hydroxy-2-methyl-propionic ester **7a** in quantitative yield (67 mg, 99%, 82% pure by RP-HPLC analysis, see General Methods, Rt = 1.67 min) utilized for the next step without purification. ESI-MS m/z 134.1 $(M+H)^+$, calcd 134.1. The crude **7a** was coupled with Ts-AlaOH (120 mg, 0.5 mmol) by using the same procedure described for the synthesis of **1a**. After the usual work up the dipeptide **8a** (140 mg, 80%, 88% pure by RP-HPLC analysis, see General Methods, Rt = 3.85 min) was isolated by flash chromatography over silica gel (eluant: EtOAc: cyclohexane 2/8). ^{1}H NMR ($CDCl_3$) δ = 1.25 (d, J=6.7 Hz, 3H, AlaMe), 1.40 (s, 3H, Me-isoSer), 2.44 (s, 3H, TsMe), 3.32 (dd, J=6.0, 14.0 Hz, isoSerHβ), 3.66-3.83 (m, 5H, AlaHα+Me-isoSerHβ+COOMe), 4.95 (br.d, J=8.4 Hz, 1H, AlaNH), 6.47 (dd, J=5.0, 6.0 Hz, 1H, isoSerNH),7.33 (m, 2H, $TsArH_{3,5}$), 7.75 (m, 2H, $TsArH_{2,6}$). ESI-MS m/z 359.3 $(M+H)^+$, calcd 359.1.

Ts-(S)-Ala-(R)-α-Me-isoSerOMe (**8b**). The reaction of nitromethane and methyl pyruvate in the same quantities as described for the preparation of **6a** in the presence of 2,2'-isopropylidenebis[(4S)-4-tert-butyl-2-oxazoline] gave **6b** in quantitative yield (87% pure by RP-HPLC analysis, Rt = 2.04 min, 89% e.e. as determined by chiral HPLC analysis of the crude mixture, see General Methods). ESI-MS m/z 186.1 $(M+Na)^+$, calcd 186.1. The reduction to β-amino ester **7b** and coupling with Ts-AlaOH gave **8b** after purification by flash chromatography (150 mg, 84%, 93% pure by RP-HPLC analysis, see General Methods, Rt = 3.85 min) was done as described for **8a**. ^{1}H NMR ($CDCl_3$) δ = 1.23 (d, J=6.7 Hz, 3H, AlaMe), 1.37 (s, 3H, Me-isoSer), 2.44 (s, 3H, TsMe), 3.20 (dd, J=4.8, 13.6 Hz, isoSerHβ), 3.66-3.83 (m, 5H, AlaHα+isoSerHβ+COOMe), 5.06 (br.d, J=8.0 Hz, 1H, AlaNH)), 6.65 (br.t, 1H, isoSerNH), 7.33 (m, 2H, $TsArH_{3,5}$), 7.75 (m, 2H, $TsArH_{2,6}$). ESI-MS m/z 359.3 $(M+H)^+$, calcd 359.1.

Ts-(S)-Ala-(S)-α-Me-isoSer-(S)-Phe-(S)-ValOMe (**9a**). The dipeptide ester **8a** (140 mg, 0.39 mmol) was dissolved in MeOH (2 mL) and treated with 1 M LiOH (1 mL) while stirring. After 6 h, pH was adjusted to 7 with 0.1 M HCl and the solvent was removed at reduced pressure, giving Ts-Ala-α-Me-isoSerOH (128 mg, 95%, 90% pure by RP-HPLC analysis, see general Methods, Rt = 2.35 min). ESI-MS m/z 345.2 $(M+H)^+$, calcd 345.1. The residue was suspended in 4:1 DCM/DMF (5 mL) and treated with HOBt, HBTU, DIPEA, and H-Phe-ValOMe under MW irradiation as described for the prepaparation of **1a**. After the usual work up, the tetrapeptide **9a** (0.20 g, 85%, 90% pure by analytical RP-HPLC, see general Methods, Rf = 4.99 min) was isolated by flash chromatography over silica gel (eluant: EtOAc). ^{1}H NMR ($CDCl_3$) δ = 0.79 (d, J=5.8 Hz, 3H, ValMe), 0.82 (d, J=6.8 Hz, 3H, ValMe), 1.09 (d, J=6.8 Hz, 3H, AlaMe), 1.22 (s, 3H, α-Me-isoSer), 2.07 (m, 1H, ValHβ), 2.36 (s, 3H, TsMe), 3.05 (dd, J=8.0, 14.8 Hz, 1H, PheHβ), 3.10 (dd, J=6.8, 14.8 Hz, 1H, PheHβ), 3.29 (d, J=5.8 Hz, 2H, isoSerHβ), 3.63 (s, 3H, OMe), 3.67 (dq, J=6.8, 7.6 Hz, 1H, AlaHα), 4.38 (dd, J=4.8, 8.0 Hz, 1H, ValHα), 4.48 (ddd, J=6.8, 7.6, 8.0 Hz, 1H, PheHα), 6.69 (d, J=7.6 Hz, 1H, AlaNH), 6.96 (d, J=8.0 Hz, 1H, ValNH), 7.17-7.27 (m, 7H, PheArH+$TsArH_{3,5}$), 7.38 (t, J=5.8 Hz, 1H, isoSerNH), 7.50 (d, J=7.6 Hz, 1H, PheNH), 7.66 (m, 2H, $TsArH_{2,6}$). ESI-MS m/z 605.5 $(M+H)^+$, calcd 605.3.

Ts-(S)-Ala-(R)-α-Me-isoSer-(S)-Phe-(S)-ValOMe (**9b**). The dipeptide ester **8b** (150 mg, 0.42 mmol) was treated with 1 M LiOH in MeOH as described for **7a**, affording the dipeptide acid (134 mg, 95%, 85% pure by RP-HPLC analysis, see general Methods, Rt = 2.38 min). after the same reaction work up. ESI-MS m/z 345.3 $(M+H)^+$, calcd 345.1. Ts-Ala-(R)-α-Me-isoSerOH was coupled with H-Phe-ValOMe, as described for the preparation of **9a**. The tetrapeptide **9b** (0.21 g, 83%, 91% pure by analytical RP-HPLC, see general Methods, Rf = 5.11 min) was isolated after the same work up described for **9a**. ^{1}H NMR ($CDCl_3$) δ = 0.87 (d, J=5.6 Hz, 3H, ValMe), 0.86 (d, J=6.8 Hz, 3H, ValMe), 1.03 (d, J=7.2 Hz, 3H, AlaMe), 1.15 (s, 3H, α-Me-isoSer), 2.06 (m, 1H, ValHβ), 2.35 (s, 3H, TsMe), 2.89 (dd, J=8.0, 14.2 Hz, 1H, PheHβ), 3.05 (dd, J=6.4, 14.2 Hz, 1H, PheHβ), 3.17 (dd, J=5.6, 13.6 Hz, 1H, isoSerHβ), 3.51 (dd, J=6.8, 13.6 Hz, 1H, isoSerHβ), 3.65 (s, 3H, OMe), 3.76 (dq, J= 7.2, 7.8 Hz, 1H, AlaHα), 4.40 (dd, J=5.8, 8.2 Hz, 1H, ValHα), 4.53 (ddd, J=6.4, 7.6, 8.0 Hz, 1H, PheHα), 6.80 (d, J=7.8

Hz, 1H, AlaNH), 7.09-7.15 (m, 3H, ValNH+PheArH$_{3,5}$), 7.18-7.26 (m, 6H, PheArH$_{2,4,6}$+TsArH$_{3,5}$$^{+}$isoSerNH), 7.35 (d, J=7.6 Hz, 1H, PheNH), 7.66 (m, 2H, TsArH$_{2,6}$). ESI-MS m/z 605.5 (M+H)$^{+}$, calcd 605.3

Ts-(S)-Ala-(S)-5-Me-Amo-(S)-Phe-(S)-ValOMe (**10a**). The cyclization of **9a** in solution as reported for **3a-g** followed by the same work-up of the reaction and isolation by semi-preparative RP-HPLC afforded **10a** (95%, 96% pure by analytical RP-HPLC, see General methods, Rt = 7.23 min). ^{1}H NMR ($CDCl_3$) δ = 0.87 (d, J=7.2 Hz, 3H, ValMe), 0.94 (d, J=7.2 Hz, 3H, ValMe), 1.14 (d, J=6.8 Hz, 3H, AlaMe), 1.31 (s, 3H, AmoMe), 2.22 (m, 1H, ValHβ), 2.42 (s, 3H, TsMe), 3.33 (dd, J=4.8, 14.4 Hz, 1H, AmoHβ), 3.49 (dd, J=7.4, 14.0 Hz, 1H, PheHβ), 3.55 (dd, J=10.4, 14.0 Hz, 1H, PheHβ), 3.67 (dd, J=7.6, 14.4 Hz, 1H, AmoHβ), 3.80 (s, 3H, OMe), 3.88 (dq, J=6.8, 8.8 Hz, 1H, AlaHα), 4.57 (dd, J=4.6, 8.2 Hz, 1H, ValHα), 4.95 (dd, J=7.4, 10.4 Hz, 1H, PheHα), 5.64 (d, J=8.8 Hz, 1H, AlaNH), 6.76 (d, J=8.2 Hz, 1H, ValNH), 6.97 (dd, J=4.8, 7.6 Hz, 1H, AmoNH), 7.24-7.36 (m, 7H, PheArH+TsArH$_{3,5}$), 7.70 (m, 2H, TsArH$_{2,6}$); ^{13}C NMR ($CDCl_3$) δ = 17.5, 19.0, 19.3, 19.7, 21.5, 31.0, 34.4, 43.5, 52.2, 52.7, 57.8, 58.1, 84.3, 127.0, 127.1, 127.9, 128.8, 128.8, 128.9, 129.1, 129.3, 129.7, 129.9, 135.0, 137.2, 143.5, 153.6, 167.7, 172.2, 172.5, 174.6. Elem. Anal. for $C_{30}H_{38}N_4O_9S$; calcd: C 57.13, H 6.07, N 8.88, S 5.08; found: C 58.27, H 6.18, N 8.81, S 4.97. ESI-MS m/z 631.1 (M+H)$^{+}$, calcd 631.2.

Ts-(S)-Ala-(R)-5-Me-Amo-(S)-Phe-(S)-ValOMe (**10b**). The cyclization of **9b** in solution as reported for **3a-g** and **9a** followed by the same work-up of the reaction and isolation by semi-preparative RP-HPLC afforded **10b** (92% 97% pure by analytical RP-HPLC, see General methods, Rt = 7.45 min). ^{1}H NMR ($CDCl_3$) δ = 0.87 (d, J=7.2 Hz, 3H, ValMe), 0.94 (d, J=7.2 Hz, 3H, ValMe), 1.13 (d, J=7.2 Hz, 3H, AlaMe), 1.23 (s, 3H, AmoMe), 2.19 (m, 1H, ValHβ), 2.44 (s, 3H, TsMe), 3.12 (dd, J= 3.6, 14.4 Hz, 1H, AmoHβ), 3.48 (dd, J=9.6, 14.0 Hz, 1H, PheHβ), 3.54 (dd, J=7.8, 14.0 Hz, 1H, PheHβ), 3.79 (s, 3H, OMe), 3.86 (dq, J= 7.2. 8.8 Hz, 1H, AlaHα), 4.09 (dd, J= 9.2, 14.4 Hz, 1H, AmoHβ), 4.51 (dd, J=4.8, 8.2 Hz, 1H, ValHα), 4.99 (dd, J=7.8, 9.6 Hz, 1H, PheHα), 6.34 (d, J=8.8 Hz, 1H, AlaNH), 6.52 (d, J=8.2 Hz, 1H, ValNH), 6.76 (dd, J= 3.6, 9.2 Hz, 1H, AmoNH), 7.19-7.32 (m, 5H, PheArH), 7.38 (m, 2H, TsArH$_{3,5}$), 7.72 (m, 2H, TsArH$_{2,6}$); ^{13}C NMR ($CDCl_3$) δ = 18.0, 18.4, 18.6, 21.1, 22.1. 31.4, 33.2, 43.0, 51.8, 52.3, 55.4, 58.0, 84.2, 126.4, 126.7, 128.3, 128.6, 129.4, 136.0, 137.0, 142.9, 156.1, 167.6, 171.8, 172.1, 173.5. Elem. Anal. for $C_{30}H_{38}N_4O_9S$; calcd: C 57.13, H 6.07, N 8.88, S 5.08; found: C 56.00, H 5.99, N 8.91, S 5.13. ESI-MS m/z 631.1 (M+H)$^{+}$, calcd 631.2.

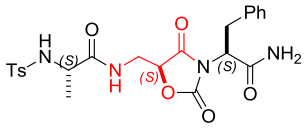
Ts
H
N
(S)
O
N
H
(S)
O
O
N
(S)
Ph
NH2
O

3a

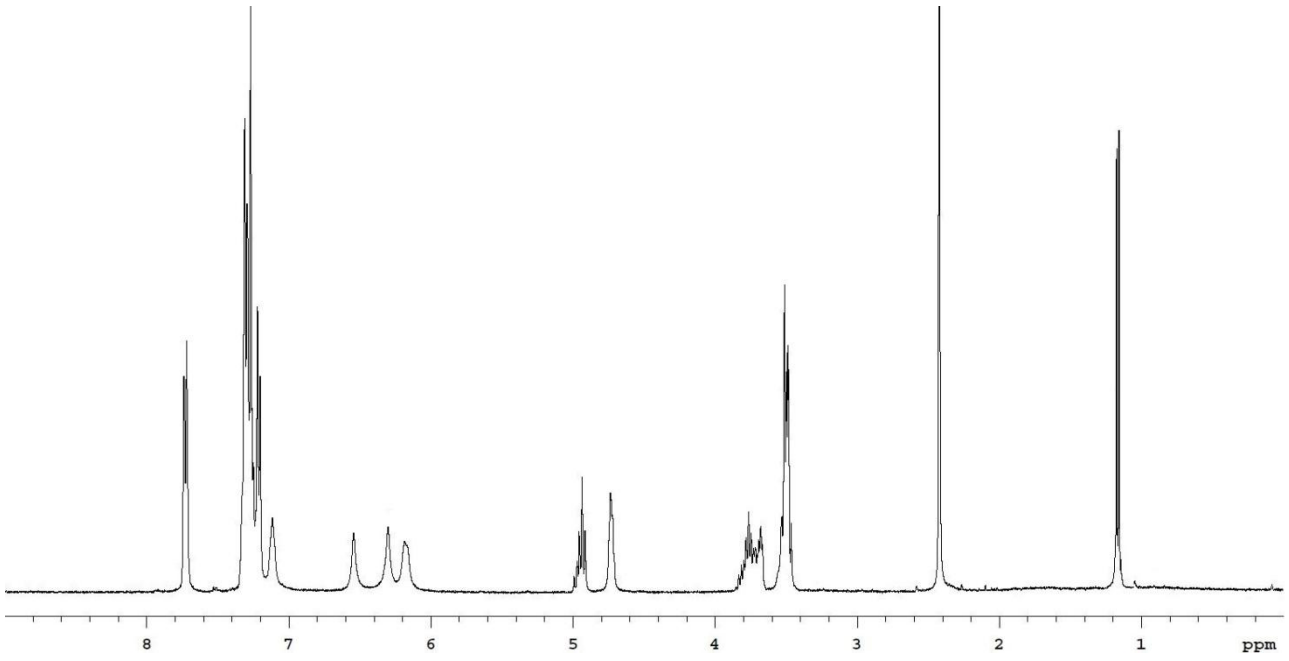
8
7
6
5
4
3
2
1
ppm

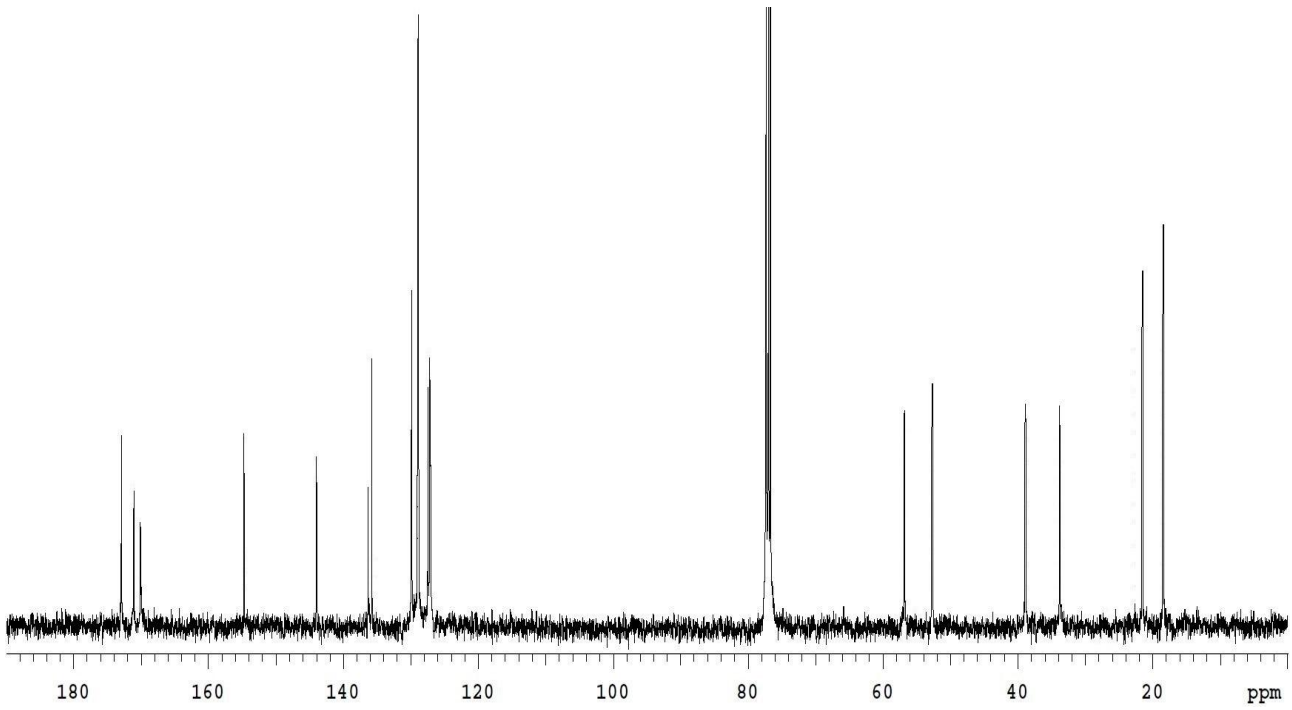
180
160
140
120
100
80
60
40
20
ppm

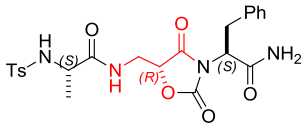
Ts
H
N
(S)
O
N
H
(R)
O
O
O
N
(S)
Ph
NH2
O

3b

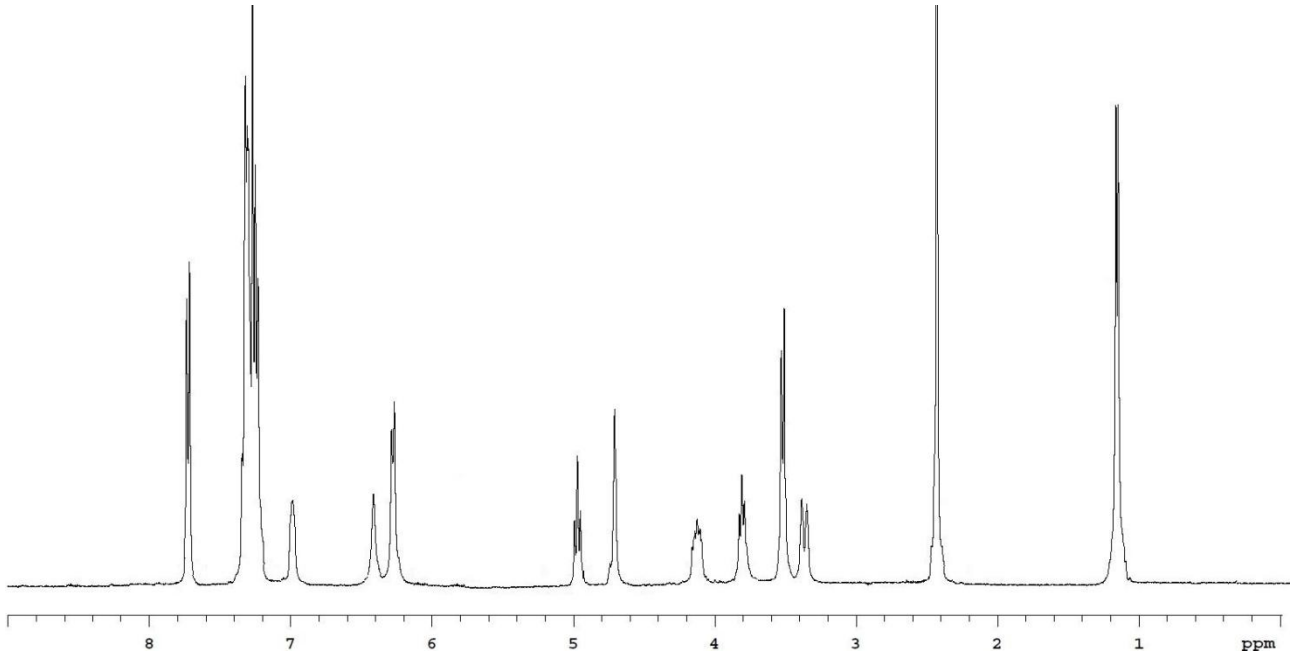
8
7
6
5
4
3
2
1
ppm

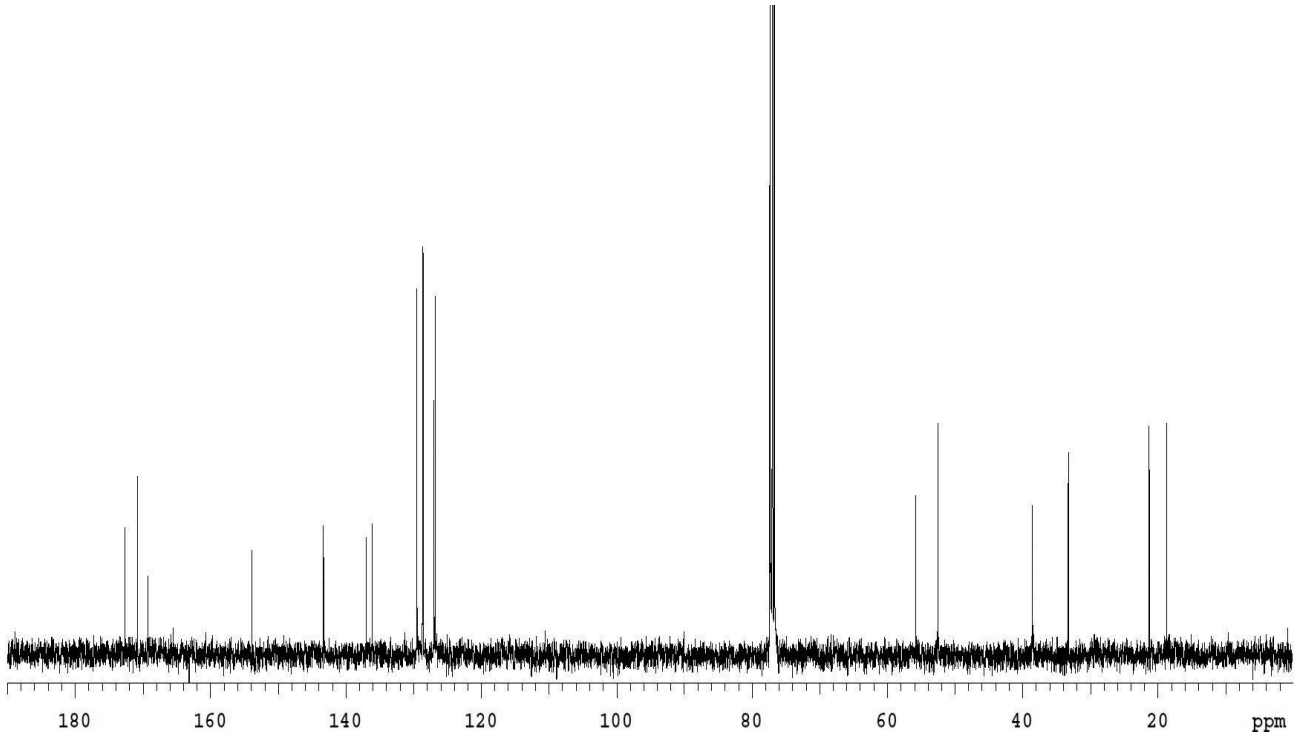
180
160
140
120
100
80
60
40
20
ppm

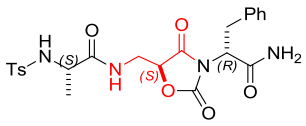
Ts
H
N
O
(S)
N
H
(S)
O
O
O
N
(R)
Ph
NH2
O

3c

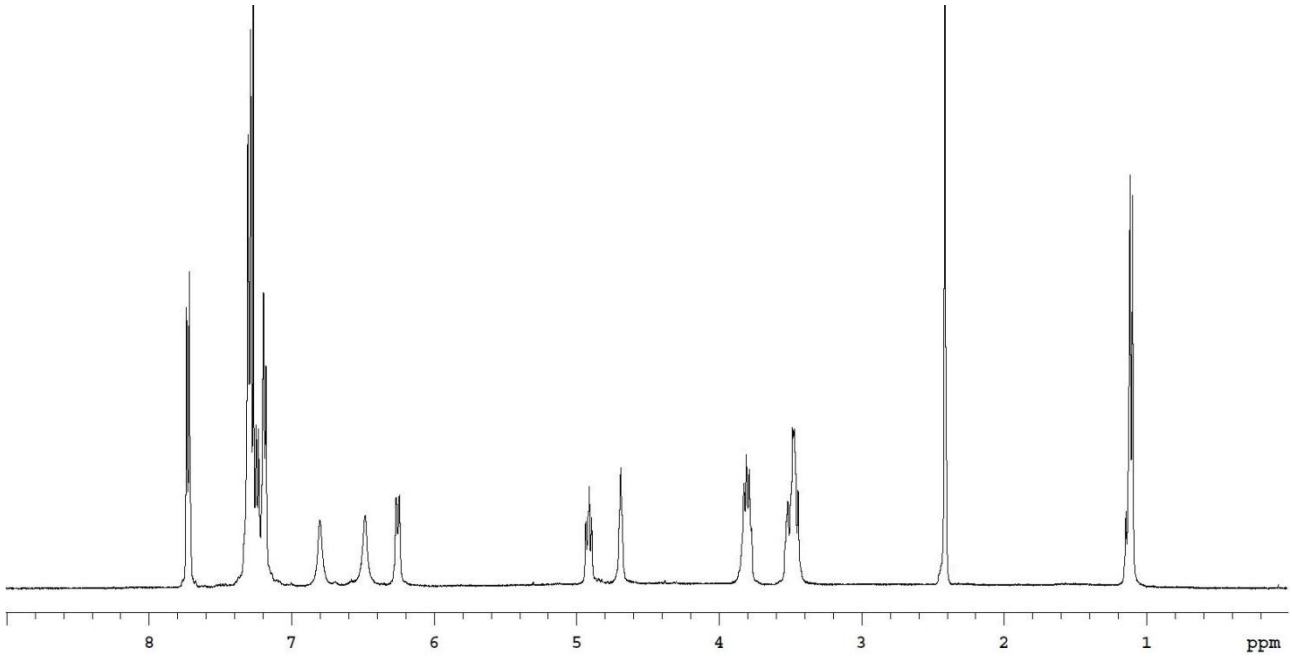
8
7
6
5
4
3
2
1
ppm

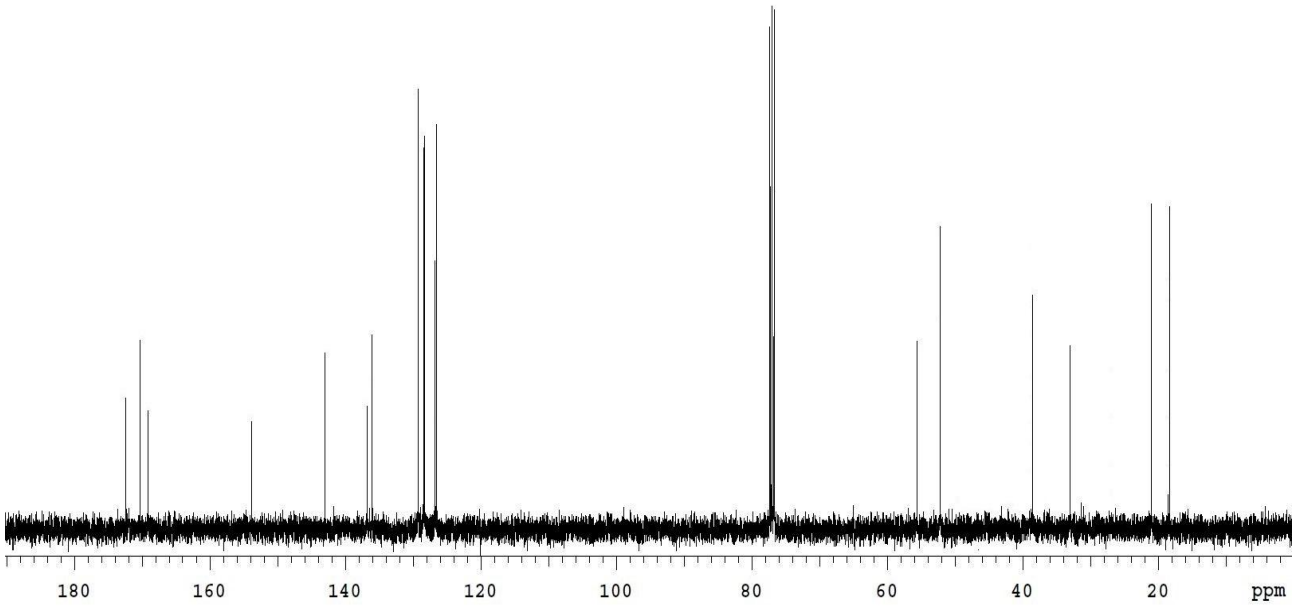
180
160
140
120
100
80
60
40
20
ppm

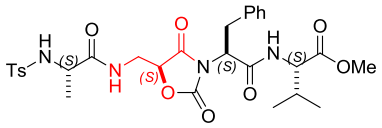
Ts
H
N
O
(S)
N
H
(S)
O
O
N
(S)
Ph
O
H
N
(S)
O
OMe

3d

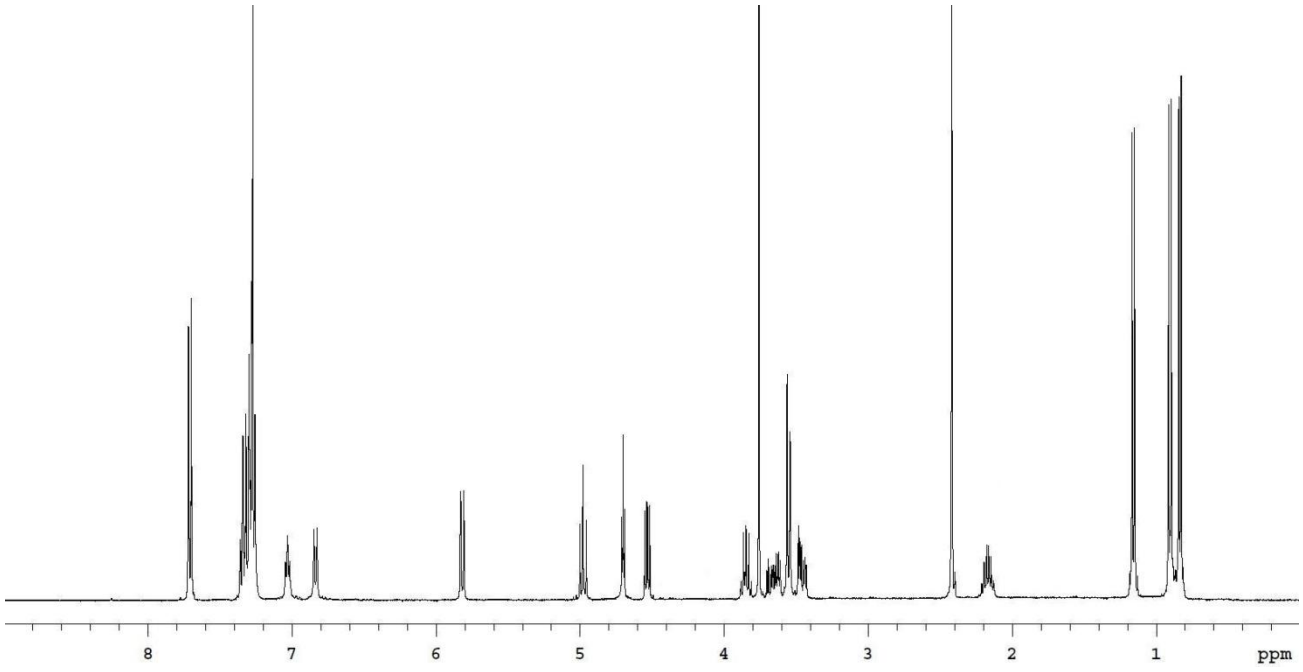
8
7
6
5
4
3
2
1
ppm

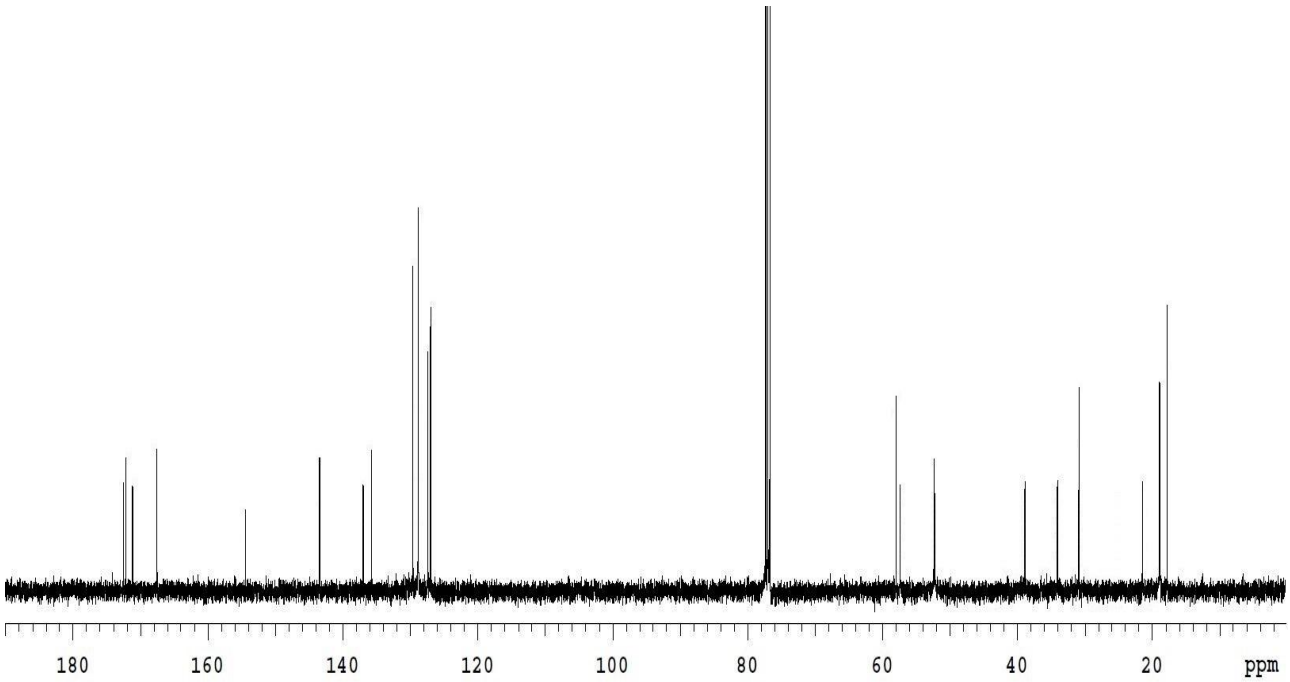
180
160
140
120
100
80
60
40
20
ppm

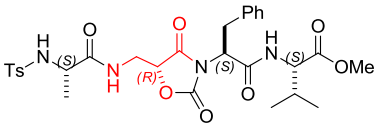
Ts
H
N
(S)
O
N
H
(R)
O
O
O
N
(S)
Ph
O
H
N
(S)
O
OMe

3e

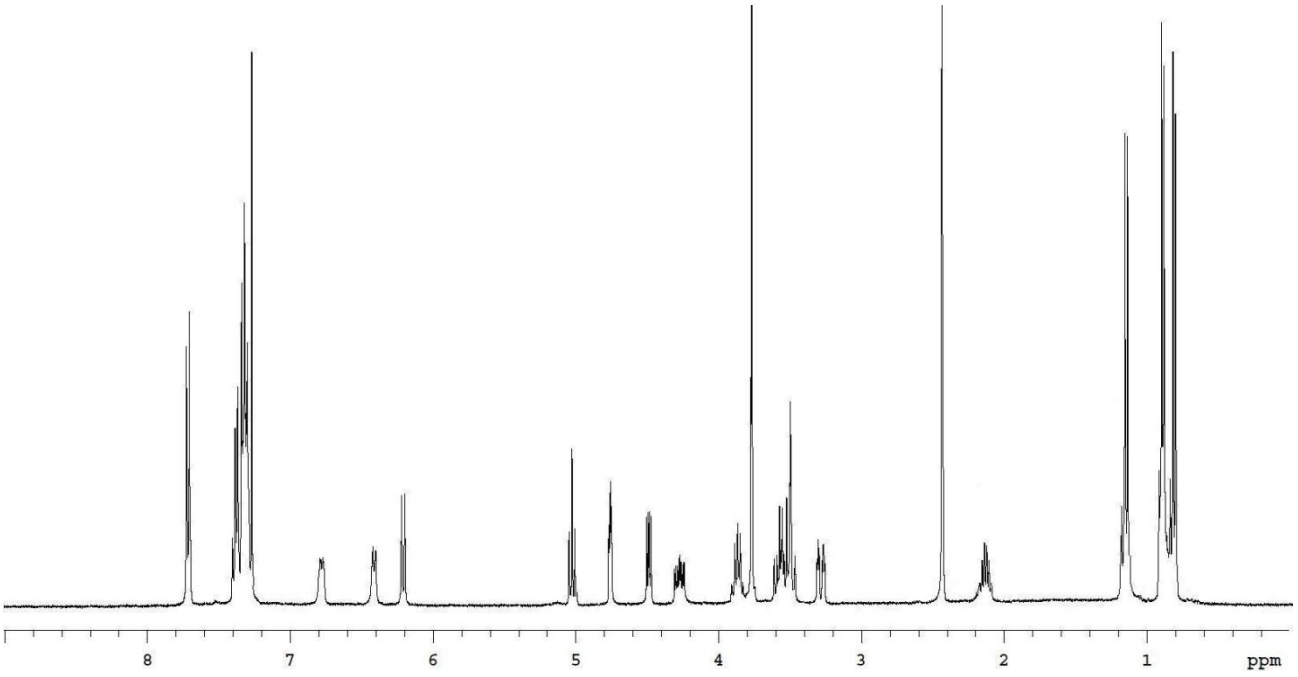
8
7
6
5
4
3
2
1
ppm

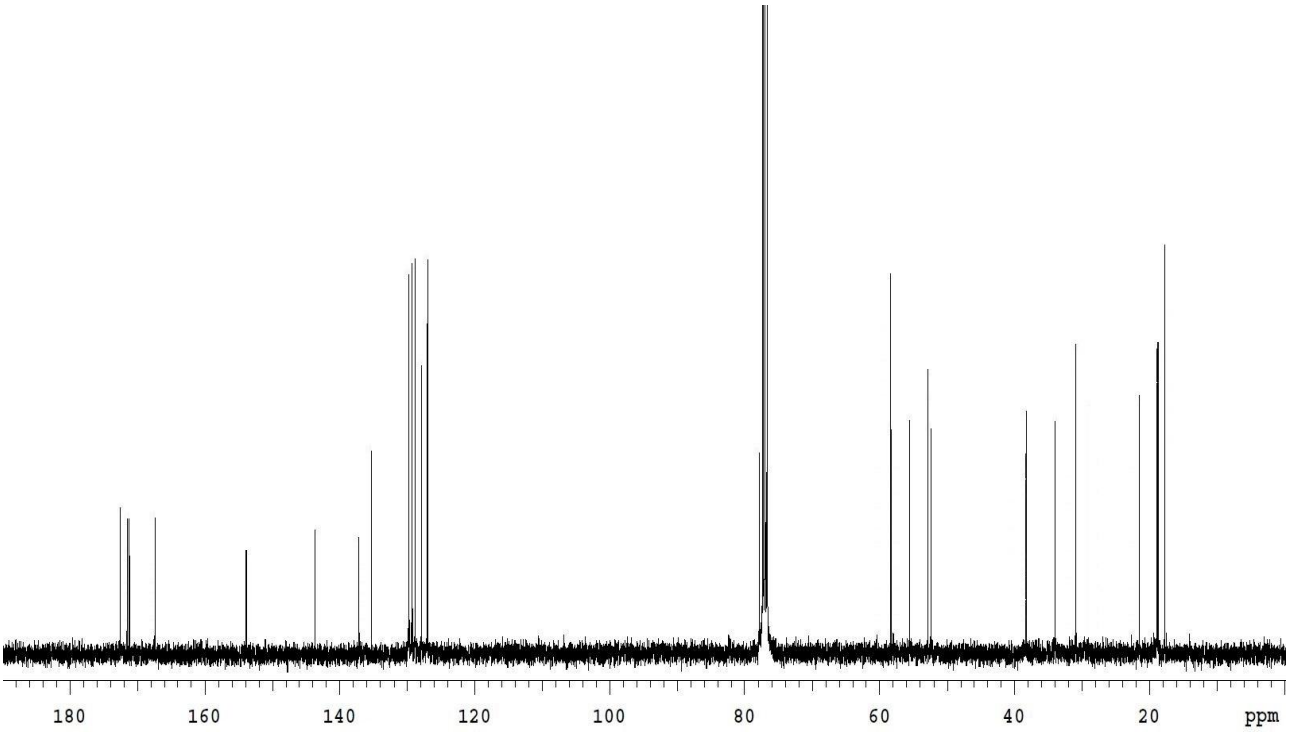
180
160
140
120
100
80
60
40
20
ppm

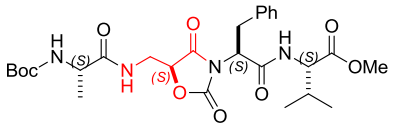
Boc
H
N
O
(S)
N
H
(S)
O
O
O
N
(S)
Ph
O
H
N
(S)
O
OMe

3f

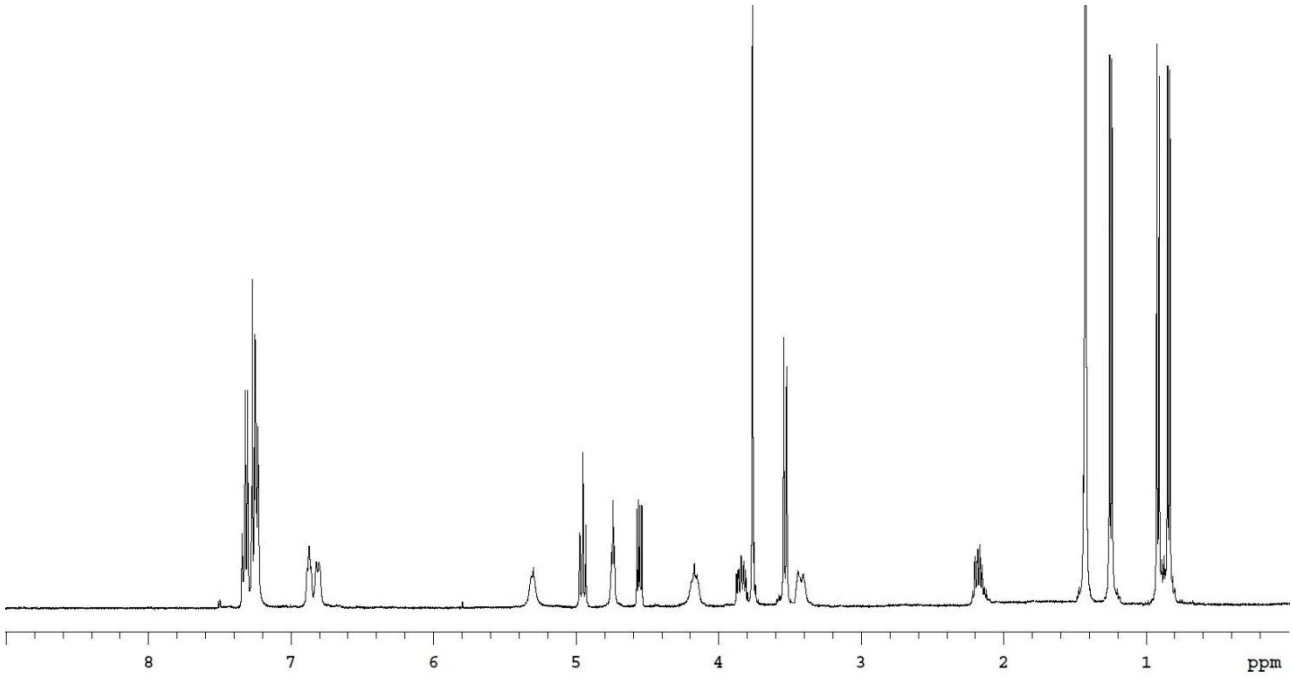
8
7
6
5
4
3
2
1
ppm

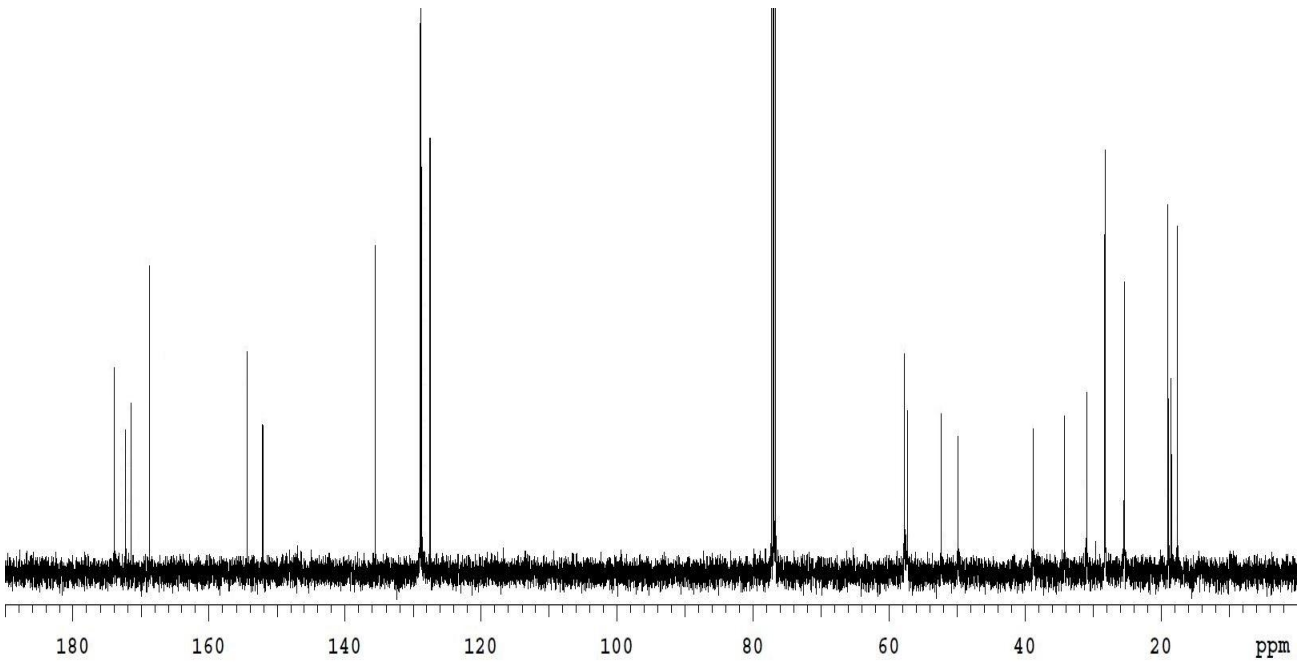
180
160
140
120
100
80
60
40
20
ppm

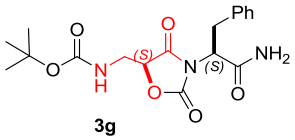
Ph
O
O
NH2
(S)
(S)
N
H
O
O
O

3g

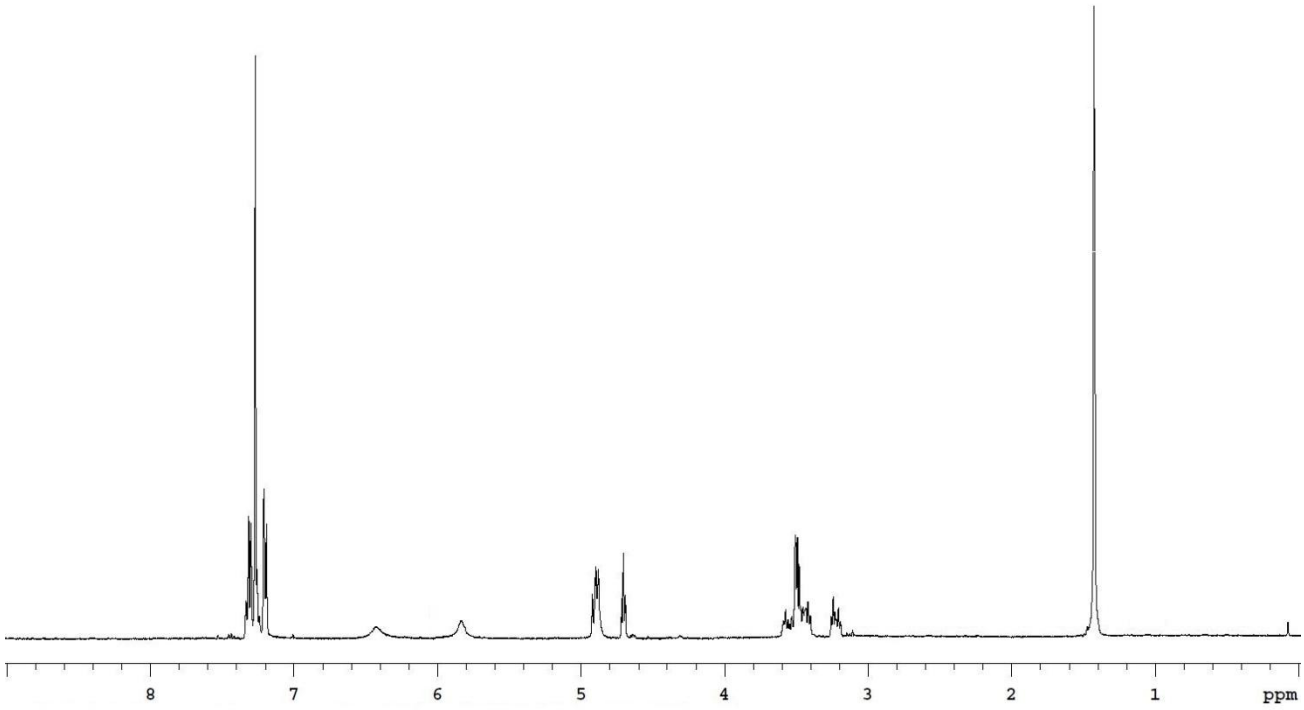
8
7
6
5
4
3
2
1
ppm

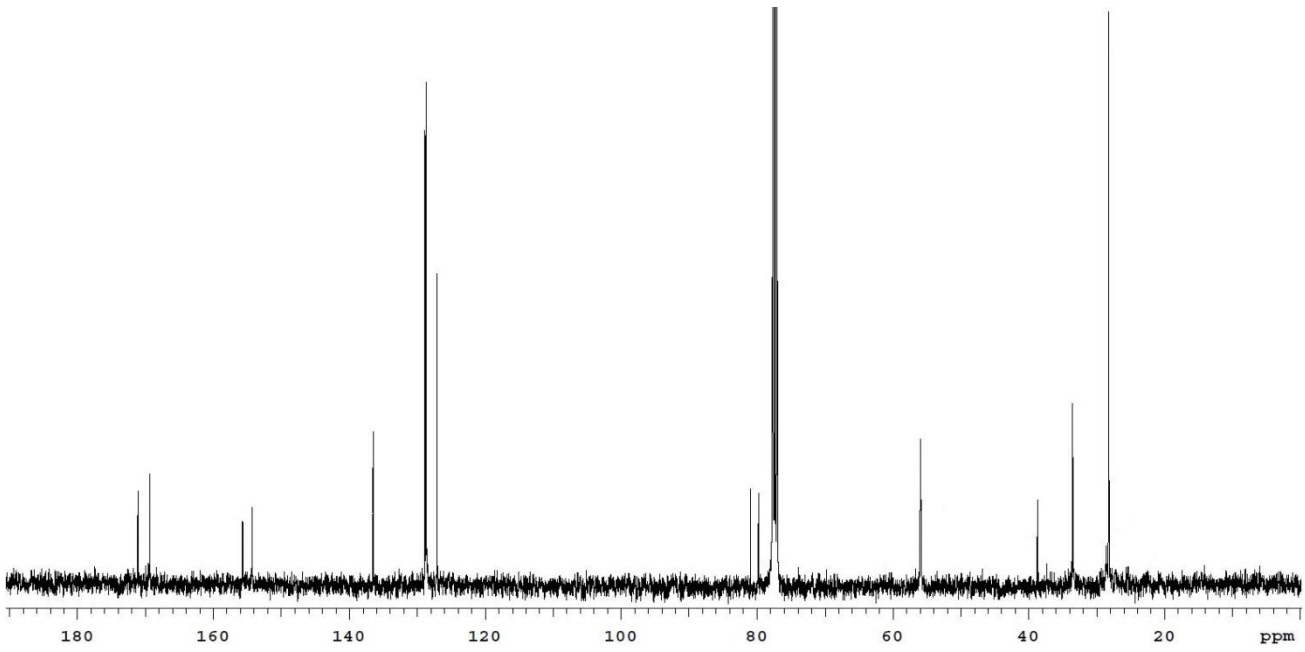
180
160
140
120
100
80
60
40
20
ppm

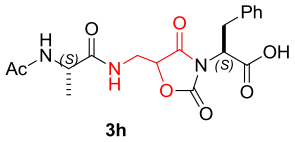
Ph
H
N
O
Ac
(S)
N
H
O
O
N
(S)
OH
O
O

3h

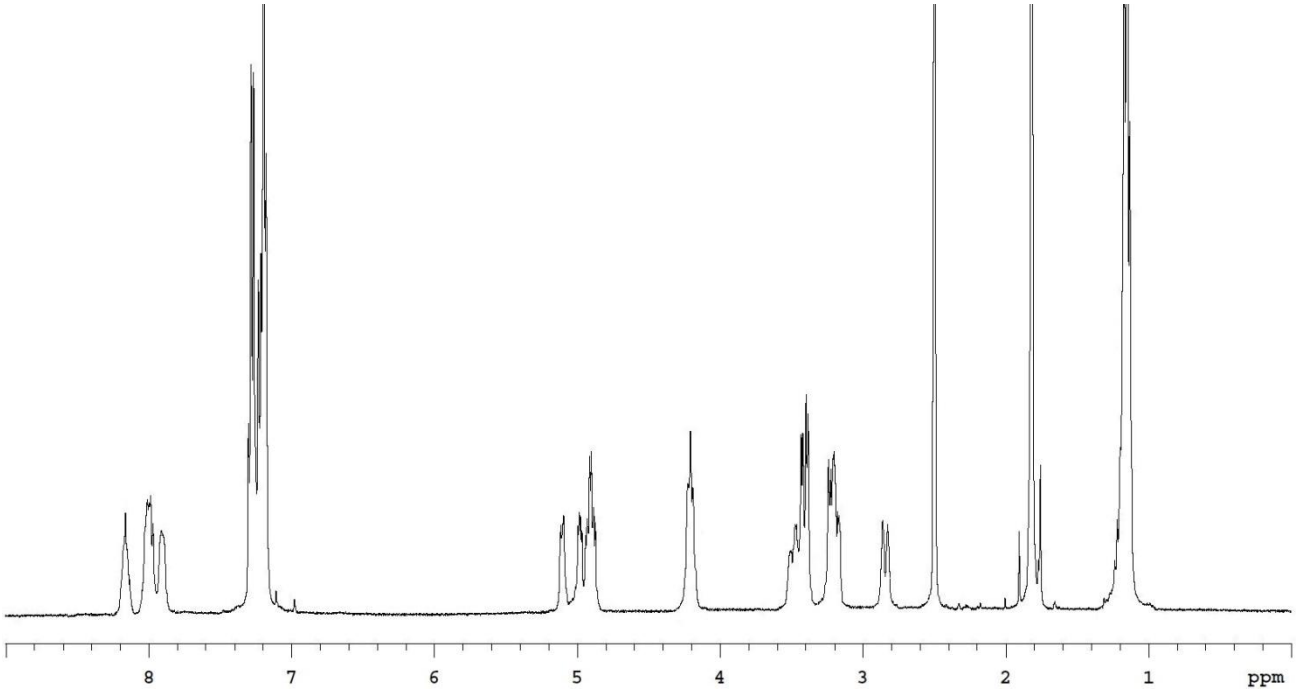
8
7
6
5
4
3
2
1
ppm

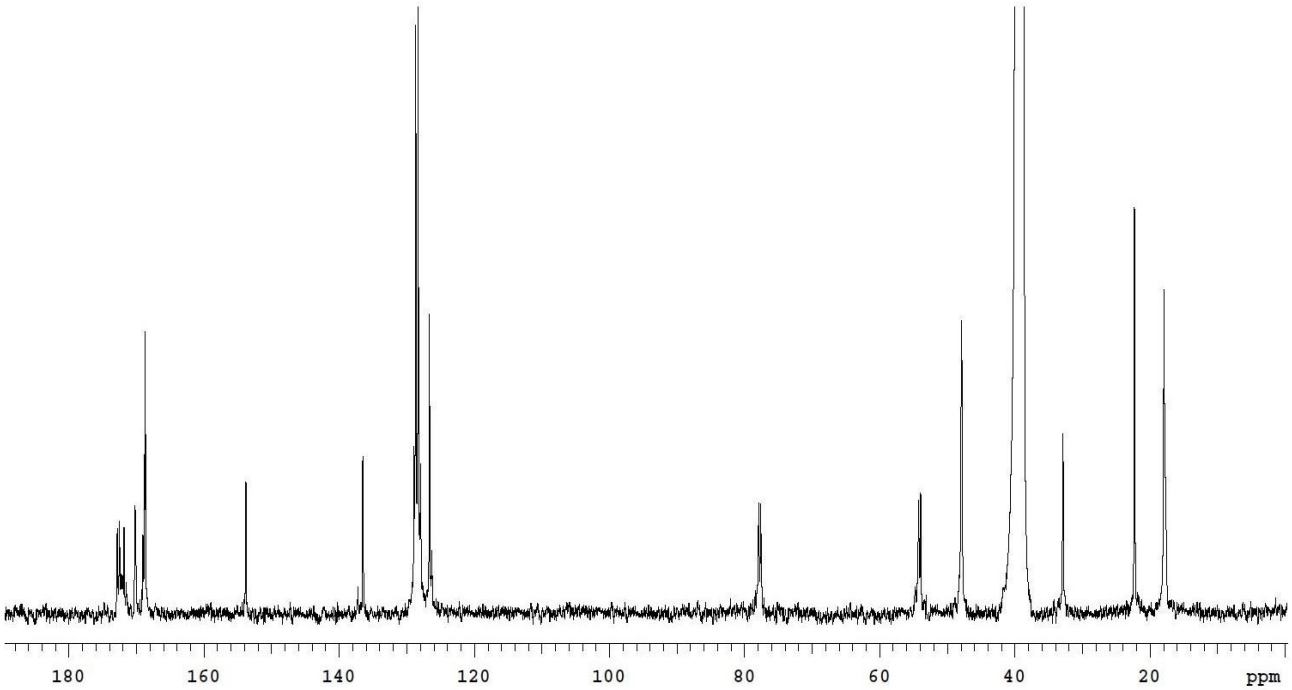
180
160
140
120
100
80
60
40
20
ppm

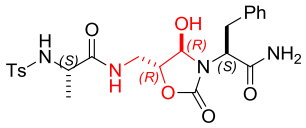
Ts
H
N
(S)
O
N
H
OH
(R)
(R)
O
O
N
(S)
Ph
NH2
O

5

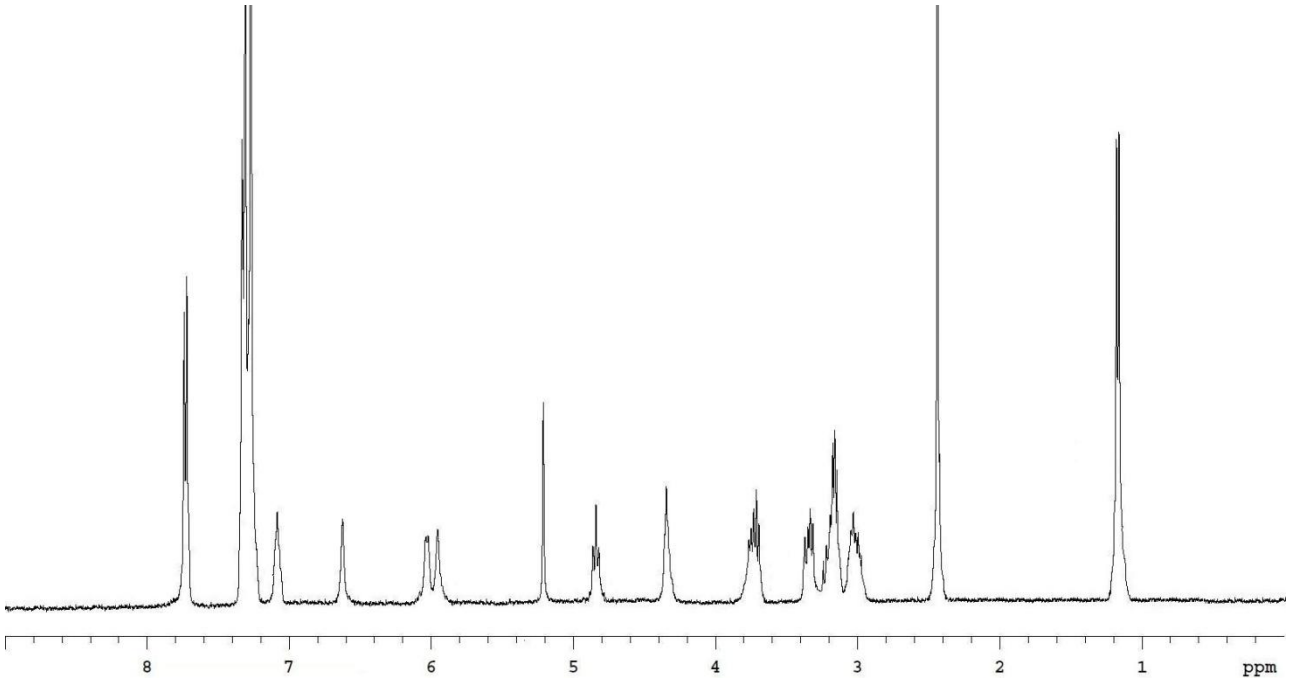
8
7
6
5
4
3
2
1
ppm

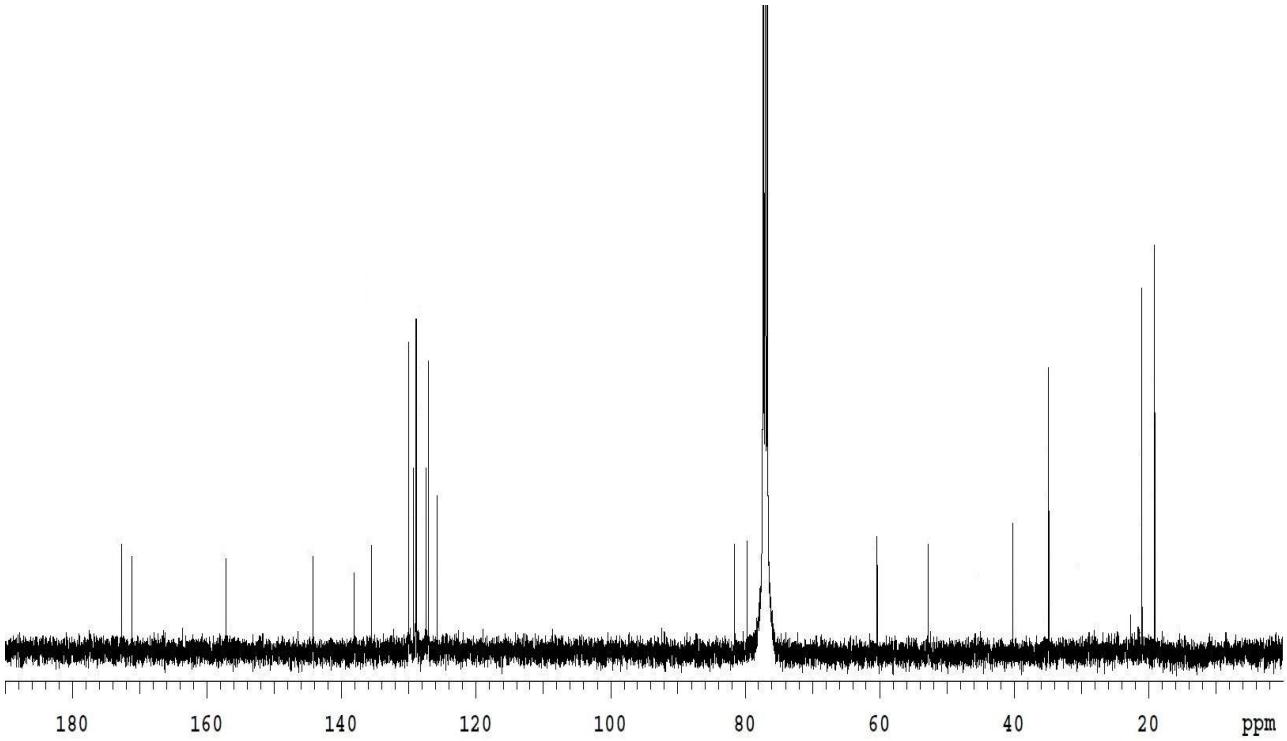
180
160
140
120
100
80
60
40
20
ppm

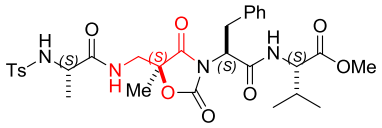

10a

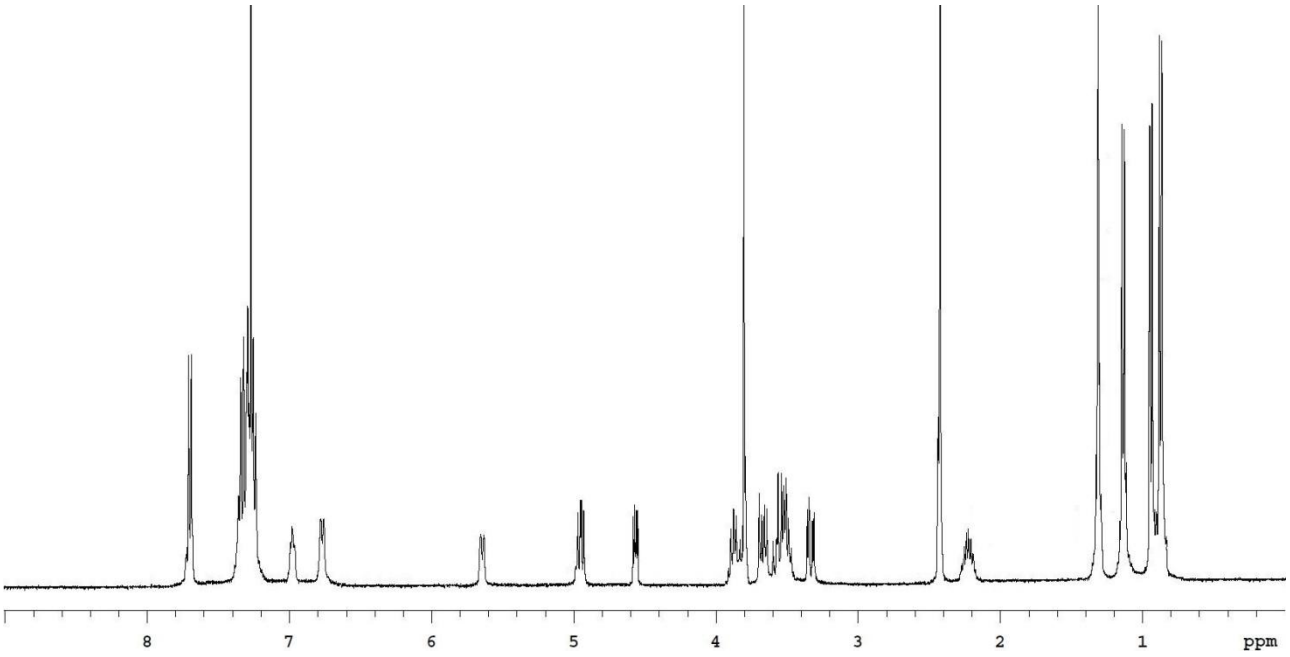

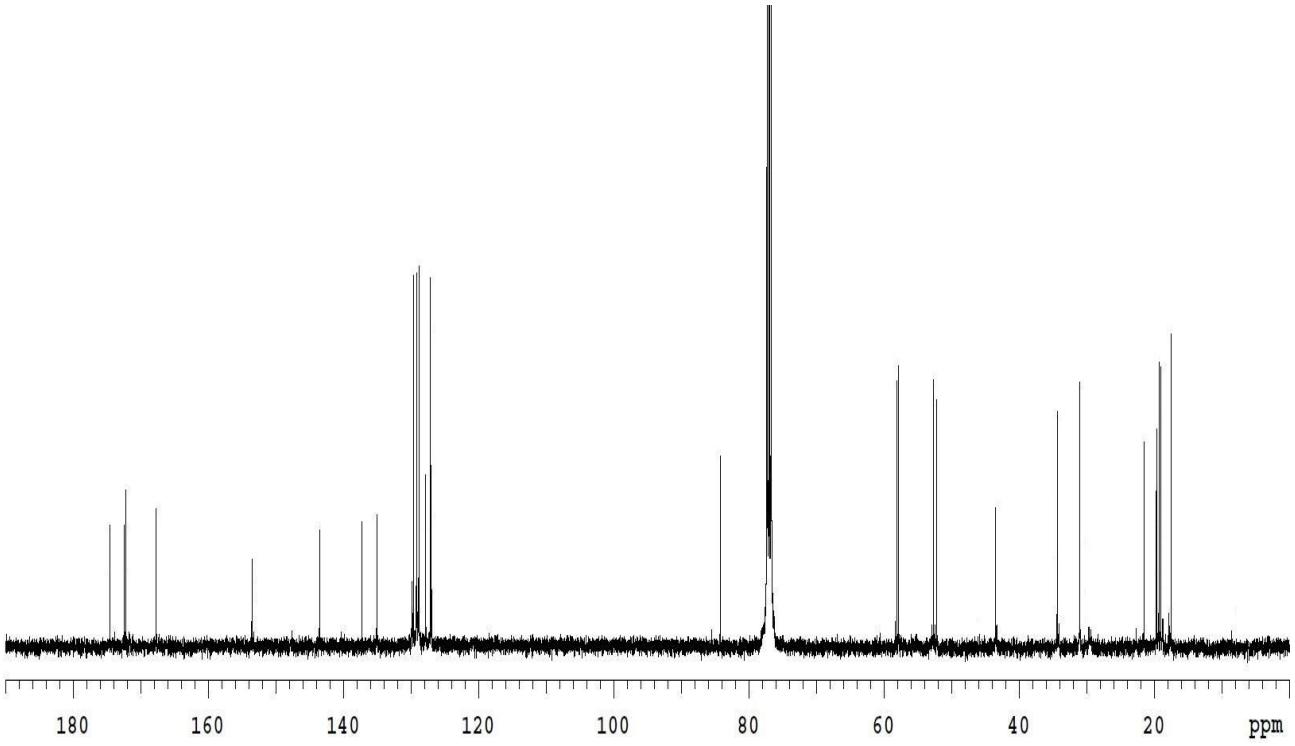

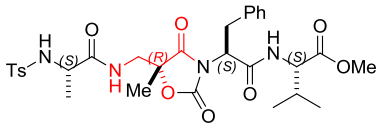

10b

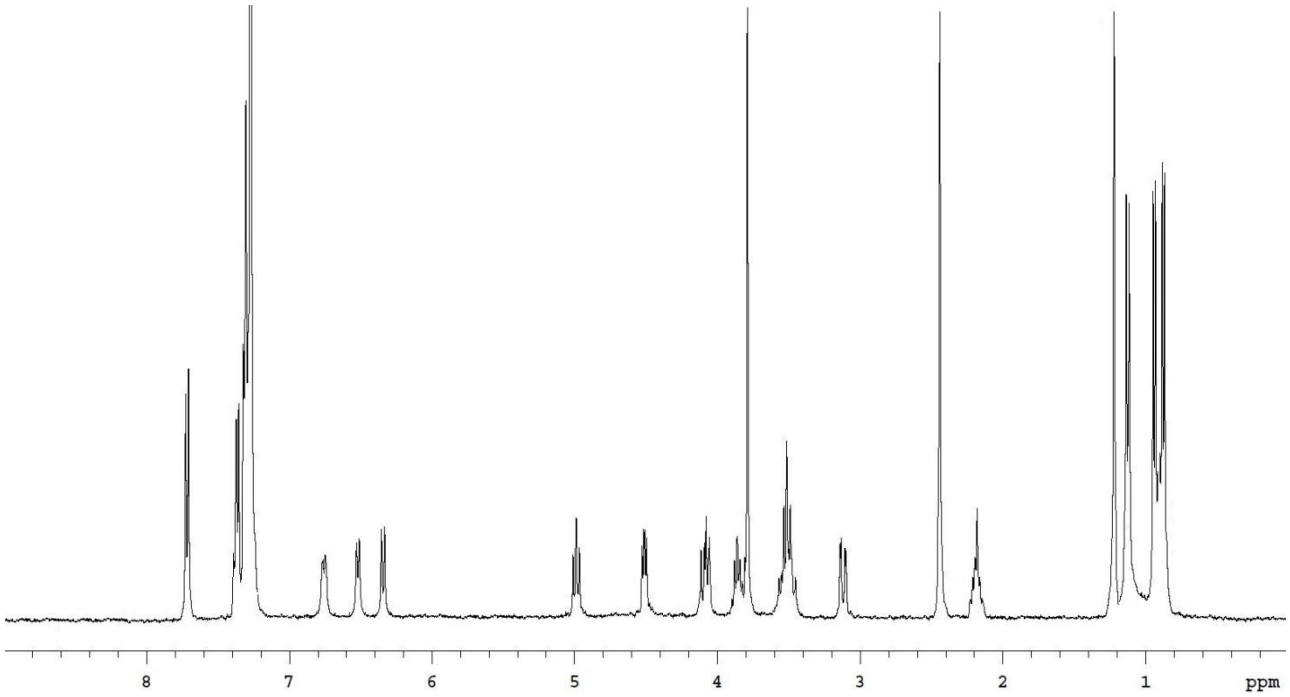

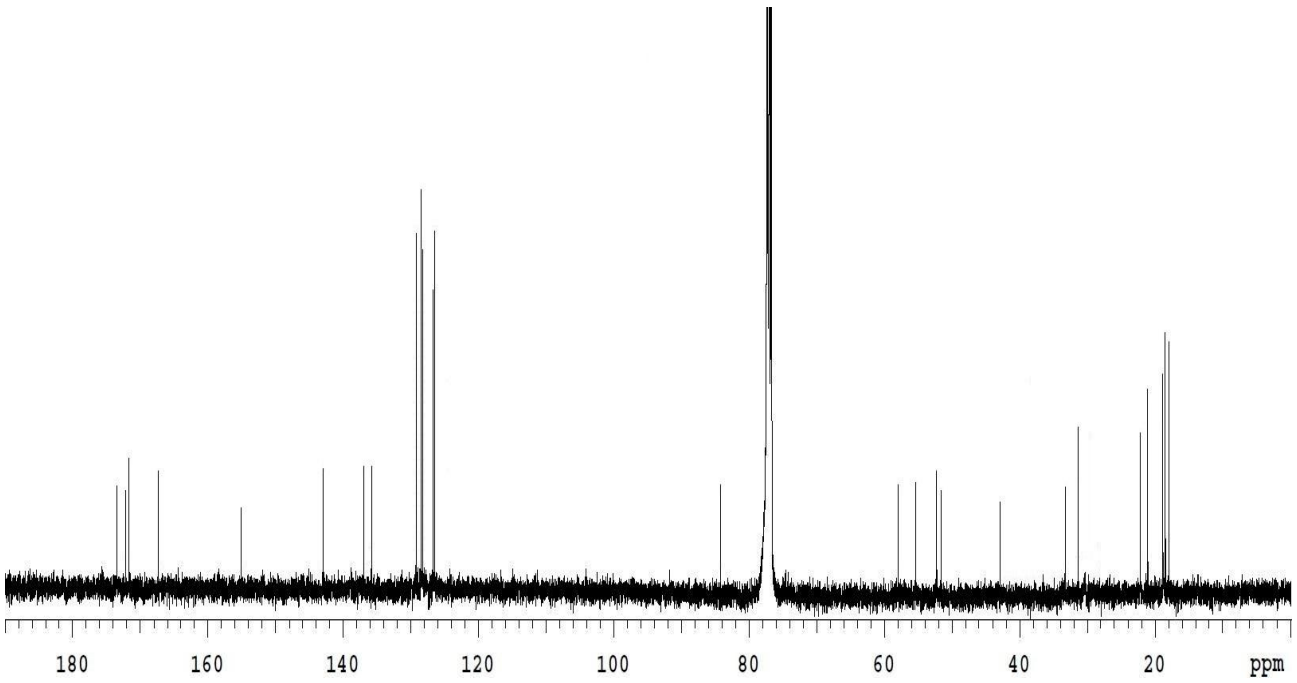

5.4.3. Conformationa analysis

ROESY and molecular dynamics. 2D ROESY experiments in 8:2 [D_6]DMSO/H_2O were performed in the phase sensitive mode at r.t., spin-locking field (γb2) was 2000 Hz, and mixing time was set to 250 ms; spectra were processed in the hypercomplex approach; peaks were calibrated on DMSO. Only ROESY-derived constraints were included in the restrained molecular dynamics.[50] Cross-peak intensities were classified very strong, strong, medium, and weak, and were associated with distances of 2.3, 2.7, 3.3, and 5.0 Å, respectively.[51] The intensities of the cross peaks arising from protons separated by known distances (e.g. geminal) were found to match with these associations. Geminal and other obvious correlations were discarded as constraints. For the absence of Hα(i, i+1) ROESY cross peaks, all of the ω bonds were set at 180° (force constant: 16 kcal mol^{-1} $Å^{-2}$).

Table 4. Non-obvious ROESY cross-peaks observed for **3d** in 8:2 [D_6]DMSO/H_2O.[a]

Cross-peak	intensity	Cross-peak	Intensity
ValNH-ValMe	vs	$PheArH_{3,5}$-$AmoH\beta_{up}$	m
ValNH-AlaMe	w	$PheArH_{3,5}$-$PheH\beta_{up}$	m
ValNH-ValHβ	s	$PheArH_{3,5}$-$PheH\beta_{dw}$	w
ValNH-TsMe	w	$PheArH_{3,5}$-ValHα	w
ValNH-$AmoH\beta_{up}$	w	$PheArH_{3,5}$-PheHα	m
ValNH-$PheH\beta_{up}$	w	$PheArH_4$-ValMe	w
ValNH-$PheH\beta_{dw}$	s	$PheArH_4$-TsMe	w
ValNH-COOMe	w	$PheArH_{2,6}$-ValMe	w
ValNH-ValHα	m	$PheArH_{2,6}$-AlaMe	w
ValNH-PheHα	vs	$PheArH_{2,6}$-TsMe	w
ValNH-AlaNH	w	$PheArH_{2,6}$-$AmoH\beta_{up}$	m
ValNH-AmoNH	w	$PheArH_{2,6}$-$PheH\beta_{up}$	vs
AmoNH-ValMe	w	$PheArH_{2,6}$-$PheH\beta_{dw}$	s
AmoNH-AlaMe	m	$PheArH_{2,6}$-PheHα	vs
AmoNH-$AmoH\beta_{up}$	s	AmoHα-AlaMe	m
AmoNH-$AmoH\beta_{dw}$	m	AmoHα-$AmoH\beta_{up}$	m
AmoNH-AlaHα	vs	AmoHα-$AmoH\beta_{dw}$	vs
AmoNH-AmoHα	m	PheHα-ValMe	w
AmoNH-$TsArH_{2,6}$	m	PheHα-ValHβ	w
AmoNH-AlaNH	m	PheHα-TsMe	w
AlaNH-ValMe	w	PheHα-$PheH\beta_{up}$	m
AlaNH-AlaMe	vs	PheHα-$PheH\beta_{dw}$	s
AlaNH-$PheH\beta_{dw}$	w	PheHα-COOMe	w
AlaNH-AlaHα	m	PheHα-ValHα	w
AlaNH-PheHα	w	ValHα-AlaMe	w
AlaNH-$TsArH_{2,4}$	w	ValHα-ValHβ	vs
$TsArH_{2,6}$-ValMe	w	ValHα-TsMe	w
$TsArH_{2,6}$-AlaMe	s	ValHα-$PheH\beta_{up}$	w
$TsArH_{2,6}$-$AmoH\beta_{up}$	w	ValHα-$PheH\beta_{dw}$	w
$TsArH_{2,6}$-$AmoH\beta_{dw}$	m	COOMe-ValHβ	m
$TsArH_{2,6}$-AlaHα	s	$PheH\beta_{dw}$-AlaMe	w

$TsArH_{2,6}$-ValHα	w	$PheH\beta_{up}$-ValMe	m
$TsArH_{2,6}$-AmoHα	w	$PheH\beta_{up}$-ValHβ	w
$TsArH_{3,5}$-ValMe	w	$AmoH\beta_{dw}$-AlaMe	w
$TsArH_{3,5}$-AlaMe	w	TsMe-ValMe	w
$TsArH_{3,5}$-$AmoH\beta_{dw}$	w	TsMe-AlaMe	w
$TsArH_{3,5}$-Val Hα	w	TsMe-ValHβ	w
$TsArH_{3,5}$-Amo Hα	w	ValHβ-AlaMe	w
$PheArH_{3,5}$-AlaMe	w	ValMe-AlaMe	w

[a] Stereochemistry has been omitted; [b] up = upfield, dw = downfield; [c] vs = very strong, s = strong, m = medium, w = weak.

Table 5. Non-obvious ROESY cross-peaks observed for **3e** in 8:2 $[D_6]$DMSO/H_2O.[a]

Cross-peak	Intensity	Cross-peak	Intensity
ValNH-ValMe	vs	$PheArH_{3,5}$-$PheH\beta_{up}$	w
ValNH-ValHβ	s	$PheArH_{3,5}$-$PheH\beta_{dw}$	w
ValNH-AmoHα	w	$PheArH_{3,5}$-Phe Hα	w
ValNH-$PheH\beta_{up}$	m	$PheArH_{2,6}$-AlaMe	w
ValNH-$PheH\beta_{dw}$	w	$PheArH_{2,6}$-$AmoH\beta_{dw}$	m
ValNH-COOMe	w	$PheArH_{2,6}$-$PheH\beta_{up}$	s
ValNH-ValHα	m	$PheArH_{2,6}$-$PheH\beta_{dw}$	vs
ValNH-PheHα	vs	$PheArH_{2,6}$-PheHα	vs
ValNH-AlaNH	w	AmoHα-ValMe	w
ValNH-AmoNH	w	AmoHα-$AmoH\beta_{up}$	m
AmoNH-ValMe	w	AmoHα-$AmoH\beta_{dw}$	m
AmoNH-AlaMe	m	AmoHα-$PheH\beta_{dw}$	w
AmoNH-$AmoH\beta_{up}$	m	AmoHα-ValHα	w
AmoNH-$AmoH\beta_{dw}$	s	PheHα-ValMe	w
AmoNH-AlaHα	vs	PheHα-ValHβ	w
AmoNH-AmoHα	w	PheHα-$PheH\beta_{up}$	s
AmoNH-AlaNH	w	PheHα-$PheH\beta_{dw}$	m
AlaNH-ValMe	w	PheHα-ValHα	w
AlaNH-AlaMe	vs	ValHα-AlaMe	m
AlaNH-AmoHα	w	ValHα-ValHβ	m
AlaNH-AlaHα	s	ValHα-ValMe	vs
AlaNH-$TsArH_{2,6}$	s	ValHα-$AmoH\beta_{dw}$	w
AlaNH-$TsArH_{3,5}$	s	ValHα-$PheH\beta_{up}$	w
$TsArH_{2,6}$-ValMe	w	ValHα-$PheH\beta_{dw}$	w
$TsArH_{2,6}$-AlaMe	m	COOMe-ValMe	w
$TsArH_{2,6}$-AlaHα	m	COOMe-ValHβ	w
$TsArH_{2,6}$-ValHα	w	COOMe-$PheH\beta_{up}$	s
$TsArH_{2,6}$-AmoHα	w	AlaHα-TsMe	w

$TsArH_{2,6}$-PheHα	w	TsMe-AlaMe	w
$TsArH_{3,5}$-ValMe	w	TsMe-ValHβ	m
$TsArH_{3,5}$-AlaMe	w	ValHβ-AlaMe	w
$PheArH_{3,5}$-$AmoH\beta_{dw}$	w	ValMe-AlaMe	w

[a] Stereochemistry has been omitted; [b] up = upfield, dw = downfield; [c] vs = very strong, s = strong, m = medium, w = weak.

Table 6. Non-obvious ROESY cross-peaks observed for **10a** in 8:2 $[D_6]DMSO/H_2O$.[a]

Cross-peak	intensity	Cross-peak	Intensity
ValNH-ValMe	vs	$PheArH_{3,5}$-AlaMe	w
ValNH-AlaMe	m	$PheArH_{3,5}$-$AmoH\beta_{up}$	m
ValNH-ValHβ	s	$PheArH_{3,5}$-$PheH\beta_{up}$	m
ValNH-TsMe	w	$PheArH_{3,5}$-$PheH\beta_{dw}$	w
ValNH-$AmoH\beta_{up}$	w	$PheArH_{3,5}$-ValHα	w
ValNH-$PheH\beta_{up}$	w	$PheArH_{3,5}$-PheHα	m
ValNH-$PheH\beta_{dw}$	s	$PheArH_4$-ValMe	w
ValNH-COOMe	w	$PheArH_4$-TsMe	w
ValNH-ValHα	m	$PheArH_{2,6}$-ValMe	w
ValNH-PheHα	vs	$PheArH_{2,6}$-AlaMe	w
ValNH-AlaNH	w	$PheArH_{2,6}$-TsMe	w
ValNH-AmoNH	w	$PheArH_{2,6}$-$AmoH\beta_{up}$	m
AmoNH-ValMe	w	$PheArH_{2,6}$-$PheH\beta_{up}$	vs
AmoNH-AlaMe	m	$PheArH_{2,6}$-$PheH\beta_{dw}$	s
AmoNH-AmoMe	m	$PheArH_{2,6}$-PheHα	vs
AmoNH-ValHβ	m	PheHα-ValMe	w
AmoNH-$AmoH\beta_{up}$	s	PheHα-ValHβ	w
AmoNH-$AmoH\beta_{dw}$	m	PheHα-TsMe	w
AmoNH-AlaHα	vs	PheHα-$PheH\beta_{up}$	m
AmoNH-ValHα	m	PheHα-$PheH\beta_{dw}$	s
AmoNH-PheHα	m	PheHα-COOMe	w
AmoNH-$TsArH_{2,6}$	m	PheHα-ValHα	w
AmoNH-AlaNH	m	ValHα-AlaMe	m
AlaNH-ValMe	m	ValHα-ValHβ	vs
AlaNH-AlaMe	vs	ValHα-TsMe	w
AlaNH-ValHβ	w	ValHα-$PheH\beta_{up}$	w
AlaNH-$PheH\beta_{dw}$	w	ValHα-AlaHα	m
AlaNH-AlaHα	m	ValHα-COOMe	m
AlaNH-ValHα	m	ValHα-$PheH\beta_{dw}$	w
AlaNH-PheHα	w	COOMe-ValHβ	m
AlaNH-$TsArH_{2,4}$	w	$PheH\beta_{dw}$-AlaMe	w
$TsArH_{2,6}$-ValMe	w	$PheH\beta_{up}$-ValMe	m
$TsArH_{2,6}$-AlaMe	s	$PheH\beta_{up}$-ValHβ	w

$TsArH_{2,6}$-AmoMe	w	$AmoH\beta_{dw}$-AlaMe	w
$TsArH_{2,6}$-$AmoH\beta_{up}$	w	TsMe-ValMe	w
$TsArH_{2,6}$-$AmoH\beta_{dw}$	m	TsMe-AlaMe	w
$TsArH_{2,6}$-AlaHα	s	TsMe-ValHβ	w
$TsArH_{2,6}$-ValHα	w	ValHβ-AlaMe	m
$TsArH_{3,5}$-ValMe	w	AmoMe-AlaMe	w
$TsArH_{3,5}$-AlaMe	w	AmoMe-$AmoH\beta_{up}$	m
$TsArH_{3,5}$-AmoMe	w	AmoMe-$AmoH\beta_{dw}$	vs
$TsArH_{3,5}$-$AmoH\beta_{dw}$	w	AlaMe-ValMe	m
$TsArH_{3,5}$-ValHα	w		

[a] Stereochemistry has been omitted; [b] up = upfield, dw = downfield; [c] vs = very strong, s = strong, m = medium, w = weak.

Table 7. Non-obvious ROESY cross-peaks observed for **10b** in 8:2 $[D_6]$DMSO/H_2O.[a]

Cross-peak	Intensity	Cross-peak	Intensity
ValNH-ValMe	vs	$PheArH_{3,5}$-$PheH\beta_{up}$	w
ValNH-AmoMe	m	$PheArH_{3,5}$-$PheH\beta_{dw}$	w
ValNH-ValHβ	s	$PheArH_{3,5}$-PheHα	w
ValNH-$PheH\beta_{up}$	m	$PheArH_{2,6}$-AlaMe	w
ValNH-$PheH\beta_{dw}$	w	$PheArH_{2,6}$-$AmoH\beta_{dw}$	m
ValNH-COOMe	w	$PheArH_{2,6}$-$PheH\beta_{up}$	s
ValNH-ValHα	m	$PheArH_{2,6}$-$PheH\beta_{dw}$	vs
ValNH-PheHα	vs	$PheArH_{2,6}$-PheHα	vs
ValNH-AlaNH	w	PheHα-ValMe	w
ValNH-AmoNH	w	PheHα-ValHβ	w
AmoNH-ValMe	w	PheHα-$PheH\beta_{up}$	s
AmoNH-AlaMe	m	PheHα-$PheH\beta_{dw}$	m
AmoNH-AmoMe	m	PheHα-ValHα	w
AmoNH-$AmoH\beta_{up}$	m	ValHα-AlaMe	m
AmoNH-$AmoH\beta_{dw}$	s	ValHα-ValHβ	m
AmoNH-AlaHα	vs	ValHα-ValMe	vs
AmoNH-AlaNH	w	ValHα-$AmoH\beta_{dw}$	w
AlaNH-ValMe	w	ValHα-$PheH\beta_{up}$	w
AlaNH-AlaMe	vs	ValHα-$PheH\beta_{dw}$	w
AlaNH-AmoMe	w	COOMe-ValMe	w
AlaNH-AlaHα	s	COOMe-ValHβ	w
AlaNH-$TsArH_{2,6}$	s	COOMe-$PheH\beta_{up}$	s
AlaNH-$TsArH_{3,5}$	s	AlaHα-TsMe	w
$TsArH_{2,6}$-ValMe	w	TsMe-AlaMe	w
$TsArH_{2,6}$-AlaMe	m	TsMe-ValHβ	m
$TsArH_{2,6}$-AmoMe	w	ValHβ-AlaMe	w

$TsArH_{2,6}$-AlaHα	m	AmoMe-ValMe	m
$TsArH_{2,6}$-ValHα	w	AmoMe-AmoHβ_{up}	m
$TsArH_{2,6}$-PheHα	w	AmoMe-AmoHβ_{dw}	m
$TsArH_{3,5}$-ValMe	w	AmoMe-PheHβ_{dw}	w
$TsArH_{3,5}$-AlaMe	w	AmoMe-ValHα	m
$PheArH_{3,5}$-AmoHβ_{dw}	w	AlaMe-ValMe	m

[a] Stereochemistry has been omitted; [b] up = upfield, dw = downfield; [c] vs = very strong, s = strong, m = medium, w = weak.

The restrained MD simulations were conducted at 300 K and 1 atm using the AMBER force field in a 30×30×30 Å box of standard TIP3P models of equilibrated water.[52] Periodic boundary conditions were applied, a dielectric constant of 1 was used, and the cutoff distance for the nonbonded interactions was 12 Å. All water molecules with atoms that come closer than 2.3 Å to a solute atom were eliminated. A 100 ps simulation at 1200 K was used for generating 50 random structures that were subsequently subjected to a 50 ps restrained MD with a 50% scaled force field at the same temperature, followed by 50 ps with full restraints (distance force constant of 7 kcal mol^{-1} $Å^{-2}$), after which the system was cooled in 20 ps to 50 K. H-bond interactions were not included, nor were torsion angle restraints. The resulting structures were minimized with 3000 cycles of steepest descent and 3000 cycles of conjugated gradient (convergence of 0.01 kcal $Å^{-1}$ mol^{-1}). The backbones of the structures were clustered by the rmsd analysis.[50]

Unrestrained MD simulations[50] were performed starting with the conformation derived from ROESY in a 30×30×30 Å box of standard TIP3P water for 10 ns at 298 K using periodic boundary conditions, at constant temperature and pressure (Berendsen scheme,[53] bath relaxation constant of 0.2). For 1-4 scale factors, van der Waals and electrostatic interactions are scaled in AMBER to half their nominal value. The integration time step was set to 0.1 fs. The system coordinates were collected every picosecond.

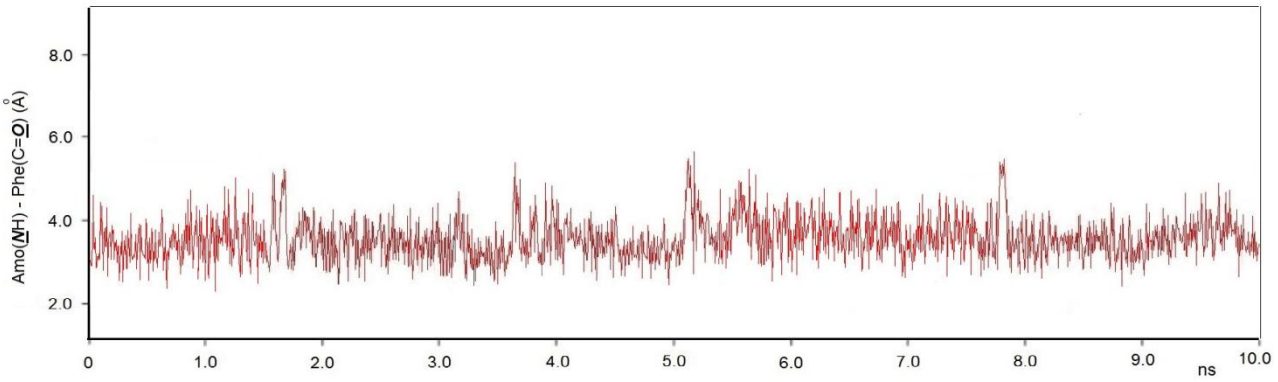

Figure 11. Distances (Å) between the amide nitrogen of Amo^2 and the carbonyl oxygen of Phe^3 sampled from a 10 ns unrestrained Molecular Dynamics simulation of **10a** calculated in a 30x30x30 Å box of equilibrated standard TIP3P water molecules, using the ROESY-derived geometry as starting structure.

Computational Methods. Theoretical calculations and full molecular geometry optimizations in the ground state have been performed in vacuo by using the Density Functional Theory (DFT)[54] Methods implemented the Gaussian 09 package of programs.[34] In particular, calculations were carried out by combining the three-parameter hybrid functional (B3) for the exchange part[55] and the Lee–Yang–Parr (LYP)[56] to the 6-311++G(d,p) basis set.

5.5. Plausible reaction pathway for the synthesis of Amo-peptides.

A plausible reaction pathway for the cyclization of the model peptide Ts-Ala-*iso*Ser-$PheNH_2$ to Ts-Ala-Amo-$PheNH_2$ with DSC and catalytic DIPEA is depicted in Scheme 8. In the proposed mechanism, the cyclization to Amo proceeds *via* the *iso*Ser-*O*-succinimidyl carbonate intermediate **A**. The intermediate **A** is deprotonated by DIPEA at PheNH, giving the 5-membered anionic intermediate **B** with endocyclic C=O (path **a**). The loss of 2,5-dioxopyrrolidin-1-olate leaving group, rapidly protonated by $DIPEAH^+$, leads to the Amo-peptide **3** and DIPEA, which can be utilized in catalytic amount. The intermediate **A** can be deprotonated at *iso*SerNH as well (path **b**); this could give access to the alternative 5-membered cyclic anionic intermediate **C** with hexocyclic C=O, precursor of a Oxd-peptide.

Preliminary computations were performed for the intermediates **B** and **C** employing Density Functional Theory; a systematic conformational analysis for the structures was done at the B3LYP/6-311++G(d,p) level. Optimization was performed by conjugate gradient algorithm, convergence at 0.001. The results indicate that the intermediate **B** is about 2.0 Kcal mol^{-1} more stable than the alternative intermediate **C**.

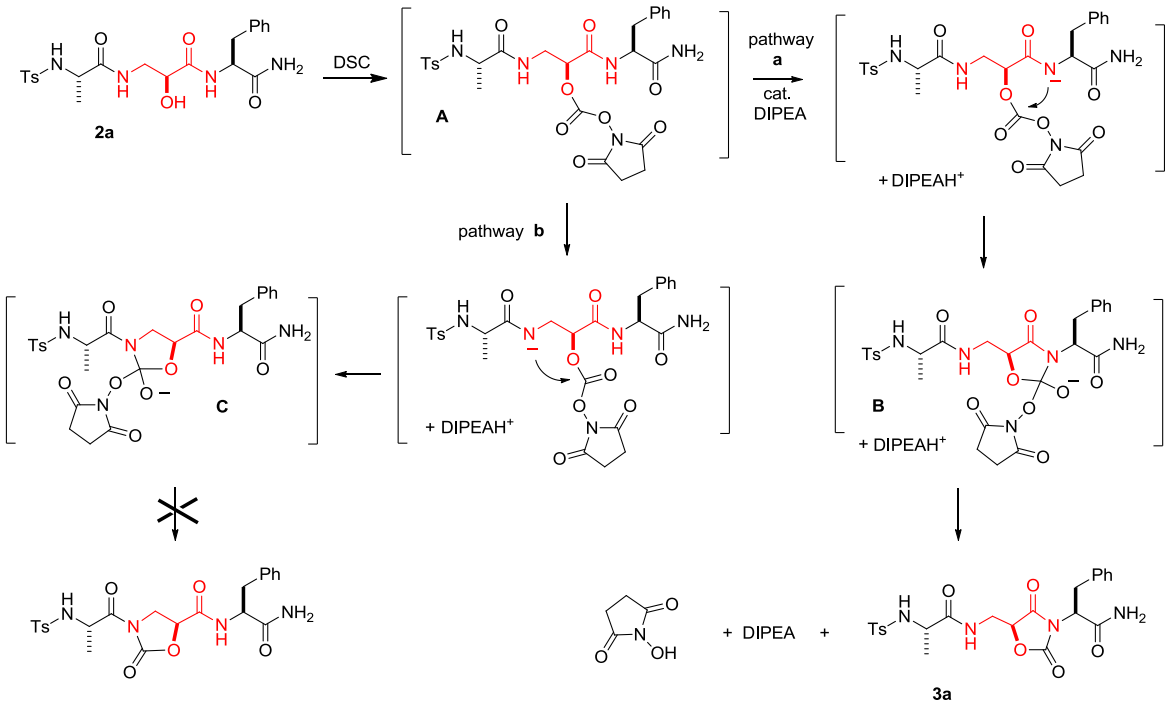

Scheme 8. Cyclization of the model peptide Ts-Ala-*iso*Ser-PheNH$_2$ **2** to Ts-Ala-Amo-PheNH$_2$ **3**.

References

1 L. Gentilucci, A. Tolomelli, F. Squassabia, *Curr. Med. Chem.* **2006**, *13*, 2449.

2 L. Gentilucci, R. De Marco, L. Cerisoli *Curr. Pharm. Des*. **2010**, *16*, 3185.

3 a) V. J. Hruby, P. M. Balse, *Curr. Med. Chem*. **2000**, *7*, 945-970. b) R. M. J. Liskamp, D. T. S. Rijkers, J. A. W. Kruijtzer, J. Kemmink. *Chem. Bio. Chem*. **2011**, *12*, 1626.

4 G. R. Gómez, J. D. A. Tyndall, B. Pfeiffer, G. Abbenante, D. P. Fairlie *Chem. Rev*. **2010,** *110*, PR1.

5 J. S. Richardson, *Adv. Protein Chem*. **1981**, *34*, 167.

6 For some reviews: a) A. J. Souers, J. A. Ellman, Tetrahedron 2001, 57, 7431. b) M. MacDonald, J. Aubé. *Curr. Org. Chem*. **2001**, *5*, 417. (c) W. A. Loughlin, J. D. A. Tyndall, M. P. Glenn, D. P. Fairlie. *Chem. Rev*. **2004**, *104*, 6085. (d) R. F. Hirschmann, K. C. Nicolaou, A. R. Angeles, J. S. Chen, A. B. Smith III. *Acc. Chem. Res.* **2009**, *42*, 1511. (e) L. R. Whitby, D. L. Boger. *Acc. Chem. Res.* **2012**, *45*, 1698. For some selected recent examples: (f) D. Blomberg, M. Hedenstro, P. Kreye, I. Sethson, K. Brickmann, J. Kihlberg, *J. Org. Chem.* **2004**, *69*, 3500. (g) G. Xuyuan, J. Ying, R. S. Agnes, E. Navratilova, P. Davis, G. Stahl, F. Porreca, H. I. Yamamura, V. J. Hruby. *Org. Lett.* **2004**, *19*, 3285. (h) U. Rosenström, C. Sköld, G. Lindeberg, M. Botros, F. Nyberg, A. Karlén, A. Hallberg. *J. Med. Chem.* **2006**, *49*, 6133. (i) L. Lomlim, J. Einsiedel, F. W. Heinemann, K. Meyer, P. Gmeiner. *J. Org. Chem.* **2008**, *73*, 3608. (l) Y. Angell, D. Chen, F. Brahimi, H. U. Saragovi, K. Burgess. *J. Am. Chem. Soc.* **2008**, *30*, 556. (m) R. Scheffelaar, R. A. K. Nijenhuis, M. Paravidino, M. Lutz, A. L. Spek, A. W. Ehlers, F. J. J. de Kanter, M. B. Groen, R. V. A. Orru, E. Ruijter. *J. Org. Chem.* **2009**, *74*, 660. (n) M. Sañudo, M. G. Valverde, S. Marcaccini, J. J. Delgado, J. Rojo, T. Torroba. *J. Org. Chem.* **2009**, *74*, 2189. (o) G. Lesma, N. Landoni, T. Pilati, A. Sacchetti, A. Silvani. *J. Org. Chem.* **2009**, *74*, 8098. (p) J. Y. Lee, I. Im, T. R. Webb, D. McGrath, M. Song, Y. Kim. *Bioorg. Chem.* **2009**, *37*, 90. (q) A. Mieczkowski, W. Koźmiński, J. Jurczak. *Synthesis* **2010**, *2*, 221. (r) A. Pinsker, J. Einsiedel, S. Harterich, R. Waibel, P. Gmeiner. *Org. Lett.* **2011**, *13*, 3502.

7 a) R. M. Freidinger, D. F. Veber, D. S. Perlow, J. R. Brooks, R. Saperstein. *Science* **1980**, *210*, 656. b) A. Perdih, D. Kikelj. *Curr. Med. Chem.* **2006**, *13*, 1525.

8 a) J. Aube. In *Advance in Amino Acid Mimetics and Peptidomimetics*; Abel, A., Ed.; JAI Press: Greenwich, **1997**, Vol. 1, 193-232. b) A.D. Piscopio, J.E. Robinson. *Curr. Opin. Chem. Biol*. **2004**, *8*, 245.

9 L. R. Whitby, Y. Ando, V. Setola, P. K. Vogt, B. L. Roth, D. L. Boger. *J. Am. Chem. Soc.* **2011,** *133*, 10184.

10 a) A. Perdih, D. Kikelj. *Curr. Med. Chem*. **2006,** *13*, 1525. b) R. M. Freidinger. *J. Org. Chem*. **1985**, *50*, 3631-3633. c) W. L. Scott, J. G. Martynow, J. C. Huffman, M. J. O'Donnell. *J. Am Chem. Soc.* **2007**, *129*, 7077.

11 a) C. Palomo, J. M. Aizpurua, A. Benito, R. Galarza, U. K. Khamrai, J. Vazquez, B. de Pascual-Teresa, P. M. Nieto, A. Linden. *Angew. Chem. Int. Ed.* **1999**, *38*, 3056. b) C. Palomo, J. M. Aizpurua, A. Benito, J. I. Miranda, R. M. Fratila, C. Matute, M. Domercq, F. Gago, S. Martin-Santamaria, A. Linden.

J. Am. Chem. Soc. **2003**, *125*, 16243. c) J.M. Aizpurua, C. Palomo, E. Balentová, A. Jimenez, E. Andreieff, M. Sagartzazu-Aizpurua, J. I. Miranda, A. Linden. *J. Org.* Chem. **2013**, 78, 224.

[12] a) L. Gentilucci, A. Tolomelli, R. De Marco, C. Tomasini, S. Feddersen. *Eur. J. Org. Chem.* **2011**, 4925. b) R. De Marco, A. Tolomelli, M. Campitiello, P. Rubini, L. Gentilucci. *Org. Biomol. Chem.* **2012**, *10*, 2307. c) R. De Marco, A. Greco, S. Rupiani, A. Tolomelli, C. Tomasini, S. Pieraccini, L. Gentilucci. *Org. Biomol. Chem.* **2013**, *11*, 4273.

[13] a) A. Polinsky, M. G. Cooney, A. Toy-Palmer, G. Osapay, M. Goodman. *J. Med. Chem*. **1992**, *35*, 4185. b) C. Bonauer, T. Walenzyk, B. König. *Synthesis* **2006**, *1*,1.

[14] a) Ö. Demir-Ordu, I. Doğan. Chirality **2010**, *22*, 641. b) G. Chen, C. Chunling Fu, S. Ma. *Org. Biomol. Chem*. **2011**, *9*, 105. c) S. Kano, T. Yokomatsu, H. Nemoto, S. Shibuya. *J. Am. Chem. Soc*. **1986**, *108*, 6746.

[15] a) G. Lelais, D. Seebach. *Biopolymers* 2004, *76*, 206. b) E. Juaristi, V. Soloshonok, Eds.; Wiley-VCH: New York, 2005. c) G. Cardillo, C. Tomasini. *Chem. Soc. Rev*. **1996**, *25*, 117.

[16] Toniolo, C. *Int. J. Peptide Protein Res.* **1990**, 35, 287.

[17] For a β2-β3-DKP scaffold: A. Sofia, M. Ressurreição, A. Bordessa, M. Civera, L. Belvisi, C. Gennari, U. Piarulli. *J. Org. Chem*. **2008**, *73*, 652.

[18] a) N. J. Ede, J. D. Rae, M. T. W. Hearn. Tetrahedron Lett. 1990, 31, 6071. b) K. Weber, P. Gmeiner. *Synlett* **1998**, 885-886. c) D. Michel, R.. Waibel, P. Gmeiner. *Heterocycles* **1999**, *51*, 365. d) T. Lehmann, D. Michel, M. Glänzel, R. Waibel, P. Gmeiner. *Heterocycles* **1999**, *51*, 1389. e) K. Weber, U. Ohnmacht, P. Gmeiner. *J. Org. Chem*. **2000**, *65*, 7406. f) P. G Hoffmann. *Synlett* **2002**, *6*, 1014.

[19] a) C. M. Goodman, S. Choi, S. Shandler, W. F. DeGrado. *Nat. Chem. Biol*. **2007**, *3*, 252. b) W. S. Horne, S. H. Gellman. *Acc. Chem. Res*. **2008**, *41*, 1399. c) L. K. Pilsl, O. Reiser. *Amino Acids* **2011**, *41*, 709. d) A. Roy, P. Prabhakaran, P. K. Baruah, G. J. Sanjayan. *Chem. Commun*. **2011**, 11593. e) T. A. Martinek, F. Fülöp. *Chem. Soc. Rev*. **2012**, *41*, 687.

[20] a) V. Santagada, F. Fiorino, E. Perissutti, B. Severino, V. De Filippis, B. Vivenzio, G. Caliendo. *Tetrahedron Lett*. **2001**, *42*, 5171. b) B. Bacsa, K. Horváti, S. Bõsze, F. Andreae, C. O. Kappe. *J. Org. Chem.* **2008**, *73*, 7532.

[21] T. Fujisawa, S. Odake, Y. Ogawa, J. Yasuda, Y. Morita, T. Morikawa. *Chem. Pharm. Bull.* **2002**, *50*, 239.

[22] a) Zlatopolskiy, B. D.; Radzom, M.; Zeeck, A.; de Meijere, A. *Eur. J. Org. Chem*. **2006**, *6*, 1525. b) Liu, S.; Yang, Y.; Liu, X.; Ferdousi, F. K.; Batsanov, Andrei S.; Whiting, A. *Eur. J. Org. Chem*. **2013**, 5692.

[23] M. Ousmer, N. A. Braun, C. Bavoux, M. Perrin, M. A. Ciufolini. *J. Am. Chem. Soc*. **2001**, *123*, 7534.

[24] A. Isidro-Llobet, M. Alvarez, F. Albericio. *Chem. Rev*. **2009**, *109*, 2455.

[25] T. Fukuyama, C. K. Jow, M. Cheung. *Tetrahedron Lett.* **1995**, *36*, 6373.

[26] G. Sabitha, B. V. S. Reddy, S. Abraham, J. S. Yadav. *Tetrahedron Lett*. **1999**, *40*, 1569.

[27] T. Ankner, G. Hilmersson. *Org. Lett*. **2009**, *11*, 503.

[28] G. Zappia, E. Gacs-Baitz, G. Delle Monache, D. Misiti, L. Nevola, B. Botta. *Curr. Org. Synth.* **2007**, *4*, 81.

[29] For some recent examples, see: a) J. E. Semple, T. D. Owens, K. Nguyen, O. E. Levy. *Org. Lett*. **2000**, *2*, 2769. b) Y. Aoyagi, R. P. Jain, R. M. Williams, *J. Am. Chem. Soc*. **2001**, *123*, 3472. c) F. Fringuelli, F. Pizzo, M. Rucci, L.Vaccaro. *J. Org. Chem*. **2003**, *68*, 7041. d) F. Gassa, A. Contini, G. Fontana, S. Pellegrino, M. L. Gelmi. *J. Org. Chem*. **2010**, *75*, 7099. e) Y. Jiang, X. Chen, Y. Zheng, Z. Xue, C. Shu, W.Yuan, X. Zhang. *Angew. Chem. Int. Ed*. **2011**, *50*, 7304-7307. f) F. Rodriguez, F. Corzana, A. Avenoza, J. H. Busto, J. M. Peregrina, M. D. M. Zurbano. *Curr. Top. Med. Chem*. **2014**, *14*, 1225.

[30] C. Christensen, K. Juhl, R. G. Hazell, K. A. Jørgensen. *J. Org. Chem*. **2002**, *67*, 4875.

[31] a) S. U. Pandya, R. S. Dickins, D. Parker. *Org. Biomol. Chem*. **2007**, *5*, 3842-3846. b) K. P. Jayakanthan, M. Y. D. Vankar. Tetrahedron 2004, 60, 397.

[32] a) J. Duan, B. W. King, C. Decicco, T. P. Jr. Maduskuie, M. E. Voss. PCT Int. Appl. (2001), WO 2001070734 A2 20010927.

[33] a) A. Banerjee, P. Balaram. *Curr. Sci. India* **1997**, *73*, 1067. b) Y.-D. Wu, D.-P. Wang, *J. Am. Chem. Soc*. **1999**, *121*, 9352; c) F. Schumann, A. Müller, M. Koksch, G. Müller, N. Sewald. *J. Am. Chem. Soc.* **2000**, *122*, 12009. d) R. Günther, H.-J. Hofmann, *Helv. Chim. Acta* **2002**, *85*, 2149 and references herein. e) S. Sagan, T. Milcent, R. Ponsinet, O. Convert, O. Tasseau, G. Chassaing, S. Lavielle O. Lequin. *Eur. J. Biochem.* **2003**, *270*, 939; f) C. Baldauf, R. Günther, H. Hofmann, *Biopolymers*, **2006**, *84*, 408. g) R. Rai, P. G. Vasudev, K. Ananda, S. Raghothama, N. Shamala, I. L. Karle, P. Balaram, *Chem. Eur. J*. **2007**, *13*, 5917. h) E. W. Guthöhrlein, M. Malešević, Z. Majer, N. Sewald. *Biopolymers* **2007**, *88*, 829. i) K. Basuroy, V. Karuppiah, N. Shamala, P. Balaram. *Helv. Chim. Acta*. **2012**, *95* 2589.

[34] M. J. Frisch, G. W. Trucks, H. B. Schlegel, G. E. Scuseria, M. A. Robb, J. R. Cheeseman, G. Scalmani, V. Barone, B. Mennucci, G. A. Petersson, H. Nakatsuji, M. Caricato, X. Li, H. P. Hratchian, Izmaylov, A. F. J. Bloino, G. Zheng, J. L. Sonnenberg, M. Hada, M. Ehara, K. Toyota, R. Fukuda, J. Hasegawa, M. Ishida, T. Nakajima, Y. Honda, O. Kitao, H. Nakai, T. Vreven, J. A., Jr. Montgomery, J. E. Peralta, F. Ogliaro, M. Bearpark, J. J. Heyd, E. Brothers, K. N. Kudin, V. N. Staroverov, R. Kobayashi, J. Normand, K. Raghavachari, A. Rendell, J. C. Burant, S. S. Iyengar, J. Tomasi, M. Cossi, N. Rega, J. M. Millam, M. Klene, J. E. Knox, J. B. Cross, V. Bakken, C. Adamo, J. Jaramillo, R. Gomperts, R. E. Stratmann, O. Yazyev, A. J.; R.; Pomelli, C.; Ochterski, J. W.; Martin, R. L.; Morokuma, K.; Zakrzewski, V. G. Austin, R. Cammi, C. Pomelli, J. W. Ochterski, R. L. Martin, K. Morokuma, V. G. Zakrzewski, G. A. Voth, P. Salvador, J. J. Dannenberg, S. Dapprich, A. D. Daniels, O. Farkas, J. B. Foresman, J. V. Ortiz, J. Cioslowski, D. J. Fox, Gaussian 09, Revision B.01; Gaussian, Inc.: Wallingford, CT, 2009.

[35] a) P. A. Temussi, D. Picone, G. Saviano, P. Amodeo, A. Motta, T. Tancredi, S. Salvadori, R. Tomatis. *Biopolymers* **1992**, *32*, 367, and references herein. b) A. Borics, G. Töth. *J. Mol. Graph. Modell*. **2010**, *28*, 495. c) E. Sikorska, M. J. Slusarz, B. Lammek, Bernard. *Biopolymers*, **2006**, *82*, 603.

[36] a) K. D. Kopple, M. Ohnishi, A. Go. *Biochemistry* **1969**, *8*, 4087. b) I.L. Karle, A. Banerjee, S. Bhattacharya, P. Balaram. *Biopolymers* **1996**, *38* 515.

[37] a) J. A. Smith, L. G. Pease. *J. Mol. Biol.* **1980**, *203*, 221. b) D. K. Chalmerst, G. R. Marshall. *J. Am. Chem. Soc*. **1995**, *117*, 5927. c) J. Venkatraman, S. C. Shankaramma, P. Balaram. *Chem. Rev*. **2001,** *101*, 3131. d) R. Rai, S. Raghothama, P. Balaram. *J. Am. Chem. Soc*. **2006**, *128*, 2675.

[38] S. Hecht, I. Huc, *Foldamers: Structure, Properties and Applications*, Wiley & Sons, **2007**, p. 456.

[39] a) C. Toniolo, E. Benedetti. *Crit. Rev. Biochem*. **1980**, *9*, 1. b) B. Imperiali, R. A. Moats, S. L. Fisher, T. J. Prins. *J. Am. Chem. Soc.***1992**, *114*, 3182. c) J. Yang, S. H. Gellman. *J. Am. Chem. Soc*. **1998**, *120*, 9090. d) I. G. Jones, W. Jones, M. North. *J. Org. Chem.* **1998**, *63*, 1505. e) L. Belvisi, C. Gennari, A. Mielgo, D. Potenza, C. Scolastico. *Eur. J. Org. Chem.* **1999**, 389.

[40] a) R. Kuroda, Y. Saito (Eds: N. Berova, K. Nakanishi, R. Woody); Wiley-VCH: New York **2000**, 601. b) O. Pieroni, A. Fissi, R. M. Jain, V. S. Chauhan. *Biopolymers* **1996**, *38*, 97. c) A. Perczel, M. Hollosi, B. M. Foxman, G. D. Fasman. *J. Am. Chem. Soc*. **1991**, *113*, 9772.

[41] M. Aschi, A. Mollica, G. Lucente, M. Paglialunga Paradisi, F. Mazza. *J. Mol. Struct*., **2006**, *785*, 176.

[42] R. Spadaccini P. A.Temussi. *Cell. Mol. Life Sci*. **2001**, *58*, 1572.

[43] K. Nguyen, M. Iskandar, D. L. Rabenstein. *J. Phys. Chem. B*, **2010**, **114**, 3387.

[44] K. Wüthrich, *NMR of Proteins and Nucleic Acids*, Wiley, New York, p. 320.

[45] W. D. Cornell, P. Cieplak, C. I. Bayly, I. R. Gould, K. M. Merz, D. M. Ferguson, D. C. Spellmeyer, T. Fox, J. W. Caldwell, P. A. Kollman. *J. Am. Chem. Soc*. **1995**, *117*, 5179.

[46] G. Srinivasulu, S. K. Kumar, G. V. M. Sharma, A. C. Kunwar. *J. Org. Chem.* **2006**, 71, 8395-8400.

[47] P. Prabhakaran, S. K. Kale, V. G. Puranik, P. R. Rajamohanan, O. Chetina, J. A. K. Howard, H.-J. Hofmann, G. J. Sanjayan. *J. Am. Chem. Soc*. **2008**, *130*, 17743.

[48] V. H. Thorat, T. S. Ingole, K. N. Vijayadas, R. V. Nair, S. S. Kale, V. V. E. Ramesh, H. C. Davis, P. Prabhakaran, R. G. Gonnade, R. L. Gawade, V. G. Puranik, P. R. Rajamohanan, G. J. Sanjayan, *Eur. J. Org. Chem*. **2013**, 3529.

[49] G. V. M. Sharma, P. Nagendar, P. Jayaprakash, P. R. Krishna, K. V. S. Ramakrishna, A. C. Kunwar, *Angew. Chem. Int. Ed*. 2005, *44*, 5878.

[50] HyperChem Release 8.0.3, Hypercube Inc., 1115 NW 4th St. Gainesville, FL 32608, USA, **2007**.

[51] M. P. Williamson, T. F. Havel, J. Wüthrich. *Mol Biol.* **1985**, *182*, 295.

[52] W. L. Jorgensen, J. Chandrasekhar, J. Madura, R. W. Impey, M. L. Klein. *J. Chem. Phys.* **1983**, *79*, 926.

[53] H. J. C. Berendsen, J. P. M. Postma, W. F. van Gunsteren, A. Di Nola, J. R. Haak. *J. Chem. Phys*. **1984**, *81*, 3684.

[54] W. Kohn, L.J. Sham. *Phys. Rev*., **1965**, *140*, A1133-A1138.

[55] A.D. Becke. *J. Chem. Phys*., **1993**, *98*, 5648.

[56] C. Lee, W. Yang, R.G. Parr. *Phys. Rev*., **1998**, B37, 785.

Chapter 6

Synthesis and conformational analysis of peptides containing the heterocycle Imd

N-heterocycles, including cyclic ureas, are useful and multi-purpose tools in medicinal chemistry, thanks to their abilities to induce conformational constraints and to confer appropriate pharmacokinetic features. Therefore, in this chapter, are proposed two different synthetic pathways for obtaining Imidazolidin-2-one rings, directly on peptide sequences. This scaffold demonstrated to be easily functionalizable and displayed the capability to induce a γ-turn, as determined by spectroscopic analyses.

6.1. Introduction

Proteins and peptides play a central role in nearly all physiological processes associated with life, this together with a diversity of chemical structure, makes them particularly attractive starting point for drug discovery programs.[1] In fact, peptides themselves have emerged relatively slowly as drugs, for example insulin in the treatment of diabetes and cyclosporin as an immunosuppressent. Their potential utilities as therapeutics are limited because of their inherent instability toward proteolytic cleavage by peptidases, lack of oral bioavailability, inability to cross the blood–brain barrier since their high molecular weight, and rapid excretion through the liver and kidneys.[2] These limitations have generated an intensive effort for overcoming these deficiencies in an attempt to develop peptidomimetics. The substitution of peptides with peptidomimetics has included a wide variety of strategies,[2c,d] that involve the chemical modification of a peptide to introduce/delete those biological and chemical properties associated with effective/ineffective drug action.[2a,b]

One of the major negative features that makes peptides inappropriate drug candidates is their flexibility. Peptide structure and conformation are strongly influenced by the nature of constituent amino acids and also the biophysical environment in which they exist. Therefore, the high conformational flexibility presents a potential problem in generating therapeutics and biological probes, since a peptide must attain a certain conformation in order to bind to its biological target, be it a receptor or an enzyme.

Folding is the process nature has selected to control the conformation of its molecular machinery and carry out unsurpassed chemical functions such as enzyme catalysis, information storage and duplication in nucleic acids, as well as energy capture and conversion. Systematic case studies have revealed that there is typically a small cluster of well ordered key residues in the peptide backbone that contributes the majority of the recognition or binding affinity.[3] Therefore, the pre-organization of peptide shape, via the introduction of a structural motif that imparts conformational restriction, can enhance binding and hence therapeutic potential, moreover, can be useful for identification of biologically active conformers.

Over the years, chemists have worked to geometrically restricted analogs that favors receptor binding surmounting the required loss of entropy for correct folding,[4] thereby, improving potency, selectivity, and stability.[5] The active conformation recognized by the receptor typically involves a turn structure (ß- or γ-turn),[6] so, small-molecules and peptides with turn constraints have been successful in targeting this class of receptors.[6,7]

With this purpose, a good deal of effort has gone into mimicking these structures using heterocyclic-based peptidomimetics. Some heterocyclic systems, called privileged scaffolds, appear frequently in bioactive products and marketed drugs. A number of common aromatic heterocycles have been employed in this context, examples used include pyrrole, tetrazole, triazole and pyrazoles.[8] Over the years, extensive improvements have been made in the development of ligands, metals, reaction conditions, and building block availability, making this method one of the most useful tools to append aromatic rings into a small molecule or peptidomimetic.[9] With this powerful tool, it is not surprising to observe an increase of aromatic ring count in the new bioactive molecules.[10] However, limitations in solubility, pharmacokinetics, and bioavailability of high-aromatic-ring-count molecules are now well recognized, leading scientists to favor saturated building blocks, especially saturated N-heterocycles.[11]

Saturated N-heterocycles are prevalent in biologically active molecules and are increasingly attractive scaffolds in the development of new pharmaceuticals. Among these usefull scaffolds we can find pseudo-Pro analogues[12] and R-amino-γ-lactams,[13] so-called Freidinger-Veber lactams, that have been commonly proven particularly effective in the design of constrained peptidomimetics for therapeutic targets.[13,14]

Amid different N-heterocycles, cyclic urea scaffolds are of great and actual interest since they induce peptide turn geometry, by combining the covalent constraints of R-amino-γ-lactams with the electronic restrictions and side-chain diversity of aza-amino acids. In fact, aza analogs of amino acids restrict backbone ψ-dihedral angle, due to the planarity of the urea moiety,

and the ϕ-dihedral angle, because of hydrazine N-N lone-pair repulsion.[15] Azapeptides utilize electronic forces to stabilize turn conformations in peptides.[16] Therefore, designed to favor turn secondary structures, aza-ciclic surrogates reserve both electronic and structural constraints to hinder rotation about the backbone ϕ-, ψ- and ω-dihedral angles, giving rise to γ- and ß- turns.[17]

Cyclic urea moieties are found in many biologically active compounds,[18] and are expected to have greater membrane solubility and increased conformational rigidity relative to the corresponding linear urea.[19]

Particularly, imidazolidin-2-ones (Imds) are utilized as structural elements in a number of inhibitors of human immunodeficiency virus (HIV) protease and HIV replication. [20] Still, Imds have utility as antitumor agents,[21] antibacterial MurB inhibitors,[22] dopamine D 4 and CGRP receptor antagonists,[23] antioxidants,[24] and unnatural base pairs.[25]

In literature, cyclic ureas such as Imds are most commonly constructed via treatment of 1,2-diamine precursors with phosgene equivalents such as carbonyl diimidazole,[19,26] via Hofmann rearrangement of Asn,[27] via ring expansion of aziridine derivatives,[28] via cyclization of aza-propargylglycinamides,[29] via alkylation of the urea nitrogen of semicarbazone residues,[30] via Pd-catalyzed urea carboamination reactions,[31] and so on.

Although a number of synthetic methods are available, many require multistep sequences for their preparation. Thus, alternative strategies for the construction of Imd would provide more facile access to derivatives that are not readily available. In addition, methods that allow for preparation of a variety of products from a common starting material would consent straightforward generation of analogues that could be used to optimize biological activity or pharmaceutical properties.

Continuing with our work toward the synthesis of constrained peptidomimetics from modified peptides (chapter 4 and 5),[12,32] in this chapter is reported the synthesis of Imd-containing peptidomimetics starting from different protected amino acid sequences.

6.2. Results and discussion

6.2.1. Synthesis

We propose two different synthetic pathways for the in-peptide synthesis of Imd rings.

The preparation of di/tri and tetra-peptides **1a-c**, **7**, **9a-b** and **11a-b** was conducted by coupling the amino acids under MW irradiation, using a microwave oven specifically designed for organic synthesis,[33] with HBTU/HOBt as activating agents. Moreover, β-amino-Ala was prepared as described in the literature.[34]

In the first route developed, the N-protected-dipeptides were treated with DSC and DIPEA, as base, for obtaining elimination to dehydroalanine (ΔAla), as illustrated in the literature (Scheme 1, **2a-c**).[35] The subsequent non-diastereoselective aza-Michael addition of different amines to ΔAla, furnished racemic compounds **3a-e**, in quantitative yields. Analysis of the crude reaction mixture by RP-HPLC and ESI-MS revealed the presence of the two diastereomeric compounds (**3a-e**) in 1:1 ratio (General Methods).

Notably, we were able to adding not only simple primary amines but also an O-ptotected amino acid (PheOBn, compound **3c**) in quantitative yield.

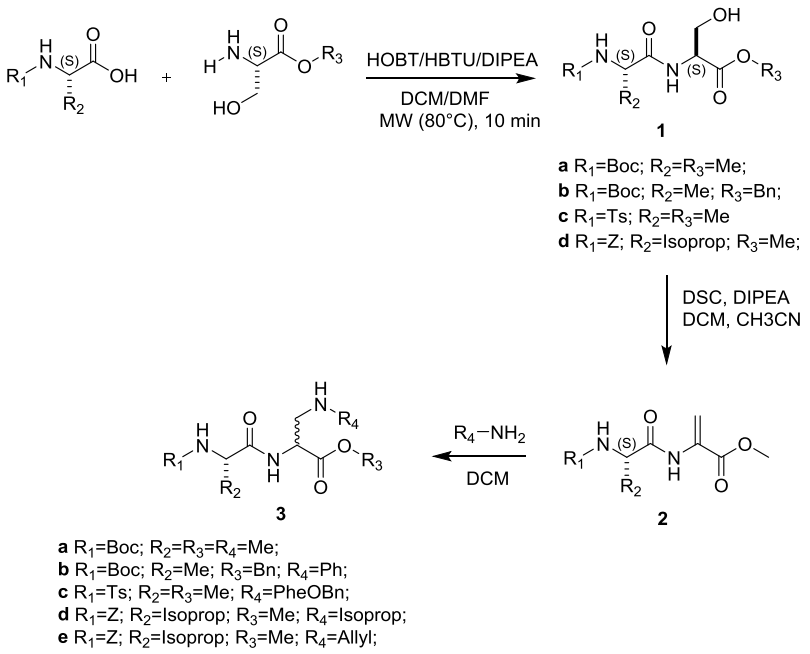

Scheme 1. Synthesis of dipeptides, elimination of Ser to ΔAla and aza-Michael reaction.

In order to optimize the cyclization of these amino peptides, we investigated the role of the carbonate, solvent, base, and protecting group, by reacting the model peptides **3a** under different conditions (Table 1).

On the basis of our precedent works (Chapter 4 and 5),[12,32] we treated compound **3a** with 1,2 eq. of DSC and catalytic amounts of DIPEA in a mixture of DCM/DMF, but the outcome of the reaction did not give the expected results (table 1, entry 1), also using larger quantities of reactants. Still, the use of an inorganic base did not influence the result (table 1 entry 2). Due to these negative results, we tried to replace the DSC carbonate with *p*-nitrobenzylchloroformate (p-NBC), that in the presence of variable amounts of DIPEA (from catalitic to excess) in DCM/DMF, gave the intermediate **4a** in traces, only when a large excess of base (10 eq.) was employed (table 1, entry 3).

On the basis of these evidences, we were been interested in Dowson et al. work,[36] who efficiently transformed *o*-aminoanilides into an aromatic N-acylurea moiety through the addition of *p*-nitrophenylchloroformate (p-NPC) and DIPEA as base.[36] Inspired by this paper, we have found that the treatment of our substrate **3a** with p-NPC and 10 eq. of DIPEA, in DCM/DMF, allows a significative, but yet insufficient, increment of the intermediate **4a** formation (table 1, entry 4). This result prompted us to attempt a better outcome by increasing the DIPEA amount and by adding DMAP as additive base (table 1, entry 5). Long last these conditions permitted the isolation of the intermediate (yield 70%) that was purified and treated with large quantities of DIPEA (10 eq) to afford the product **5a** in 80% yield (table 1, entry 6). Obviously, the found reaction conditions were not optimal, since predicted an overuse of reagents and the necessity to isolate and purify the intermediate **4a**, which in turn needed to much base for cyclization.

At this point, we tried to consider p-NPC as a constant and we used DBU as base. Fortunately, this strategy has proved successful, since 3 eq. of p-NPC and 3 eq. of DBU, in a mixture of DCM/DCM, furnished the desired product **5a** in very satisfactory yield (85%), in only 5 h of reaction and avoiding to isolate the intermediate (table 1, entry 7). Finally, using the same reagents in only DMF improves even more the final yield (table 1, entry 8).

The optimized reaction was extended also to different protected dipeptides, when N-/O-protecting groups were changed the outcome of the reaction was the same. Moreover the nature of the substituents on the amine function (R_3=alchil, allyl, aryl, aminoacid) is dimonstrated irrelevant for the cyclization reaction. This is an evident advantage since permitted to obtain Imd rings with different substituents on N1 position.

In all cases, epimerization during the cyclization of **3a-e** was excluded on the basis of the NMR and HPLC analyses (see General Methods).

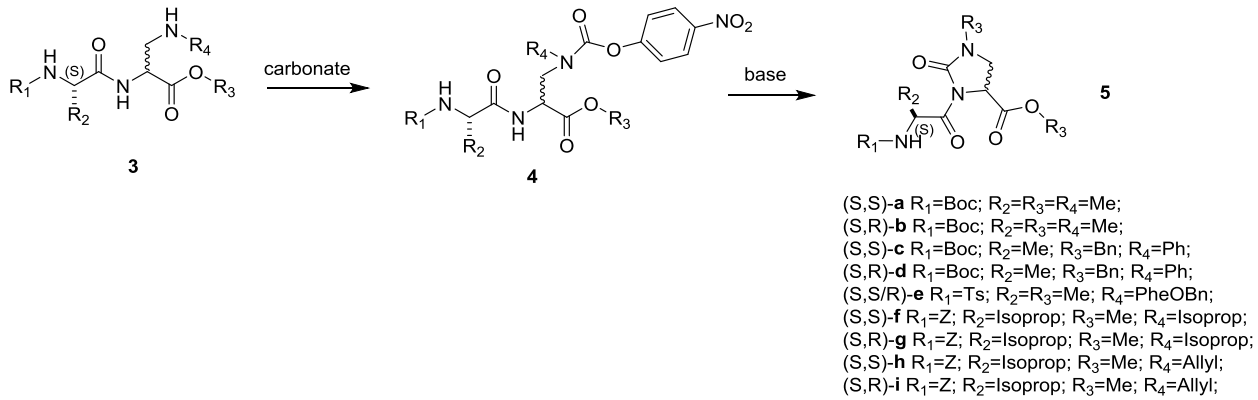

Scheme 2. Synthesis of Imd-containing dipeptides.

Table1. Cyclization of **3a**: reagents, yields and reaction times.

entry	compd	Carbonate	Base	Solvent	Product	Yield %	Time (h)
1	**3a**	DSC	DIPEA	DCM/DMF	-	-	24
2	**3a**	DSC	K_2CO_3	DCM/DMF	-	-	24
3	**3a**	p-NBC	DIPEA	DCM/DMF	**4a**	traces	24
4	**3a**	p-NPC	DIPEA	DCM/DMF	**4a**	20	12
5	**3a**	p-NPC	DIPEA+DMAP	DCM/DMF	**4a**	70	12
6	**4a**	-	DIPEA	DCM/DMF	**5a**	90	12
7	**3a**	p-NPC	DBU	DCM/DMF	**5a**	85	5
8	**3a**	p-NPC	DBU	DMF	**5a**	90	5

As mentioned earlier, all compounds were obtained in racemic form. The two different diastereoisomers, in some cases, were separated by flash chromtography (**5c-d**, **5f-i**) or by semipreparative RP-HPLC (**5a-b**).

To afford the correct assignment of the stereochemistry, compounds **5a-b** were hydrolyzed in a heated solution of MeOH and TEA, following a procedure reported in literature,[37] for obtaining **6a-b**. Since the optical rotation power of the *S* enantiomer of **6** is well known in literature,[38] we were able to identify the stereochemistry of **5a-b**. Thanks to this data we could assign the stereochemestry of the other separated diastereoisomers (**5c-d**, **5f-i**), because a distinctive trend of the ^{1}H NMR signals of *S,S* and *S,R* compounds.

Unfortunately, in some cases (**5f-i**) was not feasible the complete isolation of diastereoisomers and, specifically, for mixture **5e** the separation was impossible both with flash chromatography and semipreparative RP-HPLC.

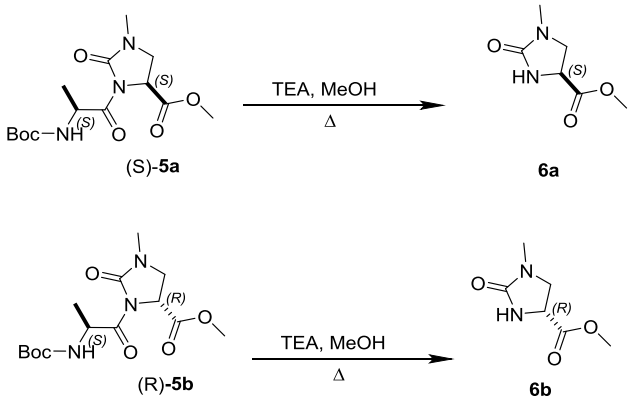

Scheme 3. Hydrolysis of compounds **5a** and **5b**.

This situation prompted us to explore an alternative route for obtaining only one diastereoisomer from the in-peptide synthesis of Imd scaffold.

The Hofmann rearrangement is a well-known reaction that easily allows the transformation of primary amides into amines,[39] utilizing bromine in aqueous basic conditions. Several methods have been described, employing different reagents that are generally able to deliver a positive halogen.[40] In the recent years, iodine(III) reagents[41] have been used to perform the same conversions under acidic conditions. The iodine(III) reagents normally employed are $PhI(OCOCF_3)_2$,[42] $PhIO–HCO_2H$[43] and PhI(OTs)OH,[44] which lead to high yields of the corresponding ammonium salts. Moreover by reacting primary amides with iodine(III) compounds in methanol under basic conditions, the corresponding methyl carbamates are obtained,[45] as methanol behaves both as a solvent and a reagent to trap the intermediate isocyanate. Furthermore, it's important to note, that the one-pot synthesis of Imd from residues of Asn is already described in literature,[27] but these approaches do not permit to obtain a full functionalization of the ring.

In our strategy, Imd can be easily obtained starting from the Hofmann rearrangment of N-protected (*S*)-Asn into β-amino-(*S*)-Ala, using $PhI(OAc)_2$ (Scheme 4),[34] the successive protection of the amino-function with Cbz, the incorporation of the residue into different di-/tri-/tetrapepide sequences (**7**, **9a-b**, **11a-b**, **13**, scheme 4) and the final cyclization that affords compounds **8**, **10** and **12a-b** in very good yields.

In the case of tetrapeptidomimetic **14**, the intermediate **11b** was first N-deprotected by catalytic hydrogenation, then the Boc-glycinale was inserted through a reductive amination. Finally, the corresponding product **13** was easily ciclized under the optimized condition to gave the three-point substituted Imd **14**.

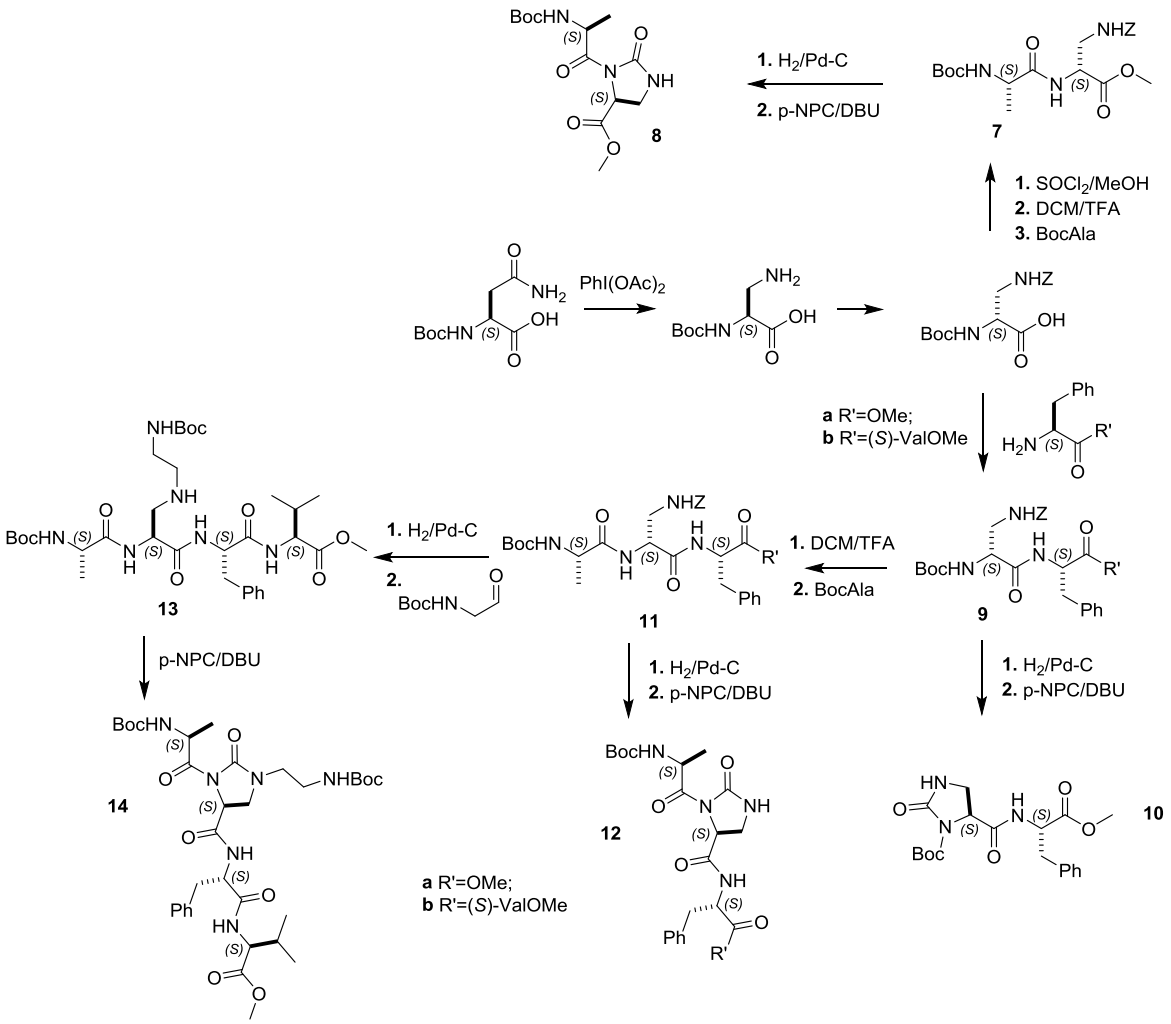

Scheme 4. Synthesis of Imd-peptides starting from Boc-(*S*)-Asn.

It's then important to underline that N1 unsubstituted Imd can be easily functionalized using acyl chloride derivatives.[46] The reactions depicted in Scheme 2 and 4represent the first synthesis of an already N-functionalized-Imd directly within a peptide sequence.

6.2.2. Conformational properties

We can speculate that the structure of compound **10** is comparable with the structures described by Tomasini et al. and analyzed by X-ray diffraction study.[27a] The molecular structure of their compounds shows that the Imd ring is almost planar and this data is in agreement with other analogous compounds reported in literature.[47]

To investigate the conformational bias exerted by the Imd in position 2 of the di-/tri-/tetrapeptides, on the overall structure of the peptide, we analyzed all compounds by NMR spectroscopy.

In particular, ^{1}H NMR analysis of all the final molecules showed a significantly downfield position in the Hα of the residue preceding the Imd (Ala or Val). For instance, the AlaHα in Boc-(*S*)-Ala-(*S*)-Imd-OMe (**5a**) it is at ca. 5.5 ppm, while in its precursor, **3a**, it is at ca. 4.2 ppm. This accounts for a strong deshielding effect exerted by Imd(C=O),[48] compatible with a non-conventional CH···O=C intramolecular hydrogen bond,[49] and confirms the *trans* conformation of the amide bond between the Imd and the preceding, deshielded residue.

The occurrence of intramolecular H-bonds in **12b** was evaluated by analyzing the variable temperature (VT)-^{1}H-NMR experiments in 8:2 DMSO-d_6/H_2O. For this compound, the comparatively lower VT-^{1}H-NMR $\Delta\delta/\Delta t$ parameters of PheNH (-0.9) with respect to AlaNH (-3.7), ImdNH (-1.9) and ValNH (-4.5) were suggestive of a significative preference for conformations having PheNH involved in a H-bond ($|\Delta\delta/\Delta t|$ < or close to 2.5 p.p.b./K).[50,51]

The described results are in agreement with the presence of a γ-turn between the PheNH and, presumably, the AlaC=O.

In to this purpose, Boger and co-workers,[52] recognizing that in the β-turn one of the folding amino acids (i+1 or i+2) often serves a structural rather than a recognition role (e.g., Pro or Gly),[53] sought to replace the two central amino acid with an N-heterocycle. From different analyzes, they found that *trans*-pyrrolidine-3,4-dicarboxamide could serve as a synthetically

accessible template upon which to display the amino acid side-chain groups. Rigidified by an intramolecular H-bond, precisely a γ-turn, the lowest energy conformation of the trans-pyrrolidine-3,4-dicarboxamide forces the lateral chains to assume the same triangle geometries that can be find in a β-turn. In fact, an overlay of the low energy conformation with the peptide backbone of a type-I β-turn demonstrates a potential mode of mimicry and yielded this conformation. In line with the design, the noncovalent constraints that stabilize the lowest energy conformer also permit a degree of flexibility to allow the compound to adopt variable H-bond donor/acceptor patterns (e.g., which the carbonyl is exo or endo in the pseudo-7-member ring) and permit the attached side chains to approximate the correct vector display of amino acid side chains in a wide range of β-turn structures.[53]

Likewise, the Imd ring can be considered an isoster of pyrrolidine and since it demonstrated to have a *trans* conformation and to induce a γ-turn, just like Boger's heterocycle, we can conclude that the insertion of Imd scaffold into a peptide sequence could lead to the same conformational advantages found for *trans*-pyrrolidine-3,4-dicarboxamide.

Significantly, the *trans*-Imd can be substituted in three different positions, that allow a very wide combination of natural and unnatural amino acid side chains, lending to the development of diversified libraries of derivatives.

6.3 Conclusions

The cyclization to Imd with p-NPC and DBU was performed with very good yields starting from short peptidic sequences containing a β-amino-α-amino acid. The latter was obtained from the aza-Michael addition of different substituted primary amine on a ΔAla, previously synthesized by Ser-containing dipeptides, or from the Hofmann rearrangement of a N-protected Asn residue. Both strategies permitted to abtain a three point functionalized Imd that, as highlighted by conformational analysis, shows a *trans* conformation and induces the formation of a well defined γ-turn.

For the simple synthetic protocol, the peculiar geometric features and the easy functionalization, the Imd ring deserves to be exploited for the design of new conformationally biased peptidomimetics or foldamers or even small molecules. These characteristics can permit not only the synthesis of potential drugs but also labeling molecules for diagnostic purposes or for instance for PNAs synthesis, that always requires functionalizable moiety.

Finally, by a purely synthetic point of view, would be interesting to explore a diastereoselective aza-Michael addition, in order to avoid the separation of diastereoisomers.

6.4. Experimental Section

6.4.1. General Methods

Standard chemicals (including Boc- or Cbz-protected α-amino acids, Boc-(*S*)-AlaOH, Z-ValOH, Boc-(*S*)-SerOH, Boc-(*S*)-PheOH, (*S*)-H-PheOMe, (*S*)-H-ValOMe, Boc-(*S*)Asn), were purchased from commercial sources and used without further purification. Flash chromatography was performed on silica gel (230-400 mesh), using mixtures of distilled solvents. Compounds purities were assessed by analytical RP-HPLC and elemental analysis. Analytical RP-HPLC was performed on an Agilent 1100 series apparatus, using a RP column Phenomenex mod. Gemini 3μ C18 110A 100x3.0 mm (P/No 00D-4439-Y0); column description: stationary phase octadecyl carbon chain-bonded silica (C18) with TMS endcapping, fully porous organo-silica solid support, particle size 3 μm, pore size 110 Å, length 100 mm, internal diameter 3 mm; DAD 210 nm; mobile phase: from a 9:1 H_2O-CH_3CN to a 2:8 H_2O-CH_3CN in 20 min at a flow rate of 1.0 mL min^{-1}, followed by 10 min at the same composition. Semi-preparative RP-HPLC was performed on an Agilent 1100 series apparatus, using a RP column ZORBAX mod. Eclipse XDB-C18 PrepHT cartridge 21.2x150 mm 7μ (P/No 977150-102); column description: stationary phase octadecyl carbon chain-bonded silica (C18), double endcapped, particle size 7 μm, pore size 80 Å, lenght 150 mm, internal diameter 21.2 mm; DAD 210 nm; mobile phase from 8:2 H_2O-CH_3CN to 100% CH_3CN in 10 min at a flow rate of 12 mL min^{-1}. Chiral HPLC analysis was performed on an Agilent 1200 series apparatus, using a CHIRALPAK IC column (P/No 83325); column description: chiral stationary phase cellulose *tris* (3,5-dichlorophenylcarbamate) immobilized on silica, particle size 5 μm, lenght 250 mm, internal diameter 4.6 mm, DAD 210/254 nm; mobile phase: 3:1 n-hexane/2-propanol, at 0.8 mL min^{-1}. ESI analysis was performed using a MS single quadrupole HP 1100MSD detector, with a drying gas flow of 12.5 l/min, nebulizer pressure 30 psgi, drying gas temp. 350°C, capillary voltage 4500 (+) and 4000 (-), scan 50-2600 amu. Elemental analyses were performer using a Thermo Flash 2000 CHNS/O analyzer. High quality IR were obtained at 2 cm^{-1} resolution using a FT-IR spectrometer and 1 mm NaCl solution cell. Electronic circular dichroism (ECD) spectra were recorded on a Jasco J-710 spectropolarimeter. The synthetic procedures by MW irradiation were performed using a microwave oven (MicroSYNTH Microwave Labstation for Synthesis) equipped with a built-in ATC-FO advanced fiber optic automatic temperature control. ^1H NMR spectra were recorded using a Varian Gemini apparatus at 400 MHz in 5 mm tubes, using 0.01 M peptide at room temperature. Solvent suppression was performed by

the solvent presaturation procedure implemented in Varian (PRESAT). ^{13}C NMR spectra were recorded at 100 MHz. Chemical shifts are reported as δ values relative to residual $CHCl_3$ δH (7.26 p.p.m.), DMSO δH (2.50 p.p.m.) and $CDCl_3$ δC (77.16 p.p.m.) as internal standards. The unambiguous assignment of ^1H NMR resonances was performed by 2D gCOSY. VT-^1H NMR experiments were performed over the range of 298-348 K; temperature calibration was done with the ethylene glycol OH-CHn chemical-shift separation method. 4.6 μm particle.

6.4.2. Synthetic procedures

*General procedure for the synthesis of peptides **1a-b**, **7**, **9a-b**, **11***. A stirred solution of N-protected amino acid (1.0 mmol) in in 4:1 DCM/DMF (5 mL, 0.2 M) was treated with HOBt (1.2 mmol) and HBTU (1.2 mmol), at r.t. and under nitrogen atmosphere. After 5 min, O-protected amino acid (1.1 mmol.) and DIPEA (2.4 mmol) were added, and the mixture was stirred under nitrogen atmosphere and under MW irradiation. The microwave-assisted reaction was performed with a initial irradiation power of 150W, and monitoring the internal reaction temperature at 80°C with a built-in ATC-FO advanced fiber optic automatic temperature control. After 10 min, the mixture was concentrated at reduced pressure, and the residue was diluted with EtOAc (25 mL). The solution was washed with 0.1 M HCl (5 mL), and a saturated solution of $NaHCO_3$ (5 mL). The organic layer was dried over Na_2SO_4 and the solvent was evaporated at reduced pressure.The peptides were isolated by flash chromatography over silica gel (eluant EtOAc/cyclohexane from 70:30 to 100:0). Yields 75-95%, 94-96 % pure by analytical RP-HPLC..

*General procedure for the synthesis of **2a-d***. To a stirred solution of **1** (1.0 mmol) in DCM/CH_3CN (2/1), DSC (1.5 mmol) and DIPEA (1.5 mmol) were added under inert atmosphere. After 3 h solvents were evaporated under reduced pressure, and the residue was diluted in EtOAc (25 mL) and washed with HCl 1 M (25 mL). The aqueous layer was extracted two more times with EtOAc (25 mL). The organic layers were dried over Na_2SO_4 and evaporated under reduced pressure. The peptides were isolated by flash chromatography over silica gel (eluant EtOAc/cyclohexane 70:30). Yield 75-85%, 94-96 % pure by analytical RP-HPLC.

General procedure for Boc deprotection. The intermediate *N*-Boc peptides (1.0 mmol) were deprotected by treatment with 25% TFA in DCM (5 mL) while stirring at r.t. After 15 min, the solution was evaporated under reduced pressure, and the treatment was repeated. The residue was suspended in ice-cold Et_2O (20 mL). The intermediate peptide-TFA salts which precipitated in almost quantitative yields were collected by centrifuge, and used for the next couplings without further purifications (80-85% pure by analytical RP-HPLC, General Methods).

General Procedure for Cbz Deprotection. The intermediates N-Cbz (1mmol) were deprotected by catalytic hydrogenation, consisting in the dissolution of peptides derivative in MeOH (5 mL) and in the addition of 10% Pd-C in the presence of H_2 atmosphere. After 8 h, the suspension was filtered over Celite® under suction, and the solvent was evaporated at reduced pressure. The residue was used for the next step without further purifications (85-90% pure by analytical RP-HPLC, General Methods).

*General procedure for the Michael addition with substituted amines **3a-e***. To a stirred solution of **2** (1 mmol) in CH_2Cl_2 (0.2 M), the substituted amine (4 mmol) was added under inert atmosphere. After 5 h solvent was evaporated under reduced pressure and the compound was used without further purification (yield up to 90%,).

*General procedure for the synthesis of Imd-peptides **5a-i**, **10**, **12a-b**, **14***. To a stirring solution of β-Ala-peptides (1 mmol) in dry DMF (0.2 M) and under inert atmosphere, *p*-NPC (3 mmol) was added. After 40 minutes DBU (3 mmol) in DMF was added. After 3 h solvent was evaporated under reduced pressure, the residue was resuspended in EtOAc (25 mL) and washed three times with HCl 1M (25 mL). The organic layer was dried over Na_2SO_4 and evaporated under reduced pressure. The diasteroisomers **5c-d**, **5f-i** were separated and compound **12b** was purified by flash-chromatography over silica gel (eluant EtOAc/cyclohexane from 30:70 to 70:30). Yields 80-95%. The diastereosimers **5a-b** were separated and compounds **8**, **10**, **12a** and **14** were purified with semipreparative RP-HPLC (yields 70-80%).

(*S*)-(N-Me)-ImdOMe **6a** and (*R*)-(N-Me)-ImdOMe **6b**. To a solution of **5a** or **5b** (0.33g, 1 mmol) in dry MeOH (3mL) under inert atmosphere, TEA (6 mmol) was added and the reaction was refluxed. After 6h solvent was evaporated under reduced pressure. The residue was purified by flash chromatography over silica gel (eluant EtOAc/cyclohexane from 50:50 to 90:10) and the product **6a** and **6b** were obtained in 70% Yield.

Boc-(*S*)-Ala-(*S*)-(NCH_2CH_2NHBoc)-βAla-(*S*)-Phe-(*S*)-ValOMe **13**. Compound **11b** (0.20g, 0.28 mmol) was deprotected following the *General Procedure for Cbz Deprotection*. The residue obtained was used for the next step without further purifications (Yield 95%, 85% pure by analytical RP-HPLC, General Methods). To a solution of deprotected-**11b** (0.20g,

0.35 mmol) in THF (5mL) were added N-Boc-2-aminoacetaldehyde (0.07g, 1.2 mmol) and 2 drops of AcOH. After 10 min $NaCNBH_3$ (0.09g, 4 mmol). After 2 h the reaction was quenched with H_2O and THF was evaporated under reduced pressure. The acqueous solution was extracted three times with EtOAc (25mL), and the organic layers were dried over Na_2SO_4. The intermediate **13** were used for the next cyclization reaction without further purifications (Yield 60%, 50% pure by analytical RP-HPLC, General Methods).

Boc-(*S*)-Ala-(*S/R*)-(N-Me)-βAlaOMe **3a**. 90% pure by RP-HPLC (General Methods), Rt = 1.44 min. ^{1}H NMR ($CDCl_3$) δ = 1.38 (d, J=6.8 Hz, 6H, AlaMe), 1.45 (s, 18H, *t*-Bu), 2.43 (s, 6H, NMe), 2.79-3.08 (m, 4H, βAlaHβ), 3.76 (s, 6H, OMe), 4.14-4.22 (m, 2H, AlaHα), 4.62-4.70 (m, 2H, βAlaHα), 5.07 (d, J=6.8 Hz, 1H, AlaNH), 5.16 (d, J=6.8 Hz, 1H, AlaNH), 7.05 (d, J=6.8 Hz, 1H, βAlaNH), 7.17 (d, J=6.8 Hz, 1H, βAlaNH). ESI-MS m/z 304.1 (M+H)+, calcd 304.2.

Boc-(*S*)-Ala-(*S/R*)-(N-Ph)-βAlaOBn **3b**. 95% pure by RP-HPLC (General Methods), Rt = 9.92 min. ^{1}H NMR ($CDCl_3$) δ = 1.34 (d, J=6.8 Hz, 3H, AlaMe), 1.35 (d, J=6.8 Hz, 3H, AlaMe), 1.44 (s, 18H, *t*-Bu), 3.60 (ddd, J=2.4, 4.8, 13.2 Hz, 2H, βAlaHβ), 3.65 (ddd, J=2.4, 4.8, 13.2 Hz, 2H, βAlaHβ), 4.14-4.17 (m, 2H, AlaHα), 4.79-4.82 (m, 2H, βAlaHα), 4.83 (d, J=6.8 Hz, 1H, AlaNH), 4.87 (d, J=6.8 Hz, 1H, AlaNH), 5.18 (s, 4H, $BnCH_2$), 6.59-6.62 (m, 4H, ArH), 6.79-6.82 (m, 10H, ArH), 6.86 (d, J=6.4, 1H, βAlaNH), 7.13-7.21 (m, 3H, βAlaNH+ArH), 7.33-7.39 (m, 4H, ArH). ESI-MS m/z 442.1 (M+H)+, calcd 442.2.

Ts-(*S*)-Ala-(*S/R*)-(N-PheOBn)-βAlaOMe **3c**. 92% pure by RP-HPLC (General Methods), Rt = 10.53 min. ^{1}H NMR ($CDCl_3$) δ = 1.21 (d, J=7.2 Hz, 3H, AlaMe), 1.25 (d, J=7.2 Hz, 3H, AlaMe), 2.37 (s, 3H, TsMe), 2.41 (s, 3H, TsMe), 2.44 (m, 1H, βAlaHβ), 2.91-3.04 (m, 4H, βAlaHβ+PheHβ), 3.10-3.19 (m, 3H, βAlaHβ+PheHβ), 3.55 (m, 1H, AlaHα), 3.59 (s, 3H, OMe), 3.67 (s, 3H, OMe), 3.76 (m, 1H, AlaHα), 3.85 (t, J=6.4, 2H, PheHα), 4.29 (ddd, J=3.6, 7.6, 11.6 Hz, 1H, βAlaHα), 4.34 (ddd, J=4, 7.6, 11.2 Hz, 1H, βAlaHα), 5.12 (s, 2H, $BnCH_2$), 5.15 (s, 2H, $BnCH_2$), 5.39 (br s, 2H, AlaNH), 6.45 (d, J=7.6 Hz, 1H, βAlaNH), 7.06 (d, J=7.6 Hz, 1H, βAlaNH), 7.12-7.38 (m, 24H, ArH), 7.70-7.75 (m, 4H, TsArH). ESI-MS m/z 582.3 (M+H)+, calcd 582.2.

Z-(*S*)-Val-(*S/R*)-(N-isopropyl)-βAlaOMe **3d**. 93% pure by RP-HPLC (General Methods), Rt = 1.52 min. ^{1}H NMR ($CDCl_3$) δ = 0.94 (d, J=6.6 Hz, 6H, ValMe), 0.99 (d, J=6.6 Hz, 6H, ValMe), 1.05-1.08 (m, 12H, N-isopropylMe), 2.14-2.21 (m, 2H, ValHβ), 2.81-2.83 (m, 2H, N-isopropylC*H*), 2.95-2.98 (m, 2H, βAlaHβ), 3.13-3.15 (m, 2H, βAlaHβ), 3.73 (s, 6H, OMe), 4.05-4.13 (m, 2H, ValHα), 4.64 (m, 2H, βAlaHα), 5.10 (s, 4H, $BnCH_2$), 5.43 (d, J=7.6 Hz, 1H, ValNH), 5.52 (d, J=7.6 Hz, 1H, ValNH), 7.07 (br s, 1H, βAlaNH), 7.27-7.36 (m, 11H, βAlaNH+ArH). ESI-MS m/z 394.2 (M+H)+, calcd 394.2.

Z-(*S*)-Val-(*S/R*)-(N-allyl)-βAlaOMe **3e**. 80% pure by RP-HPLC (General Methods), Rt = 1.40 min. ^{1}H NMR ($CDCl_3$) δ = 0.91-0.99 (m, 12H, ValMe), 2.07-2.22 (m, 2H, ValHβ), 2.90-2.94 (m, 2H, $NCH_2CH{=}CH_2$), 3.05-3.08 (m, 2H, $NCH_2CH{=}CH_2$), 3.20-3.29 (m, 4H, βAlaHβ), 3.75 (s, 6H, OMe), 4.05-4.11 (m, 2H, ValHα), 4.62 (m, 2H, βAlaHα), 5.11 (s, 4H, $BnCH_2$), 5.17-5.20 (m, 4H, $NCH_2CH{=}CH_2$), 5.36 (br s, 2H, ValNH), 5.77-5.85 (m, 2H, $NCH_2CH{=}CH_2$), 7.30-7.40 (m, 10H, ArH), 7.89 (d, J=8.4 Hz, 1H, βAlaNH), 7.97 (d, J=9.2 Hz, 1H, βAlaNH). ESI-MS m/z 392.1 (M+H)+, calcd 392.2.

Boc-(*S*)-Ala-(*S/R*)-(Me-N-COOPh(-NO_2))-βAlaOMe **4a**. 90% pure by RP-HPLC (General Methods), Rt = 7.89 min. ^{1}H NMR ($CDCl_3$) δ = 1.35 (d, J=3.2 Hz, 3H, AlaMe), 1.37 (d, J=3.2 Hz, 3H, AlaMe), 1.43 (s, 18H, *t*-Bu), 3.05 (s, 3H, NMe), 3.15 (s, 3H, NMe), 3.55-3.92 (m, 10H, βAlaHβ), 3.68 (s, 3H, OMe), 3.74 (s, 3H, OMe), 4.12-4.20 (m, 2H, AlaHα), 4.804 (ddd, J=2.8, 7.6, 10.8 Hz, 1H, βAlaHα), 4.87 (ddd, J=2.8, 7.6, 10.8 Hz, 1H, βAlaHα), 4.93 (d, J=6.0 Hz, 2H, AlaNH), 6.93 (d, J=7.6 Hz, 1H, βAlaNH), 7.10 (d, J=7.6 Hz, 1H, βAlaNH), 7.28-7.35 (m, 4H, ArH), 8.22-8.24 (m, 4H, ArH). ESI-MS m/z 491.1 (M+Na), calcd 491.2.

Boc-(*S*)-Ala-(*S*)-(N-Me)-ImdOMe **5a**. 98% pure by RP-HPLC (General Methods), Rt = 9.86 min. ^{1}H NMR ($CDCl_3$) δ = 1.42 (s, 12H, AlaMe+ *t*-Bu), 2.87 (s, 3H, NMe), 3.39 (dd, J=3.4, 9.8 Hz, 1H, $ImdH_5$), 3.71 (t, J=9.8 Hz, 1H, $ImdH_5$), 3.77 (s, 3H, OMe), 4.82 (dd, J=3.4, 9.8 Hz, 1H, $ImdH_4$), 5.08 (d, J=7.6 Hz, 1H, AlaNH), 5.51 (quint., J=7.6, 1H, AlaHα); ^{13}C NMR ($CDCl_3$) δ = 18.4, 28.3, 30.5, 46.6, 48.7, 51.9, 52.9, 79.6, 153.1, 155.3, 169.9, 174.1. ESI-MS *m/z* 352.3 (M+Na), calcd 352.2. $[\alpha]_D^{20}$ -66.6 (*c* 0.9, $CHCl_3$).

Boc-(*S*)-Ala-(*R*)-(N-Me)-ImdOMe **5b**. 95% pure by RP-HPLC (General Methods), Rt = 9.98 min. ^{1}H NMR ($CDCl_3$) δ = 1.37 (d, J=7.2, 1H, AlaMe), 1.42 (s, 9H, *t*-Bu), 2.88 (s, 3H, NMe), 3.38 (dd, J=3.4, 9.8 Hz, 1H, $ImdH_5$), 3.71 (t, J=9.8 Hz,

1H, ImdH_5), 3.76 (s, 3H, OMe), 4.70 (dd, J=3.4, 9.8 Hz, 1H, ImdH_4), 5.35 (d, J=7.6 Hz, 1H, AlaNH), 5.51 (quint., J=7.6, 1H, AlaHα); ^{13}C NMR ($CDCl_3$) δ = 19.3, 29.3, 30.6, 46.6, 48.9, 51.8, 52.9, 79.3, 153.1, 154.8, 169.7, 173.9. ESI-MS *m/z* 352.1 $(M+Na)^+$, calcd 352.2. $[\alpha]_D^{20}$ +10.3 (*c* 1.9, $CHCl_3$).

Boc-(*S*)-Ala-(*S*)-(N-Ph)-ImdOBn **5c**. 98% pure by RP-HPLC (General Methods), Rt = 10.42 min. ^{1}H NMR ($CDCl_3$) δ = 1.40 (d, J=6.8 Hz, 3H, AlaMe), 1.44 (s, 9H, *t*-Bu), 3.84 (dd, J=3.2, 9.8 Hz, 1H, ImdH_5), 4.19 (t, J=9.8 Hz, 1H, ImdH_5), 5.00 (dd, J=3.2, 9.8 Hz, 1H, ImdH_4), 5.10 (d, J=7.2, 1H, AlaNH), 5.22 (dd, J=12.0, 36.0, 2H, BnCH_2), 5.53 (quint., J=7.2 Hz, 1H, AlaHα), 7.18 (m, 2H, ArH), 7.35-7.40 (m, 6H, ArH), 7.49 (m, 2H, ArH); ^{13}C NMR ($CDCl_3$) δ = 18.2, 28.3, 45.3, 49.1, 51.6, 67.9, 79.8, 119.3, 124.9, 128.5, 128.7, 128.8, 129.1, 134.6, 137.9, 150.9, 155.3, 168.9, 174.4. ESI-MS *m/z* 468.1 $(M+H)^+$, calcd 468.2.

Boc-(*S*)-Ala-(*R*)-(N-Ph)-ImdOBn **5d**. 90% pure by RP-HPLC (General Methods), Rt = 10.69 min. ^{1}H NMR ($CDCl_3$) δ = 1.44 (d, J=6.4 Hz, 3H, AlaMe), 1.47 (s, 9H, *t*-Bu), 3.77 (dd, J=2.4, 10.0 Hz, 1H, ImdH_5), 4.23 (t, J=10.0 Hz, 1H, ImdH_5), 4.88 (dd, J=2.8, 10.0 Hz, 1H, ImdH_4), 5.23 (s, 2H, BnCH_2), 5.44 (br d, 1H, AlaNH), 5.65 (m, 1H, AlaHα), 7.19 (m, 1H, ArH), 7.35-7.41 (m, 7H, ArH), 7.49 (m, 2H, ArH); ^{13}C NMR ($CDCl_3$) δ = 19.5, 28.4, 45.3, 49.5, 52.1, 67.9, 79.6, 119.2, 125.0, 126.1, 128.3, 128.7, 129.2, 134.8, 137.8, 150.8, 154.8, 168.7, 174.2. ESI-MS *m/z* 468.1 $(M+H)^+$, calcd 468.2.

Ts-(*S*)-Ala-(*S/R*)-(N-(*S*)-PheOBn)-ImdOMe **5e**. 90% pure by RP-HPLC (General Methods), Rt = 10.92 min. ^{1}H NMR ($CDCl_3$) δ = 1.27 (s, 18H, *t*-Bu), 1.32 (d, J=6.8 Hz, 3H, AlaMe), 1.36 (d, J=6.8 Hz, 3H, AlaMe), 2.39 (s, 3H, TsMe), 2.41 (s, 3H, TsMe), 2.91-3.03 (m, 3H, PheHβ), 3.25 (dd, J=3.6, 8.4 Hz, 2H, ImdH_5), 3.38 (dd, J=4.6, 11.4 Hz, 1H, PheHβ), 3.52 (s, 3H, OMe), 3.60 (s, 3H, OMe), 3.75 (dd, J=3.6, 8.4 Hz, 2H, ImdH_5), 4.26 (dd, J=3.6, 8.4 Hz, 1H, ImdH_4), 4.38 (dd, J=3.6, 8.4 Hz, 1H, ImdH_4), 4.88 (dd, J=4.6, 11.4 Hz, 1H, PheHα), 4.97 (dd, 5.0, 11.0 Hz, 1H, PheHα), 5.06 (m, 1H, AlaHα), 5.20 (s, 2H, BnCH_2), 5.21-5.25 (m, 3H, AlaHα+BnCH_2), 5.73 (d, J=8.8 Hz, 1H, AlaNH), 5.80 (d, J=9.6 Hz, 1H, AlaNH), 7.10-7.13 (m, 3H, ArH), 7.17-7.39 (m, 21H, ArH), 7.67-7.71 (m, 4H, ArH); ESI-MS m/z 608.3 (M+H)+, calcd 608.2.

Z-(*S*)-Val-(*S*)-(N-isopropyl)-ImdOMe **5f**. 80% pure by RP-HPLC (General Methods), Rt = 9.00 min. ^{1}H NMR ($CDCl_3$) δ = 0.84 (d, J=7.2 Hz, 3H, ValMe), 0.86 (d, J=7.2 Hz, 3H, ValMe), 1.05 (d, J=6.4 Hz, 3H, CHCH_3), 1.10 (d, J=6.4 Hz, 3H, CHCH_3), 2.18 (m, 1H, ValHβ), 2.37(m, 1H, NCH), 3.32 (dd, J=3.6, 9.8 Hz, 1H, ImdH_5), 3.66 (t, J=9.8 Hz, 1H, ImdH_5), 3.76 (s, 3H, OMe), 4.69 (dd, J=3.6, 9.8 Hz, 1H, ImdH_4), 5.11 (s, 3H, BnCH_2+ValNH), 5.61 (m, 1H, ValHα), 7.33-7.37 (m, 5H, ArH); ESI-MS m/z 420.2 (M+H)+, calcd 420.2.

Z-(*S*)-Val-(*R*)-(N-isopropyl)-ImdOMe **5g**. 75% pure by RP-HPLC (General Methods), Rt = 9.05 min. ^{1}H NMR ($CDCl_3$) δ = 0.84 (d, J=7.2 Hz, 3H, ValMe), 0.86 (d, J=7.2 Hz, 3H, ValMe), 1.05 (d, J=6.4 Hz, 3H, CHCH_3), 1.10 (d, J=6.4 Hz, 3H, CHCH_3), 2.18 (m, 1H, ValHβ), 2.37(m, 1H, NCH), 3.32 (dd, J=3.6, 9.8 Hz, 1H, ImdH_5), 3.66 (t, J=9.8 Hz, 1H, ImdH_5), 3.76 (s, 3H, OMe), 4.82 (dd, J=3.6, 9.8 Hz, 1H, ImdH_4), 5.11 (s, 2H, BnCH_2), 5.39 (d, J=8.0 Hz, 1H, ValNH), 5.61 (m, 1H, ValHα), 7.33-7.37 (m, 5H, ArH); ESI-MS m/z 420.2 (M+H)+, calcd 420.2.

Z-(*S*)-Val-(*S*)-(N-allyl)-ImdOMe **5i**. % pure by RP-HPLC (General Methods), Rt = 9.19 min. ^{1}H NMR ($CDCl_3$) δ = 0.84 (d, J=6.8 Hz, 3H, ValMe), 0.87 (d, J=6.8 Hz, 3H, ValMe), 2.06 (m, 1H, ValHβ), 3.12 (d, 2H, NCH_2CH), 3.34 (dd, J=3.6, 10.2 Hz, 1H, ImdH_5), 3.67 (t, J=10.2 Hz, 1H, ImdH_5), 3.76 (s, 3H, OMe), 4.54 (dd, J=6.0, 8.8 Hz, 1H, ValHα), 4.70 (dd, J=3.6, 10.2 Hz, 1H, ImdH_4), 5.10 (s, 2H, BnCH_2), 5.22-5.31 (m, 2H, CH_2CH=CH_2), 5.59 (d, J=8.8 Hz, 1H, ValNH), 5.75 (m, 1H, CH_2C*H*=CH_2), 7.31-7.37 (m, 5H, ArH); ESI-MS m/z 418.4 (M+H)+, calcd 418.2.

Z-(*S*)-Val-(*R*)-(N-allyl)-ImdOMe **5h**. % pure by RP-HPLC (General Methods), Rt = 9.30 min. ^{1}H NMR ($CDCl_3$) δ = = 0.84 (d, J=6.8 Hz, 3H, ValMe), 0.87 (d, J=6.8 Hz, 3H, ValMe), 2.35 (m, 1H, ValHβ), 3.12 (d, 2H, NCH_2CH), 3.34 (dd, J=3.6, 10.2 Hz, 1H, ImdH_5), 3.67 (t, J=10.2 Hz, 1H, ImdH_5), 3.76 (s, 3H, OMe), 4.54 (dd, J=6.0, 8.8 Hz, 1H, ValHα), 4.83 (dd, J=3.6, 10.2 Hz, 1H, ImdH_4), 5.10 (s, 2H, BnCH_2), 5.22-5.31 (m, 2H, CH_2CH=CH_2), 5.59 (d, J=8.8 Hz, 1H, ValNH), 5.75 (m, 1H, CH_2C*H*=CH_2), 7.31-7.37 (m, 5H, ArH). ESI-MS m/z 418.4 (M+H)+, calcd 418.2.

(*S*)-(N-Me)-ImdOMe **6a**. 98% pure by RP-HPLC (General Methods), Rt = 1.74 min. ^{1}H NMR ($CDCl_3$) δ = 2.79 (s, 3H, NMe), 3.63 (dd, J=4.4, 9.6 Hz, 1H, ImdH_5), 3.66 (dd, J=2.8, 9.6 Hz, 1H, ImdH_5), 3.79 (s, 1H, OMe), 4.20 (dd, J=4.4, 9.6 Hz, 1H, ImdH_4), 5.13 (br s, 1H, ImdNH), 5.65 (m, 1H, AlaHα); ESI-MS *m/z* 159.1 $(M+H)^+$, calcd 159.1. $[\alpha]_D^{20}$ +16.9 (*c* 1.9, $CHCl_3$).

(*D*)-(N-Me)-ImdOMe **6a**. 98% pure by RP-HPLC (General Methods), Rt = 1.74 min. ^{1}H NMR ($CDCl_3$) δ = 2.79 (s, 3H, NMe), 3.63 (dd, J=4.4, 9.6 Hz, 1H, ImdH_5), 3.66 (dd, J=2.8, 9.6 Hz, 1H, ImdH_5), 3.79 (s, 1H, OMe), 4.20 (dd, J=4.4, 9.6 Hz, 1H, ImdH_4), 5.13 (br s, 1H, ImdNH), 5.65 (m, 1H, AlaHα); ESI-MS *m/z* 159.1 $(M+H)^+$, calcd 159.1. $[\alpha]_D^{20}$ -17.9 (*c* 0.9, $CHCl_3$).

Boc-(*S*)-Ala-(*S*)-(N-Cbz)-βAlaOMe **7**. 97% pure by RP-HPLC (General Methods), Rt = 7.56 min. ^{1}H NMR ($CDCl_3$) δ = 1.33 (d, J=6.8 Hz, 1H, AlaMe), 1.42 (s, 9H, *t*-Bu), 3.62-3.69 (m, 2H, βAlaHβ), 3.74 (s, 3H, OMe), 4.12 (m, 1H, AlaHα), 4.61 (dd, J=4.6, 7.2 Hz, 1H, βAlaHα), 5.08 (s, 3H, CbzNH+CbzCH_2), 5.54 (br s, 1H, AlaNH), 7.03 (d, J=4.6 Hz, 1H, βAlaNH), 7.27-7.35 (m, 5H, ArH); ESI-MS *m/z* 424.2 $(M+H)^+$, calcd 424.2.

Boc-(*S*)-(N-Cbz)-βAla-PheOMe **9**. 98% pure by RP-HPLC (General Methods), Rt = 9.79 min. ^{1}H NMR ($CDCl_3$) δ = 1.47 (s, 9H, *t*-Bu), 3.06 (dd, J=6.4, 13.8 Hz, 1H, PheHβ), 3.21 (dd, J=6.4, 13.8, 1H, PheHβ), 3.52-3.57 (m, 2H, βAlaHβ), 3.75 (s, 3H, OMe), 4.23 (m, 1H, βAlaHα), 4.86 (q, J=7.2 Hz, 1H, PheHα), 5.15 (s, 2H, CbzCH_2), 5.41 (br s, 1H, CbzNH), 5.67 (br s, 1H, βAlaNH), 7.13-7.40 (m, 11H, PheNH+ArH); ESI-MS *m/z* 522.0 (M+Na), calcd 522.2.

Boc-(*S*)-Ala-(*S*)-(N-Cbz)-βAla-(*S*)-PheOMe **11a**. 98% pure by RP-HPLC (General Methods), Rt = 9.37 min. ^{1}H NMR ($CDCl_3$) δ = 1.44 (s, 12H, AlaMe+*t*-Bu), 3.02 (dd, J=7.4, 14.2 Hz, 1H, PheHβ), 3.18 (dd, J=7.4, 14.2, 1H, PheHβ), 3.47 (dt, J=4.4, 14.0, 1H, βAlaHβ), 3.57 (dt, J=4.4, 14.0, 1H, βAlaHβ), 3.71 (s, 3H, OMe), 4.10 (m, 1H, AlaHα), 4.45 (q, J=5.6, 1H, βAlaHα), 4.78 (q, J=7.4 Hz, 1H, PheHα), 4.97 (br s, 1H, CbzNH), 5.11 (dd, J=12.4, 36.4 Hz, 2H, CbzCH_2), 5.44 (br s, 1H, Ala NH), 7.11-7.13 (m, 3H, βAlaNH+PheNH+ArH), 7.21-7.29 (m, 3H, ArH), 7.31-7.36 (m, 6H, ArH); ESI-MS *m/z* 571.2 (M+Na), calcd 571.3.

Boc-(*S*)-Ala-(*S*)-(N-Cbz)-βAla-(*S*)-Phe-(*S*)-ValOMe **11b**. 90% pure by RP-HPLC (General Methods), Rt = 9.83 min. ^{1}H NMR ($CDCl_3$) δ = 0.83 (d, J=7.0 Hz, 3H, ValMe), 0.87 (d, J=7.0 Hz, 3H, ValMe), 1.31 (d, J=6.4 Hz, 3H, AlaMe), 1.44 (s, 9H, *t*-Bu), 2.16 (m, 1H, ValHβ), 2.94 (dd, J=9.6, 14.2 Hz, 1H, PheHβ), 3.42-3.54 (m, 3H, PheHβ+βAlaHβ), 3.69 (s, 3H, OMe), 3.98 (m, 1H, AlaHα), 4.35 (m, 1H, βAlaHα), 4.46 (dd, J=6.4, 8.4 Hz, 1H, ValHα), 4.83 (m, 1H, PheHα), 4.96 (d, J=10.4 Hz, 1H, AlaNH), 5.02 (d, J=17.2 Hz, 1H, CbzCH_2), 5.17-5.20 (m, 2H, AlaNH+ CbzCH_2), 6.97 (d, J=6.4 Hz, ValNH), 7.18-7.25 (m, 5H, ArH), 7.30-7.38 (m, 6H, PheNH+ArH), 7.79 (br s, 1H, βAlaNH); ESI-MS *m/z* 670.2 $(M+H)^+$, calcd 670.3.

Boc-(*S*)-Ala-(*S*)-(NCH_2CH_2NHBoc)-βAla-(*S*)-Phe-(*S*)-ValOMe **13**. 50% pure by RP-HPLC (General Methods), Rt = 4.59 min. ESI-MS m/z 679.4 (M+H)+, calcd 670.3.

Boc-(*S*)-Ala-(*S*)-ImdOMe **8**. 70% pure by RP-HPLC (General Methods), Rt = 4.05 min. ESI-MS m/z 338.0 (M+Na), calcd 338.2.

Boc-(*S*)-Imd-(*S*)-PheOMe **10**. 50% pure by RP-HPLC (General Methods), Rt = 7.16 min. ESI-MS m/z 392.2 (M+H)+, calcd 392.2.

Boc-(*S*)-Ala-(*S*)-Imd-(*S*)-PheOMe **12a**. 70% pure by RP-HPLC (General Methods), Rt = 6.66 min. ESI-MS m/z 464.4 (M+H)+, calcd 464.2.

Boc-(*S*)-Ala-(*S*)-Imd-(*S*)-Phe-(*S*)-ValOMe **12b**. 95% pure by RP-HPLC (General Methods), Rt = 7.37 min. ^{1}H NMR ($CDCl_3$) δ = 0.83 (d, J=7.0 Hz, 3H, ValMe), 0.87 (d, J=7.0 Hz, 3H, ValMe), 1.33 (d, J=6.0 Hz, 3H, AlaMe), 1.39 (s, 9H, *t*-Bu), 2.14 (m, 1H, ValHβ), 3.06 (dd, J=5.6, 13.2 Hz, 1H, PheHβ), 3.13 (dd, J=5.6, 13.2 Hz, 1H, PheHβ), 3.58-3.66 (m, 2H, ImdH_5), 3.71 (s, 3H, OMe), 4.43 (dd, J=5.2, 8.2 Hz, 1H, ValHα), 4.67 (m, 1H, PheHα), 4.84 (m, 1H, ImdH_4), 5.15(d, J=7.2 Hz, 1H, AlaNH), 5.39 (m, 1H, AlaHα), 6.21 (d, J=8.2 Hz, ValNH), 6.97 (d, J=6.4 Hz, 1H, PheNH), 7.21-7.29 (m, 5H, PheArH); ^{1}H NMR ([D_6]DMSO) δ = 0.86 (d, J=6.6 Hz, 3H, ValMe), 0.88 (d, J=6.6 Hz, 3H, ValMe), 1.16 (d, J=7.2 Hz, 3H, AlaMe), 1.35 (s, 9H, t-Bu), 2.02 (m, 1H, ValHβ), 2.75 (dd, J=4.4, 14 Hz, 1H, PheHβ), 2.99 (dd, J=4.4, 14 Hz, 1H, PheHβ), 3.09 (dd, J=2.8, 10.8 Hz, 1H, ImdH_5), 3.59 (dd, J=2.8, 10.8 Hz, 1H, ImdH_5), 3.62 (s, 3H, OMe), 4.14 (t, J=7.2 Hz, 1H, ValHα), 4.57 (m, 1H, PheHα), 4.72 (dd, J=2.8, 10.8 Hz, 1H, ImdH_4), 5.16 (t, J=7.8 Hz, 1H, AlaHα), 7.00 (d, J=7.4 Hz, 1H, AlaNH), 7.16-7.27 (m, 5H, PheArH); 8.24 (d, J=8.0 Hz, PheNH), 8.29 (d, J=7.8 Hz, 1H, ValNH); ^{13}C NMR ($CDCl_3$) δ = 17.8, 18.8, 28.3, 29.7, 31.1, 38.1, 40.2, 52.2, 54.9, 56.0, 57.5, 79.9, 127.1, 127.2, 128.8, 129.1, 129.3, 136.0, 154.6, 155.2, 168.5, 170.2, 171.6, 175.0. ESI-MS *m/z* 562.2 $(M+H)^+$, calcd 562.3.

Boc-(*S*)-Ala-(*S*)-(NCH_2CH_2NHBoc)-Imd-(*S*)-Phe-(*S*)-ValOMe **14**. 80% pure by RP-HPLC (General Methods), Rt = 9.86 min. ESI-MS m/z 727.2 (M+Na), calcd 727.3.

6.4.3. Conformational analysis

NMR analyses. ^{1}H-NMR spectra were recorded at 400 MHz in 5 mm tubes, using 0.01 M peptide at room temperature. Solvent suppression was performed by the solvent presaturation procedure implemented in Varian (PRESAT). ^{13}C-NMR spectra were recorded at 100 MHz. Chemical shifts are reported as δ values. The unambiguous assignment of ^{1}H-NMR resonances was performed by 2D gCOSY, HMBC, and HSQC. gCOSY experiments were conducted with a proton spectral width of 3103 Hz. VT-^{1}H-NMR experiments were performed over the range of 298-348 °K. 2D spectra were recorded in the phase sensitive mode and processed using a 90°-shifted, squared sine-bell apodization.

References

[1] a) Gron, H.; Hyde-De Ruyscher, R. *Curr. Opin. Drug Discov. Devel.* **2000**, *3*, 636; b) Edwards, P. J.; La Plante, S. R. Peptides as Leads for Drug Discovery In Peptide Drug Discovery and Development: Translational Research in Academia and Industry; Wiley Publishers: Germany, 2011; pp 1–55. Chapter 1.

[2] a)Advances in Amino Acid Mimetics and Peptidomimetics; Abell, A., Ed.; JAI Press: Greenwich, 1997; Vol. 1; b)Advances in Amino Acid Mimetics and Peptidomimetics; Abell, A., Ed.; JAI Press: Greenwich, 1999; Vol. 2; c) Grauer, A.; König, B. *Eur. J. Org. Chem.* **2009**, *30*, 5099; d) Vagner, J.; HongchangQu, H.; Hruby, V. *J. Curr. Opin. Chem. Biol.* **2008**, *12*, 292.

[3] Moreira, I. S.; Fernandez, P. A.; Ramos, M. *J. Proteins: Struct., Funct., Bioinf.* **2007**, *68*, 803.

[4] Ball, J. B.; Alewood, P. F. *J. Mol. Recognit.* **1990**, *3*, 55.

[5] Smith, A. B., III; Charnley, A. K.; Hirschmann, R. *Acc. Chem. Res.* **2011**, *44*, 180.

[6] a) Ruiz_Gomez, G.; Tyndall, J. D. A.; Pfeiffer, B.; Abbenante, G.; Fairlie, D. P. *Chem. Rev.* **2010**, *110*, PR1–PR41; b) Tyndall, J. D. A.; Pfeiffer, B.; Abbenante, G.; Fairlie, D. P. *Chem. Rev.* **2005**, *105*, 793.

[7] a) Souers, A. J.; Ellman, J. A. *Tetrahedron* **2001**, *57*, 7431; b) Blakeney, J. S.; Reid, R. C.; Le, G. T.; Fairlie, D. P. *Chem. Rev.* **2007**, *107*, 2960.

[8] Etzkorn, F.A., Travins, J. M. and Hart, S.A., in A.D. Abell (Ed.), Advances in Amino Acid Mimetics and Peptidomimetics, JAI Press, Greenwich, 2, 1999, pp. 125–163.

[9] Meijere, A.; Diederich, F. Metal-Catalyzed Cross-Coupling Reactions, 2nd ed.; Wiley-VCH Verlag: Weinheim, 2004.

[10] Ritchie, T. J.; Macdonald, S. J. F. *Drug Discovery Today* **2009**, *14*, 1011.

[11] a) Ritchie, T. J.; Macdonald, S. J. F.; Young, R. J.; Pickett, S. D. *Drug Discovery Today* **2011**, *16*, 164; b) Lovering, F.; Bikker, J.; Humblet, C. *J. Med. Chem.* **2009**, *52*, 6752; c) Leeson, P. D.; St-Gallay, S. A.; Wenlock, M. C. *MedChemComm* **2011**, *2*, 91; d) Feher, M.; Schmidt, J. M. *J. Chem. Inf. Comput. Sci.* **2002**, *43*, 218.

[12] De Marco, R.; Greco, A.; Rupiani, S.; Tolomelli, A.; Tomasini, C.; Pieraccini, S.; Gentilucci, L. *Org Biomol Chem* **2013**, *11*, 4273.

[13] a) Freidinger, R. M.; Veber, D. F.; Perlow, D. S.; Brooks, J. R.; Saperstein, R. *Science* **1980**, *210*, 656; b) Freidinger, R. M.; Perlow, D. S.; Veber, D. F. *J. Org. Chem.* **1982**, *47*, 104; c) Freidinger, R. M. *J. Org. Chem.* **1985**, *50*, 3631; d) Jamieson, A. G.; Boutard, N.; Beauregard, K.; Bodas, M. S.; Ong, H.; Quiniou, C.; Chemtob, S.; Lubell, W. D. *J. Am. Chem. Soc.* **2009**, *131*, 7917; e) Boutard, N.; Jamieson, A. G.; Ong, H.; Lubell, W. D. *Chem. Biol. Drug Des.* **2010**, *75*, 40.

[14] Wolfe, M. S.; Dutta, D.; Aube, J. *J. Org. Chem.* **1997**, *62*, 654.

[15] Lee, H. J.; Song, J. W.; Choi, Y. S.; Park, H. M.; Lee, K. B. *J. Am. Chem. Soc.* **2002**, *124*, 11881.

[16] Proulx, C.; Sabatino, D.; Hopewell, R.; Spiegel, J.; Ramos, Y. G.; Lubell, W. D. *Future Med. Chem.* **2011**, *3*, 1139.

[17] a)Proulx, C.; Lubell, W. D. *Org. Lett.* **2012**, *14*, 4552; b) Proulx, C.; Lubell, W. D. *Biopolymers* **2014**, *102*, 7; c) R. Skerlj, G. Bridger, Y. Zhou, E. Bourque, E. McEachern, M. Metz, C. Harwig, T. Li , W. Yang, D. Bogucki , Y. Zhu, J. Langille, D. Veale, T. Ba, M. Bey, I. Baird, A. Kaller, M. Krumpak, D.Leitch, M. Satori, K. Vocadlo , D. Guay, S. Nan, H. Yee, J. Crawford, G. Chen, T. Wilson, B. Carpenter, D. Gauthier, R. MacFarland, R. Mosi, V. Bodart, R. Wong, S. Fricker, D. Schols, *J. Med. Chem.* **2013**, *56*, 8049.

[18] Lam, P.Y.S.; Jadhav, P.K.; Eyermann, C.J.; Hodge, C.N.; Ru, Y.; Bacheler, L.T.; Meek, J.L.; Otto, M.J.; Rayner, M.M.; Won, Y.N.; Chang, C.-H.; Weber, P.C.; Jackson, D.A.; Sharpe, T.R. *Science*, **1994**, *263*, 380.

[19] J. M. Kim, T. E. Wilson, T. C. Norman, P. G. Schultz, *Tetrahedron lett.* **1996**, *37*, 5309.

[20] Kazmierski, W. M.; Furfine, E.; Gray-Nunez, Y.; Spaltenstein, A.; Wright, L. *Bioorg. Med. Chem. Lett.* **2004**, *14*, 5685.

[21] a) Congiu, C.; Cocco, M. T.; Onnis, V. Bioorg. *Med. Chem. Lett.* **2008**, *18*, 989; b) Xue, N.; Yang, X.; Wu, R.; Chen, J.; He, Q.; Yang, B.; Lu, X.; Hu, Y. *Bioorg. Med. Chem*. **2008**, *16*, 2550.

[22] Bronson, J. J.; DenBleyker, F. L.; Falk, P. J.; Mate, R. A.; Ho, H.-T.; Pucci, M. J.; Snyder, L. B. *Bioorg. Med. Chem. Lett*. **2003**, *13*, 873.

[23] a) Carling, R. W.; Moore, K. W.; Moyes, C. R.; Jones, E. A.; Bonner, K.; Emms, F.; Marwood, R.; Patel, S.; Patel, S.; Fletcher, A. E.; Beer, M.; Sohal, B.; Pike, A.; Leeson, P. D. *J. Med. Chem.* **1999**, *42*, 2706; b) Burgey, C. S.; Stump, C. A.; Nguyen, D. N.; Deng, J. Z.; Quigley, A. G.; Norton, B. R.; Bell, I. M.; Mosser, S. D.; Salvatore, C. A.; Rutledge, R. Z.; Kane, S. A.; Koblan, K. S.; Vacca, J. P.; Graham, S. L.; Williams, T. M. *Bioorg. Med. Chem. Lett.* **2006**, *16*, 5052; c) Shaw, A.; Paone, D. V.; Nguyen, D. N.; Stump, C. A.; Burgey, C. S.; Mosser, S. D.; Salvatore, C. A.; Rutledge, R. Z.; Kane, S. A.; Koblan, K. S.; Graham, S. L.; Vacca, J. P.; Williams, T. M. *Bioorg. Med. Chem. Lett.* **2007**, *17*, 4795.

[24] a) Smith, R. C.; Reeves, J. C. *Biochem. Pharmacol*. **1987**, *36*, 1457; b) Watanabe, K.; Morinaka, Y.; Hayashi, Y.; Shinoda, M.; Nishi, H.; Fukushima, N.; Watanabe, T.; Ishibashi, A.; Yuki, S.; Tanaka, M. *Bioorg. Med. Chem. Lett.* **2008**, *18*, 1478.

[25] a) Hirao, I.; Kimoto, M.; Harada, Y.; Fujiwara, T.; Sato, A.; Yokoyama, S. *Nucleic Acids Res. Suppl.* **2002**, *2*, 37; b) Hirao, I.; Harada, Y.; Kimoto, M.; Mitsui, T.; Fujiwara, T.; Yokoyama, S. *J. Am. Chem. Soc.* **2004**, *126*, 13298.

[26] a) Sartori, G.; Maggi, R. in Science of Synthesis (Houben-Weyl Methods of Molecular Transformations); Ley, S. V., Knight, J. G., Eds.; Thieme: Stuttgart, 2005; Vol. 18, pp 665; For other recent approaches to the synthesis of cyclic ureas, see: b) Kim, M.; Mulcahy, J. V.; Espino, C. G.; Du Bois, *J. Org. Lett.* **2006**, *8*, 1073; c) Streuff, J.; Ho¨velmann, C. H.; Nieger, M.; Mun˜iz, K. *J. Am. Chem. Soc.* **2005**, *127*, 14586; d) Zabawa, T. P.; Kasi, D.; Chemler, S. R. *J. Am. Chem. Soc.* **2005**, *127*, 11250; e) Kim, M. S.; Kim, Y.-W.; Hahm, H. S.; Jang, J. W.; Lee, W. K.; Ha, H.-J. *Chem. Commun.* **2005**, 3062; and references therein. f) Bar, G. L. J.; Lloyd- Jones, G. C.; Booker-Milburn, K. I. *J. Am. Chem. Soc.* **2005**, *127*, 7308.

[27] a) G. Angelici, S. Contaldi,S. Lynn Green, C. Tomasini, Org Biomol Chem, 2008, 6, 1849; b) F. Schneider, Justus Liebigs *Ann. Chem*., **1937**, *529*,1; c) K.Hayashi, K.-i. Nunami, J. Kato, N. Yoneda, M. Kubo, T. Ochiai and R. Ishida, *J. Med. Chem*., **1989**, *32*, 289; d) H. Kubota, A. Kubo, M. Takahashi, R. Shimizu, T. Da-te, K. Okamura and K.-i. Nunami, *J. Org. Chem.*, **1995**, *60*, 6776; e) R. P. Robinson, E. R. Laird, K. M. Donahue, L. L. Lopresti-Morrow, P. G. Mitchell, M. R. Reese, L. M. Reeves, A. I. Rouch, E. J. Stam and S. A. Yocum, *Bioorg. Med. Chem. Lett.*, **2001**, *11*, 1211; f) A. Arasappan, F. G. Njoroge, T. N. Parekh, X. Yang, J. Pichardo, N. Butkiewicz, A. Prongay, N. Yao and V. Girijavallabhan, *Bioorg. Med. Chem. Lett*., **2004**, *14*, 5751. g) M. P. Doyle, Q.-L. Khou, C. E. Raab, G. H. P. Roos, S. H. Simonsen and V. Lynch, *Inorg. Chem*., **1996**, *35*, 6064; h) M. P. Doyle and J. T. Colyer, *Tetrahedron: Asymmetry*, **2003**, *14*, 3601; i) M. P. Doyle, J. P. Morgan, J. C. Fettinger, P. Y. Zavalij, J. T. Colyer, D. J. Timmons and M. D. Carducci, *J. Org. Chem*., **2005**, *70*, 5291.

[28] H. Eum, Y. Lee, S. Kim, A. Baek, M. Son, K. W. Lee, S. W.Ko, S. Kim, S. Y. Yun, W. K. Lee, H.Ha, *Bull. Korean Chem. Soc.* **2010,** *31*, 611.

[29] C. Proulx, W. D. Lubell, *Org. Lett.* **2012**, *14*, 4552.

[30] N. Doan, R. Hopewell, W. D. Lubell, *Org. Lett.* **2014**, *16*, 2232.

[31] J. A. Fritz, J. S. Nakhla, J. P. Wolfe, *Org. Lett.* **2006**, *8*, 2531.

[32] Greco, A.; Tani, S.; De Marco, R.; Gentilucci, L. *Chem. Eur. J.* **2014**, *20*, 13390.

[33] V. Santagada, F. Fiorino, E. Perissutti, B. Severino, V. De Filippis, B. Vivenzio, and G. Caliendo, *Tetrahedron Lett*., 2001, **42**, 5171; B. Bacsa, K. Horváti, S. Bõsze, F. Andreae, and C. O. Kappe, *J. Org. Chem.*, **2008**, *73*, 7532.

[34] Zhang, L. H.; Kauffman, G. S.; Pesti, J. A.; Yin, J. *J. Org. Chem*. **1997**, *62*, 6918.

[35] K. R. Rajashankar, S. Ramakumar, and V. S. Chauhan, *J. Am. Chem. Soc*., **1992**, *114*, 9225; U. Schmidt, A Lieberknecht, and J. Wild, *Synthesis*, 1988, **3**, 159; A. Polinsky, M. G. Cooney, A. Toy-Palmer, G. Osapay, and M. Goodman, *J. Med. Chem.*, **1992**, *35*, 4185; J. M. Humphrey, and A. R. Chamberlin, *Chem. Rev.*, **1997**, *97*, 2243; C. Bonauer, T. Walenzyk, and B. König, *Synthesis*, **2006**, *1*,1; R. Ramapanicker, R. Mishra, and S. Chandrasekaran, *J. Pept. Sci*., **2010**, *16*, 123.

[36] J. B. Blanco-Canosa, P. E. Dawson, *Angew. Chem.* **2008**, *120*, 6957.

[37] G. Cardillo, L. Gentilucci, A. Tolomelli, *Tetrahedron Lett*., **1999**, *40*, 8261.

[38] H. Kubota, A. Kubo, M. Takahashi, R. Shimizu, T. Da-te, K. Okamura, K.Nunami, *J. Org. Chem*. **1995**, *60*, 6776.

[39] a) A. W. Hofmann, *Ber. Dtsch. Chem. Ges.*, **1881**, *14*, 2725; b) A. W. Hofmann, *Ber. Dtsch. Chem. Ges*., **1885**, *18*, 2734.

[40] a) G. M. Loudon and M. E. Parham, *Tetrahedron Lett*., **1978**, 437; b) M. Waki, Y. Kitajima and N. Zumiya, *Synthesis*, **1981**, 266; (c) P. Pallai, M. Goodman, *J. Chem. Soc*., *Chem. Commun*., **1982**, 280; d) F. Squadrini, A. S. Verdini and G. C. Viscomi, *Gazz. Chim. Ital*., **1984**, *114*, 25; e) Y. Shimihihashi, H. Kodama, M. Waki and T. Costa, *Chem. Lett.*, **1988**, 1821.

[41] R. M. Moiarty, *J. Org. Chem*., **2005**, *70*, 2893.

[42] a) A. S. Radhakrishna, M. E. Parham, R. M. Riggs and G. M. Loudon, *J. Org. Chem*., **1979**, *44*, 1746; b) G. M. Loudon, A. S. Radhakrishna, M. R. Almond, J. K. Blodgett and R. H. Boutin, *J. Org. Chem*., **1984**, *49*, 4272; c) M. R. Almond, J. B. Stimmel, A. E. Thompson and G. M. Loudon, *Org. Synth*., **1988**, *67*, 132; d) M. Tamura, J. Jacyno and C. H. Stammer, *Tetrahedron Lett*., **1986**, *27*, 5435.

[43] a) A. S. Radhakrishna, C. D. Rao, R. K. Varma, B. B. Sing and S. P. Bhatnagar, *Synthesis*, **1983**, 538; b) C. Wasielewki, M. Topolski and M. Dembkowski, *J. Prakt. Chem*., **1989**, *331*, 507.

[44] a) I. M. Lazbin and G. F. Koser, *J. Org. Chem*., **1986**, *51*, 2669; (b) A. Vasudervan and G. F. Koser, *J. Org. Chem*., **1988**, *53*, 5158; (c) R. M. Moriarty, J. S. Khoshrowshahi, A. K. Awaathi and R. Penmaata, *Synth. Commun*., **1988**, *18*, 117.

[45] a) R. M. Moiarty, C. J. Chany, II, R. K. Vaid, O. Prakash and S. M. Tuladhar, *J. Org. Chem.*, **1993**, *58*, 2478; (b) X. Huang, M. Seid and J. W. Keillor, *J. Org. Chem*., **1997**, *62*, 7495.

[46] a) Handzlik, J.; Macia¸g, D.; Kubacka, M.; Mogilski, S.; Filipek, B.; Stadnicka, K.; Kiec´ -Kononowicz, K. *Bioorg. Med. Chem.* **2008**, *16*, 5982; b) Handzlik, J.; Szyman´ ska, E.; Ne¸dza, K.; Kubacka, M.; Siwek, A.; Mogilski, S.; Handzlik, J.; Filipek, B.; Kiec´ -Kononowicz, K. *Bioorg. Med. Chem.* **2011**, *19*, 1349; c) Handzlik, J.; Pertz, H. H.; Gornemann, T.; Jahnichen, S.; Kiec´ -Kononowicz, K. *Bioorg. Med. Chem. Lett.* **2010**, *20*, 6152; d) Kiec´ -Kononowicz, K.; Stadnicka, K.; Mitka, A.; Pekala, E.; Filipek, B.; Sapa, J.; Zygmunt, M. *Eur. J. Med. Chem*. **2003**, *38*, 555; e) Handzlik, J.; Bajda, M.; Zygmunt, M.; Maciag, D.; Dybala, M.; Bednarski, M.; Filipek, B.; Malawska, B.; Kiec -Kononowicz, K. *Bioorg. Med. Chem*. **2012**, *20*, 2290.

[47] H. Kubota, A. Kubo, M. Takahashi, R. Shimizu, T. Da-te, K. Okamura and K.-i. Nunami, *J. Org. Chem.*, **1995**, *60*, 6776;

[48] a) C. Tomasini, G. Luppi and M. Monari, *J. Am. Chem. Soc*., **2006**, *128*, 2410; b) G. Angelici, G. Luppi, B. Kaptein, Q. B. Broxterman, H. J. Hofmann, C. Tomasini, *Eur. J. Org. Chem.*, **2007**, 2713; c) G. Angelici, G. Falini, H.-J. Hofmann, D. Huster, M. Monari, C. Tomasini, *Angew. Chem., Int. Ed.*, **2008**, *47*, 8075; d) G. Angelici, G. Falini, H.-J. Hofmann, D. Huster, M. Monari and C. Tomasini, *Chem.–Eur. J.*, **2009**, *15*, 8037.

[49] P. A. Temussi, D. Picone, G. Saviano, P. Amodeo, A. Motta, T. Tancredi, S. Salvadori and R. Tomatis, *Biopolymers*, **1992**, *32*, 367.

[50] C. Toniolo, and E. Benedetti, *Crit. Rev. Biochem*., 1980, **9**, 1; B. Imperiali, R. A. Moats, S. L. Fisher, and T. J. Prins, *J. Am. Chem. Soc.*, 1992, **114**, 3182; J. Yang, and S. H. Gellman, *J. Am. Chem. Soc*., 1998, **120**, 9090; I. G. Jones, W. Jones, and M. North, *J. Org. Chem*., 1998, **63**, 1505; L. Belvisi, C. Gennari, A. Mielgo, D. Potenza, and C. Scolastico, *Eur. J. Org. Chem.*, 1999, 389.

[51] J. A. Smith, and L. G. Pease, *J. Mol. Biol*., **1980**, *203*, 221; D. K. Chalmerst, and G. R. Marshall, *J. Am. Chem. Soc*., **1995**, *117*, 5927; J. Venkatraman, S. C. Shankaramma, and P. Balaram, *Chem. Rev*., **2001**, *101*, 3131; R. Rai, S. Raghothama, and P. Balaram, *J. Am. Chem. Soc*., **2006**, *128*, 2675.

[52] L. R. Whitby, Y. Ando, V. Setola, P. K. Vogt, B. L. Roth, D. L. Boger, *J. Am. Chem. Soc.* **2011**, *133*, 10184.

[53] a) Che, Y.; Brooks, B. R.; Marshall, G. R. *J. Comput.-Aided Mol. Des.* **2006**, *20*, 109; b) Garland, S. L.; Dean, P. M. *J. Comput.-Aided Mol. Des.* **1999**, *13*, 469; c) Garland, S. L.; Dean, P. M. *J. Comput.-Aided Mol. Des.* **1999**, *13*, 485.

Chapter 7

Alternative synthesis of the antibiotic Linezolid starting from the β-amino acid Isoserine

In this chapter is described a new synthesis of the 5-aminomethyl-3-oxazolidinone core of linezolid in enantiomerically pure form. The expedient cyclization of the α-hydroxy amide derived from isoserine and 3-fluoro-4-morpholinoaniline to aminomethyl-oxazolidin-2,4-dione and the mild selective reduction at the position C(4) gave linezolid in almost quantitative overall yield.

7.1. Introduction

The development of bacterial resistance to currently available antibacterial agents is a growing global health problem.[1] In fact, the infections caused by multidrug-resistant pathogens are responsible for significant morbidity and mortality in both the hospital and community settings.[2] One possible approach to face this problem is to design novel classes of antibacterial agents employing new mechanisms of action. Such agents would exhibit a lack of cross-resistance with existing antimicrobial drugs. However, from the early 1970s to 1999 the innovative antibiotic pipeline dried up. All newly launched antibiotics were analogues of existing drugs except for mupirocin, a Gram-positive antibiotic launched in 1985. Since 2000, the situation has improved, with five more new classes of antibiotics approved and launched: linezolid (LZD, **1**),[3] daptomycin, retapamulin, fidaxomicin, and bedaquiline.[2]

Discovered in the 90's, and approved in the U.S. by FDA in 2000, LZD (Figure 1) is currently the only antibiotic commercially available in the oxazolidinone class. Compounds containing the oxazolidinone moiety are interesting because their spectrum of activity covers the important Gram-positive pathogens, particularly those which have been the cause of resistance development.[2,3]

LZD selectively inhibits bacterial protein synthesis through binding the peptidyltransferase center on the bacterial ribosome, thus forbidding the bacterial translation process.[4] This action mechanism is unique among protein synthesis inhibitors and explains why LZD retains antibacterial activity against Gram-positive organisms which are resistant to members of other classes.

When LZD came to the market, it was claimed that there would be no cross-resistance to this antibiotic and that resistance would be rare and difficult for the bacteria to develop.[5] Nevertheless, with the increased wide use of LZD and the abuse in some degree in clinic in recent years, some clinically resistant strains to LZD have been found worldwide such as *S. aureus* and *Enterococcus spp*.,[6] and although the LNZ-resistant strains (LinR) appear relatively infrequently in the clinic, the infections caused by them were found to be life-threatening.

Consequently, several researchers have recently focused on modifying the oxazolidinone structure to seek analogues with an extended spectrum of antibacterial activity covering Gram-negative organisms, activity against LinR strains, and improved safety profile. Presently, only four oxazolidinones have entered clinical development.[7] As a consequence, the identification of novel synthetic protocols to obtain the 5-aminomethyl-3-oxazolidinone core in enantiomerically pure form can be regarded of great interest for the preparation of LZD and novel analogues.

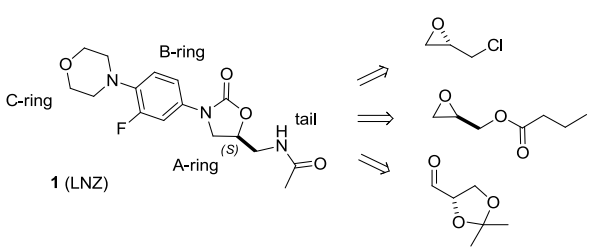

Figure 1. The syntheses of LZD (**1**) utilize chiral building blocks.

The key step of LZD synthesis is the formation of the (*S*)-configured 5-substituted oxazolidinone A ring. Most protocols described in patents or publications made use of chiral oxiranes[3,7,8] such as epichlorohydrin[9] (Figure 1), or other building

blocks, e.g. glyceraldehyde[10] (Figure 1), while very few papers reported approaches based on asymmetric protocols.[11] The optimized large-scale synthesis of LZD involves a total of 9 steps, and the oxazolidinone ring is built by adding enantiomerically pure (*S*)-3-chloropropane-1,2-diol to a Cbz-protected proper aniline (Scheme 1).[3,8]
The large majority of LZD analogs reported in the literature display modifications at the ring B or C, and/or at the C(5)-side chain.[2,3,7] By contrast, the replacement of the oxazolidinone ring A with other heterocycles has been described very few times.[12]
In this contest, herein is reported an expedient synthesis of the oxazolidinone core from the very convenient chiral reagent isoserine, taking advantage of a synthetic strategy that is suitable to furnish novel LZD analogues carrying diverse substituents at the A ring.

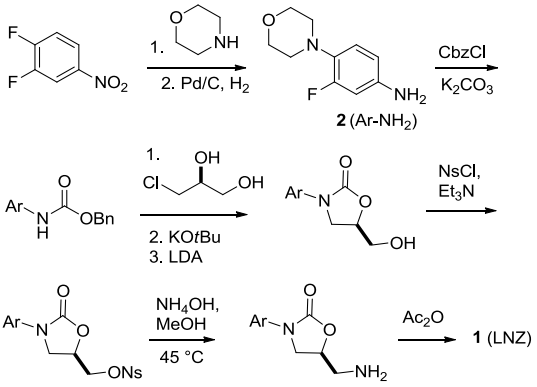

Scheme 1. Synthesis of LZD (**1**) on a process scale.

7.2. Results and Discussion

In the above chapters 3 and 4, is been reported the rapid and simple formation of 1,3-oxazolidin-2-one scaffolds for the design of β-turn-like peptidomimetics,[13] or as chiral auxiliaries for the stereoselective synthesis of unusual amino acids.[14] Interestingly, we observed that the reaction of peptide sequences containing the α-hydroxy-β^2-amino acid[15] isoserine (Isoser) with carbonate gave rise to 5-aminomethyloxazolidine-2,4-dione rings (chapter 5).[16]
These heterocycles have been described and utilized quite rarely in organic and medicinal chemistry.[17] This result prompted us to design a plausible retro-synthetic pathway for the synthesis of optically pure LZD (**1**) *via* the intermediate 5-aminomethyloxazolidine-2,4-dione, taking advantage of the very convenient commercially available chiral reagent (*S*)-isoserine (Scheme 2). The rationale for the other steps of the proposed strategy is discussed in the following sections.

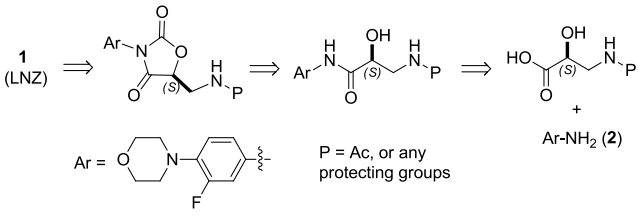

Scheme 2. Retro-synthetic approach to LZD (**1**) *via* a oxazolidine-2,4-dione intermediate, readily obtained in turn from the chiral building block isoserine.

The approach depicted in Scheme 2 could be exploited in the preparation of a number of unprecedented LZD derivatives carrying diverse substituents at the A-ring and/or at the methylacetamide tail (see Figure 1). Indeed, Isoser can be purchased also in the (*R*)-configuration, and several enantiomerically pure Isoser derivatives are commercially available.[18] Furthermore, many non-racemic substituted isoserines can be obtained from chiral starting materials or by enzymatic resolution, by the use of chiral auxiliaries,[19] or by asymmetric catalysis, for example via catalytic enantioselective Henry reactions.[20] These synthetic alternatives will be developed in due course.

According to the retrosynthetic plan, the first step corresponded to the coupling of 3-fluoro-4-morpholin-4-yl-phenylamine (**2**), prepared as reported in the literature,[3] and Isoser. Initially, we optimized the conditions for the coupling of Isoser carrying diverse protecting groups at the *N*-terminus. The reaction of **2** with *N*-Boc-IsoserOH (Scheme 3) was attempted according to a protocol described in the literature for the coupling of anilines with chiral α-hydroxy acids. This strategy

appeared as a suitable process for the synthesis of the enantiomerically pure α-hydroxy amide **3**.[21] Arylamine **2** was treated with $SOCl_2$/IMD (imidazole) to give the corresponding *N*-sulfinylarylamine, and the reaction of the latter with *N*-Boc-IsoserOH was performed in presence of 1,2,4-triazole. Despite several modifications aimed at optimizing the procedure, in our hands the reaction afforded the expected amide **3a** with moderate yields, up to 40% (Table 1, entry 1).

Consequently, the reactions of **2** and *N*-Boc-IsoserOH were conducted under various conditions (Table 1), and in different solvents (only the best results are reported in Table 1). All runs were monitored by tlc and stopped following the disappearance of the reagents, or in any case after 12 h. The reaction of **2** and the mixed anhydride obtained from *N*-Boc-IsoserOH and ethylchloroformate/TEA gave only traces of **3a** after 12 h (Table 1, entry 2). The use of EDC and HOBt as coupling activating agents in the presence of DIPEA (or TEA, not shown) at rt afforded **3a** in low yield (15%, entry 3). The use of DBU (1,8-diazabicyclo[5.4.0]undec-7-ene) gave a 40% yield (entry 4), while NMM (*N*-methylmorpholine) gave a more satisfactory 60% yield (entry 5).

On the other hand, the use of the activating agents HBTU/HOBt/NMM or HATU/HOBt/NMM at rt for 12 h led to very good yields, 96% and 94% (entries 6 and 7 in Table 1), respectively. These two reactions were accelerated by heating for 10 min at 80 °C by MW irradiation, giving **3a** in quantitative yields after isolation by flash chromatography over silica gel (entry 8 with HBTU, and entry 9 with HATU).

Noteworthy, Isoser was incorporated without a protection for the OH function. Under the reaction conditions reported above,[12] the acylation of the OH-function and thus the formation of isoserine-isoserine side products was not observed, as confirmed by the ^{1}H NMR and RP-HPLC ESI MS analyses of the crude reaction mixture.

The availability of *N*-Ac-IsoserOH offered the opportunity to synthesize a direct precursor of LZD (**1**) already equipped with the desired methylacetamide tail (Scheme 2). Therefore, we reacted **2** and *N*-Ac-IsoserOH under the best-yielding conditions determined for the preparation of **3a** at r.t. (entry 6 in Table 1), or under MW activation (entry 9 in Table 1). In particular, the use of HBTU/HOBt/NMM at r.t. gave **3b** in 97% yield after 12 h (entry 10), while HATU/HOBt/NMM at 80 °C under MW irradiation gave the same product quantitatively in 10 min (entry 11). As a reference control, we repeated the coupling with EDC/HOBt/NMM (see entry 5), and obtained a low yield (20%, entry 12). This observation confirms the efficacy of HATU/HOBt/NMM coupling reagents and MW activation.

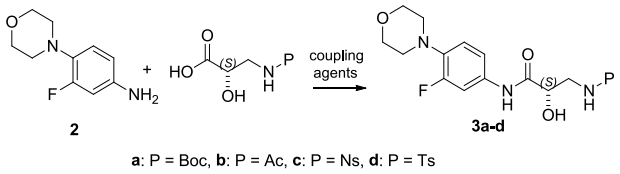

Scheme 3. Coupling of **2** and Isoser.

Table 1. Coupling reactions of isoserine and **2** to afford amides **3a-d**.

entry	P	coupling agents	Temp (°C)	solvent	3	Yield (%)[a]
1	Boc	1. $SOCl_2$/IMD	1. -30	DCM/DMF	a	40[b]
		2. triazole	2. r.t.			
2	Boc	EtOCOCl/TEA	-20-r.t.	DCM/DMF	-	-[b,c]
3	Boc	EDC/HOBt/DIPEA	0-r.t.	DCM/DMF	a	15[b]
4	Boc	EDC/HOBT/DBU	0-r.t.	DCM/DMF	a	40[b]
5	Boc	EDC/HOBt/NMM	0-r.t.	DCM/DMF	a	60[b]
6	Boc	HBTU/HOBt/NMM	0-r.t.	DCM/DMF	a	96[b]
7	Boc	HATU/HOBt/NMM	0-r.t.	DCM/DMF	a	94[b]
8	Boc	HBTU/HOBt/NMM	80 (MW)	DMF	a	98[d]
9	Boc	HATU/HOBt/NMM	80 (MW)	DMF	a	98[d]
10	Ac	HBTU/HOBt/NMM	0-r.t.	DCM/DMF	b	97
11	Ac	HATU/HOBt/NMM	80 (MW)	DMF	b	98[d]
12	Ac	EDC/HOBt/NMM	0-r.t.	DCM/DMF	b	20

13	Ts[e]	HATU/HOBt/NMM	80 (MW)	DMF	‹	97[d]
14	Ns[e]	HATU/HOBt/NMM	80 (MW)	DMF	‹	96[d]

[a] Determined after isolation by flash chromatography over silica gel. [b] Reaction time 12 h. [c] Traces. [d] Reaction time 10 min. [e] Not further examined.

We observed that *N*-Ts (tosyl)- and *N*-Ns (nosyl)-IsoserOH behaved similarly to *N*-Boc- and *N*-Ac-IsoserOH in the coupling with **2** under the same reaction conditions used in entry 9 (Table 1), giving in almost quantitative yields the corresponding α-hydroxy arylamides **3c** and **3d** (entries 13 and 14). The arylsulfonyl protecting groups might be of some interest for future developments of LZD analogues. For the comparatively simpler cleavage, the Boc protecting group represents the most convenient option.[22] Nevertheless, the literature reports several methods for the mild cleavage of arylsulfonyl groups.[23]

The following synthetic step of the strategy depicted in Scheme 2 consisted in the cyclization of the Isoser arylamides **3** to the five-membered heterocycles **4** (Scheme 4). As anticipated, we observed that oligopeptides containing Isoser underwent cyclization to 5-aminomethyloxazolidin-2,4-diones by treatment with 1.1 equiv. of DSC (*N,N′*-disuccinimidyl carbonate) and a catalytic amount of DIPEA in DMF at r.t. for 1h.[16] Under these conditions, **3a** and **3b** gave the corresponding **4a** and **4b** in very good yields, 96% (entry 1 in Table 2) and 92% (entry 2 in Table 2), respectively, after purification by flash chromatography over silica gel.

Other carbonates or dicarbonates converted **3a** to the 1,3-oxazolidin-2,4-dione **4a** in lower yields: Boc_2O 15% (Table 2, entry 3),[24] triphosgene 35% (entry 4),[24] CDI (1,1'-carbonyldiimidazole)[25] 30% (entry 5), *p*-nitrophenylchloroformate[26] 45% (entry 6). All reactions were conducted at r.t. for 12 h; increasing the equivalents of the reagents, time, and temperature, in different solvents, had scarce effects on the reactions.

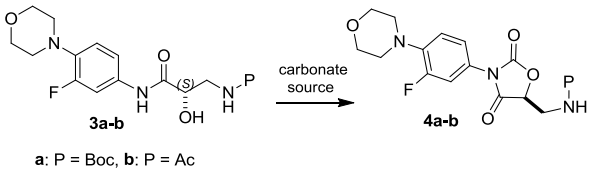

Scheme 4. Cyclization of **3a** and **3b** to 3-aryl-5-aminomethyl-1,3-oxazolidin-2,4-diones **4a** and **4b**.

Table 2. Cyclization of **3a** and **3b** to **4a** and **4b**: reagents and yields.

entry	3	carbonate	4	Yield (%)[a]
1	**a**	DSC	**a**	96[b]
2	**b**	DSC	**b**	92[b]
3	**a**	Boc_2O	**a**	15[c]
4	**a**	triphosgene	**a**	35[c]
5	**a**	CDI	**a**	30[c]
6	**a**	*p*NO_2-phenylchloroformate	**a**	45[c]

[a] Determined after isolation by flash chromatography over silica gel. [b] Reaction time 1 h. [c] Reaction time 12 h.

Having the Boc-aminomethyl **4a** and acetamidomethyl **4b** at hand, the last step towards LZD (**1**) consisted in the reduction of the carbonyl at C(4) (Scheme 5 and Table 3). This step raised some concerns for the risk of simultaneous reduction of the acetamide segment. The reduction of amides to amines under mild conditions is regarded as a highly valuable but challenging transformation; many of the reported procedures utilize costly or harmful heavy metal catalysts, high pressure and/or high temperatures.[27] The convenience of the strategy depicted in Scheme 2 was substantiated by the observations reported in the literature that in a 1,3-oxazolidine-2,4-dione, the *N*-carbamate moiety increases the reactivity of the inner amide bond towards reduction by $NaBH_4$.[14] This precedent motivated us to attempt conversion of **4b** to LZD (**1**) upon identification of a proper reducing agent (Table 3).

In effect, the 5-methylacetamide **4b** was regioselectively reduced with 1.5 equiv. of $NaBH_4$ in H_2O/THF at 0 °C, giving exclusively the 5-aminomethyl-4-hydroxy **5** (Scheme 5) with *trans* relative stereochemistry (Table 3, entry 1). This LZD

derivative might be utilized for the introduction of substituents at C(4) in the oxazolidinone ring. Yields improved to 95% in MeOH/THF (entry 2), while other solvents gave inferior results (not shown). The *trans*-relationship was confirmed by the very small coupling constant JH_4-H_5 in the ^{1}H NMR spectra; *trans*-4,5-disubstituted 1,3-oxazolidin-2-ones are characterized by coupling constants much lower than that of the *cis*-stereoisomers.[24] Interestingly, the RP-HPLC and NMR analyses excluded an equilibrium between anomers at C(4).

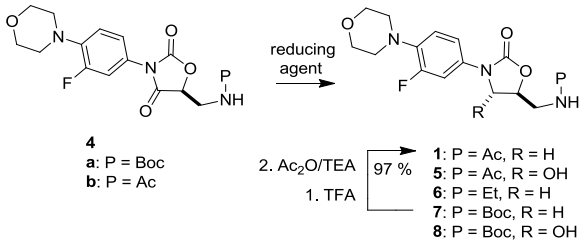

Scheme 5. Reduction of the carbonyl bond at C(4) of the 1,3-oxazolidin-2,4-dione: synthesis of LZD (**1**).

Table 3. Mild reductions of **4a** and **4b** at C(4) with several reducing agents.

Entry	4	Reducing agent	Temp (°C)	Solvent	Prod.	Yield (%)[a]
1	**b**	$NaBH_4$	0	H_2O/THF	**5**	50[b]
2	**b**	$NaBH_4$	0	MeOH/THF	**5**	95[b]
3	**b**	$LiAlH_4$	0	THF	-	-[b,c]
4	**b**	H_2/Pd-C	r.t.	MeOH	-	-[d]
5	**b**	$HCOO^-NH_4^+$/Pd-C	60	*i*-PrOH	-	-[d]
6	**b**	NH_2NH_2	100	$(HOCH_2)_2$	-	-[d]
7	**b**	$Zn(OAc)_2$/$(EtO)_3SiH$	r.t.-40	THF	-	-[d]
8	**b**	BH_3/OEt_2	0-r.t.	THF	-	-[d]
9	**b**	BH_3·DMS	0	THF	**1**	55[e]
10	**b**	BH_3·DMS/MS	0	THF	**1**	88[b]
11	**a**	BH_3·OEt_2	0-r.t.	THF	-	-[d]
12	**a**	BH_3·DMS	0	THF	**7**	64[b,f]
13	**a**	BH_3·DMS/MS	0	THF	**7**	97[b]

[a] Determined after isolation by flash chromatography over silica gel. [b] reaction time 2h. [c] Traces of **1**, and **6** as the major by-product. [d] Reaction time 24 h; **4** was recovered almost quantitatively. [e] **5** and **6** were the major by-products. [f] **8** was the major by-product.

Not unexpectedly, reaction with $LiAlH_4$ at 0 °C resulted in the reduction of both the carbonyl at C(4) and the *N*-Ac function, giving a small amount of **1**, and the 5-ethylaminomethyl **6** (Scheme 5) as the major by-product (Table 3, entry 3). Catalytic hydrogenation (entries 4 and 5),[27] Wolff-Kishner reaction (entry 6),[28] $Zn(OAc)_2$ catalyzed reduction with $(EtO)_3SiH$ (entry 7),[27d] 2M borane in diethyl ether (entry 8),[27] gave only traces of the desired product after 24 h.

On the other hand, borane dimethyl sulfide complex in anhydrous THF at 0 °C gave **1**, which was easily isolated in 55% yield by flash chromatography (entry 9 in Scheme 5). The analysis of the crude reaction mixture by RP-HPLC ESI revealed the presence of significant amounts of by-products **5** and **6** (not isolated). When the reaction was repeated in the presence of activated (dried) 4 Å molecular sieves, which effectively prevented the formation of 4-hydroxy **5**, product **1** was obtained in the very satisfactory yield of 88% (entry 10), while **6** was present in traces. Increased reaction temperature resulted in higher amounts of *N*-ethylamino **6**.

Finally, we examined the reduction of **4a** under the conditions described for entries 8-10 in Scheme 5 and Table 3. Borane in diethyl ether was again nearly ineffective (entry 11), while borane dimethyl sulfide complex gave the 1,3-oxazolidin-4-one **7**[29] (64%, entry 12) and traces of 4-hydroxy-1,3-oxazolidin-4-one **8** (Scheme 5, not isolated). By contrast, in the presence of

molecular sieves, borane dimethyl sulfide complex afforded **7** quantitatively (entry 13). The subsequent treatment with TFA followed by treatment with acetic anhydride/TEA afforded **1** in 97% yield (Scheme 5).
The enantiomeric purity of the reported compounds and intermediates was confirmed by HPLC analysis using a chiral stationary phase. The analyses of the compounds **1**, **3a**, **3b**, **4a**, **4b**, **5**, **7** performed on a CHIRALPAK IC column were compared to the analyses of the corresponding racemates obtained from *rac*-isoserine (Experimental section) As concerning the compounds **1**(LZD) and **7**, the spectroscopic characterizations and specific optical rotations nicely matched the data reported in the literature (**1**,3[11a] **7**[29], see Experimental Section).

7.3. Conclusions

We have demonstrated the feasibility of a new approach to the synthesis of LZD, based on the use of the chiral starting material *N*-acetyl-isoserine, which was efficiently coupled to 3-fluoro-4-morpholinoaniline. Cyclization of the resulting α-hydroxy-β-acetamido arylamide provided a 5-acetamidomethyl-1,3-oxazolidin-2,4-dione intermediate, which was reduced regioselectively to give LZD in very good yield under mild reaction conditions. The use of a *N*-Boc protected isoserine further improved the efficiency of the reduction, only requiring an extra deprotection/acetylation step to afford LZD. Further work could be done for the synthesis of optically pure substituted α-hydroxy-β-aminoacids of type β^2-, β^3-, $\beta^{2,3}$-, $\beta^{3,3}$-, suitable precursors of diversely A ring-substituted LZD analogues.

7.4. Experimental Section

7.4.1. General Methods

Standard chemicals, including (*S*)- and *rac*-isoserine, were purchased from commercial sources and used without further purification. **2** was prepared as reported in the literature. Flash chromatography was performed on silica gel (230-400 mesh), using mixtures of distilled solvents. Compounds purities were assessed by analytical RP-HPLC and elemental analysis. Analytical RP-HPLC was performed on an Agilent 1100 series apparatus, using a RP column Phenomenex mod. Gemini 3μ C18 110A 100x3.0 mm (P/No 00D-4439-Y0); column description: stationary phase octadecyl carbon chain-bonded silica (C18) with TMS endcapping, fully porous organo-silica solid support, particle size 3 μm, pore size 110 Å, length 100 mm, internal diameter 3 mm; DAD 210 nm; mobile phase: from a 9:1 H2O/CH3CN to a 2:8 H2O/CH3CN in 20 min at a flow rate of 1.0 mL min-1, followed by 10 min at the same composition. Epimerization of intermediates and products was excluded on the basis of chiral HPLC analysis, performed on an Agilent 1200 series apparatus, using a CHIRALPAK IC column (P/No 83325); column description: chiral stationary phase cellulose *tris*(3,5-dichlorophenylcarbamate) immobilized on silica, particle size 5 μm, lenght 250 mm, internal diameter 4.6 mm, DAD 210/254 nm; mobile phase: 1:1 *n*-hexane/2-propanol, at 0.8 mL min^{-1}. The synthetic procedures by MW irradiation were performed using a microwave oven (MicroSYNTH Microwave Labstation for Synthesis) equipped with a built-in ATC-FO advanced fiber optic automatic temperature control. ^{1}H NMR spectra were recorded using a Varian Gemini apparatus at 400 MHz in 5 mm tubes, using 0.01 M peptide at room temperature. ^{13}C NMR spectra were recorded at 100 MHz. Chemical shifts are reported as δ values relative to residual CHCl3 δH (7.26 p.p.m.), DMSO δH (2.50 p.p.m.) and $CDCl_3$ δC (77.16 p.p.m.) as internal standards. The unambiguous assignment of ^{1}H NMR resonances was performed by 2D gCOSY.

7.4.2. Synthetic procedures

4-morpholino-3-fluoroaniline (**2**).[30]A solution of morpholine (1.1 mol) in DMSO (5 mL) was slowly added to a stirred solution of 3,4-difluoronitrobenzene (1.0 mmol) in DMSO (5 mL) under inert atmosphere, and the mixture was heated at 75 °C while stirring. After 2 h, the mixture was allowed to cool to r.t. and ice-cold water (200 mL) was added. The nitro-intermediate which precipitated quantitatively from the solution was filtered and re-crystallized from ethanol. The crude nitro intermediate was dissolved in MeOH (50 mL), and treated with H_2 (1 atm) and a catalytic amount of Pd/C. The reaction was stirred for 3 h at r.t., than it was filtered through an Hirsch funnel fitted with Celite®. Solvent was evaporated at reduced pressure giving 2 as a gray solid (90%), not needing further purifications.

N-protected-isoserinearylamides **3**. 3-fluoro-4-morpholinoaniline (**2**) (1.0 mmol) was added to a stirred solution of N-protected isoserine (1.05 mmol) in 9:1 DCM/DMF (5 mL) at 0 °C. After 15 min, HOBt (1.1 mmol) and NMM (2.0 mmol) were added, followed after 30 min by HBTU, or HATU (1.1 mmol). The mixture was stirred at r.t. for 12 h. Alternatively, the reaction was performed under MW irradiation for 10 min, with an initial irradiation power of 150W, while monitoring the internal reaction temperature at 80 °C. Then the reaction mixture was concentrated at reduced pressure, and the residue

was diluted with AcOEt (30 mL), washed with 0.1 M HCl (5 mL), and a saturated solution of $NaHCO_3$ (5 mL). The organic layer was dried over Na_2SO_4 and the solvent was evaporated at reduced pressure, to afford **3** as a crude residue, which was purified (yield: see Table 1) by flash chromatography over silica gel (eluant: 40:60 cyclohexane/EtOAc).

3a. $[\alpha]_D^{20}$ = -98.6 (c 0.5, $CHCl_3$); ^{1}H NMR ($CDCl_3$) δ: 1.44 (s, 9H, tBu), 3.12 (t, J=4.4 Hz, 4H, morph$H_{3,5}$), 3.59 (ddd, J=2.2, 5.8, 14.8 Hz, 1H, CH_2N), 3.69 (ddd, J=2.2, 5.8, 14.8 Hz, 1H, CH_2N), 3.92 (t, J=4.4 Hz, 4H, morph$H_{2,6}$), 4.30 (m, 1H, CH_2CH), 5.19 (br. t, 1H, BocNH), 5.72 (br.d, 1H, OH) 6.93 (t, J=8.8 Hz, 1H, ArH_2), 7.16 (m, 1H, ArH_5), 7.58 (dd, J=2.4, 14 Hz, 1H, ArH_6), 8.85 (s, 1H, CONH); ^{13}C NMR ($CDCl_3$) δ: 28.2, 44.8, 51.0, 66.9, 71.8, 81.1, 108.6, 108.8, 115.5 118.7, 118.8, 132.3, 132.4, 136.6, 136.7, 154.2, 156.6, 170.1; ES-MS m/z $[M+H]^+$ calcd 384.2, found 384.2. Elem. anal. for $C_{18}H_{26}FN_3O_5$ calcd: C 56.39, H 6.84, F 4.96, N 10.96; found: C 56.67, H 6.89, F 5.02, N 10.90.

3b. $[\alpha]_D^{20}$ = -77.1 (c 0.7, $CHCl_3$); ^{1}H NMR ($CDCl_3$) δ: 2.04 (s, 3H, Ac), 3.07 (t, J=4.4 Hz, 4H, morph$H_{3,5}$), 3.68 (ddd, J=2.2, 5.8, 14.8 Hz, 1H, CH_2N), 3.82 (ddd, J=2.2, 5.8, 14.8 Hz, 1H, CH_2N), 3.89 (t, J=4.4 Hz, 4H, morph$H_{2,6}$), 4.32 (m, 1H, CH_2CH), 6.07 (br.s, 1H, OH), 6.45 (br.t, 1H, AcNH), 6.95 (t, J=8.6 Hz, 1H, ArH_2), 7.15 (m, 1H, ArH_5), 7.55 (m, 1H, ArH_6), 8.89 (s, 1H, CONH); ^{13}CNMR ($CDCl_3$) δ: 22.7, 44.8, 51.1, 66.9, 74.2, 108.6, 108.8, 115.5, 119.0, 127.0, 128.3, 154.2, 170.1, 174.7; ES-MS m/z $[M+H]^+$ calcd 326.2, found 326.3. Elem. anal. for $C_{15}H_{20}FN_3O_4$ calcd: C 55.38, H 6.20, F 5.84, N 12.92; found: C 55.71, H 6.25, F 5.87, N 13.00.

Synthesis of **3a**, protocol of Table 1, entry 1.[31] For the synthesis of N-sulfinyl 4-morpholino-3-fluoroaniline, a solution of 1,1'-sulfinyldiimidazole (1 mmol) in dry DCM (2.5 mL) was added dropwise to a stirred solution of **2** in anhydrous 4:1 DCM/THF (2.5 mL), under inert atmosphere at -30 °C. After 1 h, the reaction mixture was filtered still under inert atmosphere at r.t., and the filtrate was used for the next step without further purifications. The filtrate (a solution of N-sulfinyl 4-morpholino-3-fluoroaniline) was added dropwise to a solution of N-Boc-isoSerine (1 mmol) and 1,2,4-triazole (1.4 mmol) in anhydrous 4:1 DCM/DMF (5 mL) while stirring, under nitrogen atmosphere at 0 °C. The reaction mixture was stirred for 3 h at 0 °C and for 15 h at r.t. Then the solvent was removed at reduced pressure, the residues was diluted with AcOEt (25 mL), washed with 1 M HCl (5 mL) and with a saturated solution of $NaHCO_3$ (5 mL). The organic layer was dried over Na_2SO_4, filtered, and concentrated at reduced pressure to afford the product 3a as crude residue, which was isolated (yield: see Table 1) by flash chromatography over silica gel (eluant: 35:65 cyclohexane/EtOAc).

5-aminometyloxazolidin-2,4-dione **4**. DSC (1.1 mmol) was added to a stirred solution of **3** (1.0 mmol) in 3:1 DCM/DMF (4 mL), followed by DIPEA (0.1 mmol) at r.t. and under inert atmosphere. After 1 h, the solvent was distilled at reduced pressure, the residues was diluted with 1 M HCl (5 mL), and the aqueous phase was extracted three times with AcOEt (3x15 mL). The combined organic layers were dried over Na_2SO_4, filtered, and concentrated at reduced pressure. The oily residue was purified by flash chromatography over silica gel (eluant: 60:40 cyclohexane/EtOAc) giving the product 4 (yield: see Table 2).

4a. $[\alpha]_D^{20}$ = -32.4 (c 0.5, $CHCl_3$); ^{1}H NMR ($CDCl_3$) δ: 1.45 (s, 9H, tBu), 3.13 (t, J=4.4 Hz, 4H, morph$H_{3,5}$), 3.75-3.85 (m, 2H, CH_2N), 3.88 (t, J=4.4 Hz, 4H, Morph$H_{2,6}$), 4.90 (t, J=6.0, 1H, CH_2CH), 5.00 (br.t, 1H, BocNH), 7.01 (t, J=8.4 Hz, 1H, ArH_2), 7.16-7.19 (m, 2H, $ArH_{5,6}$); ^{13}C NMR ($CDCl_3$) δ: 28.2, 40.4, 40.7, 50.5, 66.7, 82.2, 113.8, 118.6, 118.7, 121.7, 124.3, 124.4, 140.4, 140.6, 153.6, 153.7, 156.1, 169.8, 172.9; ES-MS m/z $[M+H]^+$ calcd 410.2, found 410.1. Elem. anal. for $C_{19}H_{24}FN_3O_6$ calcd: C 55.74, H 5.91, F 4.64, N 10.26; found: C 56.01, H 6.05, F 4.68, N 10.32.

4b. $[\alpha]_D^{20}$ = -27.3 (c 0.6, $CHCl_3$); ^{1}H NMR ($CDCl_3$) δ: 2.06 (s, 3H, Ac), 3.13 (t, J=4.8 Hz, 4H, morph$H_{3,5}$), 3.83-3.94 (m, 6H, CH_2N+morph$H_{2,6}$), 5.05 (t, J=5.4 Hz, 1H, CH_2CH), 5.93 (br.t, 1H, AcNH), 7.01 (t, J=8.8 Hz, 1H, ArH_2), 7.15-7.19 (m, 2H, $ArH_{6,5}$); ^{13}C NMR (DMSO) δ: 23.0, 39.4, 51.0, 66.8, 79.1, 115.2, 115.5, 119.7, 124.0, 125.4, 125.5, 140.8, 153.5, 154.9, 171.1, 171.2; ES-MS m/z $[M+H]^+$ calcd 352.1, found 352.1. Elem. anal. for $C_{16}H_{18}FN_3O_5$ calcd: C 54.70, H 5.16, F 5.41, N 11.96; found: C 55.02, H 5.19, F 5.45, N 12.04.

5-acetamidomethyl-4-hydroxy-oxazolidin-2-one **5**. Fresh $NaBH_4$ (0.057 g, 1.5 mmol) was added to a stirred solution of **4b** (0.35 g, 1.0 mmol) in 1:1 MeOH/THF (5 mL) at 0 °C under inert atmosphere. The reaction was quenched after 24 h by adding acetone. The mixture was concentrated at reduced pressure, and the residue was diluted with water (5mL). The mixture was extracted twice with DCM and once with EtOAc. The organic layers were collected and dried over Na_2SO_4. The solution was filtered and solvent was evaporated at reduced pressure. The oily **5** was isolated (0.33 g, 95%) by flash chromatography over silica gel (eluant: 50:50 cyclohexane/EtOAc). $[\alpha]_D^{20}$ = +1.8 (c 0.5, $CHCl_3$); ^{1}H NMR ($CDCl_3$) δ: 1.98 (s, 3H, Ac), 3.07 (dd, J=3.0, 5.8 Hz, 4H, morph$H_{3,5}$), 3.55 (ddd, J=5.0, 9.0, 14.4 Hz, 1H, CH_2N), 3.73 (ddd, J=5.0, 9.0, 14.4 Hz, 1H, CH_2N), 3.87 (dd, J=3.0, 5.8 Hz, 4H, morph$H_{2,6}$), 4.47 (br.t, 1H, CH_2CH), 5.02 (br.s, 1H, OH), 5.60 (s, 1H, CHOH), 6.36 (t, J=6.0 Hz, 1H, AcNH), 6.93 (t, J=9.2 Hz, 1H, ArH_1), 7.22 (dd, J=2.0, 10.4 Hz, 1H, ArH_6), 7.31 (dd, J=2.2, 13.8 Hz, 1H, ArH_5); ^{13}C NMR ($CDCl_3$) δ: 22.9, 40.7, 50.9, 66.8, 80.9, 83.1, 111.0, 111.3, 118.3, 119.0, 125.5, 154.0,

154.8, 156.5, 171.9; ES-MS m/z $[M+H]^+$ calcd 354.1, found 354.0. Elem. anal. for $C_{16}H_{20}FN_3O_5$ calcd: C 54.39, H 5.71, F 5.38, N 11.89; found: C 54.67, H 5.75, F 5.36, N 11.99.

5-aminometyloxazolidin-2-ones **1** and **7**. Dry 4 Å molecular sieves (100% w/w) were added under inert atmosphere to a solution of **4** (1.0 mmol) in freshly distilled THF (10 mL). BH_3·DMS (2.0 mmol) was added to the suspension under inert atmosphere at 0 °C. After stirring for 7 hours, the reaction was quenched with 0.1 M HCl (10 mL). The mixture was concentrated at reduced pressure to half of the initial volume, and extracted 3 times with EtOAc (3x15 mL). The combined organic layers were dried over Na_2SO_4, filtered, and concentrated at reduced pressure. The products **1** or **7** (yields: see Table 3) were purified by flash chromatography over silica gel (eluant: 75:25 cyclohexane/EtOAc).

LZD (**1**).[3,11a] $[\alpha]_D^{20}$ = -9.0 (c 0.5, $CHCl_3$), lit.[11a] $[\alpha]_D^{23}$ = -9.8 (c 2.5, $CHCl_3$); ^{1}H NMR ($CDCl_3$) δ: 2.04 (s, 3H, Ac), 3.11 (t, J=4.2 Hz, 4H, morph$H_{3,5}$), 3.62 (ddd, J=3.2, 6.0, 14.8 Hz, 1H, CH_2N), 3.71(ddd, J=3.2, 6.0, 14.8 Hz, 1H, CH_2N), 3.76 (dd, J=7.2, 9.0 Hz, 1H, OxdH_4), 3.91 (t, J=4.4 Hz, 4H, morph$H_{2,6}$), 4.04 (dd, J=7.2, 9.0 Hz, 1H, OxdH_4), 4.78 (m, 1H, OxdH_5), 5.99 (br.t, J=6.0 Hz, 1H, AcNH), 7.05-7.10 (m, 2H, Ar$H_{1,6}$), 7.49 (dd, J=2.8, 15.2 Hz, 1H, ArH_5); ^{13}C NMR ($CDCl_3$) δ: 23.1, 42.1, 47.7, 51.3, 66.5, 71.9, 107.5, 107.8, 113.9, 119.8, 132.8, 133.0, 136.4, 136.5, 154.2, 154.4, 156.8, 171.1; ES-MS m/z $[M+H]^+$ calcd 338.2, found 338.2. Elem. anal. for $C_{16}H_{20}FN_3O_4$ calcd: C 56.97, H 5.98, F 5.63, N 12.46; found: C 57.23, H 6.05, F 5.61, N 12.68.

7.[29] $[\alpha]_D^{20}$ = -34.4 (c 0.3, CH_3CN), lit. $[\alpha]_D^{25}$ = -36 (c 0.71, CH_3CN); ^{1}H NMR ($CDCl_3$) δ: 1.41 (s, 9H, tBu), 3.06 (t, J=4.8 Hz, 4H, morph$H_{3,5}$), 3.46-3.54 (m, 2H, CH_2N), 3.81 (dd, J=6.6, 9.0 Hz, 1H, OxdH_4), 3.87 (t, 4.8 Hz, 4H, morph$H_{2,6}$), 4.00 (dd, J=6.6, 9.0 Hz, 1H, OxdH_4), 4.74 (m, 1H, OxdH_5), 5.02 (br.t, 1H, BocNH), 6.94 (t, J=9.0 Hz, 1H, ArH_1), 7.09 (ddd, J=1.2, 2.8, 8.8 Hz, 1H, ArH_6), 7.44 (dd, J=2.8, 14.2 Hz, 1H, ArH_5); ^{13}C NMR ($CDCl_3$) δ: 28.2, 47.5, 51.0, 66.9, 72.0, 80.3, 107.4, 107.6, 113.9, 118.9, 119.0, 133.2, 133.3, 136.4, 154.3, 156.2, 156.7; ES-MS m/z $[M+H]^+$ calcd 396.2, found 396.2. Elem. anal. for $C_{19}H_{26}FN_3O_5$ calcd: C 57.71, H 6.63, F 4.80, N 10.63; found: C 57.98, H 6.62, F 4.91, N 10.89.

Synthesis of **1** via **7**. Compound **7** (0.40 g, 1.0 mmol) was treated with 1:3 TFA/DCM (5 mL) while stirring at r.t. After 15 min, the solution was evaporated at reduced pressure, and the residue underwent the same treatment. The crude residue was suspended in Et_2O (20 mL), and the precipitate was collected by centrifuge. A stirred suspension of the crude TFA salt was suspended in 5 mL of EtOAc and treated with Ac_2O (0.14 mL, 1.5 mmol) and TEA (0.28 mL, 2.0 mmol) at r.t. After 3 h, the mixture was diluted with EtOAc (40 mL), and washed with 0.1 M HCl (5 mL) and brine (5 mL). The organic layer was dried over Na_2SO_4, filtered, and concentrated at reduced pressure. The product 1 was isolated (0.33 g, 97%) by flash chromatography over silica gel (eluant: 75:25 cyclohexane/EtOAc).

7.4.3. Determination of the enantiomeric purity of the reported compounds.

Chiral HPLC analyses of rac-**1**/(*S*)-**1**, rac-**3a**/(*S*)-**3a**, rac-**3b**/(*S*)-**3b**, rac-**4a**/(*S*)-**4a**, rac-**4b**/(*S*)-**4b**, rac-**5**/(*S*)-**5**, rac-**7**/(*S*)-**7**, performed on an Agilent 1200 series apparatus, using a CHIRALPAK IC column (P/No 83325).
Column description: chiral stationary phase cellulose *tris*(3,5-dichlorophenylcarbamate) immobilized on silica, particle size 5 μm, lenght 250 mm, internal diameter 4.6 mm. Mobile phase: 1:1 *n*-hexane/2-propanol, at 0.8 mL min^{-1}. DAD 210/254 nm.

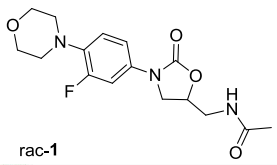

rac-**1**

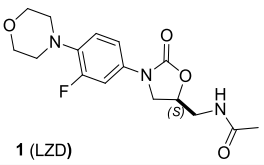

1 (LZD)

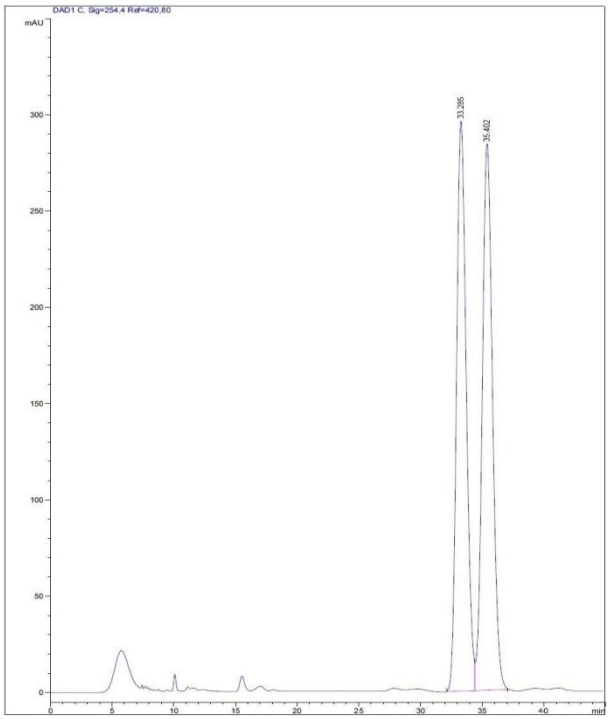
DAD1 C, Sig=254,4 Ref=420,80
mAU
33.265
36.402
min

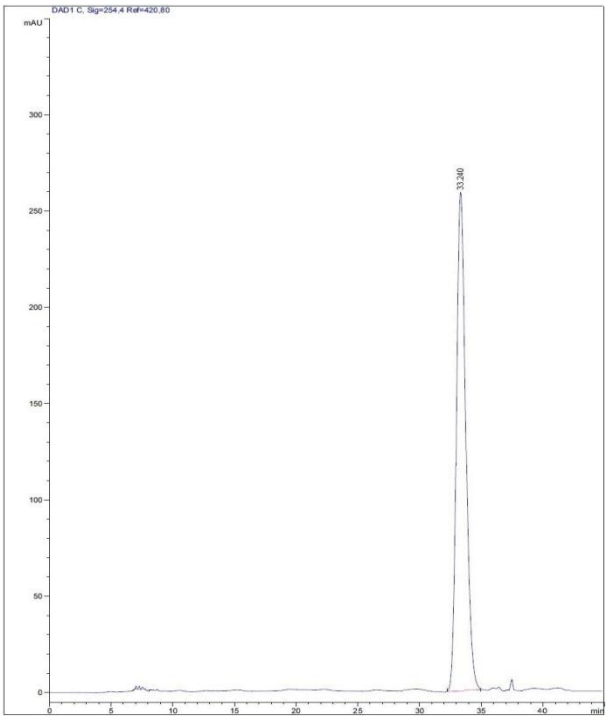
DAD1 C, Sig=254,4 Ref=420,80
mAU
33.240
min

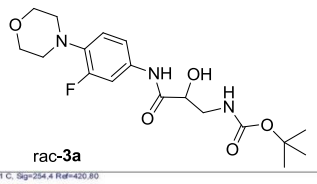

rac-**3a**

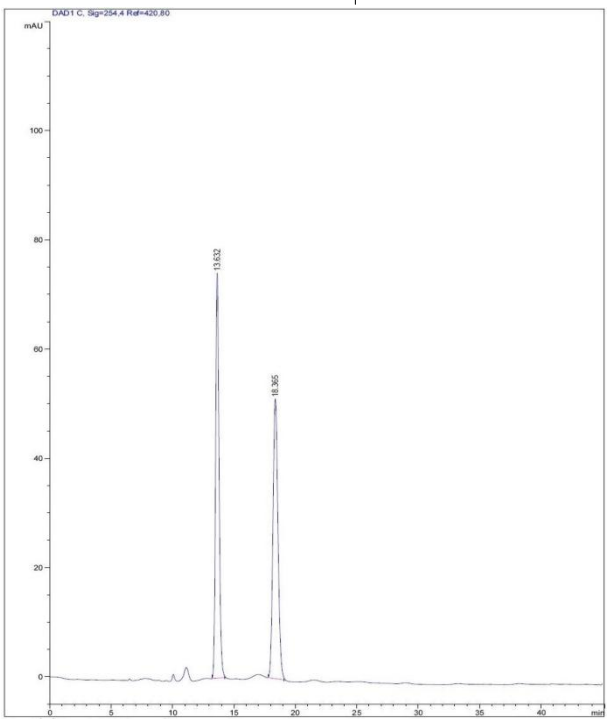

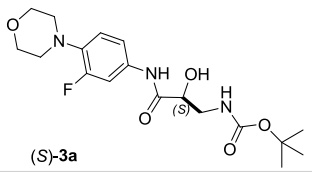

(*S*)-**3a**

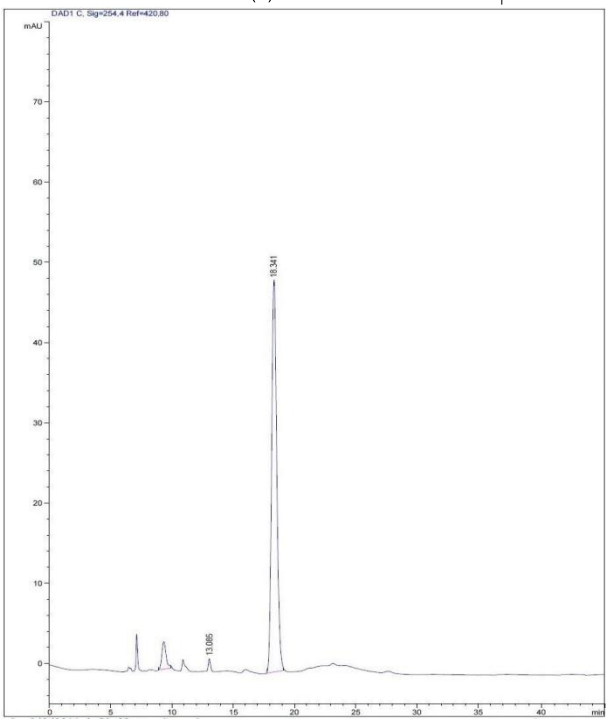

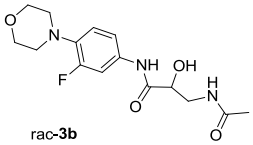

rac-**3b**

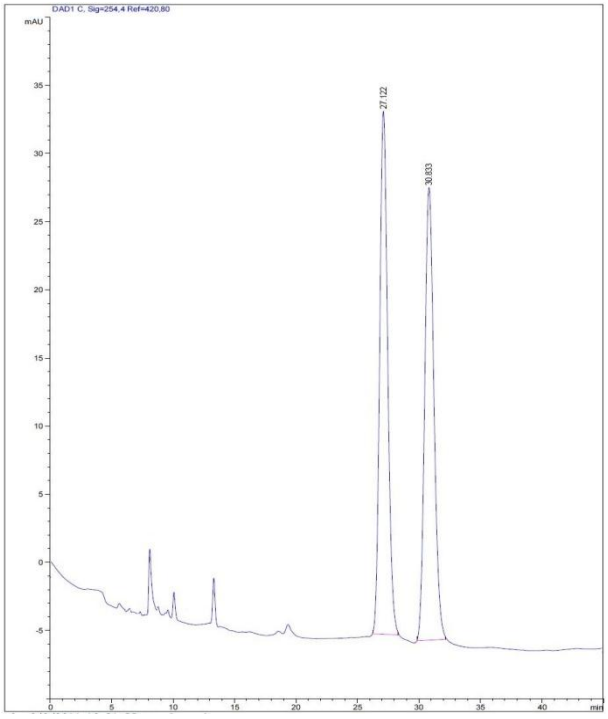

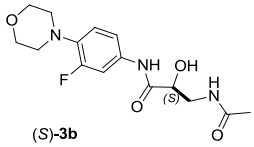

(*S*)-**3b**

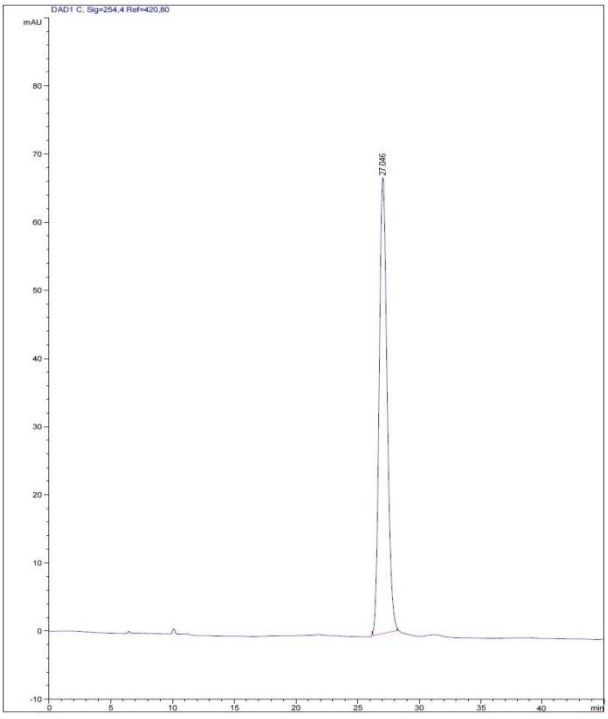

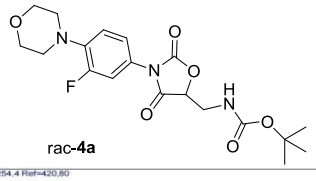

rac-**4a**

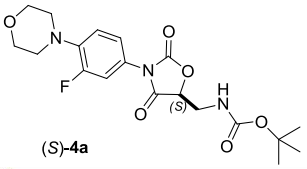

(*S*)-**4a**

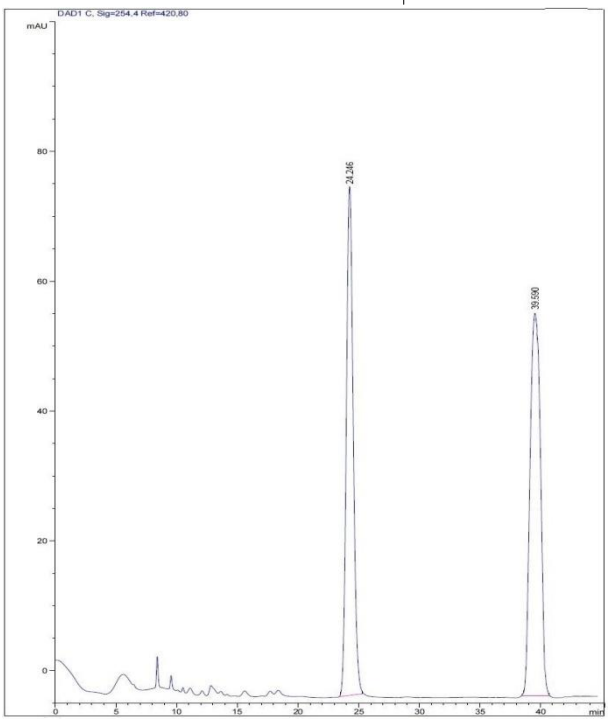

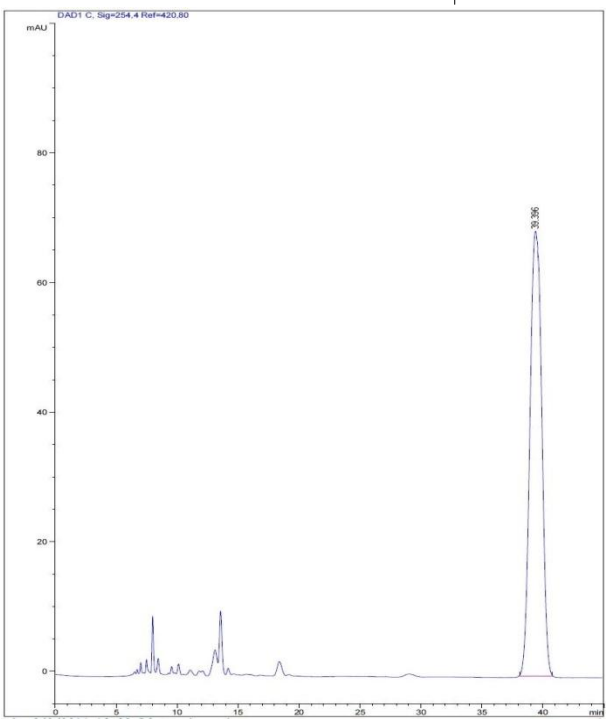

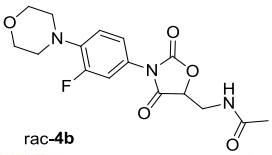

rac-**4b**

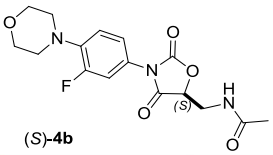

(*S*)-**4b**

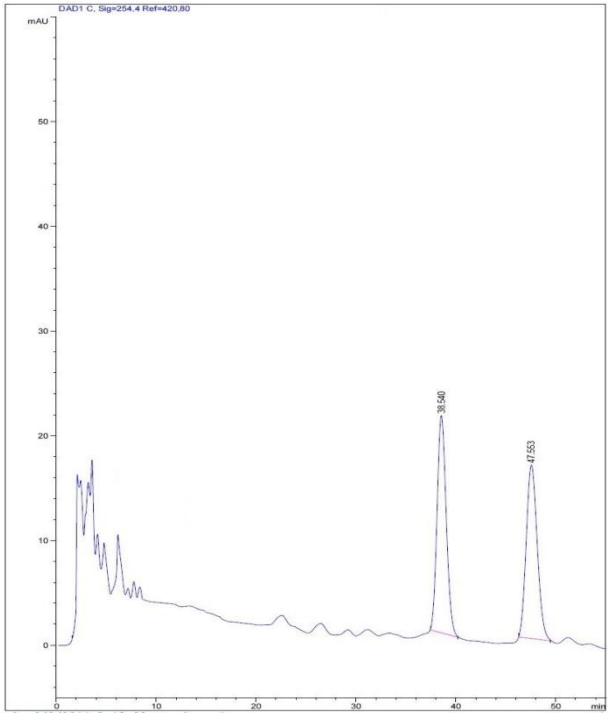

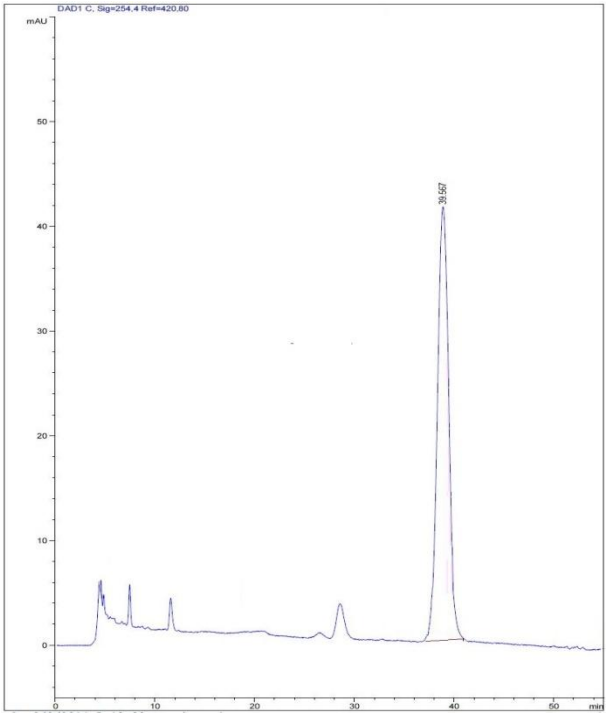

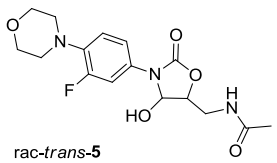

rac-*trans*-**5**

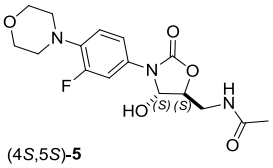

(4*S*,5*S*)-**5**

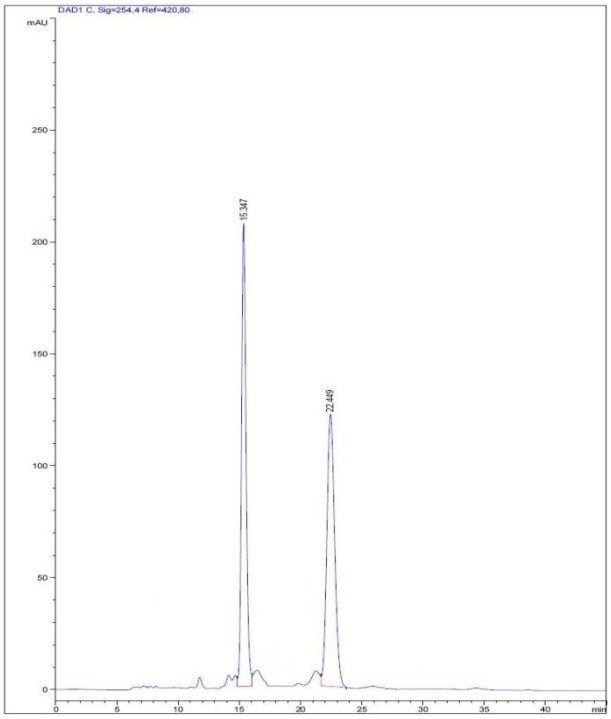

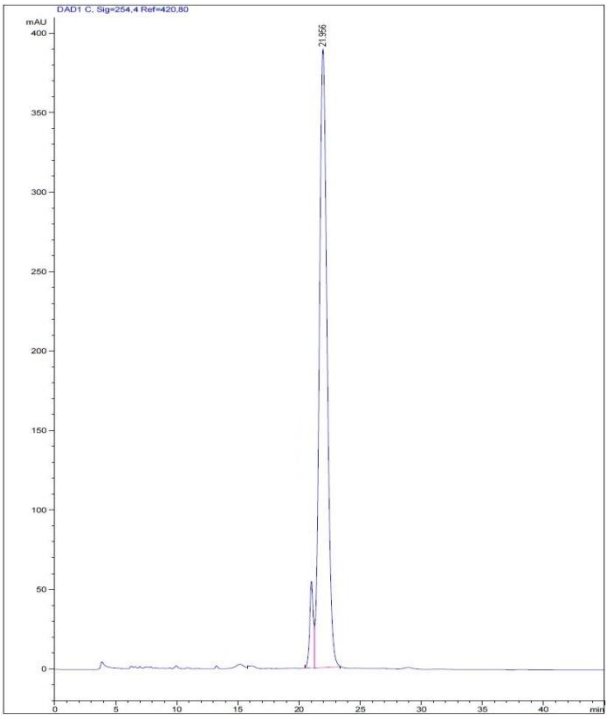

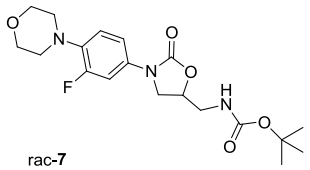

rac-**7**

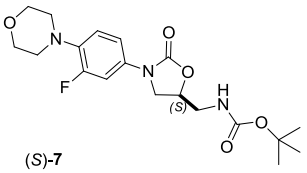

(*S*)-**7**

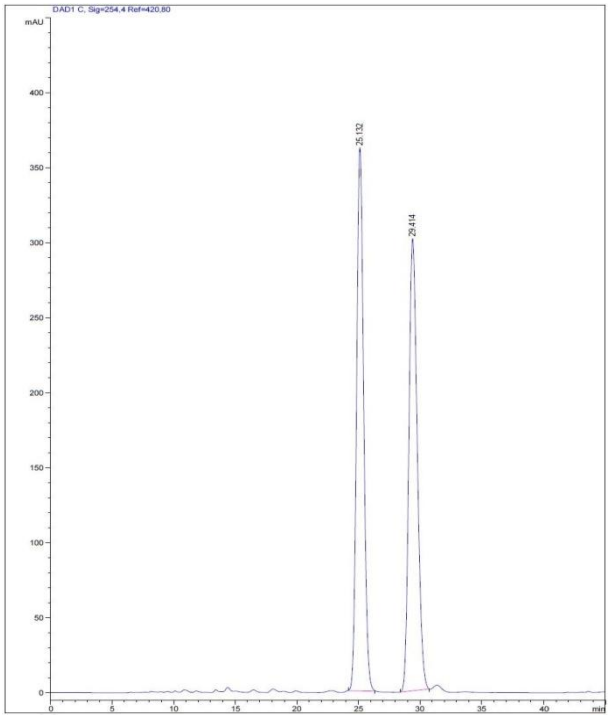

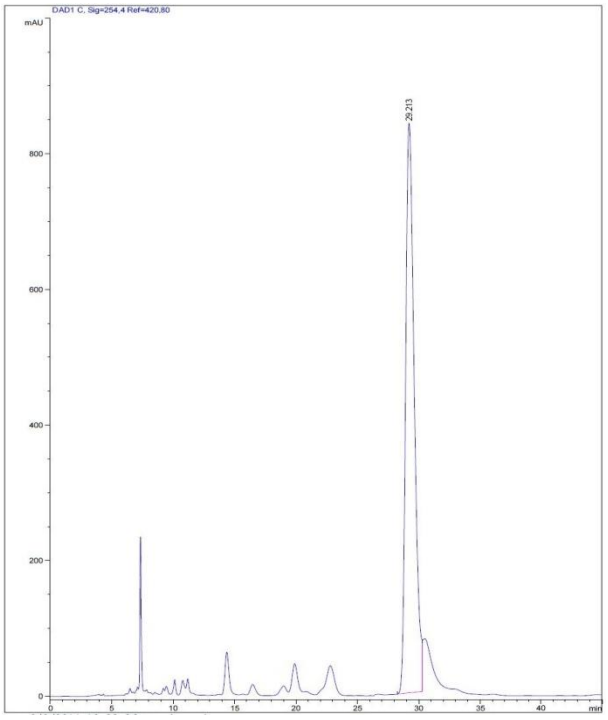

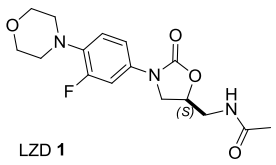

LZD **1**

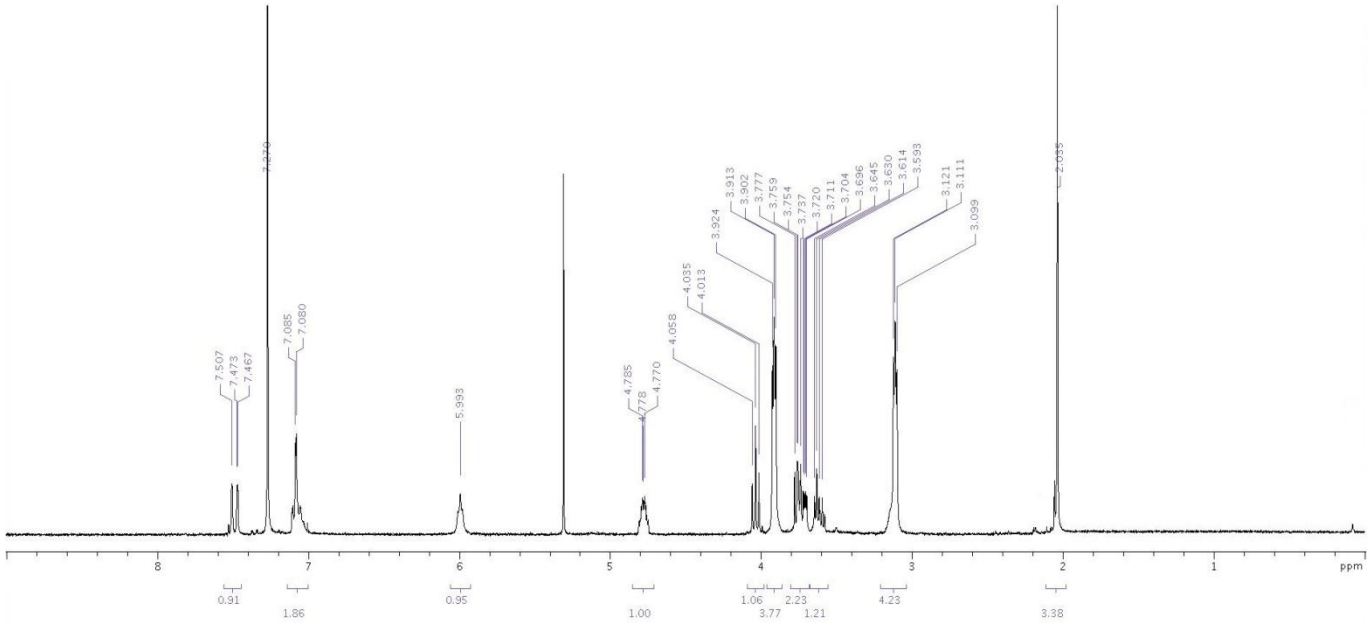
7.507
7.473
7.467
7.210
7.085
7.080
5.993
4.785
4.778
4.770
4.058
4.035
4.013
3.924
3.913
3.902
3.777
3.759
3.754
3.737
3.720
3.711
3.704
3.696
3.645
3.630
3.614
3.593
3.121
3.111
3.099
2.039
8
7
6
5
4
3
2
1
ppm
0.91
1.86
0.95
1.00
1.06
3.77
2.23
1.21
4.23
3.38

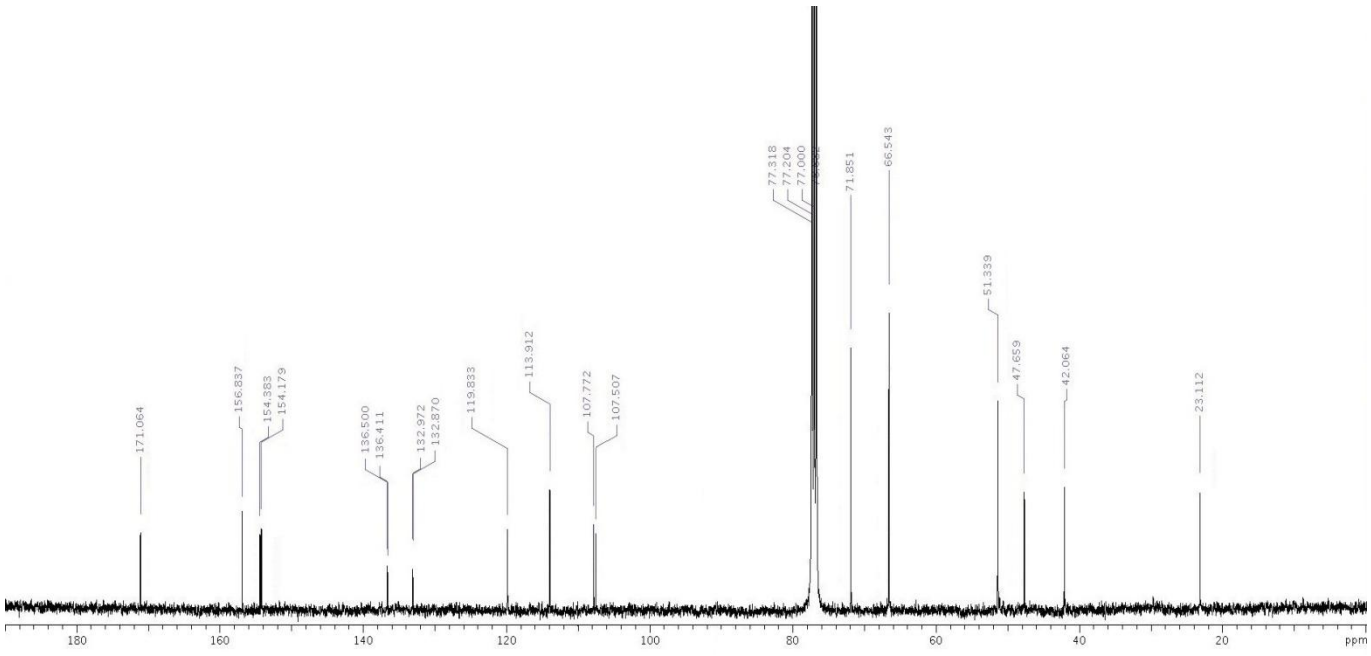
171.064
156.837
154.383
154.179
136.500
136.411
132.972
132.870
119.833
113.912
107.772
107.507
77.318
77.204
77.000
71.851
66.543
51.339
47.659
42.064
23.112
180
160
140
120
100
80
60
40
20
ppm

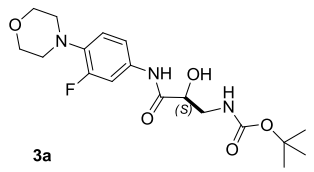
O
N
F
NH
OH
O
(S)
H
N
O
O

3a

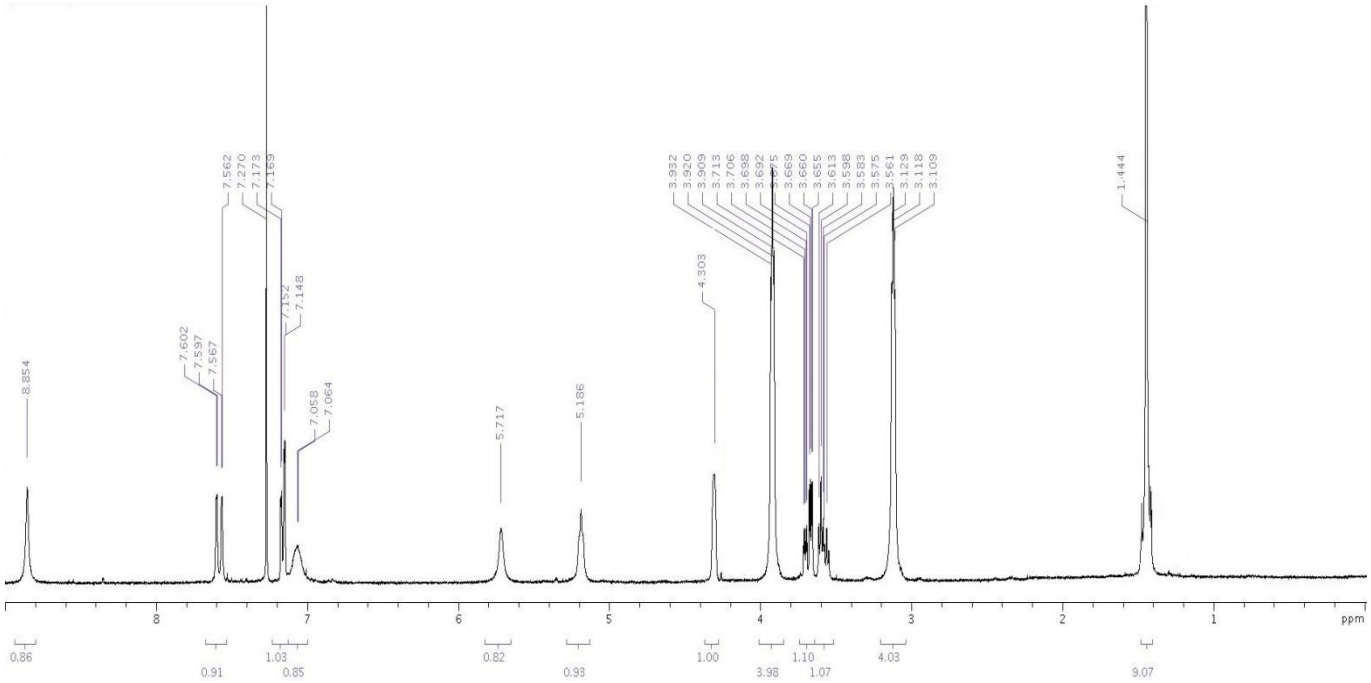
8.854
7.602
7.597
7.587
7.562
7.270
7.173
7.169
7.152
7.148
7.058
7.064
5.717
5.186
4.303
3.932
3.920
3.909
3.713
3.706
3.698
3.692
3.675
3.669
3.660
3.655
3.613
3.598
3.583
3.575
3.561
3.129
3.118
3.109
1.444
ppm
0.86
0.91
1.03
0.85
0.82
0.93
1.00
3.98
1.10
1.07
4.03
9.07

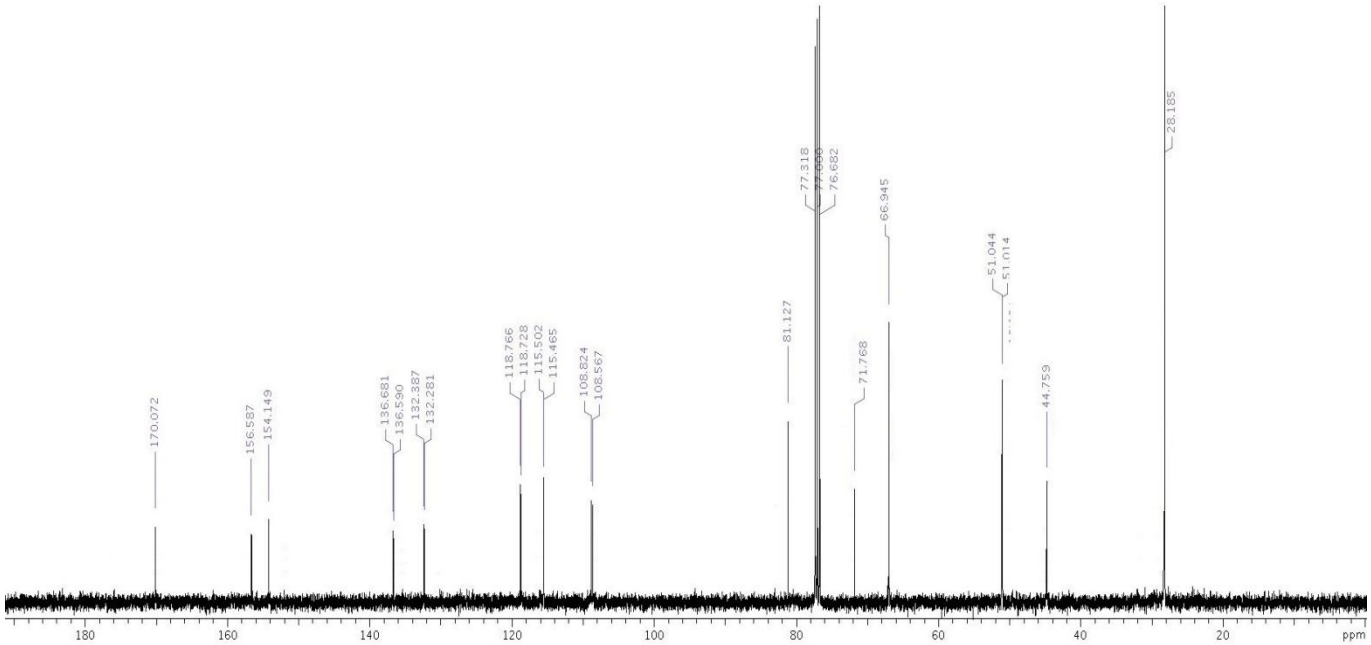
170.072
156.587
154.149
136.681
136.590
132.387
132.281
118.766
118.728
115.502
115.465
108.824
108.567
81.127
77.318
77.066
76.682
71.768
66.945
51.044
51.014
44.759
28.185
ppm

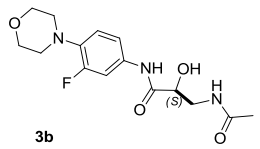
O
N
F
NH
OH
(S)
H
N
O
O

3b

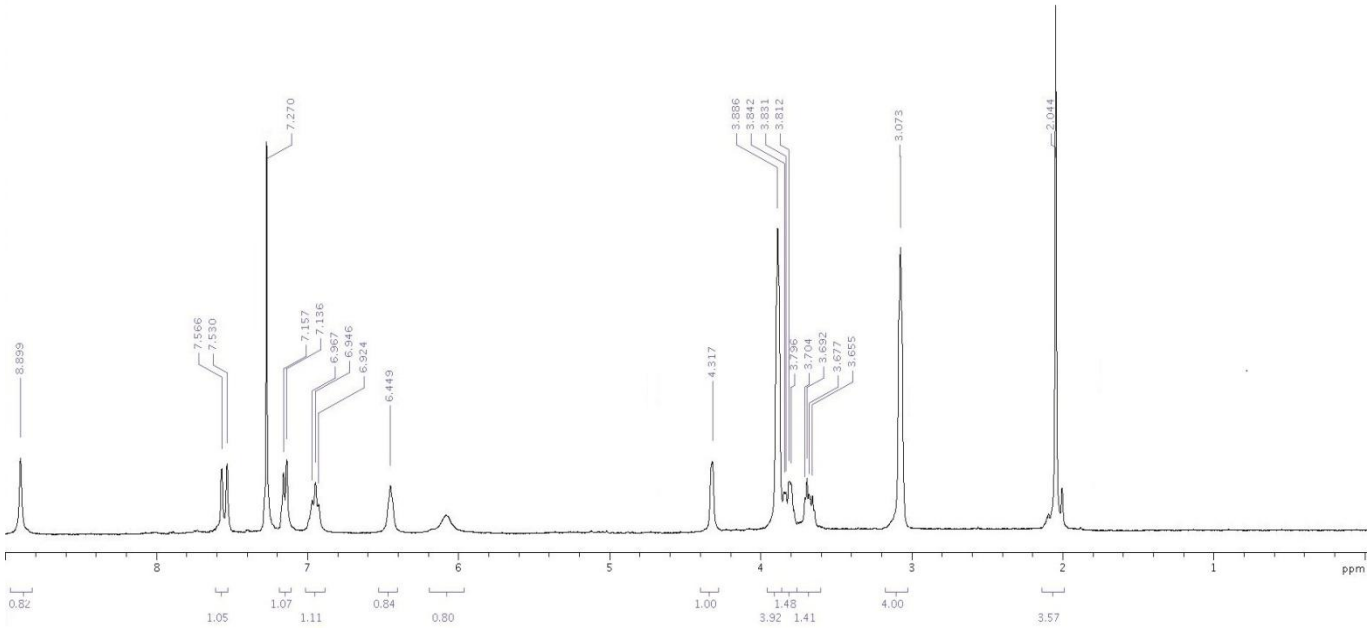
8.899
7.566
7.530
7.270
7.157
7.136
6.967
6.946
6.924
6.449
4.317
3.886
3.842
3.831
3.812
3.796
3.704
3.692
3.677
3.655
3.073
2.044
ppm
0.82
1.05
1.07
1.11
0.84
0.80
1.00
1.48
3.92
1.41
4.00
3.57

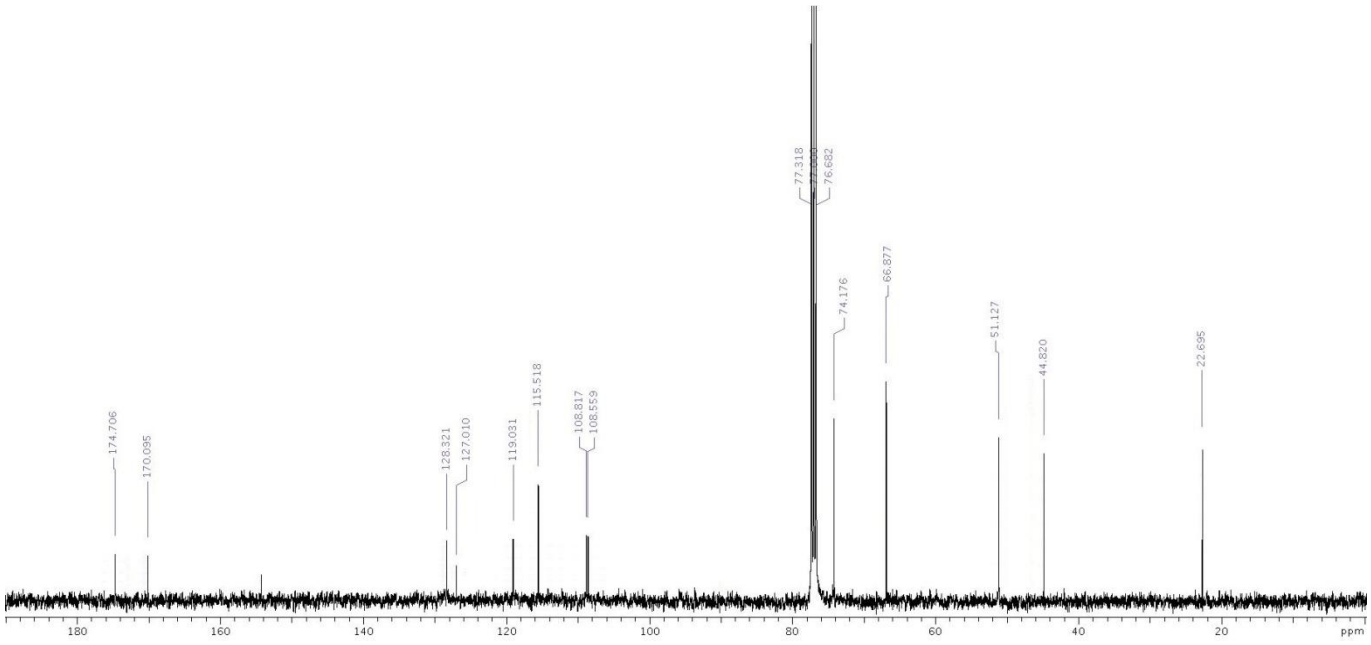
174.706
170.095
128.321
127.010
119.031
115.518
108.817
108.559
77.318
76.682
74.176
66.877
51.127
44.820
22.695
ppm

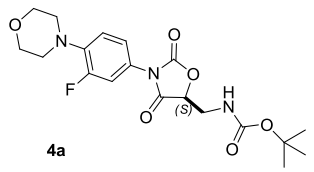

4a

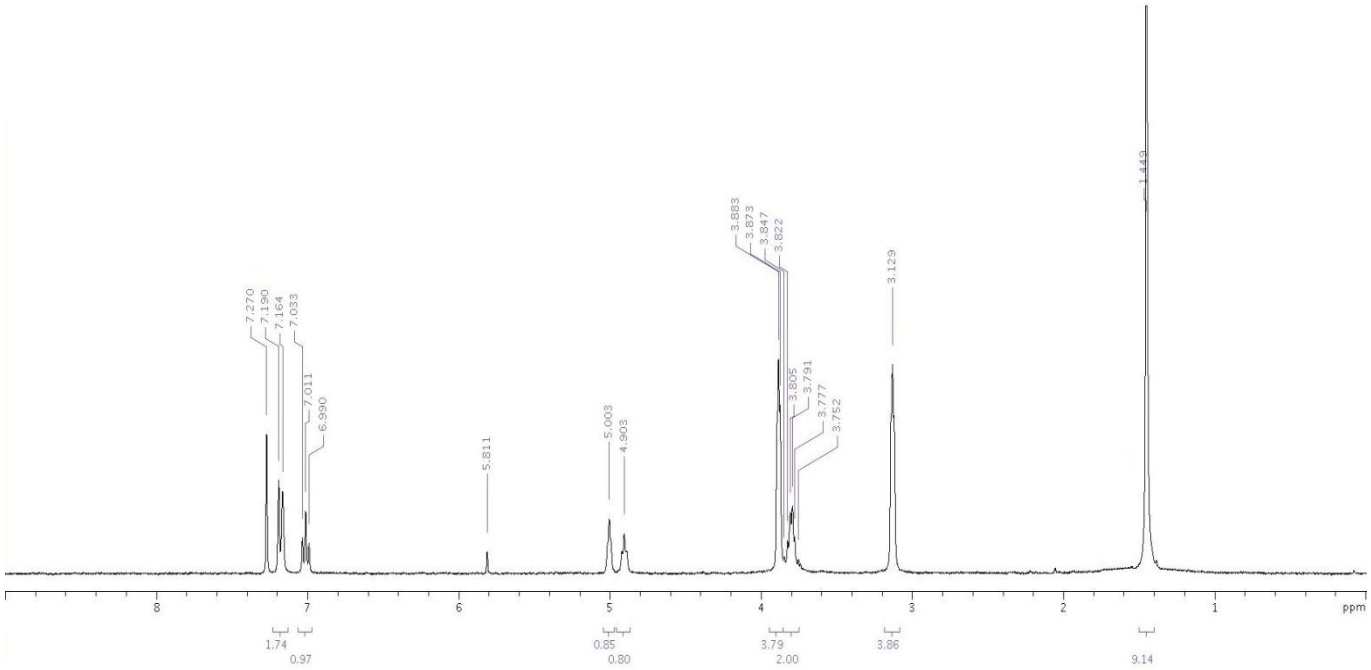
7.270
7.190
7.164
7.033
7.011
6.990
5.811
5.003
4.903
3.883
3.873
3.847
3.822
3.805
3.791
3.777
3.752
3.129
1.449
ppm
1.74
0.97
0.85
0.80
3.79
2.00
3.86
9.14

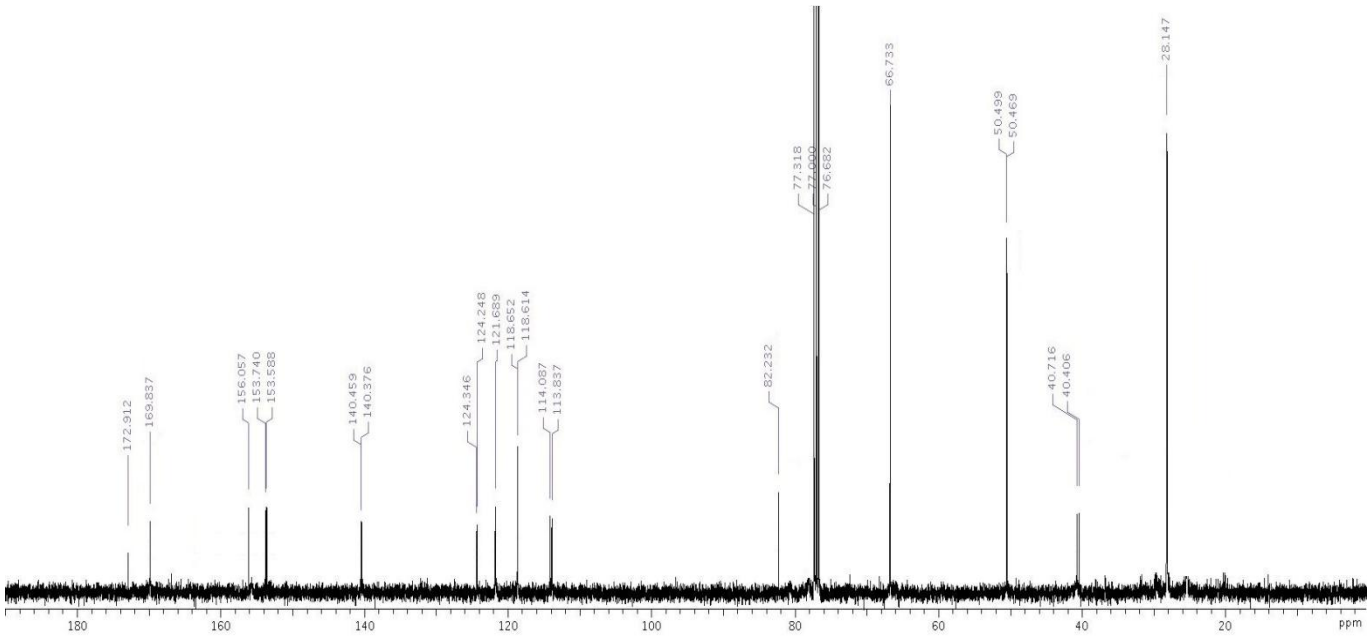
172.912
169.837
156.057
153.740
153.588
140.459
140.376
124.346
124.248
121.689
118.652
118.614
114.087
113.837
82.232
77.318
77.000
76.682
66.733
50.499
50.469
40.716
40.406
28.147
ppm

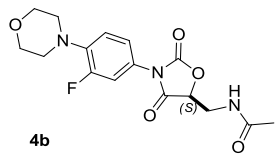

4b

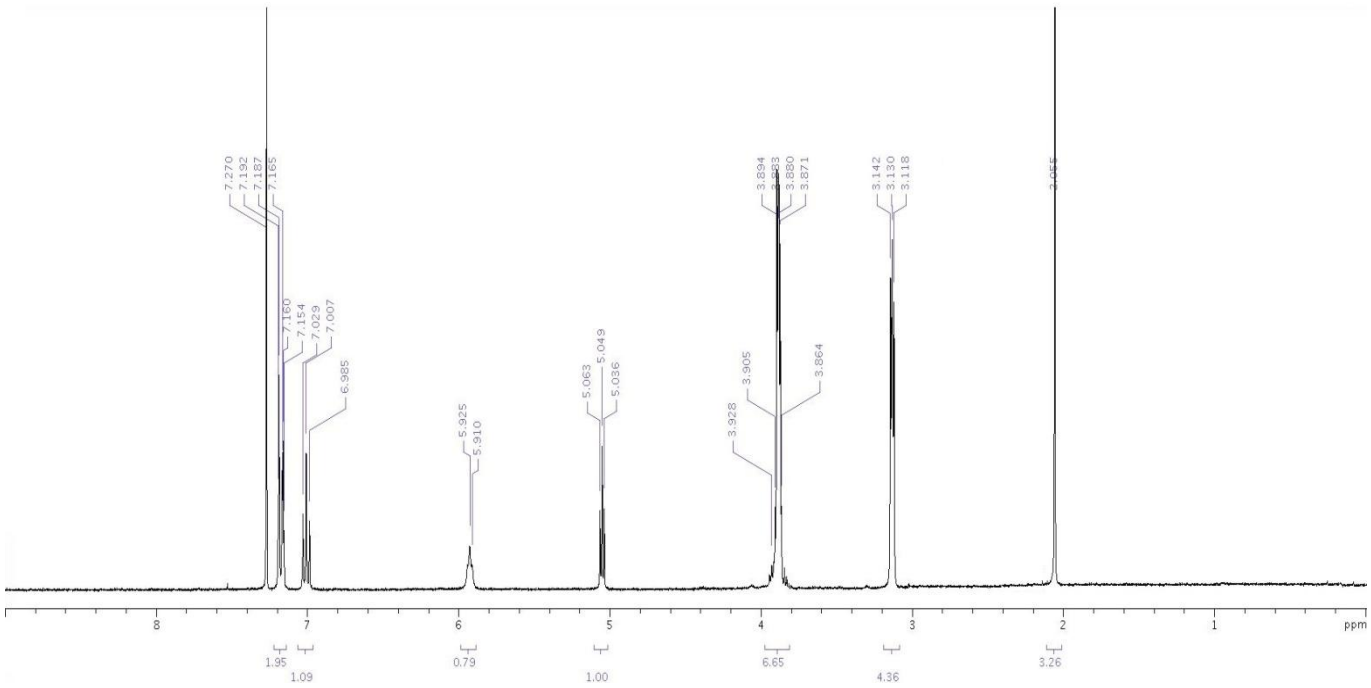
7.270
7.192
7.187
7.165
7.160
7.154
7.029
7.007
6.985
5.925
5.910
5.063
5.049
5.036
3.928
3.905
3.894
3.883
3.880
3.871
3.864
3.142
3.130
3.118
2.055
8
7
6
5
4
3
2
1
ppm
1.95
1.09
0.79
1.00
6.65
4.36
3.26

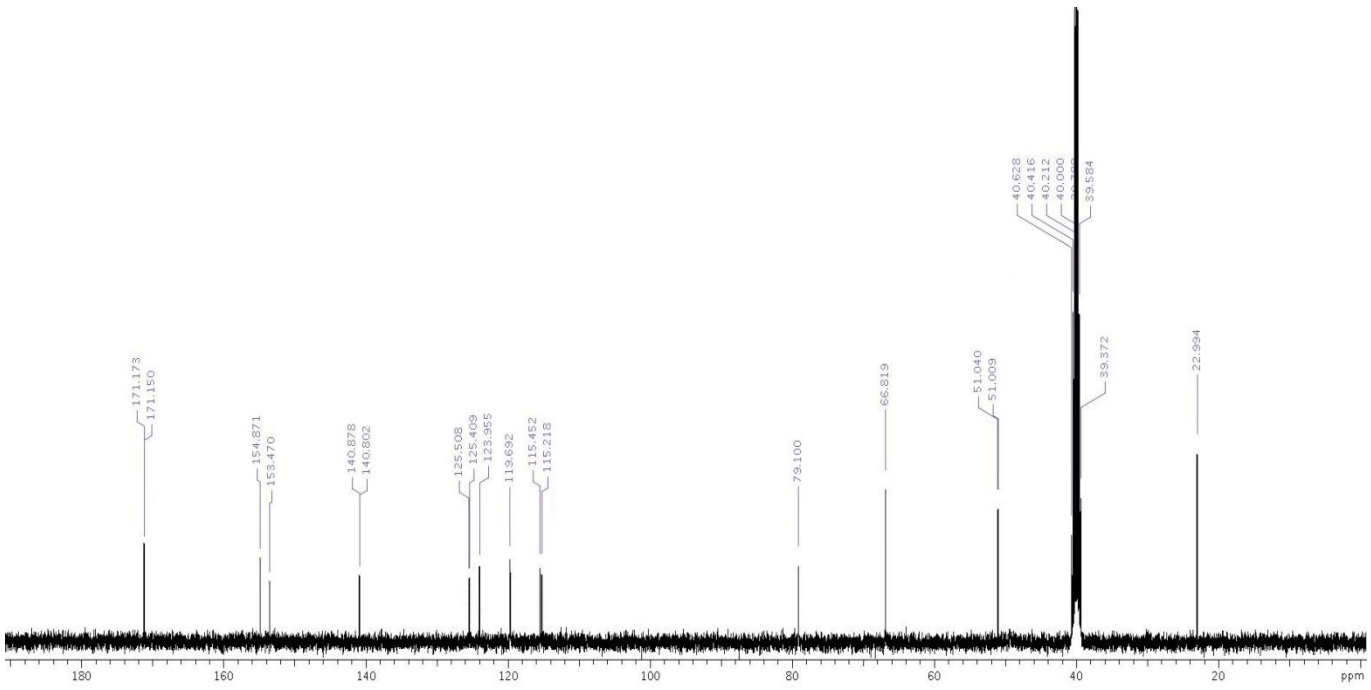
171.173
171.150
154.871
153.470
140.878
140.802
125.508
125.409
123.955
119.692
115.452
115.218
79.100
66.819
51.040
51.009
40.628
40.416
40.212
40.000
39.584
39.372
22.994
180
160
140
120
100
80
60
40
20
ppm

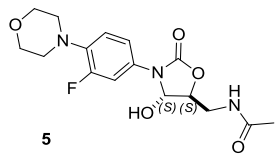

5

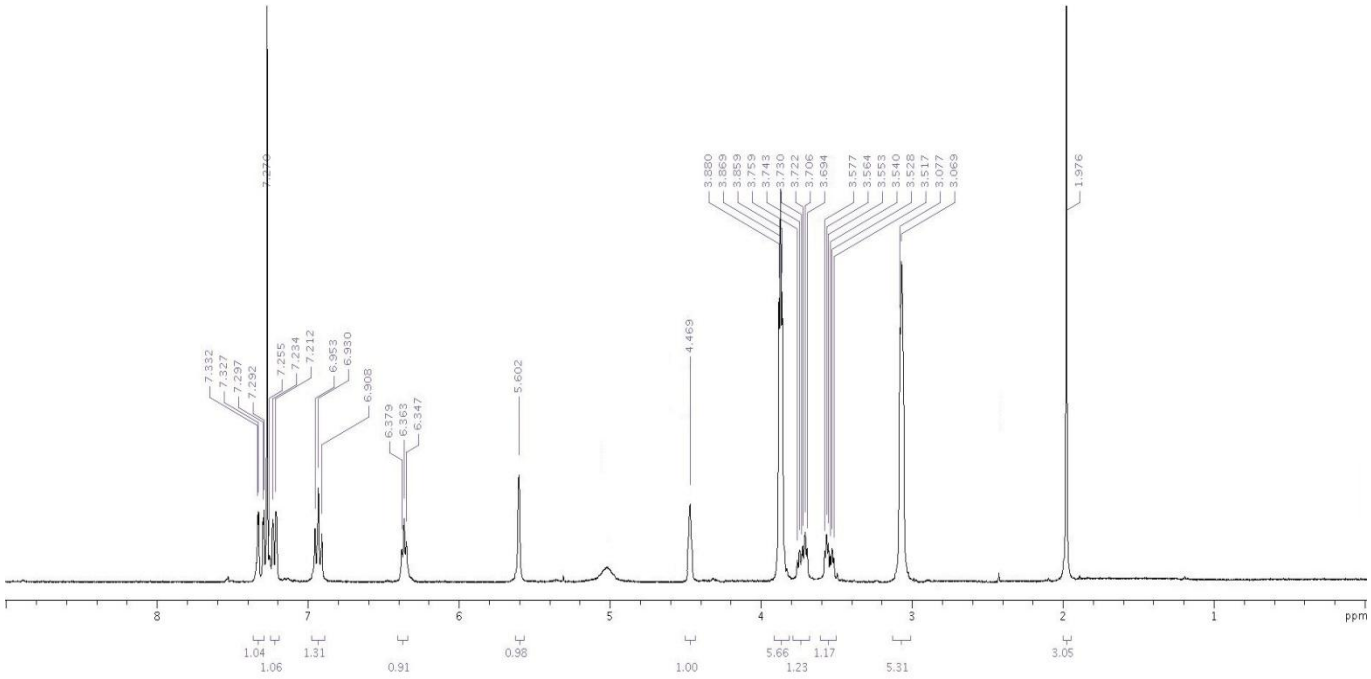
7.270
7.332
7.327
7.297
7.292
7.255
7.234
7.212
6.953
6.930
6.908
6.379
6.363
6.347
5.602
4.469
3.880
3.869
3.859
3.759
3.743
3.730
3.722
3.706
3.694
3.577
3.564
3.553
3.540
3.528
3.517
3.077
3.069
1.976
ppm
1.04
1.06
1.31
0.91
0.98
1.00
5.66
1.23
1.17
5.31
3.05

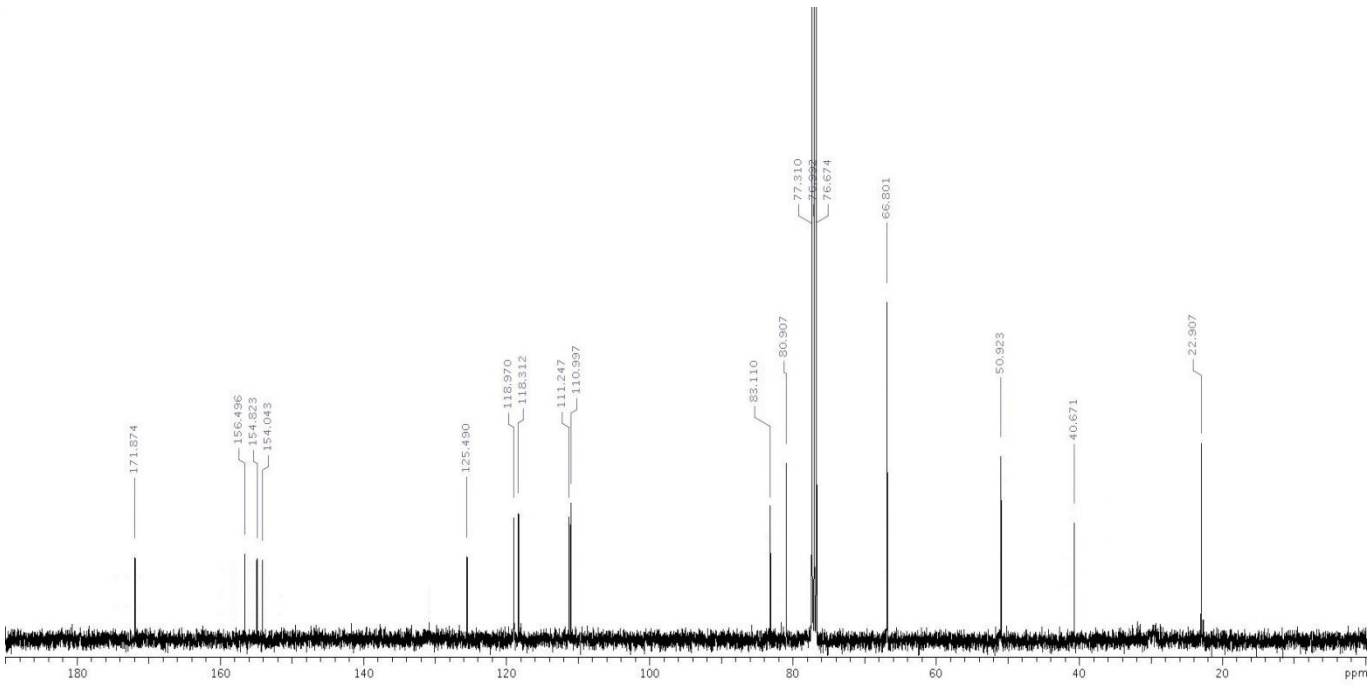
171.874
156.496
154.823
154.043
125.490
118.970
118.312
111.247
110.997
83.110
80.907
77.310
76.992
76.674
66.801
50.923
40.671
22.907
ppm

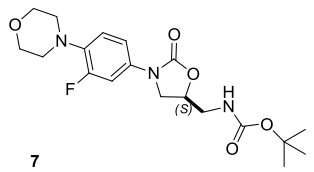

7

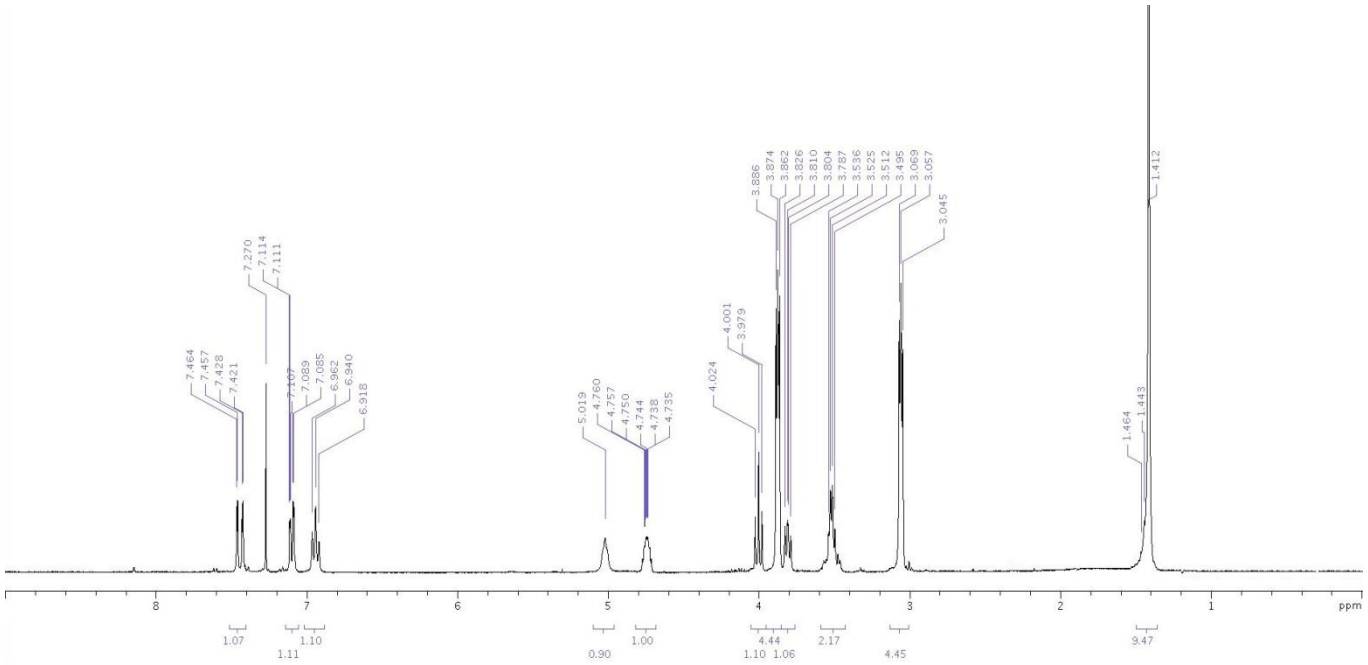
7.464
7.457
7.428
7.421
7.270
7.114
7.111
7.107
7.089
7.085
6.962
6.940
6.918
5.019
4.760
4.757
4.750
4.744
4.738
4.735
4.024
4.001
3.979
3.886
3.874
3.862
3.826
3.810
3.804
3.787
3.536
3.525
3.512
3.495
3.069
3.057
3.045
1.464
1.443
1.412
ppm
1.07
1.11
1.10
0.90
1.00
4.44
1.10
1.06
2.17
4.45
9.47

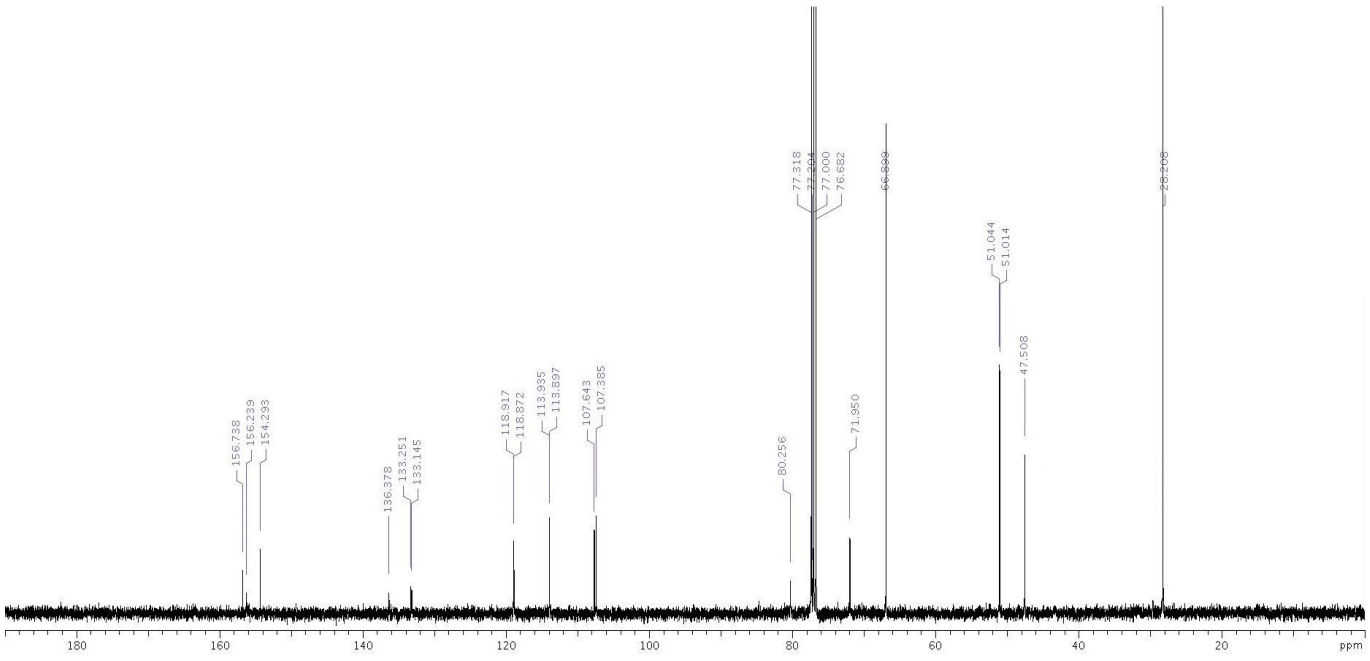
156.738
156.239
154.293
136.378
133.251
133.145
118.917
118.872
113.935
113.897
107.643
107.385
80.256
77.318
77.000
76.682
71.950
66.899
51.044
51.014
47.508
28.206
ppm

References

[1] World Health Organization 2014 , Antimicrobial resistance: global report on surveillance. http://www.who.int/drugresistance/documents/surveillancereport/en/

[2] a) J. M. Rolain, R. Canton, G. Cornaglia, *Clin. Microbiol. Infec.* **2012**, *18*, 615. b) M. S. Butler, M. A. Blaskovich, M. A. Cooper, *J. Antibiot.* **2013**, *66*, 571. c) J. Rybak, *Antimicrob. Agents Chemother*. **1998**, *42*, 721.

[3] M. R. Barbachyn, *Angew. Chem. Int. Ed.* **2003**, *42*, 2010.

[4] a) S. M. Swaney, H. Aoki, M. C. Ganoza, D. L. Shinabarger, *Antimicrob. Agents Chemother*. **1998**, *42*, 3251; b) D. N. Wilson, F. Schluenzen, J. M. Harms, A. L. Starosta, S. R. Connell, P. Fucini, *PNAS* **2008**, *105*, 13339; c) K. L. Leach, S. J. Brickner, *Ann. N.Y. Acad. Sci*. **2011**, *1222*, 49.

[5] M. Fines, R. Leclercq, *J. Antimicrob. Chemother*. **2000**, *45*, 797.

[6] a) K. S. Long, B. Vester, *Antimicrob. Agents Ch.* **2012**, *56*, 603. b) B. Gu, T. Kelesidis, S. Tsiodras, J. Hindler, R. M. Humphries, *J. Antimicrob. Chemother*. **2013**, *68*, 4.

[7] a) M. F. Gordeev, Z. Y. Yuan, *J. Med. Chem.* **2014**, *57*, 4487. b) A. R. Renslo, G. W. Luehr, M. F. Gordeev, *Bioorg. Med. Chem. Lett*. **2006**, *14*, 4227. c) K. Michalska, I. Karpiuk, M. Król, S. Tyski. *Bioorg. Med. Chem.* **2013**, *21*, 577.

[8] B. A. Pearlman, W. R. Perrault, M. R. Barbachyn, P. R. Manninen, D. S. Toops, D. J. Houser, T. J. Fleck (Upjohn), US5837870, **1998** [Chem. Abstr. 1998, 130, 25061].

[9] G. Madhusudhan, G. Om Reddy, T. Rajesh, J. Ramanatham, P. K. Dubey, *Tetrahedron Lett*. **2008**, *49*, 3060.

[10] G. Y. Xu, Y. Zhou, M. C. Xu, *Chin. Chem. Lett*. **2006**, *17*, 302.

[11] a) L. Song, X. Chen, S. Zhang, H. Zhang, P. Li, G. Luo, W. Liu, W. Duan, W. Wang, *Org. Lett*. **2008**, *10*, 5489. b) A. Palumbo Piccionello, P. Pierro, A. Accardo, S. Buscemia, A. Pace, *RSC Adv*. **2013**, *3*, 24946.

[12] A. Palumbo Piccionello, R. Musumeci, C. Cocuzza, C. G. Fortuna, A. Guarcello, P. Pierro, A. Pace, *Eur. J. Med. Chem*. **2012**, *50*, 441.

[13] a) L. Gentilucci, A. Tolomelli, R. De Marco, C. Tomasini, S. Feddersen, *Eur. J. Org. Chem.* **2011**, 4925. b) R. De Marco, A. Tolomelli, M. Campitiello, P. Rubini, L. Gentilucci, *Org. Biomol. Chem.* **2012**, *10*, 2307. c) R. De Marco, A. Greco, S. Rupiani, A. Tolomelli, C. Tomasini, S. Pieraccini, L. Gentilucci, *Org. Biomol. Chem.* **2013**, *11*, 4273.

[14] R. De Marco, L. Cavina, A. Greco, L. Gentilucci, *Amino Acids* **2014**, 46, 2823.

[15] a) G. Lelais, D. Seebach. *Biopolymers* **2004**, *76*, 206; b) *Enantioselective Synthesis of β-Amino Acids*, 2nd Ed., E. Juaristi, V. Soloshonok, Eds.; Wiley-VCH: New York, 2005.

[16] A. Greco, S. Tani, R. De Marco, L. Gentilucci, *Chem. Eur. J*. **2014**, *20*, 13390.

[17] a) Ö. Demir-Ordu, I. Doğan, *Chirality* **2010**, *22*, 641. b) G. Chen, C. Chunling Fu, S. Ma, *Org. Biomol. Chem*. **2011**, *9*, 105. c) S. Kano, T. Yokomatsu, H. Nemoto, S. Shibuya, *J. Am. Chem. Soc*. **1986**, *108*, 6746.

[18] Selected examples of commercially available isoserines: 3-phenylisoserine, isothreonine, 3-amino-2-hydroxy-2-methylpropanoic acid, 3-amino-2-hydroxy-4-methylpentanoic acid, 3-amino-2-hydroxy-4-phenylbutyric acid, 3-amino-2-hydroxy-5-methylhexanoic acid, 3-amino-2,4-dihydroxybutanoic acid, 3-amino-2-hydroxy-3-(4-hydroxyphenyl) propanoic acid, 3-amino-3-(3-fluoro-phenyl)-2-hydroxy-propionic acid.

[19] For some recent examples, see: a) J. E. Semple, T. D. Owens, K. Nguyen, O. E. Levy, *Org. Lett.* **2000**, *2*, 2769. b) Y. Aoyagi, R. P. Jain, R. M. Williams, *J. Am. Chem. Soc*. **2001**, *123*, 3472. c) F. Fringuelli, F. Pizzo, M. Rucci, L. Vaccaro, *J. Org. Chem*. **2003**, *68*, 7041. d) F. Gassa, A. Contini, G. Fontana, S. Pellegrino, M. L. Gelmi, *J. Org. Chem.* **2010**, *75*, 7099. e) Y. Jiang, X. Chen, Y. Zheng, Z. Xue, C. Shu, W.Yuan, X. Zhang, *Angew. Chem. Int. Ed*. **2011**, *50*, 7304. f) F. Rodriguez, F. Corzana, A. Avenoza, J. H. Busto, J. M. Peregrina, M. D. M. Zurbano, *Curr. Top. Med. Chem*. **2014**, *14*, 1225.

[20] C. Christensen, K. Juhl, R. G. Hazell, K. A. Jørgensen, *J. Org. Chem*. **2002**, *67*, 4875.

[21] R. Chidambaram, J. Zhu, K. Penmetsa, D. Kronenthala and J. Kant, *Tetrahedron Lett.* **2000**, *41*, 6017.

[22] A. Isidro-Llobet, M. Alvarez, F. Albericio, *Chem. Rev*. **2009**, *109*, 2455.

[23] a) T. Fukuyama, C. K. Jow, M. Cheung, *Tetrahedron Lett.* **1995**, *36*, 6373. b) G. Sabitha, B. V. S. Reddy, S. Abraham, J. S. Yadav, *Tetrahedron Lett*. **1999**, *40*, 1569-1570. c) T. Ankner, G. Hilmersson, *Org. Lett*. **2009**, *11*, 503.

[24] G. Zappia, E. Gacs-Baitz, G. Delle Monache, D. Misiti, L. Nevola, B. Botta, *Curr. Org. Synth.* **2007**, *4*, 81.

[25] S. Cutugno, G. Martelli, L. Negro, D. Savoia, *Eur. J. Org. Chem.*, **2001**, *3*, 517.

[26] J. B. Blanco-Canosa, P. E. Dawson, *Angew. Chem. Int. Ed*. **2008**, *120*, 6957.

[27] a) A. M. Smit, R. Whyman, *Chem. Rev*. **2014**, *114*, 5477. b) D. L. Dodds, D. J. Cole-Hamilton, *In Sustainable catalysis: challenges and practices for the pharmaceutical and fine chemical industries* (Eds.: P. J. Dunn, K. K. (Mimi) Hii, M. J. Krische), Wiley, **2013**, pp. 1-36. c) M. Stein, B. Breit, *Angew. Chem. Int. Ed.* **2013**, *52*, 2231. d) S. Das, D. Addis, S. Zhou, K. Junge, M. Beller, *J. Am. Chem. Soc.*, **2010**, *132*, 1770.

[28] Z. Luo, M. Naguib, *Tetrahedron Lett.* **2012**, 53, 3316.

[29] W. R. Perrault, B. A. Pearlman, D. B. Godrej, A. Jeganathan, K. Yamagata, J. J. Chen, C. V. Lu, P. M. Herrinton, R. C. Gadwood, L. Chan, M. A. Lyster, M. T. Maloney, J. A. Moeslein, M. L. Greene, M. R. Barbachyn, *Org. Process Res. Dev*. **2003**, *7*, 533.

[30] M. R. Barbachyn. *Angew. Chem. Int. Ed.* **2003**, *42*, 2010.

[31] R. Chidambaram, J. Zhu, K. Penmetsa, D. Kronenthal J. Kant. *Tetr. Lett.* **2000**, *41*, 6017.

Chapter 8

Synthesis and biological assay of retroinverse-$\alpha_4\beta_1$ integrin antagonists

In recent years, several research groups proposed new peptidomimetic antagonists of integrins αvβ3, α5β1, αIIbβ3, αvβ6, αvβ5, etc. based on retro-sequences of the classic integrin-binding motif RGD. The retro-strategy is still largely ignored for the non-RGD-binding α4β1 integrin. Herein is presented the first examples of retro-sequences for targeting this integrin, composed of Asp or *iso*Asp equipped with an aromatic cap at the *N*-terminus, (*S*)-pyrrolidine-3-carboxylic acid (β^2-Pro) as a constrained core, and the amino variant (AMPUMP) of the well known α4-targeting diphenylurea MPUPA. Moreover, it is discussed α4β1 receptor affinity (SPA), cell adhesion assays, stability in mouse serum, and conformational analysis. For their significant ability to inhibit cell adhesion and remarkable stability, the retro-peptide mimetics BnCO-Asp-β-Pro-AMPUMP (**3**) and BnCO-*iso*Asp-β-Pro-AMPUMP (**4**) represent promising candidates for designing small molecules as potential anti-inflammatory agents.

8.1. Introduction

The integrin α4β1 (VLA-4, very late activation antigen-4, CD49d/CD29) is a cell surface receptor expressed on lymphocytes (and also on monocytes, eosinophils, basophils, macrophages), that mediates cellular adhesion events crucial to leukocyte trafficking and activation during inflammatory processes.[1,2] If the condition becomes chronic, there can be a sustained extravasation of lymphocytes that can exacerbate the inflammatory condition, which in turn will continue to recruit more inflammatory cells resulting in tissue destruction.

Their involvement in disease processes prompted several pharmaceutical companies to pursue α4 integrin antagonists as potential anti-inflammatory agents.[3] Monoclonal α4 integrin antibodies have been shown to be modulators in animal models for auto-inflammatory diseases such as asthma, rheumatoid arthritis, and inflammatory bowel diseases.[4,5] The humanized monoclonal antibody Natalizumab has been approved for multiple sclerosis.[5] However, the inherent limitations of antibody therapy, high cost, potential immunogenicity, and the requirement for intravenous administration, strongly spurred efforts to develop small molecule antagonists.

The primary ligands of α4β1 integrin are vascular cell adhesion molecule (VCAM), and the extracellular matrix (ECM) protein fibronectin (FN). Their integrin binding sites contain a critical aspartic acid located within a highly conserved tripeptide sequences, Ile-Asp-Ser (IDS) in VCAM and Leu-Asp-Val (LDV) in FN.[6,7] Consequently, peptidomimetics and non-peptide mimetics of the recognition sequences can effectively inhibit the integrin.[6,7] For instance, the combination of a LDVP sequence and *N*-terminal *o*-methylphenylureaphenylacetyl group (MPUPA) lead to the potent selective BIO1211 (MPUPA-LDVP-OH **1**, Table 1).[8,9,10] However, the residual peptidic nature of **1** and related compounds resulted in rapid enzymatic hydrolysis[11,12] and clearance in vivo.[13] Among the non-peptides, the *N*-(2,6-diclorobenzoyl)-2,6-dimethoxy biphenylalanine TR-14035 was highlighted as a non-specific α4 integrin antagonist.[14] In general, the large majority of the peptidomimetic compounds share common structural features: a α4-targeting aromatic cap at the *N*-terminus (eventually an aromatic urea such as MPUPA), a suitable spacer, and a β-carboxylate mimetic of Asp.[6,7]

In search for new lead structures, the similarities between the different types of integrins prompted several research groups to test the Arg-Gly-Asp (RGD) sequence for inhibition of α4β1. This epitope, discovered several years earlier, was found on numerous ECM proteins, collagen, fibrinogen, vitronectin (VT), and FN, and was known to interact with several integrins, including αvβ3, α5β1, αIIbβ3, etc.[15] Mould et al. described the ability of peptide GRGDS and homologues to inhibit the interaction of α4β1 with the alternatively spliced type III connecting segment (IIICS) region of fibronectin,[16] and Cardarelli et al. provided evidence that RGD-containing cyclopeptide 1-adamantaneacetyl-CGRGDSPC(S-S)[17] was a inhibitor of cell adhesion mediated by α4β1. Also, Nowlin, Cardarelli, et al. showed that the RCD-containing cyclic peptide RCD(ThioP)C(S-S) inhibited α4β1 and α5β1 integrin-mediated cell adhesion,[18] and Jackson et al. observed that cyclic eptides containing RCD blocked the interaction of α4β1with VCAM-1.[19] Using atomic force microscopy measurement of monocyte-endothelial cell interaction, Elitok et al. demonstrated that a cRGD peptide inhibited their adhesion through α4β1-VCAM-1, resulting in the inhibition of monocyte/macrophage infiltration.[20]

Albeit the α4β1 receptor was not definitively documented to interact RGD peptides with high affinity, these results suggest that the strategies successfully developed for designing a variety of RGD-derived analogues[21,22] could

potentially be used to identify new α4β1 antagonists.[6,7] In this respect, we sought to investigate the opportunity to design retro sequences of the common MPUPA-spacer-Asp peptidomimetic binding-motif (see above) of the integrin α4β1 as potential antagonists. In the last few years, the use of retro-sequences of the classic RGD binding motif for αvβ3 and α5β1-integrin has became popular. Initially, Kessler et al. investigated the biological activity of retro (DGR), inverso (rGd), retro-inverso (dGr) analogues (plus their stereoisomers) of the selective and superactive αvβ3 integrin inhibitor c[RGDfV].[23] Some years later, we proposed cyclopeptides containing the partially modified retro Arg-Gly-Asp sequence ψ(NHCO)Aspψ-(NHCO)Gly-Arg.[24] Novellino, Kessler, et al., grafted the *iso*DGR motif onto c[phg-*iso*DGRG], achieving activity enhancement toward α5β1 integrin;[25,26] further, selectivity toward FN-binding integrins α5β1 and αvβ6 over VT-binding integrins αvβ3 and αvβ5 was improved changing the flanking amino acids.[26]
Some researchers have proposed that deamidation of the Asn-Gly-Arg (NGR) motif in FN into *iso*DGR might result in a gain of protein function by creating a new adhesion binding site for integrins.[27,28] However, this hypothesis was questioned in a report using recombinant FN with mutations in the NGR motif.[29] Later investigations suggested that the *iso*DGR sequence can fit into the RGD-binding pocket of integrin, establishing the same electrostatic clamp as well as additional polar interactions.[30,31,32]
These considerations prompted us to transfer the retro strategy into peptidomimetic sequences showing Asp or *iso*Asp, a central spacer, and the amino variant 1-(4-(aminomethyl)phenyl)-3-(*o*-methylphenyl)urea (AMPUMP) of the well-known α4-targeting MPUPA, giving the retro sequences Asp-spacer-AMPUMP, and *iso*Asp-spacer-AMPUMP.[6,7,8,9,10]

8.2. Results and discussion

8.2.1. Design and synthesis

The structures of the peptidomimetics **2-6** (Table 1) were designed on the basis of the models developed by 3D-QSAR analysis of large libraries of compounds containing diphenylureas such as MPUPA, or other substituted aromatic groups.[13,33,34] 3D geometries of plausible candidates were screened prior to synthesis by molecular modeling;[35] Figure 1 shows the bioactive geometries and structures of the prototypic model compounds **7**[13,36] and **8**.[2,33] This selection led to the retro sequences Asp-β^2-Pro-AMPUMP **3** and **5**, and *iso*Asp-β^2-Pro-AMPUMP **4** and **6** (β^2-Pro, (*S*)-pyrrolidine-3-carboxylic acid). The straight sequence MPUPA-β^2-Pro-Asp **2** was considered for comparison, and BIO1211 (MPUPA-Leu-Asp-Val-Pro-OH, **1**) was chosen as α4β1 integrin antagonist reference compound.

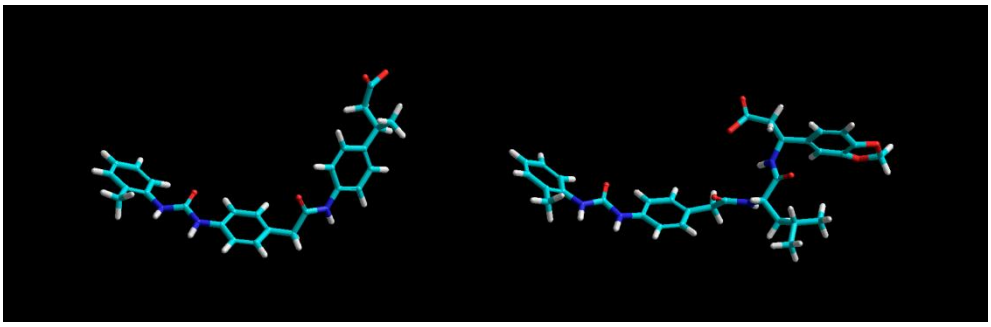

7 8

Figure 1. Structures of the model compounds **7** (and top, left) and **8** (and top, right) as reported in the literature.

The sequences **2-6** were assembled by connecting β^2-Pro to MPUPA or AMPUMP. The β^2-Pro core was chosen to increase peptide stability,[37] and for the conformational control exerted on the overall structure.[38,39,40,41] Further, we took advantage of our previous experience in the use of β^2-Pro or equivalent heterocycles[42] for preparing highly stable peptidomimetics,[43] including highly active integrin ligands.[44] Asp and *iso*Asp were equipped with aromatic substituents; it is well known that the presence of an aromatic moiety adjacent to Asp can favor integrin binding.[6,7] The compounds **3** and **4** show a phenylacetyl *N*-cap (BnCO), while **5** and **6** include the *N*-2,6-dicholorobenzoyl group, which was shown to efficiently bind to the β1-subunit, [45] and is present in many ligands, including TR-14035.[6,7,14]

After synthesis and bioassay, the coherence of the most active compounds with the geometries of the 3D-QSAR models was confirmed by 2D ROESY and molecular dynamics (see Experimental section).

As a representative example, the preparation of the BnCO-*iso*Asp-β^2-Pro-AMPUMP sequence **4** is described in Scheme 1; for the details on the intermediates, see Experimental section. Fmoc-Asp(O*t*-Bu)-OH was treated with BnBr, giving **9**, and Fmoc was replaced with the phanylacetyl group *via* **10**. The resulting fully protected Asp **11** was treated with TFA giving **12**. In parallel, Boc-4-(aminomethyl)aniline was treated with 2-methylbenzene isocyanate affording Boc-AMPUMP **13**. This was treated with TFA, and resulting AMPUMP **14** was coupled with Boc-β-Pro-OH in solution under MW irradiation and in the presence of HOBt/HBTU/DIPEA, giving **15**. Boc deprotection was followed by coupling with **12** under the same conditions as before. The resulting **17** was deprotected by catalytic hydrogenation, giving **4** in very good yield. The strategies for the syntheses of the remaining compounds are given in Experimental section. The products were purified (96-98%) by semi-preparative reversed-phase (RP) HPLC.

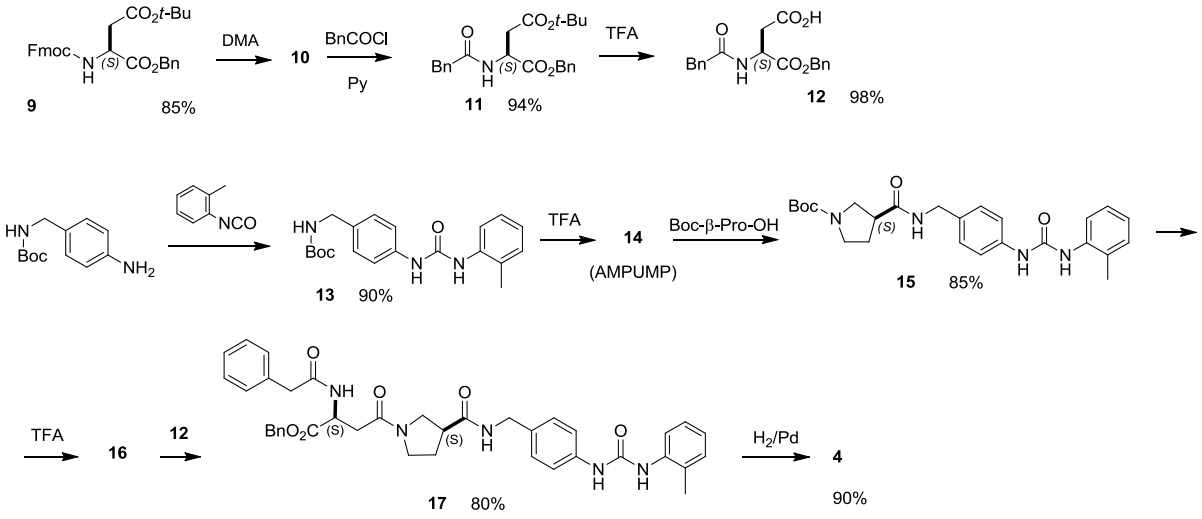

Scheme 1. Synthesis of BnCO-*iso*Asp-β^2-Pro-AMPUMP (**4**).

8.2.2. Scintillation proximity-binding assay

The binding of the peptidomimetics **1**-**6** to α4β1 integrin was measured by (SPA), using Jurkat cells stably expressing human α4 integrin, and ^{125}I-FN as the specific radioligand.[46,47] Western blot analysis of the α4β1 integrin, extracted from cell lysate and purified by chromatography, confirmed that both α4 and β1 integrin subunits were present in the eluate employed for the test (Experimental section).

Table 1. SPA binding to bead-associated α4β1 integrin and inhibition of Jurkat cell adhesion of BIO1211 (**1**) and compounds **2**-**6**.[a]

	structure	Purity (%)[b]	m/z [M+1] vs calcd	SPA IC50 (nM)	SPA Ki (nM)	α4β1/VCAM-1 IC50 (nM)	αvβ3/VT IC50 (nM)
1	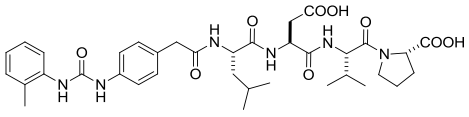	-		4.80±2.4	1.50±0.37	7.60±3.0	-
2	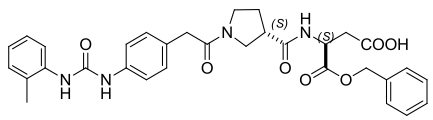	96	587.2/ 587.2	>10^5	>10^5	>10^5	-
3	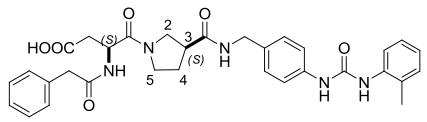	98	586.2/ 586.3	100±40	60±10	80±10	>10^5

4	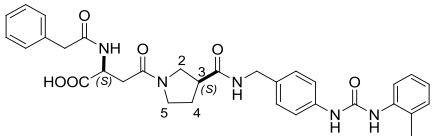	97	586.1/ 586.3	290±20	180±40	93±10	$>10^5$
5	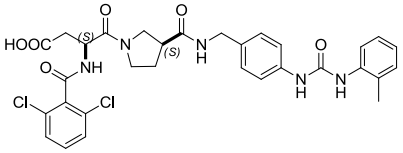	96	640.1/ 640.2	3.90±0.54 10^3	2.4±0.25 10^3	$>10^5$	-
6	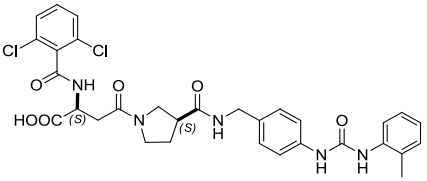	96	640.1/ 640.2	$>10^5$	$>10^5$	$>10^5$	-

[a] Mean of four determinations ± SE. [b] Determined by analytical RP-HPLC; see Materials and instruments

Specific binding of ^{125}I-FN to an antibody-captured α4 and β1 integrin was time-dependent; the signal reached a plateau in 10 h and remained constant for the rest of the 24 h incubation (Experimental section). The relatively slow kinetics of the SPA may require the establishment of equilibrium between the different components.[46,47] ^{125}I-FN specific binding to the SPA bead-associated α4β1 integrin, measured after overnight incubation, was inhibited in a concentration-dependent manner by BIO1211, MPUMP-Leu-Asp-Val-Pro-OH (**1**), with IC_{50} and Ki values of 4.8 and 1.5 nM, respectively (Table 1). Furthermore, ^{125}I-FN selective binding was blocked by an anti-human α4 integrin antibody (5 mg/tube) to capture the integrin complex (data not shown).

The straight sequence MPUMP-β^2-Pro-Asp-OBn **2** was not able to inhibit ^{125}I-FN binding. On the contrary, the retro compounds **3-5** caused concentration-dependent inhibition of ^{125}I-FN binding (Table 1). The sequence BnCO-Asp-β^2-Pro-AMPUMP **3** showed IC_{50} and Ki values (M) of 1.0×10^{-7} and 6.0×10^{-8}, respectively. The analogue of **3** containing *iso*Asp **4** showed IC_{50} of 2.9×10^{-7} and Ki of 1.8×10^{-7} M. The analogue of **3** equipped with the 2,6-dicholorobenzoyl group **5** revealed a modest affinity, in the micromolar range, while **6**, analogue of **4** with the 2,6-dicholorobenzoyl instead of the phanylacetyl (BnCO) group, did not displace ^{125}I-FN in a significant way.

8.2.3. Cell adhesion inhibition

Subsequently, we assayed the ability of **1-6** to inhibit the adhesion of α4β1 integrin-expressing Jurkat cells to VCAM-1. In a first series of experiments, we ascertained that adhesion of these cells to 96-well plates coated with human recombinant VCAM-1 was concentration-dependent and was not observed in BSA-coated wells.[46,47] The adhesion of Jurkat cells (5×10^5 cells per well) to VCAM-1 (2-25 mg/ml) ranged from 1.9 to 3.2×10^4 cells. The adhesion to VCAM-1 (10 mg/ml) was inhibited (>92%) after pretreatment with 5 mg/ml of an anti-α4 integrin antibody. As shown in Table 1, the reference compound BIO1211 (MPUPA-Leu-Asp-Val-Pro-OH, **1**) behaved as a potent α4β1 integrin ligand and inhibited Jurkat cell adhesion to VCAM-1 with a IC_{50} of 7.6 nM. Peptidomimetics **2** and **6** did not affect cell adhesion to a significant extent, confirming the results of the SPA assay. Interestingly, the retro compounds BnCO-Asp-β^2-Pro-AMPUMP (**3**) and BnCO-*iso*Asp-β^2-Pro-AMPUMP (**4**) inhibited cell adhesion with an IC_{50} of 80 and 93 nM, respectively. On the contrary, **5** failed to behave as adhesion antagonist, despite of the micromolar affinity revealed by the SPA (Table 1). In addition, **3** and **4** did not show any significant activity (IC_{50} > 100 μM) in cell adhesion assays (Table 1) aimed to evaluate any potential antagonist activity towards αvβ3 integrin (SK-MEL-24 cells coated with 10 mg/ml VT). Finally, neither compound (up to 2 mM) influenced cell viability, evaluated by Trypan blue exclusion (data not shown).

8.2.4. In vitro metabolic stability

BIO1211 (**1**) was found to be very unstable in heparinized blood, plasma and rat liver, lung and intestinal homogenates, being metabolized by hydrolytic cleavage of the terminal dipeptide moiety, giving a sequence[11,12] much less active than the parent compound.8 For their peptidomimetic nature the sequences BnCO-Asp-β^2-Pro-urea **3** and BnCO-*iso*Asp-β^2-Pro-urea **4** were supposed to be significantly more stable, in particular for the presence of the central β-Pro. The resistance of **3** and **4** to enzymatic degradation was estimated using 100% mouse serum (Sigma)[48] and compared to that of **1** under the same conditions. After 120 min, **3** was degraded to a moderate extent (about 10%),

and **4** was only slightly degraded (< 5%) after incubation in the mouse serum, while **1** was almost completely hydrolyzed, being present only in traces, as detected by RP-HPLC and ESI-MS analyses. Apparently, the presence of *iso*Asp increased the stability of **4** compared to **3**.

8.2.5. Conformational analyses

The significant biological activity of the structurally correlated BnCO-Asp-β^2-Pro-AMPUMP (**3**) and BnCO-*iso*Asp-β^2-Pro-AMPUMP (**4**) prompted us to analyze the conformations by NMR spectroscopy and MD simulations (Experimental section) in particular to check the fulfillment of the geometric requisites of the 3D models utilized for structure design (Experimental section).

As expected on the basis of the literature,[38,39,40,41] the ^{1}H-NMR of both **3** and **4** revealed two sets of resonances, in about 1:1 ratio, corresponding to the cis and trans conformers of the peptide bond linking the pyrrolidine ring. The cis conformations were assigned by detection of the NOE cross peaks between AspHα (**3**) or *iso*AspHβ (**4**) and PyrrolidineH-2, while the trans conformations were deduced by detection of the NOE cross peaks between AspHα (**3**) or *iso*AspHβ (**4**) and PyrrolidineH-5 (for this numbering, see the structures **3** and **4** in Table 1, and structures associated to Tables 2 to 5).[49]

Molecular conformations were investigated by 2D ROESY in 8:2 DMSO-d_6/H_2O; DMSO-d_6 alone or mixtures of DMSO-d_6 and H_2O have been recommended by several authors as biomimetic media.[50,51] Cross-peak intensities were ranked to infer plausible inter-proton distances as restraints. Structures consistent with ROESY were obtained by simulated annealing with restrained MD[35] in a box of explicit TIP3P water molecules. The structures were minimized with the AMBER force field and clustered by the rmsd analysis of backbone atoms (Experimental section).

For **3**, computations essentially gave one major cluster for the all-trans conformer and one cluster for the trans-cis-trans conformer, each comprising almost 95% of the structures. For each cluster, the representative geometries all-trans-**3**A and trans-cis-trans-**3**C with the lowest internal energy and no violations of the distance constraints were selected and analyzed (Figure 2).

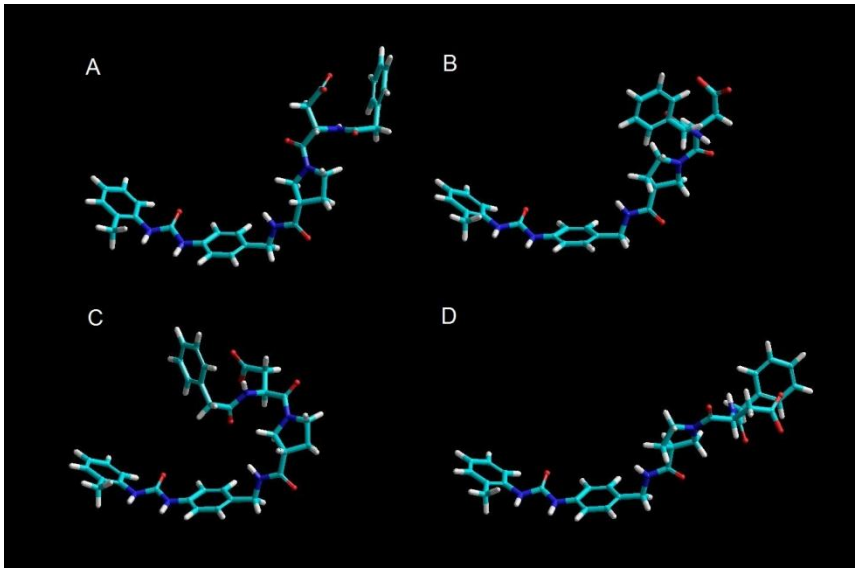

Figure 2. Representative low-energy structure all-trans-**3**A (**3**, BnCO-Asp-β^2-Pro-AMPUMP) consistent with ROESY analysis and calculated by restrained MD; alternative minor conformer **3**B (low energy structure), determined by unrestrained MD; representative low-energy structure of trans-cis-trans-**3**C calculated by restrained MD; minor conformer **3**D (low energy structure) determined by unrestrained MD. All structures obtained in a 45×45×45 Å box of standard TIP3P water molecules.

To investigate the dynamic behavior, the structures **3**A and **3**C were analyzed by unrestrained MD for 10 ns in a 45×45×45 Å box of explicit, equilibrated water molecules. Besides to the all-trans-**3**A, the analysis of the trajectories revealed the occurrence of the minor all-trans conformer **3**B, differing almost exclusively in the orientation of BnCO-Asp-β-Pro dipeptide respect to the AMPUMP group. The analysis of the trajectories of trans-cis-trans-**3**C revealed the presence of the minor conformer **3**D, showing the alternative orientation of BnCO-Asp-β-Pro respect to AMPUMP

(Figure 2). On the other hand, the conversion of the all-trans conformers into the trans-cis-trans conformers was observed very seldom.

In a similar way, computations for **4** gave one cluster for the all-trans conformer and one cluster for the trans-cis-trans conformer (> 90% of the structures). Figure 3 shows the representative low energy geometries of all-trans-**4**A and trans-cis-trans-**4**C. Unrestrained MD performed as described for **3** revealed the alternative minor conformers all-trans-**4**B and trans-cis-trans-**4**D, differing from **4**A and **4**C in the display of the Asp-β-Pro dipeptide respect to the AMPUMP group.

Despite of potentially high flexibility of the linear ligands, the β-Pro scaffold conferred them markedly bent conformations. Indeed, the conformers **A** and **C** determined by restrained MD were clearly predominant during the unrestrained MD simulations in water. Apparently, both all-trans-**A** and trans-cis-trans-**C** conformations seemed compatible with one or the other 3D model **7** or **8** (Figure 1).[2,13,33,36,52,53] For the moment, the determination of the different contribution of the cis and trans geometries to the bioactive conformations of the compounds is not possible.

The most significant differences between the corresponding conformations of **3** and **4** were related to the position of the aromatic group adjacent to Asp or *iso*Asp, respectively. This might be correlated to the slightly different IC_{50} and Ki values determined by SPA, confirming the role of the flanking aromatic substituent for efficient binding of the receptor.[23,24,25,33]

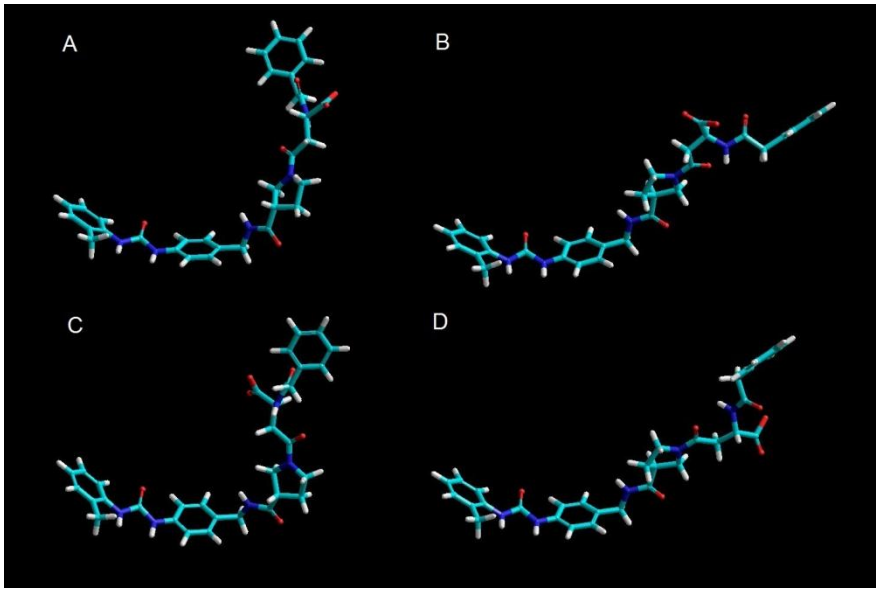

Figure 3. Representative low-energy structure all-trans-**4**A (**4**, BnCO-*iso*Asp-β^2-Pro-AMPUMP) consistent with ROESY analysis and calculated by restrained MD; alternative minor conformer **4**B (low energy structure), determined by unrestrained MD; representative low-energy structure of trans-cis-trans-**4**C calculated by restrained MD; minor conformer **4**D (low energy structure) determined by unrestrained MD. All structures obtained in a 45×45×45 Å box of standard TIP3P water molecules.

8.3. Conclusions

In summary, herein is reported the first implementation of the retro-sequence strategy for the design of new α4β1 integrin inhibitors. Starting from the well known α4β1 integrin binding motif "MPUPA-spacer-Asp", exemplified by the potent and selective ligand BIO1211 (MPUPA-Leu-Asp-Val-Pro-OH), we assembled the retro peptidomimetic sequences by connecting Asp or *iso*Asp, and the amino variant (AMPUMP) of the widely utilized diphenylurea MPUPA, to a pyrrolidine-3-carboxylate (β^2-Pro) scaffold, the latter selected by inspection of the 3D models (3D-QSAR) reported in the literature. After syntheses, the conformational analyses confirmed the good agreement with the models.

Interestingly, while the straight sequence MPUPA-β-Pro-Asp-OBn (**2**), analogue of BIO1211, was completely inactive, the retro sequences BnCO-Asp-β-Pro-AMPUMP (**3**) and BnCO-*iso*Asp-β-Pro-AMPUMP (**4**), displayed a moderate binding affinity (SPA), and efficiently inhibited the adhesion of α4β1 integrin-expressing cells to VCAM-1. Besides, the peptidomimetic nature conferred these compounds good in vitro metabolic stability (mouse serum). Albeit **3** was a

slightly more potent inhibitor than **4**, the latter was significantly more stable. These evidences support that the retro approach can furnish promising candidates for the development of a new class of peptidomimetic anti-inflammatory agents.

8.4. Experimental section

8.4.1. General methods

Unless stated otherwise, chemicals were obtained from commercial sources and used without further purification. The MW-assisted synthesis was performed using a MicroSYNTH microwave labstation. Flash chromatography was performed on silica gel (230-400 mesh), using mixtures of distilled solvents. Purities were determined to be ≥ 96% by analytical RP-HPLC and combustion analysis. Analytical RP-HPLC was performed on an C18 column (4.6 μm particle size, 100 Å pore diameter, 250 μm, DAD 210 nm, from a 9:1 H_2O/CH_3CN to a 2:8 H_2O/CH_3CN, with the addition of 0.05% TFA, in 20 min) at a flow rate of 1.0 mL/min, followed by 10 min at the same composition. Elemental analyses were performer using a Thermo Flash 2000 CHNS/O analyzer. Semipreparative RP-HPLC was performed on a C18 column (7 μm particle size, 21.2 mm×150 mm, from 8:2 H_2O/CH_3CN to 100% CH_3CN, with the addition of 0.05% TFA, in 10 min) at a flow rate of 12 mL/min. Mass analysis was done by ESI. ^{1}H NMR and ^{13}C NMR spectra were recorded at 400 and 100 MHz, respectively, in 5 mm tubes, at rt. Chemical shifts are reported as δ values relative to the solvent peak. 2D spectra were recorded in the phase sensitive mode and processed using a 90°-shifted, squared sinebell apodization.

8.4.2. Synthetic procedures

Peptide coupling, general procedure. HOBt (1.1 mmol) and HBTU (1.1 mmol) were added to a stirred solution of the acid partner (1.0 mmol) in 4:1 DCM/DMF (5 mL) at rt under inert atmosphere. After 5 min, the amino partner-TFA salt (1.1 mmol) and DIPEA (2.2 mmol) were added at rt, and the mixture was stirred under MW irradiation, keeping irradiation power fixed at 150W and monitoring the internal reaction temperature at 80 °C with a built-in ATC-FO advanced fiber optic automatic temperature control. After 10 min the mixture was diluted with DCM, and the solution was washed with 0.5 M HCl (5 mL) and saturated $NaHCO_3$ (5 mL). The organic layer was dried over Na_2SO_4, and solvent was removed at reduced pressure. The intermediates were isolated by crystallization from $EtOH/Et_2O$ or by flash chromatography over silica-gel. For the preparation of the different Asp or isoAsp derivatives and of **11**, see S.M. Compounds **2**-**6** were purified by semipreparative RP-HPLC (see 7.4.1.), (70-85% yield, 96-98% pure by analytical RP-HPLC).

Fmoc-Asp(OtBu)-OBn (**9**). A mixture of Fmoc-Asp(O*t*Bu)-OH (1.50 g, 3.65 mmol), BnBr (1.7 mL, 14.6 mmol) $NaHCO_3$ (0.92 g, 10.9 mmol) in DMF (6 mL), was stirred for 8 h. Then the mixture was diluted with water (10 mL) and extracted three times with EtOAc (20 mL). The combined organic layers were dried over Na_2SO_4, and solvent was distilled at reduced pressure. The oily residue was purified by flash chromatography over silica-gel (eluant EtOAc/cyclohexane 1:9) giving **7** (1.58 g, 85%). The analyses were in agreement with the literature.[54]

BzCO-Asp(OtBu)-OBn (**11**). **9** (0.89 g, 1.71 mmol) was treated with 2M dimethylamine in THF (4 mL) under inert atmosphere while stirring. After 10 min, the solvent was distilled at reduced pressure, and the residue was treated as before for additional 40 min. After solvent evaporation, the residue was triturated with Et_2O, and the precipitate **10** (quantitative yield) was utilized without purification. ESI-MS *m/z* 293.1 $(M+H)^+$, calcd 293.1. Crude **10** was dissolved in DCM (10 mL) and treated with BnCOCl (0.250 mL, 1.71 mmol) and pyridine (0.21 mL, 2.6 mmol) under inert atmosphere. After 4 h the reaction was diluted with EtOAc (30 mL) and washed with 0.5 M HCl (5 mL), sat. $NaHCO_3$ (5 mL), and brine (5 mL), and dried over Na_2SO_4. Solvent was distilled at reduced pressure, and the residue was purified by flash chromatography over silica-gel (eluant EtOAc/cyclohexane 2:8) giving **11** (0.64 g, 94%). ^{1}H NMR ($CDCl_3$, 200 MHz) δ (ppm): 1.40 (s, 9H, *t*-Bu), 2.73 (dd, J = 4.2, 17.1 Hz, 1H, AspHβ), 2.95 (dd, J= 4.0, 17.1 Hz, 1H, AspHβ), 3.60 (s, 2H, CH_2Ph), 4.86 (q, J = 8.2 Hz, 1H, AspHα), 5.10 (d, J = 13.0 Hz, 1H, CH_2Ph), 5.22 (d, J = 13.0 Hz, 1H, CH_2Ph), 6.51 (br.d, J = 7.2 Hz, 1H, AspNH), 7.40-7.80 (m, 10H, ArH); ESI-MS *m/z* 398.1 $(M+H)^+$, calcd 398.2.

BzCO-Asp-OBn (**12**). **11** (0.64 g, 1.61 mmol) was stirred in 1:3 TFA/DCM (4 mL). After 30 min the mixture was concentrated at reduced pressure, and the procedure was repeated. The oily residue was triturated in Et_2O, and the crude **12** which precipitated (0.54 g, 98%), was utilized without purification. ESI-MS *m/z* 342.1 $(M+H)^+$, calcd 342.1

Synthesis of Boc-AMPUMP (**13)**. 2-Methylphenyl isocyanate (0.56 mL, 4.50 mmol) was added to a stirred solution of *t-Bu*-4-aminobenzylcarbamate (1.0 g, 4.50 mmol) in DMF (8 mL) at r.t. under inert atmosphere. After 2 h the reaction was diluted with EtOAc (30 mL), giving the precipitate **13** (1.44 g, 90%) collected by filtration. ^{1}H NMR (DMSO-d6, 200 MHz) δ (ppm): 1.38 (s, 9H, *t*-Bu), 2.22 (s, 3H, CH_3Ph), 4.06 (d, J = 5.8 Hz, 2H, CH_2Ph), 4.24 (d, J = 5.4 Hz, 1H, NH), 6.86 (dd, J = 6.2, 13.2 Hz, 2H, ArH), 6.91-7.22 (m, 4H, ArH), 7.35 (d, J = 8.6 Hz, 1H, ArH), 7.76 (s, 1H, NH), 7.81 (d, J = 8.0 Hz, 1H, ArH), 8.82 (s, 1H, NH); ESI-MS *m/z* 356.1 $(M+H)^+$, calcd .356.2.

Synthesis of **15**. Boc deprotection of **13** (1.44 g, 4.05 mmol) was performed as described for the preparation of **12**. The residue was suspended in Et_2O (20 mL). The TFA-AMPUMP salt **14** which precipitated in quantitative yield was used for the next coupling without further purifications. ESI-MS *m/z* 256.1 $(M+H)^+$, calcd 256.1. The TFA salt **14** was coupled with Boc-(*S)*-β-*iso*Pro-OH (1.13 g, 5.0 mmol) under MW irradiation as described in the main text (Peptide coupling, general procedure). The residue was purified by flash chromatography over silica-gel (eluant EtOAc) giving **15** as a waxy solid (1.55 g, 85%). ^{1}H NMR ($CDCl_3$, 200 MHz) δ (ppm): 1.44 (s, 9H, *t*-Bu),1.50-1.63 (m, 1H, PyrrolidineH-4), 1.90-2.01 (m, 2H, PyrrolidineH-4+H-3), 2.13 (s, 3H, CH_3Ph), 2.76-2.90 (m, 1H, PyrrolidineH-5), 3.10-3.22 (m, 1H, PyrrolidineH-5), 3.38-3.58 (m, 2H, PyrrolidineH-2), 4.06 (d, J = 5.8 Hz, 2H, CH_2Ph), 4.24 (d, J = 5.4 Hz, 1H, NH), 6.86 (dd, J = 6.2, 13.2 Hz, 2H, ArH), 6.91-7.22 (m, 4H, ArH), 7.35 (d, J = 8.6 Hz, 1H, ArH), 7.76 (s, 1H, NH), 7.81 (d, J = 8.0 Hz, 1H, ArH), 8.82 (s, 1H, NH); ESI-MS *m/z* 475.1 $(M+Na)^+$, calcd 475.2.

Synthesis of **17**. **15** (1.55 g, 3.4 mmol) was deprotected as described for **14**; the TFA salt **16** (quantitative yield) was used without further purifications. ESI-MS *m/z* 353.1 $(M+H)^+$, calcd 353.2. Crude **16** (0.26 g, 0.73 mmol) was coupled with **12** (0.25 g, 0.73 mmol) under MW irradiation as described in the main text (Peptide coupling, general procedure). The residue was purified by flash chromatography over silica-gel (eluant EtOAc/cyclohexane 2:8) giving **17** (0.39 g, 80%). ^{1}H NMR ($CDCl_3$, 200 MHz) δ (ppm): 1.84-2.19 (m, 2H, PyrrolidineH-4), 2.19 (s, 3H, CH_3), 2.58 (m, 1H, AspHβ), 2.70-2.81 (m, 1H, PyrrolidineH-3), 2.94 (m, 1H, AspHβ), 3.20-3.30 (m, 2H, PyrrolidineH-$5_<$), 3.41-3.51 (m, 4H, CH_2Ph+PyrrolidineH-$2_>$), 3.51-3.62 (m, 2H, PyrrolidineH-$5_>$), 4.23-4.40 (m, 4H, CH_2Ph+PyrrolidineH-$2_<$), 4.82 (m, 1H, AspHα), 5.25 (m, 2H, CH_2Ph), 6.30 (br.t, 1H, NH), 6.40 (s, 1H, NH), 6.60 (br.d, 1H, AspNH), 6.70 (s, 1H, NH), 6.90 (t, J = 7.4 Hz, 1H, ArH), 6.94-7.20 (m, 9H, ArH), 7.20-7.25 (m, 5H, ArH), 7.25-7.36 (m, 2H, ArH), 7.59 (d, J = 8.0 Hz, 1H, ArH); ESI-MS *m/z* 676.2 $(M+H)^+$, calcd 676.3.

Synthesis of **4**. **17** (0.39 g, 0.58 mmol) was treated with H_2 and catalytic Pd/C in EtOH (20 mL). After 6 h, the mixture was filtered over Celite, and the solvent was evaporated at reduce pressure. The residue was purified by semi-preparative RP-HPLC (general methods) giving **4** (0.27 g, 80 %). ^{1}H NMR (8:2 DMSO-d_6/H_2O, 400 MHz) δ (ppm): 1.85 (m, 1H, PyrrolidineH-4_{cis}), 1.95-2.05 (m, 2H, PyrrolidineH-4_{trans}+PyrrolidineH-4_{cis}), 2.15 (m, 1H, PyrrolidineH-4_{trans}), 2.18 (s, 3H, CH3), 2.57 (m, 1H, AspHβ), 2.94 (m, 1H, AspHβ), 2.97 (m, 1H, PyrrolidineH-3_{trans}), 3.22 (dd, J = 6.0, 10.0 Hz, 1H, PyrrolidineH-5_{cis}), 3.39-3.48 (m, 4H, PyrrolidineH-3_{cis}+ NCH_2Ar+PyrrolidineH-2_{trans}), 3.49-3.55 (m, 3H, PyrrolidineH-5_{trans}+PyrrolidineH-5_{cis}+PyrrolidineH-2_{trans}), 3.58 (m, 1H, PyrrolidineH-5_{trans}), 4.21 (d, J = 6.0 Hz, 2H, PhCH_2CO), 4.34 (dd, J = 4.8, 8.8 Hz, 1H, PyrrolidineH-2_{cis}), 4.43 (t, J = 9.2 Hz, 1H, PyrrolidineH-2_{cis}), 4.59 (m, 1H, AspHα_{cis}), 4.63 (m, 1H, AspHα_{trans}), 6.90 (t, J = 7.2 Hz, 1H, ArH4), 7.10-7.19 (m, 4H, ArH3,5+ArH3',5'), 7.13-7.24 (m, 5H, ArH''), 7.40 (d, J = 8.2 Hz, 2H, ArH2',6'), 7.79 (d, J = 8.0 Hz, 1H, ArH6), 7.90 (s, 1H, NHa), 8.41 (br.t, 1H, NHc_{trans}), 8.45 (br.t, 1H, NHc_{cis}), 8.50 (br.d, 1H, AspNH_{trans}), 8.54 (br.d, 1H, AspNH_{cis}), 8.91 (s, 1H, NHb); ^{13}C NMR (DMSO-d6, 400 MHz) δ (ppm): 18.3, 28.3, 29.5, 29.9, 39.4, 42.4, 42.7, 44.1, 45.0, 47.7, 48.2, 49.2, 55.0, 118.4, 121.5, 126.4, 127.8, 128.4, 129.2, 129.3, 130.4, 132.7, 136.4, 137.7, 139.1, 153.1, 171.7, 172.0, 172.2, 172.3. Elem. Anal. for C32H35N5O6, calcd: C 65.63, H 6.02, N 11.96, found: C 66.94, H 6.19, N 11.72; ESI-MS m/z 586.1 (M+H)+, calcd 586.3.

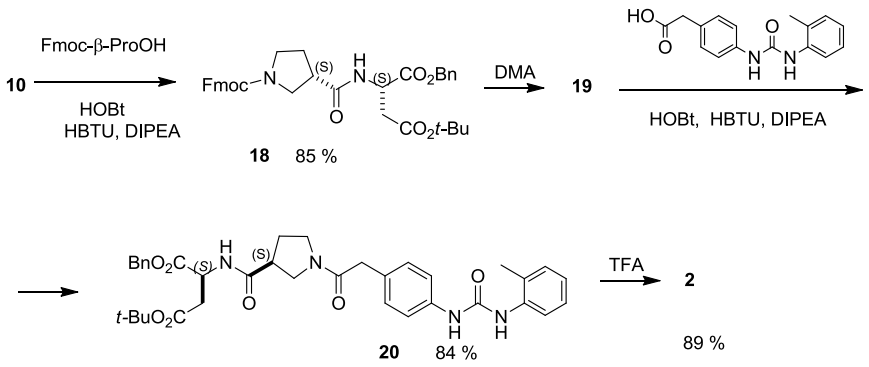

Scheme 2. Synthesis of **2**.

*Synthesis of **18***. Fmoc-(*S*)-β-*iso*Pro-OH (0.13 g, 0.38 mmol) was coupled with **10** (0.10 g, 0.34 mmol) under MW irradiation as described in the main text (Peptide coupling, general procedure). The residue was purified by flash chromatography over silica-gel (eluant EtOAc/cyclohexane 1:1) giving **18** (0.20 g, 85%). ESI-MS *m/z* 621.2 $(M+Na)^+$, calcd 621.3.

*Synthesis of **20***. Fmoc deprotection of **18** (0.20 g, 0.32 mmol) was performed as reported for the synthesis of **10**; after solvent evaporation, the residue containing **19** (quantitative yield) was utilized without purification. ESI-MS *m/z* 377.1 $(M+H)^+$, calcd 377.2. Crude **19** was coupled with 4-[N-(2-methylphenyl)ureido]phenylacetyl [55] (0.14 g, 0.50 mmol) as described in the main text (Peptide coupling, general procedure). The residue was purified by flash chromatography over silica-gel (eluant EtOAc/ cyclohexane 1:1) giving **20** (0.18 g, 84%). ^{1}H NMR ($CDCl_3$, 400 MHz) δ (ppm): (two sets of resonances: > = major conformer; < = minor conformer) 1.36 (s, 9H, *t*-Bu), 2.03 (q, J = 7.4 Hz, 1H, PyrrolidineH-4), 2.16 (s, 4H, CH_3+PyrrolidineH-4), 2.72 (dd, J = 4.6, 17.0 Hz, 1H, AspHβ), 2.82-2.98 (m, 2H, PyrrolidineH-3+AspHβ), 3.38 (m, 1H, PyrrolidineH-$5_<$), 3.40-3.50 (m, 3H, CH_2Ph+PyrrolidineH-$2_>$+PyrrolidineH-$5_<$), 3.51-3.60 (m, 6H, PyrrolidineH-$2_<$+PyrrolidineH-$2_>$+CH_2Ph+PyrrolidineH-$5_>$), 4.80 (m, 1H, AspHα), 5.10 (d, J = 12.4 Hz, 1H, CH_2Ph$_<$), 5.13 (d, J = 12.0 Hz, 1H, CH_2Ph$_>$), 5.15 (d, J = 12.4 Hz, 1H, CH_2Ph$_<$), 5.18 (d, J = 12.0 Hz, 1H, CH_2Ph$_>$), 6.76 (d, J = 8.0 Hz, 1H, AspNH$_<$), 6.87 (d, J = 8.4 Hz, 1H, AspNH$_>$), 6.93-7.04 (m, 4H, ArH), 7.04-7.14 (m, 5H, ArH), 7.21-7.33 (m, 4H, ArH+NH), 7.63 (d, J = 7.6 Hz, 1H, ArH), 7.68 (s, 1H, NH); ESI-MS *m/z* 665.2 $(M+Na)^+$, calcd 665.3

*Synthesis of **2***. The deprotection of **20** (0.18 g, 0.27mmol) was performed as described for **12** . The residue was purified by semi-preparative RP-HPLC (general methods) giving **2** (0.14 g, 89%). ^{1}H NMR ($CDCl_3$) δ (ppm): (two sets of resonances: > = major conformer; < = minor conformer) 1.95 (m, 1H, PyrrolidineH-4), 2.05-2-19 (m, 4H, CH_3+PyrrolidineH-4), 2.74 (m, 1H, AspHβ), 2.90-2.99 (m, 2H, PyrrolidineH-3+AspHβ), 3.36 (m, 2H, PyrrolidineH-$5_<$+PyrrolidineH-$2_>$), 3.41-3.50 (m, 2H, PyrrolidineH-$2_>$+PyrrolidineH-$5_<$), 3.54 (d, J = 5.2 Hz, 2H, ArCH_2CON), 3.51-3.60 (m, 4H, PyrrolidineH-$2_<$+PyrrolidineH-$5_>$), 4.78 (m, 1H, AspHα), 5.07 (br.s, 2H, CH_2Ph), 6.96 (t, J = 7.6 Hz, 1H, ArH), 7.00-7.08 (m, 3H, ArH), 7.09-7.18 (m, 5H, ArH), 7.24-7.32 (m, 4H, ArH+NH), 7.35 (d, J = 8.8 Hz, 1H, AspNH), 7.56 (s, 1H, NH), 7.60 (d, J = 8.0 Hz, 1H, ArH); ^{13}C NMR ($CDCl_3$) δ (ppm): 18.3, 28.3, 36.7, 36.4, 40.6, 42.4, 44.1, 47.7, 48.8, 48.9, 49.2, 118.4, 123.0, 126.4, 127.0, 128.0, 128.4, 129.2, 129.3, 130.4, 132.7, 136.4, 137.7, 139.1, 153.1, 169.0, 170.3, 172.0, 172.2. Elem. Anal. for $C_{32}H_{34}N_4O_7$, calcd C 65.52, H 5.84, N 9.55, found C 63.88, H 6.00, N 9.64; ESI-MS *m/z* 587.2 $(M+H)^+$, calcd 587.2.

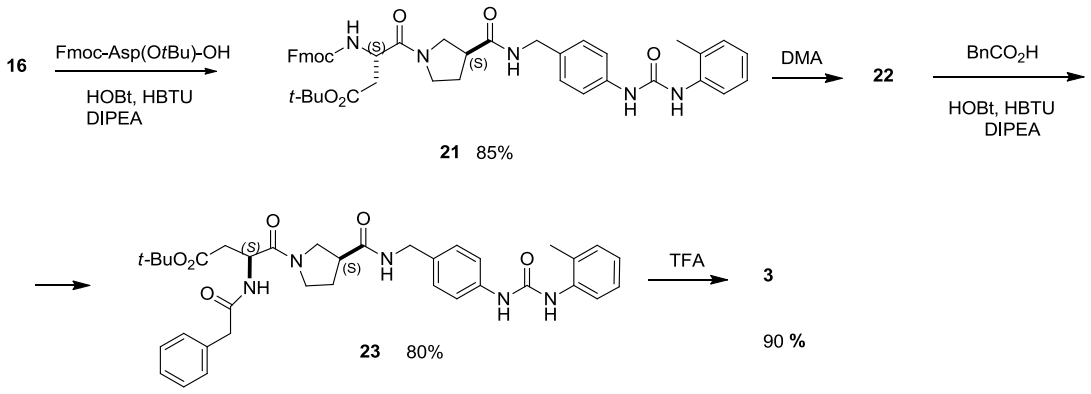

Scheme 3. Synthesis of **3**.

Synthesis of **21**. Fmoc-Asp(O*t*Bu)OH (0.321 g, 0.78 mmol) was coupled with **16** (0.25 g, 0.71 mmol) as described in the main text (Peptide coupling, general procedure). The residue was purified by flash chromatography over silica-gel (eluant EtOAc/cyclohexane 8:2) giving **21** (0.45 g, 85%). ^{1}H NMR ($CDCl_3$, 400 MHz) δ (ppm) 1:1 mixture of two conformers: 1.31+1.33 (s, 9H, *t*-Bu), 1.90 (q, J = 7.2 Hz, 1H, PyrrolidineH-4), 1.98 (m, 1H, PyrrolidineH-4), 2.04+2.05 (s, 3H, CH_3), 2.45 (m, 1H, AspHβ), 2.62-2.73 (m, 2H, PyrrolidineH-3+AspHβ), 3.22 (m, 1H, PyrrolidineH-5), 3.36-3.49 (m, 2H, PyrrolidineH-2+PyrrolidineH-5), 3.58 (dd, J = 7.0, 9.0 Hz, 1H, PyrrolidineH-2), 3.65-3.76 (m, 2H, PyrrolidineH-2+PyrrolidineH-5), 4.09, (d, J = 6.4 Hz, 2H, CH_2Ph), 4.14-4.30 (m, 3H, Fmoc), 4.78 (br.q, 1H, AspHα), 5.85+5.90 (d, J = 9.2 Hz, 1H, AspNH), 6.80 (d, 1H, J = 8.8 Hz, 1H, ArH), 6.85-6.90 (m, 2H, ArH), 6.94-7.09 (m, 5H, ArH), 7.12-7.22 (m, 2H, ArH), 7.22-7.35 (m, 3H, ArH+NH), 7.42-7.54 (m, 3H, ArH+NH), 7.64 (d, J = 8.0 Hz, 2H, ArH), 7.92 (s, 1H, NH); ESI-MS *m/z* 746.3 $(M+H)^+$, calcd 746.4.

Synthesis of **23**. Fmoc deprotection of **21** (0.32 g, 0.43 mmol) was performed as described for the preparation of **10** giving crude **22** in quantitative yield. ESI-MS *m/z* 524.3 $(M+H)^+$, calcd 524.4. The resulting residue was coupled with phenylacetic acid (0.065 g, 0.48 mmol) as described in the main text (Peptide coupling, general procedure). The residue was purified by flash chromatography over silica-gel (eluant EtOAc/cyclohexane 8:2) giving **23** (0.22 g, 80%). ^{1}H NMR ($CDCl_3$, 200 MHz) δ (ppm): (two sets of resonances: > = major conformer; < = minor conformer) 1.39 (s, 9H, *t*-Bu), 1.95-2.05 (m, 2H, PyrrolidineH-4), 2.28 (s, 3H, CH_3), 2.50 (m, 1H, AspHβ), 2.75-2.90 (m, 2H, AspHβ+PyrrolidineH-3), 3.22 (m, 1H, PyrrolidineH-$5_<$), 3.37-3.52 (m, 6H, PyrrolidineH-$2_>$+CH_2Ph+PyrrolidineH-$5_>$+PyrrolidineH-$5_<$), 3.61-3.80 (m, 3H, PyrrolidineH-$2_<$+PyrrolidineH-$5_>$), 4.15-4.25 (m, 2H, CH_2Ph), 4.99 (m, 1H, AspHα), 6.82-7.12-7.20 (m, 10H, ArH), 7.23-7.40 (m, 4H, ArH+AspNH+NH), 7.48-7.55 (m, 2H, NH), 7.65 (br.d, 1H, ArH); ESI-MS *m/z* 642.2 $(M+H)^+$, calcd 642.3.

Synthesis of **3**. **23** (0.22 g, 0.34 mmol) was deprotected as described for **12**. The residue was purified by semi-preparative RP-HPLC (general methods) giving **3** (0.18 g, 90%). ^{1}H NMR (8:2 DMSO-d_6/H_2O, 400 MHz) δ (ppm): 1.89 (m, 1H, PyrrolidineH-4_{cis}), 1.92 (m, 1H, PyrrolidineH-4_{trans}), 2.00 (m, 1H, PyrrolidineH-4_{cis}), 2.06 (m, 1H, PyrrolidineH-4_{trans}), 2.22 (s, 3H, CH_3), 2.39 (m, 1H, AspHβ), 2.72 (m, 1H, AspHβ), 2.91 (m, 1H, PyrrolidineH-3_{trans}), 2.96 (m, 1H, PyrrolidineH-3_{cis}), 3.21 (m, 1H, PyrrolidineH-5_{cis}), 3.28 (m, 1H, PyrrolidineH-2_{trans}), 3.39-3.45 (m, 3H, PyrrolidineH-5_{trans}+ NCH_2Ar), 3.45 (m, 1H, PyrrolidineH-5_{cis}), 3.54 (m, 1H, PyrrolidineH-2_{cis}), 3.56 (m, 1H, PyrrolidineH-2_{trans}), 3.63 (m, 1H, PyrrolidineH-5_{trans}), 3.75 (t, J = 8.8 Hz, 1H, PyrrolidineH-2_{cis}), 4.19 (s, 2H, PhCH_2CO$_{cis}$), 4.21 (s, 2H, PhCH_2CO$_{trans}$), 4.75 (m, 1H, AspHα$_{cis}$), 4.81 (m, 1H, AspHα$_{trans}$), 6.93 (t, J = 7.2 Hz, 1H, ArH_4), 7.09-7.18 (m, 4H, $ArH_{3,5}$+$ArH_{3',5'}$), 7.16-7.28 (m, 5H, *Ph*CH_2CON), 7.39 (d, J = 8.4 Hz, 2H, $ArH_{2',6'}$), 7.81 (d, J = 8.0 Hz, 1H, ArH_6), 7.89 (s, 1H, NHa), 8.43 (br.t, 1H, NHc$_{trans}$), 8.46 (br.t, 1H, NHc$_{cis}$), 8.54 (br.d, 1H, AspNH$_{trans}$), 8.56 (br.d, 1H, AspNH$_{cis}$), 8.98 (s, 1H, NHb); ^{13}C NMR (DMSO-d_6) δ (ppm): 18.3, 28.3, 29.9, 39.4, 40.2, 42.4, 44.1, 45.8, 46.0, 47.4, 48.8, 48.9, 49.2, 118.4, 121.5, 126.4, 126.6, 127.8, 128.4, 129.3, 130.4, 132.7, 133.0, 136.4, 137.7, 139.1, 153.1, 168.8, 170.3, 171.7, 172.0. Elem. Anal. for $C_{32}H_{35}N_5O_6$, calcd C 65.63, H 6.02, N 11.96, found C 66.20, H 6.18, N 11.70; ESI-MS *m/z* 586.2 $(M+H)^+$, calcd 586.3.

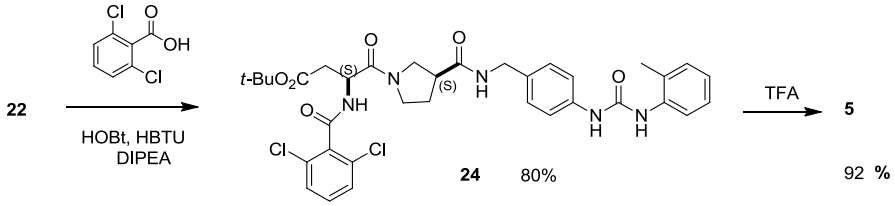

Scheme 4. Synthesis of **5**.

Synthesis of **24**. **22** was prepared as described above and in the same amount, and it was coupled with 2,6-dichlorobenzoic acid (0.090 g, 0.48 mmol) under MW irradiation as described in the main text (Peptide coupling, general procedure). The residue was purified by flash chromatography over silica-gel (eluant EtOAc/cyclohexane 8:2) giving **24** (0.24 g, 80 %). ^{1}H NMR ($CDCl_3$, 200 MHz) δ (ppm): (two sets of resonances: > = major conformer; < = minor conformer) 1.35 (s, 9H, *t*-Bu), 2.05-2.20 (m, 2H, PyrrolidineH-4), 2.39 (s, 3H, CH_3Ph), 2.52 (m, 1H, AspHβ), 2.89-2.99 (m, 2H, PyrrolidineH-3$_>$+AspHβ), 3.10 (m, 1H, PyrrolidineH-3$_<$), 3.25 (m, 1H, PyrrolidineH-5$_<$), 3.45-3.63 (m, 2H, PyrrolidineH-2$_>$+PyrrolidineH-5$_<$+PyrrolidineH-5$_>$), 3.69-3.78 (m, 2H, PyrrolidineH-2$_>$+PyrrolidineH-2$_<$), 4.09-4.10 (m, 2H, PyrrolidineH-5$_>$+PyrrolidineH-2$_<$), 4.26 (d, J = 5.7 Hz, 2H, CH_2Ph), 4.99 (m, 1H, AspHα), 6.84 (br.t, 1H, ArH), 7.05-7.15 (m, 5H, ArH+NH), 7.15-7.26 (m, 5H, ArH+AspNH+NH), 7.25-7.33 (m, 3H, ArH+NH), 7.75-7.87 (m, 2H, ArH+NH). ESI-MS *m/z* 696.1 $(M+H)^+$, calcd 696.2

Synthesis of **5**. **24** (0.24 g, 0.34 mmol) was deprotected as described for **12**. The residue was purified by semi-preparative RP-HPLC (general methods) giving **5** (0.20 g, 92%). ^{1}H NMR (DMSO-d_6, 400 MHz) δ (ppm): (two sets of resonances: > = major conformer; < = minor conformer) 2.00-2.18 (m, 2H, PyrrolidineH-4$_<$), 2.20-2.38 (m, 2H, PyrrolidineH-4$_>$), 2.39 (s, 3H, CH_3Ph), 2.58 (m, 1H, AspHβ), 2.90 (m, 1H, PyrrolidineH-3$_>$), 2.98 (m, 1H, AspHβ), 3.08 (m, 1H, PyrrolidineH-3$_<$), 3.35 (m, 1H, Proδ$_<$), 3.46 (dd, J = 8.0, 12.0 Hz, 1H, Proα$_>$), 3.59 (m, 2H, PyrrolidineH-5$_<$+ PyrrolidineH-5$_>$), 3.70 (dd, J = 8.0, 12.0 Hz, 1H, Proα$_>$), 3.79 (dd, J = 7.6, 9.2 Hz, 1H, Proα$_<$), 4.00 (m, 1H, Proδ$_>$), 4.09 (m, 1H, Proα$_<$), 4.24 (d, J = 5.6 Hz, 2H, CH_2Ph), 5.12 (m, 1H, AspHα), 6.81 (t, J = 7.6 Hz, 1H, ArH), 7.02-7.14 (m, 4H, ArH), 7.15-7.26 (m, 3H, ArH), 7.35 (t, J = 8.4 Hz, 2H, ArH), 7.58 (s, 1H, NH), 7.79 (d, J = 8.4 Hz, 1H, ArH), 7.81 (br.t, 1H, NH$_>$), 7.85 (br.t, 1H, NH$_<$), 8.40 (d, J = 7.6 Hz, 1H, AspNH$_<$), 8.55 (d, J = 7.6 Hz, 1H, AspNH$_>$), 8.62 (s, 1H, NH$_>$), 8.64 (s, 1H, NH$_<$). Elem. Anal. for $C_{31}H_{31}Cl_2N_5O_6$, calcd C 58.13, H 4.88, N 10.93 found C 57.00, H 4.81, N 10.15; ESI-MS *m/z* 640.1 $(M+H)^+$, calcd 640.2

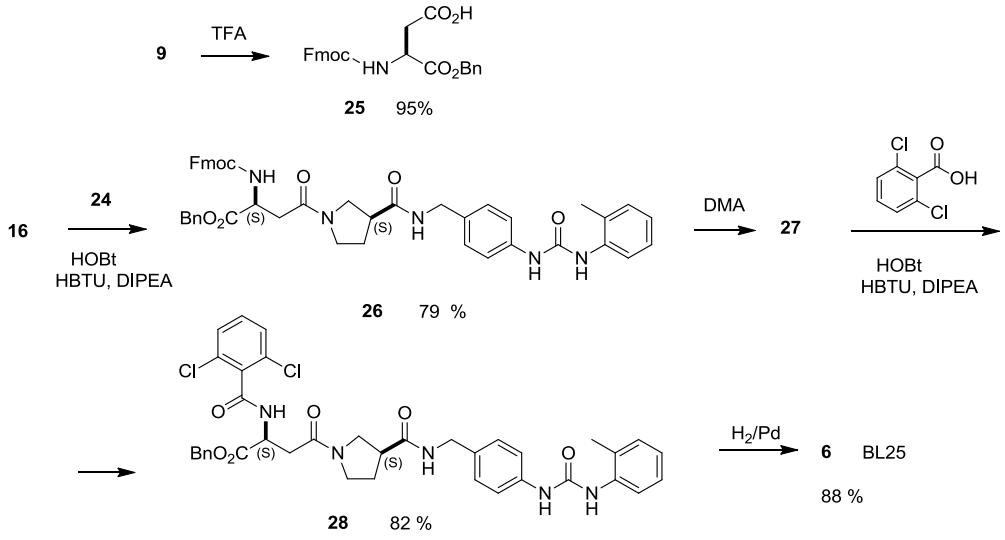

Scheme 5. Synthesis of **6**.

Synthesis of **26**. *Fmoc-Asp(Ot-Bu)-OBn* (**9**) (0.20 g, 0.39 mmol) was deprotected as described for **12**, giving **25** in quantitative yield. ESI-MS *m/z* 640.1 $(M+H)^+$, calcd 640.2. Crude **25** was coupled with **16** (0.13 g, 0.38 mmol) as described in the main text (Peptide coupling, general procedure). The residue was purified by flash chromatography over silica-gel (eluant EtOAc/cyclohexane 8:2) giving **26** (0.23 g, 79 %). ^{1}H NMR (95:5 $CDCl_3$/DMSO-d6, 400 MHz) δ (ppm): (two sets of resonances: > = major conformer; < = minor conformer) 1.99 (m, 2H, PyrrolidineH-4$_<$), 2.10 (m,

2H, PyrrolidineH-4$_{>}$), 2.20 (s, 3H, CH_3Ph), 2.66 (m, 1H, AspHβ), 2.90 (m, 1H, PyrrolidineH-3), 2.99 (m, 1H, AspHβ), 3.30 (m, 1H, PyrrolidineH-5$_{<}$), 3.42-3.60 (m, 4H, PyrrolidineH-2$_{>}$+PyrrolidineH-5$_{□}$+PyrrolidineH-5$_{>}$), 3.64 (m, 1H, PyrrolidineH-2$_{<}$), 4.00-4.13 (m, 2H, PyrrolidineH-5$_{>}$+PyrrolidineH-2$_{<}$), 4.20-4.40 (m, 5H, CH_2Ph+Fmoc), 4.61 (m, 1H, AspHα), 5.10 (br.s, 2H, CH_2Ph), 6.47 (br.d, 1H, AspNH$_{>}$), 6.52 (br.d, 1H, AspNH$_{<}$), 6.89 (br.t, 1H, ArH), 7.00-7.20 (m, 4H, ArH), 7.20-7.30 (m, 7H, ArH+NH), 7.30-7.40 (m, 4H, ArH), 7.45-7.55 (m, 3H, ArH), 7.70 (br.d, 2H, ArH), 7.75-7.82 (m, 2H, ArH+NH), 8.59 (s, 1H, NH); ESI-MS *m/z* 780.2 $(M+H)^+$, calcd 780.3

Synthesis of **28**. Fmoc deprotection of **26** (0.23 g, 0.30 mmol) was performed for the preparation of **10,** giving **27** in quantitative yield. ESI-MS *m/z* 558.2 $(M+H)^+$, calcd 558.3. The resulting crude **27** was coupled with 2,6-dichlorobenzoic acid (0.057 g, 0.30 mmol) as described in the main text (Peptide coupling, general procedure). The residue was purified by flash chromatography over silica-gel (eluant EtOAc) giving **28** (0.18 g, 82 %). ^{1}H NMR ($CDCl_3$, 200 MHz) δ (ppm): (two sets of resonances: > = major conformer; < = minor conformer) 1.90 (m, 2H, PyrrolidineH-4$_{<}$), 2.10 (m, 2H, PyrrolidineH-4$_{>}$), 2.15 (s, 3H, CH_3Ph), 2.55 (m, 1H, AspHβ), 2.90-3.00 (m, 2H, PyrrolidineH-3+AspHβ), 3.20 (m, 1H, PyrrolidineH-5$_{<}$), 3.37-3.58 (m, 3H, PyrrolidineH-2$_{>}$+PyrrolidineH-5$_{<}$+PyrrolidineH-5$_{□}$), 3.59-3.89 (m, 3H, PyrrolidineH-2$_{>}$+PyrrolidineH-2$_{<}$+PyrrolidineH-5$_{>}$), 4.10-4.27 (m, 3H, PyrrolidineH-2$_{<}$+CH_2Ph), 4.98-5.18 (m, 3H, CH_2Ph+AspHα), 6.90 (br.t, 1H, ArH), 7.01-7.14 (m, 8H, ArH+NH), 7.15-7.26 (m, 6H, ArH+AspNH), 7.26-7.34 (m, 3H, ArH+NH), 7.70 (m, 2H, ArH+NH); ESI-MS *m/z* 730.1. $(M+H)^+$, calcd 730.2

Synthesis of **6. 28** (0.18 g, 0.24 mmol) was deprotected as described for **4**. The residue was purified by semi-preparative RP-HPLC (general methods) giving **6** (0.14 g, 88 %). ^{1}H NMR (DMSO-d6, 400 MHz) δ (ppm): (two sets of resonances: > = major conformer; < = minor conformer) 1.95 (m, 2H, PyrrolidineH-4$_{<}$), 2.05 (m, 2H, PyrrolidineH-4$_{>}$), 2.29 (s, 3H, CH_3Ph), 2.56 (m, 1H, AspHβ), 2.92-2.98 (m, 2H, PyrrolidineH-3+AspHβ), 3.25 (m, 1H, Proδ$_{<}$), 3.47 (m, 1H, PyrrolidineH-2$_{>}$), 3.60 (m, 2H, PyrrolidineH-5$_{<}$+PyrrolidineH-5$_{>}$), 3.69-3.79 (m, 2H, Proα$_{>}$+Proα$_{<}$), 3.99 (m, 1H, Proδ$_{>}$), 4.11 (m, 1H, Proα$_{<}$), 4.27 (br.s, 2H, CH_2Ph), 5.09 (m, 1H, AspHα), 6.81 (br.t, 1H, ArH), 7.01-7.14 (m, 4H, ArH), 7.15-7.26 (m, 3H, ArH), 7.27-7.35 (m, 2H, ArH), 7.52 (s, 1H, NH), 7.70 (d, J = 8.4 Hz, 1H, ArH), 7.75 (br.t, 1H, NH$_{>}$), 7.81 (br.t, 1H, NH$_{<}$), 8.20 (br.d, 1H, AspNH$_{<}$), 8.25 (br.d, 1H, AspNH$_{>}$), 8.51 (s, 1H, NH); ^{13}C NMR ($CDCl_3$) δ (ppm): 18.2, 28.4, 29.5, 39.4, 42.7, 48.7, 49.0, 51.2, 118.6, 121.8, 124.1, 127.0, 128.6, 129.5, 131.0, 131.4, 132.8, 133.8, 136.6, 136.8, 138.0, 153.4, 167.4, 171.2, 172.0, 173.1. Elem. Anal. for $C_{31}H_{31}Cl_2N_5O_6$, calcd C 58.13, H 4.88, N 10.93 found C 57.60, H 4.79, N 11.13; ESI-MS *m/z* 640.1 $(M+H)^+$, calcd 640.2

8.4.3. Scintillation proximity-binding assay (SPA)

We developed a SPA assay to detect competitive binding of drugs to soluble ^{125}I-human FN (Mw approximately 440 kDa) bound to an antibody-captured integrin complex.[46,47] The assay uses microspheres coated with an anti-rabbit IgG antibody capable of binding the complex α_4 integrin anti-α_4 antibody. The radioligand binds to the $\alpha_4\beta_1$ integrin and the close proximity of the isotope to the scintillant incorporated in the beads allows the radiation energy to transfer to the scintillant where it can be detected as counts per min (cpm).

Materials employed for Scintillation proximity-binding assay (SPA) and cell adhesion assays. Cell culture media, phosphate-buffered saline (PBS) and fetal bovine serum (FBS) were from Lonza (Euroclone S.p.A, Milan, Italy); HBSS and chloromethylfluorescein diacetate (CMFDA) were from Invitrogen (Carlsbad, CA, USA). Lectin from Triticus vulgaris, soluble fibronectin (FN) from human plasma were purchased from Sigma-Aldrich (Steinheim, Germany). Jurkat clone E6.1 was obtained from the European Cell Culture Collection (ECACC, Wiltshire, UK); SK-MEL-24 cell line was from American Type Culture Collection (ATCC, Manassas, VA, USA).

Black 96-well clear-bottom plates were purchased from Corning Costar (Celbio, Milan, Italy). Soluble human VCAM-1 was purchased from R&D Systems (Minneapolis, MN, USA). BIO-1211 (N-[[4-[[[(2-methylphenyl)amino]carbonyl]amino]-phenyl]acetyl]-L-leucyl-L-aspartyl-L-valyl-L-proline) was purchased from Bachem (Weil am Rhein, Germany). Tissue Protein Extraction Reagent (TPER1) and BCA1 protein assay were purchased from Pierce (Rockford, IL, USA).

Rabbit anti-human monoclonal antibodies against the α4 subunit of α4β1 integrin was purchased from Santa Cruz Biotechnology Inc. (Santa Cruz, CA, USA). Mouse anti-human monoclonal antibody against β1 subunit (MAB 2000) was obtained from Chemicon (Millipore, Billerica, MA, USA). Secondary antibody (goat anti-mouse or goat anti-rabbit) were purchased from Santa Cruz Biotechnology Inc. Polyacrylamide gel, N,N,N0,N0-tetramethy-lethylenediamine (TEMED), ammonium persulfate (PSA) and SDS were purchased from Sigma-Aldrich. Hybond-

ECL Nitrocellulose Membrane was from Amersham Biosciences (GE Healthcare Europe, Milan, Italy). $Na^{125}I$ was obtained from PerkinElmer Inc., Waltham, Massachussets, USA). Polyvinyltoluene (PVT) anti-rabbit binding beads were supplied by Amersham Biosciences as a powder and reconstituted in distilled water. Plastic disposables were from Sarstedt (Verona, Italy). All other reagents were of analytical grade or the highest purity available, purchased from Sigma.

Scintillation proximity-binding assay (SPA). The radioligand binds to the α4β1 integrin and the close proximity of the isotope to the scintillant incorporated in the beads allows the radiation energy to transfer to the scintillant where it can be detected as counts per min (cpm). FN was labeled with Na[^{125}I] using the IodogenKit, as specified by the manufacturer (Pierce). ^{125}I-FN was purified from unincorporated iodine by gel filtration chromatography on PD-10 columns; trichloroacetic acid-precipitable radioactivity was $6.30x10^{10}$ μCi/mol. The experiments were carried out in scintillation vials; in each vial 1mg/50 μl anti-rabbit-coated beads, 400 ng of rabbit anti-α4 integrin antibody and a portion of cell eluate (containing approximately 100 μg of α4β1 integrin) were added. The α4β1integrin was extracted from Jurkat cells (cultured in RPMI 1640 medium, supplemented with L-glutamine, 10% FBS, antibiotic-antimicotycotic solution and kept in a humidified incubator at 37°C in a 5% CO_2 atmosphere). The cells were collected and then cytoplasmic proteins were extracted with the T-PER extraction buffer and α4β1 integrin was purified by affinity chromatography, as described.[56] For Western blot experiments on extracts we used antibodies against α4 and β1 integrin subunits to confirm that both integrins partitioned to the cell lysate collected from the affinity column. The binding buffer contained Tris-HCl 25 mM pH 7,5; $CaCl_2$ 1 mM; $MgCl_2$ 1 mM; $MnCl_2$ 1mM; BSA 2% (w/v); phenylmethanesulfonyl fluoride (PMSF) 1 mM; aprotinin 1 mg/ml; leupeptin 50 mM.
First, we allowed for the slow interaction between the α4 integrin protein and the compound under examination by incubating together for 1,5 hr at room temperature. Then we added the rabbit anti-human α4 integrin antibody, followed by an incubation time of 2 hours at 4°C. From this point on, all incubations were conducted at room temperature Then the anti-rabbit antibody binding beads were added, and the solution containing the four components was incubated for 2 h at room in the dark. ^{125}I-FN was added to the vials, which were then incubated overnight on a shaker in the dark.
The samples were read using a LS 6500 multipurpose scintillation counter (Beckham Coulter, Fullerton, CA, USA). The SPA procedure was optimized in preliminary experiments, as described.[57] As shown in Figure 4, western blot analysis of cell lysates, purified by a chromatographic technique already reported,[56] confirmed that both α4 and β1 integrin subunits were present in the eluate employed for the SPA. Specific binding of ^{125}I-FN to an antibody-captured α4β1 integrin was time-dependent; the signal increasing during the first 10 h, then reaching a plateau and remaining constant for the remainder of the 24 h incubation (data not shown). The relatively slow kinetics of the SPA may require the establishment of equilibrium between the different components.[58,59]

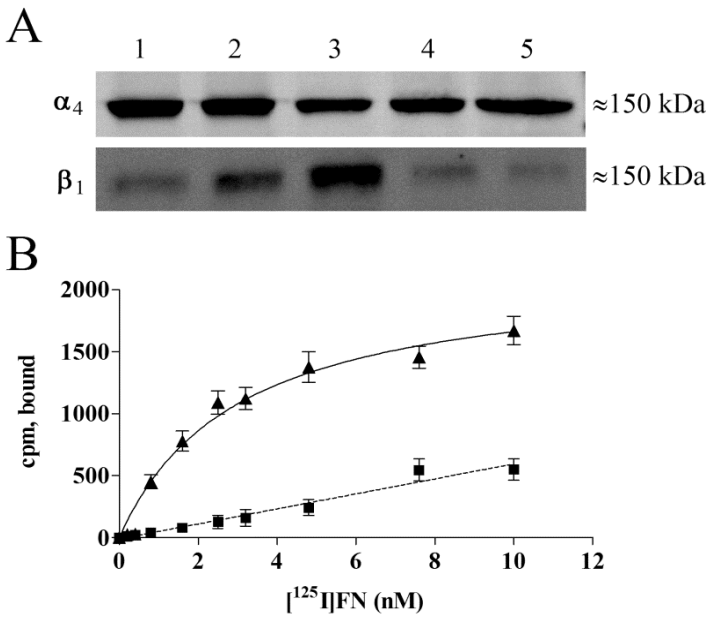

Figure 4. A. Representative autoradiogram of Western blot experiments to evaluate the α4 and β1 integrin subunits in cell lysates of Jurkat E6.1 cells endogenously expressing α4β1 integrin. The lysates were purified by affinity chromatography and fractions of approximately 0.5 ml were collected; the presence of the α4 or β1 integrin subunit was evaluated by Western blotting. **1**: total lysate; **2-5**: four eluted fractions. Fractions 2-5 were used for SPA. B. Saturation SPA binding of ^{125}I-FN to the purified α4β1 integrin extracted from Jurkat E6.1 cells and incubated with increasing concentrations of the radioligand (cpm) as described in Materials and Methods section. Nonspecific binding was determined in the presence of 100 mM unlabeled fibronectin. (■) Non-specific binding; (▲) specific binding obtained by subtraction of the non-specific binding from total binding counts. Mean ± S.E.M. of three experiments done in triplicate.

8.4.4. Adhesion assays

Jurkat cell adhesion assays were done was as described.[56,60] Briefly, 96-well plates were coated at 4°C overnight with 2 μg/ml of VCAM-1 and a saturation curve for the ligand was plotted to establish the best signal-to-noise ratio. Non-specific hydrophobic binding sites were blocked by incubation with a BSA 1%/HBSS (w/v) solution for 30 min at 37°C. The day of the assay, the cells were counted and stained with 12.5 μM CMFDA (30 min at 37°C). After three rinses with BSA/HBSS to wash away the excess dye, aliquots of 500,000 (Jurkat) cells were divided among a number of tubes corresponding to the number of treatments. For inhibition experiments, cells were mixed with the drug and pre-incubated at 37°C for 30 min to reach equilibrium before being plated. After 30 min incubation at 37°C in the coated wells, the non-specifically bound cells were washed away with BSA/HBSS solution. Adherent cells were lysed by the addition of 0.5% Triton-X-100 in PBS (30 min at 4°C). Released CMFDA was quantified by fluorescence imaging at Ex485 nm/Em535 nm (Wallac ARVO 1420 multilabel counter) and adherent cells was counted by interpolation on a standard curve. The fluorescence intensity with and without VCAM-I was taken as respectively 100% and 0%. Alternatively, the number of adherent cells was calculated by comparison with a standard curve prepared in the same plate using known concentrations of labeled cells.

SK-MEL-24 cell adhesion assays were carried out as described.[61] 96-well plates were coated by passive adsorption with FN (10 μg/ml) or nonspecific substrate poly-l-lysine (0.002 %) overnight at 4°C. Cells (routinely grown in minimum essential medium supplemented with 10% FBS, nonessential amino acids, and sodium pyruvate) were counted with a hemocytometer and pre-incubated with various concentrations of each compound for 30 min at room temperature to reach a ligand–receptor equilibrium. At the end of the incubation time, the cells were plated (50000 cells per well) and incubated at room temperature for 1 h. All the wells were then washed with PBS to remove nonadherent cells, and 50 μL hexosaminidase [4-nitrophenyl-N-acetyl-β-d-glucosaminide dissolved at a concentration of 7.5 mM in 0.09 M citrate buffer (pH 5) and mixed with an equal volume of 0.5% Triton X-100 in H_2O] was added. This product is a chromogenic substrate for β-N-acetylglucosaminidase, whereby it is transformed into 4-nitrophenol; absorbance was measured at 405 nm. The reaction was blocked by the addition of 100 μL of a stopping solution [50

mM glycine and 5 mM EDTA (pH 10.4)], and the plates were read in a Victor2 Multilabel Counter (PerkinElmer, Waltham, MA, USA).
The efficacy of putative antagonists (at least eight different concentrations were used) was determined by the reduction in adherent cells compared to the untreated control. Each experiment was conducted in quadruplicate and the data are presented as the mean ± S.E.M. of at least three independent assays.

8.4.5. Data analysis.

All data are expressed as mean ± S.E.M., for the number of experiments indicated. SPA binding data and ligand concentration-response curves were analyzed using GraphPad software (GraphPad Software Inc., San Diego, CA, USA). IC_{50} values indicate the molar ligand concentration required to inhibit the response by 50% and were converted, in SPA experiments, to Ki values using the method of Cheng and Prusoff.[62]

8.4.6. In vitro metabolic stability

Enzymatic degradation studies of **1**, **3**, and **4** were carried out in triplicate and repeated three times using mouse serum purchased from Sigma-Aldrich. Peptides were dissolved in Tris buffer pH 7.4 and 10 μL aliquots of a 10 mM peptide stock solution were added to 190 μL of serum. Incubations were carried out at 37°C for 120 min. Aliquots of 20 μL were withdrawn from the incubation mixtures and enzyme activity was terminated by precipitating proteins with 90 μL of glacial acetonitrile. Samples were then diluted with 90 μL of 0.5% acetic acid to prevent further enzymatic breakdown and centrifuged at 13,000×g for 15 min. The supernatants were collected and the stability of peptides was determined by RP-HPLC ESI-MS analysis.

8.4.7. Conformational analysis

The unambiguous assignment of ^{1}H-NMR resonances was performed by 2D gCOSY. 2D ROESY experiments were recorded in 8:2 DMSO-d_6/H_2O, with a 250 ms mixing time with a proton spectral width of 3088 Hz. Peaks were calibrated on DMSO. Only ROESY-derived constraints (force constant: 7 kcal mol^{-1}Å^{-2}) were included in the restrained molecular dynamics. Cross-peak intensities were classified very strong, strong, medium, and weak, and were associated with distances of 2.2, 2.6, 3.0, and 4.5 Å, respectively. Geminal couplings and other obvious correlations were discarded. The ω bonds were set at 180° (16 kcal mol^{-1}Å^{-2}). The restrained MD simulations were conducted using the AMBER force field in a 45×45×45 Å box of standard TIP3P models of equilibrated water.

NMR analysis. ^{1}H-NMR spectra were recorded at 400 MHz or 200 MHz in 5 mm tubes using 0.01 M peptide at r.t. ^{1}H NMR spectra of the peptides in $CDCl_3$ at 298 K were poorly resolved with very broad resonances, so the experiments were recorded in mixtures of $CDCl_3$ and DMSO-d_6; in particular, the NMR experiments on **3** and **4** were performed in the biomimetic 8:2 DMSO-d_6/H_2O. The unambiguous assignment of ^{1}H-NMR resonances was done by 2D gCOSY, conducted with a proton spectral width of 3103 Hz. 2D spectra were recorded in the phase sensitive mode and processed using a 90°-shifted, squared sine-bell apodization. 2D ROESY experiments of **3** and **4** were recorded in 8:2 DMSO-d_6/H_2O, with a 250 ms mixing time with a proton spectral width of 3088 Hz. Peaks were calibrated on DMSO. The ^{1}H-NMR of both **3** and **4** revealed two sets of resonances, in about 1:1 ratio, suggestive of a slow equilibrium between the cis and trans conformers of the peptide bond between Asp or *iso*Asp and β-Pro. The cis conformations were assigned by detection of the NOE cross peaks between AspHα (**3**) or *iso*AspHβ (**4**) and β-PyrrolidineH-2, while the trans conformations were deduced by detection of the NOE cross peaks between AspHα (**3**) or *iso*AspHβ (**4**) and β-*iso*PyrrolidineH-5.

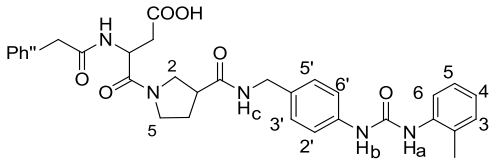

Table 2. Non-obvious ROESY cross-peaks observed for cis-**3**.[a,b,c]

Cross peak[b]	Intensity[c]	Cross peak[b]	Intensity[c]
NHb-NHa	vs	NHb-Ar$H_{2',6'}$	vs
NHb-Ar$H_{3',5'}$	w	NHb-Me	w
AspNH-AspHα	m	AspNH-CH_2Ph''	s
AspNH-AspHβ$_{dw}$	m	AspNH-AspHβ$_{up}$	m
NHc-Ar$H_{3',5'}$	m	NHc-CH_2Ph'	s
NHc-PyrrolidineH-2$_{up,un}$	w	NHc-PyrrolidineH-3	s
NHc-PyrrolidineH-4$_{dw,on}$	w	NHc-PyrrolidineH-4$_{up,un}$	w
NHa-Me	s	Ph''-AspHα	w
Ar$H_{3',5'}$-PyrrolidineH-2$_{up,un}$	w	Ar$H_{3',5'}$-PyrrolidineH-4$_{dw,on}$	w
AspHα-PyrrolidineH-2$_{dw,on}$	vs	AspHα-PyrrolidineH-2$_{up,un}$	s
AspHα-AspHβ$_{dw}$	s	AspHα-AspHβ$_{up}$	vs
CH_2Ph'-PyrrolidineH-4$_{dw,on}$	w	AspHα-CH_2Ph''	m
CH_2Ph'-AspHβ$_{dw}$	w	CH_2Ph'-PyrrolidineH-4$_{up,un}$	w
β-PyrrolidineH-2$_{dw,on}$-AspHβ$_{up}$	w	β-PyrrolidineH-2$_{dw,on}$-AspHβ$_{dw}$	w

[a] up = upfield; dw = downfield; [b] on = same side of Hβ; un = opposite side of Hβ; [c] vs = very strong, s = strong, m = medium, w =weak.

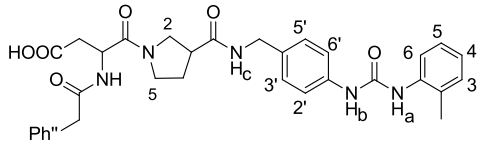

Table 3. Non-obvious ROESY cross-peaks observed for all-trans-**3**.[a,b]

Cross peak[a,b]	Intensity[c]	Cross peak[b]	Intensity[c]
NHb-NHa	vs	NHb-Ar$H_{6'}$	vs
NHb-Ar$H_{5'}$	w	NHb-Me	w
AspNH-AspHα	m	AspNH-CH_2Ph''	s
AspNH-PyrrolidineH-2$_{up,un}$	w	AspNH-AspHβ$_{dw}$	m
AspNH-AspHβ$_{up}$	m	NHc-Ar$H_{3',5'}$	m
NHc-CH_2Ph'	s	NHc-PyrrolidineH-2$_{up,un}$	w
NHc-PyrrolidineH-3	s	NHc-PyrrolidineH-4$_{dw,on}$	w
NHc-PyrrolidineH-4$_{up,un}$	w	NHa-Me	s
Ph''-AspHα	w	Ar$H_{3',5'}$-PyrrolidineH-3	w
Ar$H_{3',5'}$-PyrrolidineH-4$_{up,un}$	w	AspHα-PyrrolidineH-5$_{dw,un}$	s
AspHα-PyrrolidineH-5$_{up,on}$	s	AspHα-PyrrolidineH-2$_{up,un}$	w
AspHα-AspHβ$_{dw}$	s	AspHα-AspHβ$_{up}$	s

CH_2Ph'-PyrrolidineH-$4_{dw,on}$	w	AspHα-CH_2Ph''	m
CH_2Ph'-AspHβ_{dw}	w	CH_2Ph'-PyrrolidineH-$4_{up,un}$	w
β-PyrrolidineH-$5_{dw,un}$-AspHβ_{up}	w	CH_2Ph'-PyrrolidineH-3	w

[a] up = upfield; dw = downfield; [b] on = same side of Hβ; un = opposite side of Hβ; [c] vs = very strong, s = strong, m = medium, w =weak.

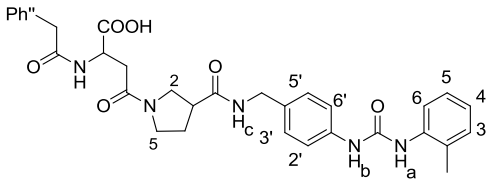

Table 4. Non-obvious ROESY cross-peaks observed for cis-**4**.[a,b]

Cross peak[a,b]	Intensity[c]	Cross peak[b]	Intensity[c]
NHb-NHa	vs	NHb-$ArH_{6'}$	vs
NHb-$ArH_{5'}$	w	NHb-Me	w
AspNH-AspHα	m	AspNH-CH_2Ph''	s
AspNH-AspHβ_{dw}	m	AspNH-AspHβ_{up}	m
NHc-$ArH_{3',5'}$	m	NHc-CH_2Ph'	s
NHc-PyrrolidineH-$2_{up,un}$	m	NHc-PyrrolidineH-3	vs
NHc-PyrrolidineH-$4_{dw,on}$	w	NHa-Me	vs
Ph''-AspHα	w	$ArH_{3',5'}$-PyrrolidineH-3	w
$ArH_{3',5'}$-PyrrolidineH-$4_{up,un}$	w	AspHα-AspHβ_{dw}	s
AspHα-AspHβ_{up}	s	AspHα-CH_2Ph''	m
CH_2Ph'-PyrrolidineH-$4_{dw,on}$	w	CH_2Ph'-PyrrolidineH-$4_{up,un}$	w
CH_2Ph'-AspHβ_{dw}	w	CH_2Ph'-PyrrolidineH-3	w
β-PyrrolidineH-$5_{dw,un}$-AspHβ_{up}	w	AspHβ_{dw}-PyrrolidineH-$2_{dw,on}$	s
AspHβ_{dw}-PyrrolidineH-$2_{up,un}$	s	AspHβ_{up}-PyrrolidineH-$2_{dw,on}$	s
AspHβ_{up}-PyrrolidineH-$2_{up,un}$	s		

[a] up = upfield; dw = downfield; [b] on = same side of Hβ; un = opposite side of Hβ; [c] vs = very strong, s = strong, m = medium, w =weak.

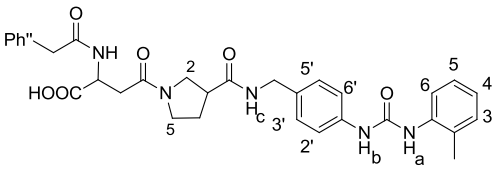

Table 5. Non-obvious ROESY cross-peaks observed for trans-**4**.[a,b]

Cross peak[a,b]	Intensity[c]	Cross peak[b]	Intensity[c]
NHb-NHa	vs	NHb-$ArH_{6'}$	vs
NHb-$ArH_{5'}$	w	NHb-Me	w
AspNH-AspHα	m	AspNH-CH_2Ph''	s
AspNH-AspHβ_{dw}	s	AspNH-AspHβ_{up}	s
NHc-$ArH_{3',5'}$	m	NHc-CH_2Ph'	s
NHc-PyrrolidineH-$2_{up,un}$	m	NHc-PyrrolidineH-3	vs

NHc-PyrrolidineH-$4_{dw,on}$	w	NHa-Me	vs
Ph''-AspHα	w	$ArH_{3',5'}$-PyrrolidineH-3	w
$ArH_{3',5'}$-PyrrolidineH-$4_{up,un}$	w	AspHα-AspHβ_{dw}	s
AspHα-AspHβ_{up}	s	AspHα-CH_2Ph''	s
CH_2Ph'-PyrrolidineH-$4_{dw,on}$	w	CH_2Ph'-PyrrolidineH-$4_{up,un}$	w
CH_2Ph'-AspHβ_{dw}	w	CH_2Ph'-PyrrolidineH-3	w
AspHβ_{dw}-PyrrolidineH-$5_{dw,un}$	s	AspHβ_{dw}-PyrrolidineH-$2_{up,on}$	s
AspHβ_{up}-PyrrolidineH-$5_{dw,un}$	s	AspHβ_{up}-PyrrolidineH-$5_{up,on}$	s

[a] up = upfield; dw = downfield; [b] on = same side of Hβ; un = opposite side of Hβ; [c] vs = very strong, s = strong, m = medium, w =weak.

Restrained molecular dynamics. Molecular conformations were investigated by 2D ROESY and restrained molecular dynamics. The intensities of the cross-peak were ranked to infer plausible inter-proton distances as restraints (Tables 2-5). Only ROESY-derived constraints were included in the restrained molecular dynamics. Cross-peak intensities were classified very strong, strong, medium, and weak, and were associated with distances of 2.2, 2.6, 3.0, and 4.5 Å, respectively. Geminal couplings and other obvious correlations were discarded. The ω bonds were set at 180° (force constant: 16 kcal $mol^{-1}Å^{-2}$).

The restrained MD simulations[63] were conducted using the AMBER [64] force field in a 45×45×45 Å box of standard TIP3P models of equilibrated water.[65] All water molecules with atoms that come closer than 2.3 Å to a solute atom were deleted. A 100 ps simulation at 1200 °K was used for generating 50 random structures that were subsequently subjected to a 50 ps restrained MD with a 50% scaled force field at the same temperature, followed by 50 ps with full restraints (distance force constant of 7 kcal mol^{-1} $Å^{-2}$), after which the system was cooled in 20 ps to 50°K. H-bond interactions were not included, nor were torsion angle restraints. The resulting structures were minimized with 3000 cycles of steepest descent and 3000 cycles of conjugated gradient (convergence of 0.01 kcal $Å^{-1}$ mol^{-1}). The backbones of the structures were clustered by the rmsd analysis module.[63]

To investigate the dynamic behavior, the ROESY-restrained structures were analyzed by unrestrained MD for 10 ns in a 45×45×45 Å box of explicit, equilibrated water molecules, at 298 °K, constant temperature and pressure (Berendsen scheme,[66] bath relaxation constant of 0.2). For 1-4 scale factors, van der Waals and electrostatic interactions are scaled in AMBER to half their nominal value. The integration time step was set to 0.1 fs.

References

1 D.M. Rose, R. Alon, M.H. Ginsberg, *Immunol. Rev*. 218 (**2007**) 126.
2 J. Singh, S. Adams, M.B. Carter, H. Cuervo, W.C. Lee, R.R. Lobb, R.B. Pepinsky, R. Petter, D. Scott,. Curr. Top. Med. Chem. 4 (2004) 1497.
3 P. Vanderslice, D.G. Woodside, Prog. Resp. Res. 39 (2010) 169.
4 R.Gonzalez-Amaro, M. Mittelbrunn, F. Sanchez-Madrid, Immunology 116 (2005) 289.
5 P.S. Rommer, R. Patejdl, U.K. Zettl, Curr. Pharm. Des. 18 (2012) 4498.
6 D.Y. Jackson, Curr. Pharm. Des. 8 (2002) 1229.
7 G.X. Yang, W.K. Hagmann, Med. Res. Rev. 23 (2003) 369.
8 K. Lin, H.S. Ateeq, S.H. Hsiung, L.T. Ching, C.N. Zimmerman, A. Castro, W.C. Lee, C.E. Hammond, S. Kalkunte, L.L. Chen, R.B. Pepinsky, D.R. Leone, A.G. Sprague, W.M. Abraham, A. Gill, R.R. Lobb, S.P. Adams, J. Med. Chem. 42 (1999) 920.
9 G.T. Bolger, BIO-1211 (Biogen). IDrugs 3 (2000) 536.
10 P.C. Astles, N.V. Harris, A.D. Morley, Bioorg. Med. Chem. 9 (2001) 2195.
11 B.V. Karanam, A. Jayra, M. Rabe, Z. Wang, C. Keohane, J. Strauss, S. Vincent, Xenobiotica 37 (2007) 487.
12 A.L. Fisher, E. DePuy, A. Jayaraj, C. Raab, M. Braun, M. Ellis-Hutchings, J. Zhang, J.D. Rogers, D.G. Musson, J. Pharm. Biomed. Anal. 27 (2002) 57.
13 J. Singh, H. Van Vlijmen, Y. Liao, W.C. Lee, M. Cornebise, M. Harris, I. Shu, A. Gill, J.H. Cuervo, W.M. Abraham, S.P. Adams, J. Med. Chem. 45 (2002) 2988.
14 I. Sircar, K.S. Gudmundsson, R. Martin, J. Liang, S. Nomura, H. Jayakumar, B.R. Teegarden, D.M. Nowlin, P.M. Cardarelli, J.R. Mah, S. Connell, R.C. Griffith, E. Lazarides, Bioorg. Med. Chem. 10 (2002) 2051.
15 M. Barczyk, S. Carracedo, D. Gullberg, Cell Tissue Res. 339 (2010) 269.
16 A.P. Mould, A. Komoriya, K.M. Yamada, M.J. Humphries, J. Biol. Chem. 266 (1991) 3579.

[17] P.M. Cardarelli, R.R. Cobb, D.M. Nowlin, W. Scholz, F. Gorcsan, M. Moscinski, M. Yasuhara, S.L. Chiang, T.J. Lobl, J. Biol Chem. 269 (1994) 18668.

[18] D.M. Nowlin, F. Gorcsan, M. Moscinski, T. Chiang, T.J. Lobl, P.M. Cardarelli, J. Biol. Chem. 268 (1993) 20352.

[19] D.Y. Jackson, C. Quan, D.R. Artis, T. Rawson, B. Blackburn, M. Struble, G. Fitzgerald, K. Chan, S. Mullins, J.P. Burnier, W.J. Fairbrother, K. Clark, M. Berisini, H. Chui, M. Renz, S. Jones, S. Fong, J. Med. Chem. 40 (1997) 3359.

[20] S. Elitok, S.V. Brodsky, D. Patschan, T. Orlova, K.M. Lerea, P. Chander, M.S. Goligorsky. Am. J. Physiol. Renal Physiol. 290 (2006) F159-F166.

[21] C. Henry, N. Moitessier, Y. Chapleur, Mini Rev. Med. Chem. 2 (2002) 531.

[22] A. Perdih, M. Sollner Dolenc, Curr. Med. Chem. 17 (2010) 2371.

[23] J. Wermuth, S.L. Goodman, A. Jonczyk, H. Kessler, J. Am. Chem. Soc. 119 (1997) 1328.

[24] L. Gentilucci, G. Cardillo, S. Spampinato, A. Tolomelli, F. Squassabia, R. De Marco, A. Bedini, M. Baiula, L. Belvisi, M. Civera, J. Med. Chem. 53 (2010) 106.

[25] A.O. Frank, E. Otto, C. Mas-Moruno, H.B. Schiller, L. Marinelli, S. Cosconati, A. Bochen, D. Vossmeyer, G. Zahn, R. Stragies, E. Novellino, H. Kessler, Angew. Chem. Int. Ed. 49 (2010) 9278.

[26] A. Bochen, U.K. Marelli, E. Otto, D. Pallarola, C. Mas-Moruno, F.S. Di Leva, H. Boehm, J.P. Spatz, E. Novellino, H. Kessler, L. Marinelli, J. Med. Chem. 56 (2013) 1509.

[27] F. Curnis, R. Longhi, L. Crippa, A. Cattaneo, E. Donossola, E. Bachi, A. Corti, J. Biol. Chem. 281 (2006) 36466.

[28] V. Takahashi, M. Leiss, M. Moser, T. Ohashi, T. Kitao, D. Heckmann, A. Pfeifer, H. Kessler, J. Takagi, H.P. Erickson, R. Fässler, J. Cell Biol. 178 (2007) 167.

[29] J. Xu, L.M. Maurer, B.R. Hoffmann, D.S. Annis, D.F. Mosher, J. Biol. Chem. 285 (2010) 8563.

[30] A. Spitaleri, M. Ghitti, S. Mari, L. Alberici, C. Traversari, G.P. Rizzardi, G. Musco, Angew. Chem. Int. Ed. 50 (2011) 1832.

[31] M. Ghitti, A. Spitaleri, B. Valentinis, S. Mari, C. Asperti, C. Traversari, G.P. Rizzardi, G. Musco, Angew. Chem. Int., Ed. 51 (2012) 7702.

[32] M. Mingozzi, A. Dal Corso, M. Marchini, I. Guzzetti, M. Civera, U. Piarulli, D. Arosio, L. Belvisi, D. Potenza, L. Pignataro, C. Gennari, Chem. Eur. J. 19 (2013) 3563.

[33] J. Singh, H. van Vlijmen, W.C. Lee, Y. Liao, K.C. Lin, H. Ateeq, J. Cuervo, v C. Zimmerman, C. Hammond, M. Karpusas, R. Palmer, T. Chattopadhyay, S.P. Adams, J. Comp. Aid. Mol. Des. 16 (2002) 201.

[34] S. Thangapandian, S. John, S. Sakkiah, K.W. Lee, Chem. Biol. Drug Des. 78 (2011) 289.

[35] HyperChem Release 8.0.3, 2012, Hypercube Inc. 1115 NW 4th St. Gainesville, FL 32608 (USA).

[36] J. Witherington, V. Bordas, A. Gaiba, P.M. Green, A. Naylor, N. Parr, D.G. Smith, A.K. Taklea, R.W. Ward, Bioorg. Med. Chem. Lett. 16 (2006) 2256.

[37] L. Gentilucci, R. De Marco, L. Cerisoli, Curr. Pharm. Des. 16 (2010) 3185.

[38] B.R. Huck, J.M. Langenhan, S.H. Gellman, Org. Lett. 1 (1999) 1717.

[39] L.M. Sandvoss, H.A. Carlson, J. Am. Chem. Soc. 125 (2003) 15855.

[40] G. Lelais, D. Seebach, Biopolymers 76 (2004) 206.

[41] Enantioselective Synthesis of β-Amino Acids, 2nd ed.; Juaristi, E., Soloshonok, V., Eds.; Wiley-VCH: New York, 2005.

[42] A. Tolomelli, L. Gentilucci, E. Mosconi, A. Viola, E. Paradisi, Amino Acids 41 (2011) 575.

[43] G. Cardillo, L. Gentilucci, A. Tolomelli, M. Calienni, A.R. Qasem, S. Spampinato, Org. Biomol. Chem. 1 (2003) 1498.

[44] A. Tolomelli, L. Gentilucci, E. Mosconi, A. Viola, S.D. Dattoli, M. Baiula, S. Spampinato, L. Belvisi, M. Civera, ChemMedChem 6 (2011) 2264.

[45] A. Macchiarulo, G. Costantino, M. Meniconi, K. Pleban, G. Ecker, D. Bellocchi, R. Pellicciari, J. Chem. Inf. Comput. Sci. 44 (2004) 1829.

[46] A.R. Qasem, C. Bucolo, M. Baiula, A. Spartà, P. Govoni, A. Bedini, D. Fascì, S. Spampinato, Biochem. Pharmacol. 76 (2008) 751, and references herein.

[47] C. Solorzano, S. Bouquelet, M.A. Pereyra, F. Blanco-Favela, M.C. Slomianny, R. Chavez, R. Lascurain, E. Zenteno, C. Algundis, Glycoconj J. 23 (2006) 591.

[48] A. Bedini, M. Baiula, L. Gentilucci, A. Tolomelli, R. De Marco, S. Spampinato, Peptides 31 (2010) 2135.

[49] PyrrolidineH-2 and H-5 correspond to β-ProHα and β-ProHδ, respectively, in the following paper: A. Katarzyńska, M. Bilska, E. Adamek, M. Zimecki, S. Jankowski, J. Zabrocki, J. Pept. Sci. 14 (2008) 1283.

[50] P.A. Temussi, D. Picone, G. Saviano, P. Amodeo, A. Motta, T. Tancredi, S. Salvadori, R. Tomatis, Biopolymers 32 (1992) 367-372, and references herein.

[51] A. Borics, and G. Töth, Structural J. Mol. Graph. Modell. (2010) 28, 495.

[52] *For a molecular docking analysis, see:* T.J. You, D.S. Maxwell, T.P. Kogan, Q. Chen, J. Li, J. Kassir, G.W. Holland, R.A.F. Dixon, Biophys. J. 82 (2002) 447.

[53] *Also on molecular docking:* C.M. Carlevaro, J.H.M. Da Silva, W. Savino, E.R. Caffarena, J. Theor. Comp. Chem. 12 (2013) 1250108/1.

[54] A.L. Larroque, J. Dubois, S. Thoret, G. Aubert, A. Chiaroni, F. Guèritte, D. Guènard, Bioorg. Med. Chem. 15 (2007) 563.

[55] K. Lin, H.S. Ateeq, S.H. Hsiung, L.T. Ching, C.N. Zimmerman, A. Castro, W.C. Lee, C.E. Hammond, S. Kalkunte, L.L. Chen, R.B. Pepinsky, D.R. Leone, A.G. Sprague, W.M. Abraham, A. Gill, R.R. Lobb, S.P. Adams, J. Med. Chem. 42 (1999) 920.

[56] A.R. Qasem, C. Bucolo, M. Baiula, A. Spartà, P. Govoni, A. Bedini, D. Fascì, S. Spampinato, Biochem. Pharmacol. 76 (2008) 751.

[57] S. Sun, J. Almaden, T.J. Carlson, J. Barker, M.R. Gehring, Metab. Eng. 7 (2005) 38.

[58] J.A. Pachter, R. Zhang, R. Mayer-Ezell, Anal. Biochem. 230 (1995)101.

[59] Y. Takada, M.J. Elices, C. Crouse, M.E. Hemler, EMBO J. 8 (1989)1361.

[60] C. Marcinkiewicz, J.J. Calvete, M.M. Marcinkiewicz, M. Raida, S. Vijay-Kumar, Z. Huang, R.R. Lobb, S. Niewiarowski, EC3, J. Biol. Chem. 274 (1999) 12468.

[61] A. Tolomelli, L. Gentilucci, E. Mosconi, A. Viola, S.D. Dattoli, M. Baiula, S. Spampinato, L. Belvisi, M. Civera, Chem. Med. Chem. 6 (2011) 2264.

[62] Y. Cheng, W.H. Prusoff, Biochem. Pharmacol. 22 (1973) 3099.

[63] HyperChem Release 8.0.3, 2012, Hypercube Inc. 1115 NW 4th St. Gainesville, FL 32608 (USA).

[64] W.D. Cornell, P. Cieplak, C.I. Bayly, I.R. Gould, K.M. Merz, D.M. Ferguson, D.C. Spellmeyer, T. Fox, J.W. Caldwell, P.A. Kollman. J. Am. Chem. Soc. 117 (1995) 5179.

[65] W.L. Jorgensen, J. Chandrasekhar, J. Madura, R.W. Impey, M.L. Klein, J. Chem. Phys. 79 (1983) 926.

[66] H.J.C. Berendsen, J.P.M. Postma, W.F. van Gunsteren, A. Di Nola, J.R. Haak, J. Chem. Phys. 81 (1984) 3684.

Chapter 9

Synthesis of active α4β1 integrin antagonists containing Amo hybrid α/β-dipeptide scaffolds as inductor of constrained conformations

Peptidomimetics represent an attractive starting point for drug discovery programs; in particular, peptidomimetics that result from the incorporation of a heterocycle may take advantage of increased enzymatic stability and higher ability to reproduce the bioactive conformations of the parent peptides, resulting in enhanced therapeutic potential. Herein are presented mimetics of the α4β1 integrin antagonist BIO1211 (MPUPA-Leu-Asp-Val-Pro-OH), containing a aminomethyloxazolidine-2,4-dione scaffold (Amo). Interestingly, the retro-sequences PhCOAsp(OH)-Amo-APUMP including either (*S*)- or (*R*)-configured Amo displayed significant ability to inhibit the adhesion of α4β1 integrin expressing cells, and remarkable stability in mouse serum. Conformational analysis confirmed that the conformational bias exerted by the Amo scaffolds determined ligand's affinity for the receptors. These peptidomimetics could be of interest for the development of small molecule agents effective against inflammatory processes and correlated autoimmune diseases.

9.1. Introduction

Many fundamental processes associated with life are mediated by interactions of peptide ligands with protein receptors.[1] Very often, events mediated by protein-protein interactions depend on the recognition of limited portions of their exposed surfaces, bringing again the matter to interactions between short peptide sequences (continuous or discontinuous epitopes).[2] Several reports have discussed the role of oligopeptide motifs in stabilizing proteins, in protein evolution, and in generating secondary structures. Evidence from the literature[3,4,5] suggested that motifs as small as three contiguous amino acids can still play important roles in biology, medicine, and biotechnology.[6]

Very few peptides can be utilized as drugs in their native state; for example, insulin in the treatment of diabetes, and cyclosporine as an immunosuppressant.[6] Generally, the utility of native peptides is limited by an instability in vivo towards hydrolysis by many proteases, and a lack of bioavailability, due to inability to cross the biological barriers.[1,6,7] One way to improve stability is represented by the peptidomimetic approach, consisting in the modification of peptide structure while maintaining or improving the biological activity.[1,6,8] For instance, peptidomimetic protease inhibitors have been obtained by substitution of the cleavable peptide bond with a moiety that resembles the transition state of its hydrolysis.[9] In azapeptides, the α-CH group of the backbone is substituted by a isoelectronic nitrogen atom, the side chains remaining unaltered.[10] The peptoids, introduced by Zuckermann and co,[11] are peptidomimetics in which the side chain of an amino acid is "shifted" to the α-amino group. The retro-inverso peptides are obtained when the normal sequence from *N*- to *C*-terminus is reversed, and the natural *L*-amino acids are changed by *D*-amino acids.[12,13] Finally, the peptidomimetics containing a isoster of one or more peptide bonds (e.g. a reduced amide CH_2-NH or a C=C) are often referred to as pseudopeptides.[1,2,6,7]

The linear native peptides also show high flexibility, that may result in scarce target affinity and/or poor selectivity. In this respect, the pre-organization of peptide shape via introduction of structural motifs that impart conformational restriction can minimize the unfavorable loss of entropy in peptide-receptor recognition, giving enhanced binding affinity and hence therapeutic potential.[1,6,7,14] To this purpose, constrained peptidomimetics[1,14] can be obtained by the incorporation of non-natural amino acids, including *D*-configured residues,[15] residues with modified side chains, *N*-alkylated amino acids, α-substituted or β-substituted α-amino acids, proline analogues,[16] etc. These specialized residues generally exert a "local" constraint, namely a significant conformational bias in the close proximity of where are situated. For instance, α,α-dialkylated residues (e.g. α-aminoisobutyric acid, Aib) tend to stabilize a 3^{10}-helix,[17,18,19] while *N*-alkyl substitution reduces the predominance of *trans* versus *cis* peptide bond configuration, and β-substitution restraints the side chain angle (χ). The introduction of a single β-amino acid is expected to increase peptide backbone flexibility, due to the presence of a extra rotating bond. Nevertheless, Seebach et al.,[20,21] Gellman et al.,[22,23,24] and others,[25] observed that short oligomers composed of β-amino acids (β-peptides), or α- and β-amino acids (hybrid α/β-peptides), folded into well-defined three dimensional structures (foldamers), similar to those of natural peptides.

"Global" constraints can be introduced by "head-to-tail" cyclization or "side-chain-to-head/tail" cyclization of the peptides. Apart from the use of (di)sulfide, amide, and other obvious bridges, strategic macrocyclizations have been achieved by ring-closing metathesis (RCM),[26] or by copper-catalyzed azide-alkyne cycloaddition reaction (click-chemistry).[27,28] For instance,

the RCM of alkene-containing dialkylated amino acids at the beginning and at the end of full turns allowed to stabilize a helix ("stapled" peptides).[29,30,31]

Constrained peptidomimetics may result from the incorporation of a heterocyclic scaffold into a peptide.[1,7,14,32] The most well-known approach for constraining a dipeptide is the Freidinger lactam,[33] consisting in the cyclization of the *i*-side chain functional group onto the *i+1* nitrogen (Figure 1). Such lactams or spirolactams have been utilized as β-turn inducers, and for preparing different classes of bioactive peptidomimetics, including peptide hormones (LHRH, GH), enkephalin, dopamine, inhibitors of ACE, or NEP, antagonists of renin, neurokinin, thrombin, etc.[34] Other constrained dipeptide analogues are differently fused Aza, thiaza, diazabicycloalkane amino acids (Figure 1),[35] widely utilized for the design of β-turn mimetics, β-lactam antibacterial peptides, NK antagonists, metalloprotease inhibitors, etc.

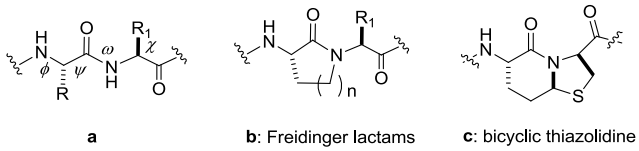

Figure 1. (**a**) Structures of a model dipeptide showing the dihedral angles ϕ (N-Cα), ψ (Cα-C=O), ω (C(O)-N), and χ (Cα-Cβ); (**b**) sketch of a Friedinger lactam; (**c**) a prototypic bicyclic turn-mimetic.

Unfortunately, the preparations of the heterocyclic scaffolds generally require multistep procedures, resulting in low overall yields. Besides, many synthetic methods lack flexibility and are therefore not suited to the introduction of diversity. Finally, the structures of the turn mimetics may lack some relevant pharmacophores for specific targets. For these reasons, many efforts have been dedicated to the expedient introduction of constrained scaffolds within a peptide sequence.[1,7,14,32,34]

In the chapter 4 is proposed the expedient cyclization of β-hydroxy-α-amino acids already embedded in a oligopeptide sequence, by treatment with disuccinimidyldicarbonate (DSC) and a base, to give oxazolidinone-peptides (Oxd).[36,37] Depending from the stereochemistry, linear peptides including two consecutive β-hydroxy-α-amino acids gave rise to sequences Oxd-Oxd or ΔAbu-Oxd; these scaffolds adopted well defined extended or folded conformations, in particular normal or inverse β-turns of type I or II. (Scheme 1).[38]

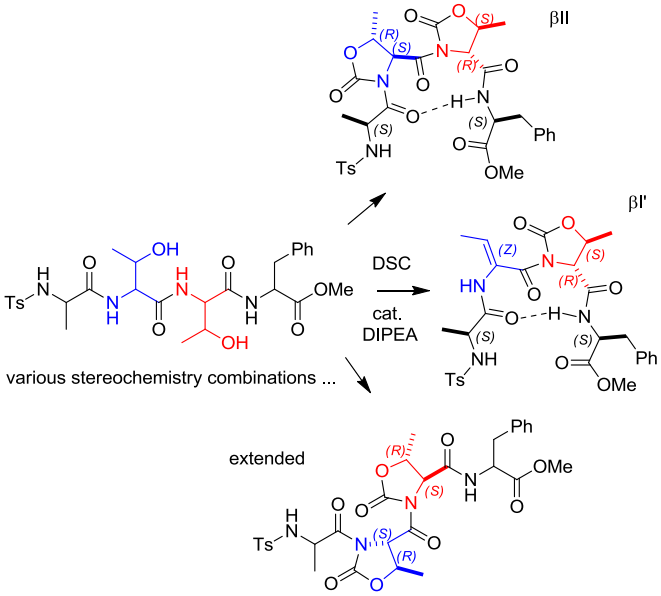

Scheme 1. The cyclization of linear peptides including two consecutive β-hydroxy-α-amino acids giave rise to Oxd-Oxd or ΔAbu-Oxd sequences, characterized by extended or folded conformations.

On the other hand, the cyclization of isoserine (*i*Ser) or other α-hydroxy-β-amino acids within oligomeric sequences afforded a 5-aminomethyloxazolidine-2,4-dione (Amo) scaffold, comprising *i*Ser and the amine function of the following residue (Chapter 5, Scheme 2).[39]

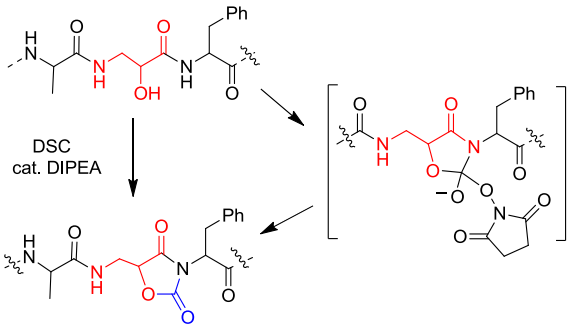

Scheme 2. The cyclization of linear peptides containing *i*Ser or other α-hydroxy-β-amino acids gives rise to a 5-aminomethyloxazolidin-2,4-dione (Amo) dipeptide scaffold.

To date, the oxazolidine-2,4-dione heterocycle has found very little use in organic and medicinal chemistry.[40,41,42] In the chapter 7, we discussed a new procedure fort the synthesis of the 5-aminomethyl-3-oxazolidinone core of the antibiotic linezolid (LNZ) in enantiomerically pure form (Scheme 3). The cyclization of the α-hydroxy amide derived from *i*Ser and 3-fluoro-4-morpholinoaniline to Amo, and the mild selective reduction at the position C(4), gave linezolid in excellent overall yield.[43]

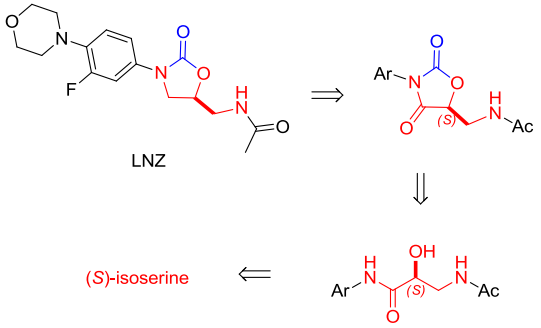

Scheme 3. Retro-synthetic approach to LZD *via* Amo intermediate, readily obtained in turn from the chiral building block *i*Ser.

From the structural point of view, the Amo dipeptide scaffold can be regarded as a unprecedented β^2-homo analogue of a Freidinger lactam (Figure 2). In the field,[44] Gmeiner and co. and others, previously combined the Freidinger lactams with β^3-amino acids (Figure 2).[45,46,47] The cyclic structure of Amo, achieved via acylation of the backbone nitrogen atom, embraces two consecutive amino acids, therefore introducing a global constraint of C(*i*)-N(*i+1*) type.[1,14] This cyclization is expected to significantly reduce the conformational space accessible to the peptide segment in which it is incorporated.[48] Finally, the Amo dipeptide might also rise potential interest for the design of hybrid oligomers composed of α- and β^2-residues,[21,22,25] being these latter less synthetically accessible respect to their β^3-counterparts (Figure 2).[49,50]

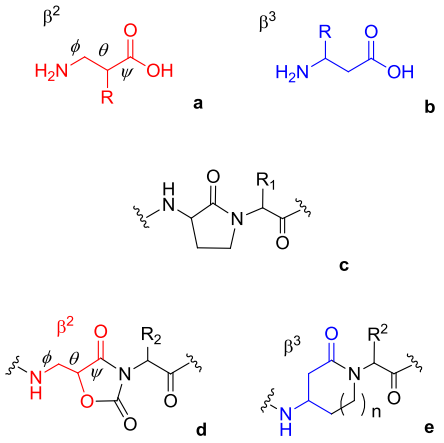

Figure 2. (**a**) Structures of β^2- and (**b**) β^3-amino acids with the soft torsional angles ϕ (N-Cβ), θ (Cβ-Cα), and ψ (see the section Conformational Analysis); (**c**) classic Freidinger lactam composed of all α-amino acids; (**d**) β^2-homo Amo variant; (**e**) Gmeiner's β^3-homo lactam.

Herein is described the use of the Amo α/β-dipeptide scaffold for the design of highly stable peptidomimetic antagonists of the integrin α4β1, or Very Late Activation antigen-4 (VLA-4), a heterodimeric cell-surface receptor expressed on lymphocytes, monocytes, eosinophils, basophils, macrophages. For the involvement of the integrin α4β1 in inflammatory processes associated to a sustained recruitment of these cells,[51] monoclonal α4 integrin antibodies[52,53] or small-molecule antagonists[54,55,56,57,58] can find applications as anti-inflammatory agents.

9.2. Results and discussion

Pepetidomimetic design. The natural ligands of α4β1 integrin are fibronectin (FN), a protein of the extracellular matrix (ECM), and the vascular cell adhesion molecule-1 (VCAM-1). FN and VCAM-1 bind to and activate the integrin by recognition of the tripeptide motifs Leu-Asp-Val (LDV), and Ile-Asp-Ser (IDS), respectively. As a consequence, several researchers designed small-molecule antagonists starting from these recognition sequences.[54,55] The peptide BIO1211, MPUPA-LDVP-OH (**1**, Figure 2) represents a prototypic example of LDV derivative.[59] It is equipped with the o-methylphenylureaphenylacetyl (MPUPA) moiety, which demonstrated a strong efficacy to target the α4 subunit. However, this peptide **1** was found to undergo rapid clearance in vivo,[60] and very unstable in heparinized blood, plasma and rat liver, lung and intestinal homogenates, being metabolized by hydrolytic cleavage of the terminal dipeptide moiety.[61,62] In search for new lead structures, several research groups proposed peptidomimetic integrin antagonists; selected examples are shown in Figure 3.

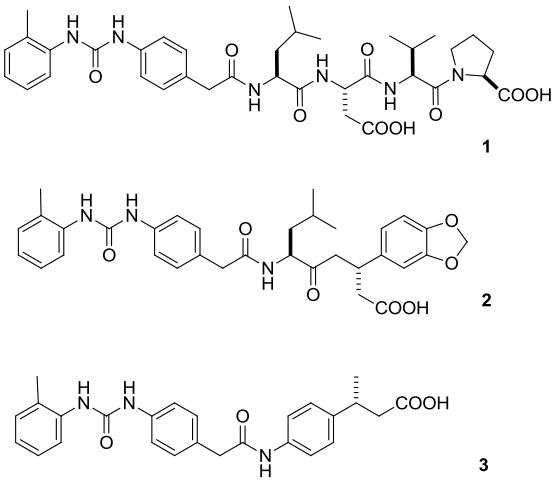

Figure 3. Structures of the peptide BIO1211 (**1**) and of the peptidomimetics **2** and **3**.

Moving from our previous experience in the field of highly stable and biologically active peptides containing β-amino acids,[63,64,65,66,67] including integrin ligands,[68,69,70,71,72,73] we envisaged the opportunity to design new peptidomimetic α4β1 integrin antagonists containing the Amo α/β-dipeptide scaffold. In this sense, we observed that the large majority of the peptidomimetic α4β1 ligands share common structural features: a α4-targeting diphenylurea moiety at the *N*-terminus, a suitable spacer, and a *C*-terminal Asp or a mimetic containing a carboxylic acid. In general, optimal distance between the *C*-terminal carboxylic acid and the urea carbonyl seems to be 14-15 bonds. Very often, the presence of an aromatic group at or adjacent to Asp favors integrin binding.[54,55]

Starting from these premises, we selected and synthesized the diastereoisomeric Amo-containing sequences MPUPA-(*S*)-Amo-(*S*)-Asp(NHPh)-OH (**4**), and MPUPA-(*R*)-Amo-(*S*)-Asp(NHPh)-OH (**5**)**,** and the diastereoisomeric PhCO-(*S*)-Asp(OH)-(*S*)-Amo-APUMP (**6**), and PhCO-(*S*)-Asp(OH)-(*R*)-Amo-APUMP (**7**) (Scheme 4); APUMP (**9**, 1-(4-(aminomethyl)phenyl)-3-(o-methylphenyl)urea),[74] represents an amino variant of MPUPA. The building blocks were chosen to maintain a 14-bond carboxylate-urea distance. Having the diphenylurea moiety at the *C*-terminus, and the Asp at the *N*-terminus, **6** and **7** can be regarded to as retro sequences[12,13] of the straight sequences **4** and **5**, respectively. Besides, while **4** and **5** appear characterized by a flexible diphenylurea-Amo junction, and a more rigid Amo-Asp portion, the compounds **6** and **7** show a more flexible Asp-Amo, and a highly rigid Amo-diphenylurea scaffold (Scheme 4).

After synthesis and bioassay as potential inhibitors of the integrin α4β1, we confirmed the coherence of the most effective compound(s) with the models developed by 3D-QSAR analysis of large libraries of compounds containing diphenylureas or other substituted aromatic groups,[56,60,75,76,77] with the aid of 2D ROESY and molecular dynamics simulations[78] (see the section Conformational Analysis).

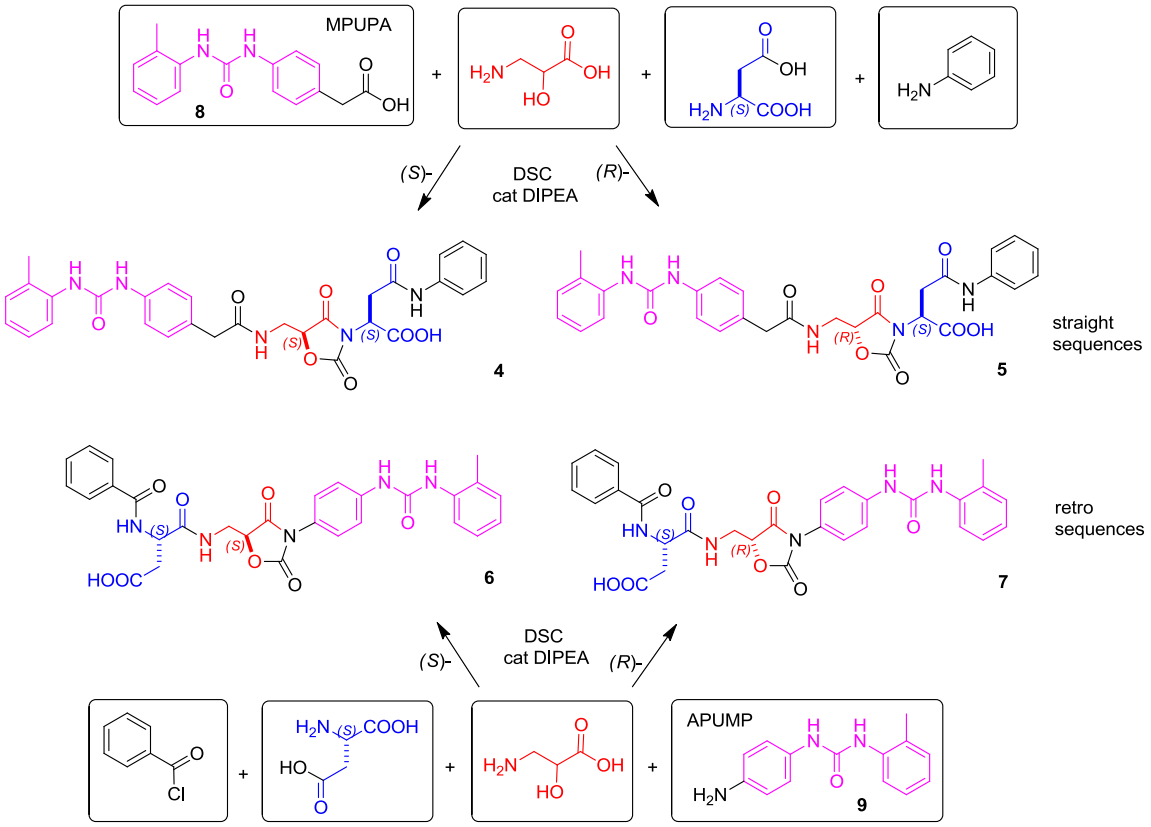

Scheme 4. Design of the straight Amo peptidomimetics MPUPA-Amo-Asp(NHPh)-OH, (*S*,*S*)-**4**, and (*R*,*S*)-**5**, and of the retro variants PhCOAsp(OH)-Amo-APUMP (*S*,*S*)-**6** and (*S*,*R*)-**7**.

Peptidomimetic synthesis. The straight Amo compounds **4** and **5** were prepared by cyclization of the corresponding precursors containing the building blocks (*S*)- or (*R*)-*i*Ser, respectively, Asp, MPUPA (**8**),[59] and aniline (Scheme 4). In a similar way, the cyclization of the linear precursors composed of a benzoyl moiety, Asp, (*S*)- or (*R*)-*i*Ser, APUMP,[74] gave **6** or **7** (Scheme 4). As a representative example, the preparation of MPUPA-(*S*)-Amo-(*S*)-Asp(NHPh)-OH (**4**) is briefly described in Scheme 5. The diastereoisomer **5** containing (*R*)-Amo was obtained using the same protocol. The *t*Bu protecting group of Fmoc-Asp(O*t*Bu)-OBn **10**[79] was removed by treatment with TFA, and the β-carboxylate functionality was reacted with aniline using HBTU, HOBt and DIPEA as coupling agents, giving the fully protected **11**. Then, this was treated with DMA to remove the Fmoc protecting group, and the intermediate was coupled with Boc-*i*Ser-OH in 10 min under MW irradiation, in the presence of HOBt/HBTU/DIPEA. The resulting **12** was treated with TFA and subsequently coupled with MPUPA (**8**) under the previous conditions, giving **13**. The cyclization to Amo **14** was done with DSC and a catalytic amount of DIPEA. Epimerization of isoserine during the cyclization was excluded on the basis of the NMR and HPLC analyses (see General Methods). After each coupling, the intermediates were isolated by flash chromatography over silica gel. The purity and identity of the intermediates was determined by RP-HPLC and ESI MS analysis and eventually by NMR. Final deprotection of the benzyl ester **14** by catalytic hydrogenation gave **4**, which was isolated > 95% pure by semi-preparative RP-HPLC (Scheme 5).

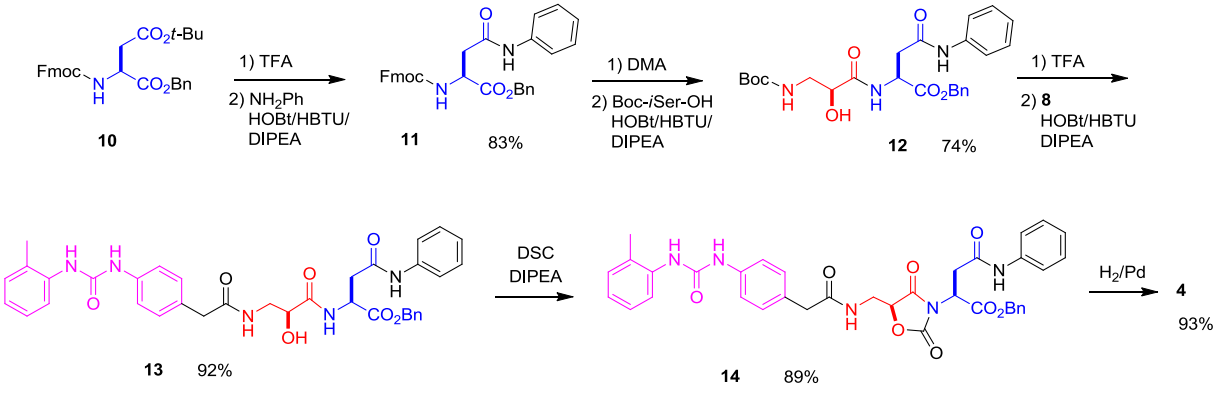

Scheme 5. Synthesis of MPUPA-Amo-Asp(NHPh)-OH (**4**).

The synthesis of PhCOAsp(OH)-Amo-APUMP (**6**) is briefly sketched in Scheme 6, while **7** was obtained from (*R*)-*i*Ser using the same protocol. APUMP (**9**) was preparing using a modified version of a procedure described in the literature,[74] from Boc-4-(aminomethyl)aniline and 2-methylbenzene isocyanate; the resulting Boc-APUMP was deprotected with TFA. The TFA salt of **9** was coupled with Boc-*i*Ser-OH in solution under MW irradiation and in the presence of HOBt/HBTU/DIPEA, giving **15**. The Boc deprotection of **15** was followed by coupling with PhCOAsp(O*t*Bu)-OH (**16**) under the same conditions as before. The resulting **17** was treated with DSC and DIPEA to give PhCOAsp(O*t*Bu)-Amo-APUMP (**18**). The latter was treated with TFA, giving **6** which was purified by semi-preparative RP-HPLC. The characterization of the final compound was done by MS, NMR, and elemental analysis.

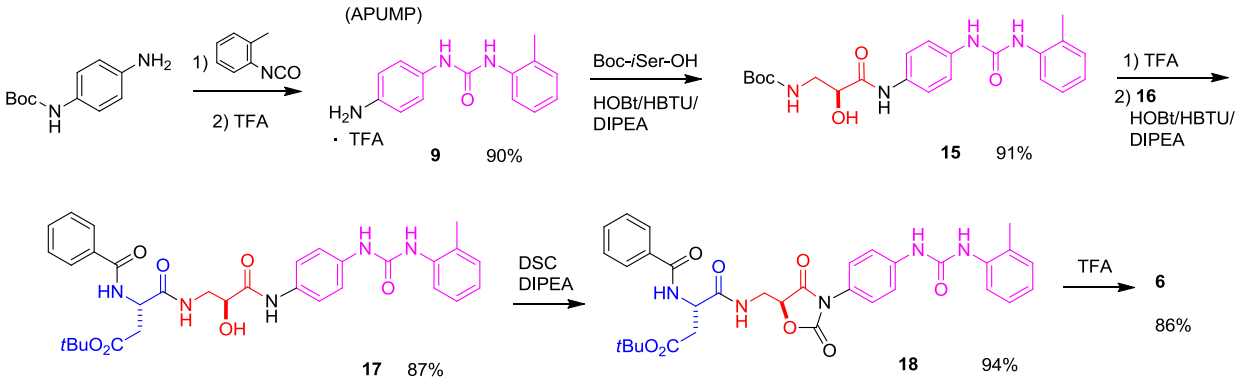

Scheme 6. Synthesis of PhCOAsp(OH)-Amo-APUMP (**6**).

In vitro enzymatic stability. The enzymatic stability of peptidomimetics **4**-**7** was estimated by incubation in mouse serum for 3 h.[80] During this period, samples of the incubation mixtures were withdrew at intervals chosen so that a kinetic curve of the hydrolysis could be constructed (Figure 6). At 180 min, compounds **4**, **5**, and **7**, were only slightly degraded (< 10 %), while **6** was degraded to a moderate extent (about 10-15 %) in the mouse serum (Table 1). On the contrary, BIO1211 (**1**) was almost completely hydrolyzed, being present only in traces, as detected by RP-HPLC and ESI-MS analyses. These data support that the presence of the Amo scaffold strongly increased the enzymatic stability of the peptidomimetics respect to **1**.

Cell adhesion inhibition. The efficacy of the compounds **4**-**7** as antagonists of the integrin α4β1 was determined by measuring their ability to inhibit the adhesion of α4β1 integrin-expressing Jurkat cells to the natural ligand VCAM-1 (Table 1). BIO1211 (MPUPA-Leu-Asp-Val-Pro-OH, **1**) was chosen as α4β1 integrin antagonist reference compound. The adhesion of these cells to 96-well plates coated with human recombinant VCAM-1 was concentration-dependent and was not observed in BSA-coated wells.[81] The adhesion of Jurkat cells (5×10^5 cells per well) to VCAM-1 (2-25 μg/ml) ranged from 1.9 to 3.2×10^4 cells. The adhesion to VCAM-1 (10 μg/ml) was inhibited (> 92%) after pretreatment with 5 μg/ml of an anti-α4 integrin antibody.

As expected,[59] the reference compound BIO1211 (MPUPA-Leu-Asp-Val-Pro-OH, **1**) behaved as a potent α4β1 integrin ligand and inhibited cell adhesion to VCAM-1 with a IC_{50} of 7.6 nM. On the contrary, peptidomimetics **4** and **5** did not affect cell adhesion to a significant extent. Possibly, the rigid Amo-Asp scaffolds prevented these compounds from adopting a 3D display of the pharmacophores (urea, carboxylate, and aromatic substituent) compatible with the bioactive conformation(s) of α4β1 integrin ligands (see Conformational Analysis). On the other hand, the retro compounds PhCO-(*S*)-Asp(OH)-(*S*)-Amo-APUMP **6**, and PhCO-(*S*)-Asp(OH)-(*R*)-Amo-APUMP **7**, inhibited cell adhesion with an IC_{50} of 19 and 148 nM, respectively. Therefore, both the compounds behaved as integrin antagonists, albeit with different affinity. Apparently, the rigid (*S*)-configured Amo-urea scaffold of **6** imposed a better overall geometry compared to the (*R*) one. The different in-solution conformations of **6** and **7** were analyzed by 2D ROESY and restrained molecular dynamics, and were compared to the 3D models determined by 3D QSAR and molecular docking (Conformational Analysis).

Table 1. HPLC and MS analysis,[a] inhibition of Jurkat cell adhesion,[b] and peptide stability (PS)[c] in mouse serum after 3 h, of BIO1211 (**1**) and compounds **4**-**7**.

n	structure	Purity (%)	m/z [M+1] vs calcd	α4β1/VCAM-1 IC50 (nM)	PS 3h (%)
1	MPUPA-Leu-Asp-Val-Pro-OH	-	-	7.60±3.0	traces
4	MPUPA-(*S*)-Amo-(*S*)-Asp(NHPh)-OH	96	588.2/588.2	$>10^4$	91±5
5	MPUPA-(*R*)-Amo-(*S*)-Asp(NHPh)-OH	98	588.3/588.2	$>10^4$	94±6
6	PhCO-(*S*)-Asp(OH) -(*S*)-Amo-APUMP	97	574.3/574.2	19±20	85±4
7	PhCO-(*S*)-Asp(OH) -(*R*)-Amo-APUMP	96	574.2/574.2	148±24	88±6

[a] Determined by analytical RP-HPLC. [b] Mean ± SE. [c] Mean amounts (%) of intact peptides ± SE after a 3 h incubation in mouse serum, determined by RP-HPLC; peak areas were normalized to 100 at *t*=0.

Conformational analysis. The significant biological activity of the structurally correlated PhCO-(*S*)-Asp(OH)-(*S*)-Amo-APUMP (**6**) and PhCO-(*S*)-Asp(OH)-(*R*)-Amo-APUMP (**7**) prompted us to analyze the in-solution conformations by NMR spectroscopy and MD simulations, to check the coherence with the 3D geometric requisites of the models reported in the literature for α4β1 antagonists.[56,60,75,76,77,82,83,84] Molecular conformations were investigated by 2D ROESY in 8:2 [D6]DMSO/H_2O; [D6]DMSO alone or mixtures of [D6]DMSO and H_2O have been recommended by several authors as excellent biomimetic media. It has been demonstrated that cryoprotective mixtures of high viscosities, such as DMSO/water, showed a remarkable ability to favor compact structures representative of the bioactive conformers over disordered structures.[85,86,87]

The ^{1}H NMR spectra showed a single set of resonances, suggestive of conformational homogeneity or a rapid equilibrium between conformers. 2D-ROESY of the model compounds in [D6]DMSO/H2O (8:2) mixture gave well analyzable cross-peaks (Tables S1 and S2). Cross-peak intensities were ranked to infer plausible inter-proton distances as restraints. The amide bonds were set at 180°; indeed, it is well established that peptides comprising only secondary amide bonds adopt all-*trans* conformations. In any case, the absence of Hα(*i*)-Hα(*i+1*) cross-peaks reasonably excluded the occurrence of *cis* amide bonds.[88] Structures consistent with ROESY were obtained by simulated annealing with restrained molecular dynamics in a box of explicit TIP3P water molecules.[89] Random structures generated by unrestrained high temperature molecular dynamics were subjected to restrained dynamics with a scaled force field at high temperature, followed by dynamics with full restraints, after which the system was cooled and minimized with the AMBER force field[90] and clustered by the rmsd analysis of backbone atoms.[78]

For both **6** and **7**, the computations gave one major cluster comprising the large majority of the structures. The representative geometries with the lowest internal energy and no violations of the distance constraints were selected and analyzed (Figure 4). Both **6** and **7** displayed a partially bent disposition of the backbone; however, the presence of (*S*)-Amo or (*R*)-Amo scaffolds conferred the compounds distinct 3D shapes (Figure 4 and 5).

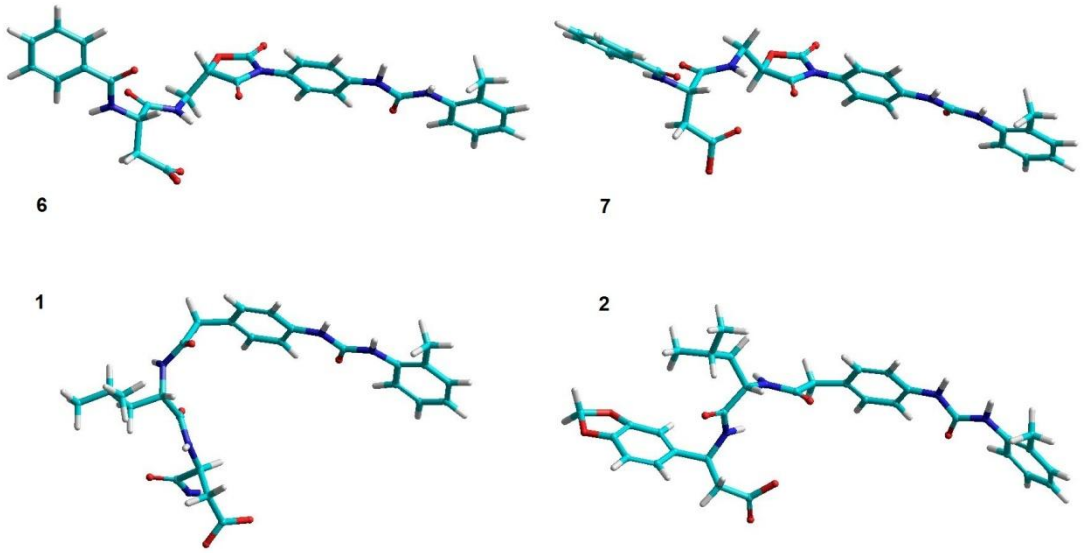

Figure 4. Top: representative low-energy structures of PhCO-(*S*)-Asp(OH)-(*S*)-Amo-APUMP (**6**), and PhCO-(*S*)-Asp(OH)-(*R*)-Amo-APUMP (**7**), consistent with ROESY analysis and calculated by restrained MD in a 45×45×45 Å box of standard TIP3P water molecules. Bottom: bioactive geometry of the prototypic model compound **1**[77] (for clarity, only urea-Leu-Asp is shown), and peptidomimetic **2** (Figure 3), as reported in the literature.[56,60,75]

Clearly, the central torsion angle between the Cβ-Cα carbons represents the most relevant geometric variable of the Amo compounds. According to the convention of Banerjee and Balaram,[91] the soft torsional degrees of freedom in a β-amino acid are defined as ϕ (N-Cβ), θ (Cβ-Cα), and ψ (Cα-C=O), respectively (Figure 2). The ROESY-derived structure of the homochiral **6** display a partially bent backbone disposition (Figure 4 and 5), and the PhCO-Asp moiety is placed below the plane of the heterocycle. The Amo residue adopts a *+g* conformation about the central dihedral angle θ, which is consistent with the calculated geometries previously reported for β^2-amino acids.[49,91,92,93] In the diastereoisomer **7**, the central dihedral angle θ of Amo adopts a *-g* conformation (due to the reversal of stereochemistry, the *–g* conformation of (*R*)-Amo corresponds to the *+g* of (*S*)-Amo), and the PhCO-Asp group is positioned on the opposite side of the Amo ring respect to **6** (Figure 5).

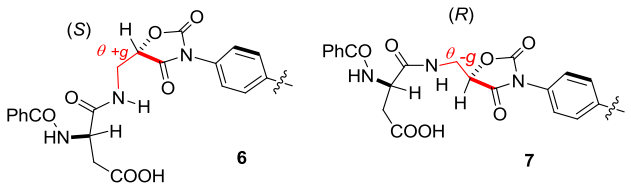

Figure 5. Sketches of the geometries about the (*S*)- or (*R*)-configured Amo rings in **6** and **7**, respectively.

Figure 4 shows also a comparison of the representative structures of **6** and **7** calculated by ROESY and restrained molecular dynamics, with the bioactive geometries of the compounds **1** and **2** as reported in the literature,[56,60,75] representative of the 3D models developed by 3D QSAR or molecular docking.[76,77,82,83,84] Both **6** and **7** tend to adopt similar semi-bent conformations; however, the relative display of the diphenylurea, the carboxylate group, and the aromatic group, imposed by the (*S*)-Amo-urea rigid scaffold of the antagonist **6**, reproduce the geometries of the pharmacophores of reference compounds more closely, accounting for the comparatively higher efficacy to inhibit Jurkat cells adhesion to VCAM-1 (Table 1).

9.3. Conclusions

In summary, herein is reported the design and synthesis of α4β1 integrin inhibitors, mimetics of the well-known BIO1211 (**1**), readily assembled by connecting a diphenylurea pharmacophore and an aryl-substituted Asp, to a (*S*)- or (*R*)-configured Amo scaffolds, obtained in turn by the expedient cyclization of the corresponding (*S*)- or (*R*)-isoserine-containing sequences. Different assemblies lead to "normal" or retro-sequences, and the resulting compounds showed remarkable chemical and

enzymatic stability, as determined by incubation in mouse serum, while under the same conditions **1** was rapidly degraded. The retro sequences PhCO-(*S*)-Asp(OH)-(*S*)-Amo-APUMP (**6**), and PhCO-(*S*)-Asp(OH)-(*R*)-Amo-APUMP (**7**), were shown to inhibit the adhesion of the α4β1 integrin-expressing Jurkat cells to the ligand VCAM in a dose-dependent manner, in particular the homochiral **6** showed IC_{50} in the low 10^{-8} M range. The comparatively higher activity of **6** compared to **7** was rationalized on the basis of the different 3D molecular geometries imposed by the (*S*)- or (*R*)-Amo scaffolds. 2D ROESY analysis in a biomimetic environment and restrained molecular dynamics gave for **6** a preferential conformation which was more compatible with the 3D requisites reported in the literature for BIO1211 and similar compounds. These results support that the Amo approach can furnish bioactive peptidomimetics, potentially useful as anti inflammatory agents.

9.4. Experimental Section

9.4.1. General Methods

Standard chemicals and biological reagents were purchased from commercial sources and used without further purification. In particular: mouse serum, lectin from Triticus vulgaris, were obtained from Sigma-Aldrich; cell culture media, phosphate-buffered saline (PBS) and fetal bovine serum (FBS), from Lonza; HBSS and chloromethylfluorescein diacetate (CMFDA) from Invitrogen; Jurkat clone E6.1 was obtained from the European Cell Culture Collection; black 96-well clear-bottom plates were purchased from Corning Costar. Soluble human VCAM-1 was purchased from R&D Systems. BIO-1211 (**1**) was purchased from Bachem. Flash chromatography was performed on silica gel (230-400 mesh), using mixtures of distilled solvents. The purities of the intermediates were determined by analytical RP-HPLC; the purities of the Amo peptides **6** and **7** were assessed also by elemental analysis. RP-HPLC was performed on an Agilent 1100 series apparatus, using a RP column Phenomenex mod. Gemini 3µ C18 110A 100x3.0 mm (P/No 00D-4439-Y0); column description: stationary phase octadecyl carbon chain-bonded silica (C18) with TMS endcapping, fully porous organo-silica solid support, particle size 3 µm, pore size 110 Å, length 100 mm, internal diameter 3 mm; DAD 210 nm; mobile phase from a 9:1 H_2O-CH_3CN to a 2:8 H_2O-CH_3CN in 20 min at a flow rate of 1.0 mL min^{-1}, followed by 10 min at the same composition (mobile phase A). The analytic RP-HPLC of compounds **4**-**7** and other intermediates with a free amino or carboxylate group was performed as reported above, with the addition of 0.1% HCOOH in the mobile phase (mobile phase B), and setting DAD at 254 nm. Semi-preparative RP-HPLC of compounds **4**-**7** was performed on an Agilent 1100 series apparatus, using a RP column ZORBAX mod. Eclipse XDB-C18 PrepHT cartridge 21.2x150 mm 7µ (P/No 977150-102); column description: stationary phase octadecyl carbon chain-bonded silica (C18), double endcapped, particle size 7 µm, pore size 80 Å, lenght 150 mm, internal diameter 21.2 mm; DAD 210 nm; mobile phase from 8:2 H_2O-CH_3CN to 100% CH_3CN, both H_2O and CH_3CN with the addition of 0.1% HCOOH, in 10 min, at a flow rate of 12 mL min^{-1}. ESI analysis was performed using a MS single quadrupole HP 1100MSD detector, with a drying gas flow of 12.5 l/min, nebulizer pressure 30 psgi, drying gas temp. 350°C, capillary voltage 4500 (+) and 4000 (-), scan 50-2600 amu. Elemental analyses were performer using a Thermo Flash 2000 CHNS/O analyzer. The synthetic procedures by MW irradiation were performed using a microwave oven (MicroSYNTH Microwave Labstation for Synthesis) equipped with a built-in ATC-FO advanced fiber optic automatic temperature control. ^{1}H NMR spectra were recorded using a Varian Gemini apparatus at 400 MHz in 5 mm tubes, using 0.01 M peptide at room temperature. For spectra in water/[D6]DMSO, solvent suppression was performed by the solvent presaturation procedure implemented in Varian (PRESAT). ^{13}C NMR spectra were recorded at 100 MHz. Chemical shifts are reported as δ values relative to residual $CHCl_3$ δH (7.26 p.p.m.), DMSO δH (2.50 p.p.m.) and $CDCl_3$ δC (77.36 p.p.m.) as internal standards. The unambiguous assignment of ^{1}H NMR resonances was performed by 2D gCOSY.

9.4.2. Synthetic procedures

MPUPA (**8**) was prepared as reported in the literature.[59] Briefly, *o*-tolyl isocyanate (0.82 mL, 6.6 mmol) was added to a stirred solution of 2-(4-aminophenyl)acetic acid (1.0 g, 6.6 mmol) in DMF (5 mL) at r.t. After 3 h, the mixture was diluted with EtOAc (40 mL) and the solid **8** which precipitated in almost quantitative yield was collected by filtration under suction, and was used without further purifications (1.75 g, 93%, 90% pure by analytical RP-HPLC, see General Methods, mobile phase B, Rt = 6.08 min). ES-MS *(m/z)* 285.0 [M+1], calcd 285.1. The analyses were in agreement with the literature.[59]

APUMP (**9**) was prepared using a modified version of a procedure reported in the literature.[74] *o*-Tolyl isocyanate (0.6 mL, 4.8 mmol) was added at r.t. to a stirred solution of *N*-Boc-*p*-phenylenediamine (1.0 g, 4.8 mmol) in DMF (5 mL). After 3h, the mixture was diluted with EtOAc (40 mL), the solid Boc-APUMP which precipitated in almost quantitative yield was collected by filtration under suction, and used without further purifications (1.44 g, 90%, 90% pure by analytical RP-HPLC, see General Methods, mobile phase A, Rt = 8.87 min). ES-MS *(m/z)* 342.0 [M+1], calcd 342.1. Boc-APUMP (1.0

g, 2.9 mmol), was treated with 25% TFA in DCM (5 mL) while stirring at r.t. After 15 min, the volatiles was removed under reduced pressure, and the treatment was repeated. The residue was triturated in Et_2O, the solid **9** (APUMP) was collected as a TFA salt by filtration in almost quantitative yield, and used for the next couplings without further purifications (0.94 g, 91%, 90% pure by analytical RP-HPLC, see General Methods, mobile phase B, Rt = 1.47 min). ES-MS *(m/z)* 241.2 [M+1], calcd 241.1.

Fmoc-Asp(O*t*Bu)-OBn (**10**) was prepared as reported in the literature.[79] Briefly, a mixture of Fmoc-Asp(O*t*Bu)-OH (1.50 g, 3.65 mmol), BnBr (1.7 mL, 14.6 mmol) $NaHCO_3$ (0.92 g, 10.9 mmol) in DMF (6 mL), was stirred for 8 h at r.t. The mixture was diluted with water (20 mL) and extracted three times with EtOAc (20 mL). The combined organic layers were dried over Na_2SO_4, and the solvent was distilled at reduced pressure. The oily residue was purified by flash chromatography over silica-gel (eluant EtOAc/cyclohexane 1:9) giving **8** (1.58 g, 85%, 94% pure by analytical RP-HPLC, see General Methods, mobile phase A, Rf = 13.7 min). ES-MS *(m/z)* 502.0 [M+1], calcd 502.2. The analyses were in agreement with the literature.[79]

Fmoc-Asp(NHPh)-OBn (**11**). The compound **10** (0.50 g, 1.0 mmol) was treated with 25% TFA in DCM (5 mL) as reported for the preparation of **9**. After the same work-up, the resulting **11** was used for the following reactions without further purifications (0.44 g, 98%, 85% pure by analytical RP-HPLC, see General Methods, mobile phase B, Rf = 1.78 min). ES-MS *(m/z)* 446.2 [M+1], calcd 446.2. The residue (0.44 g, 0.98 mmol) was dissolved in 3:1 DCM/DMF (5 mL), and HOBT (0.135 g, 1.0 mmol), HBTU (0.76 g, 2.0 mmol), DIPEA (0.52 mL, 3.0 mmol), and aniline (0.14 g, 1.5 mmol), were added while stirring. The mixture was heated under MW irradiation, keeping irradiation power fixed at 150W and monitoring the internal reaction temperature at 80 °C with a built-in ATC-FO advanced fiber optic automatic temperature control. After 10 min, the mixture was allowed to reach r.t. and diluted with DCM (20 mL), and the solution was washed with 0.5 M HCl (5 mL) and saturated $NaHCO_3$ (5 mL). The organic layer was dried over Na_2SO_4, and solvent was removed at reduced pressure. The compound **11** (0.44 g, 85%, 94% pure by analytical RP-HPLC, see General Methods, mobile phase A, Rt = 11.84 min) was isolated by flash chromatography over silica-gel (eluant EtOAc/cyclohexane 1:1). ES-MS *(m/z)* 521.3 [M+1], calcd 521.2.

Boc-*i*Ser-Asp(NHPh)-OBn (**12**). Fmoc deprotection of compound **11** (0.26 g, 0.5 mmol) was done with 2M DMA in THF (4 mL) while stirring at r.t for 20 min. After that, the volatiles were removed under reduced pressure and the residue treated again under the same conditions. The deprotected intermediate was triturated twice with ice-cold Et_2O and was utilized for the next coupling without further purifications (0.12 g, 80%, 75% pure by analytical RP-HPLC, see General Methods, mobile phase B, Rt = 1.17 min). ES-MS *(m/z)* 299.0 [M+1], calcd 299.1. The residue (0.12 g, 0.4 mmol) was coupled with Boc-*i*Ser-OH (0.1 g, 0.48 mmol) under the same conditions and work-up procedures utilized for the synthesis of **11**. The dipeptide **12** (0.18 g, 92%, 95% pure by analytical RP-HPLC, see General Methods, mobile phase A, Rt = 8.50 min) was isolated by flash chromatography over silica-gel (eluant EtOAc/cyclohexane 7:3). ES-MS *(m/z)* 486.2 [M+1], calcd 486.2.

MPUPA-*i*Ser-Asp(NHPh)-OBn (**13**). The Boc-protected **12** (0.18 g, 0.37 mmol) was treated with TFA in DCM under the same conditions and work up procedure described for the deprotection of **9**. The resulting intermediate dipeptide-TFA salt (0.18 g, 98%, 90% pure by analytical RP-HPLC, see General Methods, mobile phase B, Rt = 1.31 min), was utilized without further purifications. ES-MS *(m/z)* 386.3 [M+1], calcd 386.2. The TFA salt (0.18 g, 0.36 mmol) was reacted with MPUPA (0.12 g, 0.43 mmol) using the same coupling conditions and work up procedure described for the preparation of **11**. The residue was purified by flash chromatography over silica-gel (eluant: EtOAc) giving **13** (0.22 g, 94%, 95% pure by analytical RP-HPLC, see General Methods, mobile phase A, Rt = 8.69 min). ES-MS *(m/z)* 652.2 [M+1], calcd 652.3. ^{1}H NMR (400 MHz, [D6]DMSO) δ: 2.21 (s, 3H, Me), 2.80 (dd, J = 10.4, 15.0 Hz, 1H, AspHβ), 2.90 (dd, J = 5.6, 15.0 Hz, 1H, AspHβ), 3.23 (m, 1H, *i*SerHβ), 3.46 (m, 1H, *i*SerHβ), 3.56-3.60 (m, 2H, CH_2CON), 4.03 (m, 1H, *i*SerHα), 4.79 (ddd, J = 5.6, 8.4, 10.4 Hz, 1H, AspHα), 5.07 (d, J = 12.6 Hz, 1H, CH_2Ph), 5.13 (d, J = 12.6 Hz, 1H, CH_2Ph), 6.90 (br.t, 1H, ArH), 7.00 (m, 1H, ArH), 7.08-7.22 (m, 10H, ArH+NH), 7.23-7.31 (m, 2H, ArH), 7.32-7.39 (m, 2H, ArH), 7.57 (d, J = 7.8 Hz, 2H, ArH), 7.64 (br.t, 1H, *i*SerNH), 7.80 (s, 1H, ureaNH), 7.83 (d, J = 7.8 Hz, 1H, ArH), 8.08 (d, J = 8.4 Hz, 1H, AspNH), 8.82 (s, 1H, ureaNH).

MPUPA-Amo-Asp(NHPh)-OBn (**14**). DSC (0.092 g, 0.36 mmol) and DIPEA (12 μL, 0.07 mmol) were added to a stirred solution of **13** (0.21 g 0.33 mmol) in 3:1 DCM/DMF (4 mL) at r.t. and under inert atmosphere. After 1 h, the solvent was removed at reduced pressure, the residue was diluted with 0.1 M HCl (5 mL), and the mixture was extracted three times with DCM (10 mL). The combined organic layers were dried over Na_2SO_4, and solvent was evaporated at reduced pressure. The Amo compound **12** was isolated (0.20 g, 89%, 96% pure by analytical RP-HPLC, see General Methods, mobile phase A, Rt = 9.48 min) by flash chromatography over silica-gel (eluant EtOAc/cyclohexane 6:4). ES-MS *(m/z)* 678.0 [M+1], calcd 678.3. ^{1}H NMR (400 MHz, [D6]DMSO) δ: 2.15 (s, 3H, Me), 2.83 (m, 1H, AspHβ), 3.10 (m, 1H,

AspHβ), 3.22-3.37 (m, 2H, C*H*$_2$CON), 3.50-3.60 (m, 2H, AmoHβ), 5.06 (d, J = 12.8 Hz, 1H, C*H*$_2$Ph), 5.09-5.15 (m, 2H, C*H*$_2$Ph+AspHα), 5.16 (m, 1H, AmoHα), 6.91 (br.t, 1H, ArH), 7.02 (m, 1H, ArH), 7.06-7.21 (m, 10H, ArH+NH), 7.21-7.32 (m, 2H, ArH), 7.32-7.38 (m, 2H, ArH), 7.56 (d, J = 7.8 Hz, 2H, ArH), 7.80 (s, 1H, ureaNH), 7.83 (d, J = 7.8 Hz, 1H, ArH), 8.36 (br.t, 1H, AmoNH), 8.99 (s, 1H, ureaNH).

MPUPA-(*S*)-Amo-Asp(NHPh)-OH (**4**). The benzyl ester **14** (0.20 g, 0.29 mmol) was dissolved in MeOH (10 mL), 10% Pd-C (0.05 g) was added, and the reaction vessel was filled with H_2. After 8 h, the suspension was filtered over Celite® under suction, and the solvent was evaporated at reduced pressure. The residue was isolated (0.16 g, 93%, 97% pure by analytical RP-HPLC, see General Methods, mobile phase B, Rt = 7.92 min) by semi-preparative RP-HPLC (see General Methods, mobile phase B). ES-MS *(m/z)* 588.2 [M+1], calcd 588.2. ^{1}H NMR (400 MHz, [D6]DMSO) δ: 2.23 (s, 3H, Me), 2.90 (m, 1H, AspHβ), 3.30 (m, 1H, AspHβ), 3.33-3.40 (m, 2H, C*H*$_2$CON), 3.53 (m, 1H, AmoHβ), 3.62 (m, 1H, AmoHβ), 5.11 (br.t, 1H, AspHα), 5.21 (m, 1H, AmoHα), 6.92 (br.t, 1H, ArH), 7.01 (m, 1H, ArH), 7.09-7.19 (m, 5H, ArH+NH), 7.23-7.31 (m, 2H, ArH), 7.32-7.38 (m, 2H, ArH), 7.57 (d, J = 7.8 Hz, 2H, ArH), 7.82 (d, J = 7.8 Hz, 1H, ArH), 7.94 (s, 1H, ureaNH), 8.36 (br.t, 1H, AmoNH), 9.02 (s, 1H, ureaNH), 10.12 (br.s, 1H, COOH).

MPUPA-(*R*)-Amo-Asp(NHPh)-OH (**5**). The use of (*R*)-isoserine instead of (*S*)-isoserine, under the same reactions conditions, the same reagents, in the same quantities, and the same work-up and isolation procedures, utilized for the preparation of **4**, gave the diastereoisomer **5** (96% pure by analytical RP-HPLC, see General Methods, mobile phase B, Rt = 7.92 min). ES-MS *(m/z)* 588.3 [M+1], calcd 588.2. ^{1}H NMR (400 MHz, [D6]DMSO) δ: 2.23 (s, 3H, Me), 2.94 (m, 1H, AspHβ), 3.26 (m, 1H, AspHβ), 3.35-3.45 (m, 2H, C*H*$_2$CON), 3.53 (m, 1H, AmoHβ), 3.61 (m, 1H, AmoHβ), 5.11 (br.t, 1H, AspHα), 5.25 (m, 1H, AmoHα), 6.90 (br.t, 1H, ArH), 7.02 (m, 1H, ArH), 7.09-7.20 (m, 5H, ArH+NH), 7.23-7.30 (m, 2H, ArH), 7.31-7.37 (m, 2H, ArH), 7.56 (d, J = 7.8 Hz, 2H, ArH), 7.80 (d, J = 7.8 Hz, 1H, ArH), 7.93 (s, 1H, ureaNH), 8.38 (br.t, 1H, AmoNH), 9.01 (s, 1H, ureaNH), 10.10 (br.s, 1H, COOH).

Boc-*i*Ser-APUMP (**15**). APUMP TFA salt (**9**, 0.86 g, 2.42 mmol) was coupled with Boc-(S)-isoSerOH (0.45 g, 2.19 mmol) using the same quantities of coupling agents and under same conditions described for the synthesis of **11**. After the usual work up, **15** (0.85 g, 91%, 93% pure by analytical RP-HPLC, see General Methods, mobile phase A, Rt = 7.11 min), was isolated by flash chromatography over silica gel (eluant cyclohexane/EtOAc from 75:25). ES-MS *(m/z)* 451.0 [M+Na], calcd 451.2.

PhCO-Asp(OtBu)-OH (**16**). Fmoc-Asp(OtBu)-OH (1.0 g, 2.42 mmol) was treated with 2M DMA in THF, as reported for the Fmoc deprotection of **12**, and after the same work-up, the crude H-Asp(OtBu)-OH (0.39 g, 85%, 73% pure by analytical RP-HPLC, see General Methods, mobile phase B, Rt = 1.61 min) was used for the following step without further purifications. ES-MS *(m/z)* 190.1 [M+1], calcd 190.1. The crude H-Asp(OtBu)-OH (0.39 g, 2.0 mmol) was diluted with DCM (4 mL), and benzoyl chloride (0.35 mL, 3.0 mmol), and pyridine (0.33 mL, 3 mmol) were added while stirring at r.t. After 3 h, 1M HCl (5 mL) was added, the mixture was shaken with a separating funnel, and the organic layer was separated. The aqueous layer was extracted twice with DCM (5 mL), and the collected organic layers were dried over Na_2SO_4. The solvent was evaporated at reduced pressure, the residue was triturated twice in Et_2O, and was utilized without further purifications (0.54 g, 92%, 80% pure by analytical RP-HPLC, see General Methods, mobile phase B, Rt = 6.00 min). ES-MS *(m/z)* 293.1 [M+1], calcd 293.1.

PhCO-Asp(OtBu)-*iso*Ser-APUMP (**17**). Compound **15** (0.4 g, 0.93 mmol) was *N*-deprotected according to the procedure described for the preparation of **9**, giving H-*iso*Ser-APUMP as a TFA salt in quantitative yield, utilized without purification (0.44 g, 99%, 90% pure by analytical RP-HPLC, see General Methods, mobile phase B, Rt = 1.23 min), ES-MS *(m/z)* 329.2 [M+1], calcd 329.2. The crude salt (0.16 g, 0.36 mmol) was coupled with **16** (0.11 g, 0.37 mmol) using the same quantities and under same conditions described for the preparation of **11**, affording compound **17**. After the usual work up, **17** was isolated (0.19 g, 88%, 94% pure by analytical RP-HPLC, see General Methods, mobile phase A, Rt = 7.95 min) by flash chromatography over silica gel (eluant cyclohexane/EtOAc 20:80). ES-MS *(m/z)* 604.2 [M+1], calcd 604.3. ^{1}H NMR (400 MHz, [D6]DMSO) δ: 1.34 (s, 9H, *t*Bu), 2.21 (s, 3H, Me), 2.65 (dd, J = 7.4, 15.8 Hz, 1H, AspHβ), 2.80 (dd, J = 6.4, 15.8 Hz, 1H, AspHβ), 3.40 (m, 1H, *i*SerHβ), 3.58 (m, 1H, *i*SerHβ), 4.16 (m, 1H, *i*SerHα), 4.89 (ddd, J = 6.4, 7.4, 8.0 Hz, 1H, AspHα), 6.85 (br.t, 1H, ArH), 7.00-7.08 (m, 3H, ArH), 7.09-7.20 (m, 5H, ArH), 7.24-7.32 (m, 4H, ArH+NH), 7.60 (d, J = 8.0 Hz, 1H, ArH), 7.64 (br.t, 1H, *i*SerNH), 8.00 (s, 1H, ureaNH), 8.22 (d, J = 8.0 Hz, 1H, AspNH), 9.02 (s, 1H, ureaNH).

PhCO-Asp(OtBu)-Amo-APUMP (**18**). The cyclization of **17** (0.19 g, 0.31 mmol) was performed with DSC and DIPEA according to the same conditions and work-up procedures utilized for the synthesis of **14**, giving **18** (0.18 g 95%, 92% pure by analytical RP-HPLC, see General Methods, mobile phase A, Rt = 8.87 min) after flash chromatography over silica

gel (eluant cyclohexane/EtOAc from 20:80). ES-MS *(m/z)* 630. [M+1], calcd 630.3. ^{1}H NMR (400 MHz, [D6]DMSO) δ: 1.21 (s, 9H, *t*Bu), 2.18 (s, 3H, Me), 2.55-2.62 (m, 2H, AspHβ), 3.53 (m, 1H, AmoHβ), 3.65 (m, 1H, AmoHβ), 4.75 (m, 1H, AspHα), 5.12 (br.t, 1H, AmoHα), 6.96 (t, J = 7.4 Hz, 1H, ArH), 7.12-7.20 (m, 2H, ArH), 7.29 (d, J = 8.0 Hz, 2H, ArH), 7.46 (br.t, 2H, ArH), 7.53-7.60 (m, 3H, ArH), 7.75 (d, J = 8.0 Hz, 1H, ArH), 7.90 (d, J = 7.6 Hz, 2H, ArH), 7.98 (s, 1H, ureaNH), 8.30 (br.t, 1H, AmoNH), 8.44 (br.d, 1H, AspNH), 9.03 (s, 1H, ureaNH).

PhCO-Asp(OH)-(S)-Amo-APUMP (**6**). The intermediate **18** (0.185 g 0.29 mmol) was deprotected with TFA according to the same procedure described for **9**, giving **6** (0.14 g 86%, 96% pure by analytical RP-HPLC, see General Methods, mobile phase B, Rt = 7.02 min) after isolation by semi-preparative RP-HPLC (see General Methods, mobile phase B). ES-MS *(m/z)* 574.3 [M+1], calcd 574.2. ^{1}H NMR (400 MHz, 8:2 [D6]DMSO/H_2O) δ: 2.25 (s, 3H, Me), 2.66-2.75 (m, 2H, AspHβ), 3.62 (ddd, J = 4.2, 8.0, 14.8 Hz, 1H, AmoHβ), 3.80 (ddd, J = 4.2, 8.0, 14.8 Hz, 1H, AmoHβ), 4.81 (m, 1H, AspHα), 5.20 (br.t, 1H, AmoHα), 6.96 (t, J = 7.4 Hz, 1H, ureaAr$H_{4'}$), 7.12-7.20 (m, 2H, ureaAr$H_{3',+5'}$), 7.30 (d, J = 8.0 Hz, 2H, ureaArH_2), 7.46 (dd, J = 7.2, 7.6 Hz, 2H, BzArH_{3+5}), 7.53 (t, J = 7.2 Hz, 1H, BzArH_4), 7.56 (d, J = 8.0 Hz, 2H, ureaArH_3), 7.82 (d, J = 8.0 Hz, 1H, ureaAr$H_{6'}$), 7.87 (d, J = 7.6 Hz, 2H, BzArH_{2+6}), 8.02 (s, 1H, ureaNH'), 8.45 (br.t, 1H, AmoNH), 8.66 (d, J = 8.6 Hz, 1H, AspNH), 9.23 (s, 1H, ureaNH); ^{13}C NMR (100 MHz, [D6]DMSO) δ: 17.9, 36.1, (40), 50.2, 78.2, 118.1, 121.3, 123.0, 124.6, 126.2, 127.3, 127.6, 127.8, 128.2, 130.3, 131.4, 134.0, 137.2, 140.23, 152.6, 154.4, 166.3, 170.6, 171.7, 171.8. Elem. Anal. for $C_{29}H_{27}N_5O_8$; calcd: C 60.73, H 4.74, N 12.21; found: C, 60.95; H, 4.69; N, 12.11.

PhCO-(S)-Asp(OH)-(R)-Amo-APUMP (**7**). The use of (*R*)-isoserine instead of (*S*)-isoserine, under the same reactions conditions, the same reagents, in the same quantities, and the same work-up and isolation procedures, described for the preparation of **6**, gave the diastreoisomer **7** (95 % pure by analytical RP-HPLC, see General Methods, mobile phase B, Rt = 7.02 min). ^{1}H NMR (400 MHz, 8:2 [D6]DMSO/H_2O) δ: 2.24 (s, 3H, Me), 2.67 (dd, J = 8.0, 14.6 Hz, 1H, AspHβ), 2.75 (dd, J = 4.4, 14.6 Hz, 1H, AspHβ), 3.69 (m, 1H, AmoHβ), 3.72 (m, 1H, AmoHβ), 4.82 (ddd, J = 4.4, 8.0, 8.6 Hz, 1H, AspHα), 5.20 (br.t, 1H, AmoHα), 6.98 (t, J = 7.4 Hz, 1H, ureaAr$H_{4'}$), 7.11-7.19 (m, 2H, ureaAr$H_{3',+5'}$), 7.29 (d, J = 8.0 Hz, 2H, ureaArH_2), 7.46 (dd, J = 7.2, 7.6 Hz, 2H, BzArH_{3+5}), 7.54 (t, J = 7.2 Hz, 1H, BzArH_4), 7.56 (d, J = 8.0 Hz, 2H, ureaArH_3), 7.82 (d, J = 8.0 Hz, 1H, ureaAr$H_{6'}$), 7.87 (d, J = 7.6 Hz, 2H, BzArH_{2+6}), 8.00 (s, 1H, ureaNH'), 8.43 (br.t, 1H, AmoNH), 8.65 (d, J = 8.6 Hz, 1H, AspNH), 9.25 (s, 1H, ureaNH); ^{13}C NMR (100 MHz, [D6]DMSO) δ: 17.9, 36.1, (40), 50.2, 78.4, 118.0, 121.3, 123.0, 124.6, 126.2, 127.3, 127.6, 127.8, 128.2, 130.3, 131.4, 133.9, 137.2, 140.23, 152.6, 154.4, 166.3, 170.6, 171.6, 171.8 . Elem. Anal. for $C_{29}H_{27}N_5O_8$; calcd: C 60.73, H 4.74, N 12.21; found: C 60.62, H 4.78, N 12.29.

Cell adhesion assay. Jurkat cell adhesion assay was done as described.[94,95] Briefly, 96-well plates were coated at 4 °C overnight with 2 μg/ml of VCAM-1 and a saturation curve for the ligand was plotted to establish the best signal-to-noise ratio. Non-specific hydrophobic binding sites were blocked by incubation with a BSA 1 % /HBSS (w/v) solution for 30 min at 37°C. The day of the assay, the cells were counted and stained with 12.5 μM CMFDA (30 min at 37 °C). After three rinses with BSA/HBSS to wash away the excess dye, aliquots of 500,000 (Jurkat) cells were divided among a number of tubes corresponding to the number of treatments. For inhibition experiments, cells were mixed with the drug and pre-incubated at 37 °C for 30 min to reach equilibrium before being plated. After 30 min incubation at 37 °C in the coated wells, the non-specifically bound cells were washed away with BSA/HBSS solution. Adherent cells were lysed by the addition of 0.5 % Triton-X-100 in PBS (30 min at 4°C). Released CMFDA was quantified by fluorescence imaging at Ex485 nm/Em535 nm (Wallac ARVO 1420 multilabel counter) and adherent cells was counted by interpolation on a standard curve. The fluorescence intensity with and without VCAM-I was taken as respectively 100% and 0%. Alternatively, the number of adherent cells was calculated by comparison with a standard curve prepared in the same plate using known concentrations of labeled cells. The efficacy of putative antagonists (at least eight different concentrations were used) was determined by the reduction in adherent cells compared to the untreated control.

Data analysis. Three independent experiments were run in quadruplicate; all data are expressed as mean ± S.E.M. IC_{50} values indicate the molar ligand concentration required to inhibit the response by 50%. Data were analyzed using GraphPad software 5.0 (GraphPad Software Inc., San Diego, CA, USA).

In vitro enzymatic stability. Enzymatic degradation studies of **1**, **4**-**7** were carried out in triplicate and repeated three times using mouse serum purchased from Sigma-Aldrich. Peptides were dissolved in Tris buffer pH 7.4 and 10 μL aliquots of a 10 mM peptide stock solution were added to 190 μL of serum. Incubations were carried out at 37°C for 120 min. Aliquots of 20 μL were withdrawn from the incubation mixtures and enzyme activity was terminated by precipitating proteins with 90 μL of glacial acetonitrile. Samples were then diluted with 90 μL of 0.5% acetic acid to prevent further enzymatic

breakdown and centrifuged at 13,000×g for 15 min. The supernatants were collected and the stability of peptides was determined by RP-HPLC ESI-MS analysis.

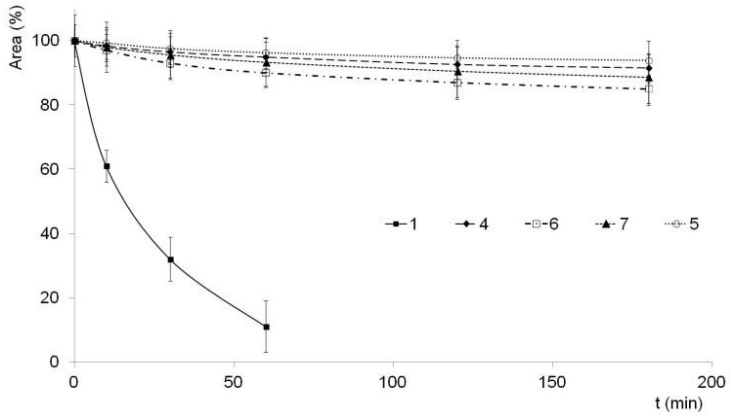

Figure 6. Stability curves of BIO1211 (**1**) and compounds **4**-**7** in mouse serum. Sampling intervals were chosen so that a kinetic curve could be constructed. Peak areas were normalized to 100 at *t*=0. Each hydrolysis experiment was repeated 3 times, and the reported data are mean values. Error ranges were estimated on the basis of the standard deviation.

9.4.3. Conformational analysis

ROESY and molecular dynamics. 2D ROESY experiments in 8:2 [D_6]DMSO/H_2O were performed in the phase sensitive mode at r.t., spin-locking field (γb2) was 2000 Hz, and mixing time was set to 250 ms; spectra were processed in the hypercomplex approach; peaks were calibrated on DMSO. Only ROESY-derived constraints were included in the restrained molecular dynamics.[78] Cross-peak intensities were classified very strong, strong, medium, and weak, and were associated with distances of 2.3, 2.7, 3.3, and 5.0 Å, respectively.[96] The intensities of the cross peaks arising from protons separated by known distances (e.g. geminal) were found to match with these associations. Geminal and other obvious correlations were discarded as constraints. For the absence of Hα(*i*, *i+1*) ROESY cross peaks, all of the ω bonds were set at 180° (force constant: 16 kcal mol^{-1} $Å^{-2}$).

The restrained MD simulations were conducted at 1 atm using the AMBER force field in a 45×45×45 Å box of standard TIP3P models of equilibrated water.[89] Periodic boundary conditions were applied, a dielectric constant of 1 was used, and the cutoff distance for the nonbonded interactions was 12 Å. All water molecules with atoms that come closer than 2.3 Å to a solute atom were eliminated. A 100 ps simulation at 1200 K was used for generating 50 random structures that were subsequently subjected to a 50 ps restrained MD with a 50% scaled force field at the same temperature, followed by 50 ps with full restraints (distance force constant of 7 kcal mol^{-1} $Å^{-2}$), after which the system was cooled in 20 ps to 50 K. H-bond interactions were not included, nor were torsion angle restraints. The resulting structures were minimized with 3000 cycles of steepest descent and 3000 cycles of conjugated gradient (convergence of 0.01 kcal $Å^{-1}$ mol^{-1}). The backbones of the structures were clustered by the rmsd analysis.[78]

Table 2. Non-obvious ROESY cross-peaks observed for **6**[a] in 8:2 [D_6]DMSO/H_2O.

Cross-peak[b]	Intensity[c]	Cross-peak[b]	Intensity[c]
Me-ureaNH	w	AmoHβ$_{dw}$-AmoHα	s
Me-ureaNH’	vs	AmoHβ$_{dw}$-AmoNH	m
AspHβ-AmoHβ$_{up}$	w	AmoHβ$_{dw}$-AspNH	w
AspHβ-AmoHβ$_{dw}$	w	AspHα-AmoHα	w
AspHβ-AspHα	s	AspHα-BzArH$_{2+6}$	w
AspHβ-BzArH$_{2+6}$	w	AspHα-AmoNH	vs
AspHβ-AmoNH	m	AspHα-AspNH	m
AspHβ-AspNH	s	AmoHα-ureaArH$_2$	w
AmoHβ$_{up}$-AspHα	w	AmoHα-AmoNH	m
AmoHβ$_{up}$-AmoHα	m	ureaArH$_2$-AmoNH	w

AmoHβ$_{up}$-ureaArH$_2$	w	ureaArH$_3$-ureaArH$_{6'}$	w
AmoHβ$_{up}$-AmoNH	vs	BzArH$_{2+6}$-AspNH	vs
AmoHβ$_{up}$-AspNH	w	ureaNH'-ureaNH	vs
AmoHβ$_{dw}$-AspHα	w	AmoNH-AspNH	w

[a] Stereochemistry has been omitted; [b] up = upfield, dw = downfield, Bz = benzoyl; [c] vs = very strong, s = strong, m = medium, w = weak.

Table 3. Non-obvious ROESY cross-peaks observed for **7**[a] in 8:2 [D$_6$]DMSO/H$_2$O.

Cross-peak[b]	Intensity[c]	Cross-peak[b]	Intensity[c]
Me-ureaNH	w	AmoHβ$_{dw}$-AspHα	w
Me-ureaNH'	vs	AmoHβ$_{dw}$-AmoHα	m
AspHβ$_{up}$-AmoHβ$_{up}$	w	AmoHβ$_{dw}$-AmoNH	s
AspHβ$_{up}$-AspHα	m	AspHα-AmoHα	w
AspHβ$_{up}$-BzArH$_{2+6}$	w	AspHα-BzArH$_{2+6}$	w
AspHβ$_{up}$-AmoNH	w	AspHα-AmoNH	vs
AspHβ$_{up}$-AspNH	s	AspHα-AspNH	m
AspHβ$_{dw}$-AspHα	s	AmoHα-ureaArH$_2$	w
AspHβ$_{dw}$-BzArH$_{2+6}$	w	AmoHα-AmoNH	m
AspHβ$_{dw}$-AmoNH	w	ureaArH$_2$-AmoNH	w
AspHβ$_{dw}$-AspNH	m	ureaArH$_3$-ureaArH$_{6'}$	w
AmoHβ$_{up}$-AspHα	w	BzArH$_{2+6}$-AspNH	vs
AmoHβ$_{up}$-AmoHα	s	ureaNH'-ureaNH	vs
AmoHβ$_{up}$-AmoNH	m	AmoNH-AspNH	w
AmoHβ$_{up}$-AspNH	w		

[a] Stereochemistry has been omitted; [b] up = upfield, dw = downfield, Bz = benzoyl; [c] vs = very strong, s = strong, m = medium, w = weak.

References

1 Liskamp, R. M. J; Rijkers, D. T. S.; Kruijtzer, John A. W.; Kemmink, *J. Chem Bio Chem* **2011**, *12*, 1626.
2 Shiba, K. *Chem Soc Rev* **2010**, *39*, 117.
3 Ung, P.; Winkler, D. A. *J Med Chem* **2011**, *54*, 1111.
4 De Marco, R.; Bedini, A.; Spampinato, S.; Gentilucci, L. *J Med Chem* **2014**, *57*, 6861.
5 De Marco, R.; Tolomelli, A.; Spampinato, S.; Bedini, A.; Gentilucci, L. *J Med Chem.* **2012**, *55*, 10292.
6 Gentilucci, L.; Tolomelli, A.; Squassabia, F. *Curr Med Chem* **2006**, *13*, 2449.
7 Gentilucci, L.; De Marco, R.; Cerisoli, L. *Curr Pharm Des* **2010**, *16*, 3185.
8 Gante, *J. Angew Chem Int Ed Engl* **1994**, *33*, 1699.
9 Toniolo, C. Houben-Weyl Methods of Organic Chemistry, Vol E22c, Synthesis of Peptides and Peptidomimetics (Ed.: M. Goodman), Thieme, Stuttgart, 2004; Chapter 10.
10 Zega A. *Curr Med Chem* **2005**, *12*, 589.
11 Zuckermann, R. N.; Kerr, J. M.; Kent, S. B. H.; Moos, W. H. *J Am Chem Soc* **1992**, *114*, 10646.
12 Fletcher, M. D.; Campbell, M. M. *Chem Rev* **1998**, *98*, 763.
13 Chorev, M. *Biopolymers* **2005**, *80*, 67.
14 Hruby, V. J.; Balse, P. M. *Curr Med Chem* **2000**, *7*, 945.
15 Durani, S. *Acc Chem Res* **2008**, *41*, 1301.
16 Thamm, P.; Musiol, H. J.; Moroder, L. Methods of organic chemistry: synthesis of peptides and peptidomimetics (Goodman, M. Ed.). Thieme Verlag, Stuttgart, 2003; vol. 22.
17 Toniolo, C; Crisma, M.; Formaggio, F.; Valle, C.; Cavicchioni, G.; Précigoux, G.; Aubry, A.; Kamphuis, J. *Biopolymers* **1993**, *33*, 1061.
18 Toniolo, C.; Crisma, M.; Formaggio, F.; Peggion, C. *Pept Sci* **2001**, *60*, 396.

[19] Toniolo, C.; Formaggio, F.; Kaptein, B.; Broxterman, Q. B. *Synlett* **2006**, 1295.
[20] Seebach, D.; Overhand, M.; Kühnle, F. N. M.; Martinoni, B.; Oberer, L.; Hommel, U.; Widmer, H. *Helv Chim Acta* **1996**, *79*, 913.
[21] Seebach, D.; Beck, A. K.; Bierbaum, D. *J. Chem Biodiversity* **2004**, *1*, 1111.
[22] Gellman, S. H. *Acc Chem Res* **1998**, *31*, 173.
[23] Appella, D. H.; Christianson, L. A.; Karle, I. L.; Powell, D. R.; Gellman, S. H. *J Am Chem Soc* **1996**, *118*, 13071.
[24] Cheng, R. P.; Gellman, S. H.; DeGrado, W. F. *Chem Rev* **2001**, *101*, 3219.
[25] Goodman, C. M.; Choi, S.; Shandler, S.; DeGrado, W F. *Nature Chem Biol*, **2007**, *3*, 252.
[26] Miller, S. J.; Blackwell, H. E.; Grubbs, R. H. *J Am Chem Soc* **1996**, *118*, 9606.
[27] Cantel, S.; Le Chevalier Isaad, A.; Scrima, M.; Levy, J. J.; DiMarchi, R. D.; Rovero, P.; Halperin, J. A.; D'Ursi, A. M.; Papini, A. M.; Chorev, M. *J Org Chem* **2008**, *73*, 5663.
[28] Ingale, S.; Dawson, P. *Org Lett* **2011**, *13*, 2822.
[29] Blackwell, H. E.; Grubbs, R. H. *Angew Chem Int Ed* **1998**, *37*, 3281.
[30] Schafmeister, C. E.; Po, J.; Verdine, G. L. *J Am Chem Soc* **2000**, *122*, 5891.
[31] Walensky, L. D.; Kung, A. L.; Escher, I.; Malia, T. J.; Barbuto, S.; Wright, R. D.; Wagner, G.; Verdine, G. L.; Korsmeyer, S. J. *Science* **2004**, *305*, 1466.
[32] Abell, A. D. *Lett Pept Sci*, **2002**, *8*, 267.
[33] Freidinger, R. M.; Schwenk Perlow, D.; Veber, D. F. *J Org Chem* **1982**, *47*, 104.
[34] Aubé, J. Advance in Amino Acid Mimetics and Peptidomimetics, Vol. 1 (Ed.: A. Abel), JAI Press, Greenwich, 1997; 193–232.
[35] Hanessian, S.; McNaughton-Smith, G.; Lombart, H.-G.; Lubell, W. D. *Tetrahedron*, **1997**, *53*, 12789.
[36] Gentilucci, L.; Tolomelli, A.; De Marco, R.; Tomasini, C.; Feddersen, S. *Eur J Org Chem* **2011**, 4925.
[37] De Marco, R.; Tolomelli, A.; Campitiello, M.; Rubini, P.; Gentilucci, L. *Org Biomol Chem* **2012**, *10*, 2307.
[38] De Marco, R.; Greco, A.; Rupiani, S.; Tolomelli, A.; Tomasini, C.; Pieraccini, S.; Gentilucci, L. *Org Biomol Chem* **2013**, *11*, 4273.
[39] Greco, A.; Tani, S.; De Marco, R.; Gentilucci, L. *Chem Eur J* **2014**, *20*, 13390.
[40] Demir Ordu, Ö.; Doğan, I. *Chirality* **2010**, *22*, 641.
[41] Chen, G.; Chunling Fu, C.; Ma, S. *Org Biomol Chem* **2011**, *9*, 105.
[42] Kano, S.; Yokomatsu, T.; Nemoto, H.; Shibuya, S. *J Am Chem Soc* **1986**, *108*, 6746.
[43] Greco, A.; De Marco, R.; Tani, S.; Giacomini, D.; Galletti, P.; Tolomelli, A.; Juaristi, E.; Gentilucci, L. *Eur J Org Chem* **2014**, *34*, 7614.
[44] For a β^2-β^3-diketopiperazine scaffold, see: Ressurreição, A. S. M.; Bordessa, A.; Civera, M.; Belvisi, L.; Gennari, C.; Piarulli, U. *J Org Chem* **2008**, *73*, 652.
[45] For a β^2-β^3-diketopiperazine scaffold, see: Ressurreição, A. S. M.; Bordessa, A.; Civera, M.; Belvisi, L.; Gennari, C.; Piarulli, U. *J Org Chem* **2008**, *73*, 652.
[46] Weber, K.; Gmeiner, P. *Synlett* **1998**, 885.
[47] Weber, K.; Ohnmacht, U.; Gmeiner, P. *J Org Chem* **2000**, *65*, 7406.
[48] Toniolo, C. *Int J Pept Prot Res* **1990**, *35*, 287.
[49] Lelais, G.; Seebach, D. *Biopolymers* **2004**, *76*, 206.
[50] Juaristi, E. Enantioselective synthesis of β-amino acids, 2nd ed. (Soloshonok, V., Ed.), Wiley-VCH: New York, 2005.
[51] Rose, D. M.; Alon, R.; Ginsberg, M. H. *Immunol Rev* **2007**, *218*, 126.
[52] Gonzalez-Amaro, R.; Mittelbrunn, M.; Sanchez-Madrid, F. *Immunology* **2005**, *116*, 289.
[53] Rommer, P. S.; Patejdl, R.; Zettl, U. K. *Curr Pharm Des* **2012**, *18*, 4498.
[54] Jackson, D. Y. *Curr Pharm Des* **2002**, *8*, 1229.
[55] Yang, G. X.; Hagmann, W. K. *Med Res Rev* **2003**, *23*, 369.
[56] Singh, J.; Adams, S.; Carter, M. B.; Cuervo, H.; Lee, W. C.; Lobb, R. R.; Pepinsky, R. B.; Petter, R.; Scott, D. *Curr Top Med Chem* **2004**, *4*, 1497.
[57] Vanderslice, P.; Woodside, D. G. *Prog Respir Res* **2010**, *39*, 169.
[58] Baiula, M.; Bedini, A.; Carbonari, G.; Dattoli, S. D.; Spampinato, S. *Front Pharmaco*. **2012**, *26*, *203*, 1.
[59] Lin, K.; Ateeq, H. S.; Hsiung, S. H.; Ching, L. T.; Zimmerman, C. N.; Castro, A.; Lee, W. C.; Hammond, C. E.; Kalkunte, S.; Chen, L. L.; Pepinsky, R. B.; Leone, D. R.; Sprague, A. G.; Abraham, W. M.; Gill, A.; Lobb, R. R.; Adams, S. P. *J Med Chem 1999*, **42**, 920.
[60] Singh, J.; Van Vlijmen, H.; Liao, Y.; Lee, W. C.; Cornebise, M.; Harris, M.; Shu, I.; Gill, A.; Cuervo, J. H.; Abraham, W. M.; Adams, S.P. *J Med Chem* **2002**, *45*, 2988.
[61] Karanam, B. V.; Jayra, A.; Rabe, M.; Wang, Z.; Keohane, C.; Strauss, J.; Vincent, S.; *Xenobiotica* **2007**, *37*, 487.
[62] Fisher, A. L.; DePuy, E.; Jayaraj, A.; Raab, C.; Braun, M.; Ellis-Hutchings, M.; Zhang, J.; Rogers, J. D.; Musson, D. G. *J Pharm Biomed Anal* **2002**, *27*, 57.
[63] Cardillo, G.; Gentilucci, L.; Melchiorre, P.; Spampinato, S. Bioorg *Med Chem Lett* **2000**, *10*, 2755.
[64] Cardillo, G.; Gentilucci, L.; Qasem, A. R.; Sgarzi, F.; Spampinato, S. *J Med Chem* **2002**, *45*, 2571.
[65] Tolomelli, A.; Gentilucci, L.; Mosconi, E.; Viola, A.; Paradisi, E. *Amino Acids* **2011**, *41*, 575.
[66] Spampinato, S.; Qasem, A. R.; Calienni, M.; Murari, G.; Gentilucci, L.; Tolomelli, A.; Cardillo, G. *Eur J Pharmacol* **2003**, *469*, 89.
[67] Cardillo, G.; Gentilucci, L.; Tolomelli, A.; Calienni, M.; Qasem, A. R.; Spampinato, S. *Org Biomol Chem* **2003**, *1*, 1498.
[68] Tolomelli, A.; Gentilucci, L.; Mosconi, E.; Viola, A.; Dattoli, S. D.; Baiula, M.; Spampinato, S. Belvisi, L.; Civera, M. *Chem Med Chem* **2011**, *6*, 2264.
[69] Tolomelli, A.; Baiula, M.; Belvisi, L.; Viola, A.; Gentilucci, L.; Troisi, S.; Dattoli, S. D.; Spampinato, S.; Civera, M.; Juaristi, E.; Escudero, M. *Eur J Med Chem* **2013**, *66*, 258.
[70] Galletti, P.; Soldati, R.; Pori, M.; Durso, M.; Tolomelli, A.; Gentilucci, L.; Dattoli, S. D.; Baiula, M.; Spampinato, S.; Giacomini, D. *Eur J Med Chem* **2014**, *83*, 284.
[71] Dattoli, S. D.; De Marco, R.; Baiula, M.; Spampinato, S.; Greco, A.; Tolomelli, A.; Gentilucci, L. *Eur J Med Chem* **2014**, *73*, 225.
[72] Gentilucci, L.; Cardillo, G.; Tolomelli, A.; De Marco, R.; Garelli, A.; Spampinato, S.; Spartà, A.; Juaristi, E. *Chem Med Chem* **2009**, *4*, 517.
[73] Gentilucci, L.; Cardillo, G.; Spampinato, S.; Tolomelli, A.; Squassabia, F.; De Marco, R.; Bedini, A.; Baiula, M.; Belvisi, L.; Civera, M. *J Med Chem* **2010**, *53*, 106.

[74] McClellan, W. J.; Dai, Y.; Abad-Zapatero, C.; Albert, D. H.; Bouska, J. J.; Glaser, K. B.; Magoc, T. J.; Marcotte, P. A.; Osterling, D. J.; Stewart, K. D.; Davidsen, S. K.; Michaelides, M. R. *Bioorg Med Chem Lett* **2011**, *21*, 5620.

[75] Singh, J.; van Vlijmen, H. W.; Lee, C.; Liao, Y.; Lin, K. C.; Ateeq, H.; Cuervo, J.; Zimmerman, C.; Hammond, C.; Karpusas, M.; Palmer, R.; Chattopadhyay, T.; Adams, S. P. *J Comp Aid Mol Des* **2002**, *16*, 201.

[76] Thangapandian, S.; John, S.; Sakkiah, S.; Lee, K. W. *Chem Biol Drug Des* **2011**, *78*, 289.

[77] Martins da Silva, J. H.; Dardenne, L. D.; Savino, W.; Caffarena, E. R. *J Braz Chem Soc* **2010**, *21*, 546.

[78] HyperChem Release 8.0.3, 2012, Hypercube Inc. 1115 NW 4th St. Gainesville, FL 32608 (USA).

[79] Larroque, A.L.; Dubois, J.; Thoret, S.; Aubert, G.; Chiaroni, A.; Guèritte, F.; Guènard, D. *Bioorg Med Chem* **2007**, *15*, 563.

[80] Bedini, A.; Baiula, M.; Gentilucci, L.; Tolomelli, A.; De Marco, R.; Spampinato, S. *Peptides* **2010**, *31*, 2135.

[81] Qasem, A.R.; Bucolo, C.; Baiula, M.; Spartà, A.; Govoni, P.; Bedini, A.; Fascì, D.; Spampinato, *S. Biochem Pharmacol* **2008**, *76*, 751.

[82] You, T. J.; Maxwell, D. S.; Kogan, T. P.; Chen, Q.; Li, J.; Kassir, J.; Holland, G. W.; Dixon, R. A. F. *Biophys J* **2002**, *82*, 447.

[83] Carlevaro, C. M.; Da Silva, J. H. M.; Savino, W.; Caffarena, E.R. *J Theor Comp Chem* **2013**, *12*, 1250108/1.

[84] Macchiarulo, A.; Costantino, G.; Meniconi, M.; Pleban, K.; Ecker, G.; Bellocchi, D.; Pellicciari, R. *J Chem Inf Comput Sci* **2004**, *44*, 1829.

[85] Temussi, P.A.; Picone, D.; Saviano, G.; Amodeo, P.; Motta, A.; Tancredi, T.; Salvadori, S.; Tomatis, R. *Biopolymers* **1992**, *32*, 367, and references herein.

[86] Spadaccini, R.; Temussi, P. A. *Cell Mol Life Sci* **2001**, *58*, 1572.

[87] Borics, A.; Töth, G. *J Mol Graph Modell* **2010**, *28*, 495.

[88] Wthrich, K. NMR of Proteins and Nucleic Acids, Wiley, New York, p. 320.

[89] Jorgensen, W. L.; Chandrasekhar, J.; Madura, J.; Impey, R. W.; Klein M. L. *J Chem Phys* **1983**, *79*, 926.

[90] Cornell, W. D.; Cieplak, P.; Bayly, C. I.; Gould, I. R.; Merz, K. M.; Ferguson, D. M.; Spellmeyer, D. C.; Fox, T.; Caldwell, J. W.; Kollman, P. A. *J Am Chem Soc* **1995**, *117*, 5179.

[91] Banerjee, A.; Balaram, P. *Curr Sci India* **1997**, *73*, 1067.

[92] Baldauf, C.; Gunther, R.; Hofmann, H. *Biopolymers* **2006**, *84*, 408.

[93] Rai, R.; Vasudev, P. G.; Ananda, K.; Raghothama, S.; Shamala, N.; Karle, I. L.; Balaram, P. *Chem Eur J* **2007**, *13*, 5917.

[94] Qasem, A. R.; Bucolo, C.; Baiula, M.; Spartà, A.; Govoni, P.; Bedini, A.; Fascì, D.; Spampinato, S. *Biochem Pharmacol* **2008**, *76*, 751.

[95] Marcinkiewicz, C.; Calvete, J. J.; Marcinkiewicz, M. M.; Raida, M.; Vijay-Kumar, S.; Huang, Z.; Lobb, R. R.; Niewiarowski, S. *J Biol Chem* **1999**, *274*, 12468.

[96] Williamson, M. P.; Havel, T. F.; Wüthrich. *J. Mol Biol* **1985**, *182*, 295.

Chapter 10

Self-Assembled monolayers of zeolite L nanocrystals functionalized with the integrin ligand c[RGDfK] as model devices for the specific detection of cancer cells

In this chapter is reported the preparation of nanostructured substrate, readily obtained by immobilizing the cyclic c[RGDfK] targeting ligand onto patterned zeolite L monolayers. The functionalized surface allows fast and specific entrapment of cancer cells *via* integrin-mediated cell adhesion. With its high specificity towards cancer cells and fast adhesion ability, this biocompatible monolayer candidates itself as promising platform for implementation in diagnostics and personalized therapy formulation devices.

10.1. Introduction

Integrins are heterodimeric glycoproteinic adhesion receptors that mediate cellular attachment to the extracellular matrix (ECM) and to other cells.[1] Upon interaction with specific substrates (*i.e.* fibrinogen, fibronectin, plasminogen, *etc*.) they also regulate various cellular functions, such as cell adhesion, migration, invasion, proliferation and survival/anoikis.[1,2] Recent studies have demonstrated the crucial role of integrins (*e.g*. αvβ3, αvβ5, αvβ1, α6β4, α4β1, *etc*.) in the development of invasive tumors that preferentially metastasize to bone, such as breast and prostate carcinomas.[2,3] For example, studies examining the expression of αvβ3 integrin in various breast cancer tissues have evidenced a correlation between the overexpression of integrin αvβ3 and the formation of bone metastases in breast cancer patients.[4] In pancreatic tumor, the increased expression of αvβ3 integrin is associated with an increased activation of MMP-2 and lymph node metastases,[5] and in prostate carcinoma again to bone metastases formation.[3,4]

Since the discovery of the Arg-Gly-Asp (RGD) tripeptide as the prominent minimal recognition motif for many integrins (including αvβ3, αvβ5, and αvβ1),[1,2,6] this sequence has been employed for the development of small-molecule antagonists, focused on the use of RGD-mimetics,[3,4,7] which efficiently led to important results in blocking tumor progression.[8] Nowadays, interest has also focused on the construction of RGD-functionalized bio-active substrates for the preparation of integrin-mediated cell adhesion surfaces to be employed for biomedical applications, especially for the bio-integration of implant materials.[9] The successful design of these scaffolds relies on understanding the interactions of the cells with the coating components. Cell adhesion, migration, proliferation, and differentiation onto bio-active substrates are quite sensitive to the bioactivity, tether length, interspacing, and density of the biological ligands attached to the surface.[9,10] An attractive way to improve the organization and consequently the efficacy of cell-binding substrates, regards the intercalation between the bioactive recognition moiety and the support surface of self-assembled monolayers (SAM) of nanoparticles (NPs). The large surface area of SAMs superficially functionalized with bioactive molecules, provides a large number of contact points in a confined surface (high density of ligands on the NP's surface), which can be exploited for a more effective binding to biological systems.[10] Furthermore, the organization of the biomolecules on the SAMs can be controlled thanks to a series of micro-fabrication techniques recently developed that allow the creation of pre-definite morphologies, dimensions, and molecular orientations (*i.e.* soft lithography and microcontact printing).[11] In this respect, it has been demonstrated that zeolite L SAMs can be successfully employed as nano-motif for the functional patterning of glass for biotechnological applications.[11] The formation of the monolayer is achieved by a chemical functionalization[12] of the channel entrances of this porous material, allowing the control of the crystals orientation.

Based on these premises, in this chapter is reported the preparation and the preliminary biological assays of an integrin-targeted patterned SAM of disk-shaped zeolite L on glass substrates for cancer cell adhesion. By coating with a cyclic RGD peptide (c[RGDfK]) the surface of the zeolite SAM a faster, more spatially controlled, and more selective adhesion of cancer cells is achieved. This interaction could hence be exploited for diagnostic purposes for the entrapment and study of an important biomarker, namely circulating tumor cells (CTCs).[13] CTCs are cells that have shed into the vasculature from a primary tumor, constituting seeds for subsequent growth of metastasis.[14] Their importance in cancer diagnostic has grown[15] as their concentration in the blood may represent an indicator of a tumor's invasiveness, as well as its sensitivity/resistance to a specific therapy.

Moreover, CTCs could serve as "liquid biopsy" by providing representative tumor tissue, essential for biomarker identification and subsequent formulation of a personalized therapeutic treatment.[16]

10.2. Results and discussion

To construct our bio-compatible substrate we have employed ultra-flat disk-shaped zeolite L crystals approximately 1000 nm width and 250 nm height (Figure 1a; see also synthetic procedures section).[17] The crystals were first loaded with a fluorescent dye, *N,N'*-bis(2,6-dimethylphenyl)perylene-3,4,9,10-tetracarboxylic acid diimide (DXP; λ_{exc} = 490 nm; λ_{em} = 564 nm), for visualization purposes (**DXP-Zeo**) and subsequently their surface functionalized with 3-(isocyano)propyltriethoxysilane (ICPTES; **DXP-Zeo-IC**) for both the synthesis of the monolayer, and successive grafting of the RGD-peptide. Qualitative and quantitative characterization of the functionalized zeolites was performed by means of X-ray photoelectron spectroscopy (XPS) and thermogravimetric analysis (TGA). The first technique allowed detection of the modifications of the elemental composition of the material along with the synthetic modifications. Indeed, upon DXP insertion first, and surface functionalization with ICPTES later (see synthesis section), the relative atomic percentages (At%) of the elements composing the materials change. The signals of C(1s) and N(1s), very low for the pristine zeolites (C(1s): 6.1 At%; N(1s) 0.7 At%), increased significantly and consequentially in **DXP-Zeo** and **DXP-Zeo-IC** (C(1s): 20.7 and 33.0 At%; N(1s) 2.0 and 5.5 At%; Figure 8, Table 1). TGA further confirmed the occurrence of each step of the functionalization by displaying an increasing weight loss passing from zeolites (negligible weight loss in the analyzed temperature range) to **DXP-Zeo** and **DXP-Zeo-IC** (1.7 and 5.7 % respectively; contribution of water excluded), confirming an always more important ratio of organic material in the hybrids (Figure 9, Supporting Information). Ultimately, scanning electron microscopy (SEM) analysis demonstrated that the morphology of the zeolites (important for fostering efficient cellular adhesion) was preserved throughout the functionalization steps (Figure 10).

The SAMs were then prepared according to a protocol developed in our laboratories (Figure 1).[11] Specifically, activated silica plates where functionalized with aminopropyltriethoxysilane (APTES; see synthesis section for details) to obtain amino functional groups on the surface for reaction with **DXP-Zeo-IC**. This coupling step, key to the formation of the monolayer, was then performed by sonicating the amino-functionalized glass substrates in a suspension of **DXP-Zeo-IC** (1 mg/mL) in toluene for 30 minutes. To pattern the zeolite SAMs a stripe-patterned (50 μm) elastomeric poly(dimethyl siloxane) (PDMS) stamp was pressed on the monolayer for about 30 s and peeled off quickly.[11,12] Stripes of about 50 μm of SAMs remained on the surface of the glass. This topography was chosen to better prove the attachment of the cells only on the zeolites functionalized with the peptide, thus highlighting the specificity of its action.

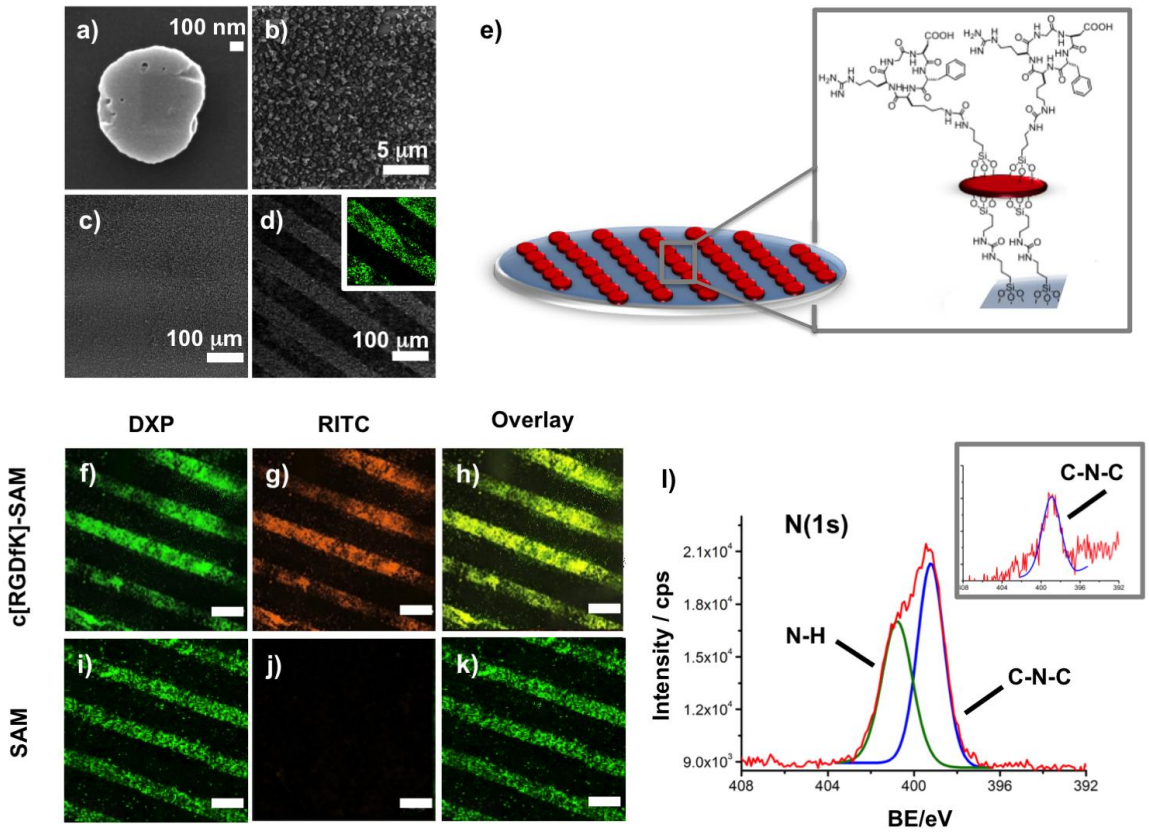

Figure 1. a-d) SEM images of: a) zeolite L crystals employed in the preparation of the SAM; b) close-up image of the prepared SAM, displaying the **DXP-Zeo-IC** covalently attached on the surface; the SAM before (c) and after (d) PDMS patterning; in the inset of (d) the confocal image of the printed SAM (λ_{exc} = 490 nm); e) graphical representation of the cRGD-SAM bound onto a glass substrate; f-h) confocal images of **c[RGDfK]-SAM** after reaction with RITC dye. i-k) As control for the lack of reaction of the RITC in absence of **c[RGDfK]**, also naked SAM was tested. f,i) DXP channel (green): λ_{exc}= 490 nm; g,j) RITC channel (orange): λ_{exc}= 540 nm; h,k) overlay. Scale bar = 200 µm; l) high resolution N(1s) XPS analysis of **c[RGDfK]-SAM**. In the inset the high-resolution N(1s) XPS analysis of the naked SAM.

Once prepared, to enable the SAM to promote efficient cell adhesion, the printed substrate was coupled with the αvβ3 integrin ligand c[RGDfK], developed by Kessler *and co-workers.*[18] This sequence was specifically chosen since RGD-containing cyclopeptides (cRGD) were shown to be more resistant to chemical degradation, more effective, and more selective than the linear equivalents.[7,19] Moreover, c[RGDfK] allows conjugation to the isocyanate-functionalized monolayer thanks to the presence of the amino group in the lysine.[20] The ligand c[RGDfK] was readily prepared by cyclization of the linear precursor H-Asp(O*t*Bu)-D-Phe-Lys(Boc)-Arg(Mtr)-Gly-OH, obtained in turn by solid phase peptide synthesis using the acid-labile 2-chlorotrityl resin and TBTU/HOBt/DIPEA as coupling agents under controlled microwave heating, according to a recently optimized procedure (Synthesis section).[21] After peptide cleavage with AcOH/CF_3CH_2OH (TFE) in DCM, the cyclization step was performed by slowly adding (12 h) the linear peptide to a solution of HATU/DIPEA *via* a temporized syringe. The final deprotection with TFA in the presence of scavengers afforded the crude cyclopeptide, purified (>95 %) by semi-preparative RP-HPLC. Bio-conjugation of the peptide to the printed monolayer was thus ultimately performed upon immersion of the patterned SAMs into a solution of c[RGDfK] (1 mg/mL) in TEA and DMF (1:100) heated at 35 °C for 3 h.

Effective functionalization of the monolayers with the peptide was assessed by XPS analysis and by selective functionalization with rhodamine B isothiocyanate (Figure 1 and Synthetic procedures section). In the latter experiment, both a c[RGDfK]-functionalized SAM and a naked one, used as control, were reacted with rhodamine B isothiocyanate (RITC). Due to its isothiocyanate group, this dye can react with the amino group present on the peptide (*i.e.* arginine residue), resulting to its covalent binding to the **c[RGDfK]-SAM**. Such reaction cannot occur on the naked SAM, presenting on its surface only isocyanate groups. Indeed, as shown in

Figure 1f-h, confocal imaging of the two substrates showed that only **c[RGDfK]-SAM** presents the characteristic emission of RITC, perfectly superimposable with the signal of the DXP entrapped in the zeolites channels. As expected, the signal of the rhodamine dye is not present on the naked SAM (Figure 1i-k), clearly indicating that the presence of the RITC signal in the **c[RGDfK]-SAM** cannot be due to non specific adsorption on the zeolites. Moreover, the images in Figure 1f-h show the homogeneous distribution of the dye exclusively along the stripes of the monolayer surface, highlighting at the same time both the successful patterning as well as the homogenous coverage obtained for the bio-coating. XPS analysis of the two substrates further indicated the presence of the peptide on the zeolites surface. In fact, the relative amount of C(1s) and N(1s) increased in the peptide-derivatized SAM, in comparison to the naked monolayer (C(1s): 30.6 and 5.1; N(1s) 42.6 and 8.7 % for SAM and **c[RGDfK]-SAM** respectively). Moreover, the high resolution XPS analysis of the N(1s) peak for **c[RGDfK]-SAM** displays a modification of its shape as compared to SAM (Figure 1l and inset). Indeed it results composed of two components, one at 399 eV (present also in **SAMs**) corresponding to the isocyanate form of N(1s) and one at 402 eV assigned to the peptidic and urea form of N(1s).
Once confirmed the morphology and the effective surface functionalization of the SAMs, adhesion experiments were performed with the integrin expressing cancer cells lines HeLa and Glioma C6. Specifically, 1×10^5 cells of each cell line were stained (DiO staining, λ_{exc}= 484 nm; λ_{em} = 501 nm) and seeded on both naked and c-RGD-functionalized SAMs in order to evaluate the effect of the peptide on the binding activity of the monolayers. After 30 min incubation at 37 °C, cells were washed, and fixed with paraformaldehyde (PFA). Confocal microscope images showed that the adhesion behavior on the SAMs of the cancerous cell lines is dramatically different depending on the presence of the bio-active cRGD on the monolayer surface. As shown in Figure 2, the population of both HeLa and Glioma C6 cells on **c[RGDfK]-SAMs** resulted much higher than the population on the naked monolayers. Accurate counting of the number of cells on the cRGD-functionalized versus the naked SAMs showed a 3.5 and 18.4 fold increase of population, for HeLa and Glioma C6 respectively. These results demonstrate that cancer cells undergo an efficient integrin-mediated adhesion onto the zeolite monolayers, already in the short time interval (30 min) employed for the incubation. Interestingly, the primary endothelial cells T-293 (DiD staining, λ_{exc}= 644 nm; λ_{em} = 665 nm) were also tested on both the c[RGDfK]-functionalized and the naked monolayer, and did do not bind to either types of SAMs .

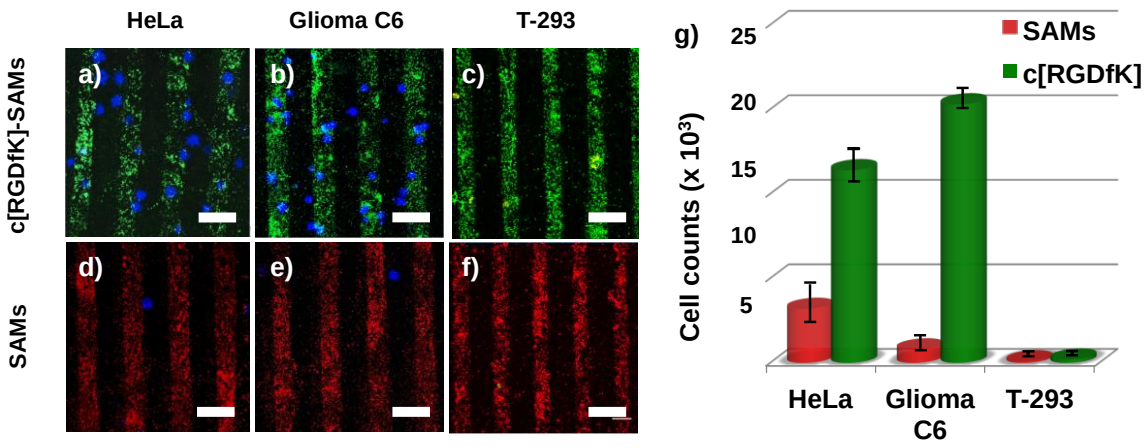

Figure 2. a-f) Confocal images of the **c[RGDfK]-SAM** (DXP, green channel, λ_{exc}= 490 nm) and naked **SAM** (DXP, red channel, λ_{exc} = 490 nm) after cancer cell adhesion experiments (1×10^5, incubation 30 min at 37 °C); cells are visualized in blue (DiO staining, λ_{exc} = 484 nm); scale bar = 100 μm. The emission of the DXP is represented either as green (a-c) or red (d-f), depending if the monolayer is coated or not by the c[RGDfK] peptide respectively. Cancer cells are visualized in blue (DiO, λ_{exc} = 484 nm), primary endothelial cells in yellow (DiD, λ_{exc} = 644 nm); g) quantitative data of adhered cells on c[RGDfK]-functionalized and naked SAMs (analyzed area: 0.0025 cm^2; cell count values normalized to an area of 1 cm^2).

To show that the selectivity of the here reported **c[RGDfK]-SAMs** could be used for specific cancer cell detection, we further tested the capacity of **c[RGDfK]-SAM** to sense cancer cells in presence of a heterogeneous mixed cell population. Cancer cells and primary cells (HeLa/T-293 and Glioma C6/T-293 1:1 ratio, 1×10^5 cells

each) were labeled with different fluorescent stains (for cancer cells DiO staining, λ_{exc}= 484 nm; λ_{em} = 501 nm; for primary cells DiD staining λ_{exc}= 644 nm; λ_{em} = 665 nm) and seeded on both naked and **c[RGDfK]-SAMs**. Analysis of the cell adhesion by confocal microscopy (Figure 3a-d) confirmed a very low healthy cell binding on both substrates. Most importantly, the number of cancer cells on the peptide coated SAMs is much higher compared to the non bio-compatible surfaces confirming the role of the cyclic peptide on the recognition of the overexpressed integrin receptors present in cancer cells. Indeed, as graphically represented in Figure 3e, the ratio cancer/primary cells resulted increased from 4.5 and 3 to 8.5 and 20.7 for HeLa and Glioma C6, respectively, when passing from the naked to the **c[RGDfK]-SAMs**. These results further confirm the ability of the substrate to capture a large number of cancer cells when the cyclic peptide is bound to the surface, and more interestingly to have a very effective adhesion, of mainly cancer cells, in the presence of the same amount of healthy cells.

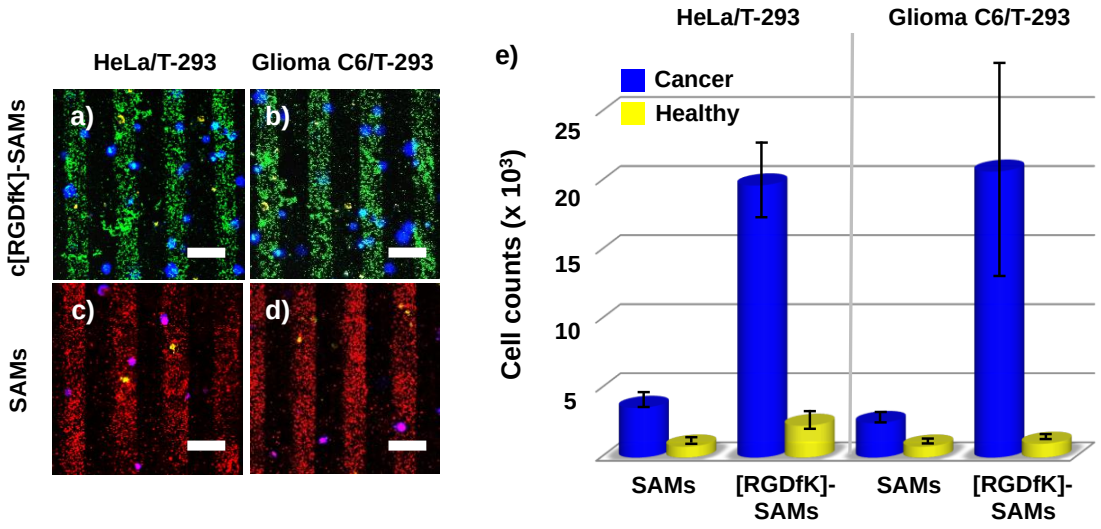

Figure 3. a-d) Confocal images of the c[RGDfK]-functionalized (DXP, green channel, λ_{exc}= 490 nm) and naked SAMs (DXP, red channel, λ_{exc} = 490 nm) after mixed population cell adhesion experiments (1×10^5 of each cell line, incubation 30 min at 37 °C); cancer cells are visualized in blue (DiO, λ_{exc} = 484 nm), primary endothelial cells in yellow (DiD, λ_{exc} = 644 nm); scale bar = 100 μm; g) quantitative data of adhered cells on c[RGDfK]-functionalized and naked SAMs (analyzed area: 0.0025 cm^2; cell count values normalized to an area of 1 cm^2).

10.3. Conclusion

In conclusion, we have demonstrated the efficiency of our new bio-selective substrate based on zeolite L SAMs conjugated to the integrin ligand c[RGDfK], for the adhesion of cancer cells. This adhesion resulted very efficient for both the cancer cell lines tested, HeLa and Glioma C6, even upon rapid incubation (only 30 min.). Finally, we challenged our new biocompatible surface with a mixed population of cancer and primary endothelial cells and, in these incubation conditions, almost exclusive adhesion of cancer cells was observed, thus demonstrating the high affinity of the c[RGDfK] peptide for the integrin proteins abundantly present on the surface of cancer cells.

Perspectives. Further studies on the sensitivity and the tailoring of the surface coating of these monolayers are currently on going. Indeed, this substrate might represent a potential candidate for the development of new diagnostic kits or even implantable diagnostic devices capable to specifically recognize and trap CTCs present into biological fluids, thus enabling a significant advance in the early detection and study of cancer and other integrin-related diseases. In this context, we are now developing surfaces loaded with $\alpha_4\beta_1$ integrin ligands in order to study inflammatory processes such as asthma and autoimmune diseases.
Finally, since porous nanoparticles like zeolite L are very popular for drug delivery applications, we have already synthesized zeolite L crystals approximately 200 nm width and 50 nm height, loaded with DXP dye and functionalized with different integrin antagonists and cytotoxic peptides. These constructs are now under

investigation for their theranostic abilities, which means high capacity to ferry cargo and loads onto them both imaging and therapeutic functions.

10.4. Experimental Section

10.4.1. General Methods

Standard chemicals, including protected amino acids, were purchased from commercial sources and used without further purification. Flash chromatography was performed on silica gel (230-400 mesh), using mixtures of distilled solvents. The purity of c[RGDfK] and its synthetic precursors was assessed by analytical RP-HPLC performed with an Agilent 1100 series apparatus, using a RP column [Phenomenex mod. Gemini 3µ C18 110A 100x3.0 mm (P/No 00D-4439-Y0)]; column description: stationary phase octadecyl carbon chain bonded silica (C18) with TMS end capping, fully porous organosilica solid support, particle size 3 mm, pore size 110 Å, length 100 mm, internal diameter 3 mm; DAD 210 nm; mobile phase: from 9:1 H_2O/CH_3CN to 2:8 H_2O/CH_3CN with the addition of 0.1 % TFA, in 20 min at a flow rate of 1.0 mL/min, followed by 10 min at the same composition. Semi-preparative RP-HPLC was performed with an Agilent 1100 series apparatus, using a RP column [ZORBAX mod. Eclipse XDBC18 PrepHT cartridge 21.2 x 150 mm 7µ (P/No 977150-102)]; column description: stationary phase octadecyl carbon chain bonded silica (C18), double end capped, particle size 7 µm, pore size 80 Å, length 150 mm, internal diameter 21.2 mm; DAD 210 nm; mobile phase from 8:2 H_2O/CH_3CN to 100 % CH_3CN with the addition of 0.1 % TFA, in 10 min at a flow rate of 12 mL/min. MS (ESI) analysis was performed using a MS single quadrupole HP 1100 MSD detector, with a drying gas flow of 12.5 L/min, nebulizer pressure 30 psgi, drying gas temp. 350 °C, capillary voltage 4500 (+) and 4000 (-), scan 50-2600 amu. The synthetic procedures by MW irradiation were performed with a microwave oven (Micro-SYNTH Microwave Labstation for Synthesis) equipped with a built-in ATC-FO advanced fiber optic automatic temperature control. ^{1}H NMR spectrum of c[RGDfK] was recorded with a Varian Gemini apparatus at 400 MHz in a 5 mm tube, using 0.01 M peptide at RT.

Zeolites were prepared according to a standard procedure previously reported in the literature.[22] 3-isocyanatepropyltriethoxysilane, 3-aminopropyltriethoxysilane, TEA, DMF, Toluene, PFA, DiO, DiD, DiL, DXP were purchased from Sigma Aldrich. PDMS was obtained from Dow Corning corporation (184 silicon elastomer base, SYLGARD). Glass plates (⦸ 1.2 cm) used for zeolite monolayers were purchased from Servoprax GmbH. Dulbecco's modified culture medium (DMEM), FBS, penicillin, glutamine, trypsin and PBS solution (pH 7.2) were purchased from Gibco (Life Technologies). HeLa cells and Glioma C6 were obtained from ATCC/LGC Standards GmbH (Wesel, Germany) and cultivated according to the provider's protocol. T-293 cells were kindly provided by Dr. Eric Robinet at the IHU, Hopital Civil Strasbourg. XPS analyses were performed using a K-Alpha™+ X-ray Photoelectron Spectrometer (XPS) System (Thermo Scientific). Monochromatic Al K alpha X-rays were used (15 keV, 72 W, 200 µm spot diameter). Spectra were measured using a pass energy of 200 eV for survey spectra and 50 eV for core level spectra. The analyzed zeolite samples were prepared by drop-casting an ethanolic dispersion (0.1 mg/mL) of the particles onto a glass coverslip pre-coated with Au (Emitech K575X peltier cooled) for 3 min at 60 mA. The monolayers were analyzed as they were, without further treatment. TGA analyses were conducted on a TGA 1 STAR System Mettler Toledo machine under nitrogen atmosphere. The samples (0.1 – 2 mg) were kept at 50 °C for 30 minutes for stabilization, then heated from 50 to 750 °C at a speed of 10 °C/min, and held at this temperature for further 30 minutes before cooling. The analyses were performed under a gas flow of N_2 at 50 mL/min. SEM images were recorded with a FEI Quanta FEG 250 instrument (FEI corporate, Hillsboro, Oregon, USA) at an operating distance of 10 mm and with an acceleration voltage of 5 kV. The zeolite samples were prepared by drop-casting a dispersion of particles in EtOH onto a glass cover slip, subsequently sputter coated with Au (Emitech K575X peltier cooled) for 60 s at 60 mA prior to fixation on an Al support. SAMs monolayers were analyzed without further manipulation. Powder X-ray diffraction (PXRD) measurements were performed on a Bruker D2 PHASER diffractometer using a Cu Kα-radiation (1.54184 Å) and a Ni Kβ-filter at 300 W (30 kV, 10 mA) power with a LYNXEYE scintillation detector. Samples were mounted on a zero background silicon sample holder. The measurement was performed from a 2θ value from 5 to 45 ° with exposure time of 1.5 second per step. All measurements were performed at room pressure and RT. Confocal images were obtained with a Zeiss LSM 710 microscope system, 63X magnification, numerical aperture 1.3 of Zeiss LCI Plan-NEOFLUAR water immersion objective lens (Zeiss GmbH). All image processing was performed with the ZEN 2011 software.

10.4.2. Synthetic procedures

Synthesis of H-Asp(OtBu)-D-Phe-Lys(Boc)-Arg(Mtr)-Gly-OH. The linear pentapeptide precursor of c[RGDfK] was assembled on the commercially-available Gly-preloaded 2-chlorotrityl resin (Gly loading 1.1 mmol/g resins). The resin (0.5 g) was swollen in 1:2 DMF/dimehylpirrolidone (5 mL) for 30 min before use. Fmoc-amino acid (3 equiv), the coupling reagents TBTU (3 equiv), HOBt (3 equiv), DIPEA (6 equiv), were added to the resin and the mixture was reacted for 10 min under MW irradiation (50 W, 50 ^{o}C). The resin was washed 3 times with DMF (5 mL) and MeOH (5 mL). Deprotection of Fmoc group was carried out by treatment of 20 % piperidine/DMF for 3 min under MW irradiation (50 W, 50 ^{o}C). After that, the resin was washed 3 times with DMF (5 mL) and MeOH (5 mL). The resulted peptidyl resin was treated with AcOH and TFE in CH_2Cl_2 (1:1:4 v/v/v, 15 mL) for 90 min at RT. The solution of the cleaved cyclic peptide was concentrated at reduced pressure. The residue was lyophilized to afford 0.32 g of crude peptide. The purity of the product was determined 85 % by reversed-phase (RP) HPLC (see General Methods); Rt = 6.55 min. MS (ESI) *m/z*: $[M + H]^+$ calcd for $C_{46}H_{71}N_9O_{13}S$, 990.5; found, 990.8.

Synthesis of c[Asp(OtBu)-D-Phe-Lys(Boc)-Arg(Mtr)-Gly]. The linear peptide (0.32 g, *circa* 0.32 mmol) in DMF (10 mL) was added dropwise at RT using a temporized syringe in 12 h, to a stirred solution of HATU (3 equiv) and DIPEA (6 equiv) in DMF (40 mL). The reaction mixture was stirred for other 12 h. The solvent was evaporated at reduced pressure, the residue diluted with water (5 mL) was extracted 3 times with EtOAc (15 mL). The residue was purified by flash chromatography over silica gel (eluent: 100 % EtOAc) giving the cyclopeptide (205 mg, 66 %), 90% pure by RP-HPLC (General Methods). Rt = 9.69 min. MS (ESI) *m/z*: $[M + H]^+$ calcd for $C_{46}H_{69}N_9O_{12}S$, 972.5; found, 972.8.

Procedure for the final deprotection to c[RGDfK]. The fully-protected cyclopeptide (0.2 g mg, 0.20 mmol) was dissolved in TFA-TIS-H_2O (95:2.5:2.5 v/v/v, 20 mL) and the solution was stirred at RT for 2 h. The solution was concentrated at reduced pressure and the residue was lyophilized to afford the crude peptide. The product c[RGDfK] was isolated by semi-preparative RP-HPLC (General Methods) as a TFA salt (121 mg, 85 %), >95% pure as determined by analytical RP-HPLC, see General Methods; Rt = 1.00 min. MS (ESI) *m/z*: $[M + H]^+$ calcd for $C_{27}H_{41}N_9O_7$, 604.3; found, 604.5. ^{1}H NMR was found to match with the literature[2] (400 MHz, D_2O, δ): 0.67-0.73 (m, 2H, LysHγ), 1.27-1.56 (m, 7H, LysHβ, LysHδ, ArgHγ, ArgHβ), 1.73 (m, 1H, ArgHβ), 2.40 (dd, J = 7.2, 15.6 Hz, 1H, AspHβ), 2.51 (dd, J = 6.9, 15.6 Hz, 1H, AspHβ), 2.69-2.73 (m, 2H, LysHε), 2.80 (m, 1H, PheHβ), 2.95 (dd, J = 5.2, 13.2 Hz, 1H, PheHβ), 3.050-3.09 (m, 2H, ArgHδ), 3.30 (d, J = 14.2 Hz, 1H, GlyHα), 3.73 (m, 1H, LysHα), 4.05 (d, J = 14.2 Hz, 1H, GlyHα), 4.26 (m, 1H, ArgHα), 4.40 (dd, J = 5.2, 10.4 Hz, 1H, PheHα), 4.55 (m, 1H, AspHα), 7.10-7.24 (m, 5H, PheArH).

Zeolite synthesis. Zeolite L nanocrystals were synthesized according to a procedure largely described in literature.[17]

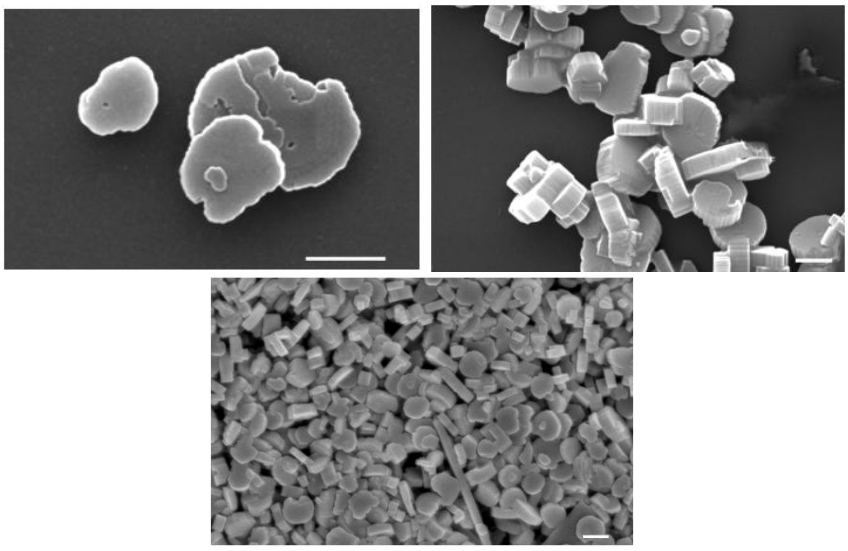

Figure 4. SEM image of disk-shaped zeolite L crystals; scale bar = 500 nm.

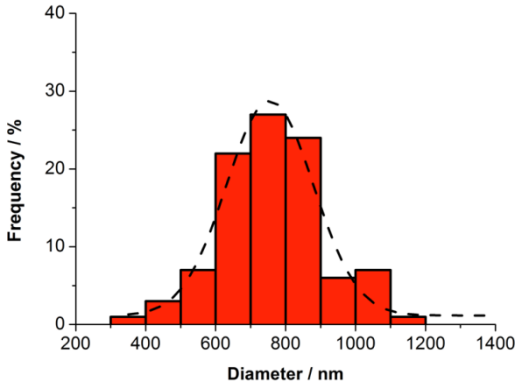

Figure 5. Size distribution diagram of disk-shaped zeolite L (derived from SEM images).

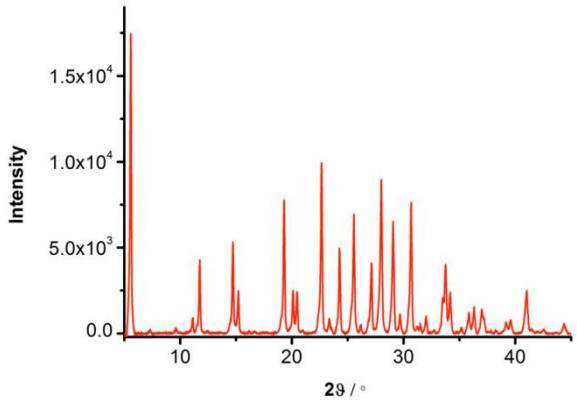

Figure 6. Powder XRD diffraction pattern of zeolite L.

*Zeolite loading with DXP 170 dye (**Zeo-DXP**).* Zeolites[S1] (300 mg) and DXP (6.23 mg) were kept overnight under high vacuum. The solid mixture was then introduced in a sealed flask and heated in a rotary furnace at 300 °C for 48 h. The flask was then opened and the powder washed and centrifuged (30 min, 40 krcf) in butan-1-ol until the supernatant ceased UV emission. The material was characterized by means of XPS, TGA, and SEM.

*Functionalization of **Zeo-DXP** with 3-Isocyanopropyltriethoxysilane (**IC-Zeo-DXP**).* **Zeo-DXP** (50 mg) were suspended in a 50 mL flask containing a mixture of toluene (5 mL) and TEA (0.2 mL), and sonicated for 15 min until the precipitate was dissolved. Then 3-(triethoxysilyl)propyl isocyanate (0.8 mL) was added, and the mixture further sonicated for 3 h. The suspension was then cooled to RT and centrifuged for 20 min at 40 krcf. The precipitate was then redispersed by sonication in toluene and centrifuged three times to remove unreacted silane. The material was characterized by means of XPS, TGA, and SEM.

*Preparation of **IC-Zeo-DXP** SAMs.* Glass plates were introduced into a 100 mL flask and activated with 3:1 H_2SO_4/H_2O_2 (10 mL) at 100 °C for 1 h. The solution was removed and the plates were washed with bi-distilled water (3 × 30 mL) followed by ethanol (3 × 20 mL) and finally dried under nitrogen flow. The plates were then fixed onto a Teflon support to avoid any surface overlap and the system was placed into a 100 mL round bottom flask containing toluene (30 mL). APTES (0.8 mL) and TEA (0.2 mL) were added and the flask was heated at 115 °C overnight. Subsequently, the plates were removed from the solution and washed with toluene (5 mL) and ethanol (5 mL) and dried with nitrogen flow. The plates were then placed into a suspension of isocyanate-functionalized zeolites in toluene (1 mg/mL, 2 mL), and sonicated for 30 minutes, before recovering the plates, rinsing them with toluene (5 mL) and air-drying them before use. The SAM was characterized by means of SEM.

*Preparation of the PDMS elastomeric stamp and patterning of **IC-Zeo-DXP** SAMs.* The monomeric silicon elastomer and the activator agent were introduced in a plastic test tube (10:1 w/w). The components were mixed and the mixture was spilled into a Petri dish containing three patterned Si wafers (50 μm × 50 μm, width × depth). The viscous liquid on Petri dish was degassed at reduced pressure, then heated at 50 °C for 3 h. Finally, the polymer was cut around the negative stamp, the latter was removed, and the resulting elastomeric stamp employed for the soft lithography of the SAMs. The elastomeric stamp was pressed onto the monolayer for 30 sec. Effective patterning was analyzed by SEM.

*Functionalization of **IC-Zeo-DXP** SAMs with c[RGDfK].* c[RGDfK] (1 mg) and TEA (10 μL) were dissolved in DMF (1 mL). The solution was sonicated for 5 min to favor the complete dissolution of the peptide. A plate of patterned monolayer composed of DXP-loaded zeolite NPs was immersed in the solution and heated at 35 °C for 3 h. Finally, the plate was removed from the solution and washed with DMF (5 mL) and EtOH (5 mL), then air dried. The SAM was characterized by means of XPS, and SEM.

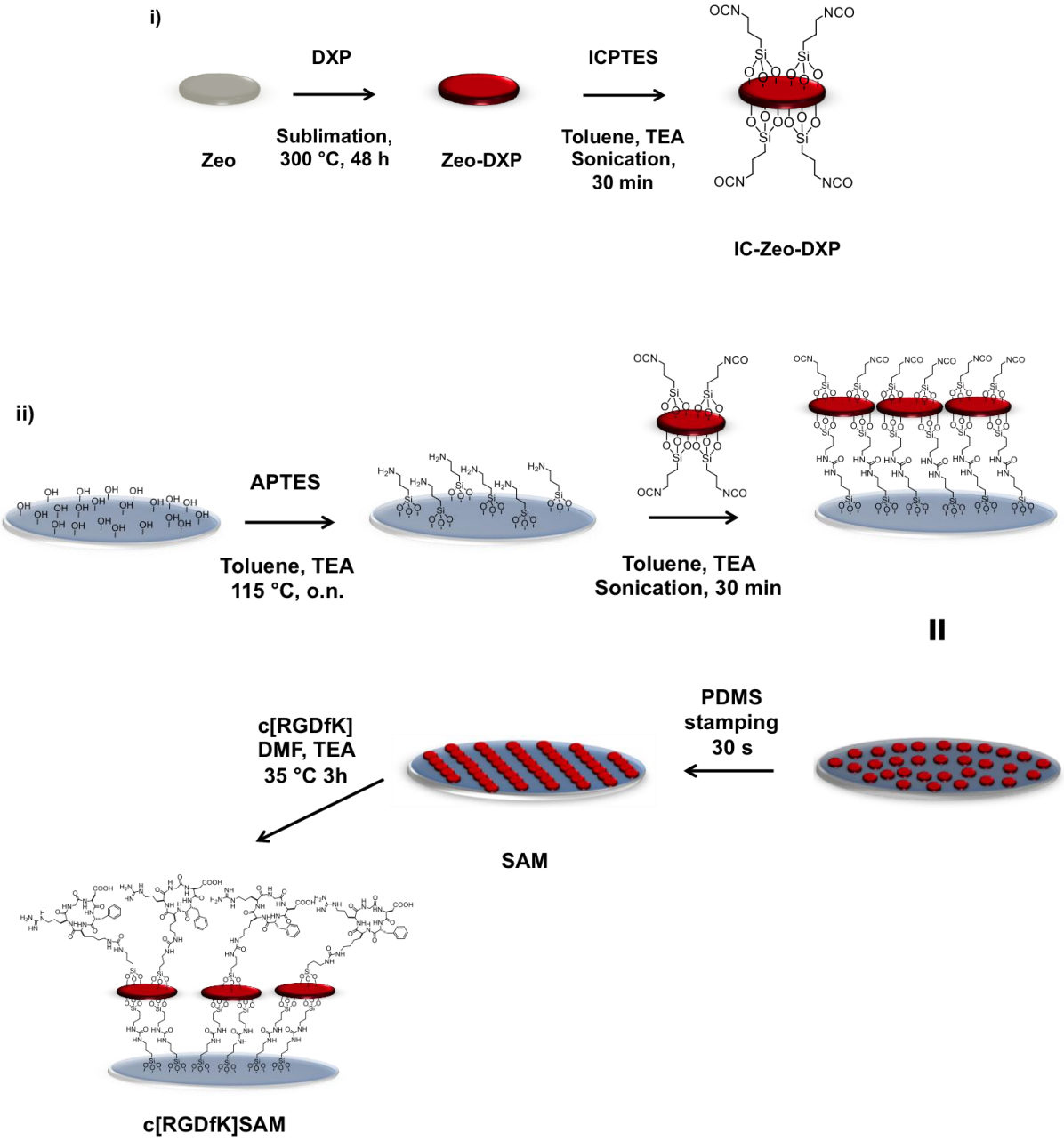

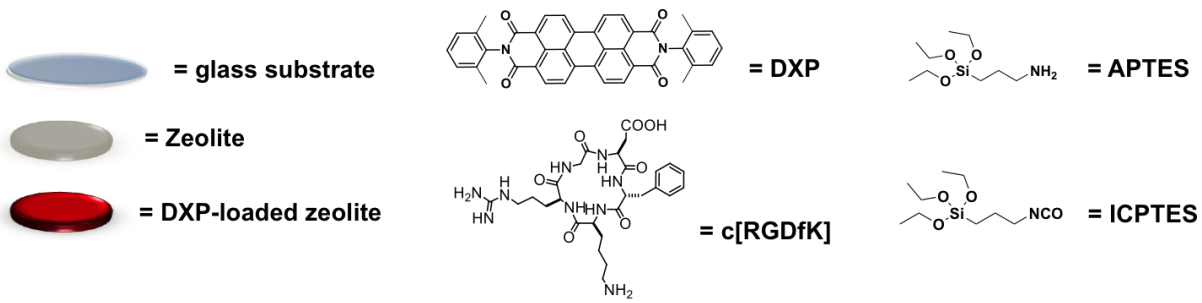

Figure 7. Preparation of DXP-loaded c[RGDfK]-functionalized patterned SAMs of zeolite L crystals: i) synthesis of **IC-Zeo-DXP** used for the monolayer preparation; ii) **c[RGDfK]-SAM** preparation.

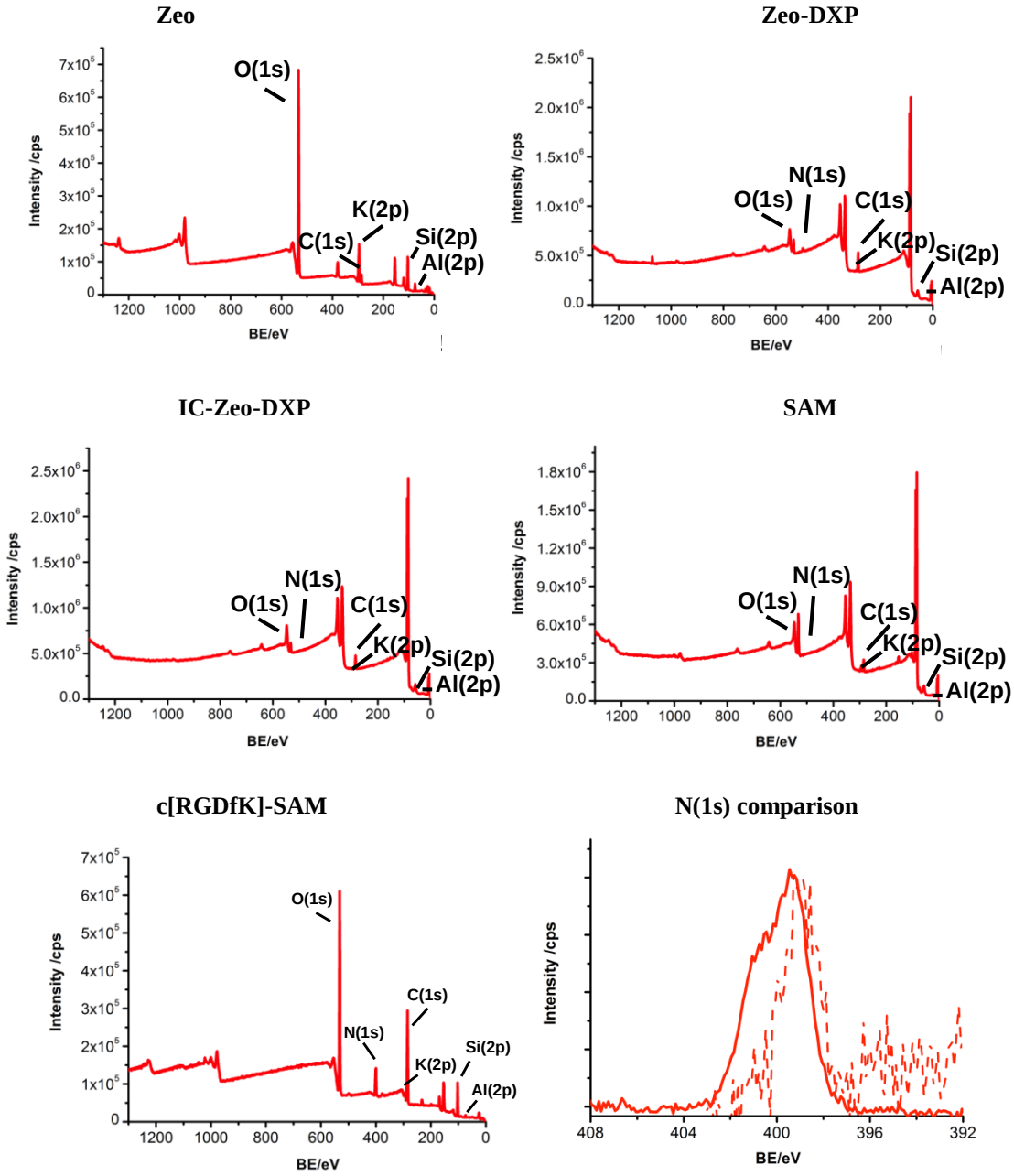

Figure 8. XPS survey spectra for the pristine, the derivatized, and the monolayers of zeolite L materials, and comparison of the high resolution XPS analysis of N(1s) of the **SAM** (dashed line) and c**[RGDfK]-SAM** (full line) samples.

Table 1. XPS analysis results for the pristine, the derivatized and the monolayers of zeolite L materials.*

	Si(2p)**	Al(2p)**	O(1s)**	K(2p)**	C(1s)**	N(1s)**
Zeo	21.4 ± 0.1	6.9 ± 0.8	58.4 ± 0.7	6.5 ± 1.0	6.1 ± 1.0	0.7 ± 0.2
Zeo-DXP	18.9 ± 2.5	8.7 ± 3.3	44.0 ± 5.8	5.6 ± 0.7	20.7 ± 3.7	2.0 ± 0.1
IC-Zeo-DXP	16.0 ± 2.3	12.7 ± 1.6	29.3 ± 3.6	3.5 ± 1.2	33.0 ± 6.7	5.5 ± 0.8
SAM	17.5 ± 3.1	7.5 ± 0.9	37.2 ± 0.1	2.1 ± 1.2	30.6 ± 2.9	5.1 ± 2.8
c[RGDfK]-SAM	14.2 ± 2.1	1.5 ± 0.7	32.8 ± 3.1	0.2 ± 0.2	42.6 ± 4.7	8.7 ± 1.2

* Data not to be considered quantitative.
**Atomic %.

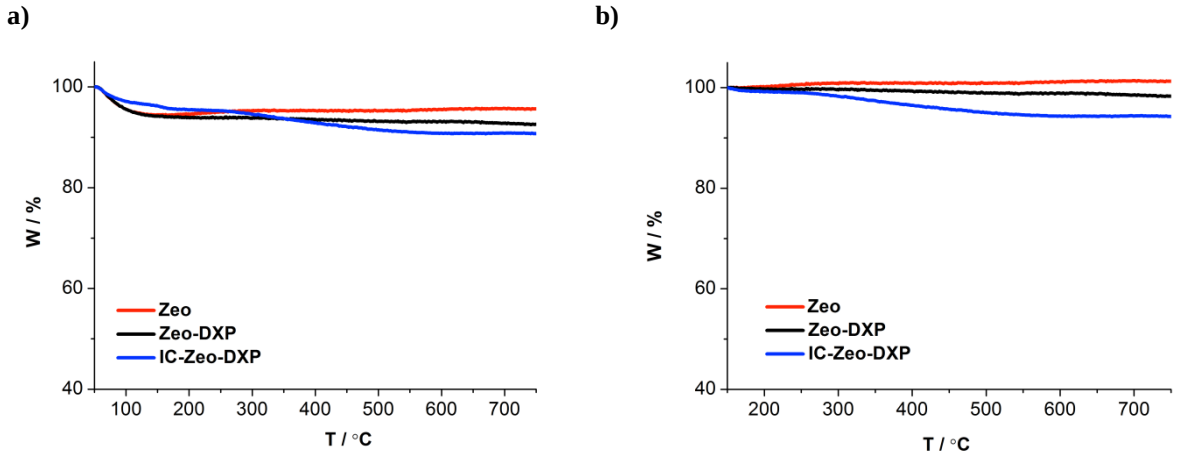

Figure 9. a) TGA analysis of the pristine and the derivatized zeolite L materials; b) normalization of the TGA curves after removing the contribution of the water present in the zeolite materials (pristine zeolites used as reference).

Zeo-DXP

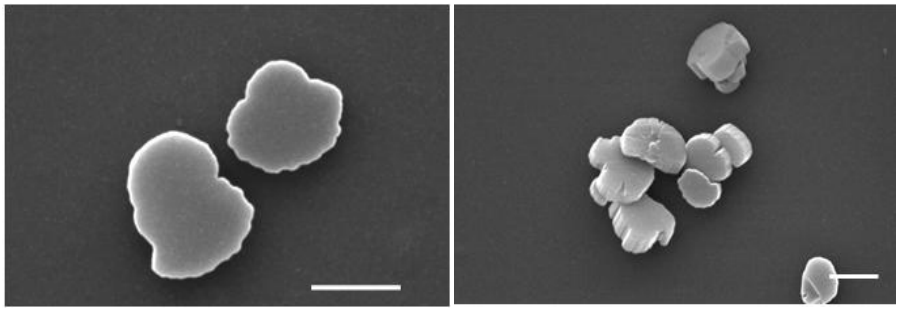

IC-Zeo-DXP

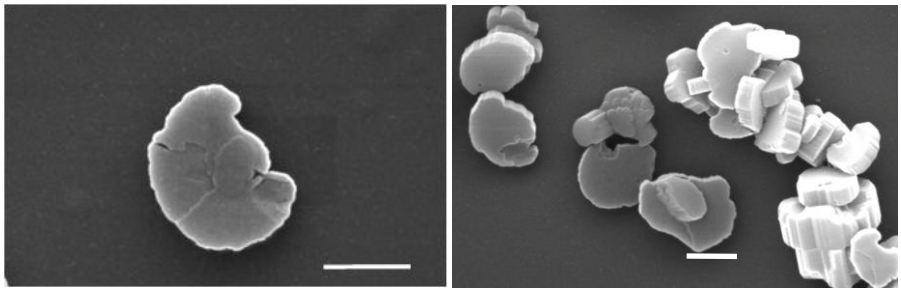

Figure 10. SEM images of the functionalized particles: **Zeo-DXP** and **IC-Zeo-DXP**. Scale bar = 500 nm.

*Functionalization of **c[RGDfK]-SAMs** with rhodamine B isothyocyanate isomer I.* A c[RGDfK]-functionalized SAMs was immersed in a solution of rhodamine B isothiocyanate in EtOH (10 mg/mL) at RT for 30 min. Finally the plate was removed from the solution and washed in EtOH (5 mL) and air dried. The SAM was characterized by means of XPS, and confocal microscope.

10.4.3. Biological methods

Cell culture. Complete culture media was prepared as following: 88 % Dulbecco's Modified Eagle Medium (DMEM), 10 % Fetal Bovine Serum, 1 % Penicillin-Streptomycin and 1 % L-Glutamine 200 nM. The cell culture flask was washed twice with PBS, trypsinated and incubated for 5 min before neutralization of the trypsin with an equal volume of CCM. The cells suspension was then centrifuged 3 min at 1000 rpm and hence re-suspended in fresh CCM until a homogenous dispersion was obtained. 1 mL of the cell suspension was added to a new flask and diluted with 10 mL of CCM, before returning in the incubator.

Cell staining. Cells (1×10^6/mL) were suspended in a serum-free culture medium, and the dye (5 μL/mL) was added. Glioma C6 and HeLa cells were stained with DiO while T-293 cells were stained with DiD. The suspension was then gently mixed and incubated for 10-20 minutes at 37 °C, before being centrifuged at 1500 rpm for 5 min. The supernatant was finally removed, and the cells gently resuspended in fresh medium at 37 °C. The washes were repeated twice.

Cell adhesion and counting. The monolayers were washed with PBS solution to remove all the impurities. The printed DXP SAMs, either naked or functionalized with the peptide, were placed in a 24 well plate and seeded with cells (1×10^5 HeLa, Glioma C6, or T-293 cells). Each plate was covered with the culture medium (2 mL) and incubated for 30 min. Then the culture medium was removed, the plates washed twice with PBS (5 mL) and fixed with PFA (3 mL). After 10 minutes, PFA was removed, and the plates were washed twice with bi-distilled water (5 mL) and mounted on microscopy glass for confocal microscope analysis. The cells counting is an average of three values each referred to a surface of 0.0025 cm^2. This averaged value is then normalized to the total area of the monolayer, 1 cm^2.

a)

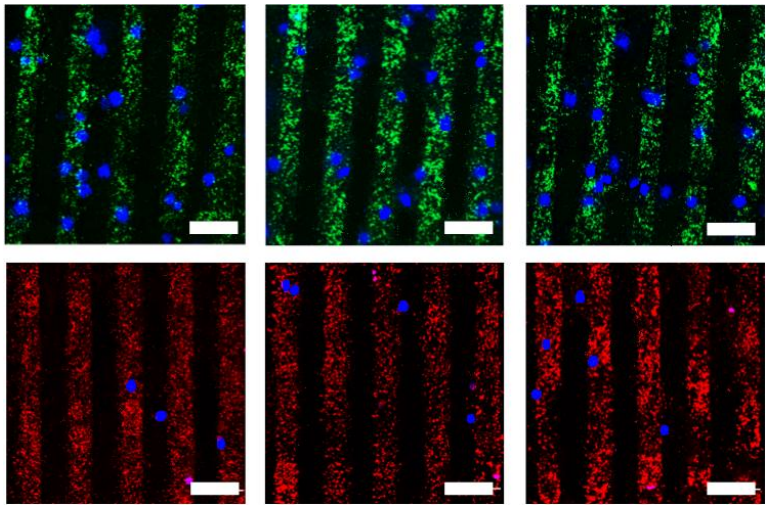

b)

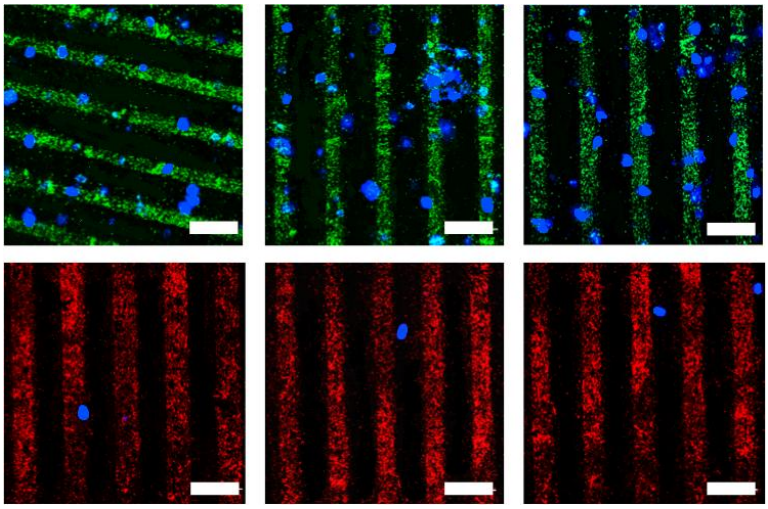

c)

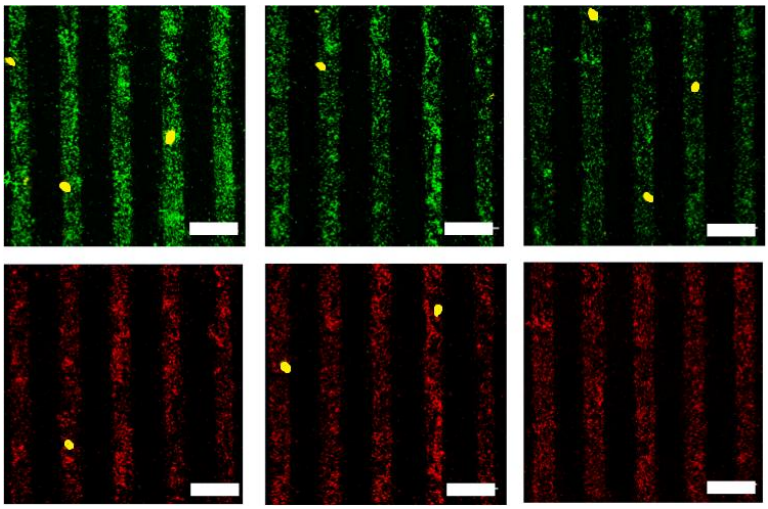

Figure 11. Representative confocal microscopy images for the adhesion experiments of HeLa (a), Glioma C6 (b) and T-293 cells (c) on isocyanate-functionalized SAMs (in red; DXP λ_{exc}= 490 nm) and c[RGDfK]-functionalized SAMs (in green; DXP λ_{exc}= 490 nm): HeLa and Glioma C6 cells are visualized in blue (DiO staining, λ_{exc}= 484 nm); T-293 in yellow (DiD staining, λ_{exc}= 644 nm). Scale bar = 100 μM.

Table 2. Cell counting analysis for the single population adhesion experiments.*

Surface	HeLa**	Glioma C6**	T-293**
SAM	3.2 ± 1.1	0.8 ± 0.4	0.1 ± 0.05
c[RGDfK]-SAM	11.4 ± 0.8	15.3 ± 0.5	0.2 ± 0.05
ratio cells on **c[RGDfK]-SAM/SAM**	3.5	19.1	2

* Total area monitored = 0.0025 cm^2; cell count values normalized to an area of 1 cm^2
**x 10^3

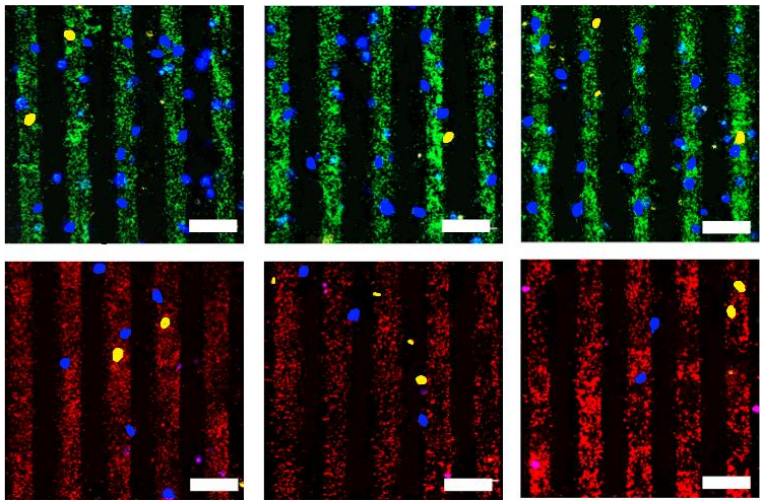

Figure 12. Representative confocal microscopy images for the adhesion experiment of HeLa and T-293 cells (DiO and DiD staining, respectively; DiO λ_{exc} = 484 nm; DiD λ_{exc}= 644 nm) on naked (top) or on c[RGDfK]-functionalized SAMs (bottom): HeLa cells are visualized in blue; T-293 in yellow. Scale bar = 50 μM.

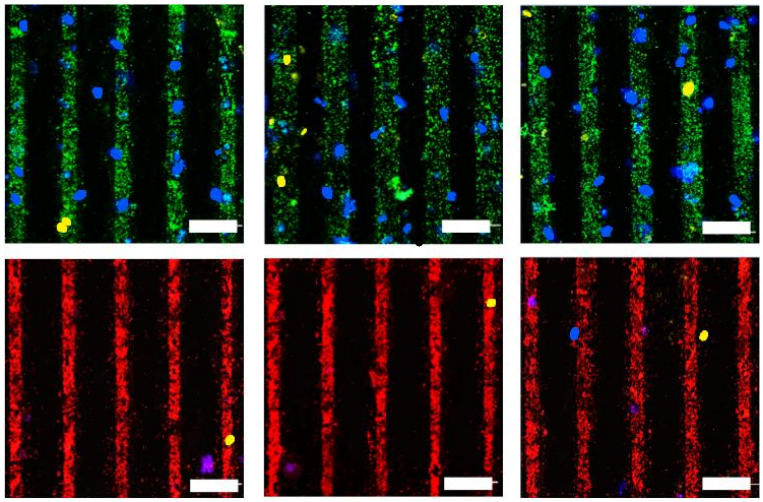

Figure 13. Confocal microscopy image for the adhesion experiment of Glioma C6 and T-293 cells (DiO and DiD staining, respectively; DiO λ_{exc} = 484 nm; DiD λ_{exc}= 644 nm) onto isocyanate-functionalized SAMs (top) or c[RGDfK]-functionalized SAMs (bottom): Glioma C6 cells are visualized in blue; T-293 in yellow. Scale bar = 50 μM.

Table 3. Cell counting analysis for the mixed population adhesion experiments.

Surface	**HeLa/ T-293**		**Glioma C6/T293**	
	HeLa**	T-293**	Glioma C6**	T-293**
SAM	3.6 ± 0.4	0.8 ± 0.1	2.5 ± 0.3	0.8 ± 0.1
c[RGDfK]-SAM	19.7 ± 2.2	2.3 ± 0.5	20.7 ± 6.6	1.0 ± 0.2
cancer/primary cells on c**[RGDfK]-SAM**	8.5		20.7	

* Total area monitored = 0.0025 cm^2; cell count values normalized to an area of 1 cm^2
**x 10^3

References

[1] a) F. G. Giancotti, E. Ruoslahti, *Science* **1999**, *285*, 1028; b) H. Liapis, A. Flath, S. Kitazawa, *Diagn. Mol. Pathol.* **1996**, *5*,127; c) C. R. Cooper, C.H. Chay, K. J. Pienta, *Neoplasia* **2002**, *4*, 191.

[2] H. M. Sheldrake, L. H. Patterson, *Curr. Cancer Drug Targets* **2009**, *9*, 519.

[3] a) J. S. Desgrosellier, D. A. Cheresh, D. S. Missan, *Nat. Rev. Cancer* **2010**, *10*, 9; b) M. Di Persio, *Crit. Rev. Eukaryot. Gene Expr.* **2012**, *22*, 309.

[4] S. Takayama, S. Ishii, T. Ikeda, S. Masamura, M. Doi, M. Kitajima, *Anticancer Res.* **2005**, *25*, 79.

[5] R. Hosotani, M. Kawaguchi, T. Masui, T. Koshiba, J. Ida, K. Fujimoto, M. Wada, R. Doi, M. Imamura, *Pancreas* **2002**, *25*, e30.

[6] E. Ruoslahti, M. D. Pierschbacher, *Science* **1987**, *238*, 491.

[7] a) C. Henry, N. Moitessier, Y. Chapleur, *Mini Rev. Med. Chem.* **2002**, *2*, 531; b) K. Temming, R. M. Schiffelers, G. Molema, R. J. Kok, *Drug Resist.* **2005**, *8*, 381.

[8] a) R. E. Hewitt, D. G. Powe, K. Morrell, E. Balley, I. H. Leach, I. O. Ellis, D. R. Turner, *Br. J. Cancer* **1997**, *75*, 221; b) M. Rolli, E. Fransvea, J. Pilch, A. Saven, B. Felding-Habermann, *Proc. Natl. Acad. Sci. USA* **2003**, *100*, 9482; c) M. M. Zutter, H. Sun, S. A. Santoro; *J. Mammary Gland Biol. Neoplasia* **1998**, *3*, 191.

[9] a) F. Rechenmacher, S. Neubauer, C. Mas-Moruno, P. M. Dorfner, J. Polleux, J. Guasch, B. Conings, H. G. Boyen, A. Bochen, T. R. Sobahi, R. Burgkart, J. P. Spatz , R. Fässler, H. Kessler, *Chem. Eur. J.* **2013**, *19*, 9218; b) K. D. Belfield, *Biomacromolecules* **2011**, *12*, 441.

[10] a) J. Park, S. Bauer, K. von der Mark, P. Schmuki, *Nano Lett.* **2007**, *7*, 1686; b) L. Ferreira, J. M. Karp, L. Nobre, R. Langer, *Cell Stem Cell* **2008**, *3*, 136.

[11] a) N. S. Kehr, A. Schaefer, B. J. Ravoo, L. De Cola, *Nanoscale*, **2010**, *2*, 601; b) J. El-Gindi, K. Benson, L. De Cola, H. J. Galla, N. S. Kehr, *Angew. Chem. Int. Ed.* **2012**, *51*, 3716; c) N. S. Kehr, K. Riehemann, J. El-Gindi, A. Schäfer, H. Fuchs, H. J. Galla, L. De Cola, *Adv. Funct. Mater.* **2010**, *20*, 2248.

[12] K. B. Yoon, *Acc. Chem. Res.* **2007**, *40*, 29.

[13] T. Ashworth, *Australian Med. J.* **1869**, *14*, 146.

[14] G. P. Gupta, J. Massagué, *Cell*, **2006**, *127*, 679.

[15] B. Mostert, S. Sleijfer, J. A. Foekens, J. W. Gratama, *Cancer Treat. Rev.*, **2009**, *35*, 463.

[16] E. A. Punnoose, S. K. Atwal, J. M. Spoerke, H. Savage, A. Pandita A, R. F. Yeh, A. Pirzkall, B. M. Fine, L. C. Amler, D. S. Chen, M. R. Lackner, *PLoS ONE*, **2010**, *5*, e12517.

[17] A. Devaux, G. Calzaferri, I. Miletto, P. Cao, P. Belser, D. Brühwiler, O. Khorev, R. Häner, A. Kunzmann, *J. Phys. Chem. C*, **2013**, *117*, 23034.

[18] a) R. Haubner, D. Finsinger, H. Kessler, *Angew. Chem. Int. Ed. Engl.* **1997**, *36*, 1374; b) M. Kantlehner, D. Finsinger, J. Meyer, P. Schaffner, A. Jonczyk, B. Diefenbach, B. Nies, H. Kessler, *Angew. Chem, Int. Ed.* **1999**, *38*, 560.

[19] L. Gentilucci, G. Cardillo, S. Spampinato, A. Tolomelli, F. Squassabia, R. De Marco, A. Bedini, M. Baiula, L. Belvisi, M. Civera, *J. Med. Chem.* **2010**, *53*, 106.

[20] a) F. Danhier, A. Le Breton, V. Préat, *Mol. Pharmaceutics* **2012**, *9*, 2961; b) D. Arosio, C. Casagrande, L. Manzoni, *Curr. Med. Chem.* **2012**, *19*, 3128.

[21] K. Yamada, I. Nagashima, M. Hachisu, I. Matsuo, H. Shimizu, *Tetrahedron Lett.* **2012**, *53*, 1066.

[22] A. Devaux, G. Calzaferri, I. Miletto, P. Cao, P. Belser, D. Brühwiler, O. Khorev, R. Häner, A. Kunzmann, *J. Phys. Chem. C*, **2013**, *117*, 23034.

Conclusions

This thesis work deals, principally, with the development of different chemical protocols ranging from environmental sustainability peptide synthesis to asymmetric synthesis of modified tryptophans to a series of straightforward procedures for constraining peptide backbones without the need for a pre-formed scaffold.
Much efforts have been dedicated to the structural analysis in a biomimetic environment, fundamental for predicting the *in vivo* conformation of compounds, as well as for giving a rationale to the experimentally determined bioactivity. The conformational analyses in solution has been done mostly by NMR (2D gCosy, Roesy, VT, titration experiments, molecular dynamics, etc.), FT-IR and ECD spectroscopy.
As a practical application, 3D rigid scaffolds have been employed for the synthesis of biological active compounds based on peptidomimetic and retro-mimetic structures. These mimics have been investigated for their potential as antiflammatory agents and actually the results obtained are very promising.
Moreover, the synthesis of Amo ring permitted the development of an alternative high effective synthetic pathway for obtaining Linezolid antibiotic.
The final section is, instead, dedicated to the construction of a new biosensor based on zeolite L SAMs functionalized with the integrin ligand c[RGDfK], that has showed high efficiency for the selective detection of tumour cells. Such kind of sensor could, in fact, enable the convenient, non-invasive detection and diagnosis of cancer in early stages, from a few drops of a patient's blood or other biological fluids.
In conclusion, the researches described herein demonstrate that the peptidomimetic approach to 3D definite structures, allows unambiguous investigation of the structure-activity relationships, giving an access to a wide range bioactive compounds of pharmaceutical interest to use not only as potential drugs but also for diagnostic and theranostic applications.